

Construction of robust *Escherichia coli* strains for large-scale production

Dissertation

Von der Fakultät 4 Energie-, Verfahrens- und Biotechnik der Universität Stuttgart
zur Erlangung der Würde eines
Doktors der Naturwissenschaften (Dr. rer. nat.)
genehmigte Abhandlung

Vorgelegt von

Martin Ziegler

aus Stuttgart

Hauptberichter:	Prof. Dr.-Ing. Ralf Takors
Mitberichter:	Prof. Dr. Georg Sprenger
Tag der mündlichen Prüfung:	10. Februar 2022

Institut für Bioverfahrenstechnik der Universität Stuttgart

2022

Titel in deutscher Sprache:

**Konstruktion robuster *Escherichia coli* Stämme für die
Produktion in großvolumigen Reaktoren**

Meinem Vater

Acknowledgements

This manuscript is the culmination of several years of scientific work. Many people were involved and supported me during this time. I would like to express my gratitude and appreciation.

First and foremost, I want to thank Prof. Dr.-Ing. Ralf Takors for the opportunity to work on this project – none of this would have been possible without his trust in my abilities. His continued support has shaped this project and guided me through the academic world. I would also like to thank the members of the audit committee of this thesis: Prof. Dr. Georg Sprenger and Prof. Dr. Bernhard Hauer. Furthermore, I would like to thank Prof. Dr. Ingrid Weiß, Jun. Prof. Dr. Michael Heymann, and apl. Prof. Dr. habil. Martin Siemann-Herzberg for their participation in the circulation procedure.

I am deeply grateful for the support of many colleagues during the realization of this project: Andreas Ankenbaur, Andreas Freund, Alex Dietrich, Salaheddine Laghrami, Andrea Seipel, Martina Schweikert, Eugenia Münch, Mira Lenfers-Lücker, Attila Teleki, Maike Kuschel, Prof. Dr. Bastian Blombach, Steven Minden, Robert Nitschel, Richard Schäfer, Christoph Schaal, Maria Aniolek, Silke Reu, Maren Lösch, Anina Buchmann and Adrian Eilingsfeld.

My special thanks go to my colleague Julia Zieringer who collaborated with me on several joint research projects. Her continued support and the enlightening discussions in our shared office have helped to shape this project and broadened my understanding of computational biology.

I would further like to acknowledge the support of students who have written their thesis under my supervision: Teresa Gäbele, Clarissa-Laura Döring, Liv Paul, Lukas Madenach, Simon Leuben and Theresa Raisch. I would also like to thank the iGEM team of the University of Stuttgart – we had an amazing time!

I would like to thank my close friend Nicholas Cole for proof-reading this thesis.

Finally, I would like to thank my family and friends for their continued support through all these years. My special gratitude lies with my closest family, and my late father Dr. Klaus Ziegler – I wish you could have seen the completion of this work.

Declaration of Authorship

I declare that this thesis has been written by me. Thoughts, results, and citations from other authors have been marked with references according to scientific standards. The presented results are based on my own research activities or on joint activities with other scientists in which case I have indicated the individual contributions. Contents of the electronic version of this thesis are identical to the printed version.

Hiermit erkläre ich, dass ich die vorliegende Arbeit selbstständig angefertigt habe. Gedanken, Forschungsergebnisse und Zitate anderer Autoren wurden wissenschaftlichen Standards entsprechend im Text mit Quellenangaben gekennzeichnet. Die präsentierten Forschungsergebnisse beruhen auf meiner eigenen Forschungsaktivität oder gemeinsamen Forschungsaktivitäten mit anderen Wissenschaftlern, in welchem Fall ich die einzelnen Beiträge kenntlich gemacht habe. Die elektronische Version dieser Thesis ist inhaltlich identisch zur gedruckten Form.

Ort, Datum

Martin Ziegler

Table of Contents

Acknowledgements	4
Declaration of Authorship	5
Table of Contents	6
List of Figures	10
List of Tables.....	15
Abbreviations and Symbols	16
Abstract	19
Zusammenfassung	21
1. Introduction	24
1.1 Challenges in biochemical engineering – motivation for this thesis.....	25
2. Scientific background.....	27
2.1 Microbial fermentations	27
2.1.1 Monod kinetics and Pirt’s maintenance coefficient	27
2.1.2 Batch fermentations.....	28
2.1.3 Continuous cultivations.....	29
2.2 Scale-up of microbial processes	31
2.2.1 Scale-down reactors	31
2.3 <i>Escherichia coli</i> as a host for microbial fermentations	33
2.3.1 General physiology	33
2.3.2 Transcriptional regulation	34
2.3.3 The Stringent Response.....	35
2.3.4 Glucose limitation	36
2.3.5 Nitrogen limitation	38
2.3.6 Adenylate Energy Charge	39
2.3.7 Scale-up of <i>E. coli</i> fermentations	40

2.4 Genetic engineering of <i>Escherichia coli</i>	42
2.4.1 Plasmids and pJOE4056.2.....	42
2.4.2 Recombineering	42
2.4.3 Genome reduction	43
2.4.4 CRISPRi.....	45
3. Objectives and research questions of this thesis	48
4. Publications	50
4.1 Transcriptional profiling of the stringent response mutant strain <i>E. coli</i> SR reveals enhanced robustness to large-scale conditions.....	51
4.1.1 Summary	52
4.1.2 Introduction	53
4.1.3 Results	56
4.1.4 Discussion	71
4.1.5 Materials and methods	76
4.1.6 Acknowledgements	82
4.2 Engineering of a robust <i>Escherichia coli</i> chassis and exploitation for large-scale production processes	83
4.2.1 Abstract	84
4.2.2 Introduction	85
4.2.3 Materials and methods	88
4.2.4 Results	97
4.2.5 Discussion	110
4.2.6 Conclusion.....	116
4.2.7 Acknowledgements	117
4.3 CRISPRi enables fast growth followed by stable aerobic pyruvate formation in <i>Escherichia coli</i> without auxotrophy.....	118
4.3.1 Practical application	119

4.3.2 Abstract	120
4.3.3 Introduction	121
4.3.4 Materials and methods	124
4.3.5 Results	132
4.3.6 Discussion	141
4.3.7 Acknowledgements	146
5. Materials and Methods – additional experiments	147
5.1 Contributions	147
5.2 General molecular biology methods	147
5.2.1 Buffer and media	147
5.2.2 Polymerase Chain Reaction (PCR)	148
5.2.3 Agarose gel electrophoresis	148
5.2.4 Cloning	148
5.2.5 Transformation	149
5.3. Protein production in <i>E. coli</i> MG1655, <i>E. coli</i> CD202 and <i>E. coli</i> SR	150
5.3.1 Strains	150
5.3.2 Cloning of p006_kan_eGFP	151
5.3.3 Shaking flask experiments	151
5.4 Pyruvate production in <i>E. coli</i> SR	153
6. Results – additional experiments	154
6.1 Production of eGFP by <i>E. coli</i> strains	154
6.2 Cultivation of <i>E. coli</i> SR pdCas9 psgRNA_aceE_234_pdhR_329	156
7. Discussion	157
7.1 Robustness of <i>E. coli</i> RM214 and <i>E. coli</i> SR to heterogeneous conditions	160
7.2 Simulating large-scale conditions with scale-down reactors	163
7.3 Modulating global cellular regulation – the case of <i>E. coli</i> SR	167

Table of Contents

7.4 Nitrogen-limitation as a process strategy	169
7.5 Outlook: Engineering hosts for large-scale conditions	171
8. Conclusion.....	174
9. References	175
Attachments.....	214

List of Figures

- Fig. 1:** Phases of a batch fermentation. Data shown is from a batch fermentation of *E. coli* MG1655 pdCas9 psgRNA_aceE_234_pdhR_329. Error bars indicate SEM (n = 5). The limiting nutrient was ammonium. A: pre-exponential phase, B: exponential phase, C: limited phase, D: stationary phase 29
- Fig. 2:** Dilution of original volume elements in a chemostat experiment..... 30
- Fig. 3:** Basic scale-down reactor designs. A: STR with installed discs to reduce mixing efficacy. B: STR operated with oscillating cultivation conditions. C: STR-STR two-compartment reactor. D: STR-PFR two-compartment reactor. 32
- Fig. 4:** Experimental design of the two-compartment system. The fermenter consists of a stirred tank reactor (STR) as the primary cultivation vessel and a plug-flow reactor (PFR) connected by an active pump. The ammonium-limited chemostat was operated at a dilution rate of $D = 0.2 \text{ h}^{-1}$ with the feeding point placed in the STR. The STR served as a limitation zone and the PFR formed a starvation zone. The setup was designed to resolve different timescales of cellular response. Oxygen saturation was measured by three oxygen probes and recorded by the process control system (01, 02, 03). V_{STRref} : Reference Volume without connection of PFR (constant volume)..... 57
- Fig. 5:** Physiological measurements. **A.** Cell dry weight. Concentration of cell dry weight after at least 25 h chemostat process before connecting the plug-flow reactor (0 h) and after 28 h of chemostat process with connected PFR (28 h). **B.** Ammonium. Concentration of residual ammonium in the supernatant. **C.** Carbon Balance. Columns show efflux fractions of total C-mol based on carbon influx. The final fraction represents undetermined dissolved organic substances in the fermentation broth, as measured by the difference of all efflux carbon detected by exhaust gas or total carbon analysis and the sum of the individually measured efflux components. Error bars indicate SEM (n = 2) of individual components (A, B and C). 59
- Fig. 6:** Number of UP (black) and DOWN (gray) regulated genes (DEGs). Long-term (left) and short-term (right) response to repeated nitrogen starvation for *E. coli* MG1655 (WT) and *E. coli* SR (SR) and given process times..... 61
- Fig. 7:** Principal component analysis of transcript data of *E. coli* MG1655 (WT) (top) and *E. coli* SR (bottom) obtained from STR (S) and PFR (port 5, P5) at three process time points (0 h, 5 min, and 28 h). Covered measurement variance of each principal component (PC) is

indicated. Ellipses cluster samples of STR and PFR. PC1 accounts for ‘sample port location’, PC2 for ‘process time’.....	62
Fig. 8: Alarmone accumulation along the PFR. Concentration of ppGpp measured from samples drawn along the plug flow reactor (P1 to P5) relative to the concentration measured in the stirred tank reactor (S, all values set to 1) for <i>E. coli</i> MG1655 (WT) and <i>E. coli</i> SR (SR). Error Bars represent SEM (n = 2).	64
Fig. 9: Venn diagrams representing partially overlapping sets of DEGs of <i>E. coli</i> MG1655 (WT) and <i>E. coli</i> SR. The number of significantly up- (UP) and downregulated (DOWN) genes in each set is indicated by numbers. Left: Short-term responses 5 min after PFR connection. Right: Short-term responses 28 h after PFR connection. Complete gene lists of the Venn diagrams are available in the supplementary data.	65
Fig. 10: Top: Transcriptional patterns grouped into COG categories of <i>E. coli</i> MG1655 (WT) and <i>E. coli</i> SR (SR). Left: short-term patterns to the PFR stimulus 5 min after PFR connection. Right: short-term patterns to the PFR stimulus 28 h after PFR connection. Bottom: Sigma factor activities of <i>E. coli</i> MG1655 (WT, grey) and <i>E. coli</i> SR (SR, black). Left: Short-term response to the PFR stimulus 5 min after PFR connection. Right: Short-term response to the PFR stimulus 28 h after PFR connection. Significant categories are indicated with an asterix.	66
Fig. 11: Significant GO categories after 5 min and 28 h of both <i>E. coli</i> SR (left) and <i>E. coli</i> MG1655 (right). Downregulated categories are arranged at the top and upregulated GO terms at the bottom. 5 min: Short-term response of <i>E. coli</i> SR (left) and <i>E. coli</i> MG1655 (right) after 5 min of PFR action. Only the Top 20 out of 102 significantly downregulated categories are shown. Neither strain had significantly upregulated categories for this time-point. 28 h: Short-term response of <i>E. coli</i> SR (left, light grey) and <i>E. coli</i> MG1655 (right, light grey) after 28 h of PFR action. For <i>E. coli</i> SR only the Top 20 out of 24 significantly upregulated categories are shown. For <i>E. coli</i> MG1655 only the Top 20 out of 95 significantly downregulated categories are shown. No significantly upregulated categories were found for this time-point.	69
Fig. 12: Reactor Setup. The primary reactor was a standard laboratory reactor operated as a fully aerobic glucose limited chemostat at 37 °C (left scheme). For measurements of the well mixed STR reference state the entire biosuspension was in the primary reactor ($V_{STR} = 1.60$ l). Scale-down conditions were installed by connecting a secondary plug-flow reactor (PFR). An active pump then constantly circulated $V_{PFR} = 0.38$ l fermentation broth between STR and PFR reducing the volume fraction in the STR to $V_{STR-PFR} = 1.22$ l (right scheme). Labels STR and	

P1 to P5 designate sampling ports with the respective average residence time of biosuspension after leaving the STR. Fermentations were carried out in two phases each lasting for at least five volumetric residence times: First, a homogenous STR reference state was established, followed by a subsequent heterogeneous STR-PFR phase. 97

Fig. 13: Basic growth parameters of deletion strains. Deletion strains CD101 to RM214 were cultivated in minimal glucose medium in shaking flask fermentations. The maximum specific growth rate (blue) and biomass yield (yellow) were determined. The parent strain *E. coli* MG1655 was cultivated in parallel, and all data collected normalized to its growth parameters. Error bars indicate SEM (n = 3). The dashed line is a visual aid indicating reference values of 1. 99

Fig. 14: Determination of maintenance coefficients under heterogeneous STR-PFR conditions. *E. coli* MG1655 (grey squares, dashed line) and *E. coli* RM214 (orange triangles, solid line) were cultivated in the STR-PFR system (glucose limited chemostats, $D = 0.05 \text{ h}^{-1}$, 0.1 h^{-1} , 0.2 h^{-1} , 0.3 h^{-1}). Maintenance coefficients m_s (slope) and true biomass yields Y_{XS}^{true} (intersection) were determined from the linear regression of data points. The difference of the maintenance coefficients is statistically significant ($\Delta m_s = -0.038 \text{ g}_{\text{Glucose}} * \text{g}_{\text{CDW}}^{-1} * \text{h}^{-1}$, $p < 0.05$). Error bars indicate technical standard deviation. 101

Fig. 15: EGFP yield on substrate and proportion of cells with high eGFP content. *E. coli* MG1655 *rhaB*⁻ pJOE4056.2_tetA (grey) and *E. coli* RM214 *rhaB*⁻ pJOE4056.2_tetA (orange) were cultivated in the STR-PFR system (glucose limited chemostat, $D = 0.2 \text{ h}^{-1}$). Samples were collected from the primary vessel. Error bars indicate SEM (n = 4), statistical indicators: * $p < 0.05$, ** $p < 0.01$, *** $p < 0.001$. Left: eGFP yield on substrate declines for both strains after PFR connection. Simultaneously, the difference between the strains gradually increases. Statistics: two-tailed t-tests comparing means of a single strain at later time points to the STR mean of the strain; and comparing the means of both strains at each time point to each other. Right: The proportion of cells with high eGFP content declines towards the end of the fermentation and is lower for *E. coli* MG1655 *rhaB*⁻ pJOE4056.2_tetA than for *E. coli* RM214 *rhaB*⁻ pJOE4056.2_tetA. Statistics: one-tailed t-tests comparing the presumably lower mean of *E. coli* MG1655 *rhaB*⁻ pJOE4056.2_tetA to that of *E. coli* RM214 *rhaB*⁻ pJOE4056.2_tetA at each time point. 104

Fig. 16: Carbon Balance. *E. coli* MG1655 *rhaB*⁻ pJOE4056.2_tetA (grey) and *E. coli* RM214 *rhaB*⁻ pJOE4056.2_tetA (orange) were cultivated in the STR-PFR system (glucose limited

chemostat, $D = 0.2 \text{ h}^{-1}$). Columns show efflux fractions of individual substances. Error bars indicate SEM ($n = 4$). For raw data see Supplementary Tables S5.A and S5.B.	106
Fig. 17: Adenylate Energy Charge in the STR and during PFR passage. <i>E. coli</i> MG1655 rhaB ⁻ pJOE4056.2_tetA and <i>E. coli</i> RM214 rhaB ⁻ pJOE4056.2_tetA were cultivated in the STR-PFR system (glucose limited chemostat, $D = 0.2 \text{ h}^{-1}$). The adenylate energy charge of cultures was determined shortly after PFR connection (STR-PFR 5 min, upper panel) and after five volumetric residence times (STR-PFR 25 h, lower panel). Samples were drawn from the primary reactor (0 s) and the five sampling ports along the axis of the PFR (35 s, 52 s, 77 s, 102 s, 128 s). Error bars indicate SEM ($n = 4$).	108
Fig. 18: sgRNA binding sites. Four binding sites (232, 233, 234 and 235) were chosen for CRISPRi targeting <i>aceE</i> and three binding sites (327,328 and 329) for CRISPRi against <i>pdhRp</i>	133
Fig. 19: Pyruvate yield in shaking flask fermentations of <i>E. coli</i> MG1655 pdCas9 with different psgRNAs. Data is grouped into four series. Error bars indicate SEM ($n = 3$; * $n = 2$). A: wild-type reference (no plasmids) and first series, silencing of <i>aceE</i> . B: second series, combinatorial silencing of <i>aceE</i> . C: third series, simultaneous silencing of <i>aceE</i> and <i>pdhR</i> . D: fourth series, silencing of <i>pdhR</i>	134
Fig. 20: Shaking flask fermentations of the single knockdown strain <i>E. coli</i> pdCas9 psgRNA_aceE_234. The experiments were conducted with addition of the inducer anhydrotetracycline (left) or without anhydrotetracycline (right). Error bars indicate SEM ($n = 3$).	135
Fig. 21: Bioreactor cultivations of knockdown strains. The aerobic lab-scale fermentations were carried out with excessive glucose. Depletion of ammonia initiates the nitrogen-limited second process phase. Error bars indicate SEM. Left: The best single knockdown strain from the 1 st series <i>E. coli</i> MG1655 pdCas9 psgRNA_aceE_234 ($n = 3$). Right: The best double knockdown strain from the 3 rd series <i>E. coli</i> MG1655 pdCas9 psgRNA_aceE_234_pdhR_329 ($n = 5$). ..	137
Fig. 22: Shaking flask fermentations of the double knockdown strain <i>E. coli</i> MG1655 pdCas9 psgRNA_aceE_232_aceE_235. Error bars indicate SEM ($n = 3$).	139
Fig. 23: Shaking flask fermentations of the single knockdown strain <i>E. coli</i> MG1655 pdCas9 psgRNA_aceE_pdhR_329. Error bars indicate SEM ($n = 3$).	141

Fig. 24: Production of eGFP in *E. coli* SR. The indicated strains were cultivated in aerobic shaking flasks in minimal medium. Inducer was added 4 h after inoculation. Error bars represent SEM (n = 3)..... 155

Fig. 25: Fermentation profile of *E. coli* SR pdCas9 psgRNA_aceE_234_pdhR_329 with inducer anhydrotetracycline (+ Atc). Error bars indicate SEM (n = 3)..... 156

List of Tables

Table 1: Sigma factors	35
Table 2: Physiological measurements	60
Table 3: Bacterial strains used in this study.	76
Table 4: Bacterial strains used in this study.	89
Table 5: Fermentation parameters ^a of the eGFP production processes.	109
Table 6: Strains used in this study.	126
Table 7: Primers used in this study.	128
Table 8: Yield coefficients and fermentation parameters of bioreactor fermentations with extended nitrogen-limited production phase.	138
Table 9: Strains used in the protein production experiments	150
Table 10: Primer for cloning of p006_kan_eGFP	151
Table 11: Strains used in the pyruvate production experiments.	153
Table 12: Scientific output	158

Abbreviations and Symbols

Abbreviation	Full Designation
AEC	Adenylate Energy Charge
AMP	adenosine monophosphate
ADP	adenosine diphosphate
Atc	anhydrotetracycline
ATP	adenosine triphosphate
AxP	adenosine phosphate(s)
cAMP	cyclic adenosine monophosphate
CDW	cell dry weight
crRNA	CRISPR RNA
CRISPR	Clustered Regularly Interspaced Short Palindromic Repeats
CRISPRi	CRISPR interference
CRP	cAMP response protein
Da	Dalton
dCas9	dead Cas9
DNA	deoxyribonucleic acid
dsDNA	double stranded DNA
<i>E. coli</i>	<i>Escherichia coli</i>
<i>E. coli</i> MG1655	<i>Escherichia coli</i> K-12 MG1655
EDTA	Ethylenediaminetetraacetic acid
EMP	Embden-Meyerhoff-Parnas

Abbreviations and Symbols

Abbreviation	Full Designation
eGFP	enhanced green fluorescent protein
GDP	guanosine diphosphate
GTP	guanosine triphosphate
IPTG	Isopropyl- β -D-thiogalactopyranosid
MAGE	multiplex automated genome engineering
Mb	Megabases
MEP	2C-methyl-d-erythritol-4-phosphate
OD	optical density
Osm	Osmotic concentration (formerly known as Osmolarity)
PAM	protospacer adjacent motif
PHA	polyhydroxyalkanoates
PCR	polymerase chain reaction
PFR	plug-flow reactor
ppGpp	guanosine 3',5'-bis(diphosphate)
pppGpp	guanosine 3'-diphosphate 5'-triphosphate
(p)ppGpp	ppGpp and pppGpp
RNA	ribonucleic acid
RNAP	RNA polymerase
SEM	standard error of the mean
sgRNA	single guide RNA
ssDNA	single stranded DNA
STR	stirred tank reactor

Abbreviations and Symbols

Abbreviation	Full Designation
tracrRNA	trans-activating crRNA
TRIS	tris(hydroxymethyl)aminomethane

Symbol	Designation	Dimension
c_s	substrate concentration	$\text{g}_{\text{Substrate}} / \text{l}$
K_s	substrate uptake kinetic constant	$\text{g}_{\text{Substrate}} / \text{l}$
m_s	maintenance coefficient	$\text{g}_{\text{Substrate}} / \text{g}_{\text{CDW}} / \text{h}$
n	number of observations	-
p	error probability	-
μ	specific growth rate	h^{-1}
μ_{max}	maximum specific growth rate	h^{-1}
$Y_{\text{XS},\mu}$	biomass yield	$\text{g}_{\text{CDW}} / \text{g}_{\text{Substrate}}$

Abstract

The biotechnical production of many fine chemicals, proteins or pharmaceuticals depends on large-scale microbial cultivations. Due to limited mixing, heterogeneities in process relevant parameters such as nutrient concentrations arise in such fermentations. *Escherichia coli* (*E. coli*) is a model organism frequently used in the biotechnological industry. If *E. coli* is cultivated under heterogeneous conditions, biological reactions of the microorganism result in reduced process performance. Since large-scale fermentations are not economically feasible in academic settings, scale-down reactors that mimic aforementioned heterogeneities are used to investigate heterogenous fermentations. Previous studies in scale-down reactors unraveled that, depending on the process strategy, the unstable supply of a limiting primary carbon or nitrogen source such as glucose or ammonium is one of the underlying causes of process performance loss. Low concentrations of glucose or ammonium elicit the stringent response as a biological starvation reaction which comprises extensive transcriptional reactions.

In the first project that contributes to this thesis, the regulatory and transcriptional reactions of the strains *E. coli* MG1655 and *E. coli* SR to repeated exposure to ammonium starvation zones were examined in a scale-down reactor. The scale-down reactor followed a two-compartment approach and consisted of a stirred tank reactor and a plug-flow reactor simulating passage through a starvation zone. *E. coli* SR is a strain with modulated stringent response. It was observed that short-term starvation stimuli do not trigger this regulatory program in *E. coli* SR and the transcriptional reaction was noticeably reduced. Long-term adaptation of the strain to repeated cycles of limitation and starvation also clearly differed from *E. coli* MG1655. Despite lack of the stringent response, *E. coli* SR showed no deficits in the assimilation of the limiting ammonium or in biomass yield on ammonium.

In the second project of this thesis, a series of deletion strains with robust phenotype against glucose starvation zones were constructed. Candidate genes were identified and successively removed from the genome of *E. coli* MG1655 by Recombineering. The fundamental growth parameters of the strains were determined in shaking flask fermentations and no noticeable differences compared to *E. coli* MG1655 were found. Chemostat cultivations in a scale-down reactor with glucose as the limiting nutrient source revealed that the final strain of the deletion series, *E. coli* RM214, had a significantly lower maintenance coefficient under heterogeneous conditions than *E. coli* MG1655. Moreover, in an exemplary heterologous protein production

scenario *E. coli* RM214 *rhaB*⁻ pJOE4056.2_{tetA} proved to be more robust to heterogeneities and showed a significantly higher product yield than *E. coli* MG1655 *rhaB*⁻ pJOE4056.2_{tetA}.

In the third project of this thesis, the production of pyruvate in *E. coli* MG1655 by inhibition of pyruvate dehydrogenase through CRISPR interference was investigated. A central goal was to achieve the stable production in nitrogen-limited conditions. For this, different target sequences in the operon *pdhR-aceEF-lpd* were tested and the strains cultivated in shaking flask fermentations. All tested target sequences were generally suitable to trigger the accumulation of pyruvate. Combined CRISPR interference against two target sequences did not lead to an increased pyruvate yield in most cases. In addition, the strains *E. coli* MG1655 pdCas9 psgRNA_{aceE_234} and *E. coli* MG1655 pdCas9 psgRNA_{aceE_234_pdhR_329} were characterized in two phase fermentations in lab-scale reactors. The initial phase was an unlimited exponential growth phase and was followed by an ammonium-limited production phase. *E. coli* MG1655 pdCas9 psgRNA_{aceE_234} only produced pyruvate during the exponential phase, and reuptake of pyruvate occurred in the second phase. In contrast, *E. coli* MG1655 pdCas9 psgRNA_{aceE_234_pdhR_329} stably produced pyruvate during the exponential and the ammonium-limited phase and is a potential chassis strain for the growth-decoupled production of pyruvate derived bioproducts.

The overarching research issues of the projects were the characterization of strains in heterogeneous conditions and the development of new strategies to improve their performance. The collected data leads me to conclude that the construction of robust microbial strains for large-scale applications is both expedient and feasible. Tailored genetic modifications are the method of choice to achieve this goal. Furthermore, suitable genetic constructs offer promising possibilities for the stable growth-decoupled production of chemicals in nitrogen-limited conditions.

Zusammenfassung

Die biotechnische Herstellung zahlreicher Produkte wie Feinchemikalien, Proteine oder Pharmazeutika beruht auf großvolumigen Fermentationsansätzen. In diesen Fermentationen entstehen aufgrund imperfekter Durchmischung Heterogenitäten in prozessrelevanten Parametern wie Nährstoffkonzentrationen. *Escherichia coli* (*E. coli*) ist ein in der biotechnologischen Industrie häufig verwendeter Modellorganismus. Wenn *E. coli* unter heterogenen Bedingungen kultiviert wird, führen biologische Reaktionen des Mikroorganismus zu sinkenden Leistungsparametern des Prozesses. Da großvolumige Fermentationen im akademischen Kontext aus Kostengründen nicht möglich sind, werden zur Erforschung heterogener Bedingungen stattdessen *scale-down* Reaktoren verwendet, die einzelne Bedingungen des Großmaßstabs im Labormaßstab nachbilden. Frühere Untersuchungen in *scale-down* Reaktoren zu den Ursachen von Prozessverlusten ergaben unter anderem, dass, abhängig von der Prozessstrategie, die schwankende Verfügbarkeit einer limitierenden primären Kohlenstoff- oder Stickstoffquelle wie Glukose oder Ammonium hierfür mit verantwortlich ist. Niedrige Konzentrationen von Glukose oder Ammonium rufen hierbei die stringente Antwort als biologische Hungerreaktion hervor, die umfassende transkriptionelle Reaktionen beinhaltet.

Im Rahmen eines der Forschungsprojekte, die diese Thesis bilden, wurden die regulatorischen und transkriptionellen Reaktionen der Stämme *E. coli* MG1655 und *E. coli* SR bei wiederholter Exposition zu Ammonium-Hungerzonen in einem *scale-down* Reaktor untersucht. *E. coli* SR ist ein Stamm mit modulierter stringenter Antwort. Der verwendete *scale-down* Reaktor bestand aus zwei Kompartimenten: Einem Rührkesselreaktor und einem Rohrreaktor, welcher die Passage durch eine Hungerzone simulierte. Es wurde beobachtet, dass kurzfristige Hungerstimuli keine stringente Antwort in *E. coli* SR auslösten und die transkriptionelle Reaktion deutlich reduziert war. Die langfristige Adaption des Stammes an wiederholte Limitations- und Hungerzyklen unterschied sich zudem deutlich zu der von *E. coli* MG1655. Trotz der fehlenden stringenten Antwort wies *E. coli* SR keine Defizite in der Assimilation des limitierenden Ammoniiums oder der Biomasseausbeute auf.

Im zweiten Forschungsprojekt dieser Thesis wurde eine Serie von Deletionsstämmen erstellt, deren Stämme robustere Eigenschaften gegenüber Glukose-Hungerzonen aufwiesen. Hierzu wurden Kandidatengene ausgewählt und sukzessive mittels *Recombineering* aus dem Genom

von *E. coli* MG1655 entfernt. Die grundlegenden Wachstumsparameter der Stämme der Deletionsserie wurden in Schüttelkolben untersucht und keine auffälligen Unterschiede zu *E. coli* MG1655 festgestellt. Chemostat-Kultivierungen in einem *scale-down* Reaktor mit Glukose als limitierender Nährstoffquelle ergaben, dass der finale Stamm der Deletionsserie, *E. coli* RM214, unter heterogenen Bedingungen einen signifikant niedrigeren Erhaltungsstoffwechselkoeffizient hatte als *E. coli* MG1655. Der verwendete *scale-down* Reaktor bestand wie im ersten Projekt aus einem Rührkessel und einem Rohrreaktor. Ferner konnte in einem beispielhaften heterologen Proteinproduktionsszenario gezeigt werden, dass *E. coli* RM214 *rhaB*⁻ pJOE4056.2_{tetA} robuster auf Heterogenitäten reagierte als *E. coli* MG1655 *rhaB*⁻ pJOE4056.2_{tetA}, was an einer signifikant höheren Produktausbeute erkennbar war.

Im dritten Forschungsprojekt dieser Thesis wurde die Produktion von Pyruvat in *E. coli* MG1655 durch Inhibition der Pyruvatdehydrogenase mittels CRISPR-Interferenz untersucht. Ein wesentliches Ziel war hierbei die stabile Produktion unter stickstofflimitierten Bedingungen. Hierzu wurden verschiedene Zielsequenzen im Operon *pdhR-aceEF-lpd* getestet und die Stämme in Schüttelkolben kultiviert. Es zeigte sich, dass alle gewählten Zielsequenzen grundsätzlich geeignet waren, um die Akkumulation von Pyruvat auszulösen. Kombinierte CRISPR-Interferenz gegen zwei Zielsequenzen führte jedoch in den meisten Fällen nicht zu einer Erhöhung der Pyruvatausbeute. Des Weiteren wurden zwei Stämme, *E. coli* MG1655 pdCas9 psgRNA_{aceE_234} und *E. coli* MG1655 pdCas9 psgRNA_{aceE_234_pdhR_329}, in zweistufigen Fermentationen mit einer unlimitierten exponentiellen Wachstumsphase und einer darauffolgenden ammoniumlimitierten Produktionsphase im Labormaßstab charakterisiert. Im Fall von *E. coli* MG1655 pdCas9 psgRNA_{aceE_234} konnte Pyruvat nur in der exponentiellen Phase produziert werden und wurde in der zweiten Prozessphase wieder aufgenommen. *E. coli* MG1655 pdCas9 psgRNA_{aceE_234_pdhR_329} produzierte hingegen Pyruvat stabil sowohl in der exponentiellen als auch in der ammoniumlimitierten Phase und ist daher ein potenzieller Plattformstamm für die wachstumsentkoppelte Produktion von Bioprodukten, die aus Pyruvat gebildet werden.

Die Untersuchung des Verhaltens von Stämmen in heterogenen Bedingungen und die Entwicklung neuer Strategien zur Verbesserung ihrer Leistung waren die übergreifenden Problemstellungen der vorliegenden Projekte. Aus der Gesamtheit der gesammelten Daten kann geschlussfolgert werden, dass die Erstellung robuster Stämme für den Einsatz in

großvolumigen Reaktoren möglich und zielführend ist. Maßgeschneiderte genetische Modifikationen sind hierfür das Mittel der Wahl. Ferner bieten passende genetische Konstrukte aussichtsreiche Möglichkeiten zur stabilen wachstumsentkoppelten Produktion von Chemikalien unter Stickstofflimitierung.

1. Introduction

In 2019 the global market for biotechnological products achieved a volume exceeding 449 billion US-\$ (Polaris Market Research, 2020). Products from the biotech industry have broad applications in pharmacy, agriculture, and chemical industry. Many products are obtained by fermentation using recombinant microorganisms. Traditionally, fermentation products are classified as either small molecules, characterized by a molecular weight not exceeding 1000 Da, or large molecules with higher molecular weight. While small molecules comprise basic and fine chemicals as well as a plethora of pharmaceutically active substances, large molecules are typically peptides or proteins.

Fermentative production enjoys a series of inherent advantages making it both economically and ecologically compelling. From an economic point of view, a central advantage is the autocatalytic nature of microorganisms; in other words, their ability to replicate and grow which enables simple generation of large amounts of catalyst. Fermentations usually also do not require high temperatures or high pressure. They are conducted in aqueous media avoiding the use of expensive solvents unless necessary for product recovery. For many complex bioproducts such as enzymes or antibodies, fermentation is the only economically viable source. Regarding the ecological implications, educts of microbial processes are naturally occurring, renewable resources which in principle enable processes entirely independent of fossil resources. There are limitations though: Process parameters are dictated in a narrow corridor by the natural abilities and limitations of the microorganism used, many fermentation products are inhibitory or toxic at high concentrations and efficient catalysis requires the existence and optimization of suitable enzymes.

The fermentative production of foodstuffs such as wine or vinegar is usually achieved using naturally occurring microorganisms. In contrast, large-scale production of chemicals or pharmaceuticals requires genetically modified microorganisms, termed hosts. Hosts are modified by introducing heterologous expression systems and removing or inactivating inherent disadvantageous genetic sequences. Appropriate choice of a host organism, necessary modifications to its genetic information and introduction of a suitable expression system depend on the requirements of process and product.

1.1 Challenges in biochemical engineering – motivation for this thesis

Industrial bioprocesses must fulfill economic constraints to be viable. Key performance indicators for upstream processing and fermentation are yield coefficient, carbon conversion, productivity and final product titer in the fermentation broth (Lee and Kim, 2015). Achieving competitive parameters generally requires comprehensive rational strain engineering and in parallel process development targeted at upscaling and cost reduction.

Lee and Kim (2015) proposed ten strategies enabling successful process development. Among other strategies, they suggested removing unfavorable cellular regulatory elements, optimization of metabolic fluxes towards the product, and system-wide improvement of the host strain. Since process conditions depend on size, any of the strategies must be connected to scale-up to achieve stable and good results. The following paragraphs briefly describe typical challenges associated with process development and how the research projects that form this thesis addressed these issues.

The central challenge of scale-up is stable transfer of process parameters over several orders of magnitude to the production scale. Process development is conducted in small laboratory reactors with perfect mixing and little to no gradient formation. In large-scale aerobic fed-batch fermentations, nutrient gradients arise in the reactor and these heterogeneities can negatively impact strain performance (Bylund et al., 1998). In the laboratory, scale-down reactors can be used to mimic defined aspects of large-scale reactors and observe the effects of heterogeneous conditions on strain performance (Oosterhuis et al., 1983).

As a part of this thesis, a series of *E. coli* deletion strains were engineered for increased robustness to heterogeneous processes. The performance of these strains was evaluated in an exemplary protein production scenario in glucose-limited chemostats in a scale-down reactor.

Cellular regulation is essential for microorganisms at all stages of their lifecycle to prevent loss of vitality and enable adaptation. During a bioprocess cellular regulation can have ambivalent effects. While some regulatory programs can help to maintain cellular viability in inhibiting conditions, for instance resulting from high product titers, others such as feedback inhibition can adversely affect productivity. Within the context of scale-up, regulatory modules can be activated differently in large-scale reactors than in laboratory reactors which can lead to unexpected behavior and loss of productivity at production scale (Hewitt et al., 2000).

As a part of this thesis, transcriptional profiles of *E. coli* strains in nitrogen-limited conditions in a scale-down reactor were monitored to unravel their regulatory dynamics in response to the heterogeneous environment.

A prerequisite for any successful microbial bioprocess is the existence of a strain with good production phenotype. The process of improving a strain for the production of a biomolecule through genetic engineering is termed Metabolic Engineering, for which Gregory Stephanopoulos proposed the following definition: “Metabolic engineering is the directed improvement of cellular properties through the modification of specific biochemical reactions or the introduction of new ones, with use of recombinant DNA technology.” (Stephanopoulos, 1999). A key component of successful strain engineering is the improvement of precursor supply from central metabolism for production of the target molecule. Many competing reactions can be removed permanently by deletion of the respective genes. In case of process-relevant genes deletions can be detrimental to the overall process performance. The expression of such genes can be altered by methods such as CRISPR interference or metabolic toggle switches enabling dynamic control (Soma et al., 2014).

As a part of this thesis, strains that produce pyruvate in nitrogen-limited batch fermentations were constructed by transcriptional knockdown via CRISPRi and characterized in lab-scale reactors. These strains could potentially serve as chassis strains for the production of pyruvate-derived products such as terpenoids.

At high cell densities technical constraints in oxygen transfer and cooling capacity require limiting the metabolic activity in large-scale reactors. Commonly, this is achieved by fed-batch process strategies with limited supply of the primary carbon substrate. Alternatively, if the target product is primarily made up of carbon, reduced metabolic activity can be achieved by limited supply of another element such as nitrogen or phosphorous (Chubukov and Sauer, 2014; Schuhmacher et al., 2014). This approach has the added benefit that production is decoupled from biomass formation, which can improve overall product yield and carbon conversion. However, depending on the limitation used, specific substrate uptake rates can be low and in the extreme case decrease to the maintenance coefficient.

To explore the applicability of nitrogen limitation, transcriptional profiles of *E. coli* strains in nitrogen-limited conditions in a scale-down reactor were monitored as stated above. Moreover, strains producing pyruvate were cultivated in extended nitrogen-limited batch fermentations.

2. Scientific background

2.1 Microbial fermentations

Microbial fermentations can be categorized into batch, fed-batch and continuous processes. Aerobic processes include molecular oxygen as terminal electron acceptor while anaerobic processes are conducted in the absence of oxygen. Aerobic fed-batch fermentations are the standard practice for many industrial applications. A bioprocess is divided into upstream processing which includes the process steps until the product is generated during fermentation and downstream processing which comprises the remaining steps until the formulated product is finished.

2.1.1 Monod kinetics and Pirt's maintenance coefficient

Frequently, growth of microbial cultures in bioreactors depends on the concentration of a single limiting substrate. If a microorganism has only one active transport system in the regarded concentration range, then its growth can be approximated by the empirical Monod kinetics (Monod, 1949).

$$(1) \quad \mu = \mu_{max} * \frac{c_S}{K_S + c_S}$$

In (1), μ is the specific growth rate of the microorganism, μ_{max} is its maximum specific growth rate in the given circumstances attainable by full saturation with the limiting substrate S, c_S is the actual concentration of the substrate, and K_S is a kinetic parameter equal to the substrate concentration at which half of the maximum specific growth rate is observed.

If the limiting substrate is also the microorganism's energy source, it requires a constant supply for the maintenance of basic cellular functions. This phenomenon is termed maintenance metabolism or maintenance demand. According to Pirt, the Monod kinetics (1) can be expanded by adding a maintenance coefficient m_s to reflect this demand (Pirt, 1965). In stable cultivation conditions the parameter can be regarded as approximately constant.

$$(2) \quad \mu = \mu_{max} * \frac{c_S}{K_S + c_S} - m_S * Y_{XS,\mu}$$

In (2) m_S is the maintenance coefficient and $Y_{XS,\mu}$ is the yield coefficient describing biomass formation from substrate.

The experimentally observable value of the maintenance coefficient depends on the cultivation conditions and generally increases when conditions are unfavorable for the microorganism or when metabolic burden occurs as a result of heterologous expression (Bhattacharya and Dubey, 1995).

2.1.2 Batch fermentations

The simplest mode of microbial cultivations is batch fermentation. A sterilized medium is inoculated, and the bioprocess is conducted without addition of further media during the process. Batch fermentations are frequently used in scientific research, either in shaking flasks, laboratory bioreactors, or microtiter plates. A typical *Escherichia coli* batch fermentation can be divided into four phases if growth is limited by a single substrate: pre-exponential phase, exponential phase, limited phase, and stationary phase (**Fig. 1**). If preculture and process conditions are different, the pre-exponential phase may be further subdivided into lag phase and transitional phase. If the bioprocess is not aborted and no energy providing substrate is available for cells, the stationary phase transitions into a final phase characterized by strongly reduced cellular viability and cell death.

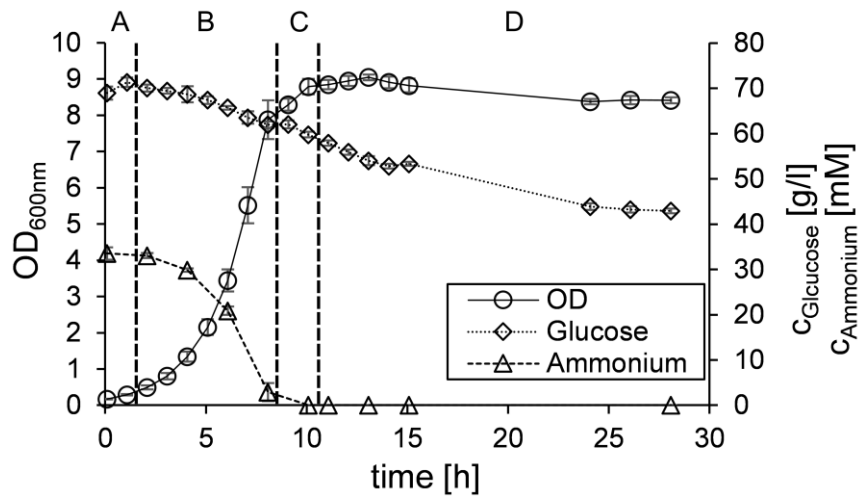


Fig. 1: Phases of a batch fermentation. Data shown is from a batch fermentation of *E. coli* MG1655 pdCas9 psgRNA_aceE_234_pdhR_329. Error bars indicate SEM (n = 5). The limiting nutrient was ammonium. A: pre-exponential phase, B: exponential phase, C: limited phase, D: stationary phase

2.1.3 Continuous cultivations

For conducting scientific research, continuous bioprocesses offer the advantage that a steady state can be approximated if the process time is chosen appropriately. The primary characteristics of this steady state are constant physiological and process parameters. A steady state serves as a reference state and changes to it in response to an external stimulus can be monitored well isolated from potential disruptive factors. The most commonly used implementations of continuous processes are based on the principle of chemostats (Monod, 1950; Novick and Szilard, 1950). A microbial culture in a stirred tank reactor is constantly fed a substrate solution including an essential nutrient in limited concentration while keeping its volume constant by continuous harvesting. Stable concentrations of cell dry weight and fermentation products result which depend on the microorganism's yield coefficients. The setup allows to experimentally assess the microorganism's physiology at a defined growth rate with a given limiting substrate (Kjeldgaard et al., 1958).

However, as pointed out by Ferenci (2006), chemostats suffer from certain limitations. Total replacement of all volume elements is never possible in a bioreactor in which volume is

2. Scientific background

replaced by dilution. The generally accepted convention is that five volumetric residence times are needed to attain a steady state in a chemostat. Assuming perfect mixing of the bioreactor, this corresponds to replacing more than 99% of the initial volume elements of the reactor (**Fig. 2**). After introduction of a constant stimulus, a new steady state is reached when five additional volumetric residence times have passed.

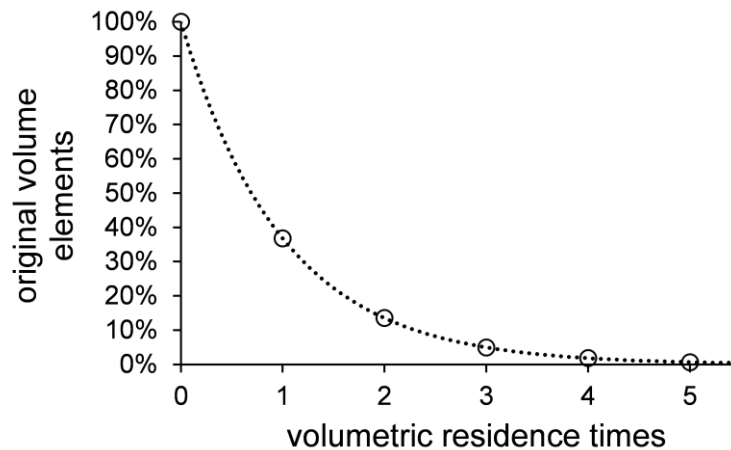


Fig. 2: Dilution of original volume elements in a chemostat experiment.

A second limitation of chemostats results from the necessity of microbial growth to maintain a steady state: the occurrence of mutations is inevitable. Consequently, different genotypes will exist in any chemostat and evolutionary mechanisms commence (Ferenci, 2006). Owing to its inherent evolutionary dynamics, a multicellular biological system cannot reach a true steady state even if the practical limitations preventing perfect dilution are disregarded. The analysis of major works in the field by Gresham and Hong (2015) shows that there is an ample mutational supply in typical chemostat experiments. However, their analysis also implies that if the number of generations is low, the bulk of a population will still be formed by cells with the initial genotype (Gresham and Hong, 2015). Nevertheless, chemostat experiments must be designed carefully to use appropriate generation numbers and control for potential mutations. If strong selective pressure is expected, even low generation numbers can be sufficient for mutants to form a non-negligible proportion of the population (Notley-McRobb et al., 2002).

2.2 Scale-up of microbial processes

The scale-up of microbial bioprocesses is a key challenge during their development (Lee and Kim, 2015). During bioprocess development the reaction volume can be scaled-up by more than 8 orders of magnitude, from less than 1 ml in microtiter plate screenings to more than 100.000 l in large-scale reactors. Typically, strains are thoroughly characterized in lab-scale reactors operating with a working volume around 1 – 10 l. Such small reactors provide a homogeneous environment with close to perfect mixing. As the scale increases, the appearance of heterogeneities is inevitable: The circulation and mixing times of reactors increase and hydrostatic pressure differences influence the solubility of gasses (Lara et al., 2006a). In standard aerobic fed-batch fermentations zones with high nutrient and low oxygen concentration arise close to the feeding point of the reactor and the reverse situation exists at the far end of the vessel (Enfors et al., 2001). Heterogeneities can also arise for pH and the concentrations of carbon dioxide and its dissolved species (Amanullah et al., 2001; Buchholz et al., 2014). As cells follow the liquid flow through the reactor, they are repeatedly subjected to concentration gradients and regime transitions which trigger adaptive cellular responses and can induce population heterogeneity (Haringa et al., 2017; Kuschel et al., 2017; Kuschel and Takors, 2020). Inhomogeneous conditions in bioprocesses typically result in reduced process performance due to the accumulation of overflow products, anaerobic byproduct formation, reduced biomass yield or reduced product yield (Bylund et al., 2000; Bylund et al., 1998; Neubauer et al., 1995b; Sandoval-Basurto et al., 2005).

From the biological point of view, the generation number of cells can introduce additional differences between scales since obtaining sufficient biomass for a large-scale reactor requires many more divisions than for a lab-scale reactor (Rugbjerg et al., 2018). Genetic stability and population homogeneity of production strains depend on the number of cellular divisions, so an appropriate number of passages in small-scale fermentation experiments is required to accurately reflect large-scale conditions.

2.2.1 Scale-down reactors

The enormous costs associated with maintenance and use of large-scale equipment prohibit their use during bioprocess development or in academic settings. As an alternative, scale-down reactors have been developed that are designed to mimic selected aspects of large-scale reactors

2. Scientific background

(Lara et al., 2006a; Takors, 2012). The central aspects guiding the design of a scale-down reactor are the kinds of heterogeneities under investigation, the volumetric fractions and average residence time in each regime, and the frequency of transitions between regimes. To meet these criteria scale-down reactors often consist of multiple compartments representing reactor zones with different regimes. **Fig. 3** schematically shows some commonly used setups.

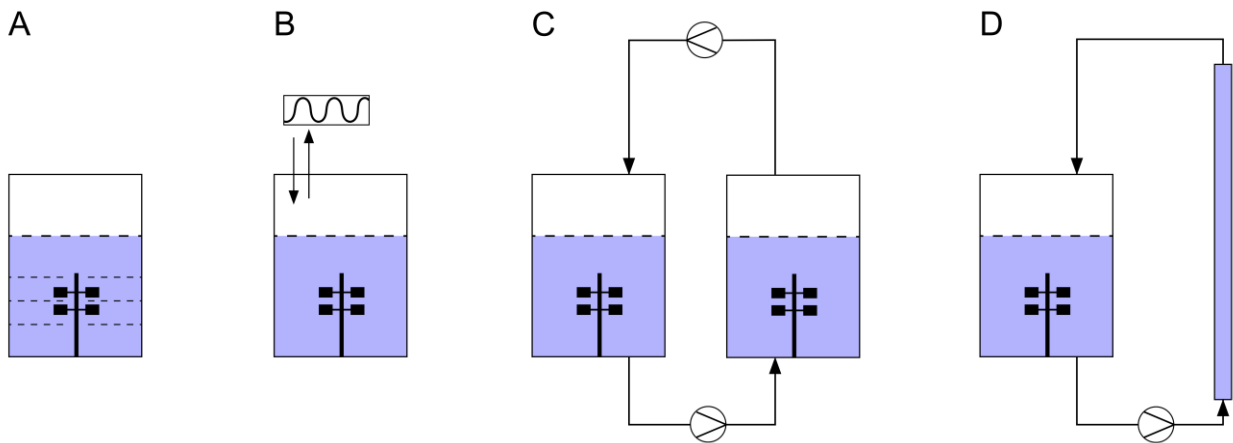


Fig. 3: Basic scale-down reactor designs. A: STR with installed discs to reduce mixing efficacy. B: STR operated with oscillating cultivation conditions. C: STR-STR two-compartment reactor. D: STR-PFR two-compartment reactor.

In most setups, a stirred tank reactor (STR) is used as the primary cultivation compartment and connected to one or more plug-flow reactors (PFR) or additional STRs (**Fig. 3** C and D). Using PFRs has the advantage of a narrow residence time distribution in the secondary compartment which allows precise control over the duration of a stimulus and enables time-resolved observations of physiological responses to the PFR passage (George et al., 1993). Using STRs in turn likely better reflects the stochastic residence time distribution of cells in a regime and may thus be more representative of actual large-scale conditions (Haringa et al., 2017). Mixed combinations of multiple compartments have also been proposed for accurate scale-down (Kuschel and Takors, 2020). Some scale-down concepts can be realized in a single STR – in this case intermittent feeding or intermittent aeration simulate repeated transitions between regimes – or fixtures are installed that artificially reduce mixing efficacy (Schilling et al., 1999; Vasilakou et al., 2020).

2.3 *Escherichia coli* as a host for microbial fermentations

One of the most well characterized microorganisms is *Escherichia coli*. *E. coli* is a gram-negative heterotrophic facultative anaerobic bacterium naturally occurring in the human gut. A plethora of *E. coli* strains is used in biotechnological research and industrial production. A commonly used group of strains termed *Escherichia coli* K-12 originated from an isolate obtained in 1922 (Bachmann, 1972). In 1997 the complete genomic sequence of the model organism *E. coli* K-12 MG1655 was presented (Blattner et al., 1997). Industrially, *E. coli* is used both for the production of small molecules such as 1,4-butanediol (Van et al., 2010) as well as large molecules with biopharmaceutical application, in particular insulin and its derivatives (Rubroder et al., 2001).

2.3.1 General physiology

E. coli is a chemoheterotroph gram-negative generalist organism capable of using a variety of small compounds for growth. *E. coli* utilizes many different sugars, small organic acids, and alcohols, with glucose as its preferred carbon source (Aidelberg et al., 2014; Wang et al., 2019b). Potential nitrogen sources for *E. coli* are ammonium, nitrite, nitrate, amino acids and many other nitrogen-containing compounds (Brons and Zehnder, 1990; Yuan et al., 2006). *E. coli* is a mesophilic organism with a temperature optimum around 37.5 °C degrees (Barber, 1908). Fermentations of *E. coli* are typically conducted at 37 °C, 30 °C or at lower temperatures if required for product stability. *E. coli* prefers neutral to slightly acidic pH and low osmolarity around 300 Osm (Cayley et al., 1991; Mueller et al., 2019; Record Jr et al., 1998). Under optimal conditions, growth of *E. coli* in rich medium can be very fast with a doubling time lower than 20 min (Barber, 1908). In minimal medium with glucose as a carbon source, maximum specific growth rates up to $\mu = 0.7 \text{ h}^{-1}$ can be achieved (LaCroix et al., 2015). Glucose degradation is achieved through the Embden-Meyerhoff-Parnas (EMP) pathway. In anaerobic bioprocesses *E. coli* metabolism is characterized by mixed acid fermentation including the excretion of acetate, lactate, succinate, formate and ethanol (Clark, 1989). In aerobic fermentations growth on glucose at high growth rates leads to a metabolic overflow phenomenon with acetate as the primary byproduct (Meyer et al., 1984). *E. coli* has a secondary terpenoid metabolism fueled by the 2C-methyl-d-erythritol-4-phosphate (MEP) pathway (Hunter, 2007).

2.3.2 Transcriptional regulation

Bacterial metabolism is highly regulated on the level of gene expression and protein activity. Gene expression is controlled by transcriptional and translational regulation. As transcription is the first step in expressing a genetic trait, measurements of the cellular transcriptome provide valuable information on how the cellular network reacts to an external stimulus. Transcriptional regulation in *E. coli* has been the subject of intense research since the discovery of the regulatory functions of the *lac* operon (Pardee et al., 1959). Due to the enormous amount of information available, a comprehensive overview of the many elements of transcriptional regulation would far exceed the scope of this thesis (Balleza et al., 2009; Treviño-Quintanilla et al., 2013). Only the most fundamental concepts will be outlined in the following paragraph.

Transcriptional initiation in *E. coli* requires the interaction of a sigma factor with the RNA polymerase (RNAP) core enzyme to form the RNAP holozyme (Murakami et al., 2002; Travers and Burgess, 1969). The activity and availability of sigma factors is controlled by their synthesis, anti-sigma factors inactivating them, and the competition of various species of sigma factors for RNAP (Jishage et al., 1996; Jishage and Ishihama, 1998; Maeda et al., 2000). Other transcription factors can promote or prevent the binding of RNAP to the promoter region of a single operon or a large set of operons (Martínez-Antonio and Collado-Vides, 2003), and some transcription factors like Fis even have dual-regulatory functions that depend on their concentration and the nucleotide sequence of their binding site on the DNA (Weinstein-Fischer and Altuvia, 2007). Transcription factors often respond to external signals transmitted by regulatory molecules and their interactions with sigma factors and other transcription factors form the transcriptional regulatory network (Fang et al., 2017). **Table 1** lists the most important sigma factors in *E. coli*, the functions they are generally associated with and a review or publication summarizing research on the respective sigma factor.

Table 1: Sigma factors

Sigma factor	Gene	Primary function	Recommended literature
σ^{70} (σ^D)	<i>rpoD</i>	housekeeping/growth	(Mazumder and Kapanidis, 2019)
σ^{54} (σ^N)	<i>rpoN</i>	nitrogen metabolism	(Merrick, 1993)
σ^{38} (σ^S)	<i>rpoS</i>	general stress response	(Landini et al., 2014)
σ^{32} (σ^H)	<i>rpoH</i>	heat shock	(Arsène et al., 2000)
σ^{28} (σ^F)	<i>fliA</i> (<i>rpoF</i>)	flagellation/chemotaxis	(Fitzgerald et al., 2014)
σ^{24} (σ^E)	<i>rpoE</i>	cell envelope stress	(Ades et al., 2003)
σ^{19} (σ^{FecI})	<i>fecI</i>	ferric citrate uptake	(Visca et al., 2002)

2.3.3 The Stringent Response

Transcriptional regulation enables cells to dynamically respond to environmental variables. One of the most important regulatory functions to maintain cellular homeostasis is the adaption of cellular growth to available nutrients. In *E. coli* the alarmone guanosine 3',5'-bis(diphosphate), short ppGpp, connects nutrient availability and growth rate (Potrykus et al., 2011). Rapid accumulation of ppGpp in response to nutrient depletion triggers a global regulatory program called the stringent response enabling quick growth reduction upon nutrient depletion (Gaca et al., 2015; Hauryliuk et al., 2015; Steinchen and Bange, 2016). During the stringent response massive transcriptional reprogramming occurs to reduce the expression of rRNA and tRNA genes in favor of amino acid biosynthesis and stress resistance proteins (Barker et al., 2001; Gentry et al., 1993; Jishage et al., 2002). Adaptive cellular regulation occurs over a wide range of ppGpp concentrations from 1 to 1000 μ M (Steinchen et al., 2020). The stringent response has been the subject of microbiological research for decades. A literature mining study identified more than 250 relevant articles in 2009, with the number ever increasing (Carneiro et al., 2011). The following sections will thus focus only on molecular key players and essential information in the context of this thesis.

Two key enzymes, RelA and SpoT are responsible for maintaining appropriate cellular ppGpp levels. In case of carbon or nitrogen starvation the binding of uncharged tRNAs to the ribosome activates the ribosome-associated RelA which rapidly initiates synthesis of ppGpp or guanosine

2. Scientific background

3'-diphosphate 5'-triphosphate (pppGpp), collectively referred to as (p)ppGpp, by transferring a diphosphate moiety from ATP to guanosine diphosphate (GDP) or guanosine triphosphate (GTP) (Haseltine and Block, 1973). The phosphatase GPP then processes pppGpp into ppGpp by removing one phosphate group making ppGpp the dominant species in *E. coli* (Mechold et al., 2013; Somerville and Ahmed, 1979). SpoT is a bifunctional enzyme containing domains for both (p)ppGpp synthesis and hydrolysis. SpoT can initiate (p)ppGpp synthesis as a response to a variety of starvation stimuli such as iron limitation, phosphate starvation and carbon limitation sensed via interaction with acyl carrier protein (Battesti and Bouveret, 2006; Bougdour and Gottesman, 2007; Vinella et al., 2005). Additionally, the (p)ppGpp synthesis activity of SpoT maintains basal ppGpp levels necessary for normal cellular growth in minimal medium (Montero et al., 2014). Its second function, ppGpp hydrolysis, is essential for terminating the stringent response and resuming growth, illustrated by the synthetic lethality of *spoT* deletions in *relA*⁺ strains (Montero et al., 2014; Somerville and Ahmed, 1979).

The accumulation of ppGpp triggers the stringent response by modulating the affinity of RNAP to different sigma factors and directly influencing open complex formation at specific promoters (Jishage et al., 2002). Consensus sequences for promoters regulated by ppGpp have been described (Sanchez-Vazquez et al., 2019). Transcriptional regulation by ppGpp is enhanced by its interaction with DksA (Doniselli et al., 2015; Molodtsov et al., 2018). Increased transcription of genes regulated by σ^{38} and σ^{54} in the presence of ppGpp further promotes survival of cells by activation of stress responses (Jishage et al., 2002; Kvint et al., 2000; Laurie et al., 2003). In addition to its transcriptional regulatory effects ppGpp also directly binds > 50 proteins in *E. coli* and modulates the activity of many proteins such as the primase DnaG to achieve cell cycle arrest (Maciag et al., 2010; Wang et al., 2019a).

As part of this thesis, regulation of the strain *E. coli* SR was characterized (Ziegler et al., 2021b). *E. coli* SR is a strain with modulated stringent response lacking *relA* and carrying a charge reversal in SpoT. *E. coli* SR does not accumulate ppGpp in nitrogen-limited conditions (Michalowski et al., 2017).

2.3.4 Glucose limitation

Since the discovery of transcriptional regulation, the central carbon metabolism in *E. coli* has been studied extensively to accurately describe the contributions of individual molecular actors

2. Scientific background

(Pastan and Adhya, 1976; Shimizu, 2013). Despite the importance of central carbon metabolism for cellular growth and survival, more than 90% of differential regulation in a wide array of different growth conditions depends only on the cellular growth rate and the activity of two transcription factors: cAMP-CRP and Cra (Kochanowski et al., 2017). Most remaining genes of central carbon metabolism are subject to limited regulation in presence of a specific carbon source. As carbon-limited fed-batch fermentations are the standard operation mode of most industrial microbial bioprocesses expedient understanding of the regulation of the central carbon metabolism is required. Frequently, glucose or raw substrates with high glucose content are used as the primary carbon source. Hardiman *et al.* (2007) showed that under glucose-limited fed-batch conditions the alarmone cyclic adenosine monophosphate (cAMP) and ppGpp are formed (Hardiman et al., 2007). The concentration of ppGpp rose transiently at the onset of carbon limitation and then stabilized on an elevated level, in accordance with its concentration-dependent regulatory functions (Steinchen et al., 2020). The concentration of cAMP in turn increased hyperbolically until saturation was reached (Hardiman et al., 2007). The primary regulatory role of cAMP-CRP at very low growth rates has been confirmed in other studies (Nanchen et al., 2008).

The regulatory functions of the cAMP-CRP regulon are closely connected to glucose transport by the phosphotransferase system (PTS) in *E. coli* (Görke and Stülke, 2008; Shimizu, 2013). One of its primary functions is catabolite repression, a mechanism that serves to ensure the hierarchical use of carbon sources in the order of maximum possible growth rate (Aidelberg et al., 2014). The phosphotransferase system consists of the non-sugar-specific proteins EI (encoded by *ptsI*) and HPr (*ptsH*), and the sugar-specific proteins EIIA^{Glc} (*crr*) and EIIBC^{Glc} (*ptsG*) for glucose. A phosphate group from phosphoenolpyruvate, forming pyruvate, serves to phosphorylate EI. The phosphate group is then relayed via HPr to EIIA^{Glc} and EIIBC^{Glc} which transports and phosphorylates glucose yielding glucose-6-phosphate. The phosphorylation state of EIIA^{Glc} depends on the glucose influx and the ratio of phosphoenolpyruvate to pyruvate and is the molecular sensor for catabolite repression (Shimizu, 2013). When *E. coli* grows on ample glucose, EIIA^{Glc} is mostly dephosphorylated. In this state EIIA^{Glc} binds and inactivates transporters of alternative carbon sources, effectively preventing their entry into the cytosol (Saier et al., 1978). As this also prevents the activation of the respective catabolic operons, the mechanism has been termed “inducer exclusion” (Saier and Crasnier, 1996). On the contrary, when glucose availability decreases, EIIA^{Glc} is predominantly phosphorylated and activates

2. Scientific background

adenylate cyclase (*cyaA*) which triggers the accumulation of cAMP (Reddy and Kamireddi, 1998). The transcription factor CRP binds cAMP and activates the cAMP-CRP regulon which enhances the expression of catabolic functions for alternative carbon sources and many other processes (Gosset et al., 2004). The cAMP-CRP regulon is large, comprises > 180 genes and many of these genes are subject to intricate layered regulation (Kochanowski et al., 2017; Zheng et al., 2004). One of the catabolic functions activated by cAMP-CRP is rhamnose degradation (Egan and Schleif, 1993; Wickstrum et al., 2005). The rhamnose expression system which was used in some experiments of this research projects is activated by cAMP-CRP as well (see: **2.4.1 Plasmids and pJOE4056.2**).

The protein Cra, also referred to as FruR, is the second major regulatory player in *E. coli* central carbon metabolism. Early studies already revealed that Cra can function both as a transcriptional activator and repressor depending on the position of its binding site at a promoter (Ramseier et al., 1993). The Cra regulon is large, comprising almost 100 genes, and significant crosstalk and antagonistic regulation between the Cra and cAMP-CRP regulons exist (Kim et al., 2018; Zhang et al., 2014). The function of Cra can be best described as a director of carbon flow in central metabolism controlling the expression of genes involved in the TCA cycle, glyoxylate shunt, Entner-Doudoroff pathway, and gluconeogenic functions in response to gluconeogenic or glycolytic conditions (Sarkar et al., 2008). This is exemplified by metabolic defects and low growth rates of Δ *cra* strains if grown on gluconeogenic substrates such as glycerol (Kim et al., 2018; Zhang et al., 2014).

2.3.5 Nitrogen limitation

In carbon-limited fermentations about 12% of the cell dry mass in *E. coli* is nitrogen (Taymaz-Nikerel et al., 2010). In fermentations of *E. coli* ammonium is frequently used as the primary nitrogen source and for pH titration. AmtB is the primary ammonium transporter in *E. coli* which uses a two-lane mechanism for coupled proton and ammonia transport (Williamson et al., 2020). Depending on ammonium availability the incorporation of ammonium is accomplished directly by the glutamate dehydrogenase GdhA via amination of 2-oxoglutarate or by the GS-GOGAT system (van Heeswijk et al., 2013). The GS-GOGAT system consists of the glutamine synthetase GlnA, which achieves ammonium assimilation by glutamine synthesis from glutamate, and a complex heterooligomer glutamate synthetase formed by GltB and GltD,

2. Scientific background

which subsequently transfers an amine group from glutamine to 2-oxoglutarate (Liaw and Eisenberg, 1994; Miller and Stadtman, 1972). In both assimilation pathways 2-oxoglutarate is effectively the cellular acceptor for ammonium linking carbon and nitrogen metabolism and enabling their coordination (Huergo and Dixon, 2015).

Nitrogen limitation is first sensed by accumulation of 2-oxoglutarate and depletion of the glutamine pool which by intricate interactions of PII uridylyltransferase / uridylyl removing enzyme (encoded by *glnA*), nitrogen regulatory protein PII-1 (*glnB*) and nitrogen regulator PII-2 (*glnK*) activate the sensor histidine kinase / phosphatase NtrB of the two-component NtrBC system (Atkinson et al., 1994; Doucette et al., 2011). Activation of NtrB (*glnL*) results in phosphorylation of NtrC (*glnG*) enabling transcription from σ^{54} dependent promoters (Zimmer et al., 2000). Many σ^{54} controlled operons encode functions for the transport of alternative nitrogen-containing compounds and concomitant expression of *nac* couples NtrBC regulation to σ^{70} dependent promoters also involved in nitrogen scavenging (Muse and Bender, 1998; Zimmer et al., 2000). Additionally, activation of σ^{54} controlled transcription involves increased transcription of *relA* forming a direct link between NtrBC regulation and the stringent response (Brown et al., 2014). If nitrogen starvation results in amino acid limitation, uncharged tRNAs bind to the ribosome and trigger ppGpp synthesis by *relA* which further strengthens expression from σ^{38} and σ^{54} dependent promoters (see: **2.3.3 The Stringent Response**). In consequence, nitrogen limitation can lead to similar global transcriptional reprogramming as glucose limitation. However, some regulatory functions occur exclusively in either conditions and the extent of the cellular response to nitrogen starvation is generally smaller (Löffler et al., 2017).

2.3.6 Adenylate Energy Charge

The adenylate energy charge (AEC) is used as a measure of the cellular energetic state (Atkinson, 1968; Atkinson and Walton, 1967). It is defined as a quotient of the concentrations of the three adenosine phosphates (AxP): adenosine monophosphate (AMP), adenosine diphosphate (ADP), and adenosine triphosphate (ATP).

$$(3) \quad AEC = \frac{ATP + 0.5 * ADP}{ATP + ADP + AMP}$$

2. Scientific background

The interpretation of the AEC as a measurement for energetic availability in the cell is based on the observation that the activity of many metabolic enzymes depends on the concentration of one or more AxP species and is supported by observed correlations between AEC and cellular viability (Atkinson, 1968; Chapman et al., 1971). For *E. coli*, typical AEC values are around 0.8 in favorable environmental conditions, while AEC values below 0.5 indicate loss of cellular viability (Chapman et al., 1971). The AEC is a highly dynamic value that can quickly react to changes in the outer circumstances because the turnover of the ATP pool in aerobically growing *E. coli* occurs on a time-scale < 1 s (Holms et al., 1972). *E. coli* can maintain AEC values close to 0.8 in glucose-limited fed-batch fermentations as long as substrate is constantly available, but complete exhaustion of substrate supply results in rapid reduction of the AEC (Hardiman et al., 2007; Löffler et al., 2016).

2.3.7 Scale-up of *E. coli* fermentations

Section **2.2 Scale-up of microbial processes** describes the general principles guiding scale-up and scale-down of microbial bioprocesses. For the model organism *E. coli*, the effects of large-scale heterogeneities have been the subject of intense research.

The primary factors for process performance loss in heterogeneous fermentations of *E. coli* are glucose excess and oxygen limitation close to the feeding point of fed-batch reactors, which typically result in reduced biomass and recombinant protein yield (Bylund et al., 2000; Enfors et al., 2001; Lara et al., 2006b; Sandoval-Basurto et al., 2005; Schweder et al., 1999). Glucose overflow leads to the accumulation of acetate and formate even in fully aerobic conditions, while oxygen limitation triggers anaerobic mixed acid fermentation. Since both phenomena often occur concomitantly when high glucose uptake leads to high oxygen demand, and similar consequences are observed in both cases, it can be difficult to accurately delimit anaerobic mixed acid fermentation from overflow metabolism. Lara et al. (2009) examined the different responses of *E. coli* to glucose excess pulses in an aerobic or anaerobic plug-flow reactor. In both cases, the metabolic response was remarkably fast and resulted in the accumulation of acetate and formate within seconds after entry into the new regime. However, in anaerobic conditions lactate, succinate and ethanol were produced as well and much higher biomass specific production rates for the byproducts were observed (Lara et al., 2009). Interestingly, multiple studies using aerated glucose pulse experiments in stirred-tank reactors observed the

2. Scientific background

accumulation of only acetate and formate despite transient dissolved oxygen tensions close to 0% which emphasizes an important distinction between oxygen limitation and full anaerobiosis (Sunya et al., 2013; Sunya et al., 2012a). Oxygen limitation has also been connected to plasmid instability, which may contribute to reduced process performance (Hopkins et al., 1987).

The seminal scale-down study by Neubauer et al. (1995b) highlighted that not only transient carbon excess but also carbon starvation was highly relevant for the performance of *E. coli* processes (Neubauer et al., 1995b). In a related study it was found that the alarmone ppGpp accumulated during transient starvation (Neubauer et al., 1995a). Later, multiple research projects examined the role of the σ^{38} regulon under such conditions and found induction of σ^{38} controlled genes and population heterogeneity (Delvigne et al., 2009; Sunya et al., 2012b). Löffler et al. (2016) further investigated the regulatory responses to repeated glucose starvation and confirmed the central role of the stringent response in cellular short- and long-term adaptation. Moreover, it was estimated that the repeatedly induced transcriptional responses lead to an increased ATP demand of up to 50%, offering a link between regulatory effects and reduced process performance (Löffler et al., 2016). Results from a follow-up simulation study indicated that these results were likely representative for a 54 m³ bioreactor (Zieringer et al., 2020). Similar but less pronounced effects were observed under nitrogen limitation (Simen et al., 2017).

Most of the described research projects focused on the short-term effects of starvation zones. To investigate the long-term adaptation of cells, Vasilakou et al. (2020) employed a repeated feast-famine regime. The conditions of their feeding cycle were extreme – 20 s feeding time and 380 s starvation at a dilution rate of only 0.044 h⁻¹ – but the observed reduction in biomass yield of almost one third compared to constant feeding conditions clearly demonstrated the consequences of substrate heterogeneities (Vasilakou et al., 2020).

In contrast to the strong effects of oxygen heterogeneities, gradients of dissolved CO₂ are generally well tolerated by *E. coli*, even at exposure times of several minutes (Baez et al., 2011). Similarly, *E. coli* appears to be quite robust to mild pH gradients. When used for plasmid DNA production exposure for up to 60 s to a pH difference of about 0.3 units was well tolerated. Substantial losses were only observed at prolonged exposure to pH > 8 (Cortés et al., 2016).

2.4 Genetic engineering of *Escherichia coli*

2.4.1 Plasmids and pJOE4056.2

Plasmids are circular mobile genetic elements that enable horizontal gene transfer between individual cells. Molecular techniques to engineer, isolate and transfer plasmids are well established, and their use is standard practice in genetic engineering. Plasmids used in genetic engineering such as pUC19 usually contain at least three functional elements: an origin of replication, a selective marker and a multiple cloning site containing the sequence-of-interest (Bolivar et al., 1977).

Plasmid pJOE4056.2 is a plasmid designed for heterologous protein expression in glucose-limited fermentations of *E. coli* (Wegerer et al., 2008). It contains an expression cassette for the fluorescent reporter protein eGFP (Zhang et al., 1996). Transcription is driven by the promoter *rhap* and translation is initiated from the ribosome binding site of gene *10* of bacteriophage T7. Expression of eGFP is thus initiated by cAMP-CRP regulation at low glucose concentrations in the presence of the inducer rhamnose. The expressed variant of eGFP additionally carries a hexahistidin-tag which enables isolation of the protein by metal-chelate affinity chromatography (Hochuli et al., 1987). Furthermore, pJOE4056.2 carries an expression cassette for ampicillin resistance and various stabilizing genetic elements. No plasmid loss could be observed over more than 50 generations in liquid culture indicating high genetic stability (Wegerer et al., 2008).

In the experiments described in this thesis, pJOE4056.2 was modified by replacing the ampicillin resistance with a tetracycline resistance encoded by *tetA* (Ziegler et al., 2021a). TetA is a class B tetracycline exporter, so resistance is mediated by drug efflux (McMurry et al., 1980). The action of TetA does not degrade the antibiotic tetracycline which enables sustained selective pressure against plasmid loss.

2.4.2 Recombineering

Recombineering is a technique used to make genetic modifications based on recombination between homologous DNA sequences (Court et al., 2002; Papa and Shoulders, 2019). Recombineering allows the insertion or removal of large DNA sequences and thus effective

2. Scientific background

engineering of the bacterial chromosome. In *E. coli* efficient recombineering functions can be provided by heterologous expression of the *exo*, *bet* and *gam* genes of phage λ . Gam prevents degradation of the DNA template introduced for recombineering by cellular nucleases, Exo degrades linear double stranded DNA (dsDNA) to a single stranded DNA (ssDNA) intermediate and Beta binds the ssDNA to protect it from cellular nucleases and promote annealing to the homologous region on the target DNA molecule (Cassuto et al., 1971; Kulkarni and Stahl, 1989; Marsić et al., 1993). Recombination then proceeds via integration of the ssDNA intermediate into a replicating DNA template (Maresca et al., 2010; Mosberg et al., 2010). Selection for successful recombineering events proceeds via integration of selective markers, phenotypic alterations, DNA cutting, or by sequencing of individual clones (Datsenko and Wanner, 2000; Yu et al., 2008; Yu et al., 2000). Using dual-selectable recombineering cassettes like the *tetA-sacB* cassette enables scarless marker recycling if multiple rounds of genetic engineering are intended (Li et al., 2013).

2.4.3 Genome reduction

The idea to reduce the genome of microorganisms to obtain advantageous traits or unravel the essential genes of life was postulated even before the first genomes were fully sequenced (Koob et al., 1994). From an evolutionary biology perspective, genome reduction promises assistance in elucidating the fundamentals of life such as DNA replication, cell division and protein synthesis. Within the context of metabolic engineering, Ziegler and Takors (2020) offered the following definition:

„Genome reduction is the repeated deletion of irrelevant genes by methods of genetic engineering with the purpose of constructing a functionalized cell for a selected application.” (Ziegler and Takors, 2020)

This definition encompasses not only the requirement for genetic engineering methods but also assumes a purpose. Which genes are considered irrelevant entirely depends on the purpose (Noack and Baumgart, 2018; Unthan et al., 2015).

The field of genome reduction nowadays encompasses countless studies on diverse economically relevant species such as *Escherichia coli*, *Bacillus subtilis*, *Pseudomonas putida*, *Corynebacterium glutamicum*, *Saccharomyces cerevisiae* and *Streptomyces avermitilis*. The

2. Scientific background

author of this thesis has previously compiled relevant studies and reflected them in an application-oriented context (Ziegler and Takors, 2020). The most important findings for the exemplary case of *Escherichia coli* will be briefly summarized in the following section.

The generation of strains with a strongly reduced genome is laborious and frequently multiple scientific publications report the progress in a particular project. The most well-known series of deletion strains is probably the MDS series originating from *E. coli* K-12 MG1655. The 4.6 Mb genome of *E. coli* MG1655 (Blattner et al., 1997) was repeatedly reduced, finally yielding the strain MDS69 with a 20.3% smaller genome than *E. coli* MG1655 (Karcagi et al., 2016; Kolisnychenko et al., 2002; Pósfai et al., 2006). In the process, strain specific genomic islands, mobile genetic elements, pseudogenes, and genes for cellular surface structures were removed. With increasing number of deletions, it became apparent that despite the rational choice of targets physiological parameters, e. g. maximum specific growth rate and biomass yield, and the competitiveness of the strains worsened (Karcagi et al., 2016). Indeed, strains of the MDS series also displayed clear advantages: Due to the removal of many mobile genetic elements the strains were well suited to replicate and carry heterologous DNA. As a result, plasmids were genetically stabilized even if they contained repetitive sequences or conferred a high metabolic burden to the cell (Chakiath and Esposito, 2007; Umenhoffer et al., 2010). Depending on the goal, these advantageous traits can outweigh the shortcomings of the strains. Umenhoffer et al. (2017) then partially transferred some of the genome reduced sequences into *E. coli* BL21(DE3) generating a chassis strain with remarkable properties for heterologous protein production (Umenhoffer et al., 2017).

A second series of genome reduced *E. coli* strains is the MGF series originating from *E. coli* K-12 W3110 (Mizoguchi et al., 2008; Mizoguchi et al., 2007). Initially, candidate regions were identified from comparison of the *E. coli* K-12 genome to *Buchnera* species. The regions were individually deleted and, if deemed suitable, transferred into a single strain. While first results indicated beneficial traits of the MGF-strains, in-depth phenotyping painted a similar picture as seen with the MDS strains: The genome reduced strains suffered from reduced maximum specific growth rate, reduced biomass yield and increased mutational rates (Kurokawa et al., 2016; Nishimura et al., 2017). However, complementary studies showed that the negative traits could be alleviated through laboratory evolution or rational strain engineering (Hirokawa et al., 2013; Nishimura et al., 2017).

2. Scientific background

The observations that genome reduced microorganisms tend to suffer from physiological shortcomings are similar in other species. On the other hand, genome reduced strains often also display beneficial traits that are interesting for selected applications. In conclusion, genome reduction should be rational and conducted with caution to achieve a desired phenotype with minimal side-effects. With respect to potential applications, the intended research target should not be to remove as much DNA as possible from the genome just because it is practically possible. A prime example for successful genome reduction is *Pseudomonas putida* EM383, a derivative of *P. putida* KT2440, lacking hand-picked genes from flagellar biosynthesis and prophage genes (Martínez-García et al., 2015; Martínez-García et al., 2014a; Martínez-García et al., 2014b). The overall scope of the genome reduction was small compared to other genome reduction projects and comprised only 4.3% of the *P. putida* KT2440 genome. Comprehensive characterization of *P. putida* EM383 under process conditions revealed that the strain surpassed its parent strain in any physiologically relevant parameter: maximum specific growth rate, biomass yield, maintenance metabolism, byproduct formation, AEC, plasmid stability, and protein productivity (Lieder et al., 2015). The study proves that targeted genome reduction of a small set of irrelevant genes can substantially improve the physiological performance of a microorganism in the target application scenario. Similarly, Valgepea et al. (2015) proposed that attractive targets for genome reduction are characterized by a high metabolic burden despite being irrelevant for the intended application of a strain (Valgepea et al., 2015).

Based on transcriptional studies with *E. coli*, a list of genes with high metabolic costs in heterogeneous fermentation scenarios of *E. coli* was compiled (Löffler et al., 2016; Simen et al., 2017). As a part of the scientific work presented in this thesis, genes were chosen from this list which were deemed irrelevant in the context of an industrial bioprocess. They primarily consisted of chemotaxis genes, transporters, and metabolic enzymes. The chosen genes were then removed from the genome of *E. coli* MG1655 by recombineering.

2.4.4 CRISPRi

Many bacteria and archaea use an adaptive immune system to defend against exogenous DNA: CRISPR/Cas (Clustered Regularly Interspaced Short Palindromic Repeats/CRISPR-associated). Repetitive nucleic acid elements termed CRISPR maintain a record of prior contact with foreign DNA and work in conjunction with Cas proteins to prevent future infections by

2. Scientific background

cleavage of foreign DNA (Barrangou et al., 2007; Garneau et al., 2010). The Cas9 protein from *Streptococcus pyogenes* requires interaction with a CRISPR RNA (crRNA) and a trans-activating crRNA (tracrRNA) to exert DNA cleavage *in vivo* but an artificial single guide RNA (sgRNA) can combine these functions, effectively enabling targeted DNA cleavage (Jinek et al., 2012). The cleavage site is then determined by base pairing of the sgRNA seed sequence and the target site, also referred to as protospacer. In total, an sgRNA consists of three elements: 20 variable nucleotides (nt) determining the target specificity, 42 nt required for the interaction with Cas9 and formation of a hairpin structure, as well as 40 nt of an *S. pyogenes* transcriptional terminator. A strict requirement limiting the target space of the system is the presence of a protospacer adjacent motif (PAM) located directly next to the target site (Mojica et al., 2009). When using Cas9 in conjunction with a sgRNA, the canonical PAM is NGG (Jinek et al., 2012).

CRISPR interference (CRISPRi) is a modification of this system using a catalytically inactive variant, dead Cas9 (dCas9) in conjunction with an sgRNA to enable targeted DNA binding and steric inhibition of transcription (Bikard et al., 2013; Qi et al., 2013). The missing catalytic activity of dCas9 results from two mutations in its nuclease domains: D10A in the RuvC1-like domain and H840A in the HNH nuclease domain (Jinek et al., 2012). Transcription of a DNA sequence can be blocked either by inhibition of transcription initiation or transcription elongation. Transcription initiation in prokaryotes is inhibited by binding of the sgRNA-dCas9 complex to promoter regions required for binding of transcription factors or RNA polymerase, e.g. the -35 to -10 region of a promoter. Blocking transcription initiation can be achieved by targeting either the coding or the non-coding DNA strand and is equally effective regardless of the strand chosen (Qi et al., 2013). In contrast, blocking transcription elongation is only effective if the sgRNA is complementary to the non-coding strand. In this orientation dCas9 is located between the sgRNA bound to the protospacer and a transcribing RNA polymerase forming a transcriptional roadblock. Otherwise, if the sgRNA is complementary to the coding strand, the advancing RNA polymerase can potentially remove it through its helicase activity, resulting in dCas9 dissociation and ineffective inhibition (Qi et al., 2013).

The efficacy of CRISPRi is primarily determined by the complementarity of sgRNA and target sequence. Even single mismatches or oversized complementary regions can reduce the repression efficiency substantially (Bikard et al., 2013; Larson et al., 2013; Qi et al., 2013). Due to the system's high sensitivity to mismatches, the probability of off-target effects with imperfect matches is relatively low. However, potential side effects can never be entirely

2. Scientific background

excluded since as little as 9 nt of perfect complementarity can be sufficient for measurable effects. Moreover, some sgRNA seeds beginning with certain nucleotide sequences always lead to growth inhibition in *E. coli* if dCas9 is expressed strongly (Cui et al., 2018). Recently, nucleotide patterns surrounding the PAM have been identified which can also modulate the effectiveness of CRISPRi (Calvo-Villamañán et al., 2020).

If dCas9 is sufficiently expressed, CRISPRi can be applied with multiple sgRNAs targeting any number of genes simultaneously (Qi et al., 2013). If multiple sgRNAs target the same gene, the joint repression strength can be higher than with any individual gene, provided the binding sites do not overlap. Using several sgRNAs targeting different genes enables multiplex CRISPRi to regulate metabolic fluxes and rates as well as the specific growth rate (Kim et al., 2020; Landberg et al., 2020). Particularly successful strategies were the repression of competing pathways, improved precursor supply and the repression of pathways that serve to degrade a substance (Li et al., 2020a; Tian et al., 2019; Wu et al., 2015).

3. Objectives and research questions of this thesis

The overarching objective of this thesis is the development of strategies for the generation of strains with advantageous traits for large-scale production. The scientific studies compiled in this thesis are based on previous investigations conducted at the Institute of Biochemical Engineering which are shortly summarized in the subsequent paragraphs.

Studies on the transcriptional regulation of *E. coli* W3110 by repeated exposure to glucose or ammonium starvation in a STR-PFR scale-down reactor revealed repeated initiation of the stringent response (Löffler et al., 2016; Simen et al., 2017). Model calculations indicated that in consequence cellular energy demand increased and the proportional impact of single genes on this increase was estimated.

In an independent study the phenotype of strains with modulated stringent response was investigated (Michalowski et al., 2017). A strain with modulated stringent response, *E. coli* SR, did not synthesize ppGpp, the hallmark of the stringent response, in reaction to nitrogen starvation and displayed an increased specific glucose uptake rate during nitrogen starvation. Strain *E. coli* HGT which additionally carries a point mutation in *aceE* leading to reduced pyruvate dehydrogenase activity was capable of accumulating pyruvate during nitrogen starvation and had even higher specific glucose uptake rates (Michalowski et al., 2017).

Based on these findings three research projects were drafted to complement the existing studies and construct strains with beneficial properties for biotechnological production. The projects were centered around the following research questions and experimental approaches:

- A. How does the regulatory response of *E. coli* SR to repeated transient nitrogen limitation differ from that of its parent strain *E. coli* MG1655? Is *E. coli* SR a potential chassis strain for large-scale applications?

To answer these questions, the strains were cultivated in a two-compartment scale-down reactor. Their basic fermentation characteristics and the transcriptomic fluctuations in response to the heterogeneous environment were compared.

- B. Is it possible to engineer a chassis strain for large-scale applications by deletions of genes that cause high energetic costs? What are the benefits of such a strain in general, or in a production scenario?

3. Objectives and research questions of this thesis

Based on *E. coli* MG1655 a series of deletion strains was engineered lacking genes with high metabolic costs under conditions of repeated exposure to nutrient starvation. The maintenance coefficients of *E. coli* MG1655 and the final strain of the deletion series, *E. coli* RM214, were determined in a scale-down reactor simulating repeated glucose starvation. The ability of the strains to produce a heterologous protein under such conditions was compared.

- C. How can the activity of the pyruvate dehydrogenase be reduced to achieve stable pyruvate production in *E. coli* MG1655? How does such a strain perform under nitrogen limitation and how does it compare to *E. coli* HGT? CRISPRi was applied to trigger aerobic pyruvate production and the effects of different sgRNAs were tested. Strains were characterized in two phase fermentations with an initial exponential batch phase and a subsequent nitrogen-limited phase.

4. Publications

Any of the attached publications were prepared in co-authorship with other researchers as indicated prior to the main text of the manuscripts. Smaller contributions are declared at the end of each publication in the respective *Acknowledgements* section.

The following three manuscripts are presented:

- Transcriptional profiling of the stringent response mutant strain *E. coli* SR reveals enhanced robustness to large-scale conditions
- Engineering of a robust *Escherichia coli* chassis and exploitation for large-scale processes
- CRISPRi enables fast growth followed by stable aerobic pyruvate formation in *Escherichia coli* without auxotrophy

Prior to the main text of each manuscript the status of the manuscript at the time of submission of this thesis is indicated. The manuscripts' contents may slightly differ from the final version in peer-reviewed journals due to corrections or modifications made at the revision or post-acceptance stage. Formatting of the manuscripts has been adapted in all cases to fit the formatting of this thesis and all references sections have been merged into the reference section of this thesis. Numberings of figures and tables have been adapted to ensure unique consecutive designations of each element. Sections not containing information related to the primary investigation have been shortened or removed and can be found in the attached original manuscripts.

The original publications or manuscripts and the supplementary materials provided with them are attached to this thesis. Due to the size and format of some supplementary data not all supplementary information is included (see Attachments). All supplements are available from the publishing journal's website or on demand from a paper's corresponding author or the author of this thesis.

4.1 Transcriptional profiling of the stringent response mutant strain *E. coli* SR reveals enhanced robustness to large-scale conditions

The manuscript was jointly penned by Martin Ziegler and Julia Zieringer. Martin Ziegler and Julia Zieringer share co-first authorship. Prof. Dr.-Ing. Ralf Takors contributed to the manuscript's content by selected additions and reviewed it. Prof. Dr.-Ing. Ralf Takors is the corresponding author.

Martin Ziegler planned and conducted all experiments in this study. Martin Ziegler collected and analyzed the primary experimental data. Julia Zieringer conducted the transcriptomic analysis. Prof. Dr.-Ing. Ralf Takors supervised the research.

This manuscript has been accepted and published in Microbial Biotechnology:

Ziegler, M., Zieringer, J., Takors, R., 2021. Transcriptional profiling of the stringent response mutant strain *E. coli* SR reveals enhanced robustness to large-scale conditions. *Microbial biotechnology* 14, 993–1010. <https://doi.org/10.1111/1751-7915.13738>.

4.1.1 Summary

In large-scale fed-batch production processes microbes are exposed to heterogeneous substrate availability caused by long mixing times. *Escherichia coli*, the most common industrial host for recombinant protein production, reacts by recurring accumulation of the alarmone ppGpp and energetically wasteful transcriptional strategies. Here, we compare the regulatory responses of the stringent response mutant strain *E. coli* SR and its parent strain *E. coli* MG1655 to repeated nutrient starvation in a two-compartment scale-down reactor. Our data shows that *E. coli* SR can withstand these stress conditions without a ppGpp mediated stress response maintaining fully functional ammonium uptake and biomass formation. Furthermore, *E. coli* SR exhibited a substantially reduced short-term transcriptional response compared to *E. coli* MG1655 (less than half as many differentially expressed genes). *E. coli* SR proceeded adaptation via more general SOS response pathways by initiating negative regulation of transcription, translation, and cell division. Our results show that locally induced stress responses propagating through the bioreactor do not result in cyclical induction and repression of genes in *E. coli* SR, but in a reduced and coordinated response, which makes it potentially suitable for large-scale production processes.

4.1.2 Introduction

Heterogeneities in large-scale fed-batch bioprocesses have long been recognized as a cause for process performance loss at industrial scale compared to homogeneous processes at lab scale (Bylund et al., 1998). Due to physical, economical, and engineering constraints the generation of gradients in large-scale reactors is inevitable. Hydrostatic pressure influences the solubility and transfer of gasses and the mixing time of large reactors can be orders of magnitude higher than that of laboratory reactors producing strong measurable chemical gradients (Delvigne et al., 2006; Enfors et al., 2001; Junker, 2004; Larsson et al., 1996). Common consequences of spatial heterogeneities are loss of productivity, reduced biomass yield, increased byproduct formation and genetic or plasmid instability (Bylund et al., 2000; Bylund et al., 1998; George et al., 1993; Hopkins et al., 1987; Jonge et al., 2011; Neubauer et al., 1995b). Reduced process performance is not limited to a single species but can be observed for many industrial workhorse organisms like *Escherichia coli*, *Saccharomyces cerevisiae*, *Penicillium chrysogenum*, and *Bacillus subtilis* (George et al., 1993; Jonge et al., 2011; Junne et al., 2011; Larsson and Enfors, 1988).

Due to the enormous costs associated with using and maintaining large-scale equipment, few experiments in the context of academic research have been performed in industrial scale bioreactors (Bylund et al., 2000; Bylund et al., 1999; Enfors et al., 2001). In consequence, researchers have relied on the use of computational fluid dynamics (CFD) to simulate reactor flow fields and on scale-down reactors to experimentally investigate selected scenarios (Kelly, 2008; Takors, 2012). Various designs of scale-down reactors exist and have been extensively reviewed elsewhere (Delvigne et al., 2017; Delvigne et al., 2006; Neubauer and Junne, 2010). One of the commonly used scale-down reactors follows a multi-compartment approach: A primary stirred tank reactor (STR) is coupled to a secondary plug flow reactor (PFR). The STR is operated as a well-mixed compartment under standard limited growth conditions and the PFR simulates a feeding, starvation or anaerobic zone providing the stimulus to be investigated (Lara et al., 2006a).

Many studies have focused on experimentally simulating the zone close to the feeding point which is usually characterized by substrate excess and potentially oxygen limitation (Enfors et al., 2001; Junne et al., 2011; Lara et al., 2009). For a variety of hosts, common observations in this scenario include the formation of small organic acids and solvents as overflow metabolites

or as anaerobic fermentation products (George et al., 1993; Neubauer et al., 1995b). Ultimately, byproduct formation may lead to process performance loss even if reuptake of byproducts occurs in the well-mixed limited growth zone (Enfors et al., 2001).

Occasionally, starvation zones have attracted attention as well (Neubauer et al., 1995b; Neubauer et al., 1995a). From CFD simulation and measured data it is known that distant from the feeding point or close to the reactor walls poorly mixed zones with very low nutrient concentrations exist. An early scale-down study with *E. coli* employing oscillatory feeding protocols revealed the involvement of the stringent response in the cellular reaction to transient glucose starvation (Neubauer et al., 1995a).

The stringent response is a global regulatory program usually preparing *E. coli* for entry into the stationary phase (Gaca et al., 2015; Haurlyliuk et al., 2015; Magnusson et al., 2005). Its hallmark is the synthesis of the alarmone (p)ppGpp on short time-scales by the ribosome-associated protein RelA or on longer time-scales by the bifunctional enzyme SpoT (Atherly, 1979; Gallant et al., 1970; Murray and Bremer, 1996). ppGpp acts primarily as a transcription factor by binding to RNA polymerase and modulating its affinity to transcription initiation sites and alternative sigma factors. Additionally, ppGpp directly modulates the activity of certain proteins (Dalebroux and Swanson, 2012; Kanjee et al., 2011).

The fast and reversible initiation of the stringent response to oscillatory substrate supply was later confirmed by measurements of ppGpp in continuous glucose chemostat cultivations in a two-compartment stirred tank-plug flow reactor (STR-PFR) setup (Löffler et al., 2016). The feeding point was placed in the STR creating a starvation zone in the PFR, which allowed to resolve the timescale of cellular response. Moreover, it was shown that extensive transcriptional responses take place as cells move transiently through a nutrient poor zone. From theoretical calculations of ATP costs Löffler *et al.* estimated that an increase in maintenance energy demand of more than 30% was caused by the repeated exposure of cells to the nutrient gradient offering a new explanation for performance losses in large-scale bioprocesses (Löffler et al., 2016). Analogous experiments with ammonium as the limiting nutrient revealed similar, yet less pronounced, regulation patterns affirming the importance of the stringent response for global regulation in *E. coli* in a scenario of oscillating starvation stimuli (Simen et al., 2017). Fed-batch processes limited by ammonium or other nitrogen sources are interesting fermentation scenarios for the production of small molecules which mainly consist of carbon

such as fatty alcohols (Chubukov et al., 2017). Nitrogen limitation is commonly used to enhance the accumulation of cellular carbon storage products such as polyhydroxyalkanoates used for bioplastic synthesis (Oliveira-Filho et al., 2019; Wen et al., 2010), including *E. coli* as a potential host (Wang et al., 2009). As nitrogen forms a relatively large part of cells, nitrogen limitation can be easily explored during process development. During scale-up, such processes will likely suffer from similar issues as carbon-limited processes (Simen et al., 2017).

Recently, the strains *E. coli* SR and *E. coli* HGT with modulated stringent response were constructed in our laboratory (Michalowski et al., 2017). The strains lack *relA* which is primarily responsible for rapid ppGpp synthesis upon nutrient depletion and carry modifications in the bifunctional enzyme SpoT. It was shown that they do not react to the exhaustion of ammonium supply by ppGpp synthesis (Michalowski et al., 2017). Strain *E. coli* SR displays no negative phenotypic differences in batch cultivations compared to its parent strain *E. coli* K-12 MG1655. However, under conditions of ammonium limitation, *E. coli* SR was found to have an elevated specific glucose consumption rate which is beneficial for two-stage processes involving product formation in the nitrogen limited phase (Jarmander et al., 2015; Perez-Zabaleta et al., 2016).

The combination of properties displayed by *E. coli* SR indicates that this strain can potentially be developed as a platform strain for robust scale-up from lab to production. In this work, we compared the phenotypic and transcriptional responses of *E. coli* SR and its parent strain *E. coli* MG1655 in a two-compartment scale-down reactor. We focused our investigation on the regulatory differences between these strains in the response to repeated short-term stimuli. The primary stirred tank reactor was operated as an ammonium-limited chemostat while a plug flow reactor simulated a nitrogen starvation zone.

4.1.3 Results

Continuous cultivation with periodic nutrient depletion

We cultivated *E. coli* SR and *E. coli* MG1655 in two independent continuous fermentations each in a previously described scale-down reactor consisting of a primary stirred tank reactor (STR) and a secondary plug-flow reactor (PFR), schematically shown in **Fig. 4** (Ankenbauer et al., 2020; Löffler et al., 2016; Simen et al., 2017). *E. coli* SR is a strain with modulated stringent response that was engineered to alleviate the induction of the stringent response and the general stress response upon nutrient depletion (Michalowski et al., 2017). The chemostat was operated at a dilution rate of $D = 0.2 \text{ h}^{-1}$ and ammonium was chosen as the limiting nutrient. After establishment of a steady state in the STR alone, a reference sample (S0, $t = 0 \text{ h}$) was taken and the PFR connected. Periodic passage from the STR (average residence time $\overline{\tau}_{STR} = 6.2 \text{ min}$) through the PFR (average residence time $\overline{\tau}_{PFR} = 2.6 \text{ min}$) then created a repeated short nitrogen starvation stimulus. The average residence times represent worst-case scenarios that are still consistent with mixing studies (Noorman, 2011; Vrabel et al., 2000) and the volume ratio STR to PFR was approximately 3:1 to represent existing simulation results (Haringa et al., 2017; Lapin et al., 2006). The long-term response of cells was investigated from additional samples taken from the STR shortly after connection of the PFR (S5, $t = 5 \text{ min}$) and after establishment of a new steady-state (S28, $t = 28 \text{ h}$) in the two-compartment cultivation. The short-term response of cells to the PFR stimulus was monitored by sampling from five ports along the primary axis of the PFR at identical timepoints. Transcript samples for the PFR were taken from port 5 (P5_5 and P5_28).

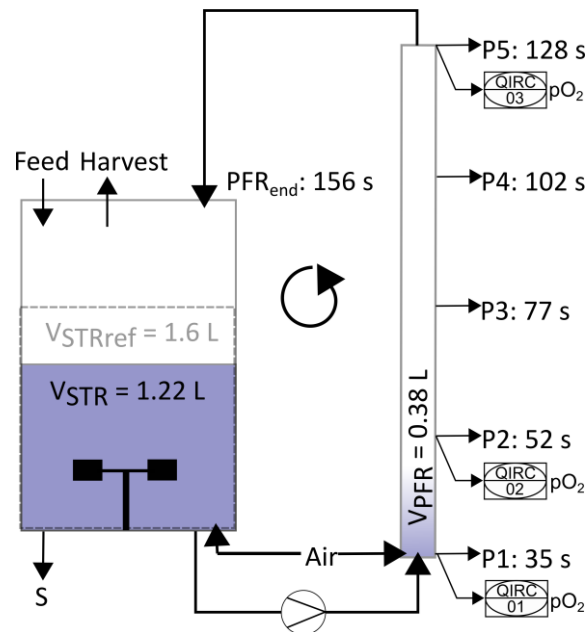


Fig. 4: Experimental design of the two-compartment system. The fermenter consists of a stirred tank reactor (STR) as the primary cultivation vessel and a plug-flow reactor (PFR) connected by an active pump. The ammonium-limited chemostat was operated at a dilution rate of $D = 0.2 \text{ h}^{-1}$ with the feeding point placed in the STR. The STR served as a limitation zone and the PFR formed a starvation zone. The setup was designed to resolve different timescales of cellular response. Oxygen saturation was measured by three oxygen probes and recorded by the process control system (01, 02, 03). V_{STRref} : Reference Volume without connection of PFR (constant volume).

Basic growth and fermentation data confirmed earlier results that there are no detrimental differences in fundamental physiological parameters (**Table 2**) between *E. coli* MG1655 and *E. coli* SR under nitrogen-limited conditions (Michalowski et al., 2017). There were no statistically significant differences in any parameter (two-tailed t-test, $p > 0.1$). Both strains reached practically identical biomass yields on ammonium and depleted ammonium to equally low levels regardless of process time and PFR action (**Fig. 5**). The most noteworthy difference between *E. coli* MG1655 and *E. coli* SR was a reduced concentration of excess glucose in the fermentation broth of *E. coli* SR. Consequently, we calculated a lower biomass yield on glucose for *E. coli* SR (**Table 2**). Under conditions of long-term nitrogen starvation in batch

fermentations *E. coli* SR had previously displayed a relaxation in glucose and nitrogen uptake coupling and we thus suspected an increased specific glucose uptake rate (Michalowski et al., 2017). The calculated specific glucose uptake rate was higher for *E. coli* SR, but the difference was not statistically significant in our experiments (two-tailed t-test, p-value > 0.1). Data from the fermentation broth supernatant showed that both strains converted comparable amounts of substrate into acetate as the primary byproduct. Carbon balancing revealed an increased fraction of unknown substances among the fermentation products of *E. coli* SR which were identified as dissolved organic substances in the fermentation supernatant by total dissolved carbon analysis. The elevated glucose uptake rate of *E. coli* SR likely leads to higher byproduct formation of typical overflow metabolites such as lactate, pyruvate, formate and the regulator 2-oxoglutarate, all of which are known to accumulate under nitrogen-limited conditions with glucose excess (Hua et al., 2004). Apart from the primary byproduct acetate, individual small carbon byproducts were not measured as the overall total carbon efflux/influx balancing was in good agreement for both strains. Carbon recovery was $101 \pm 2\%$ for *E. coli* MG1655 and $102 \pm 1\%$ for *E. coli* SR indicating that in sum all relevant substances were detected.

In general, process time and the periodic PFR stimulus hardly affected global process parameters which is in accordance with former observations made in this reactor setup for nitrogen limitation and K-12 strains (Simen et al., 2017). In sharp contrast, we found substantial regulatory differences between the two strains both in the short-term and in the long-term transcriptional responses to the periodic starvation stimulus.

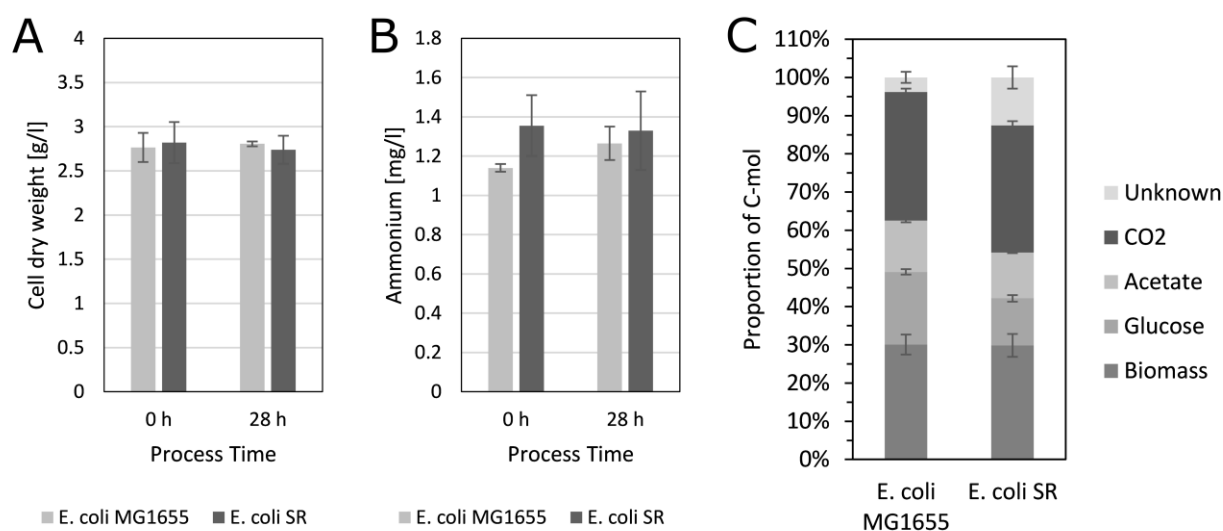


Fig. 5: Physiological measurements. **A.** Cell dry weight. Concentration of cell dry weight after at least 25 h chemostat process before connecting the plug-flow reactor (0 h) and after 28 h of chemostat process with connected PFR (28 h). **B.** Ammonium. Concentration of residual ammonium in the supernatant. **C.** Carbon Balance. Columns show efflux fractions of total C-mol based on carbon influx. The final fraction represents undetermined dissolved organic substances in the fermentation broth, as measured by the difference of all efflux carbon detected by exhaust gas or total carbon analysis and the sum of the individually measured efflux components. Error bars indicate SEM ($n = 2$) of individual components (A, B and C).

Table 2: Physiological measurements

		<i>E. coli</i> MG1655	<i>E. coli</i> SR
Y_{XN}	$\left[\frac{g_{CDW}}{g_{NH_4^+}} \right]$	4.63 ± 0.12^a	4.62 ± 0.27
Y_{XS}	$\left[\frac{g_{CDW}}{g_{Glucose}} \right]$	0.32 ± 0.01	0.28 ± 0.01
$c_{Glucose,STR}$	$\left[\frac{g_{Glucose}}{l} \right]$	2.07 ± 0.25	1.49 ± 0.06
$c_{Acetate,STR}$	$\left[\frac{g_{Acetate}}{l} \right]$	1.39 ± 0.11	1.29 ± 0.14
$q_{NH_4^+}$	$\left[\frac{g_{NH_4^+}}{g_{CDW} * h} \right]$	0.04 ± 0.01	0.05 ± 0.01
q_S	$\left[\frac{g_{Glucose}}{g_{CDW} * h} \right]$	0.63 ± 0.05	0.77 ± 0.14
q_{Ac}	$\left[\frac{g_{Acetate}}{g_{CDW} * h} \right]$	0.10 ± 0.01	0.10 ± 0.01
q_{CO_2}	$\left[\frac{mmol_{CO_2}}{g_{CDW} * h} \right]$	8.73 ± 1.06	9.98 ± 2.23
q_{O_2}	$\left[\frac{mmol_{O_2}}{g_{CDW} * h} \right]$	9.28 ± 0.47	10.9 ± 2.02
RQ	$\left[\frac{mol_{CO_2}}{mol_{O_2}} \right]$	0.95 ± 0.16	0.91 ± 0.04
q_{ATP}	$\left[\frac{mmol_{ATP}}{g_{CDW} * h} \right]$	29.23 ± 0.62^b	34.73 ± 6.39
D	$\left[\frac{1}{h} \right]$	0.20 ± 0.01	0.21 ± 0.03

^aErrors indicate SEM (n = 2). All rates were calculated from averaged values collected over the entire STR-PFR process time. ^bEstimated values assuming a P/O-Ratio of 1.2.

Transcriptomic analysis: Overview

RNA-seq-based transcriptomic data to examine potentially important genes for the ammonium stress response of *E. coli* WT and *E. coli* SR was analyzed. After filtering, 4037 predicted *E. coli* genes remained for further analysis (see supplementary data). The fast tactical transcriptional response to ammonia shortage was determined by comparing PFR port 5

samples to STR samples taken at the same process time points. Long-term responses were studied by comparing post-perturbation samples from the STR after 5 min (S5) and 28 h (S28) to the reference sample (S0). The statistical threshold for significance was set for adjusted p-value < 0.01 and $\log_2FC > |1|$. 54 differentially expressed genes (DEGs) (UP: 14, DOWN: 40) formed the long-term response of *E. coli* MG1655. The short-term response was more pronounced comprising 837 DEGs (UP: 242, DOWN: 595). *E. coli* SR disclosed a similar number of 61 DEGs for the long-term response (UP: 12, DOWN: 49), but substantially less DEGS as short term response (Total: 387, UP: 161, DOWN: 226) (**Fig. 6**). \log_2FC values range from -4.69 to 4.96 (WT) and -3.90 to 5.13 (SR). **Fig. 6** depicts an overview of transcriptional dynamics outlining the halved response of *E. coli* SR 5 min after repeated nitrogen limited perturbation compared to WT.

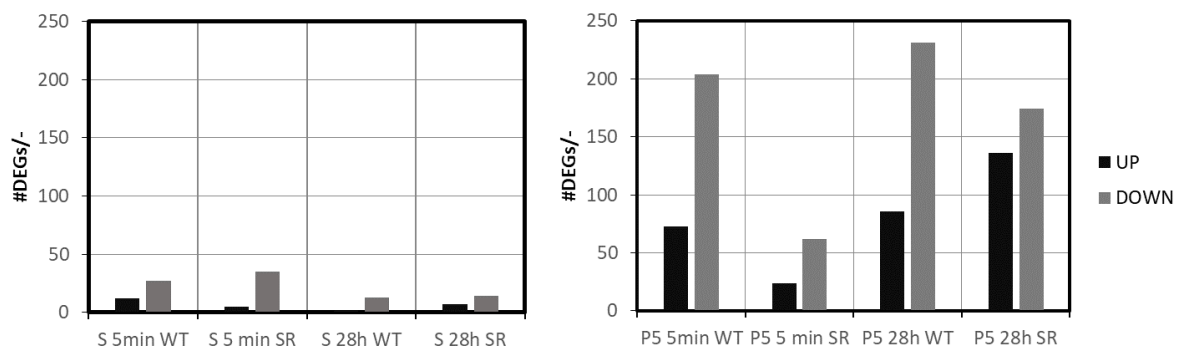


Fig. 6: Number of UP (black) and DOWN (gray) regulated genes (DEGs). Long-term (left) and short-term (right) response to repeated nitrogen starvation for *E. coli* MG1655 (WT) and *E. coli* SR (SR) and given process times.

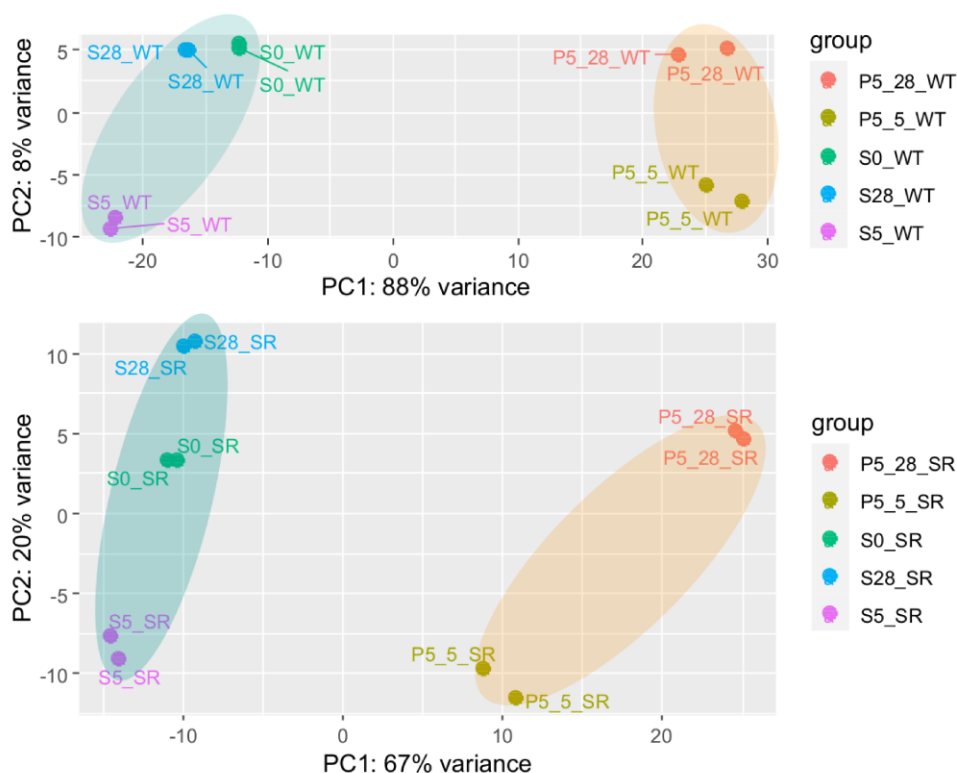


Fig. 7: Principal component analysis of transcript data of *E. coli* MG1655 (WT) (top) and *E. coli* SR (bottom) obtained from STR (S) and PFR (port 5, P5) at three process time points (0 h, 5 min, and 28 h). Covered measurement variance of each principal component (PC) is indicated. Ellipses cluster samples of STR and PFR. PC1 accounts for ‘sample port location’, PC2 for ‘process time’.

Fig. 7 shows that the multi-transcript response of each strain could be well described by 2-dimensional PCA covering 96% and 87% of total variance for *E. coli* WT and *E. coli* SR, respectively. Notably, biological duplicates were found in close proximity. PC1 accounts for the sample port location, PC2 for the time course. Unique and clearly distinguishable differences between STR and PFR transcript patterns were observed already after 5 min of repeated nitrogen starvation for both strains (**Fig. 7, A1**). In particular, principal component 1 (PC1) disclosed major differences between the samples of each strain accounting for 88% and 67% regarding *E. coli* WT and *E. coli* SR, respectively. The PCA finding is in agreement with the reduced number of DEGs observed for *E. coli* SR. The impact of PC2 is more pronounced

for *E. coli* SR although almost identical numbers of DEGs were found as long-term response in both strains. However, given the low impact of PC1 for *E. coli* SR, similar DEG values affect the relative principal component analysis stronger.

As long-term responses of both strains were similar (see Appendix: supplementary information B) and weaker than short-term responses (**Fig. 7**) further analysis focused on short-term transcript patterns. Notably, changes between long- and short-term responses of both strains were dominated by counteracting transcript dynamics resetting perturbations after PFR passages (MG1655: 5 min and 28 h). Observations are in line with similar findings (Chang et al., 2002). Additional differences were found in the upregulation of carbohydrate transport (SR: 5 min) and catabolic processes (SR: 28 h) (see Fig. A5 and A6).

Regulatory response to short-term ammonium limitation

Preceding investigations of *E. coli* K-12 strains in STR-PFR scale-down reactors revealed the rapid accumulation of the alarmone ppGpp upon entry into the nutrient limited zone under both glucose and ammonium limitation (Löffler et al., 2016; Simen et al., 2017). Concomitantly, an extensive transcriptional reprogramming of cells occurred. In standard batch fermentations *E. coli* SR in turn did not react to ammonium depletion by ppGpp synthesis (Michalowski et al., 2017). We therefore measured intracellular ppGpp levels from samples taken from the five ports of the PFR along its primary axis (**Fig. 8**). During the PFR passage *E. coli* MG1655 accumulated ppGpp to levels 2 – 3 fold higher than measured in the STR, displaying the same behavior as previously observed for the closely related K-12 strain *E. coli* W3110 (Simen et al., 2017). In contrast, *E. coli* SR had no elevated levels of ppGpp at any point during the PFR passage regardless of process time. These results complement previous findings for the case of repeated short stimuli and confirm the strain's resilience to ammonium exhaustion.

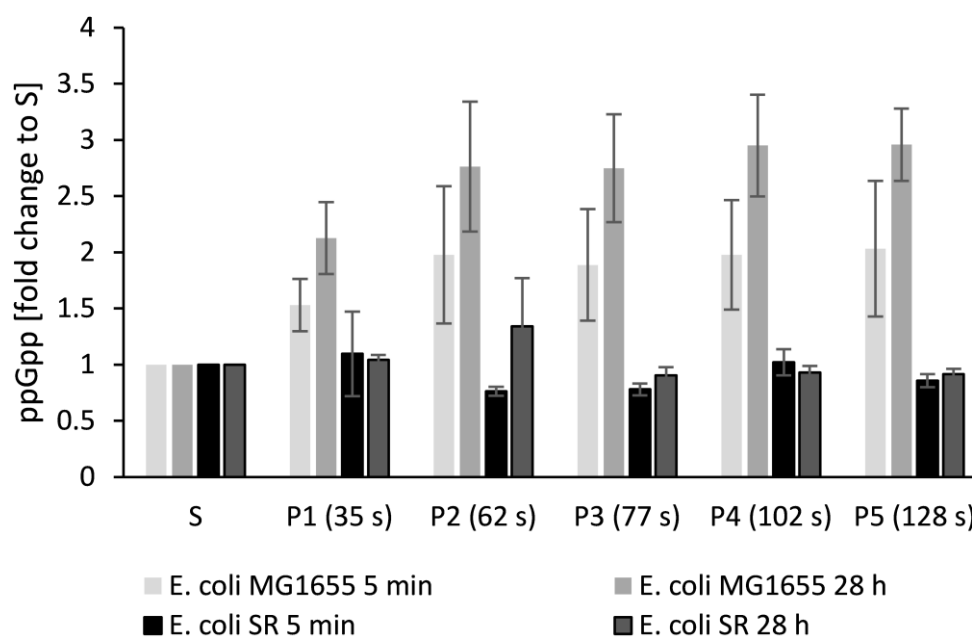


Fig. 8: Alarmone accumulation along the PFR. Concentration of ppGpp measured from samples drawn along the plug flow reactor (P1 to P5) relative to the concentration measured in the stirred tank reactor (S, all values set to 1) for *E. coli* MG1655 (WT) and *E. coli* SR (SR). Error Bars represent SEM (n = 2).

Based on these encouraging findings, we focused our investigation on the short-term transcriptional response of both strains along the PFR axis. We compared data from samples drawn from port 5 of the PFR to samples drawn from the STR at identical process time points. Short-term changes revealed a significantly different response of *E. coli* SR compared to *E. coli* MG1655 not only in the amount of DEGs (**Fig. 6**), but also in the function of these genes (**Fig. 7**, **Fig. 9**). To elucidate patterns in the transcriptional responses, we searched for common DEGs, investigated the behavior of gene clusters of orthologous groups (COGs), and compared sigma factor (σ) activities. The gene expression patterns of each strain individually were assigned to 21 functional categories based on the COG database (Tatusov et al., 2003). In total 3532 of the 4037 genes (87.5%) could be annotated to COG. For each COG category, the resulting t-values are represented in a lollipop plot (**Fig. 10**). Significant changes were defined with a FDR-corrected p-value < 0.01. Furthermore, the activation and deactivation of sigma

factors over time were investigated (**Fig. 10**). In this case, 3935 out of 4037 genes could be assigned to the sigma factor-gene interaction database from RegulonDB (Santos-Zavaleta et al., 2019).

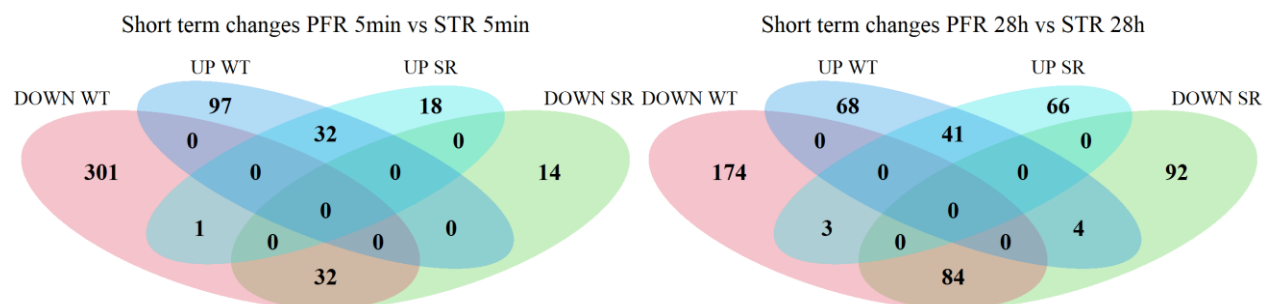


Fig. 9: Venn diagrams representing partially overlapping sets of DEGs of *E. coli* MG1655 (WT) and *E. coli* SR. The number of significantly up- (UP) and downregulated (DOWN) genes in each set is indicated by numbers. Left: Short-term responses 5 min after PFR connection. Right: Short-term responses 28 h after PFR connection. Complete gene lists of the Venn diagrams are available in the supplementary data.

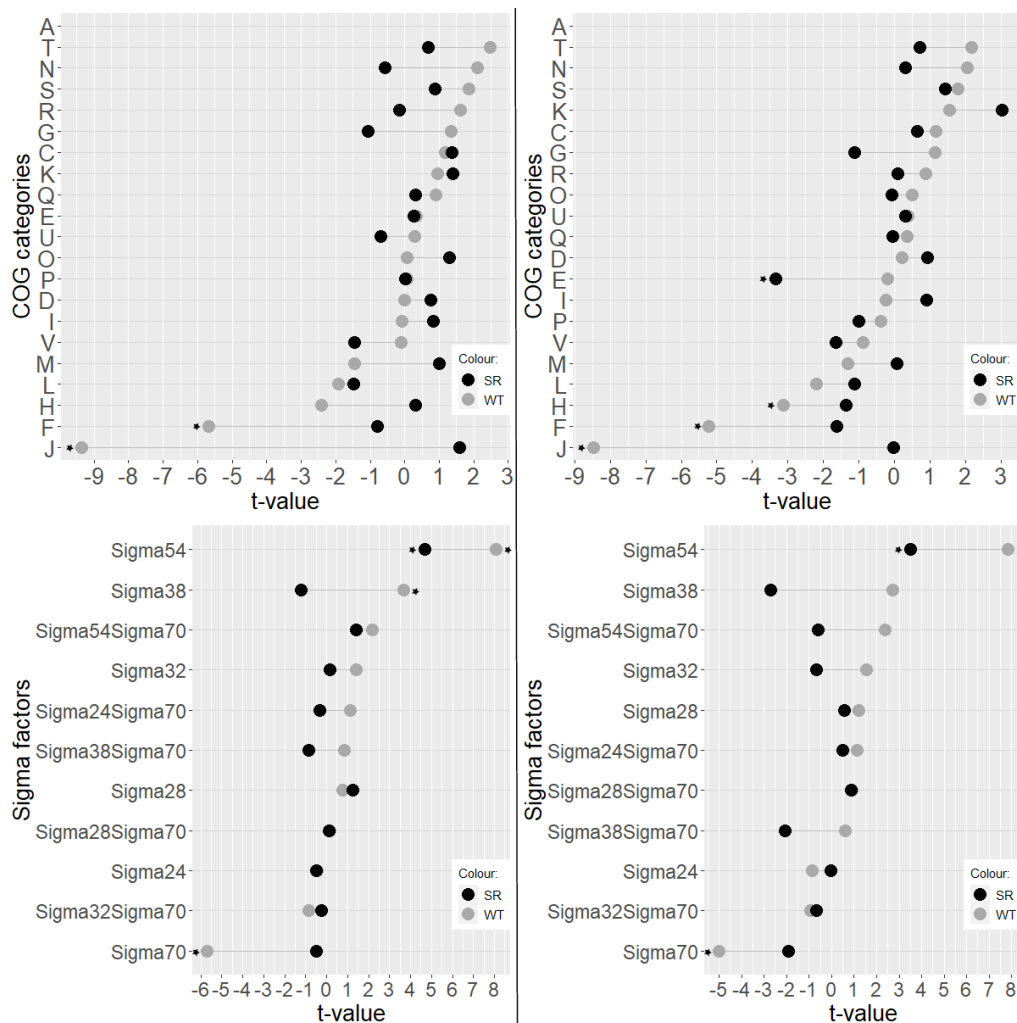


Fig. 10: Top: Transcriptional patterns grouped into COG categories of *E. coli* MG1655 (WT) and *E. coli* SR (SR). Left: short-term patterns to the PFR stimulus 5 min after PFR connection. Right: short-term patterns to the PFR stimulus 28 h after PFR connection. Bottom: Sigma factor activities of *E. coli* MG1655 (WT, grey) and *E. coli* SR (SR, black). Left: Short-term response to the PFR stimulus 5 min after PFR connection. Right: Short-term response to the PFR stimulus 28 h after PFR connection. Significant categories are indicated with an asterix.

After the first 5 min of PFR action *E. coli* MG1655 and *E. coli* SR exhibited substantially different transcriptional responses. The strains had only 64 DEGs in common, split equally between up- and down regulation (**Fig. 9** left). Hence, these genes mirror the transcriptional response to short-term starvation irrespective of a functional stringent response, in which 14

out of the 32 common upregulated genes are associated with the Ntr-reponse (e.g. *glnK*, *amtB*, *glnAHPQ*, *rutA*). Downregulated genes consist of genes responsible for amino acid biosynthesis (e.g. *argCF*, *metABFINR*) and other cellular functions such as DNA cleavage, transporters, and oxidoreductases. The only oppositely regulated gene was *guaC* coding for the GMP reductase GuaC. Transcriptional control of the *guaC* promoter by the stringent response was proposed after its initial discovery and is clearly supported by our data (Andrews and Guest, 1988). Individual, strain-specific short-term regulation was observed for 398 (*E. coli* MG1655) and 32 (*E. coli* SR) specific DEGs after 5 min, clearly demonstrating the effect of the stringent response on the *E. coli* transcriptome.

Gene expression along the PFR after 28 h of PFR action differs strongly from the early response. 125 DEGs, mostly downregulated, are shared by both strains and the number of individually regulated genes is similar with 242 genes for *E. coli* MG1655 and 158 genes for *E. coli* SR (**Fig. 9** right). Additionally, seven genes are oppositely regulated. Three of them (*tolQ*, *guaC*, *purM*) are upregulated in *E. coli* SR and downregulated in *E. coli* MG1655. These genes correspond to cell envelope integrity during cell division (Gerding et al., 2007), nucleotide metabolism (Kanjee et al., 2012) and purine *de novo* biosynthesis (Mueller et al., 1999). While purine *de novo* biosynthesis is actively inhibited by ppGpp via inhibition of GuaB, GTP synthesis solely originates from purine salvage pathways with *xdhA* significantly increased in *E. coli* MG1655 (Xi et al., 2000). The residual four oppositely regulated DEGs (*csiD*, *glnL*, *lhgO*, *yeaH*) predominantly play a role in the adaptation to nitrogen starvation and except for *glnL* are known to be induced by ppGpp. NtrB encoded by *glnL* is an essential part of the Ntr response cascade to nitrogen starvation and *yeaG* positively impacts *rpoS* transcription and translation under prolonged nitrogen starvation (Brown et al., 2014). Despite these differences in adaptation to nitrogen limitation, we observed no alterations in the uptake or utilization of ammonium which indicates that the additional regulatory adaptations of *E. coli* MG1655 are irrelevant in the context of a bioprocess.

Transcriptional patterns could be identified by functional enrichments of groups based on COG categories and sigma factor activities. COG groups J (Translation, ribosomal structure, and biogenesis) and F (nucleotide transport and metabolism) were significantly down regulated as part of the stringent response of *E. coli* MG1655 after both 5 min and 28 h (**Fig. 10**). For the 28 h sampling point, group H (coenzyme transport and metabolism) was also significantly downregulated. As already indicated by the oppositely regulated genes (**Fig. 10**) σ^{54} mediated

genes responsible for the activation of the Ntr stress response including *yeaG/H* via NtrBC were induced in *E. coli* MG1655, as well as the σ^{38} regulon as part of the general stress response (Brown et al., 2014; Figueira et al., 2015) (**Fig. 10**). Due to the limited amount of RNA-Polymerase (RNAP) core enzymes, σ^{70} competes with σ^{54} , resulting in an antiproportional expression of their mediated genes (Jishage et al., 1996). In contrast, *E. coli* SR only increased the expression of genes regulated by σ^{54} after 5 min and no significant COG category was identified at this time-point. The absence of the stringent response in *E. coli* SR is clearly visible in an overall dampened regulatory response. The only significantly regulated group is E (amino acid transport and metabolism) after 28 h of PFR action, and the significantly downregulated genes in this group are predominantly ABC-transporters.

To unravel more detailed patterns in the transcriptional responses we assigned genes to the up-to-date gene ontology (GO) gene sets using GAGE (Luo et al., 2009). 3345 out of 4037 genes (83%) could be mapped to GO Terms. As shown in **Fig. 6** the majority of significant DEGs for *E. coli* MG1655 were downregulated. This is mirrored by the results of the identified top 20 GO categories which were uniformly downregulated (**Fig. 11**). *E. coli* MG1655 predominantly downregulated genes related to ribosomal biosynthesis and translation after 5 min and 28 h as expected for a stringent phenotype (**Fig. 11**). These transcriptional changes are counteracted in the long-term response observed from the STR (Fig. A3 - A6) which indicates looping induction and repression of the genes. Patterns from *E. coli* SR were less pronounced and grouped differently. After 5 min we observed decreasing gene expression of ATP-demanding processes such as ABC transporters and ATPase complexes (**Fig. 11**). After 28 h the PFR passage mainly induced an increased negative regulation of transcription and metabolic processes (**Fig. 11**). Care must be taken in the interpretation of this group though. General categories affecting transcription (GO:0006351, GO:0045892, GO:0097659, GO:1903507) or RNA processes (GO:0032774, GO:1902679, GO:0051253, GO:0051252) are represented as simultaneously negatively and positively regulated. Moreover, all negative regulators included in these terms, such as members of the CRP family, are also capable of positive regulation. Other negative regulation categories involve genes which actively inhibit translation and belong to SOS signals like DNA damage, prevention of cell division and programmed cell death (PCD). *E. coli* SR thereby focuses on σ^{38} regulated genes, as well as toxin and antitoxin systems (*mazEF* and *mqsRA*) possibly resulting in arrested growth and a dormant cell state or even PCD. As growth arrest is usually a primary outcome of the stringent response, which is absent in

E. coli SR, we hypothesize that this pattern might provide an alternative way for *E. coli* SR to achieve cell cycle arrest.

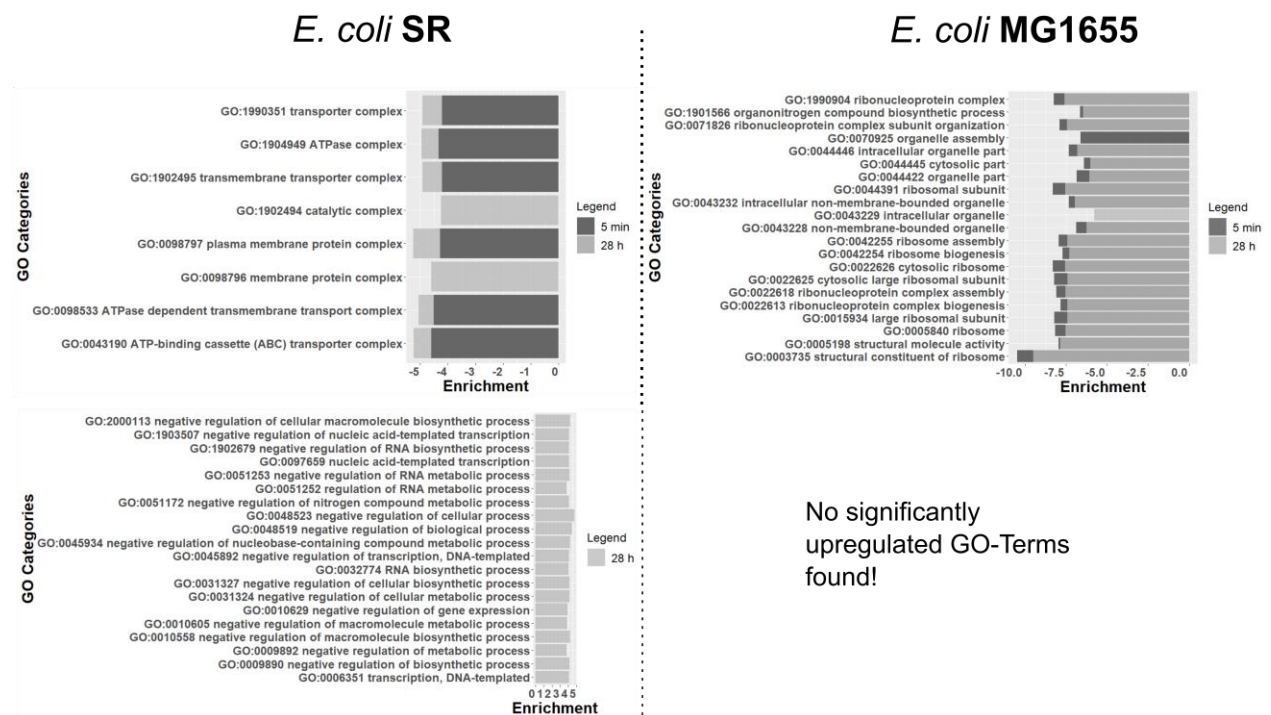


Fig. 11: Significant GO categories after 5 min and 28 h of both *E. coli* SR (left) and *E. coli* MG1655 (right). Downregulated categories are arranged at the top and upregulated GO terms at the bottom. 5 min: Short-term response of *E. coli* SR (left) and *E. coli* MG1655 (right) after 5 min of PFR action. Only the Top 20 out of 102 significantly downregulated categories are shown. Neither strain had significantly upregulated categories for this time-point. 28 h: Short-term response of *E. coli* SR (left, light grey) and *E. coli* MG1655 (right, light grey) after 28 h of PFR action. For *E. coli* SR only the Top 20 out of 24 significantly upregulated categories are shown. For *E. coli* MG1655 only the Top 20 out of 95 significantly downregulated categories are shown. No significantly upregulated categories were found for this time-point.

In summary, the short-term response transcriptional patterns of *E. coli* MG1655 were extensive and dominated by the stringent response and the Ntr regulon. The major activated sigma factors were σ^{54} and σ^{38} . Overall, the transcription of ribosomal genes and other genes necessary for growth was inhibited, while genes involved in the transport and fixation of ammonia were

induced. Our observations reflect well-known regulatory patterns exerted by *E. coli* K-12 when facing nitrogen starvation (Chang et al., 2002; Simen et al., 2017; Traxler et al., 2011; Traxler et al., 2008; Wang and Levin, 2009). In contrast, the transcriptional short-term response of *E. coli* SR is dampened both in the number of DEGs and the patterns observed, especially shortly after connection of the PFR. The only significantly activated sigma factor is σ^{54} indicating a functional but attenuated Ntr response in the absence of ppGpp accumulation. Adaptation to ongoing starvation was possibly attempted via negative regulation of metabolic processes and SOS pathways.

4.1.4 Discussion

In the present study, we investigated the regulatory responses of the stringent response mutant strain *E. coli* SR when exposed to repeated short starvation stimuli in a scale-down reactor. The comparison with its wild-type parent *E. coli* MG1655 unraveled dampened regulatory patterns which are potentially beneficial for the application of *E. coli* SR in industrial large-scale reactors. The reduced regulatory patterns might be beneficial for heterologous protein expression as well as the production of small molecules as less interference with engineered metabolic pathways may occur and energy otherwise spent for adaptive responses is available for product formation.

An important finding of our study is that despite the regulatory differences *E. coli* SR displayed no dysfunctionalities in handling the shortage of ammonium. *E. coli* SR reached the same biomass yield on ammonium as *E. coli* MG1655 both with and without PFR action. Moreover, both strains depleted ammonium to comparable levels of about 1.2 mg/l or 67 $\mu\text{mol/l}$, well in line with previously reported values for *E. coli* K-12 strains in nitrogen limited chemostats (Hua et al., 2004). The low remaining ammonium concentration indicates that uptake in both strains is mediated actively by AmtB with $K_m = 0.8$ mM (Williamson et al., 2020) and incorporation is accomplished by the GS-GOGAT System with GS $K_m = 0.1$ mM (Alibhai and Villafranca, 1994). This is supported by our transcriptional data which revealed that *amtB*, *gltB* and *gltD* were significantly enriched for both strains over all time-points. Transcripts of *glnA* were also always significantly enriched except for the time point 28 h of *E. coli* SR. Concomitantly, we identified transcriptional patterns typical for the σ^{54} and NtrBC mediated responses to nitrogen starvation (Reitzer, 2003). 13 out of 21 known NtrC-regulated operons (Brown et al., 2014) were induced at PFR port 5 in *E. coli* MG1655 at all time points (Table S2). For *E. coli* SR, the Ntr response was slightly reduced, with 9 out of 21 operons induced (Table S3) and lower overexpression of σ^{54} transcribed genes. These findings lead to the conclusion of an active, but diminished Ntr response of *E. coli* SR that still allowed fully functional ammonium assimilation. Additionally, the energy consumption as maintenance add-on for both strains was calculated according to Löffler et al. (2016) assuming *de novo* synthesis of all upregulated DEGs over the whole process time (28 h). The resulting energy savings of *E. coli* SR due to weaker transcriptional response added up to around 46.5 %. In terms of microbial productivity, the reduced maintenance demand potentially increases the amount of available ATP for biomass-specific productivities and improves cell fitness.

In a previous study, a significantly elevated specific glucose consumption rate under ammonium limitation was observed in *E. coli* SR (Michalowski et al., 2017). Similarly, we observed reduced excess glucose and the accompanying formation of dissolved byproducts in the fermentation supernatant. In *E. coli* K-12 strains, the consumption of glucose is usually tightly coupled to the availability of nitrogen on the level of metabolite control by the interaction of 2-oxoglutarate with PtsI (Doucette et al., 2011). The exact mechanism by which coupling of nitrogen and glucose uptake rates are relaxed in *E. coli* SR is not clear as the strain is isogenic to *E. coli* MG1655 except for the deletion of *relA* and the modifications in *spoT*. However, we found an increased transcription of *ptsI*, *ptsH* and *ptsG* in *E. coli* SR compared to *E. coli* MG1655 (Table S6). Artificially increased expression of *ptsI* has been shown to increase specific glucose uptake rates in nitrogen limited conditions (Chubukov et al., 2017). We presume that the increased glucose uptake rate in *E. coli* SR might be caused by deregulated expression of *ptsI*, potentially connected to the absence of the stringent response by the action of CRP whose transcription is negatively regulated by ppGpp (Johansson et al., 2000). It remains to be clarified whether *E. coli* SR has altered cytoplasmic 2-oxoglutarate levels or the action of ppGpp influences the coupling of glucose consumption to nitrogen availability, potentially by the proposed mechanism. Increased specific glucose uptake rates in conjunction with higher respiratory activity have also been observed in *E. coli* MG1655 subjected to repeated glucose feast-famine cycles (Vasilakou et al., 2020). Future studies should thus examine how *E. coli* SR reacts to varying availability of glucose or other carbon sources.

In view of these differences in carbon metabolism, we hypothesized that biological energy availability might be unequal for *E. coli* MG1655 and *E. coli* SR. From oxygen and glucose uptake rates the specific ATP production rate q_{ATP} was estimated (**Table 2**). q_{ATP} greatly depends on the effective P/O ratio and current scientific consensus estimates realistic P/O ratios between 1.0 and 1.5 for *E. coli* (Noguchi et al., 2004; Szenk et al., 2017). For our estimations of q_{ATP} we assumed a conservative P/O ratio of 1.2 and 2 moles of ATP per mol glucose from glycolysis. The result indicates that *E. coli* SR might have an increased availability of ATP compared to its wild-type parent under the applied experimental conditions. Given that the respiratory capability and thus the ATP production capability of K-12 strains is not exhausted at a dilution rate of $D = 0.2 \text{ h}^{-1}$ it appears that the increased glycolytic flux to byproducts displayed by *E. coli* SR was also not a result of increased energy demand. Moreover, increased glucose uptake has been reported previously for *E. coli* SR under conditions of ammonia

limitation despite high adenylate energy charge (Michalowski et al., 2017). Carbon and redox homeostasis at elevated glycolytic flux would then be maintained by byproduct excretion and increased respiration, possibly involving the dissipation of surplus energy by uncoupling of the electron transport chain (Bekker et al., 2009).

Nitrogen limitation inducing the stringent response is a well-documented phenomenon in *E. coli*. Multiple previous studies predominantly observed heavily increased gene expression corresponding to amino acid transport and metabolism (Barker et al., 2001; Brown et al., 2014; Durfee et al., 2008a; Simen et al., 2017; Traxler et al., 2011; Traxler et al., 2008). Conversely, we observed almost equally distributed up- and downregulated genes for amino acid transport and metabolism (see supplementary data: Transcriptomics), which was only reported by few research groups (Chang et al., 2002; Traxler et al., 2008). As a result, no overall significant statistical trend was detectable for this category (**Fig. 10**). We suggest that the individual operons do not solely respond to ppGpp, but rather depend on other signals and regulatory networks which were not found to be significantly expressed in this study such as the Lrp regulon. Additionally, caution is advised when comparing transcriptomic analyzes originating from different studies as they greatly depend on the transcriptional reference state and thus the details of the experimental design.

In general, the amount of DEGs of *E. coli* K-12 MG1655 was similar to the numbers found in the analogous study of Simen *et al.* (2017) who employed the closely related *E. coli* K-12 W3110 confirming the validity of our data. The amount of DEGs is also less than observed during the related study of glucose starvation by Löffler *et al.* (2016) which points towards significant potential of *E. coli* SR to preserve energy in glucose starvation conditions. An interesting difference to the former studies in this scale-down reactor setup is the absence of increased motility in the STR after PFR connection (Löffler et al., 2016; Simen et al., 2017). Our dataset contains no upregulated flagellar or sigma factor 28 mediated gene patterns from the STR at any time-point (**Fig. 10**). We first hypothesized that the cause might be genetic differences affecting motility which are well documented between MG1655 and W3110 and even between different MG1655 isolates (Barker et al., 2004; Hayashi et al., 2006). However, sequencing of our MG1655 isolate revealed the presence of the canonical IS-1 insertion upstream of *flhD* which confers motility and our MG1655 isolate displayed vivid spreading in motility agar (Supplementary information D, Fig. A7). An alternative explanation could be derived by the interplay of quorum sensing and flagellar regulation through the action of

autoinducer-2 (AI-2) and the motility quorum sensing regulator MqsR. While transcript levels of *luxS* (LuxS synthesizes AI-2) remain unchanged, the expression of *mqsR* is significantly enriched at PFR port 5 and MqsR is known to induce the flagellar synthesis cascade (González Barrios et al., 2006). However, cell dry weight (CDW) was always below 3 g/l in our experiments whereas Simen *et al.* worked with around 10 g/l CDW. Higher biomass should lead to increased AI-2 levels and may cause a preconditioned phenotype that rapidly initiates flagellar biosynthesis when encountering nutrient stress. Thus, rapid induction of motility genes might become more pronounced during high cell density processes in large-scale reactors and remains to be examined in further studies. Additionally, as introduced by Löffler et al. (2016) during glucose fluctuation, genes of the category cell motility were identified as one of the most prominent energy consumers and might therefore be candidates for genome reduction (Löffler et al., 2016).

Analysis of gene expression patterns (**Fig. 10** and **Fig. 11**) revealed that both strains individually adapted to repeated nitrogen starvation. *E. coli* MG1655 adjusted by utilizing the ppGpp-mediated general stress response including activation of toxin/antitoxin (TA) systems like *mqsRA* and *mazEF*. This strategy intends to arrest the cell cycle and form persister cells (Balaban et al., 2004). Persister cell formation is not yet fully understood and usually only involves a small fraction of cells (Chowdhury et al., 2016; Gerdes and Maisonneuve, 2012; Korch et al., 2015). Thus, it seems to be only of minor importance for industrial processes but some persister genes affect persister level due to altered growth rates rather than contributing to a mechanism of cell cycle arrest and might have a significant impact on bioprocess performance (Allison et al., 2011). Nonetheless two common dependencies affecting persister formation, ppGpp and TA systems, are known which is in line with our findings (Aizenman et al., 1996; Chowdhury et al., 2016; González Barrios et al., 2006; Sun et al., 2017; Wang and Levin, 2009). Persister formation benefits from increased ppGpp concentrations but is still possible at lower rates in the absence of ppGpp by proteins which simply reduce growth (Chowdhury et al., 2016). The nucleotide pyrophosphohydrolase MazG which is negatively regulated by the *mazEF* system is able to initiate cell cycle arrest and was significantly upregulated in *E. coli* SR after 28 h (Lee et al., 2008). Additionally, *E. coli* SR initiated negative regulation of transcription, translation, and cell division processes as part of the SOS response (**Fig. 11**). Most likely, the SOS pathways were activated due to ongoing DNA replication during starvation conditions which might ultimately result in DNA damage and inhibited cell division

(Bi and Lutkenhaus, 1993; Joseleau-Petit et al., 1999; Traxler et al., 2008). As part of the SOS response and as a key gene involved in filamentation *sulA* was significantly upregulated in *E. coli* SR. SulA inhibits the initiation of cellular division by repressing the assembly of FtsZ into the Z ring (Fonville et al., 2010; Huisman et al., 1984). Simultaneously with the overexpression of *sulA*, *lexA* was significantly increased which acts as a major repressor of SOS signals. LexA regulates the response strength and is actively involved in the occurrence of persister cells in bacterial populations (Butala et al., 2011). These results indicate a coordinated and rather complex SOS response in *E. coli* SR to form persister cells which is not yet fully understood.

The natural regulation of *E. coli* has evolved towards optimality in its lifestyle as a gut bacterium and is not honed for the demands of a large-scale bioprocess. The absence of the stringent response and the conservation of the ability to grow efficiently in minimal medium suggest that *E. coli* SR has the potential to become a platform strain for applications in large-scale reactors. Our transcriptional analysis shows that the short-term response of *E. coli* SR to ammonium depletion is dampened but a functional Ntr/ σ 54 response remains. Regarding glucose-limited fermentations, we hypothesize that *E. coli* SR has significant potential to preserve energy in such conditions since the regulatory responses are usually even more pronounced and centered around the stringent response (Hardiman et al., 2007; Löffler et al., 2016). We therefore propose to confirm the suitability of *E. coli* SR for large-scale applications in multi-compartment scale-down reactors employing exemplary small-molecule production scenarios. These should include standard glucose-limited fed-batches as well as ammonium limited fed-batches with a prolonged nitrogen-limited production phase to exploit its elevated glucose consumption.

4.1.5 Materials and methods

Bacterial Strains and Media

Strains *E. coli* MG1655 or *E. coli* SR were used in all experiments (**Table 3**).

2xYT agar plates were prepared by autoclaving 16 g/l tryptone, 10 g/l yeast extract, 5 g/l NaCl and 18 g/l agar-agar dissolved in demineralized water. Minimal media for precultures consisted of 4 g/l glucose, 0.96 g/l NaH₂PO₄·2H₂O, 3.51 g/l K₂HPO₄, 2.4 g/l (NH₄)₂SO₄, 0.01 g/l thiamine hydrochloride and 0.2% (V/V) trace elements stock solution. Minimal media for batch cultivation in the bioreactor consisted of 19 g/l glucose, 1.50 g/l NaH₂PO₄·2H₂O, 3.9 g/l K₂HPO₄, 5.7 g/l (NH₄)₂SO₄ and 0.2% (V/V) trace elements stock solution. 200 µl of antifoaming agent Struktol J647 (Schill + Seilacher, Hamburg, Germany) was added to the batch medium prior to inoculation. Minimal media for continuous chemostat cultivation in the bioreactor consisted of 11.4 g/l glucose, 1 g/l NaH₂PO₄·2H₂O, 2.6 g/l K₂HPO₄, 2.28 g/l (NH₄)₂SO₄ and 0.2% (V/V) trace elements stock solution. Throughout the chemostat phase 50 µl/h of antifoaming agent Struktol J647 were added continuously to the fermentation medium. The composition of trace element stock solution was 4.175 FeCl₃·6H₂O, 0.045 g/l ZnSO₄·7H₂O, 0.025 g/l MnSO₄·H₂O, 0.4 g/l CuSO₄·5H₂O, 0.045 g/l CoCl₂·6H₂O, 2.2 g/l CaCl₂·2H₂O, 50 g/l MgSO₄·7H₂O and 55 g/l sodium citrate dihydrate. Stock solutions of salts, trace elements and glucose were autoclaved separately, and stock solutions of thiamine hydrochloride were filter sterilized and stored at 4 °C. All compounds were combined just before the experiments to prevent possible aging of media.

Table 3: Bacterial strains used in this study.

Strain	Genotype/Strain Information	Reference
<i>Escherichia coli</i> K-12 MG1655 (“wild type” strain, abbrev. WT)	F-, λ-, ilvG-, rfb-50, rph-1	(Michalowski et al., 2017)
<i>Escherichia coli</i> SR	MG1655 ΔrelA, SpoT[R290E;K292D]	(Michalowski et al., 2017)

Bioreactor Setup

Cultivations were carried out in a two-compartment scale-down reactor. The primary reactor was a stirred tank reactor (STR), and a plug flow reactor (PFR) was used as the secondary compartment mimicking a starvation zone. The plug flow reactor was connected to the stirred tank reactor after establishment and sampling of a steady state in the chemostat phase. The basic technical setup has been characterized previously (Löffler et al., 2016; Simen et al., 2017). Minor modifications to the original setup have been made and are described elsewhere (Ankenbauer et al., 2020).

The primary reactor was a 3 l bioreactor (Bioengineering, Wald, Switzerland) equipped with flow baffles and two six-blade Rushton type impellers operated at 1000 rpm. A constant aeration rate of 2.0 standard liters of ambient pressurized air per minute was employed and the system operated at a total pressure of 1.5 bar. Temperature was monitored by a platinum resistance thermometer and regulated by electrical heating or water cooling. Temperature was set to 28 - 30 °C for the batch phase and to 37 °C for the continuous chemostat phase. The reactor was equipped with a pH sensor (Mettler Toledo, Columbus, USA) to control pH and a pO₂ sensor for monitoring dissolved oxygen tension (PreSens, Regensburg, Germany). During all fermentation stages pH was set to 7.0 and regulated by automated addition of 3 M NaOH or 2.5 M H₃PO₄. Dissolved oxygen tension was not regulated but maintained values above 70% saturation to 1.5 bar ambient air throughout the entire cultivation. In the exhaust gas stream, the concentration of oxygen and carbon dioxide was measured by gas sensors (BlueSens, Herten, Germany). During the chemostat phase the feed was constantly added to the reactor by a peristaltic pump (Watson-Marlow, Falmouth, United Kingdom). The feed flow was monitored by a balance recording the weight of the stirred feed barrel and manually adjusted if necessary. The harvesting pump operated as a slave pump set to maintain a constant weight of the bioreactor. For this purpose, the stirred tank reactor was installed on a balance as well.

The secondary compartment was a plug-flow reactor with an inner tube diameter of 20 mm and a total volume of approximately 380 ml. Five ports along the primary axis were used to take samples throughout the cultivation. Oxygen saturation in the PFR was monitored close to ports P1, P2, and P5, and additional aeration of 0.15 standard liters per minute was provided next to port P1 to ensure levels above 30% saturation to ambient air conditions throughout the entire PFR passage. Temperature in the PFR was maintained at 36 – 37 °C by water heating and isolation material. A diaphragm metering pump (Sigma/1, ProMinent, Heidelberg, Germany)

was used to transfer biosuspension from the stirred tank reactor to the plug flow reactor after connection of the two reactors.

Preculture, Batch Cultivation and Continuous Cultivation

A small amount of glycerol stock seed culture was spread onto 2xYT agar plates and incubated at 37 °C for 24 h. A single colony was picked to inoculate 500 ml baffled shaking flasks with 50 ml of preculture minimal medium. Flasks were then incubated at 37 °C on an orbital shaker set to 150 rpm for 16 hours. In the next morning 500 µl of biosuspension were transferred to 1000 ml baffled shaking flasks containing 100 ml preculture minimal medium and incubated at 37 °C on an orbital shaker set to 150 rpm for 8 hours. 50 ml of this culture were used to inoculate the bioreactor. Total volume in the bioreactor was 1.6 l after inoculation. Batch fermentation in the bioreactor ensued at 28 – 30 °C overnight. In the next morning feed and harvest trains were connected and a constant feed/harvest rate at 5.33 ml/min corresponding to a dilution rate of 0.2 h⁻¹ established. After 25 h (five volumetric residence times) of STR cultivation a reference sample was taken. The plug-flow reactor was then connected to the primary reactor via a diaphragm metering pump effectively circulating about one-quarter of the total fermentation broth from the STR through the PFR and back into the STR. In the following 28 h samples were taken at predefined time points from the STR and the five PFR ports. After 28 h of STR-PFR cultivation the fermentation was aborted, and the final broth volume measured. This value was used for all volumetric calculations during data analysis.

Determination of Optical Density and Biomass

In preliminary experiments with identical setup correlation factors of optical density and biomass as cell dry weight (CDW) were determined for *E. coli* MG1655 and *E. coli* SR (supplementary information A, Table S1). The resulting correlation factors for converting OD_{600nm} values to g/l cell dry weight were 0.324 for *E. coli* MG1655 and 0.321 for *E. coli* SR. In the main cultivations optical density was measured from appropriately diluted broth on a spectrophotometer at 600 nm and converted into biomass concentration.

Determination of Acetic acid, Ammonium and Glucose Concentrations

5 ml of biosuspension was directly sampled into a syringe connected to a single-use 0.45 µm sterile filter and immediately sterile filtered. The clear supernatant was flash frozen in liquid nitrogen and stored at -70 °C until analysis. Glucose concentration was determined by D-Glucose UV-Test Kit (R-Biopharm, Darmstadt, Germany) and acetic acid concentration by

Acetic acid UV-Test Kit (R-Biopharm, Darmstadt, Germany). Ammonium concentration was determined by Ammonium cuvette test LCK 304 (Hach Lange, Düsseldorf, Germany). At the end of the cultivation feed samples were taken and processed identically.

Analysis of Total Carbon, Inorganic Carbon and Biomass Composition

For total carbon and inorganic carbon analysis 0.5 ml biosuspension sample were mixed with 50 μ l of 5 M KOH to prevent loss of dissolved carbonate. The suspension was then diluted 1:20 with demineralized water and stored at 4 °C until analysis. Analysis was performed with a multi N/C 2100 S composition analyzer (Analytik Jena, Jena, Germany) to yield the total concentration of carbon and inorganic carbon in the fermenter effluent stream. At the end of the cultivation feed samples were taken and processed identically.

To determine biomass composition 1.0 ml of biosuspension was centrifuged at 4 °C and 14000 rpm (20817 g) for 3 min. The supernatant was discarded, the pellet resuspended in 1.0 ml of freshly prepared 0.9% NaCl solution and centrifuged again. The pellet was resuspended in 5 ml 0.9% NaCl, flash frozen in liquid nitrogen and stored at -70 °C until analysis. Analysis was performed with a multi N/C 2100 S composition analyzer (Analytik Jena, Jena, Germany) and the carbon content of the biomass calculated from these values.

Measurement of ppGpp

2 ml of biosuspension was sampled directly into 0.5 ml of precooled (< -20°C) quenching solution and incubated at 6 °C on a shaker for 15 min. Quenching solution consisted of 80 μ M EDTA dissolved in 35% (V/V) perchloric acid. 500 μ l 1M K₂HPO₄ was added and the sample briefly vortexed. 550 μ l 5 M KOH was added and the sample vortexed again. To remove precipitating potassium perchlorate samples were then centrifuged at 4 °C and 7830 rpm (7197 g) for 5 min. 1.5 ml of supernatant was carefully transferred to new tubes, flash frozen in liquid nitrogen and stored at -70 °C. Prior to analysis samples were thawed and their pH adjusted to 6.95 – 7.05 with 5 M KOH or 35% (V/V) perchloric acid. Samples were centrifuged again to remove all potassium perchlorate precipitate. HPLC analysis was carried out as described previously (Löffler et al., 2016). If necessary, quantification was conducted by ppGpp standard addition (TriLink, California, USA). Samples from one time-point were analyzed directly in sequence and the data normalized to the sample drawn from the STR to eliminate differences caused by column aging.

Transcriptome Analysis

0.5 ml broth was sampled from the bioreactor and directly flash-frozen in liquid nitrogen. Frozen broth was then stored at -70 °C until the day of RNA isolation. Total RNA was isolated using RNeasy Mini Kit (Qiagen, Germany) according to the manufacturer's instructions. Isolated RNA was DNase treated and shipped to commercial sequencing partner GENEWIZ® on dry ice. Samples were treated for rRNA depletion, sequencing libraries prepared and Illumina HiSeq 2x150 bp sequencing performed. Raw FASTQ files were obtained for bioinformatic analysis. Trimmomatic v. 0.32 (Bolger et al., 2014) was used to remove adapters and low-quality reads (<Q20) checked by fastqc reports. Genes were aligned to the NCBI *E. coli* K-12 MG1655 reference genome (RefSeq: NC_000913.3) using the RNA-sequencing aligner Bowtie2 v. 2.3.2.2 (Langmead and Salzberg, 2012). On average the mapping of the reads covered 96.2%. Aligned reads were counted for each gene based on the corresponding annotation available from the NCBI database for the chosen reference sequence applying HTseq-count v. 0.6.1 in the union mode (Anders et al., 2015). On average 86.4% of the sequenced reads could be assigned uniquely to annotated features. Sequencing depth was around 27 million reads per sample on average with a mean quality phred score of 37.63.

Differential gene expression analysis was performed with the R-package DESeq2 v. 1.26.0 (Love et al., 2014) available from Bioconductor (Gentleman et al., 2004). Prior to statistical analysis, all residual non-protein encoding RNA molecules (tRNA, rRNA and sRNA) were removed from the HTseq-derived raw count data and a non-specific filter was applied to remove low coverage genes with fewer than two counts per million (54 reads on average). All filtering steps caused deviations from the raw data of less than 6 %. Samples were grouped by replicates and an experimental design was chosen that used sample time and location (STR or PFR port 5) as a combined environmental factor. To normalize read counts for the comparison of sequencing depth and RNA composition, DESeq2 uses the median of ratios method to derive a scaling factor. Dividing the original read counts by the scaling factor generated normalized count values. No outliers were observed in the two biological replicates using pearson correlation. Resulting p-values were adjusted for multiple testing according to control the false discovery rate (FDR) (Benjamini and Hochberg, 1995). Genes were identified as significantly differentially expressed by applying FDR adjusted p-values < 0.01 and a log₂ fold change ≥ |1|.

A principal component analysis was used to display the sample-to-sample distances calculated within the DESeq2 package (negative binomial distribution model). Principal component

analysis was performed using `plotPCA.san` available on Github (<https://gist.github.com/sansense/3399064897f1252d31b23ea5178c033c>).

Gene set enrichment and overrepresentation analysis of up- and downregulated genes were performed using Bioconductors' R-package GAGE v. 2.36.0 (Luo et al., 2009). GAGE tests whether the mean fold-change of a gene subset is significantly different from the background using a two-tailed t-test. Genes were selected as significantly different with an FDR adjusted p -value < 0.01 (Benjamini and Hochberg, 1995). Functional annotations were derived from the Cluster of Orthologous Groups (COG) database (Tatusov et al., 2003), the experimental sigma factor-gene interaction dataset from RegulonDB v. 10.6.3 (Santos-Zavaleta et al., 2019) and the Gene Ontology (GO) Groups database with the function `go.gsets` from GAGE (Luo et al., 2009). Furthermore, Venn diagrams were used to identify significant genes shared by both strains and differences in gene expression regulation (Chen and Boutros, 2011).

The RNA sequencing data derived from periodic ammonia starvation experiments have been deposited in NCBI's Gene Expression Omnibus (GEO) and are accessible through GEO series accession number GSE158198 (Edgar et al., 2002). Raw counts and processed data can be found in the Supplementary information. Data analysis was performed using the free statistical computing environment R v. 3.6.2.

4.1.6 Acknowledgements

The authors would like to thank the group of Computational Biology at the Institute of Biochemical Engineering for the use of the Galaxy-Server.

4.2 Engineering of a robust *Escherichia coli* chassis and exploitation for large-scale production processes

The manuscript was penned by Martin Ziegler. Martin Ziegler is the first author. Prof. Dr.-Ing. Ralf Takors contributed to the manuscript's content by selected additions and reviewed it. Prof. Dr.-Ing. Ralf Takors is the corresponding author.

Martin Ziegler planned the genomic alterations in this study and partially conducted them. Clarissa Döring contributed to establishing the recombineering method used in the laboratory supervised by Martin Ziegler. Clarissa Döring and Liv Paul contributed to the generation of recombinant strains supervised by Martin Ziegler. Martin Ziegler planned and conducted all shaking flask and fermentation experiments in this study. Christoph Schaal conducted the transcriptional measurements. Martin Ziegler collected and analyzed the primary experimental data. Julia Zieringer prepared the genomic sequencing data and content analysis was conducted by Martin Ziegler. Prof. Dr.-Ing. Ralf Takors supervised the research.

This manuscript has been accepted and published in *Metabolic Engineering*:

Ziegler, M., Zieringer, J., Döring, C.-L., Paul, L., Schaal, C., Takors, R., 2021. Engineering of a robust *Escherichia coli* chassis and exploitation for large-scale production processes. *Metab. Eng.* <https://doi.org/10.1016/j.ymben.2021.05.011>.

4.2.1 Abstract

In large-scale bioprocesses microbes are exposed to heterogeneous substrate availability reducing the overall process performance. A series of deletion strains was constructed from *E. coli* MG1655 aiming for a robust phenotype in heterogeneous fermentations with transient starvation. Deletion targets were hand-picked based on a list of genes derived from previous large-scale simulation runs. Each gene deletion was conducted on the premise of strict neutrality towards growth parameters in glucose minimal medium. The final strain of the series, named *E. coli* RM214, was cultivated continuously in an STR-PFR (stirred tank reactor – plug flow reactor) scale-down reactor. The scale-down reactor system simulated repeated passages through a glucose starvation zone. When exposed to nutrient gradients, *E. coli* RM214 had a significantly lower maintenance coefficient than *E. coli* MG1655 ($\Delta m_s = 0.038 \text{ g}_{\text{Glucose}}/\text{g}_{\text{CDW}}/\text{h}$, $p < 0.05$). In an exemplary protein production scenario *E. coli* RM214 remained significantly more productive than *E. coli* MG1655 reaching 44% higher eGFP yield after 28 h of STR-PFR cultivation. This study developed *E. coli* RM214 as a robust chassis strain and demonstrated the feasibility of engineering microbial hosts for large-scale applications.

4.2.2 Introduction

Large-scale fed-batch bioprocesses often suffer from reduced process performance compared to lab-scale experiments conducted during process development (Bylund et al., 2000; Enfors et al., 2001). The physical and engineering constraints in large-scale reactors inevitably lead to the formation of spatial heterogeneities of relevant process parameters such as nutrient availability, concentrations of dissolved oxygen, carbon dioxide, and pH (Bylund et al., 1998; Cortés et al., 2016). Heterogeneities of nutrient availability are caused by long mixing times of large-scale reactors (Delvigne et al., 2006; Noorman, 2011). Studies employing computational fluid dynamics (CFD) have revealed that in fed-batch processes this typically results in the formation of zones with high nutrient concentrations close to the feeding point and zones depleted of nutrients at the far end of the reactor (Haringa et al., 2017; Kuschel and Takors, 2020). Depending on the mixing time and their position in the reactor cells frequently move through different zones on a timescale of seconds to minutes and cellular regulatory programs ranging from overflow metabolism to starvation responses are repeatedly triggered and shut down (Kuschel et al., 2017). Due to the delay of transcriptional responses, regulatory consequences of stress stimuli may be effective distant from the spot of stress induction which finally creates a heterogeneous population status (Nieß et al., 2017; Zieringer et al., 2020). There is evidence from an increasing number of studies that the performance of many industrial workhorse organisms such as *Escherichia coli*, *Bacillus subtilis*, *Corynebacterium glutamicum*, *Saccharomyces cerevisiae* and *Penicillium chrysogenum* is negatively affected when facing process heterogeneities (George et al., 1993; Jonge et al., 2011; Junne et al., 2011; Larsson and Enfors, 1988; Olughu et al., 2020; Vasilakou et al., 2020).

Substantial effort has been made by the scientific community to understand microbial responses to the different zones occurring in large-scale reactors (Lara et al., 2006a; Lara et al., 2006b; Löffler et al., 2016; Olughu et al., 2019). In academic laboratories, the conditions of industrial reactors are commonly simulated using multi-compartment scale-down reactors (Delvigne et al., 2017; Neubauer and Junne, 2010; Takors, 2012). Typically, nutrient pulsing or secondary vessels are employed to deliver a stimulus representative for the conditions under investigation (Bylund et al., 1999). The design of a scale-down reactor also serves to control the circulation of the microbial population and its residence time in stimulus zones. A commonly used design follows the two-compartment approach comprising a primary stirred tank reactor (STR) coupled to a secondary plug-flow reactor (PFR). While the STR represents the bulk of the

fermentation broth, the plug-flow compartment represents a stimulus zone with a defined residence time. Together, the STR-PFR two-compartment reactor enables the study of cellular behavior in heterogeneous environments.

Zones with low nutrient concentration but high oxygen availability occur in reactor segments far away from the feeding point. The effects of such transient starvation conditions on the performance and intracellular regulation of microbial populations can be studied in C-limited scale-down reactors. In the case of *Escherichia coli* K-12 repeated passages of cells through starvation zones were found to negatively impact process performance which could be observed as a reduced biomass yield (Neubauer et al., 1995b). In parallel, regulatory responses such as the stringent response and the general stress response are rapidly initiated (Delvigne et al., 2009; Löffler et al., 2016; Neubauer et al., 1995a; Simen et al., 2017; Sunya et al., 2012b). Noteworthy, these cellular responses serve rather long-term than short-term needs and appear to be futile if cells enter zones of nutrient access shortly after the induction of the strategic precaution measure. Transcriptional investigations in a carbon-limited STR-PFR system offered a potential link between futile regulation and reduced process performance: Frequent transcriptional reprogramming was proposed to cause high secondary metabolic costs from aberrant transcription and translation (Löffler et al., 2016). It was estimated that an increased maintenance of up to 30 – 40% was caused by the transcriptional oscillations and a substantial fraction of this originated from the expression of open reading frames whose products appeared to bestow no apparent benefit in a controlled bioprocess employing standard glucose minimal medium.

The data collected by Löffler et al. (2016) led us to propose a novel design approach for production strains: We reasoned that an intelligently engineered deletion strain might have advantages in conditions that repeatedly induce wasteful expression of process-irrelevant genes. A heterogeneous fermentation with repeated transient starvation could then be a suitable testing environment. The choice of deletion targets would have to be based on the estimated effect of the deletion and be restricted by the requirements of neutrality towards growth and global regulation. The design process differs from previous considerations on the creation of lean-proteome strains in the regard that savings only become apparent due to fluctuating induction (Valgepea et al., 2015). Secondary metabolic costs can traditionally be assessed through Pirt's maintenance coefficient (Pirt, 1965). We hypothesized that the deletion of a suitable set of genes should lead to a reduced maintenance coefficient under scale-down

conditions representing starvation zones. The resulting strain could then serve as a base strain for the construction of robust production strains.

We identified deletion candidates matching the defined criteria and constructed a series of deletion strains from *E. coli* MG1655. The final strain of the series, named *E. coli* RM214, was fermented in continuous cultivations in an STR-PFR system simulating starvation zones. *E. coli* RM214 had a significantly lower maintenance coefficient than *E. coli* MG1655 under simulated large-scale conditions. We then characterized *E. coli* RM214 in an exemplary protein production scenario using eGFP as a model product. Compared to *E. coli* MG1655, the deletion strain showed an increased resilience towards the scale-down conditions as evidenced by reduced productivity losses and a higher fraction of producing cells.

4.2.3 Materials and methods

Bacterial Strains, Media, and Buffer Solutions

All strains used in this study are listed in **Table 4**.

2xYT medium was prepared by autoclaving 16 g/l tryptone, 10 g/l yeast extract, 5 g/l NaCl dissolved in demineralized water. For agar plates 18 g/l agar-agar was added prior to autoclavation. For pH indicator plates 0.03 g/l of neutral red and 10 g/l Rhamnose were supplemented from sterile stock solutions directly before pouring. SOC medium was prepared as described previously (Hanahan, 1983). Agar plates for *tetA-sacB* counterselection were prepared as described previously (Li et al., 2013). If strains with antibiotic resistance markers were cultivated, antibiotics were added to media after autoclavation in the following concentrations: Chloramphenicol 20 µg/ml, Tetracycline hydrochloride 10 µg/ml, disodium Carbenicillin 100 µg/ml.

Minimal media for shaking flask experiments and the precultures for bioreactor experiments consisted of 4 g/l glucose, 3.2 g/l NaH₂PO₄·2H₂O, 11.7 g/l K₂HPO₄, 8 g/l (NH₄)₂SO₄, 0.01 g/l thiamine hydrochloride and 0.2 % (V/V) trace elements stock solution. Minimal media for batch cultivation in the bioreactor consisted of 13.4 g/l glucose, 1 g/l NaH₂PO₄·2H₂O, 2.6 g/l K₂HPO₄, 9 g/l (NH₄)₂SO₄ and 0.2 % (V/V) trace elements stock solution. In the experiments with strains carrying pJOE4056.2_ *tetA* for GFP production 10 µg/ml Tetracycline hydrochloride and 1 g/l Rhamnose were supplemented. Towards the end of the batch phase about 100 µl of antifoaming agent Struktol J647 was added to prevent foaming upon glucose depletion. Minimal media for continuous chemostat cultivation in the bioreactor consisted of 13.14 g/l glucose, 1 g/l NaH₂PO₄·2H₂O, 2.6 g/l K₂HPO₄, 9 g/l (NH₄)₂SO₄ and 0.2 % (V/V) trace elements stock solution. In the experiments with strains carrying pJOE4056.2_ *tetA* for GFP production 10 µg/ml Tetracycline hydrochloride and 1 g/l Rhamnose were supplemented. Throughout the chemostat phase 50 µl/h of antifoaming agent Struktol J647 were added continuously to the fermentation medium.

The composition of trace element stock solution was 4.175 g/l FeCl₃·6H₂O, 0.045 g/l ZnSO₄·7H₂O, 0.025 g/l MnSO₄·H₂O, 0.4 g/l CuSO₄·5H₂O, 0.045 g/l CoCl₂·6H₂O, 2.2 g/l CaCl₂·2H₂O, 50 g/l MgSO₄·7H₂O and 55 g/l sodium citrate dihydrate. Stock solutions of salts, trace elements, and sugars were autoclaved separately, and stock solutions of thiamine

hydrochloride and the antibiotics were filter sterilized and stored at 4°C. All compounds were combined just before the experiments to prevent potential aging of media.

PBS-MgCa for the measurement of eGFP fluorescence and flow cytometry analysis contained 8 g/l NaCl, 0.2 g/l KCl, 1.44 g/l Na₂HPO₄, 0.24 g/l KH₂PO₄, 1 mM MgSO₄ and 0.1 mM CaCl₂. Prior to use PBS-MgCa was filtered with a sterile filter (pore size < 0.2 µm) to reduce particle load (Tomasek et al., 2018).

Table 4: Bacterial strains used in this study.

Strain	Genotype/Strain Information	Reference/Source
<i>Escherichia coli</i> K-12 MG1655	F ⁻ , λ ⁻ , <i>ilvG</i> ⁻ , <i>rfb</i> -50, <i>rph</i> -1 ("wild type" strain, abbrev. WT)	(Michalowski et al., 2017)
<i>Escherichia coli</i> DH5α <i>λpir</i>	<i>supE44</i> , Δ <i>lacU169</i> (Φ80 <i>lacZ</i> ΔM15), <i>recA1</i> , <i>endA1</i> , <i>hsdR17</i> , <i>thi</i> -1, <i>gyrA96</i> , <i>relA1</i> , <i>λpir</i> phage lysogen	(Michalowski et al., 2017)
<i>Escherichia coli</i> DH10B pSIM5	F ⁻ <i>mcrA</i> Δ(<i>mrr</i> - <i>hsdRMS</i> - <i>mcrBC</i>) φ80 <i>lacZ</i> ΔM15 Δ <i>lacX74</i> <i>recA1</i> <i>endA1</i> <i>araD139</i> Δ(<i>ara-leu</i>)7697 <i>galU</i> <i>galK</i> λ ⁻ <i>rpsL</i> (Str ^R) <i>nupG</i>	(Datta et al., 2006)
<i>T-SACK</i>	W3110 <i>araD</i> ◊ <i>tetA-sacB-amp</i> <i>fliC</i> ◊ <i>cat</i> <i>argG::Tn5</i>	(Li et al., 2013)
<i>Escherichia coli</i> CD101	MG1655 Δ <i>flk</i>	This study
<i>Escherichia coli</i> CD201	MG1655 Δ <i>flk</i> Δ <i>fliA</i>	This study
<i>Escherichia coli</i> CD202	MG1655 Δ <i>flk</i> Δ <i>fliA</i> Δ <i>fliC</i>	This study
<i>Escherichia coli</i> CD203	MG1655 Δ <i>flk</i> Δ <i>fliA</i> Δ <i>fliC</i> Δ <i>flgNMABCDEFGHIJKL</i>	This study
<i>Escherichia coli</i> CD204	MG1655 Δ <i>flk</i> Δ <i>fliA</i> Δ <i>fliC</i> Δ <i>flgNMABCDEFGHIJKL</i> Δ <i>fliEFGHIJKLMNOPQR</i>	This study
<i>Escherichia coli</i> CD205	MG1655 Δ <i>flk</i> Δ <i>fliA</i> Δ <i>fliC</i> Δ <i>flgNMABCDEFGHIJKL</i> Δ <i>fliEFGHIJKLMNOPQR</i> Δ <i>flhEABcheZYBRtaptarcheWAmotBA</i>	This study

4. Publications

Strain	Genotype/Strain Information	Reference/Source
<i>Escherichia coli</i> RM206	MG1655 $\Delta flk \Delta fliA \Delta fliC$ $\Delta flgNMABCDEFGHIJKL$ $\Delta fliEFGHIJKLMNOPQR$ $\Delta flhEABcheZYBRtaptarcheWAmotBA$ $\Delta cspD$	This study
<i>Escherichia coli</i> RM207	MG1655 $\Delta flk \Delta fliA \Delta fliC$ $\Delta flgNMABCDEFGHIJKL$ $\Delta fliEFGHIJKLMNOPQR$ $\Delta flhEABcheZYBRtaptarcheWAmotBA$ $\Delta cspD \Delta alda$	This study
<i>Escherichia coli</i> RM208	MG1655 $\Delta flk \Delta fliA \Delta fliC$ $\Delta flgNMABCDEFGHIJKL$ $\Delta fliEFGHIJKLMNOPQR$ $\Delta flhEABcheZYBRtaptarcheWAmotBA$ $\Delta cspD \Delta alda \Delta gatABCDR$	This study
<i>Escherichia coli</i> RM209	MG1655 $\Delta flk \Delta fliA \Delta fliC$ $\Delta flgNMABCDEFGHIJKL$ $\Delta fliEFGHIJKLMNOPQR$ $\Delta flhEABcheZYBRtaptarcheWAmotBA$ $\Delta cspD \Delta alda \Delta gatABCDR \Delta uhpTCBA$	This study
<i>Escherichia coli</i> RM210	MG1655 $\Delta flk \Delta fliA \Delta fliC$ $\Delta flgNMABCDEFGHIJKL$ $\Delta fliEFGHIJKLMNOPQR$ $\Delta flhEABcheZYBRtaptarcheWAmotBA$ $\Delta cspD \Delta alda \Delta gatABCDR \Delta uhpTCBA$ $\Delta yeeL$	This study
<i>Escherichia coli</i> RM214	MG1655 $\Delta flk \Delta fliA \Delta fliC$ $\Delta flgNMABCDEFGHIJKL$ $\Delta fliEFGHIJKLMNOPQR$ $\Delta flhEABcheZYBRtaptarcheWAmotBA$ $\Delta cspD \Delta alda \Delta gatABCDR \Delta uhpTCBA$ $\Delta yeeL \Delta flxA$	This study
<i>Escherichia coli</i> BW3110 pJOE4056.2	W3110 $rhaB^-$	(Wegerer et al., 2008)
<i>Escherichia coli</i> DH5 α λ pir pJOE4056.2_tetA	$supE44$, $\Delta lacU169$ ($\Phi 80lacZ\Delta M15$), $recA1$, $endA1$, $hsdR17$, $thi-1$, $gyrA96$, $relA1$, λ pir phage lysogen	This study
<i>Escherichia coli</i> K-12 MG1655 $rhaB^-$	F^- , λ^- , $ilvG^-$, $rfb-50$, $rph-1$, $rhaB^-$	This study

4. Publications

Strain	Genotype/Strain Information	Reference/Source
<i>Escherichia coli</i> RM214 rhaB ⁻	MG1655 $\Delta flk \Delta fliA \Delta fliC$ $\Delta flgNMABCDEFGHIJKL$ $\Delta fliEFGHIJKLMNOPQR$ $\Delta flhEABcheZYBRtaptarcheWAmotBA$ $\Delta cspD \Delta aldA \Delta gatABCDR \Delta uhpT \Delta yeeL$ $\Delta flxA rhaB^-$	This study
<i>Escherichia coli</i> K-12 MG1655 rhaB ⁻ pJOE4056.2_tetA	F ⁻ , λ^- , <i>ilvG</i> ⁻ , <i>rfb</i> -50, <i>rph</i> -1, <i>rhaB</i> ⁻	This study
<i>Escherichia coli</i> RM214 rhaB ⁻ pJOE4056.2_tetA	MG1655 $\Delta flk \Delta fliA \Delta fliC$ $\Delta flgNMABCDEFGHIJKL$ $\Delta fliEFGHIJKLMNOPQR$ $\Delta flhEABcheZYBRtaptarcheWAmotBA$ $\Delta cspD \Delta aldA \Delta gatABCDR \Delta uhpT \Delta yeeL$ $\Delta flxA rhaB^-$	This study

Construction of Deletion Strains

Chromosomal modifications were conducted using recombineering methods that have been comprehensively described and reviewed previously (Murphy, 2016). The *tetA-sacB* cassette and lambda recombineering functions provided by pSIM5 were used to perform chromosomal modifications with base-pair precision (Datta et al., 2006; Li et al., 2013). Deletions of single genes were designed to span the coding sequence only and deletions of operons or larger genomic regions were designed to begin with the coding sequence of the first gene and end with the coding sequence of the final gene. All deletions were verified by sequencing. **Table S1** contains an annotated list of primers used in this study and **Supplementary Information S2** a more detailed description of the recombineering method used.

Construction of GFP production strains

The protein expression system used for the bioreactor fermentations closely resembles previously described systems based on pJOE4056.2 (Wegerer et al., 2008; Wilms et al., 2001). For additional stability, the *bla* resistance cassette from plasmid pJOE4056.2 was exchanged for a *tetA* resistance cassette yielding pJOE4056.2_tetA to enable continuous selective pressure under the conditions of a chemostat. Use of pJOE4056.2_tetA requires induction with the rare sugar rhamnose at low glucose concentrations. Prior to plasmid transformation, we thus

inactivated the chromosomal copy of *rhaB* encoding rhamnulokinase in *E. coli* MG1655 and *E. coli* RM214 to yield *rhaB*⁻ strains incapable of utilizing the rare sugar rhamnose. **Supplementary Information S2** contains a more detailed description of the procedure.

Shaking Flask Cultivations

For growth experiments glycerol stock cultures were streaked on 2xTY agar plates and incubated overnight at 37 °C. For precultures, a single colony was picked to inoculate 15 ml minimal medium in a 50 ml baffled shaking flask and incubated at 37 °C on an orbital shaker set to 130 rpm overnight. On the following morning, an inoculum of the preculture was transferred into 50 ml minimal medium in a 500 ml baffled shaking flask to reach a starting OD of 0.2 and the culture incubated at 37 °C on an orbital shaker set to 130 rpm. Samples were drawn hourly using a fixed needle reaching through the attached cotton plug and a syringe. In all shaking flask experiments the wild type strain *E. coli* MG1655 was cultivated in parallel as a reference and data collected from other strains was normalized to this reference data.

Bioreactor Setup

Bioreactor fermentations were carried out in a two-compartment scale-down reactor. The primary reactor was a stirred tank reactor, and a plug flow reactor was used as the secondary compartment mimicking a starvation zone. The plug flow reactor was connected to the stirred tank reactor only after establishment and sampling of a steady state in the chemostat phase. The technical setup has been characterized previously and includes the modifications described by Ankenbauer *et al.* (Ankenbauer *et al.*, 2020; Löffler *et al.*, 2016). A schematic overview of the two-compartment reactor is shown in **Fig. 12** and **Supplementary Information S2** contains a comprehensive description of the setup.

Preculture, Batch Cultivation and Continuous Cultivation

100 µl of glycerol stock seed culture were directly used to inoculate 300 ml of preculture minimal medium in a 3 l baffled shaking flasks and incubated at 37 °C on an orbital shaker set to 130 rpm overnight. The next morning 160 ml of preculture were used to inoculate the bioreactor complementing the total volume in the bioreactor to 1.6 l fermentation broth. Batch fermentation in the bioreactor ensued at 37 °C. Upon depletion of glucose, indicated by a sharp increase in dissolved oxygen tension, feed and harvest lines were connected. The reactor was refilled with feed medium to 1.6 l broth and a constant feed/harvest rate was established. For GFP production experiments with strains carrying pJOE4056.2_tetA the feed rate was set to

5.33 ml/min corresponding to a dilution rate of 0.2 h⁻¹. For bioreactor cultivations aimed at investigating genomic stability and determining the maintenance coefficient of *E. coli* MG1655 and *E. coli* RM214 the batch phase was shortened, and feed rates were set to 8.00 ml/min, 5.33 ml/min, 2.67 ml/min or 1.33 ml/min corresponding to dilution rates of 0.3 h⁻¹, 0.2 h⁻¹, 0.1 h⁻¹ or 0.05 h⁻¹. After cultivation for at least five volumetric residence times a reference sample was taken. Then, the plug-flow reactor was connected to the primary reactor via a diaphragm metering pump effectively circulating about one-quarter (380 ml) of the total fermentation broth from the primary reactor through the plug-flow reactor and back into the stirred tank reactor. In the following five to six volumetric residence times samples were taken at predefined time points from the STR and the five PFR ports. Afterwards the fermentation was aborted, and the actual final broth volume measured. This value was used for all volumetric calculations during data analysis.

Determination of Optical Density and Biomass dry weight

Optical density of fermentation broth appropriately diluted with 0.9% NaCl from the primary reactor was measured in triplicates at 600 nm on a spectrophotometer (Amersham Biosciences/GE Healthcare, Amersham, United Kingdom). For measurement of biomass dry weight quadruplicates of 5 ml broth were centrifuged in weighted glass tubes at 2500 g and 4 °C for 7.5 min. Supernatant was immediately decanted and the pellet washed by resuspending in 5 ml of freshly prepared 150 mM NH₄HCO₃ held at 4°C. The suspension was centrifuged again, and the washing repeated once. After a final centrifugation, the remaining liquid was decanted carefully, the pellet dried at 105 °C and glass tubes containing dried pellets were weighted again.

Determination of Acetic acid, Ammonium and Glucose concentrations in fermentation supernatant and feed

5 ml of biosuspension was directly sampled into a syringe connected to a single-use 0.45 µm sterile filter and immediately filtered. The clear supernatant was flash frozen in liquid nitrogen and stored at -70 °C until analysis. Glucose concentration was determined by D-Glucose UV-Test Kit (R-Biopharm, Darmstadt, Germany) and acetic acid concentration by Acetic acid UV-Test Kit (R-Biopharm, Darmstadt, Germany). Ammonium concentration was determined by Ammonium cuvette test LCK 303 or LCK 304 (Hach Lange, Düsseldorf, Germany). At the end of the cultivation feed samples were taken directly from the feed line, flash frozen in liquid nitrogen and processed as described.

Analysis of Total Carbon, Inorganic Carbon and Biomass Composition

For total carbon and inorganic carbon analysis 0.5 ml biosuspension sample were mixed with 50 µl of 5 M KOH to prevent loss of dissolved carbonate. Then, the suspension was diluted 1:20 with demineralized water, flash frozen in liquid nitrogen, and stored at -70 °C until analysis. Analysis was performed with a multi N/C 2100 S composition analyzer (Analytik Jena, Jena, Germany) to yield the total concentration of carbon and inorganic carbon in the fermenter effluent stream.

To determine biomass composition 1.0 ml of biosuspension was centrifuged at 4 °C and 14000 rpm (20817 g) for 3 min. The supernatant was discarded, the pellet resuspended in 1.0 ml of 0.9% NaCl solution and centrifuged again. The pellet was resuspended in 5 ml 0.9% NaCl, flash frozen in liquid nitrogen and stored at -70 °C until analysis. Analysis was performed with a multi N/C 2100 S composition analyzer (Analytik Jena, Jena, Germany) and the carbon and nitrogen content of the biomass calculated from these values.

Measurement of Nucleotides

2 ml of biosuspension was sampled directly into 0.5 ml of precooled (< -20°C) quenching solution and incubated at 6 °C on a shaker for 15 min. Quenching solution consisted of 80 µM EDTA dissolved in 35% (V/V) perchloric acid. 500 µl 1 M K₂HPO₄ was added, and the sample was briefly vortexed. 550 µl 5 M KOH was added and the sample was vortexed again. To remove precipitating potassium perchlorate samples were then centrifuged at 4 °C and 7830 rpm (7197 g) for 5 min. 1.5 ml of supernatant was carefully transferred to new tubes, flash frozen in liquid nitrogen, and stored at -70 °C. Prior to analysis samples were thawed and centrifuged for 10 min at 4°C and 7197 g. 1 ml of supernatant was transferred to new tubes and their pH adjusted to 6.95 – 7.05 with 5 M KOH or 35% (V/V) perchloric acid. Samples were centrifuged again for 30 min at 4°C at 18000 g to remove potassium perchlorate precipitate from neutralization. 500 µl of supernatant were then transferred into RotiSpin Mini 3 kDa MWCO tubes and centrifuged again for 30 min at 4°C at 18000 g. HPLC analysis was carried out as described previously (Löffler et al., 2016).

Measurement of eGFP Fluorescence

Freshly sampled biosuspension was flash-frozen in liquid nitrogen and stored at -70°C until analysis. On the day of analysis all samples were thawed and diluted 1:100 with ice-cold PBS-MgCa. 200 µl of diluted sample were transferred into a black 96 well-plate with

transparent bottom and lid and the fluorescence (excitation 485 nm, emission 535 nm) was quantified in a SLT SpectraFluor plate-reader (Tecan, Switzerland). Then, the measured fluorescence values were converted into absolute eGFP concentrations using a calibration curve recorded with purified protein (see **Supplementary Information S2**).

Flow Cytometry Analysis

Freshly sampled biosuspension was diluted with PBS-MgCa to yield an OD of approximately 0.04. Diluted biosuspension was passed through a 30 µM CellTrics® filter to reduce particle content and analyzed in a BD Accuri™ C6 Plus Flow Cytometer. The excitation laser had a wavelength of 488 nm and a 533/30 nm emission filter was used to capture GFP fluorescence. Particle signals with a forward scatter height (FSC-H) signal less than 2500 were ignored and 250000 events collected. Events with an eGFP area signal less than 10 were excluded from the analysis to remove dust and cell debris, usually resulting in 235000 – 249000 remaining events. Cells from events with an eGFP area less than 2000 were defined to form the non-producing population, while cells from events with an eGFP area equal or greater than 2000 were defined to form the producing population. Histograms of all samples can be found in **Supplementary Figure S3**.

Genomic DNA Sequencing

1 ml of biosuspension was sampled, flash-frozen in liquid nitrogen and stored at -70 °C. On the day of extraction samples were thawed and total DNA extracted with DNeasy Blood and Tissue Kit (Qiagen). Isolated DNA was shipped to and sequenced by the commercial sequencing partner Eurofins Genomics resulting in approximately 5 to 6 million paired end reads (150 bp) per sample. Data was delivered as fastqc files and assembly of the reads conducted with Unicycler 0.4.8 with the following settings: min contig length 300 bp, min contig coverage 5 (Wick et al., 2017). The obtained contigs were processed with Mauve version 20150226 build 10 using the reference sequence NC_0000913.3 from the NCBI database (Darling et al., 2004). Finally, small nucleotide polymorphisms were detected using snippy (<https://github.com/tseemann/snippy>) and the output manually examined using Geneious Prime 2020.2.3 (<https://www.geneious.com>). **Supplementary Data S9** contains lists of all SNPs found.

RT-qPCR

1.5 ml of freshly drawn biosuspension were immediately flash frozen in liquid nitrogen and stored at $-70\text{ }^{\circ}\text{C}$. Frozen liquid cell suspensions were thawed on ice and 200 μl each were transferred into bead bashing tubes prefilled with 700 μl Lysis buffer. Cells were disrupted with a *Precellys® homogenisator* for 2 x 20 s. RNA was extracted using the *Quick-RNA Fungal/Bacterial Kit* (Zymo Research) following the manufacturer's instructions. The RNA concentrations were measured by Nanodrop. 10 μg RNA each was treated with 2 units *TURBO DNase* (Thermo Fisher Scientific) in 50 μl reactions for 60 min, with additional 2 units enzyme after 20 and 40 min, respectively. RNA from the DNase reactions were purified with *Zymo Clean & Concentrator™-5* (Zymo Research) according to the manufacturer's protocol and were then measured by Nanodrop. cDNA synthesis with *SuperScript® IV reverse transcriptase* (Invitrogen) was carried out according to the protocol for random hexamers as primers. 1 μg RNA was used as starting input for 20 μl reactions, but no RNase inhibitor was added. A no reverse transcriptase control was included. For the qPCR reactions, the cDNA reaction mixes were diluted with 100 μl nuclease free water. 2 μl from all cDNA reactions were pooled together and a dilution series was prepared (1, 1:10, 1:100, 1:1000) for determination of PCR efficiency for each primer pair during each PCR run. For 15 μl reactions 7.5 μl *ORA™ qPCR Green ROX L Mix* (highQu), 0.4 μl forward primer, 0.4 μl reverse primer (f.c. 266 nM, each), 4.7 μl H₂O and 2 μl of diluted cDNA reactions were mixed. *eGFP* was amplified using primers eGFP2-forward and eGFP2-reverse (amplicon length: 248 bp), for *cysG* primers *cysG_housekeeping_fwd* and *cysG_housekeeping_reverse* (amplicon length: 197 bp) were used. All reactions were performed as triplicates. Reactions were carried out on a *Biorad CFX96* in 96 well plates. Program parameters were 95 $^{\circ}\text{C}$, 3 min; 39x (95 $^{\circ}\text{C}$, 5 sec; 59 $^{\circ}\text{C}$, 15 sec; 72 $^{\circ}\text{C}$, 15 sec); 65 $^{\circ}\text{C}$ to 95 $^{\circ}\text{C}$ (0,5 $^{\circ}\text{C}$ increment). Data was analyzed with Biorad CFX Manager 3.1. Relative expression of eGFP to *cysG* was calculated from the c_q numbers measured by the instrument adjusted for amplification efficiency. Relative expressions from time points STR-PFR 25 h and STR-PFR 28 h were normalized to the corresponding STR sample.

4.2.4 Results

Engineering of *E. coli* deletion strains

Our primary goal was to engineer a series of deletion strains based on *E. coli* MG1655 with physiological advantages under heterogeneous conditions with nutrient depleted zones. Strains would ultimately be assayed in a scale-down reactor consisting of a primary stirred tank reactor (STR) and a secondary plug-flow reactor (PFR) mimicking a starvation zone (**Fig. 12**).

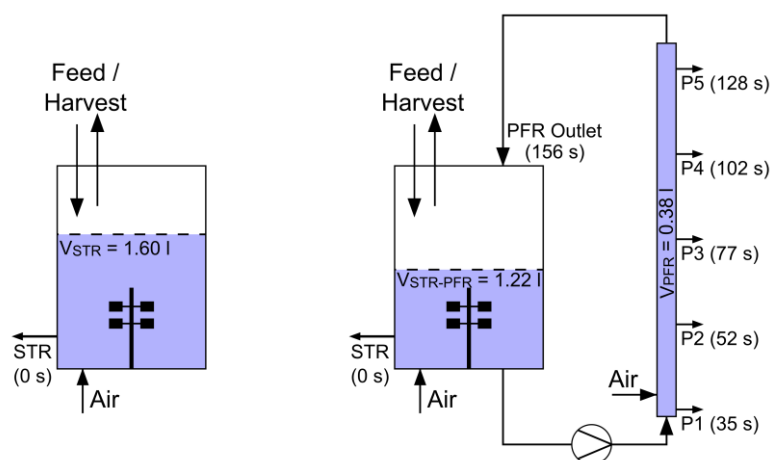


Fig. 12: Reactor Setup. The primary reactor was a standard laboratory reactor operated as a fully aerobic glucose limited chemostat at 37 °C (left scheme). For measurements of the well mixed STR reference state the entire biosuspension was in the primary reactor ($V_{STR} = 1.60$ l). Scale-down conditions were installed by connecting a secondary plug-flow reactor (PFR). An active pump then constantly circulated $V_{PFR} = 0.38$ l fermentation broth between STR and PFR reducing the volume fraction in the STR to $V_{STR-PFR} = 1.22$ l (right scheme). Labels STR and P1 to P5 designate sampling ports with the respective average residence time of biosuspension after leaving the STR. Fermentations were carried out in two phases each lasting for at least five volumetric residence times: First, a homogenous STR reference state was established, followed by a subsequent heterogeneous STR-PFR phase.

We began with defining criteria for the choice of handpicked deletion targets: First, only genes that cause relevant metabolic burden in the context of a large-scale bioprocess should be chosen. We thus based our choice of targets primarily on the list of genes with high add-on maintenance under repeated transient starvation published by Löffler et al. (2016) and selected genes with

an estimated add-on maintenance > 0.05 %. Except for *fliC* none of the chosen genes had an estimated maintenance add-on > 1 %, so we expected very little contribution of most single deletions. It was thus clear that multiple deletions would be necessary to achieve reasonably measurable effects. To maximize potential savings, we removed the entire operon if a candidate gene was part of a functionally connected operon. Second, any deletion must not be detrimental to basic growth parameters in glucose minimal medium. In the past, *E. coli* deletion strain series such as the MDS or the MGF series, had suffered from biological fitness losses (Karcagi et al., 2016; Kurokawa et al., 2016). Learning from these studies, any genes involved in primary carbon metabolism or basic cellular functions were outright excluded and we aimed for a highly selective approach with a strictly limited scope. Third, global regulatory programs must be left intact to avoid potential side effects. This included the general stress response, SOS responses and the stringent response. The stringent response had previously been identified as the major repeatedly induced regulatory program but strains with modulated ppGpp availability already exist and have dampened regulatory patterns in nutrient-limited conditions (Michalowski et al., 2017; Ziegler et al., 2021b). In this study, one of our goals was to work orthogonally to cellular regulation.

With these criteria in mind, we developed a set of planned deletions containing most parts of the flagellar apparatus, the chemotaxis systems, and multiple other handpicked genes (with add-on to maintenance > 0.05 %): *cspD*, *aldA*, *flxA*. CspD is a toxin of dispensable function, AldA is irrelevant in glucose-limited medium as its essential function is complemented by PrpC and FlxA is a protein from the Qin prophage. All of these genes are non-essential (Baba et al., 2006). Using lambda recombineering with the *tetA-sacB* cassette we sequentially engineered the strains starting from *E. coli* MG1655 until completion of the final strain *E. coli* RM214 (**Table 4**). We assayed any new deletion strain from the series for its basic growth parameters in shaking flask fermentations cultivating *E. coli* MG1655 as a benchmark in parallel. None of the deletion strains had major advantages or deficits in maximum specific growth rate or biomass yield in glucose minimal medium affirming our choice of deletion targets (**Fig. 13**). Conducting the genomic deletions required a high number of total passages until *E. coli* RM214 was completed. We sequenced both the genome of *E. coli* MG1655 and *E. coli* RM214 and identified no problematic mutations (**Supplementary Information S2, Supplementary Data S9**). As we expected little impact of single deletions, we decided to focus our characterization

only on the final strain of the series, *E. coli* RM214, and compared it to its parent wild-type strain *E. coli* MG1655.

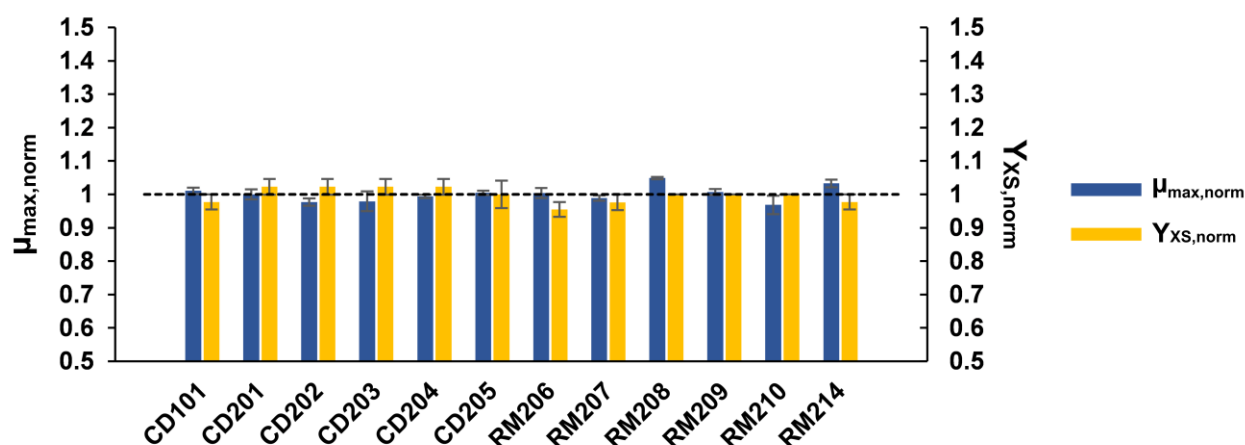


Fig. 13: Basic growth parameters of deletion strains. Deletion strains CD101 to RM214 were cultivated in minimal glucose medium in shaking flask fermentations. The maximum specific growth rate (blue) and biomass yield (yellow) were determined. The parent strain *E. coli* MG1655 was cultivated in parallel, and all data collected normalized to its growth parameters. Error bars indicate SEM ($n = 3$). The dashed line is a visual aid indicating reference values of 1.

Maintenance coefficient and genomic stability in scale-down fermentations

To test the initial hypothesis of a reduced maintenance coefficient in heterogeneous conditions and unravel potential benefits of *E. coli* RM214, we cultivated *E. coli* MG1655 and *E. coli* RM214 in two-compartment scale-down fermentations. Continuous chemostat cultivations with two phases were used to enable accurate assessment of fermentation parameters. In the first phase, strains were cultivated in standard well-mixed conditions employing only a STR (**Fig. 12**, left scheme). After five volumetric residence times this reference state was sampled and the secondary PFR compartment connected to the STR. A diaphragm metering pump then continuously circulated about one-fourth of the fermentation broth from the STR through the PFR and back into the STR. As feeding occurred only in the STR, the PFR simulated repeated passages of fractions of the population through a starvation zone (**Fig. 12**, right scheme). After continued cultivation for another five volumetric residence

times the new STR-PFR steady state was sampled. Therefore, the total process time always exceeded ten volumetric residence times.

We cultivated *E. coli* MG1655 and *E. coli* RM214 at four different dilution rates (0.05 h⁻¹, 0.1 h⁻¹, 0.2 h⁻¹, 0.3 h⁻¹) each. We measured biomass concentrations in the well mixed STR reference state and during the heterogeneous STR-PFR phase. *E. coli* RM214 had a slightly increased biomass yield on substrate, especially under STR-PFR conditions and at $D = 0.05 \text{ h}^{-1}$. We estimated Pirt's maintenance coefficient m_s of both strains by linear regression of Y_{XS}^{-1} vs D^{-1} (**Fig. 14**). We found no statistically significant differences under well mixed STR conditions, but the maintenance coefficient of *E. coli* RM214 was significantly lower than that of *E. coli* MG1655 under STR-PFR conditions ($\Delta m_s = -0.038 \text{ g}_{\text{Glucose}} * \text{g}_{\text{CDW}}^{-1} * \text{h}^{-1}$, $p < 0.05$). Differences in the true biomass yield Y_{XS}^{true} were not significant under any conditions ($p > 0.05$). The results confirm the initial hypothesis and the effectiveness of our tailored deletion strategy for the targeted environment.

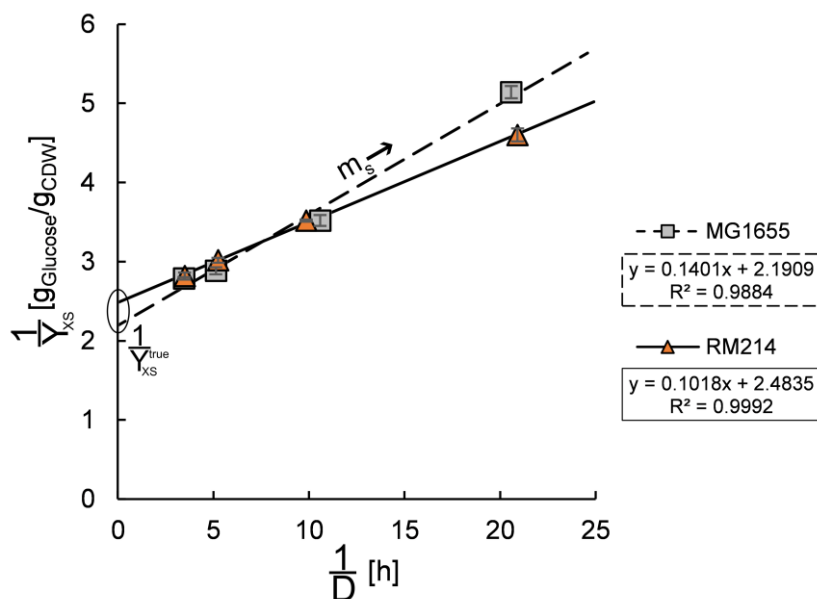


Fig. 14: Determination of maintenance coefficients under heterogeneous STR-PFR conditions. *E. coli* MG1655 (grey squares, dashed line) and *E. coli* RM214 (orange triangles, solid line) were cultivated in the STR-PFR system (glucose limited chemostats, $D = 0.05 \text{ h}^{-1}$, 0.1 h^{-1} , 0.2 h^{-1} , 0.3 h^{-1}). Maintenance coefficients m_s (slope) and true biomass yields Y_{XS}^{true} (intersection) were determined from the linear regression of data points. The difference of the maintenance coefficients is statistically significant ($\Delta m_s = -0.038 \text{ g}_{\text{Glucose}} * \text{g}_{\text{CDW}}^{-1} * \text{h}^{-1}$, $p < 0.05$). Error bars indicate technical standard deviation.

We sequenced the strains' genomes from the STR-PFR samples from all fermentations to investigate potential genomic instability that may have influenced the observations due to the long fermentation time ($> 200 \text{ h}$ at $D = 0.05 \text{ h}^{-1}$). In *E. coli* MG1655, we found SNPs in *insH5* in samples from all dilution rates but no other mutations. We also found SNPs in *insH5* in all samples from *E. coli* RM214 and additional mutations in *ycfk* and *stfE* of the inactive $\epsilon 14$ prophage (**Supplementary Data S9**). Apart from these minor alterations, the strains were remarkably stable. They showed no accumulation of mutations in any regulatory genes or genes involved in central metabolism confirming that the engineered deletions bestowed the reduced maintenance coefficient to *E. coli* RM214.

Construction of eGFP production strains

Based on these encouraging findings we hypothesized that *E. coli* RM214 should better withstand the stressful conditions of an exemplary heterogeneous production scenario including transient starvation than its ancestor strain *E. coli* MG1655. We chose to produce eGFP as an easily measurable proxy for industrially relevant intracellularly accumulated proteins such as insulin varieties or other biopharmaceuticals commonly produced in *E. coli* (Baeshen et al., 2015; Baeshen et al., 2014).

A suitable expression system to produce proteins in glucose-limited fermentations is the rhamnose-inducible expression system from pJOE4056.2 (Wegerer et al., 2008). Expression from the rhamnose promoter occurs in the presence of non-toxic rhamnose and is enhanced by low levels of glucose sensed by cAMP-CRP signaling. However, the use of rhamnose as a stable inducer requires the absence of rhamnose catabolism (Wilms et al., 2001). We therefore inactivated the chromosomal copy of *rhaB* by replacing the original gene in *E. coli* MG1655 and *E. coli* RM214 with an inactive frameshift copy from *E. coli* BW3110 by recombineering with the *tetA-sacB* cassette. The resulting strains were termed *E. coli* MG1655 *rhaB*⁻ and *E. coli* RM214 *rhaB*⁻. The absence of rhamnose catabolism was additionally confirmed by streaking the strains on 2xTY pH indicator agar plates containing Rhamnose. *E. coli* MG1655 *rhaB*⁻ and *E. coli* RM214 *rhaB*⁻ formed white colonies meaning that no acidification of the medium caused by rhamnose degradation occurred.

We then exchanged the *bla* resistance gene from pJOE4056.2 for the *tetA* resistance gene from *E. coli* T-SACK generating pJOE4056.2_ *tetA* (**Supplementary Figure S2A**). TetA is a tetracycline exporter and thus enables continuous selective pressure in the presence of tetracycline during prolonged cultivations. Transformation of the *rhaB*⁻ strains with pJOE4056.2_ *tetA* yielded *E. coli* MG1655 *rhaB*⁻ pJOE4056.2_ *tetA* and *E. coli* RM214 *rhaB*⁻ pJOE4056.2_ *tetA* (**Table 4**).

Scale-down fermentations with eGFP production

E. coli MG1655 *rhaB*⁻ pJOE4056.2_ *tetA* and *E. coli* RM214 *rhaB*⁻ pJOE4056.2_ *tetA* were then fermented in quadruplicates each in the STR-PFR scale-down reactor in continuous chemostat cultivations at a dilution rate of $D = 0.2 \text{ h}^{-1}$. Heterogeneities were introduced by using the two-compartment STR-PFR reactor in the same setting as described above (**Fig. 12**). Again, this included a well-mixed STR only chemostat phase, and a subsequent STR-PFR chemostat

phase to enable direct observation of the short-term and long-term influence of the nutrient-limited zone.

Under well-mixed STR conditions, we observed no substantial differences between the fermentations of *E. coli* MG1655 *rhaB*⁻ pJOE4056.2_tetA and *E. coli* RM214 *rhaB*⁻ pJOE4056.2_tetA. They reached comparable cell dry weight and eGFP yield on glucose (**Fig. 15**). In fact, the strains had virtually identical fermentation and production parameters in any parameter measured (**Table 5**). The primary product eGFP formed a considerable fraction of the total biomass and we detected only trace amounts of acetate byproduct as expected for glucose-limited fermentations. We also determined the proportion of cells with high eGFP content by flow cytometry and found these to be practically identical for both strains in the STR reference steady-state (**Fig. 15**). As *E. coli* RM214 was specifically engineered to have advantageous traits in heterogenous fermentations including starvation zones these findings were not surprising and instead proved that our genomic deletions did not interfere with the basic fermentation traits of *E. coli* K-12 strains.

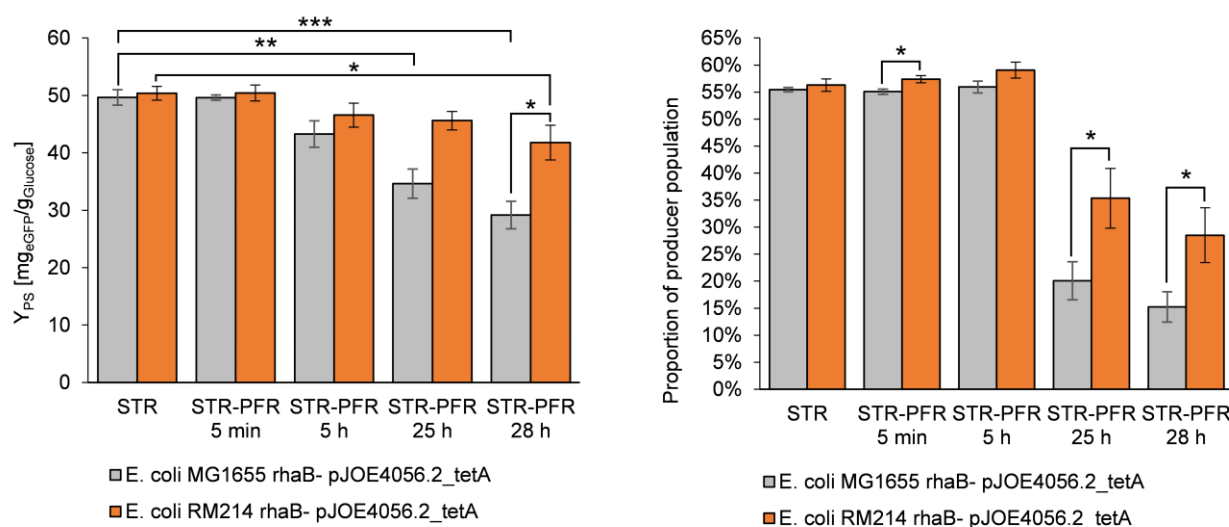


Fig. 15: EGFP yield on substrate and proportion of cells with high eGFP content. *E. coli* MG1655 rhaB⁻ pJOE4056.2_tetA (grey) and *E. coli* RM214 rhaB⁻ pJOE4056.2_tetA (orange) were cultivated in the STR-PFR system (glucose limited chemostat, $D = 0.2 \text{ h}^{-1}$). Samples were collected from the primary vessel. Error bars indicate SEM ($n = 4$), statistical indicators: * $p < 0.05$, ** $p < 0.01$, *** $p < 0.001$. Left: eGFP yield on substrate declines for both strains after PFR connection. Simultaneously, the difference between the strains gradually increases. Statistics: two-tailed t-tests comparing means of a single strain at later time points to the STR mean of the strain; and comparing the means of both strains at each time point to each other. Right: The proportion of cells with high eGFP content declines towards the end of the fermentation and is lower for *E. coli* MG1655 rhaB⁻ pJOE4056.2_tetA than for *E. coli* RM214 rhaB⁻ pJOE4056.2_tetA. Statistics: one-tailed t-tests comparing the presumably lower mean of *E. coli* MG1655 rhaB⁻ pJOE4056.2_tetA to that of *E. coli* RM214 rhaB⁻ pJOE4056.2_tetA at each time point.

Upon connecting the PFR the process performance of both strains started to decline, but this phenomenon occurred remarkably slower and much less pronounced in *E. coli* RM214 rhaB⁻ pJOE4056.2_tetA than in *E. coli* MG1655 rhaB⁻ pJOE4056.2_tetA. Five hours after connection of the PFR both strains still had similar fractions of producing cells and reached comparable biomass concentration. However, first differences in cellular eGFP content and product yield already became apparent. Over the remaining process time production parameters increasingly

diverged. After 28 h of STR-PFR continuous cultivation we observed a 43% higher product yield for *E. coli* RM214 rhaB⁻ pJOE4056.2_tetA than for *E. coli* MG1655 rhaB⁻ pJOE4056.2_tetA ($\Delta Y_{PS} = 13 \text{ mg}_{eGFP}/\text{g}_{\text{Glucose}}$, two-tailed t-test, $p < 0.05$). Instead, biomass concentration increased in *E. coli* MG1655 rhaB⁻ pJOE4056.2_tetA indicating a shift from production to biomass formation (**Supplementary Fig. S7A**). Noteworthy, we found a linear correlation describing the tradeoff between eGFP production and biomass formation using data from both *E. coli* MG1655 rhaB⁻ pJOE4056.2_tetA and *E. coli* RM214 rhaB⁻ pJOE4056.2_tetA (**Supplementary Fig. S7C** and **Supplementary Fig. S7D**). We suspected that the divergence may be caused by a reduced fraction of producing cells for *E. coli* MG1655 rhaB⁻ pJOE4056.2_tetA compared to *E. coli* RM214 rhaB⁻ pJOE4056.2_tetA and measured the fluorescence of individual cells by flow cytometry. Similar to the eGFP yield, the proportion of actively producing cells shrank rapidly in *E. coli* MG1655 rhaB⁻ pJOE4056.2_tetA and more slowly in *E. coli* RM214 rhaB⁻ pJOE4056.2_tetA. At the final time point the fraction of producing cells was significantly higher for *E. coli* RM214 rhaB⁻ pJOE4056.2_tetA than for *E. coli* MG1655 rhaB⁻ pJOE4056.2_tetA (one-tailed t-test, $p > 0.05$). To check whether differential expression of eGFP might be responsible for the reduction of eGFP yield in the heterogeneous conditions in general or for the differences between the two strains, we conducted RT-qPCR using the housekeeping gene *cysG* as a reference. However, we found no clear indication for differential expression of eGFP towards the end of the fermentation or between the two strains (**Supplementary information S10**).

After connection of the PFR we observed alterations in the respiratory parameters of both strains. Initially, cells reacted with a short spike of increased respiratory activity which then dropped rapidly in the following hour. The oxygen uptake rate Q_{O_2} and the carbon dioxide formation rate Q_{CO_2} recovered over the next two volumetric residence times and then slowly drifted towards new steady states but never reached the initial STR only values (**Supplementary Fig. S6**). We calculated total carbon balances but the deviations in the respiratory rates caused only minor redistributions between the STR reference status and the STR-PFR 28 h sample (**Fig. 16, Table S5.A** and **Table S5.B**). Apart from small gains in the biomass (CDW) fraction and small reductions in the carbon dioxide formation no major differences occurred. Declining productivity was hence accompanied by slightly declining respiration and increased biomass formation. From all collected indications we conclude that the primary factor for loss of productivity of both strains was a restructuring of the biomass

composition towards lower eGFP content (**Fig. S7B**). This is supported by our observations using flow cytometry. The proportion of cells with high eGFP content dropped substantially in the late fermentation stages (**Fig. 15**). We presume that the reduced cellular eGFP content then led to lower metabolic burden and thus enabled slightly higher biomass yields. In all parameters measured, *E. coli* RM214 rhaB⁻ pJOE4056.2_tetA proved to be more robust to the STR-PFR conditions and maintained productive for a longer period than *E. coli* MG1655 rhaB⁻ pJOE4056.2_tetA. Since the only clearly different parameter between the two strains is the maintenance coefficient, we propose that *E. coli* RM214 rhaB⁻ pJOE4056.2_tetA benefits from a small surplus of substrate that can be used to meet the high precursor and ATP demand of heterologous protein synthesis.

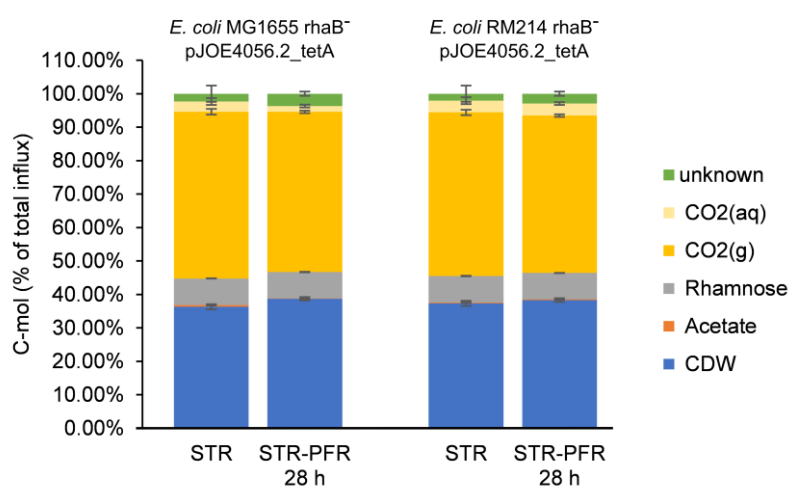


Fig. 16: Carbon Balance. *E. coli* MG1655 rhaB⁻ pJOE4056.2_tetA (grey) and *E. coli* RM214 rhaB⁻ pJOE4056.2_tetA (orange) were cultivated in the STR-PFR system (glucose limited chemostat, $D = 0.2 \text{ h}^{-1}$). Columns show efflux fractions of individual substances. Error bars indicate SEM ($n = 4$). For raw data see Supplementary Tables S5.A and S5.B.

The energetic state of cells during cultivations can be assessed by calculating the Adenylate Energy Charge (AEC) from measured nucleotide concentrations (Chapman et al., 1971). Initially, in the well-mixed STR only phase, the concentration of all nucleotides and the AEC was comparable for both strains (**Supplementary Fig. S4A**). After connection of the PFR, we

then simultaneously sampled cells from the STR and the five ports along the primary axis of the PFR to obtain a time-resolved profile of the short-term AEC changes during PFR passage (**Fig. 17**). As expected during passage through a nutrient starvation zone, the AEC of cells dropped rapidly after leaving the STR and continued to decline towards a plateau. Shortly after PFR connection, the pattern was highly similar for both strains (**Fig. 17**, upper panel). After 25 h of cultivation under scale-down conditions, the AEC of both strains in the STR and at all sampling ports of the PFR was higher than before (**Fig. 17**, lower panel). Here, differences between the strains also became apparent as the AEC of *E. coli* MG1655 rhaB⁻ pJOE4056.2_tetA was higher than that of *E. coli* RM214 rhaB⁻ pJOE4056.2_tetA at all sampling points. We then compared the AEC of samples drawn from the primary vessel at different time points to unravel long-term effects of the heterogeneous conditions. Both strains individually showed statistically significant increases in the AEC between time points STR and STR-PFR 25 h (two-tailed t-tests, $p < 0.05$; see **Supplementary Table S4B**). In fact, the AEC of *E. coli* MG1655 rhaB⁻ pJOE4056.2_tetA sampled from the primary fermentation vessel (**Fig. 17**, 0 s) at time point STR-PFR 25 h was the highest recorded value from all samples indicating that the strain was possibly trying to adapt to the unfavorable conditions. The coincidence with its reduced productivity and slightly increased biomass yield at the late fermentation stages points towards the preservation of cellular energy at the expense of heterologous protein productivity. The data from *E. coli* RM214 rhaB⁻ pJOE4056.2_tetA indicates a similar but less pronounced trend. Comparing the two strains to each other reveals a marginally significant difference ($p = 0.077$; see **Supplementary Table S4B**) of the AEC values measured in samples from the STR at STR-PFR 25 h which is reflected by the generally slightly lower AEC values of the deletion strain at this time point (**Fig. 17**, lower panel). It is noteworthy that the total AxP levels of both strains were comparable for all samples and only the distribution among ATP, ADP and AMP varied (**Supplementary Figure S4A**).

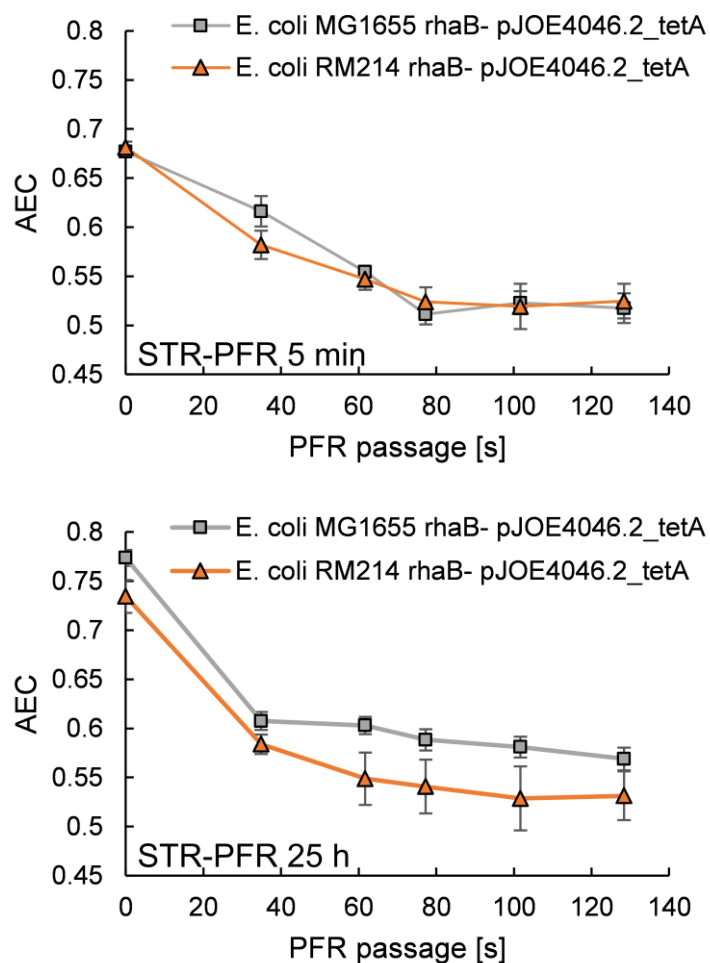


Fig. 17: Adenylate Energy Charge in the STR and during PFR passage. *E. coli* MG1655 rhaB⁻ pJOE4056.2_tetA and *E. coli* RM214 rhaB⁻ pJOE4056.2_tetA were cultivated in the STR-PFR system (glucose limited chemostat, $D = 0.2 \text{ h}^{-1}$). The adenylate energy charge of cultures was determined shortly after PFR connection (STR-PFR 5 min, upper panel) and after five volumetric residence times (STR-PFR 25 h, lower panel). Samples were drawn from the primary reactor (0 s) and the five sampling ports along the axis of the PFR (35 s, 52 s, 77 s, 102 s, 128 s). Error bars indicate SEM ($n = 4$).

Table 5: Fermentation parameters^a of the eGFP production processes.

		<i>E. coli</i> MG1655 rhaB ⁻ pJOE4056.2_tetA		<i>E. coli</i> RM214 rhaB ⁻ pJOE4056.2_tetA	
		STR	STR-PFR 28 h	STR	STR-PFR 28 h
c_x	$\left[\frac{g_{CDW}}{l}\right]$	4.02 ± 0.066	4.28 ± 0.024	4.02 ± 0.053	4.13 ± 0.024
c_P	$\left[\frac{mg_{eGFP}}{l}\right]$	630 ± 20	370 ± 32	650 ± 11	540 ± 41
Y_{XS}	$\left[\frac{g_{CDW}}{g_{Glucose}}\right]$	0.315 ± 0.0048	0.3360 ± 0.00075	0.314 ± 0.0032	0.322 ± 0.0034
Y_{PS}	$\left[\frac{mg_{eGFP}}{g_{Glucose}}\right]$	50 ± 1.3	29 ± 2.4	50 ± 1.2	42 ± 3.0
$c_{Acetate,STR}$	$\left[\frac{g_{Acetate}}{l}\right]$	0.14 ± 0.040	0.017 ± 0.0072	0.010 ± 0.0061	0.07 ± 0.030
$c_{NH_4^+}$	$\left[\frac{g_{NH_4^+}}{l}\right]$	1.64 ± 0.025	1.6 ± 0.12	1.57 ± 0.058	1.52 ± 0.033
q_S	$\left[\frac{g_{Glucose}}{g_{CDW} * h}\right]$	0.64 ± 0.013	0.60 ± 0.012	0.62 ± 0.020	0.60 ± 0.018
q_P	$\left[\frac{mg_{eGFP}}{g_{CDW} * h}\right]$	32 ± 1.4	18 ± 1.7	31 ± 1.2	25 ± 2.0
Q_{CO_2}	$\left[\frac{mmol_{CO_2}}{h}\right]$	73.5 ± 0.70	70.6 ± 0.54	72.6 ± 0.49	69.8 ± 0.64
Q_{O_2}	$\left[\frac{mmol_{O_2}}{h}\right]$	69.9 ± 0.90	67 ± 1.2	69.8 ± 0.90	65.6 ± 0.44
RQ	$\left[\frac{mol_{CO_2}}{mol_{O_2}}\right]$	1.05 ± 0.019	1.06 ± 0.013	1.04 ± 0.011	1.06 ± 0.010
$eGFP\ content$	$\left[\frac{mg_{eGFP}}{g_{CDW}}\right]$	158 ± 6.5	87 ± 7.3	161 ± 4.6	130 ± 10
Proportion of producing population	[%]	55.4 ± 0.43	15 ± 2.8	56 ± 1.2	28 ± 5.1
D	$\left[\frac{1}{h}\right]$	0.201 ± 0.0026		0.194 ± 0.0028	

^aErrors indicate SEM (n = 4).

4.2.5 Discussion

In this study, we created a series of deletion strains lacking genes with high add-on maintenance under heterogeneous conditions with repeated starvation. The final strain of the series, *E. coli* RM214 had a significantly lower maintenance coefficient than its parent *E. coli* MG1655 in an STR-PFR scale-down reactor. Moreover, *E. coli* RM214 rhaB⁻ pJOE4056.2_tetA proved to be more robust to the influence of heterogeneities in an exemplary protein production scenario reaching a significantly higher product yield in the STR-PFR phase.

The core concept of our deletion approach was to remove genes that are wastefully expressed under transient starvation conditions. The expected individual contribution of each single gene was very low (Löffler et al., 2016). The only remarkable exception was *fliC* whose expression alone was estimated to cause add-on maintenance of 3.10%, by far exceeding the expected add-on maintenance of 0.55% for the second-in-line *aldA* (Löffler et al., 2016). Multiple other flagellar and chemotaxis genes were also candidates, so the removal of these systems formed a major fraction of the deletions conducted in the creation of *E. coli* RM214. As the goal of this study was to investigate the fundamental usefulness of the whole design approach and each individual deletion had likely little effect, we did not attempt to experimentally assess the individual contributions or potential interactions. The data collected in this study thus serves to prove the general applicability of the approach but is insufficient to test the quantitative reliability of the individual metabolic cost predictions by Löffler et al. (2016). An in-depth study focusing on the effects of subsets or individual deletions would allow judging the predictions and the parallel investigation of fundamental effects and potential interactions. This is particularly interesting as the magnitude of effects observed by us exceeds the sum of all individual contributions from transcriptional and translational metabolic costs as estimated by Löffler et al. (2016). The calculations by Löffler et al. (2016) were thus either very conservative or other effects such as the actual absence of the expressed proteins provided additional secondary benefits. Investigating such secondary benefits could be helpful in refining the target selection among transiently expressed process-irrelevant genes. A potential secondary benefit enjoyed by *E. coli* RM214 could for example arise from the absence of the motility system which could save proton motive force otherwise used for flagellar rotation. On the other hand, we can confidently exclude the possibility that the slightly reduced genome of *E. coli* RM214 had a major impact due to reduced replication cost. The combined size of the deletions in

E. coli RM214 was only about 50 kb, just slightly more than 1% of the *E. coli* K-12 genome, and the metabolic demand of DNA replication is per se very low (Stouthamer, 1973).

Key findings of our study are the reduced maintenance demand of *E. coli* RM214 compared to its parent strain and the slower product yield decline of *E. coli* RM214 rhaB⁻ pJOE4056.2_tetA under STR-PFR conditions. Both differences must be caused by the genotype of *E. coli* RM214 but do these findings relate to each other by a causative link or did we observe correlated phenomena? The overall eGFP transcript levels in the production scenario were fairly stable (**Supplementary Information S10**), so it appears unlikely that differential expression of eGFP from pJOE4056.2_tetA causes the different yields. The flow cytometry data indicate that microbial individuality may play a role, but without a plausible mechanism we must assume that this is a correlated observation. Instead, we opine that a connecting mechanism can be drawn from the overall balances and the strains' cultivation parameters. Substrate consumed for maintenance demand is, by definition, not available for biomass formation. It is commonly assumed that it is fully converted into terminal products and the energy available from this conversion harnessed by the cells as ATP to meet their maintenance demand (Stouthamer and Bettenhausen, 1973). Thus, a logical link between maintenance coefficient and protein yield exists: A reduced maintenance coefficient means that more substrate is available for biomass or product formation including potential secondary ATP costs that may arise from a high foreign protein content. A simple estimation allows us to test the quantitative feasibility of a causative relation by comparing the magnitude of the reduced maintenance coefficient to the difference in protein yield: Given that there were no significant differences in Y_{XS}^{true} we can assume that Δm_s is entirely available for the additional production of eGFP in *E. coli* RM214 rhaB⁻ pJOE4056.2_tetA. Using Y_{XS} from STR-PFR 28 h and an assumed protein content of roughly 65% (Taymaz-Nikerel et al., 2010) the difference in maintenance demand could sustain an additional eGFP production rate of no more than $\Delta q_{p,ms} = 9.3 \text{ mg}_{\text{eGFP}}/\text{g}_{\text{CDW}}/\text{h}$. The experimental difference of $\Delta q_{p,ms} = 7 \text{ mg}_{\text{eGFP}}/\text{g}_{\text{CDW}}/\text{h}$ falls well within that range. A causative relation between the two observations is thus quantitatively feasible, and in our opinion likely. In this case up to 82% of the saved substrate due to lower m_s could have been used for the formation of additional eGFP in *E. coli* RM214 rhaB⁻ pJOE4056.2_tetA.

The connection between maintenance demand, energy availability and eGFP production is also supported by the AEC data collected. We found a declining AEC during PFR passage for both *E. coli* RM214 rhaB⁻ pJOE4056.2_tetA and *E. coli* MG1655 rhaB⁻ pJOE4056.2_tetA at all time

points, which is similar to the pattern observed in a preceding study with non-producing *E. coli* K-12 (Löffler et al., 2016). However, it is important to note that we measured lower AEC values in the STR and a steeper decline in the PFR, putatively due to heterologous protein production. In the heterogeneous fermentation phase, when productivity declined, we measured increased AEC values, especially in samples of the less productive *E. coli* MG1655 rhaB⁻ pJOE4056.2_tetA (**Supplementary Information S4**). The AEC is a measurement of the energetic state of cells and usually tightly balanced in a range between 0.7 and 0.9 (Chapman et al., 1971). The activity of many cellular processes is connected to the AEC and a lower AEC is associated with the activation of catabolic enzymes to meet cellular energy demands (Atkinson, 1968). Substrate depletion generally causes a reduction of the AEC (Chapman and Atkinson, 1977). Conversely, reduced AEC values have been reported in conditions when cells experienced high anabolic demand or high secondary metabolic costs, for instance caused by cultivation at their maximum specific growth rate, or induction of motility (Lieder et al., 2015; Martínez-García et al., 2014b). Heterologous protein induction is known to cause increased ATP maintenance demand (Weber et al., 2002). We thus propose that the AEC values measured from samples drawn from the primary reactor at different time points of the fermentations can be explained by the ATP demands associated with eGFP productivity. It appears likely that the generally lower AEC measured in this study compared to data from non-producing *E. coli* K-12 cultivated under similar conditions is caused by the production of eGFP. The significant increases of the AEC values of both strains towards the end of the fermentations are then a consequence of their diminishing eGFP productivity. This also explains the more pronounced AEC increase and concomitant eGFP yield decrease of *E. coli* MG1655 rhaB⁻ pJOE4056.2_tetA compared to the deletion strain. The question then arises to what extent the lower maintenance coefficient of *E. coli* RM214 rhaB⁻ pJOE4056.2_tetA under scale-down conditions influences the AEC values. From data collected in the maintenance study (**Fig. 14**) and the eGFP production fermentations we can roughly estimate the ATP demand for eGFP production of both strains at time point STR-PFR 25 h (**Supplementary Data S8**). About 13% of the total ATP demand of *E. coli* MG1655 rhaB⁻ pJOE4056.2_tetA and 22% of the total ATP demand of *E. coli* RM214 rhaB⁻ pJOE4056.2_tetA can be attributed to eGFP production. Despite its lower maintenance coefficient the combined ATP demand for maintenance plus eGFP production of the highly productive *E. coli* RM214 rhaB⁻ pJOE4056.2_tetA then still

exceeds the respective values of *E. coli* MG1655 rhaB⁻ pJOE4056.2_tetA which is reflected by its lower AEC at this time point.

A secondary observation made in this study was that loss of productivity in the STR-PFR condition was accompanied by a decline in the proportion of highly productive cells (**Fig. 15**). Microbial population heterogeneity is a subject of intense research (Binder et al., 2017) and our data provides no clear explanation why this shift occurs. Two things should be noted: First, the population heterogeneity for both *E. coli* MG1655 rhaB⁻ pJOE4056.2_tetA and *E. coli* RM214 rhaB⁻ pJOE4056.2_tetA is of the bimodal kind (**Supplementary Figure S3**) and the fractions of producing cells in the homogeneous STR cultivation phase are practically identical for both strains. Second, once the PFR is activated, we saw a decrease in the fraction of highly productive cells in all fermentations (**Fig. 15, Supplementary Figure S3**) but the decrease was faster and more consistent for *E. coli* MG1655 rhaB⁻ pJOE4056.2_tetA. The overall level of population heterogeneity is generally high since only slightly more than half of all cells are strongly accumulating eGFP. We presume this is caused by the interplay of our expression system and the fermentation conditions. The regulation of rhamnose catabolism is autocatalytic and thus bimodality might be caused by a similar mechanism as in the case of expression from the arabinose promoter P_{BAD} (Khlebnikov et al., 2000). However, transcript measurements by RT-qPCR did not lead to a concise pattern that would explain both the differences between the two strains and the declining eGFP yield of each individual strain over the course of the heterogeneous fermentation phase. Given the fairly stable expression of eGFP and the continuous selective advantage provided by *tetA*, it also appears unlikely that plasmid loss or mutations were the underlying cause. Moreover, the general stability of eGFP expression from pJOE4056.2 has been determined to be perfect for over 50 generations in earlier studies (Wegerer et al., 2008).

The deletion approach in this study differs from previous works because target selection was based on existing expression data and limited to candidates that imposed a high metabolic burden but were irrelevant under the specified conditions (Valgepea et al., 2015). Large-scale genomic deletions, the contrary approach, have been conducted before in *E. coli* K-12, for instance as part of the construction of the MDS strains (Pósfai et al., 2006). These strains had little benefits in standard protein production scenarios over their wild-type parent and were even inferior in basic process parameters, potentially caused by disrupted regulation (Karcagi et al., 2016; Sharma et al., 2007b; Sharma et al., 2007a). It needs to be emphasized that our deletion

strategy only provided advantages in the specified conditions of a heterogeneous bioprocess with transient starvation as *E. coli* RM214 had no benefit compared to *E. coli* MG1655 under well-mixed conditions. In this regard, it also appears clear that the deletion targets chosen by us cannot be directly transferred to other hosts or conditions since the naturally evolved regulation might be divergent. This is exemplified by an interesting comparison of our results to existing data from *Pseudomonas putida*. The exposure of *P. putida* KT2440 to heterogeneous STR-PFR conditions led to an increased and potentially wasteful expression of *fliC* similarly as in the case of *E. coli* (Ankenbauer et al., 2020). However, the deletion of the flagellar apparatus in *P. putida* EM329 led to significant improvements of basic fermentation and protein production parameters already under well mixed conditions (Lieder et al., 2015; Martínez-García et al., 2014b). This demonstrates not only the diverging regulation of motility between different microbes, but also implies that a strain like *P. putida* EM329 might unintentionally display additional beneficial traits in heterogeneous fermentations with starvation zones.

A premise of our study was to work orthogonally to global cellular regulation. The general stress response, stringent response and SOS responses were not modified as they might provide important functions for cellular adaptation and some expression systems depend on intracellular signaling molecules of global regulatory circuits. Examples include not only the CRP-cAMP dependent system used in this study but also novel adaptive expression systems that autoregulate cellular stress (Lo et al., 2016). Interestingly, in a former study, the rapid inactivation of *rpoS* in homogeneous chemostat cultivations was reported, which pointed to a large selective advantage of mutants (Notley-McRobb et al., 2002). In contrast, we did not find any mutations in genes involved in the stringent response or the general stress response for neither *E. coli* MG1655 nor *E. coli* RM214 at any growth rate. We conclude that under heterogeneous conditions the selective pressure on inactivating global regulatory programs is either very low or their activation may even be favorable for cellular viability which affirms our neutral approach to cellular regulation. However, this does not mean that modulating cellular regulation could not be beneficial for process or production parameters. Recently, several *E. coli* knock out strains lacking hand-picked genes that are connected to post-induction stress responses were presented (Sharma et al., 2020). These strains have advantageous traits for protein production which could be integrated into *E. coli* RM214.

Our study design focused on the influence of starvation zones on microbial culture performance. The carbon limited STR contained a substrate-limited growth and production zone representing

the bulk of large-scale fermentations. The PFR served to introduce a transient starvation stimulus representative of repeated passages through a hunger zone as predicted to occur in large-scale reactors (Haringa et al., 2017; Kuschel and Takors, 2020). Since our experimental setup was specifically chosen for the study of transient starvation, it does not capture the effects of other heterogeneities, in particular transient substrate excess. It is well-known that close to the feeding point, substrate excess and concomitant oxygen limitation dominate the environment in large-scale fed-batch processes. *E. coli* typically reacts to such conditions with the production of solvents or small organic acids caused by overflow metabolism or anaerobic fermentation (Lara et al., 2009). The formation of byproducts then results in process performance losses even if reuptake in zones with lower nutrient concentration is possible (Enfors et al., 2001; Neubauer et al., 1995b). Since our deletion approach was only aimed at reducing the additional metabolic costs of transient starvation, *E. coli* RM214 probably responds to glucose excess like other *E. coli* K-12 strains. In principle, copying the design approach to construct an *E. coli* strain with reduced additional maintenance in excess zones appears to be feasible as the transcriptional response of *E. coli* MG1655 to glucose excess is large and involves many potentially process-irrelevant genes (Veit et al., 2007). However, the resulting genetic modifications would not reduce process performance loss from byproduct formation which is likely the dominating issue in substrate excess conditions. Various strategies to alleviate byproduct metabolism have been developed by other research groups, such as the use of alternative substrate transporters, knock-outs or the expression of recombinant *Vitreoscilla* hemoglobin (Anda et al., 2006; Eiteman and Altman, 2006; Pablos et al., 2014). Given that our strain design approach avoids modifications to global regulation or central carbon metabolism, we are confident that it is compatible with these existing strategies and their combination could result in chassis strains for generally robust scale-up. A limitation of our study originates from the focus on the model protein eGFP. However, recombinant protein production is frequently limited by the availability of cellular precursors and ATP, so it is not far-fetched to expect similar effects with other protein products (Glick, 1995; Heyland et al., 2011). The reduced maintenance coefficient of *E. coli* RM214 should also be helpful to produce molecules formed in ATP-intensive pathways such as terpenoids (Li and Wang, 2016; Ward et al., 2018). Potential advantages could also occur when the accumulation of toxic products causes increased ATP demand for product export, membrane maintenance or pH homeostasis (Sun et al., 2011; Tsukagoshi and Aono, 2000). On the other hand, it may be less helpful when

the formation of a small molecule product is connected to net ATP synthesis. Glycolytic flux depends on the ATP requirements of cells and in such cases enforced ATP wasting can even increase the production rate (Boecker et al., 2019; Koebmann et al., 2002).

With the increasing knowledge about cellular metabolism and its interplay with the heterogeneous conditions of large-scale processes new possibilities to improve process performance arise. In a recent review Wehrs et al. (2019) emphasized that strains should be engineered specifically for the demands of large-scale production (Wehrs et al., 2019). In this context, our series of deletion strains is the first step towards host strains robust against the repeated exposure to starvation zones.

4.2.6 Conclusion

Large-scale fermentations often suffer from process performance loss due to heterogeneous environments. *E. coli* RM214 was engineered to obtain a deletion strain with reduced maintenance and superior production properties in fermentations with starvation zones. Our study is the first that aimed to improve a microbe by repeated genomic deletions for enhanced robustness towards heterogeneous conditions. The exemplified application of *E. coli* RM214 for eGFP production demonstrates the cellular capacity to exploit the maintenance advantage for preventing non-wanted performance loss in heterogeneously mixed industrial production scenarios. Although only showcased for eGFP, the strain offers the capacity to serve as a platform for a variety of different products. Notably, this complements classical scale-up engineering and should be a highly valuable tool to prevent non-wanted performance of essential Titer-Rate-Yield values under industrial production conditions.

4.2.7 Acknowledgements

The authors acknowledge the support of the Computational Biology Group at IBVT Stuttgart: Richard Schäfer and Prof. Björn Voß for providing access to a Galaxy Server.

The authors acknowledge the support of Dr. rer. nat. habil. Jürgen Dippon for assistance with statistical analysis.

The authors acknowledge the support of Florian Hiering and apl. Prof. Martin Siemann-Herzberg for assistance with the purification and quantification of eGFP.

The authors acknowledge the support of Andreas Freund for technical assistance.

The authors would like to thank the staff of the Court laboratory at the National Cancer Institute in Frederick, MD USA for providing the strains *T-SACK* and *E. coli* DH10B pSIM5.

The authors would like to thank apl. Prof. Martin Siemann-Herzberg and Dr. Josef Altenbuchner for providing the strain *E. coli* BW3110 pJOE4056.2.

4.3 CRISPRi enables fast growth followed by stable aerobic pyruvate formation in *Escherichia coli* without auxotrophy

The manuscript was penned by Martin Ziegler. Martin Ziegler is the first author. Teresa Gäbele and Prof. Dr.-Ing. Ralf Takors contributed to the manuscript's content by selected additions and reviewed it. Prof. Dr.-Ing. Ralf Takors is the corresponding author.

Martin Ziegler and Teresa Gäbele planned the genomic alterations in this study. Teresa Gäbele generated the recombinant strains supervised by Martin Ziegler. Martin Ziegler planned the shaking flask and fermentation experiments in this study. Teresa Gäbele conducted the shaking flask and fermentation experiments supervised by Martin Ziegler. The primary experimental data was collected and analyzed by Martin Ziegler and Teresa Gäbele. Prof. Dr.-Ing. Ralf Takors supervised the research.

This manuscript has been submitted to Engineering in Life Sciences.

The published version of this article can be accessed from the publishing journal's homepage:

Ziegler, M., Hägele, L., Gäbele, T., Takors, R., 2021. CRISPRi enables fast growth followed by stable aerobic pyruvate formation in *Escherichia coli* without auxotrophy. Eng. Life Sci., elsc.202100021. <https://doi.org/10.1002/elsc.202100021>.

4.3.1 Practical application

Pyruvate is an important cellular precursor at the intersection of glycolysis and tricarboxylic acid cycle (TCA). Reduced pyruvate flux into the TCA improves its availability for the formation of pyruvate-derived products such as terpenoids synthesized via the methylerythritol-4-phosphate (MEP) pathway in *E. coli*. In this study, balanced reduction of pyruvate dehydrogenase activity by CRISPR interference was explored to trigger the accumulation of pyruvate while maintaining robust cellular growth and avoiding acetate auxotrophy. We demonstrate the applicability of the approach in exemplary aerobic fermentations including an extended nitrogen-limited production phase. The strategy has the potential to improve titer and carbon conversion in the biotechnical production of pyruvate-derived products.

Abbreviations: TCA, tricarboxylic acid; **sgRNA**, single-guide RNA; **CRISPR**, Clustered Regularly Interspaced Short Palindromic Repeats; **CRISPRi**, CRISPR interference; **Atc**, anhydrotetracycline; *E. coli*, *Escherichia coli*;

4.3.2 Abstract

CRISPR interference (CRISPRi) was applied to enable the aerobic production of pyruvate in *Escherichia coli* MG1655 under glucose excess conditions by targeting the promoter regions of *aceE* or *pdhR*. Knockdown strains were cultivated in aerobic shaking flasks and the influence of inducer concentration and different sgRNA binding sites on the production of pyruvate was measured. Targeting the promoter region of *aceE* triggered pyruvate production during the exponential phase. In lab-scale bioreactor fermentations, an *aceE* silenced strain successfully produced pyruvate under fully aerobic conditions during the exponential phase, but loss of productivity occurred during a subsequent nitrogen-limited phase. Combinatorial use of two sgRNAs targeting *aceE* did not improve the production phenotype. However, simultaneous silencing of *aceE* and *pdhR* in *E. coli* MG1655 pdCas9 psgRNA_aceE_234_pdhR_329 enabled the stable aerobic production of pyruvate with non-growing cells at $Y_{P/S} = 0.36 \pm 0.029$ g_{Pyruvate}/g_{Glucose} in lab-scale bioreactors throughout an extended nitrogen-limited production phase. Further experiments revealed that targeting *pdhR* alone was sufficient to enable strong pyruvate production in shaking flasks.

4.3.3 Introduction

Pyruvate is a small metabolite at the intersection of glycolysis and the tricarboxylic acid (TCA) cycle. The production of pyruvate by biotechnical means is well established, for example by Toray Industries using *Torulopsis glabrata* (Miyata et al., 1987; Sawai et al., 2011). Processes with high titer, yield and productivity have been described not only for *T. glabrata* but also for *E. coli* (Li et al., 2001b; Zelić et al., 2004; Zhu et al., 2008). The economic feasibility of *E. coli* as a pyruvic acid producer from glucose has been examined in a case study (Biber et al., 2005). However, applications of pyruvate are relatively few compared to other small organic acids: Pyruvate primarily serves as an additive for the synthesis of small-volume specialty chemicals or pharmaceuticals such as L-DOPA and is sold as a food additive (Li et al., 2001a; Yuan et al., 2020). Potential medical dietary benefits have been scientifically investigated but so far could not be confirmed beyond doubt (Onakpoya et al., 2014). The importance of pyruvate for biotechnological applications therefore originates from its position in the central carbon metabolism serving as a precursor for other small molecule compounds. Bioproducts derived from pyruvate include the amino acids alanine, isoleucine, leucine and valine (Ma et al., 2018), small carbon molecules such as lactate or isobutanol (Wess et al., 2019) and isoprenoids synthesized by the methylerythritol-4-phosphate (MEP) pathway (Rohmer et al., 1996). The production of isoprenoids in *E. coli* by the native MEP pathway has received considerable attention in the past years (Patil et al., 2021; Ward et al., 2018).

An important factor in engineering the productivity of heterologous pathways branching from pyruvate is the balance of precursor availability for growth and production. Pyruvate is usually produced from glucose and gene deletions or mutations with high impact on the catalytic activity of the pyruvate dehydrogenase complex result in acetate auxotrophy in aerobic conditions (Tomar et al., 2003). Whereas this enables decoupling of growth and pyruvate production, it also implies that any demand for reducing power and ATP exceeding the supply provided from glycolysis must be met by the co-consumption of acetate which is a more expensive substrate than glucose (Biber et al., 2005). Several studies have thus explored the possibility of throttling the flux from pyruvate to acetyl-CoA to trigger the accumulation of pyruvate while maintaining a low level of flux through the TCA cycle to avoid acetate auxotrophy. The regulation of pyruvate dehydrogenase complex activity could be achieved by point mutations modulating catalytic activity (Michalowski et al., 2017). Alternatively, gene expression was controlled by promoter engineering (Ma et al., 2018) or by regulated expression

of antisense RNA (Nakashima et al., 2014). Strains accumulating pyruvate while maintaining an acceptable growth phenotype have the potential to serve as chassis for pyruvate-derived products.

Another possibility to reduce the expression of genes is through steric hindrance by a DNA binding protein. In recent years targeted binding of DNA sequences has become readily available in *E. coli* K-12 by using CRISPR-Cas derived systems. The endogenous CRISPR system of *E. coli* K-12 can be repurposed by deletion of *cas3* to yield a DNA binding system lacking nuclease activity (Chang et al., 2016; Rath et al., 2015). Alternatively, CRISPRi which uses the exogenous catalytically inactive protein dCas9 from *S. pyogenes* can be introduced in conjunction with single-guide RNAs (Bikard et al., 2013; Qi et al., 2013). A single-guide RNA (sgRNA) forms a stable complex with dCas9 which can then bind to a DNA region with complementarity to the targeting sequence and a protospacer adjacent motif (PAM). If the complex targets a region close to the transcription start of a single gene or operon, it may prevent binding of RNA polymerase which effectively represses the expression of the downstream genes. The repression strength in CRISPRi may vary over several orders of magnitude and depends primarily on the distance of the binding site to the transcription start, the target strand, and mismatches in the targeting sgRNA (Larson et al., 2013; Qi et al., 2013). CRISPRi has already been applied successfully to improve the microbial production of a plethora of small compounds (Schultenkämper et al., 2020). The technique is of particular interest for metabolic engineers because it facilitates the fine-tuning of gene expression which is helpful to find an optimal balance between competing processes such as growth and production (Sander et al., 2019b).

Fed-batch processes are the standard fermentation mode in white biotechnology. To further improve process performance complementary techniques such as the possibility to decouple growth and production phases or *in situ* product removal are actively investigated (Lo et al., 2016; Zelić et al., 2004). These techniques include dual-phase fermentations, extended production phases with resting cells, or processes limited by other compounds than the primary carbon source (Lange et al., 2017; Perez-Zabaleta et al., 2019). Nitrogen-limited processes are particularly attractive as nitrogen is a major component of biomass, nitrogen sources such as ammonia are usually cheap and easy to measure and the interplay of glucose and nitrogen metabolism in industrial hosts such as *E. coli* and *S. cerevisiae* is well characterized (Aon and Cortassa, 2001; Huergo and Dixon, 2015). In the case of a small molecule carbon-based product

nitrogen is not required for product formation and nitrogen limitation thus enables the decoupling of growth and production.

In this study, we designed sgRNAs for the silencing of *aceE* in aerobic fermentations of *E. coli* MG1655 by targeting the promoters *aceEp* and *pdhRp*. The repression of *aceEp* alone enabled the production of pyruvate in aerobic pH-controlled fermentations during the exponential phase. However, it was not sufficient to create a stable production phenotype throughout an extended nitrogen-limited production phase. The simultaneous repression of both *aceEp* and *pdhRp* overcame this limitation and allowed the production of pyruvate during the batch phase and a consecutive nitrogen-limited production phase. Repression of *pdhR* alone also triggered the accumulation of pyruvate in shaking flask experiments.

4.3.4 Materials and methods

Media and Buffer Solutions

2xTY medium was prepared by autoclaving 16 g/l tryptone, 10 g/l yeast extract, 5 g/l NaCl dissolved in demineralized water. For agar plates 18 g/l agar-agar were added prior to autoclavation. SOC medium was prepared as described previously (Hanahan, 1983). All cultivations were performed at 37 °C.

Minimal medium for shaking flask experiments consisted of 20 g/l glucose, 2.0 g/l NaH₂PO₄·2H₂O, 5.2 g/l K₂HPO₄, 4.56 g/l (NH₄)₂SO₄, 15 g/l 3-(*N*-morpholino)propanesulfonic acid (MOPS) and 0.4 % (V/V) trace elements stock solution.

N-lim minimal medium for precultures of bioreactor experiments consisted of 10 g/l glucose, 1.0 g/l NaH₂PO₄·2H₂O, 2.6 g/l K₂HPO₄, 2.2 g/l (NH₄)₂SO₄, 15 g/l 3-(*N*-morpholino)propanesulfonic acid (MOPS) and 0.2 % (V/V) trace elements stock solution.

N-lim minimal medium for bioreactor experiments consisted of 70 g/l glucose, 1.0 g/l NaH₂PO₄·2H₂O, 2.6 g/l K₂HPO₄, 2.2 g/l (NH₄)₂SO₄ and 0.2 % (V/V) trace elements stock solution.

If strains with antibiotic resistance markers were cultivated in any liquid media or on 2xTY agar plates, appropriate antibiotics were added to media in the following concentrations: Chloramphenicol 25 µg/ml, disodium Carbenicillin 100 µg/ml. If necessary, inducers were added to minimal media in the following concentrations unless stated otherwise: Isopropyl β-d-1-thiogalactopyranoside (IPTG) 1 mM, Anhydrotetracycline (Atc) 0.1 µg/ml.

The composition of trace element stock solution was 4.175 g/l FeCl₃·6H₂O, 0.045 g/l ZnSO₄·7H₂O, 0.025 g/l MnSO₄·H₂O, 0.4 g/l CuSO₄·5H₂O, 0.045 g/l CoCl₂·6H₂O, 2.2 g/l CaCl₂·2H₂O, 50 g/l MgSO₄·7H₂O and 55 g/l sodium citrate dihydrate. Stock solutions of salts, trace elements and sugars were autoclaved separately, and stock solutions of antibiotics were filter sterilized and stored at -20 °C. All compounds were combined just before the experiments to prevent potential aging of media.

Bacterial Strains and Cloning of Plasmids for CRISPR interference

All strains used in this study are listed in **Table 6** and all primers used in this study are listed in

Table 7.

Cloning of psgRNA plasmids was conducted as described previously (Hawkins et al., 2015). Briefly, primers were 5' phosphorylated using T4 polynucleotide kinase. Next, pgRNA-bacteria or a psgRNA plasmid was amplified by inverse PCR (iPCR) using a reverse primer binding the plasmid in the promoter region of the sgRNA expression cassette and a forward primer containing the complementary 20 nucleotide target binding sequence for CRISPR interference to be introduced flanked by an annealing region to the plasmid. After purification of the PCR reaction, DpnI degradation of the plasmid template, and separation of products on an agarose gel, bands at 2.6 kb were extracted and the purified DNA fragments circularized by blunt-end ligation using T4 DNA ligase. *E. coli* DH5 α λ *pir* was transformed with 2 μ l of the ligation reaction by electroporation and regenerated in SOC medium. Cells were then plated on 2xTY agar plates and incubated at 37 °C overnight. Cells from a single colony were grown in 2xTY, the plasmids extracted using E.Z.N.A.® Plasmid DNA mini Kit I (omega BIO-TEK) according to the manufacturer's instructions and the insert coding for the sgRNA verified by sequencing.

Cloning of psgRNA plasmids containing more than one sgRNA was performed using iPCR and BioBrick assembly cloning as described elsewhere (Larson et al., 2013; Shetty et al., 2008). In short, the donor sgRNA plasmid was digested using EcoRI and BamHI and the recipient plasmid digested with EcoRI and BglII. Fragments were separated on agarose gels, extracted, purified, and ligated using T4 DNA ligase. *E. coli* DH5 α λ *pir* was transformed with 5 μ l of the ligation reaction by electroporation and regenerated in SOC medium. Cells were then plated on 2xTY agar plates and incubated at 37 °C overnight. Cells from a single colony were grown in 2xTY, the plasmids extracted using E.Z.N.A.® Plasmid DNA mini Kit I (omega BIO-TEK) according to the manufacturer's instructions and the insert coding for the sgRNA verified by sequencing.

Table 6: Strains used in this study.

Strains	Strain Information / CRISPRi targets	Reference
<i>Escherichia coli</i> DH5 α λ <i>pir</i>	cloning strain	(Michalowski et al., 2017)
<i>E. coli</i> MG1655	wild-type strain	(Michalowski et al., 2017)
<i>E. coli</i> Top10 pdCas9	contains dCas9 inducible by anhydrotetracycline	(Qi et al., 2013) ^a
<i>E. coli</i> Top10 pgRNA-bacteria	empty guideRNA plasmid	(Qi et al., 2013) ^b
<i>E. coli</i> MG1655 psgRNA_lacZ_236 pdCas9	<i>lacZ</i> (TTGGGAAGGGCGATCGGTGC)	(Qi et al., 2013) ^c
<i>E. coli</i> MG1655 psgRNA_lacZ_237 pdCas9	<i>lacZ</i> (GGCCAGTGAATCCGTAATCA)	This study
<i>E. coli</i> MG1655 psgRNA_lacZ_238 pdCas9	<i>lacZ</i> (AAGCATAAAGTGTAAGCCT)	This study
<i>E. coli</i> MG1655 psgRNA_lacZ_239 pdCas9	<i>lacZ</i> (AGCGGATAACAATTTACAC)	This study
<i>E. coli</i> MG1655 psgRNA_neg_241 pdCas9	-	This study
<i>E. coli</i> MG1655 psgRNA_aceE_232 pdCas9	<i>aceE</i> (ACCTGTCTTATTGAGCTTTC)	This study
<i>E. coli</i> MG1655 psgRNA_aceE_233 pdCas9	<i>aceE</i> (CTGTCCCATTGAACTCTCGC)	This study
<i>E. coli</i> MG1655 psgRNA_aceE_234 pdCas9	<i>aceE</i> (TCTAATAACGTTGAGTTTTC)	This study
<i>E. coli</i> MG1655 psgRNA_aceE_235 pdCas9	<i>aceE</i> (AGCCAGTCGCGAGTTTCGAT)	This study
<i>E. coli</i> MG1655 psgRNA_aceE_232_aceE_234 pdCas9	<i>aceE</i> (ACCTGTCTTATTGAGCTTTC, TCTAATAACGTTGAGTTTTC)	This study
<i>E. coli</i> MG1655 psgRNA_aceE_232_aceE_235 pdCas9	<i>aceE</i> (ACCTGTCTTATTGAGCTTTC, AGCCAGTCGCGAGTTTCGAT)	This study
<i>E. coli</i> MG1655 psgRNA_aceE_233_aceE_234 pdCas9	<i>aceE</i> (CTGTCCCATTGAACTCTCGC, TCTAATAACGTTGAGTTTTC)	This study

4. Publications

Strains	Strain Information / CRISPRi targets	Reference
<i>E. coli</i> MG1655 psgRNA_aceE_233_aceE_235 pdCas9	<i>aceE</i> (CTGTCCCATTGAACTCTCGC, AGCCAGTCGCGAGTTTCGAT)	This study
<i>E. coli</i> MG1655 psgRNA_pdhR_327 pdCas9	<i>pdhR</i> (TCAAAACCTGTATGGACATA)	This study
<i>E. coli</i> MG1655 psgRNA_pdhR_328 pdCas9	<i>pdhR</i> (TATTCACCTTATGTCCATAC)	This study
<i>E. coli</i> MG1655 psgRNA_pdhR_329 pdCas9	<i>pdhR</i> (AGCCACTTGCCGAAGTCAAT)	This study
<i>E. coli</i> MG1655 psgRNA_aceE_233_pdhR_327 pdCas9	<i>aceE + pdhR</i> (CTGTCCCATTGAACTCTCGC, TCAAAACCTGTATGGACATA)	This study
<i>E. coli</i> MG1655 psgRNA_aceE_233_pdhR_328 pdCas9	<i>aceE + pdhR</i> (CTGTCCCATTGAACTCTCGC, TATTCACCTTATGTCCATAC)	This study
<i>E. coli</i> MG1655 psgRNA_aceE_233_pdhR_329 pdCas9	<i>aceE + pdhR</i> (TCTAATAACGTTGAGTTTTTC, AGCCACTTGCCGAAGTCAAT)	This study
<i>E. coli</i> MG1655 psgRNA_aceE_234_pdhR_327 pdCas9	<i>aceE + pdhR</i> (TCTAATAACGTTGAGTTTTTC, TCAAAACCTGTATGGACATA)	This study
<i>E. coli</i> MG1655 psgRNA_aceE_234_pdhR_328 pdCas9	<i>aceE + pdhR</i> (TCTAATAACGTTGAGTTTTTC, TATTCACCTTATGTCCATAC)	This study
<i>E. coli</i> MG1655 psgRNA_aceE_234_pdhR_329 pdCas9	<i>aceE + pdhR</i> (TCTAATAACGTTGAGTTTTTC, AGCCACTTGCCGAAGTCAAT)	This study

a: pdCas9-bacteria was a gift from Stanley Qi (Addgene plasmid # 44249; <http://n2t.net/addgene:44249>; RRID: Addgene_44249)

b: psgRNA-bacteria was a gift from Stanley Qi (Addgene plasmid # 44251; <http://n2t.net/addgene:44251>; RRID: Addgene_44251)

c: Strain was constructed in this study according to information provided in the given reference.

Table 7: Primers used in this study

No	Primer name	Sequence 5' → 3' (<u>binding sequence</u>)	Function
23 6	lacZ_236	<u>TTGGGAAGGGCGATCGGTGCGTTT</u> TAGAGCTAGAAAT AGCAAGTTAAAATAAGGC	fwd primer for iPCR (Qi et al., 2013)
23 7	lacZ_237	<u>GGCCAGTGAATCCGTAATCAGTTTT</u> AGAGCTAGAAATA GCAAGTTAAAATAAGGC	fwd primer for iPCR
23 8	lacZ_238	<u>AAGCATAAAGTGTAAGCCTGTTT</u> TAGAGCTAGAAATA GCAAGTTAAAATAAGGC	fwd primer for iPCR
23 9	lacZ_239	<u>AGCGGATAACAATTTACACGTTTT</u> AGAGCTAGAAATA GCAAGTTAAAATAAGGC	fwd primer for iPCR
23 2	aceE_232	<u>ACCTGTCTTATTGAGCTTTCGTTTT</u> AGAGCTAGAAATAG CAAGTTAAAATAAGGC	fwd primer for iPCR
23 3	aceE_233	<u>CTGTCCCATTGAACTCTCGCGTTTT</u> AGAGCTAGAAATAG CAAGTTAAAATAAGGC	fwd primer for iPCR
23 4	aceE_234	<u>TCTAATAACGTTGAGTTTTTCGTTTT</u> AGAGCTAGAAATAG CAAGTTAAAATAAGGC	fwd primer for iPCR
23 5	aceE_235	<u>AGCCAGTCGCGAGTTTCGATGTTTT</u> AGAGCTAGAAATA GCAAGTTAAAATAAGGC	fwd primer for iPCR
32 7	pdhR_327	<u>TCAAAACCTGTATGGACATAGTTTT</u> AGAGCTAGAAATA GCAAGTTAAAATAAGGC	fwd primer for iPCR
32 8	pdhR_328	<u>TATTCACCTTATGTCCATACGTTTT</u> AGAGCTAGAAATAG CAAGTTAAAATAAGGC	fwd primer for iPCR
32 9	pdhR_329	<u>AGCCACTTGCCGAAGTCAATGTTTT</u> AGAGCTAGAAATA GCAAGTTAAAATAAGGC	fwd primer for iPCR
24 0	sgRNA_r	ACTAGTATTATACCTAGGACTGAG CTAGC	rev primer for iPCR (Larson et al., 2013)

No	Primer name	Sequence 5' → 3' (<u>binding sequence</u>)	Function
24 1	sgRNA_neg	GTTTTAGAGCTAGAAATAGCAAGT TAAAATAAGGC	fwd primer for iPCR (Larson et al., 2013)
24 2	sgRNA_seq_col_f	GGGTTATTGTCTCATGAGCGGATA CATATTTG	sequencing of psgRNA (Larson et al., 2013)

To construct the actual production strains, *E. coli* MG1655 was transformed with 1 µl of purified psgRNA plasmid by electroporation, regenerated in SOC medium, plated on 2xTY agar plates, and incubated at 37 °C overnight. Electrocompetent cells were prepared from a single colony and transformed with 5 µl of pCas9 using identical procedures. The resulting strains carrying two plasmids were grown in 2xTY and stored as glycerol stocks at -70 °C.

β-Galactosidase Assay

The activity of β-galactosidase, the product of *lacZ*, was assayed according to Jeffrey Miller's protocol with minor adaptations (Miller, 1972). Baffled 100 ml shaking flasks containing 10 ml 2xTY medium were inoculated with a single colony from an agar plate streak and incubated with appropriate antibiotics at 37 °C and 130 rpm. After 30 min, isopropyl-β-D-thiogalactopyranosid (IPTG) was added to a final concentration of 1 mM. Cells were grown to mid-log phase and the optical density at 600 nm measured. 2 ml of biosuspension were harvested by centrifugation for 2 min at 12000 g, the supernatant discarded, and the cell pellet resuspended in 2 ml of Z-buffer (60 mM Na₂HPO₄·2H₂O, 40 mM NaH₂PO₄·H₂O, 10 mM KCl, 1 mM MgSO₄, 50 mM β-mercaptoethanol, pH adjusted to 7.0 with NaOH / H₃PO₄ prior to addition of β-mercaptoethanol). An appropriate volume of resuspended cell suspension was further diluted in Z-buffer to yield 1 ml of assay sample solution. 1 ml of diluted cells were lysed with 50 µl of chloroform and 25 µl of 0.1 % sodium dodecyl sulfate (SDS) solution. After incubation for 5 min, 200 µl of substrate solution (4 g/l o-Nitrophenyl-β-D-galactopyranoside (OPNG) dissolved in Z-buffer) were added and the time until the sample turned yellow was recorded. The reaction was stopped by adding 500 µl stop solution (1 M Na₂CO₃ in deionized water) and the samples centrifuged for 7 min at 12000 g. The supernatant was transferred into PMMA semi-micro cuvettes and the absorption at 420 nm was measured. Miller units were

calculated according to the following equation, where t is the time of reaction in minutes and V the volume of cell suspension used to correct for dilution of samples in Z-buffer:

$$\beta\text{-galactosidase activity [miller units]} = (\text{OD}_{420} \times 1000) / (\text{OD}_{600} \times t \times V)$$

Shaking flask cultivations

Strains were streaked from glycerol stock cultures on 2xTY agar plates and grown overnight at 37 °C. For precultures, a 100 ml baffled shaking flask containing 20 ml minimal medium was inoculated with a single colony and incubated at 37 °C on a rotary shaker set to 130 rpm for 16 – 40 h. For main cultures, a 500 ml baffled shaking flask containing 55 ml of minimal medium was inoculated with preculture to a starting OD of 0.2 and cultivated at 37 °C on a rotary shaker set to 130 rpm.

Bioreactor cultivations

Precultures for bioreactor experiments were inoculated from glycerol stock cultures by transferring 333 μl of glycerol stock culture into a 100 ml baffled shaking flask containing 20 ml N-lim minimal medium. Precultures were incubated at 37 °C on a rotary shaker set to 130 rpm overnight. On the next morning, a glass bioreactor containing 200 ml of N-lim minimal medium was inoculated with preculture to a starting OD of 0.2. Glass bioreactors were equipped with a temperature control set to 37 °C and magnetic stirrers set to 500 rpm. Throughout the cultivation stirring speed and gassing were kept constant at 500 rpm and 300 ml/min. DO tension was monitored and never dropped below 30 % saturation to ambient air partial oxygen pressure. The pH was kept constant at 7.0 by automated addition of 3 M NaOH. Prior to fermentation start a single droplet (about 10 μl) of Struktol J647 antifoaming agent was added to the vessel to prevent potential foaming.

Analytical Procedures

Bacterial growth was monitored by measurements of optical density at 600 nm. Biosuspension samples were appropriately diluted with 0.9 % NaCl solution and cell dry weight calculated from these values assuming a correlation factor of 0.3 (Michalowski et al., 2017).

2 ml of freshly sampled biosuspension were centrifuged at 12000 g for 2 min and aliquots of the resulting supernatant frozen until further analysis. Isocratic HPLC using a RI detector (1200Series, Agilent) with a Rezex ROA-Organic acid H⁺ column (Phenomenex) for separation was used to measure glucose, acetic acid, lactate, 2-oxoglutarate, ethanol, formate and succinate as described previously (Michalowski et al., 2017). Glucose concentration was alternatively determined by D-Glucose UV-Test Kit (R-Biopharm, Darmstadt, Germany) and acetic acid concentration by Acetic acid UV-Test Kit (R-Biopharm, Darmstadt, Germany). Ammonium concentration was determined by Ammonium cuvette test LCK 303 or LCK 304 (Hach Lange, Düsseldorf, Germany). Pyruvate was determined by an enzymatic assay measuring the consumption of NADH upon conversion of pyruvate to lactate by L-lactate dehydrogenase (LDH). L-lactate dehydrogenase suspension (L2500, Merck) was diluted 1:10 in 2.5 M (NH₄)₂SO₄ solution. 500 µl of 100 mM tris (pH 7.4), 100 µl of 2 mM NADH and 290 µl deionized water were mixed in an acryl cuvette and 100 µl of appropriately diluted sample was added. The absorbance at 365 nm was measured and 10 µl of LDH suspension was added to initiate the reaction. After incubation for 10 min at room temperature the absorbance at 365 nm was measured again and the resulting difference in absorbance used to calculate the pyruvate content of the sample.

4.3.5 Results

Our goal was to apply CRISPRi to throttle the flux from pyruvate to the TCA cycle. We aimed for a strain that accumulated pyruvate aerobically while maintaining an acceptable growth phenotype without acetate auxotrophy. The target phenotype can be obtained by balanced reduction of the activity of the pyruvate dehydrogenase complex (Michalowski et al., 2017). Therefore, our primary knockdown target was *aceE* which encodes a subunit of the pyruvate dehydrogenase complex. Additionally, we planned on using the strain in two-phase fermentations with an initial growth phase and a subsequent nitrogen-limited production phase. To achieve these goals, we created in total four series of knockdown strains each based on different silencing strategies. In the first series, single silencing of *aceE* was tested. Knockdown strains of the second series were subject to combinatorial silencing of *aceE*. The third series was engineered for simultaneous silencing of *aceE* and *pdhR*. For the fourth and final series, we tested single silencing of *pdhR*. Strains of all four series were tested in aerobic shaking flasks. One knockdown strain from the first and third series each was characterized in lab-scale reactors including a nitrogen-limited production phase.

Identification of binding sites for CRISPR interference

For CRISPRi, we used the two-plasmid system described by Qi et al. (2013) employing pdCas9 with an anhydrotetracycline inducible dCas9 and psgRNA containing constitutively expressed sgRNA templates (Qi et al., 2013). The crucial factor for gene silencing by CRISPRi is the design of sgRNAs. As the scope of our experiments was limited, we manually examined the DNA sequence around the transcription start site of promoters for suitable target sites and used BLAST to exclude candidates with potential off-target effects based on sequence similarity. To verify this simplistic approach, we designed three sgRNAs targeting *lacZp* and conducted beta-galactosidase assays to gain an estimate of repression efficiencies in induced or non-induced state. All sgRNAs targeting *lacZp* lead to strong reduction of β -galactosidase activity and thus were sufficient to knock-down *lacZ* (Supporting Information S1).

We then designed sgRNAs for the silencing of *aceE*. The *E. coli* gene *aceE* is part of the *pdhR-aceEF-lpd* operon which is primarily transcribed from *pdhRp* with minor contributions from the internal promoter *aceEp*, potentially involving σ^S (Olvera et al., 2009; Quail et al., 1994). PdhR represses the entire operon and autoregulates its own synthesis by binding to the

pdhR promoter region. Repression by PdhR is relieved by pyruvate and PdhR controls an additional small regulon of about 20 genes (Anzai et al., 2020). CRISPRi can inhibit transcription by blocking initiation or elongation. When inhibiting transcriptional elongation, targeting the non-template strand is in general more effective than targeting the template strand (Qi et al., 2013). We drafted two potential approaches: First, CRISPRi targeting *aceEp* should block both initiation from *aceEp* as well as hinder elongation of transcripts originating from *pdhRp*. Second, CRISPRi targeting *pdhRp* should effectively block initiation for the entire *pdhR-aceEF-lpd* operon while mimicking the regulatory effects of a *pdhR* deletion (Maeda et al., 2017). To explore diverse target sites, we chose three sites around *aceEp* (232, 233 and 234), one on the template-strand and two on the non-template strand, and an additional target site close to the start of the coding region of *aceE* (235) on the non-template strand (**Fig. 18**). We then identified three target sites around *pdhRp* (327, 328 and 329) which we deemed suitable for blocking transcriptional initiation from this promoter. We opted to test CRISPRi against *aceEp* first to avoid potential side-effects of *pdhR* repression.

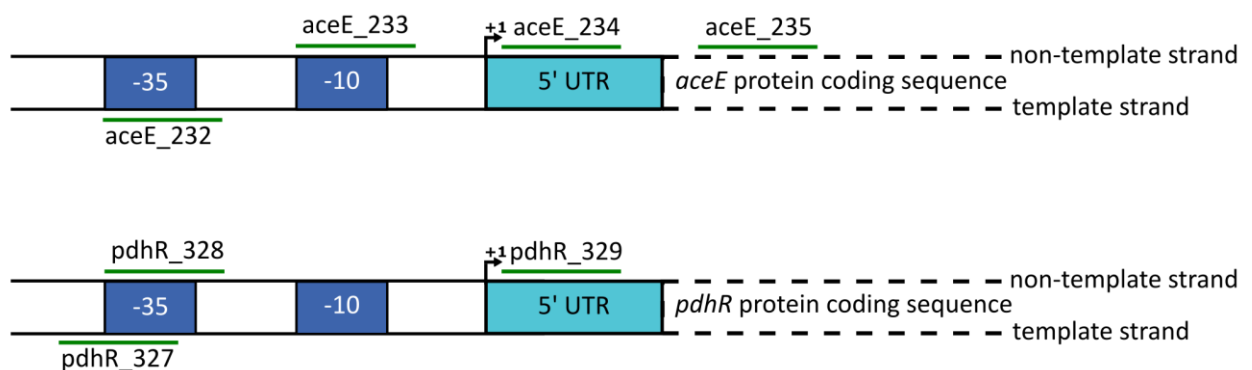


Fig. 18: sgRNA binding sites. Four binding sites (232, 233, 234 and 235) were chosen for CRISPRi targeting *aceE* and three binding sites (327,328 and 329) for CRISPRi against *pdhRp*.

Silencing of *aceE*

The four sgRNAs (232, 233, 234 and 235) targeting *aceE* were individually cloned into psgRNA and transformed into *E. coli* MG1655. Transformation with pdCas9 yielded the first series of knockdown strains. The strains were cultivated in aerobic shaking flasks in minimal medium with 0.1 $\mu\text{g/ml}$ anhydrotetracycline. Over the course of the fermentations the accumulation of pyruvate, the concomitant consumption of glucose, and the acidification of the

medium were regularly measured. Cell growth was monitored by optical density. All four sgRNAs triggered the accumulation of pyruvate, but pyruvate yield from glucose varied considerably (**Fig. 19 A**). *E. coli* MG1655 pdCas9 psgRNA_aceE_234 showed the strongest pyruvate production among strains of the first series (**Fig. 20** left panel). As we had observed leakiness of the expression system before (Supporting Information S1) we also performed shaking flask fermentations of *E. coli* MG1655 pdCas9 psgRNA_aceE_234 without addition of anhydrotetracycline but observed only minor accumulation of pyruvate (**Fig. 20** right panel).

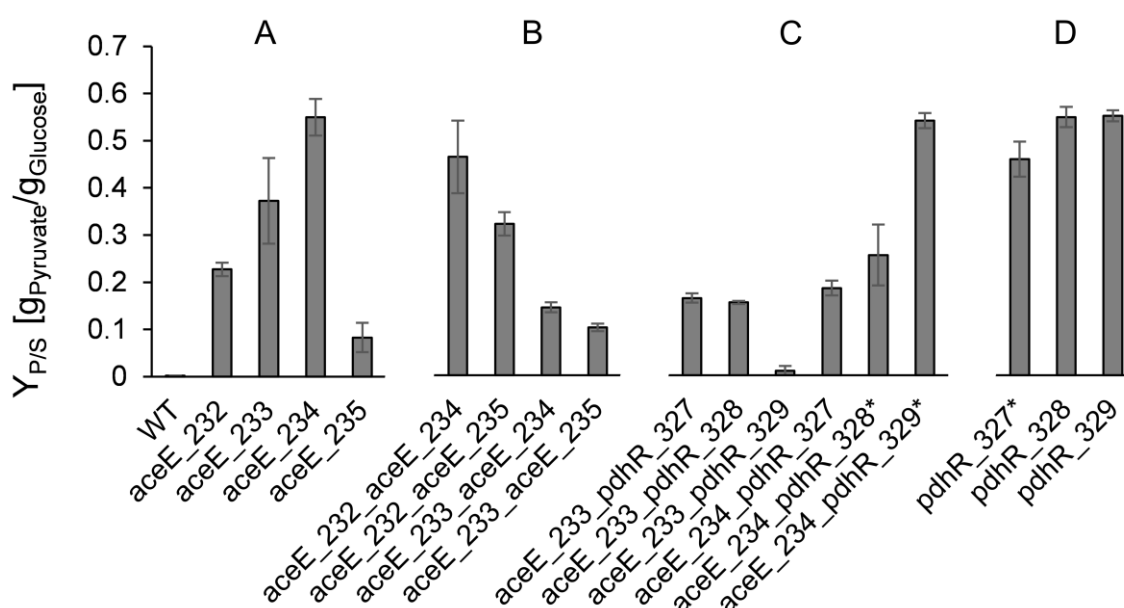


Fig. 19: Pyruvate yield in shaking flask fermentations of *E. coli* MG1655 pdCas9 with different psgRNAs. Data is grouped into four series. Error bars indicate SEM (n = 3; *n = 2). **A:** wild-type reference (no plasmids) and first series, silencing of *aceE*. **B:** second series, combinatorial silencing of *aceE*. **C:** third series, simultaneous silencing of *aceE* and *pdhR*. **D:** fourth series, silencing of *pdhR*.

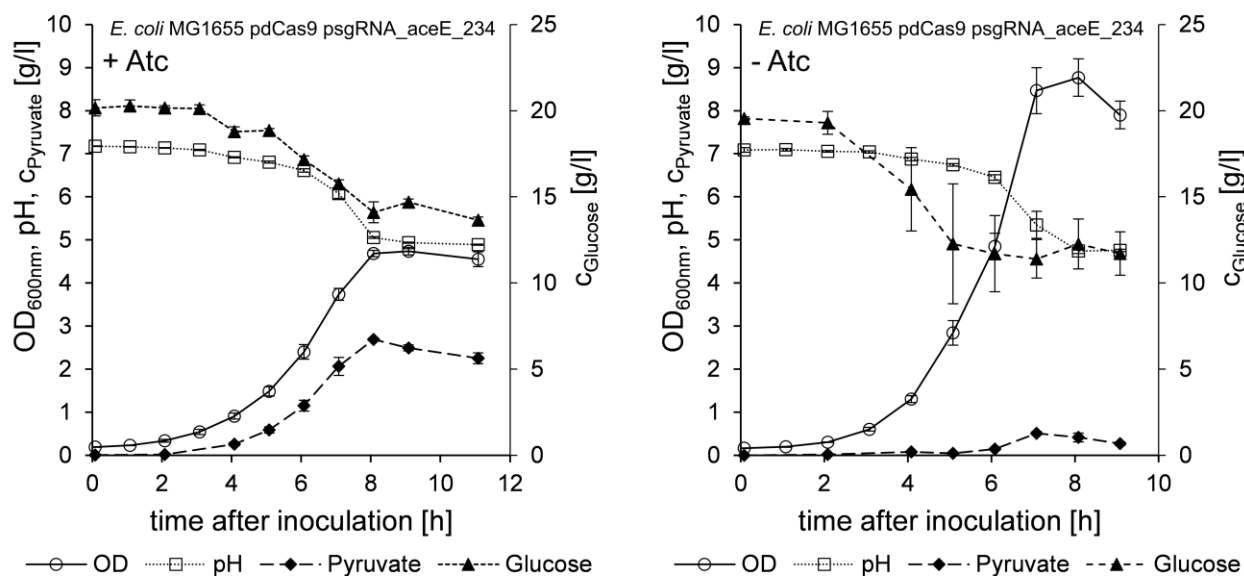


Fig. 20: Shaking flask fermentations of the single knockdown strain *E. coli* pdCas9 psgRNA_aceE_234. The experiments were conducted with addition of the inducer anhydrotetracycline (left) or without anhydrotetracycline (right). Error bars indicate SEM ($n = 3$).

To clarify the influence of anhydrotetracycline concentration on the silencing efficacy we cultivated another strain of the first series, *E. coli* MG1655 pdCas9 psgRNA_aceE_233, with varying anhydrotetracycline concentrations. The addition of as little as $0.01 \mu\text{g/ml}$ anhydrotetracycline was sufficient to induce the system and trigger the accumulation of pyruvate at the expense of biomass formation (**Supporting Information S2**). Concentrations up to $0.5 \mu\text{g/ml}$ of anhydrotetracycline were well tolerated, but at $1.0 \mu\text{g/ml}$ anhydrotetracycline growth inhibition without additional pyruvate production occurred. Small amounts of pyruvate were produced even in the absence of inducer. We concluded that the initially chosen $0.1 \mu\text{g/ml}$ anhydrotetracycline was well within the working range and continued to use this concentration.

Loss of productivity in bioreactor cultivations of *E. coli* MG1655 pdCas9 psgRNA_aceE_234

One of our goals was to enable the production of pyruvate during an extended nitrogen-limited production phase. As *E. coli* MG1655 pdCas9 psgRNA_aceE_234 had achieved the highest specific pyruvate production in the shaking flask experiments of the first series, we chose to characterize the strain in aerobic lab-scale fermentations with controlled pH. The composition of the minimal medium included excessive glucose and trace elements, with ammonium as the limiting nutrient. During the initial exponential batch-phase *E. coli* MG1655 pdCas9 psgRNA_aceE_234 grew fast and accumulated a maximum of 2.91 g/l pyruvate (**Fig. 21** left panel). However, upon depletion of ammonium the production of pyruvate stopped, and slow reuptake and consumption occurred over the remaining course of the fermentation (**Table 8**). In parallel *E. coli* MG1655 pdCas9 psgRNA_aceE_234 produced 2-oxoglutarate to a final concentration of 3.6 g/l and formed small amounts of lactate and acetate as further byproducts. We concluded that the CRISPRi silencing efficacy by single targeting of *aceE* was insufficient to maintain pyruvate production and prevent its consumption at low metabolic rates.

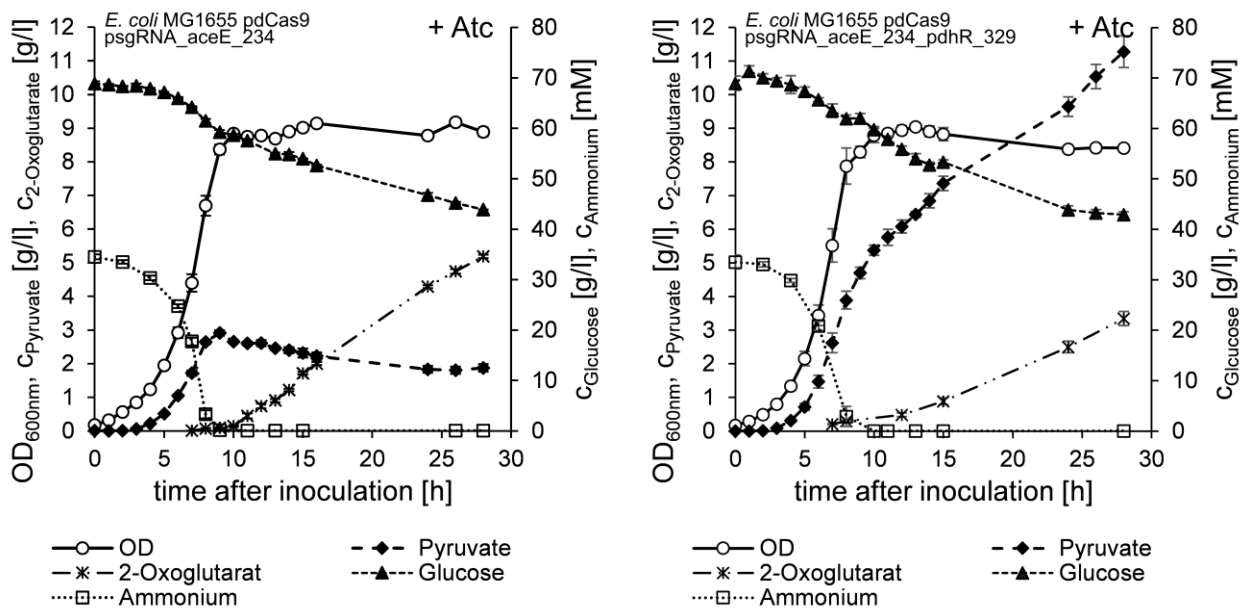


Fig. 21: Bioreactor cultivations of knockdown strains. The aerobic lab-scale fermentations were carried out with excessive glucose. Depletion of ammonia initiates the nitrogen-limited second process phase. Error bars indicate SEM. Left: The best single knockdown strain from the 1st series *E. coli* MG1655 pdCas9 psgRNA_aceE_234 (n = 3). Right: The best double knockdown strain from the 3rd series *E. coli* MG1655 pdCas9 psgRNA_aceE_234_pdhR_329 (n = 5).

Table 8: Yield coefficients and fermentation parameters of bioreactor fermentations with extended nitrogen-limited production phase.

symbol	unit	<i>E. coli</i> MG1655 pdCas9 psgRNA_aceE_234		<i>E. coli</i> MG1655 pdCas9 psgRNA_aceE_234_pdhR_329	
		exp. phase	N-lim. phase	exp. phase	N-lim. phase
μ	$[h^{-1}]$	0.414 ± 0.0042^a	-	0.472 ± 0.0078	-
$Y_{X/S}$	$\left[\frac{g_{CDW}}{g_{Glucose}} \right]$	0.270 ± 0.0072	-	0.29 ± 0.036	-
q_s	$\left[\frac{g_{Glucose}}{g_{CDW} * h} \right]$	1.53 ± 0.046	0.30 ± 0.011	1.8 ± 0.24	0.38 ± 0.013
$Y_{P/S}$	$\left[\frac{g_{Pyruvate}}{g_{Glucose}} \right]$	0.40 ± 0.018	-	0.50 ± 0.065	0.36 ± 0.029
q_p	$\left[\frac{g_{Pyruvate}}{g_{CDW} * h} \right]$	0.61 ± 0.012	-0.021 ± 0.0026	0.83 ± 0.023	0.135 ± 0.0095
$Y_{2-Oxo/S}$	$\left[\frac{g_{2-Oxoglutarate}}{g_{Glucose}} \right]$	0.010 ± 0.0018	0.332 ± 0.0073	0.0390 ± 0.0065	0.16 ± 0.012
q_{2-Oxo}	$\left[\frac{g_{2-Oxoglutarate}}{g_{CDW} * h} \right]$	0.016 ± 0.0029	0.010 ± 0.0016	0.063 ± 0.0022	0.062 ± 0.0054

a: Errors indicate SEM, *E. coli* MG1655 pdCas9 psgRNA_aceE_234 (n = 3), *E. coli* MG1655 pdCas9 psgRNA_aceE_234_pdhR_329 (n = 5).

Combinatorial silencing of *aceE*

We hypothesized that stronger repression of *aceE* might be sufficient to prevent the complete decarboxylation of pyruvate in the TCA cycle at low metabolic rates. In shaking flask experiments of the first series of knockdown strains each sgRNA alone was sufficient to enable the production of pyruvate (**Fig. 19 A**), so we presumed that a combinatorial repression of *aceE* by CRISPRi with two sgRNAs might be beneficial for the stabilization of pyruvate production. Multiplex CRISPRi against a single gene or multiple genes was successfully applied in other studies to obtain desired phenotypes (Gao et al., 2018; Zhang et al., 2018a). We thus constructed a second series of strains with four different combinations of sgRNAs targeting *aceE* (232+234, 232+235, 233+234 and 233+235). However, cultivation in shaking flask fermentations revealed that none of the strains showed beneficial properties surpassing those of the first series (**Fig.**

19 B). On the contrary, the combinatorial silencing approach appeared to be detrimental in general. Except for *E. coli* MG1655 pdCas9 psgRNA_aceE_232_aceE_235 (Fig. 22) none of the combinatorial knockdown strains could reach the pyruvate yield of the respective single knockdown strains. We suspected that close binding of multiple sgRNA-dCas9 complexes to *aceEp* could cause the declining pyruvate yield, so targeting multiple more distant sites might be a feasible alternative. As the promoter of *pdhR* strongly drives expression of *aceE* in presence of pyruvate, we hypothesized that simultaneously targeting *pdhRp* and *aceEp* might lead to effective repression of *aceE*.

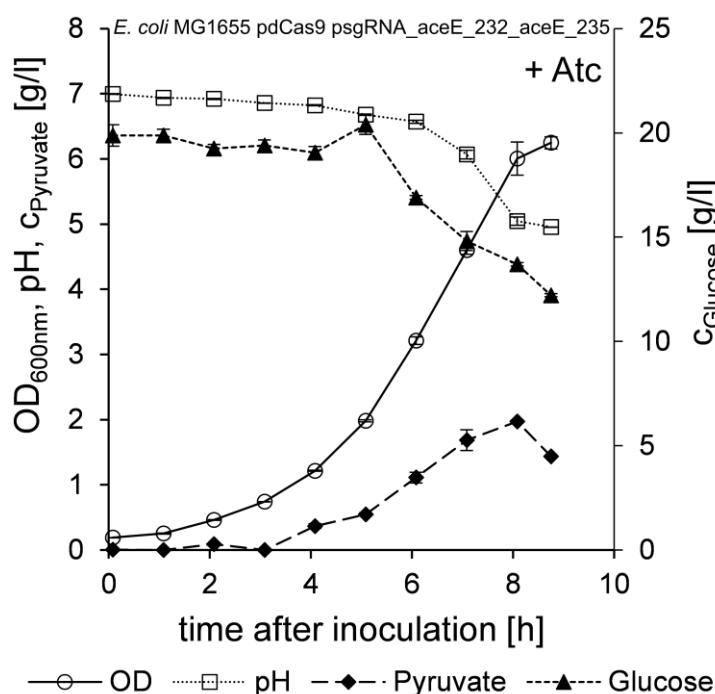


Fig. 22: Shaking flask fermentations of the double knockdown strain *E. coli* MG1655 pdCas9 psgRNA_aceE_232_aceE_235. Error bars indicate SEM (n = 3).

Simultaneous silencing of *aceE* and *pdhR* enables stable pyruvate production in extended bioreactor cultivations

We tested six different combinations of sgRNAs targeting *aceEp* and *pdhRp* (233+327, 233+328, 233+329, 234+327, 234+328 and 234+329) in a third series of knockdown strains in shaking flask experiments (Fig. 19 C). Surprisingly, most of the double knockdown strains were clearly inferior to the single *aceE* knockdown variants from the first series. However, one

strain, *E. coli* MG1655 pdCas9 psgRNA_aceE_234_pdhR_329, retained the ability to strongly produce pyruvate while benefitting from a high maximum specific growth rate. We therefore decided to characterize the strain in lab-scale bioreactors to determine its ability to produce pyruvate in an extended nitrogen-limited production phase using identical conditions as described before: excessive glucose was provided, and ammonium was used as the limiting nutrient (**Fig. 21** right panel, **Table 8**). During the exponential batch phase *E. coli* MG1655 pdCas9 psgRNA_aceE_234_pdhR_329 accumulated about 4 g/l pyruvate. When the nitrogen supply was exhausted and growth ceased, the strain continued to produce pyruvate constantly over the entire remaining process time for more than 15 h. After 28 h the final fermentation sample was drawn, and a pyruvate content of 11.28 g/l was measured. Despite the accumulation of 2-oxoglutarate as the primary byproduct the specific pyruvate production rate was stable during the nitrogen-limited phase, albeit much lower than during the exponential phase. 2-oxoglutarate accumulated to a final concentration of 3.34 g/l. Other organic acids were produced in much smaller amounts: The final titer for lactate was 0.40 g/l and the final titer for acetate 0.37 g/l. No ethanol or formate were detected in the final fermentation sample.

Compared to the performance of *E. coli* MG1655 pdCas9 psgRNA_aceE_234 the double knockdown strain *E. coli* MG1655 pdCas9 psgRNA_aceE_234_pdhR_329 was clearly superior. Not only did it achieve the stable production of pyruvate during the nitrogen-limited phase but also had significantly higher maximum specific growth rate (two-tailed t-test, $p < 0.01$) and biomass specific pyruvate productivity (two-tailed t-test, $p < 0.01$) during the exponential phase. Probably owing to constant pyruvate production it also had a significantly higher specific glucose consumption rate during the nitrogen limited phase (two-tailed t-test, $p < 0.01$).

Silencing of *pdhR*

Based on our observations with strains from the third series, we were intrigued whether targeting only the promoter region of *pdhR* would be sufficient to trigger strong accumulation of pyruvate. We thus tested a fourth series of knockdown strains with the three different sgRNAs (327, 328 and 329) targeting the promoter region of *pdhR* (**Fig. 18**). Exemplary shaking flask fermentation data from *E. coli* MG1655 pdCas9 psgRNA_pdhR_329 is shown in **Fig. 23**. All three strains carrying a sgRNA targeting *pdhRp* exhibited a similar phenotype and

strongly produced pyruvate (**Fig. 19 D**). In fact, pyruvate yield was higher than for most strains from the third series and comparable to that of *E. coli* MG1655 pdCas9 psgRNA_aceE_234 and *E. coli* MG1655 pdCas9 psgRNA_aceE_234_pdhR_329 in the shaking flask experiments. Future studies may reveal whether the strains from the fourth series share the stable pyruvate production phenotype of *E. coli* MG1655 pdCas9 psgRNA_aceE_234_pdhR_329 during a nitrogen-limited production phase.

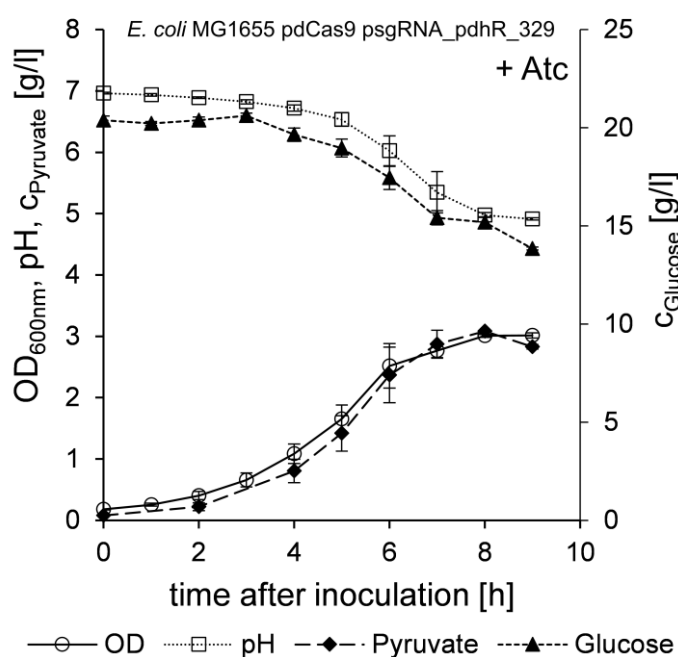


Fig. 23: Shaking flask fermentations of the single knockdown strain *E. coli* MG1655 pdCas9 psgRNA_aceE_pdhR_329. Error bars indicate SEM (n = 3).

4.3.6 Discussion

CRISPRi enables the rapid targeted silencing of virtually any non-essential gene for the purpose of metabolic engineering. In this study, we applied CRISPRi to reduce the expression of *aceE* resulting in the accumulation of pyruvate in aerobic fermentations. All sgRNAs tested enabled pyruvate production in shaking flasks, but at substantially differing yields. The simultaneous targeting of *aceE* and *pdhR* in *E. coli* MG1655 pdCas9 psgRNA_aceE_234_pdhR_329 lead

to the stable production of pyruvate at low metabolic rates during a nitrogen-limited production phase.

The sgRNAs targeting *aceE* were designed to block transcript elongation originating from *pdhRp* and initiation from *aceEp*. Given that construct psgRNA_aceE_235, designed to only block elongation, showed the poorest performance we conclude that effective silencing is most easily accomplished by targeting promoter regions. Construct psgRNA_aceE_232 was clearly less effective than psgRNA_aceE_233 and psgRNA_aceE_234 confirming the importance of targeting the non-template strand. In the case of *pdhRp* all target sites were located close to the transcription initiation site and appeared well suited. These observations are well in line with previously published findings concerning the choice of CRISPRi targets (Qi et al., 2013). Besides the good silencing efficacy, we observed substantial repression in the absence of inducer and even the lowest tested anhydrotetracycline concentration of 0.01 µg/ml was sufficient to exert repression (Supporting Information S2). We conclude that silencing efficacy should be fine-tuned by sgRNA design rather than by expression level of dCas9 if a specific level of activity is desired. Low cellular dCas9 levels are in principle desirable anyway, as toxic effects can occur if sgRNAs with certain seed sequences are used in conjunction with high dCas9 concentration (Cui et al., 2018).

Attempts to improve silencing of *aceE* by combinatorial CRISPRi against multiple target sites in *aceEp* were largely unsuccessful. In fact, there were detrimental effects, and except for *E. coli* MG1655 pdCas9 psgRNA_aceE_232_aceE_235 we could not achieve relevant improvements in any of the *aceE* double knockdown strains. Targeting the coding region of a gene with multiple sgRNAs was successful in other studies if the two target sites were sufficiently apart (Qi et al., 2013; Zhang et al., 2018a). It appears that these observations cannot be generally transferred to multiple targets within promoter regions. Regarding the distance between multiple target sites, data collected with Cas9 nickase showed that an offset of 8 base pairs was sufficient to allow the binding of multiple Cas9 complexes (Ran et al., 2013). This condition was fulfilled by all double knockdown strains except *E. coli* MG1655 pdCas9 psgRNA_aceE_233_aceE_234. The inefficacy of most silencing combinations targeting *aceEp* and *pdhRp* was even more puzzling. While *E. coli* MG1655 pdCas9 psgRNA_aceE_234_pdhR_329 achieved the phenotype we were aiming for, mechanistic investigations, which were out of the scope of this study, are necessary to unravel why only this specific combination worked. A first approach could be to measure transcript levels of *aceE*

and *pdhR* and investigate plasmid stability and integrity to exclude inactivation of the system. In-depth studies could then unravel interactions between the individual sgRNAs.

The stable production of pyruvate by *E. coli* MG1655 pdCas9 psgRNA_aceE_234_pdhR_329 during the nitrogen-limited production phase in the bioreactor fermentations was achieved by simultaneously targeting both *aceEp* and *pdhRp*. Pyruvate accumulation and the repression of *pdhR* can potentially influence cellular regulatory cascades. In wild-type *E. coli* PdhR autoregulates its own synthesis and serves as a regulator to 16 – 23 other genes (Anzai et al., 2020). Its central function is to relieve the repression of *pdhRp* at high pyruvate concentrations, thereby enhancing the expression of *pdhR*, *aceE* and *aceF* which accelerates pyruvate degradation to acetyl-CoA. Moreover, the PyrSR and BtsSR systems also sense pyruvate and each alters the expression of a small set of regulated genes (Miyake et al., 2019; Ogasawara et al., 2019). Despite the repression of *pdhR* in several knockdown strains and the concomitantly high pyruvate concentration, we did not observe detrimental effects due to altered regulation in any strain. Given the binary outer circumstances – glucose excess and complete nitrogen starvation – during the nitrogen-limited phase in the bioreactor fermentations of *E. coli* MG1655 pdCas9 psgRNA_aceE_234_pdhR_329 we presume that other regulatory responses such as the Ntr regulon dominated cellular adaptation. On the level of metabolite control, the concentration of 2-oxoglutarate controls glucose uptake by competition with phosphoenolpyruvate for its binding site at the phosphotransferase system and limits the metabolic rates in prolonged nitrogen starvation (Huergo and Dixon, 2015). Glucose uptake was strongly reduced in the fermentations of both *E. coli* MG1655 pdCas9 psgRNA_aceE_234 and *E. coli* MG1655 pdCas9 psgRNA_aceE_234_pdhR_329 during the extended production phase compared to the exponential phase. However, despite the continued accumulation of 2-oxoglutarate in the fermentation broth during the entire nitrogen-limited phase, the specific glucose uptake rates were constant. Glucose uptake was thus either enabled by continued 2-oxoglutarate export or through the activation of other mechanisms. In another study, glucose uptake reduction in nitrogen-limited conditions was alleviated by moderate overexpression of *ptsI* which indicates that the cellular levels of 2-oxoglutarate, PtsI and phosphoenolpyruvate are naturally tightly balanced (Chubukov et al., 2017).

Even though *E. coli* MG1655 pdCas9 psgRNA_aceE_234_pdhR_329 accumulated less 2-oxoglutarate than *E. coli* MG1655 pdCas9 psgRNA_aceE_234 during the nitrogen-limited production phase, a substantial flux into the TCA cycle remained as proven by the continued

formation of 2-oxoglutarate. Additional repression of pyruvate dehydrogenase activity and subsequently increased pyruvate yield from glucose could potentially be achieved by CRISPRi targeting the coding sequence of *aceF*. Deletions or repression of *poxB* and *ldhA* would likely further increase pyruvate yield from glucose and reduce the accumulation of lactate. Since the experimental yields observed during the fermentations of *E. coli* MG1655 pdCas9 psgRNA_aceE_234_pdhR_329 were lower in the nitrogen-limited fermentation phase, pyruvate yield appeared to be dependent on the specific glucose uptake rate. We suggest that pyruvate productivity could be indirectly improved by increasing specific glucose uptake, for instance by engineering *ptsI* overexpression from a promoter induced in nitrogen-limited conditions.

The use case and metabolic behavior of our strains are similar to those from the studies of Michalowski et al. (2017), so direct comparison of our strains with *E. coli* HGT is feasible. During the exponential phase pyruvate yield and biomass specific pyruvate production rate of *E. coli* MG1655 pdCas9 psgRNA_aceE_234_pdhR_329 were comparable to values reported for *E. coli* HGT and *E. coli* MG1655 pdCas9 psgRNA_aceE_234_pdhR_329 achieved a higher maximum specific growth rate (Michalowski et al., 2017). However, specific pyruvate productivity was lower during the second production phase with resting cells which indicates that stronger repression of pyruvate dehydrogenase or higher glucose uptake rates on the level of *E. coli* HGT may be necessary to improve the production phenotype of *E. coli* MG1655 pdCas9 psgRNA_aceE_234_pdhR_329. Extending the comparison to acetate auxotrophic strains, *E. coli* MG1655 pdCas9 psgRNA_aceE_234_pdhR_329 has clearly lower metabolic rates, but does not suffer from the disadvantage of dependence on acetate addition (Zhu et al., 2008). Limiting the supply of acetate may lead to reduced productivity and even pyruvate reuptake in auxotrophic strains (Zelić et al., 2003).

A potential advantage of CRISPRi compared to other genetic modifications to lower gene expression or enzymatic activity is its inherent flexibility to switch off or tune metabolic pathways during a process. A promising strategy for regulating access of different metabolic pathways to the pyruvate pool is the addition of dynamic control circuits (Brockman and Prather, 2015). Both a circuit based on PdhR and a dynamic CRISPRi silencing strategy have been applied successfully in *Bacillus subtilis* and the principle can likely be transferred to *E. coli* (Wu et al., 2020; Xu et al., 2020). Integration of a pyruvate-sensing circuit based on PdhR would require initial modifications of the genomic elements of the *pdhR*, *aceE* and *aceF*

loci but would then enable rapid phenotyping of dynamic control strategies by modulated transcription of dCas9 or sgRNAs targeting key genes of competing pathways.

In conclusion, we successfully engineered CRISPRi knockdown strains for the stable production of pyruvate during two-phase bioreactor fermentations. An important finding is that targeting *aceEp* with multiple sgRNAs was not successful despite sufficient distance between the target sites. Simultaneously repressing *aceEp* and *pdhRp* improved pyruvate accumulation during the exponential phase and was sufficient to enable constant pyruvate production during a nitrogen-limited phase. Furthermore, targeting *pdhR* alone was sufficient to enable strong pyruvate production in shaking flasks. Our study provides a foundation for controlled production of pyruvate and pyruvate-derived products in *E. coli*, and *E. coli* MG1655 pdCas9 psgRNA_aceE_234_pdhR_329 may serve as a chassis in future investigations.

4.3.7 Acknowledgements

The authors acknowledge the support of Prasika Arulrajah for assistance with sample analysis.

5. Materials and Methods – additional experiments

This section briefly covers selected experimental procedures for experiments that were not reported in the attached publications but provided helpful insight into the major issues of this thesis. Descriptions of material or procedures already covered in the attached publications are not repeated here and referenced where applicable.

5.1 Contributions

Data presented in this thesis which was not covered in any of the attached publications was analyzed by Martin Ziegler. Some research activities were conducted by students directly supervised by Martin Ziegler:

- Clarissa Döring (Bachelor Thesis)
- Lukas Madenach (Bachelor Thesis)
- Liv Paul (Master Thesis)
- Teresa Gäbele (Master Thesis)
- Jan Notheisen (Assistant Researcher)
- Prasika Arulrajah (Assistant Researcher)

5.2 General molecular biology methods

5.2.1 Buffer and media

Growth media were prepared with deionized water and sterilized by autoclavation or filtration. The composition of trace element solution, 2xTY medium, agar plates and antibiotics is given in the attached publications (Ziegler et al., 2021a; Ziegler et al., 2021b). The working concentration of Kanamycin was 50 µg/ml. SOC medium was prepared as described previously (Hanahan, 1983).

For glycerol seed cultures 700 µl of exponentially growing culture was directly added to 300 µl sterile glycerol, briefly vortexed and stored at – 70 °C.

5. Materials and Methods – additional experiments

5.2.2 Polymerase Chain Reaction (PCR)

PCR was conducted either with Phusion High Fidelity DNA Polymerase (Thermo Scientific, F530S) or Q5 Polymerase (New England Biolabs, M0491) according to the manufacturer's instructions. Colony PCR was conducted with Taq Polymerase S (Genaxxon bioscience, M3001.0000) using Coral Red Buffer Dye solution (Genaxxon bioscience, M3309.0005) according to the manufacturer's instructions. If necessary, additives were used and modifications to protocols as recommended by the manufacturers were made. After PCR, if fragments originated from a plasmid and were intended for plasmid cloning, template DNA was digested with DpnI (New England Biolabs, R0176) in a digestion reaction as recommended by the manufacturer. Fragments were cleaned with NucleoSpin Gel and PCR Clean-up, Mini Kit (Macherey-Nagel, 740609.50) or separated by gel electrophoresis.

5.2.3 Agarose gel electrophoresis

DNA fragments were separated by agarose gel electrophoresis using TAE-buffer (1 mM EDTA (Ethylenediaminetetraacetic acid), 0.02 M acetic acid, 0.04 M TRIS (tris(hydroxymethyl)aminomethane)). DNA was loaded on an agarose gel (10 g/l agarose dissolved in TAE-buffer, briefly boiled, then cooled until solid) and electrophoresis was conducted at 90 – 130 V for 45 – 60 min. Bands of the expected size were extracted with NucleoSpin Gel and PCR Clean-up, Mini Kit (Macherey-Nagel, 740609.50) and DNA concentration measured at 260 nm on a NanoDrop 1000 Spectrophotometer (Thermo Scientific).

5.2.4 Cloning

Plasmids were isolated from overnight cultures using E.Z.N.A.® Plasmid DNA Mini Kit I (omega BIO-TEK, D6942-01). Genomic DNA was isolated using DNeasy Blood & Tissue Kit (Qiagen, 69504).

One-step isothermal DNA assembly (commonly known as “Gibson assembly”) was conducted as described elsewhere (Gibson, 2011; Gibson et al., 2009). The reaction mixture was desalted with deionized water for 20 min on a MF-Millipore™ Membrane Filter, 0.025 µm pore size (Merck, VSWP02500) and directly used for transformation.

5. Materials and Methods – additional experiments

5.2.5 Transformation

For electrocompetence, cells were grown in 15 ml 2xTY medium at 30 °C or 37 °C until reaching an optical density (OD) between 0.1 and 0.6 and centrifuged at 4 °C and 5000 rpm for 15 min. The supernatant was discarded, cells resuspended in 20 – 25 ml sterile ice-cold deionized water and centrifuged again. This procedure was repeated once, and the resulting pellet resuspended in 100 µl sterile ice-cold deionized water. Transformation was conducted with around 100 ng of DNA in 2 mm cuvettes (VWR Peqlab, 732-2920DE) in an Eppendorf Eporator (Eppendorf, 4309000019) set to 2.5 kV and 5 ms. After transformation cells were regenerated at 37 °C in SOC medium on a heating block set to 300 rpm for 1 – 4 h and plated on 2xTY agar plates.

5.3. Protein production in *E. coli* MG1655, *E. coli* CD202 and *E. coli* SR¹

5.3.1 Strains

Table 9: Strains used in the protein production experiments

Strain	Genotype/strain information	Reference
<i>E. coli</i> MG1655	F ⁻ , λ ⁻ , <i>ilvG</i> ⁻ , <i>rfb</i> -50, <i>rph</i> -1	(Michalowski et al., 2017)
<i>E. coli</i> SR	MG1655 Δ <i>relA</i> , <i>spoT</i> [R290E;K292D]	(Michalowski et al., 2017)
<i>E. coli</i> DH5α λ pir	<i>supE44</i> , Δ <i>lacU169</i> (Φ80 <i>lacZ</i> ΔM15), <i>recA1</i> , <i>endA1</i> , <i>hsdR17</i> , <i>thi</i> -1, <i>gyrA96</i> , <i>relA1</i> , λpir phage lysogen	(Michalowski et al., 2017)
<i>E. coli</i> CD202	MG1655 Δ <i>flk</i> Δ <i>fliA</i> Δ <i>fliC</i>	(Ziegler et al., 2021a)
<i>E. coli</i> DH10B p006kanGFP	Complex, see (Durfee et al., 2008b)	Addgene #58534
<i>E. coli</i> DH5α λ pir p006_kan_eGFP	<i>supE44</i> , Δ <i>lacU169</i> (Φ80 <i>lacZ</i> ΔM15), <i>recA1</i> , <i>endA1</i> , <i>hsdR17</i> , <i>thi</i> -1, <i>gyrA96</i> , <i>relA1</i> , λpir phage lysogen	This work
<i>E. coli</i> MG1655 p006_kan_eGFP	F ⁻ , λ ⁻ , <i>ilvG</i> ⁻ , <i>rfb</i> -50, <i>rph</i> -1	This work
<i>E. coli</i> SR p006_kan_eGFP	MG1655 Δ <i>relA</i> , <i>spoT</i> [R290E;K292D]	This work
<i>E. coli</i> CD202 p006_kan_eGFP	MG1655 Δ <i>flk</i> Δ <i>fliA</i> Δ <i>fliC</i>	This work

¹ These experiments were planned by Martin Ziegler and conducted in collaboration with Lukas Madenach.

5. Materials and Methods – additional experiments

5.3.2 Cloning of p006_kan_eGFP

Plasmid p006kanGFP was a gift from Jaroslaw Bryk (Addgene plasmid # 58534 ; <http://n2t.net/addgene:58534> ; RRID:Addgene_58534) and isolated from *E. coli* DH10B p006kanGFP. pOCEx1-eGFP was kindly provided by Sebastian Grenz.

Table 10: Primer for cloning of p006_kan_eGFP

Primer	Sequence 5' -> 3'
MZ_15 3	TTTTTACCTCCTTAAAAGTTAAACAAA
MZ_15 4	CCCCAAGGGCGACAC
MZ_15 5	AATTTTGTTTAACTTTTAAGGAGGTAAAAAATGAGTAAAGGAGAAGAAGCTTT TC
MZ_15 6	CGGGCTAATTAGGGGGTGTCCGCCCTTGGGGTTATTTGTATAGTTCATCCATG CC

The backbone of p006kanGFP was amplified by PCR with Phusion High Fidelity DNA Polymerase using primer pair MZ_153 and MZ_154 and eGFP was amplified from pOCEx1-eGFP using primer pair MZ_155 and MZ_156. Approximately 60 ng of each fragment were joined and circularized in a 10 µl Gibson assembly reaction. The desalted mixture was used for transformation of electrocompetent *E. coli* DH5α λ pir. Large colonies were restreaked on 2xTY agar containing 1 mM IPTG. A colony showing strong fluorescence upon exposure to UV light was picked and grown at 37 °C in 2xTY medium on a rotary shaker at 120 rpm overnight. Plasmid p006_kan_eGFP was isolated and verified by sequencing. Electrocompetent *E. coli* MG1655, *E. coli* SR and *E. coli* CD202 were prepared and transformed with p006_kan_eGFP.

5.3.3 Shaking flask experiments

Glycerol seed cultures were streaked onto 2xTY agar plates (16 g/l tryptone, 10 g/l yeast extract, 5 g/l NaCl) and incubated at 37 °C overnight. A single colony was used to inoculate

5. Materials and Methods – additional experiments

50 ml of shaking flask medium LM (4 g/l glucose, 1.06 g/l NaH₂PO₄•H₂O, K₂HPO₄, 2.66 g/l (NH₄)₂SO₄, 0.01 g/l Thiamine, and 0.2 % (V/V) trace element solution (Ziegler et al., 2021b)) in a 500 ml baffled shaking flask and incubated at 37 °C and 120 rpm on a rotary shaker overnight. The next morning, three 500 ml baffled shaking flasks each containing 50 ml of shaking flask medium LM were inoculated to an OD of approximately 0.1 and the cultures incubated at 37 °C and 120 rpm on a rotary shaker. Samples for analysis were drawn each hour. After four hours 50 µl of 1 M IPTG were added to induce protein expression. Kanamycin was added to a final concentration of 50 µg/ml to all cultivations employing strains carrying p006_kan_GFP.

Samples were diluted with deionized water and OD 600 nm was measured in polystyrol half-micro-cuvettes (Sarstedt, 67.742) on an Ultrospec 10 Cell Density Meter (Amersham Biosciences). 200 µl of freshly samples biosuspension were transferred into clear 96 flat-bottom well plates and fluorescence was measured in a Synergy 2 Microplate Reader (BioTek) using the following wavelength filters: excitation: 485/20, emission: 528/20.

5.4 Pyruvate production in *E. coli* SR²**Table 11:** Strains used in the pyruvate production experiments

Strain	Genotype/strain information	Reference
<i>E. coli</i> MG1655 pdCas9 psgRNA_aceE_234_pdhR_329	F ⁻ , λ ⁻ , <i>ilvG</i> ⁻ , <i>rfb-50</i> , <i>rph-1</i>	Attached manuscript
<i>E. coli</i> SR	MG1655 Δ <i>relA</i> , <i>spoT</i> [R290E;K292D]	(Michalowski et al., 2017)
<i>E. coli</i> SR pdCas9 psgRNA_aceE_234_pdhR_329	MG1655 Δ <i>relA</i> , <i>spoT</i> [R290E;K292D]	This work

Plasmids were isolated from *E. coli* MG1655 pdCas9 psgRNA_aceE_234_pdhR_329 and electrocompetent *E. coli* SR was co-transformed with both plasmids. Multiple colonies were picked and cultivated in shaking flasks as described in the attached manuscript. After 8 hours pyruvate concentration was measured and a strain that had accumulated more than 3 g/l pyruvate was stored as a glycerol seed culture. *E. coli* SR pdCas9 psgRNA_aceE_234_pdhR_329 was then cultivated in aerobic two-phase batch fermentations in lab-scale bioreactors as described in the attached manuscript.

² These experiments were planned by Martin Ziegler and conducted in collaboration with Teresa Gäbele.

6. Results – additional experiments

This section covers experimental results for experiments that were not reported in the attached publications but provided helpful insight into the major issues of this thesis.

6.1 Production of eGFP by *E. coli* strains

The ability of *E. coli* SR to produce heterologous proteins was compared to that of *E. coli* CD202 and their common parent strain *E. coli* MG1655. *E. coli* CD202 is an early intermediate strain from the deletion series aimed at engineering a robust *E. coli* chassis strain for large-scale fermentations (Ziegler et al., 2021a). The fluorescent protein eGFP was chosen as an easily measurable proxy for heterologous protein production. Therefore, all three strains carried p006_kan_eGFP encoding eGFP under transcriptional control of the T5 promoter and LacI. Cultivation of the strains in shaking flasks revealed that *E. coli* MG1655 and *E. coli* CD202 produced similar amounts of eGFP during the exponential phase and continued to accumulate eGFP even after growth had ceased (**Fig. 24**). In the final fermentation sample, drawn 24 h after inoculation, there was no significant difference in fluorescence between these two strains. On the other hand, *E. coli* SR clearly produced less eGFP during the exponential phase and fluorescence even declined at the end of the exponential phase indicating degradation of eGFP. Fluorescence measured in the final fermentation sample of *E. coli* SR was significantly lower than in the samples from *E. coli* MG1655 (two-tailed t-test, $p < 0.01$) or *E. coli* CD202 (two-tailed t-test, $p < 0.01$).

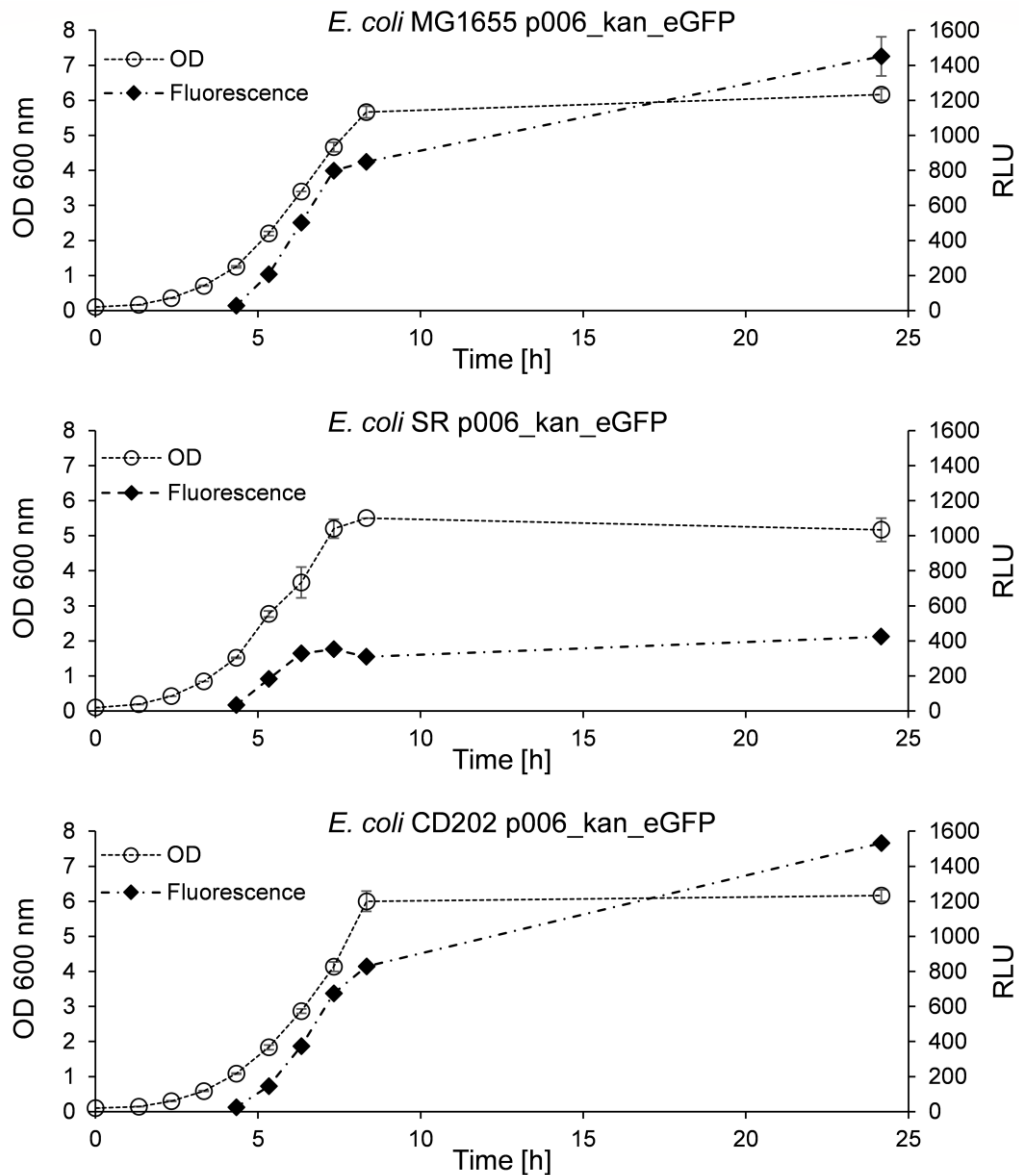


Fig. 24: Production of eGFP in *E. coli* SR. The indicated strains were cultivated in aerobic shaking flasks in minimal medium. Inducer was added 4 h after inoculation. Error bars represent SEM (n = 3).

6.2 Cultivation of *E. coli* SR pdCas9 psgRNA_aceE_234_pdhR_329

Small-scale laboratory fermentations of *E. coli* SR pdCas9 psgRNA_aceE_234_pdhR_329 were conducted to investigate the potential of this strain to produce pyruvate. Fermentations were conducted in minimal medium with excess glucose and ammonium as the limiting nutrient. Cells grew exponentially until ammonium was exhausted and produced small amounts of pyruvate during this phase (**Fig. 25**). After growth ceased, the strain continued to consume glucose, but no additional pyruvate was formed, and the optical density declined continuously until the end of the process.

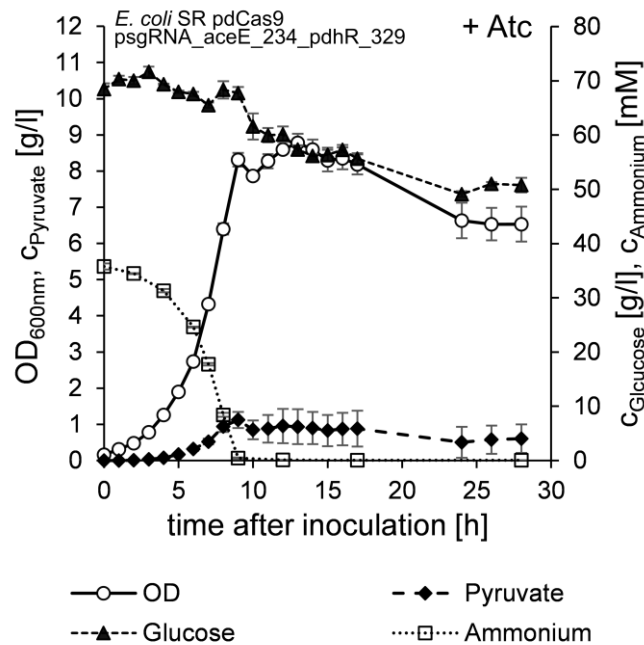


Fig. 25: Fermentation profile of *E. coli* SR pdCas9 psgRNA_aceE_234_pdhR_329 with inducer anhydrotetracycline (+ Atc). Error bars indicate SEM (n = 3).

7. Discussion

The central research questions addressed in this thesis concerned the engineering and characterization of potential *E. coli* chassis strains and process concepts for large-scale cultivations (see: **3. Objectives and research questions of this thesis**). **Table 12** provides a short summary of the scientific output of the peer-reviewed publications that form the core of this thesis as well as the additional data presented in the preceding chapter. For simplicity, the projects are referred to as **P-I**, **P-II**, **P-III** and **P-A** as indicated in **Table 12**.

The following sections embed the findings of this thesis in a broader scientific context and discuss how they relate to each other. Major emphasis is put on connecting and extending the common scientific aspects of the research projects. Since discussions of the individual results of each project are already part of the attached publications, these are only superficially touched upon here.

Table 12: Scientific output

No.	Project	Central findings
P-I	Transcriptional profiling of the stringent response mutant strain <i>E. coli</i> SR reveals enhanced robustness to large-scale conditions	<p><i>E. coli</i> SR exhibited a reduced short-term transcriptional response to repeated exposure to nitrogen-starvation compared to <i>E. coli</i> MG1655. <i>E. coli</i> SR did not accumulate ppGpp in such conditions and activated more general SOS responses instead of the stringent response. <i>E. coli</i> SR maintained fully functional ammonium assimilation and biomass formation (Ziegler et al., 2021b).</p> <p>In conclusion, modified global regulation allows restructured transcriptional responses and can dampen undesirable cellular adaptation to heterogeneous conditions.</p>
P-II	Engineering of a robust <i>Escherichia coli</i> chassis and exploitation for large-scale production processes	<p>A series of deletion strains lacking genes with high metabolic costs in repeated starvation conditions was constructed. <i>E. coli</i> RM214 had a lower maintenance coefficient than <i>E. coli</i> MG1655 when exposed to repeated glucose starvation. <i>E. coli</i> RM214 <i>rhaB</i>⁻ pJOE4056.2_tetA had lower productivity losses than <i>E. coli</i> MG1655 <i>rhaB</i>⁻ pJOE4056.2_tetA when producing eGFP under heterogeneous conditions (Ziegler et al., 2021a).</p> <p>The strain design approach tested in this study allowed the engineering of a robust strain and has the potential to be applied to other strenuous conditions.</p>

Table 5: Scientific Output (continued)

No.	Project	Central findings
P-III	CRISPRi enables fast growth followed by stable aerobic pyruvate formation in <i>Escherichia coli</i> without auxotrophy	<p>CRISPRi was used to reduce the expression of pyruvate dehydrogenase which resulted in the aerobic accumulation of pyruvate. The strain <i>E. coli</i> MG1655 pdCas9 psgRNA_aceE_234_pdhR_329 produced pyruvate during both the exponential phase and an extended nitrogen-limited production phase.</p> <p>CRISPR interference was shown to be a flexible and useful tool for the construction of production strains. The design of sgRNAs was critical for the repression efficiency and the stability of the production phenotype.</p>
P-A	Additional results shown in this document	<p><i>E. coli</i> SR produced significantly less eGFP than <i>E. coli</i> MG1655 or <i>E. coli</i> CD202 and degraded eGFP after growth ceased. <i>E. coli</i> SR pdCas9 psgRNA_aceE_234_pdhR_329 accumulated only minor amounts of pyruvate during the exponential phase and did not produce additional pyruvate during the nitrogen-limited second process phase.</p> <p>The differences between <i>E. coli</i> SR and other <i>E. coli</i> strains regarding their applicability for production processes indicates that the modulated regulation of <i>E. coli</i> SR interferes with standard expression systems. The development of new expression systems may be necessary to enable efficient production in <i>E. coli</i> SR.</p>

7.1 Robustness of *E. coli* RM214 and *E. coli* SR to heterogeneous conditions

The strains *E. coli* RM214 and *E. coli* SR were each compared to their parent strain *E. coli* MG1655 regarding potential benefits in heterogeneous fermentations with repeated exposure to starvation zones (**P-I** and **P-II**). Early studies in the field had shown that *E. coli* reacted to repeated glucose starvation by rapid initiation of the stringent response and that the biomass yield was decreased under such conditions (Neubauer et al., 1995b; Neubauer et al., 1995a). These findings were later extended to nitrogen starvation and it was proposed that wasteful expression of a large number of specific genes due to repeated initiation and abortion of the stringent response may cause an increase in maintenance demand (Löffler et al., 2016; Simen et al., 2017). For the construction of a robust chassis strain two possible strategies were apparent: First, a strain with modulated stringent response could potentially profit from the complete absence of the regulatory program. *E. coli* SR was identified as a suitable strain to test this approach (Michalowski et al., 2017). Second, a tailored deletion strain lacking genes that were presumably responsible for an increase in maintenance demand could benefit from a reduced metabolic demand while maintaining the overall regulatory program. This second approach was realized by construction of the deletion strain series as part of **P-II**.

Data collected in **P-I** and **P-II** shows that both approaches have generally resulted in more robust strains, however, in quite different regard. *E. coli* RM214 had a lower maintenance coefficient in STR-PFR conditions using glucose as a limiting substrate. This trait proved to be beneficial in an exemplary production process where the strain remained significantly more productive when facing repeated glucose starvation stimuli. The robustness of *E. coli* RM214 is thus expressed on the proteomic and metabolic level and can be harnessed to improve the performance of a bioprocess. In case of *E. coli* SR potential advantages over its wild-type parent were less directly observed on the level of transcriptional regulation. Due to the absence of the stringent response, *E. coli* SR showed a reduced transcriptional short-term response to nitrogen starvation but maintained fully functional ammonium uptake and biomass formation in minimal medium. Long-term adaptation, possibly including alternative pathways to achieve growth arrest, occurred through negative transcriptional regulation and SOS pathways. It was estimated that the reduced regulatory patterns could enable maintenance savings of up to 46.5% compared to *E. coli* MG1655. No significant differences in physiological process parameters were found,

but it must be considered that the scenario chosen for the transcriptomic studies was not designed to assess potential advantages that *E. coli* SR might exhibit in a production scenario. As this issue remains open, the general usability of *E. coli* SR for biotechnological production is comprehensively discussed in subchapter **7.3 Modulating global cellular regulation – the case of *E. coli* SR**.

This begs the question of which approach is superior and whether they are complementary or mutually exclusive in nature. Judging from the available data, only *E. coli* RM214 showed a phenotype that was beneficial beyond doubt. Technically, the mutations in *spoT* and the deletion of *relA* which result in the phenotype of *E. coli* SR could be transferred into *E. coli* RM214, but it appears unlikely that major beneficial effects could be achieved. The deletions realized in *E. coli* RM214 already cover most of the clearly irrelevant high-impact targets that were identified in the preceding study by Löffler *et al.* (2016). Additional savings by reduced global regulation would thus mostly originate from reduced regulation of process relevant genes. Potential side-effects are a general drawback of modulating large cellular regulons that can only be circumvented by intelligent choice of targets.

The work of Lastiri-Pancardo *et al.* (2020) demonstrates a middle path between the conflicting strategies used in the design of *E. coli* RM214 and *E. coli* SR. The authors established a method termed ReProMin, which aims to free proteomic resources by deletion of a small set of transcription factors predicted to not interfere with major relevant genes. Strain PFC carrying deletions of *phoB*, *flhC* and *cueR* displayed improved heterologous protein production. The study demonstrates the major advantage when targeting transcriptional regulators: a small number of genetic modifications can lead to relatively large performance increases. However, the inherent limitation is also apparent: There are only very few transcription factors in *E. coli* that have both a major impact and do not regulate process-relevant genes in a typical heterologous protein production scenario in glucose minimal medium. In fact, even the PFC variant carrying deletions of only three minor transcription factors had a significantly lower specific growth rate than its wild-type strain in minimal medium (La Cruz *et al.*, 2020). Considering the progress made in the last years in the field of genomic engineering, it appears short-sighted to regard the number of modification steps necessary to achieve a desired phenotype as the limiting factor. Even complex projects encompassing > 50 genomic modifications can be reliably handled in workflows such as CRISPR/Cas-selected MAGE (Umenhoffer *et al.*, 2017).

Another alternative approach was presented by Sharma *et al.* (2020), who attempted to reduce cellular stress responses by targeted deletion of genes that are commonly upregulated post induction. This strategy is similar to the approach used when constructing *E. coli* RM214 in **P-II**. The deletion of only two handpicked genes, *elaA* and either *cysW* or *cueR*, was sufficient to double the final titer of recombinant asparaginase (Sharma et al., 2020). A limitation of this study is that cells were cultivated in complex media in milliliter scale, so it remains to be shown how the performance of these strains transfers across scales and into a fed-batch process.

In conclusion, it appears that a tailored strategy targeting individual hand-picked genes compares favorably to approaches aimed at abolishing large regulatory circuits. While deleting regulatory circuits has the advantage of simultaneously altering the expression level of many genes, potential side-effects are difficult to predict and can negatively influence key physiological parameters. Moreover, regarding the case of repeated exposure to starvation zones, which was investigated in **P-I** and **P-II**, it remains to be investigated whether the presence of a functional stringent response may be beneficial for *E. coli* strains despite an increased maintenance coefficient. To test this hypothesis production strains of *E. coli* SR and *E. coli* MG1655 could be compared in glucose-limited STR-PFR fermentations. Alternatively, the performance of *E. coli* MG1655 carrying genetic constructs for CRISPRi against *relA* or a control locus could be compared under scale-down conditions.

7.2 Simulating large-scale conditions with scale-down reactors

In **P-I** and **P-II** *E. coli* strains were examined under heterogeneous conditions in a two-compartment scale-down reactor designed to simulate starvation zones as encountered in large-scale conditions. The average residence time in the plug-flow reactor simulating a glucose (**P-II**) or nitrogen (**P-I**) starvation zone was 156 s and about 23.75% of the total reaction volume circulated through the PFR. The question needs to be addressed whether these values are representative for large-scale industrial reactors. Studies in the field have employed vastly different residence times ranging from less than 1 min to more than 3 min in the PFR of a two-compartment reactor to study biological effects of the installed stimulus (Delvigne et al., 2009; Lara et al., 2006b; Neubauer et al., 1995b; Neubauer et al., 1995a). This diversity reflects that the circulation time and mixing time of bioreactors greatly depend on the working volume and reactor setup, so in principle no single scale-down reactor can accurately reflect all possible configurations (Delvigne et al., 2006; Noorman, 2011).

The biologically relevant measure for accurate scale-down is the average residence time in a specified regime such as a starvation zone. Studies on the flow field in bioreactors by particle image velocimetry are scarce, so simulations currently provide the best estimate. In a seminal study, Haringa *et al.* (2017) described simulations of a well-studied 22 m³ reactor used for aerobic fermentation of *S. cerevisiae* and proposed guidelines for the design of a representative scale-down reactor. This design comprises three interconnected stirred-tank reactors each representing one nutrient regime. The starvation zone makes up about 35% of the total reaction volume with a mean residence time of only about 35 s. However, given the stochastic nature of mixing in an STR, a single cell could face starvation much longer, in an example scenario > 2 min (Haringa et al., 2017). The conditions used in the experiments presented in **P-I** and **P-II** thus represent scenarios with very long continued exposure to starvation zones, bordering worst-case scenarios. The choice of a PFR as a second compartment likely reduces the representativeness, as the system lacks frequent transitions of cells with only short residence time in each compartment, but it provides the practical advantage of enabling the study of biological responses over stimulus exposure time. In **P-I** this property was critical for the collection of representative transcriptional data and in **P-II** measurements of the AEC would otherwise not have been possible. As a sidenote, using an excessively long residence time as a stimulus may even be advantageous from a scientific point of view. It facilitates the observation of biological adaptation and the discovery of new mechanisms that might otherwise be masked

by compensatory mechanisms or lost in analysis due to insufficient statistical power. For instance, installing a residence time of 3.6 min was necessary to reveal the full kinetics of short-term ppGpp formation in *E. coli* (Neubauer et al., 1995a).

The cultivations carried out in **P-I** and **P-II** were operated as continuous chemostats. In industrial settings, the use of chemostats is rare. Fed-batch fermentations are preferred, as the high biomass concentrations that can be achieved allow high volumetric rates and product titers which in turn facilitate downstream processing. How valid is it to transfer data collected with chemostats to fed-batch scenarios? When studying physiological responses, the outer circumstances and intracellular fluxes define the cellular state. Cells that are cultivated in both fed-batch or chemostat processes are in a balanced growth state. Chemostats are defined by the property that no changes in concentrations or fluxes occur unless an external stimulus is introduced. Concentrations are dynamic in fed-batch cultivations, but biomass specific fluxes change only slowly and can even be constant if an exponential feeding strategy is used. Therefore, it is feasible to transfer chemostat data from scale-down experiments to fed-batch fermentations if a central limitation is kept in mind: The heterogeneities in an actual fed-batch reactor are time-dependent because reaction volume, biomass concentration and power input all change over the course of the fermentation.

Differences between process scales as well as between chemostats and fed-batch fermentations are also caused by the evolutionary aspects of any microbiological process. Bioprocesses select for cells with growth advantages which can lead to the emergence of non-producer populations (Rugbjerg et al., 2018; Sleight and Sauro, 2013). In order to be representative, scale-down studies should thus consider an appropriate generation number. Rugbjerg *et al.* (2018) estimated that a large-scale microbial process requires in total 63 generations from strain construction to final OD for a reactor with a working volume of 10 m³, and 67 generations for a working volume of 200 m³. Of this number, 25 to 30 generations pass during preculture and the actual fermentation. The remainder already accumulates during strain construction until a master cell bank is available (Rugbjerg et al., 2018).

The required generation numbers are sufficiently high to dictate caution when planning lab-scale chemostats: Notley-McRobb *et al.* (2001) conducted glucose und nitrogen-limited chemostat cultivations and screened for the appearance of *rpoS* mutations. Excluding preculture and batch-phase, *rpoS* defects emerged after 10 – 40 generations depending on the installed

dilution rate (Notley-McRobb et al., 2002). Therefore, as a part of **P-II**, sequencing data was collected from samples of STR-PFR cultivations conducted to determine the maintenance coefficients of *E. coli* MG1655 and *E. coli* RM214 to check for potential mutations in global regulatory programs. Sequencing data from cryostocks and samples drawn at the end of the scale-down fermentations were compared. About 30 – 32 generations, 15 of them in the chemostat phase, passed between cryostocks and fermentation samples and no mutations in *rpoS* were found, regardless of dilution rate. Consequently, mutations leading to aberrant global regulation could be ruled out as a potential disruptive factor in the determination of maintenance coefficients.

In the heterologous protein production scenario employing *E. coli* MG1655 *rhaB*⁻ pJOE4056.2_tetA and *E. coli* RM214 *rhaB*⁻ pJOE4056.2_tetA that was investigated in **P-II**, the total generation number from strain construction to the final process sample was around 70, close to the 67 generations calculated to be necessary for a process volume of 200 m³ (Rugbjerg et al., 2018). The overall design of the experiment placed the occurrence of heterogeneities at a similar generation number as expected for a large-scale process: The PFR was connected after approximately 62 generations which are expected to be reached on a scale of around 1 to 10 m³ in an industrial process. Towards the end of the cultivations the proportion of producing cells dropped for both strains, but faster for *E. coli* MG1655 *rhaB*⁻ pJOE4056.2_tetA than for *E. coli* RM214 *rhaB*⁻ pJOE4056.2_tetA. With the available data, the potential effects of the generation number cannot be isolated from that of the scale-down conditions, but due to the matching design any effect or interdependency would likely be representative for an actual large-scale production scenario.

Picking up the issue of transferring data collected in chemostats to fed-batch fermentations again, there is indeed a limitation with respect to generation number originating from the nature of chemostats: Due to constant harvesting of a chemostat, a non-producer mutant could be stochastically removed before it can replicate. However, it is extremely unlikely that wash-out of mutants was a relevant factor in the experimental designs of **P-II** since only the final 15 generations grew in a continuous chemostat. Even mutants with a 50% increase in relative fitness require more than 25 generations to form the majority of a population (Gresham and Hong, 2015). If any mutants had had a significant impact on the overall culture performance, they would have had to emerge prior to the chemostat phase. The transferability of the

scale-down experiments of **P-II** thus remains valid in this regard and the same applies to the experiments of **P-I** that used a similar experimental design.

7.3 Modulating global cellular regulation – the case of *E. coli* SR

In the subchapter 7.1 **Robustness of *E. coli* RM214 and *E. coli* SR to heterogeneous conditions** a comparison between the approach to modulate global regulation versus the deletion of individual genes has been made. A major drawback of interfering with global cellular regulation are the potential unintended side-effects. For the case of *E. coli* SR this is illustrated by data collected in not previously published experiments that are reported in this thesis (**P-A**). *E. coli* SR p006_kan_eGFP failed to efficiently produce eGFP compared to *E. coli* MG1655 p006_kan_eGFP or *E. coli* CD202 p006_kan_eGFP (**Fig. 24**). Moreover, when growth ceased, eGFP was degraded by *E. coli* SR p006_kan_eGFP. Similarly, *E. coli* SR pdCas9 psgRNA_aceE_234_pdhR_329 failed to efficiently produce pyruvate (**Fig. 25**) and could not achieve a comparable performance to *E. coli* MG1655 pdCas9 psgRNA_aceE_234_pdhR_329 as seen in **P-III**. The low pyruvate production is even more remarkable as *E. coli* HGT, which has an identical genotype as *E. coli* SR with an additional mutation in *aceE*, accumulated substantial amounts of pyruvate during growth in glucose minimal medium (Michalowski et al., 2017). *E. coli* HGT proves that ppGpp modulated strains are not per se unsuitable for production, but the question arises why *E. coli* SR was unable to achieve a satisfying performance in the examined cases. Given that the only difference to *E. coli* MG1655 is the modulated stringent response, it is likely that regulatory effects of low ppGpp levels are the cause.

The central mechanism of ppGpp action is transcriptional reprogramming. Transcriptional regulation by ppGpp is mediated by its interaction with RNAP and consensus sequences for promoters inhibited or activated in the presence of ppGpp have been described (Ross et al., 2016; Sanchez-Vazquez et al., 2019). If expression of eGFP from p006_kan_eGFP was driven by a promoter activated by ppGpp, then the low productivity of *E. coli* SR p006_kan_eGFP would have been a direct consequence. However, eGFP is expressed from a T5 promoter regulated by multiple lac operator sites and the promoter contains no elements that would support activation by ppGpp. In contrast, it has some resemblance to promoters inhibited by ppGpp (Sanchez-Vazquez et al., 2019). It thus appears unlikely that the low accumulation of eGFP by *E. coli* SR was caused by insufficient transcription from p006_kan_eGFP as a direct consequence of ppGpp levels. Another possible explanation for the low productivity of *E. coli* SR p006_kan_eGFP can be derived from the research of Zhu and Dai (2019) who proposed that reduced ppGpp levels generally lower the expression of catabolic proteins including

constitutively expressed proteins that are not specifically regulated by ppGpp. The underlying cause is inappropriate cellular resource allocation resulting in an excess of ribosomes (Zhu and Dai, 2019). The observed reduction and even degradation of eGFP in *E. coli* SR p006_kan_eGFP could thus be caused by a putative inability of the strain to sufficiently lower ribosome synthesis at low growth rates leading to increased proteolysis to meet the resulting cellular demand for precursors. Concerning the low level of pyruvate accumulation by *E. coli* SR pdCas9 psgRNA_aceE_234_pdhR_329, more fundamental investigations regarding transcriptional levels and metabolic fluxes must be conducted to avoid jumping to false conclusions. The data collected so far indicates that CRISPRi is in principle functional in *E. coli* SR pdCas9 psgRNA_aceE_234_pdhR_329 but less effective than in *E. coli* MG1655 pdCas9 psgRNA_aceE_234_pdhR_329.

It is important to state that the data from **P-A** does not mean *E. coli* SR is generally not a useful production host. On the contrary, strains with reduced ppGpp levels have been patented for heterologous protein or plasmid DNA production (Dassler et al., 2009; Huber et al., 2009). Data collected in **P-I** indicates that strains with modulated stringent response may be beneficial for large-scale nitrogen-limited processes and *E. coli* HGT proves that the production of at least small metabolites from central carbon metabolism should be possible (Michalowski et al., 2017). However, the experiments described in **P-A** clearly illustrate that limitations exist. Expression systems and processes designed for wild-type *E. coli* strains do not necessarily work in stringent response modulated strains. It thus may be necessary to explore other expression systems or production conditions that can capitalize from the aberrant regulation of stringent response mutant strains. Generalizing this conclusion reveals a central issue that researchers will face in future studies with stringent response modulated strains: ppGpp transcriptional regulation affects several hundreds of promoters (Sanchez-Vazquez et al., 2019) and it exhibits allosteric modulatory effects on many cellular proteins (Zhang et al., 2018b). The sheer scope of its effects impedes accurate prediction of the behavior of stringent response modulated strains and may mask observations from regulatory studies. Only genome-scale models including the transcriptional regulatory network and its many interactions with metabolites hold the potential to make such predictions (Grimbs et al., 2019; Lempp et al., 2019).

7.4 Nitrogen-limitation as a process strategy

Fed-batch fermentations using the primary carbon source as the limiting nutrient are the standard process strategy in aerobic fine chemical fermentation and heterologous protein production. Limiting growth reduces byproduct accumulation and enables tight control of heat generation. An ideal process strategy also enables decoupling of biomass and product formation, which theoretically allows higher product yield and carbon conversion. A plethora of strategies from classical biotin auxotrophy in *Corynebacterium glutamicum* to sophisticated molecular circuits inhibiting cell division have been developed for this purpose (Li et al., 2020b; Shiiro et al., 1962). A simple alternative process strategy is to use a nitrogen source as the limiting nutrient if the product does not contain nitrogen. The transcriptional analysis conducted in **P-I** demonstrates that *E. coli* SR is potentially a superior host for large-scale fermentations with ammonium as the limiting nutrient. In **P-III** strains were constructed that can accumulate pyruvate in nitrogen-limited production scenarios.

Examples for products that are readily produced under nitrogen-limited conditions include next-generation biofuels, polyhydroxyalkanoates (PHA) and many small carbon molecules derived from central metabolism (Linton and Musgrave, 1983; Monot and Engasser, 1983; Oliveira-Filho et al., 2019; Stephenson et al., 2010; Wen et al., 2010). In **P-III** pyruvate was chosen as a product to explore the possibility of enhancing precursor supply by applying CRISPRi to reduce carbon flux into central metabolism. Such strains could be beneficial to improve the carbon conversion of terpenoid production strains which currently ranges at about 5% (Patil et al., 2021). As pointed out by Linton and Musgrave (1983), the two main challenges for competitive nitrogen-limited processes are achieving a high specific carbon substrate uptake rate and preventing wasteful combustion of carbon to CO₂. With the current knowledge, both issues can in principle be solved for the model organism *E. coli*. Known strategies to increase carbon uptake rates include regulatory intervention or artificially increased ATP demand (Chubukov et al., 2017; Koebmann et al., 2002; Michalowski et al., 2017). Channeling carbon into a product can either occur from natural regulation as in the case of PHA accumulation or by redirecting fluxes through metabolic engineering as exemplified in **P-III**. If a two-stage process with a nitrogen-limited production phase is used, the induction or repression of metabolic pathways can potentially be coupled to natural regulation occurring on the onset of nitrogen starvation. Data from **P-I** shows that NtrBC-mediated transcriptional regulation is fully functional in *E. coli* SR and thus a suitable candidate for both wild-type and stringent

response modulated strains. Integrating a NtrC dependent expression system into *E. coli* SR for nitrogen-limited production could potentially also overcome the low productivity of strains observed in **P-A**. Finally, as the cellular regulatory responses to repeated nitrogen or glucose limitation are similar (Löffler et al., 2016; Simen et al., 2017) *E. coli* RM214 may also hold the potential to be a chassis strain for a robust scale-up of nitrogen-limited fermentations. Based on the predicted impact of nitrogen limitation on the maintenance coefficient by Simen *et al.* (2017) it appears likely that *E. coli* is sufficiently sensitive to repeated nitrogen starvation to examine this in scale-down experiments as conducted in **P-II**.

7.5 Outlook: Engineering hosts for large-scale conditions

The central issue of this thesis was the engineering and evaluation of *E. coli* host strains for large-scale applications. In **P-I** regulatory differences between a stringent response modulated strain and its wild-type parent in heterogeneous nitrogen-limited conditions were investigated. In **P-II** a series of deletion strains was engineered and the robustness of the final strain to heterogeneous glucose-limited conditions was compared to that of the original strain. In **P-III** strains were modified to enable balanced and stable production in nitrogen-limited conditions. Scale-up is a central issue in bioprocess development and the results collected in this thesis lay the foundation for increasingly robust transfer across scales as well as the development of new process strategies.

Testing potential host strains for industrial application in large-scale reactors is not economically feasible, and this situation is unlikely to change. Considering the fast advancements in strain construction and metabolic engineering over the past years the number of potential candidate strains for scale-up will rather increase than decrease in future. The availability and automation level of scale-down reactors must be increased in parallel to meet the rising demand for robust process transfer across scales. Paradoxically, the most promising approach is likely the miniaturization of scale-down reactors following the general trend towards small cultivation volumes in strain development. A central task for biochemical engineers will be to improve the designs of scale-down reactors to accurately reflect as many different heterogeneities as possible in low-maintenance and small-volume scale-down reactors. Improved availability of scale-down reactors will be a key prerequisite for the further development of robust host strains. The design of scale-down experiments also needs to be improved to accurately reflect an industrial bioprocess. As discussed in section **7.2 Simulating large-scale conditions with scale-down reactors** the generation number and process time at which heterogeneities occur in a large-scale process should be considered. Of course, most time-dependent conditions cannot be realized in a chemostat. Chemostats should thus primarily serve to fundamentally study single stimuli. Operating a multi-compartment scale-down reactor in fed-batch mode would allow to establish relevant regimes and to follow the dynamics of their volumetric proportions based on simulation data. Depending on the process, the dynamics of relevant concentrations such as biomass and products should also be varied accordingly if they change significantly over the course of the fermentation.

The findings in **P-I** concerning different global regulation of stringent response modulated *E. coli* strains can likely be transferred to other industrially relevant microbial hosts as the stringent response is an evolutionary remarkably conserved mechanism among bacteria. While the molecular actors in ppGpp metabolism differ between organisms, regulatory patterns in response to starvation occur in many other hosts such as *Pseudomonas putida*, *Bacillus subtilis* and *Corynebacterium glutamicum* (Ankenbauer et al., 2020; Kriel et al., 2014; Ruwe et al., 2019; Yang et al., 2020). Ankenbauer *et al.* (2020) showed that *Pseudomonas putida* reacts by accumulating ppGpp when exposed to transient starvation (Ankenbauer et al., 2020). Modulating the stringent response or engineering deletion strains following similar principles as used in **P-II** could further enhance the robustness of *P. putida* and potentially other hosts. If hosts appear particularly vulnerable to carbon source limitation or such limitation should be avoided for other reasons, nitrogen-limited processes as demonstrated in **P-III** are an alternative process mode that permits the use of higher carbon source concentrations. Nitrogen-limited processes are particularly attractive if hosts have no tendency of accumulating an undesirable byproduct and the target product does not require nitrogen, but engineering of the host metabolism may be necessary as described in **7.4 Nitrogen-limitation as a process strategy**.

Various approaches have been described to handle inhomogeneities and their consequences occurring in large-scale fermentations. Examples for the model organism *E. coli* focus on the reduction of overflow metabolism and anaerobic by-product formation (Lara et al., 2006c; Pablos et al., 2014; Soini et al., 2008). All of these strategies are likely compatible with the deletion approach that led to *E. coli* RM214. A key step forward would be the integration of multiple strategies into a single host to yield a complete chassis strain for scale-up. Deletion series are also a promising strategy for further improvements: With the ever-increasing availability of transcriptional and metabolic data the identification of process-irrelevant genes becomes increasingly feasible. Engineering of tailored deletion strains not suffering from the many drawbacks of early deletion strain series then becomes a realistic scenario. However, the deletion of genes will not always be the most suitable approach: many genes are process-relevant but excessively expressed, for example in pre-adaptive responses (Fischer and Sauer, 2005; Sander et al., 2019a). Modulating global regulation like in *E. coli* SR offered a simple high-impact approach aimed at reducing excessive regulation (Michalowski et al., 2017) but it is not a sufficiently precise tool regarding tailored microbial hosts. The methods of synthetic biology permit the rewiring of gene regulation to optimal levels or the introduction of

artificial dynamic circuits. Artificial circuits may in future endow cells with tailored regulation that did not evolve to enable survival of the organism in a natural habitat but that was fine-tuned for the demands of industrial production (Brockman and Prather, 2015; Xu et al., 2020; Zhang et al., 2020). From a current perspective, engineering powerful chassis strains for large-scale applications will in future require multiple complementary approaches – and interdisciplinary collaboration of molecular biologists, bioinformaticians and biochemical engineers.

8. Conclusion

In the research projects that form this thesis, different approaches to increase the robustness of strains to heterogeneous fermentation environments were tested, and the possibilities of nitrogen-limited fermentations were explored.

CRISPRi was tested to evaluate the nitrogen-limited production of pyruvate. Knockdown of *aceE* proved to be an effective way to trigger pyruvate accumulation and the stable production of pyruvate during a nitrogen-limited production phase was achieved by simultaneously targeting two promoters in the strain *E. coli* MG1655 pdCas9 psgRNA_aceE_234_pdhR_329. In conclusion, the experiments show the applicability of CRISPRi for redirecting fluxes towards product formation but also demonstrate the difficulties of achieving tight repression at low metabolic rates in nitrogen-limited conditions.

To investigate the consequences of heterogeneous fermentation conditions, the modified regulatory patterns of the stringent response mutant strain *E. coli* SR were characterized. Transcriptional regulation was reduced but phenotypic advantages were not apparent, indicating that further investigations with production strains are necessary to finally evaluate the potential of the strain. However, production experiments with *E. coli* SR have shown that standard expression systems may not be suitable for this strain, so the development of new expression systems is required.

In contrast, the tailored deletion strain *E. coli* RM214 had superior characteristics in heterogeneous scale-down fermentations including significant production advantages. The increased robustness was also quantified as a reduction in the maintenance coefficient proving the presumption that heterogeneous environments cause additional ATP demand. In conclusion, the results demonstrate the effectiveness and feasibility of tailored strain engineering as a strategy to achieve robust chassis strains for scale-up and the construction of *E. coli* RM214 may serve as a blueprint for the design of future chassis strains.

9. References

- Ades, S.E., Grigorova, I.L., Gross, C.A., 2003. Regulation of the alternative sigma factor sigma(E) during initiation, adaptation, and shutoff of the extracytoplasmic heat shock response in *Escherichia coli*. *J. Bacteriol.* 185, 2512–2519.
<https://doi.org/10.1128/JB.185.8.2512-2519.2003>.
- Aidelberg, G., Towbin, B.D., Rothschild, D., Dekel, E., Bren, A., Alon, U., 2014. Hierarchy of non-glucose sugars in *Escherichia coli*. *BMC systems biology* 8, 133.
<https://doi.org/10.1186/s12918-014-0133-z>.
- Aizenman, E., Engelberg-Kulka, H., Glaser, G., 1996. An *Escherichia coli* chromosomal "addiction module" regulated by guanosine corrected 3',5'-bispyrophosphate: a model for programmed bacterial cell death. *Proceedings of the National Academy of Sciences of the United States of America* 93, 6059–6063. <https://doi.org/10.1073/pnas.93.12.6059>.
- Alibhai, M., Villafranca, J.J., 1994. Kinetic and mutagenic studies of the role of the active site residues Asp-50 and Glu-327 of *Escherichia coli* glutamine synthetase. *Biochemistry* 33, 682–686. <https://doi.org/10.1021/bi00169a008>.
- Allison, K.R., Brynildsen, M.P., Collins, J.J., 2011. Heterogeneous bacterial persisters and engineering approaches to eliminate them. *Current opinion in microbiology* 14, 593–598.
<https://doi.org/10.1016/j.mib.2011.09.002>.
- Amanullah, A., McFarlane, C.M., Emery, A.N., Nienow, A.W., 2001. Scale-down model to simulate spatial pH variations in large-scale bioreactors. *Biotechnol. Bioeng.* 73, 390–399.
<https://doi.org/10.1002/bit.1072>.
- Anda, R. de Lara, A.R., Hernández, V., Hernández-Montalvo, V., Gosset, G., Bolívar, F., Ramírez, O.T., 2006. Replacement of the glucose phosphotransferase transport system by galactose permease reduces acetate accumulation and improves process performance of *Escherichia coli* for recombinant protein production without impairment of growth rate. *Metab. Eng.* 8, 281–290. <https://doi.org/10.1016/j.ymben.2006.01.002>.
- Anders, S., Pyl, P.T., Huber, W., 2015. HTSeq--a Python framework to work with high-throughput sequencing data. *Bioinformatics (Oxford, England)* 31, 166–169.
<https://doi.org/10.1093/bioinformatics/btu638>.

- Andrews, S.C., Guest, J.R., 1988. Nucleotide sequence of the gene encoding the GMP reductase of *Escherichia coli* K12. *The Biochemical journal* 255, 35–43.
<https://doi.org/10.1042/bj2550035>.
- Ankenbauer, A., Schäfer, R.A., Viegas, S.C., Pobre, V., Voß, B., Arraiano, C.M., Takors, R., 2020. *Pseudomonas putida* KT2440 is naturally endowed to withstand industrial-scale stress conditions. *Microbial biotechnology* 13, 1145–1161. <https://doi.org/10.1111/1751-7915.13571>.
- Anzai, T., Imamura, S., Ishihama, A., Shimada, T., 2020. Expanded roles of pyruvate-sensing PdhR in transcription regulation of the *Escherichia coli* K-12 genome: fatty acid catabolism and cell motility. *Microb. Genom.* 6, e000442.
<https://doi.org/10.1099/mgen.0.000442>.
- Aon, J.C., Cortassa, S., 2001. Involvement of nitrogen metabolism in the triggering of ethanol fermentation in aerobic chemostat cultures of *Saccharomyces cerevisiae*. *Metab. Eng.* 3, 250–264. <https://doi.org/10.1006/mben.2001.0181>.
- Arsène, F., Tomoyasu, T., Bukau, B., 2000. The heat shock response of *Escherichia coli*. *International Journal of Food Microbiology* 55, 3–9. [https://doi.org/10.1016/S0168-1605\(00\)00206-3](https://doi.org/10.1016/S0168-1605(00)00206-3).
- Atherly, A.G., 1979. *Escherichia coli* mutant containing a large deletion from *relA* to *argA*. *J. Bacteriol.* 138, 530–534. <https://doi.org/10.1128/jb.138.2.530-534.1979>.
- Atkinson, D.E., 1968. The energy charge of the adenylate pool as a regulatory parameter. Interaction with feedback modifiers. *Biochemistry* 7, 4030–4034.
<https://doi.org/10.1021/bi00851a033>.
- Atkinson, D.E., Walton, G.M., 1967. Adenosine triphosphate conservation in metabolic regulation. Rat liver citrate cleavage enzyme. *The Journal of biological chemistry* 242, 3239–3241. [https://doi.org/10.1016/S0021-9258\(18\)95956-9](https://doi.org/10.1016/S0021-9258(18)95956-9).
- Atkinson, M.R., Kamberov, E.S., Weiss, R.L., Ninfa, A.J., 1994. Reversible uridylylation of the *Escherichia coli* PII signal transduction protein regulates its ability to stimulate the dephosphorylation of the transcription factor nitrogen regulator I (NRI or NtrC). *Journal of Biological Chemistry* 269, 28288–28293. [https://doi.org/10.1016/S0021-9258\(18\)46926-8](https://doi.org/10.1016/S0021-9258(18)46926-8).
- Baba, T., Ara, T., Hasegawa, M., Takai, Y., Okumura, Y., Baba, M., Datsenko, K.A., Tomita, M., Wanner, B.L., Mori, H., 2006. Construction of *Escherichia coli* K-12 in-frame, single-

- gene knockout mutants: the Keio collection. *Molecular systems biology* 2, 2006.0008. <https://doi.org/10.1038/msb4100050>.
- Bachmann, B.J., 1972. Pedigrees of some mutant strains of *Escherichia coli* K-12. *Bacteriological Reviews* 36, 525–557. <https://doi.org/10.1128/br.36.4.525-557.1972>.
- Baeshen, M.N., Al-Hejin, A.M., Bora, R.S., Ahmed, M.M.M., Ramadan, H.A.I., Saini, K.S., Baeshen, N.A., Redwan, E.M., 2015. Production of Biopharmaceuticals in *E. coli*: Current Scenario and Future Perspectives. *Journal of microbiology and biotechnology* 25, 953–962. <https://doi.org/10.4014/jmb.1412.12079>.
- Baeshen, N.A., Baeshen, M.N., Sheikh, A., Bora, R.S., Ahmed, M.M.M., Ramadan, H.A.I., Saini, K.S., Redwan, E.M., 2014. Cell factories for insulin production. *Microb. Cell Factories* 13, 141. <https://doi.org/10.1186/s12934-014-0141-0>.
- Baez, A., Flores, N., Bolívar, F., Ramírez, O.T., 2011. Simulation of dissolved CO₂ gradients in a scale-down system: a metabolic and transcriptional study of recombinant *Escherichia coli*. *Biotechnology journal* 6, 959–967. <https://doi.org/10.1002/biot.201000407>.
- Balaban, N.Q., Merrin, J., Chait, R., Kowalik, L., Leibler, S., 2004. Bacterial persistence as a phenotypic switch. *Science* 305, 1622–1625. <https://doi.org/10.1126/science.1099390>.
- Balleza, E., López-Bojorquez, L.N., Martínez-Antonio, A., Resendis-Antonio, O., Lozada-Chávez, I., Balderas-Martínez, Y.I., Encarnación, S., Collado-Vides, J., 2009. Regulation by transcription factors in bacteria: beyond description. *FEMS Microbiol Rev* 33, 133–151. <https://doi.org/10.1111/j.1574-6976.2008.00145.x>.
- Barber, M.A., 1908. The Rate of Multiplication of *Bacillus coli* at Different Temperatures. *The Journal of Infectious Diseases* 5, 379–400. <https://doi.org/10.1093/infdis/5.4.379>.
- Barker, C.S., Prüss, B.M., Matsumura, P., 2004. Increased motility of *Escherichia coli* by insertion sequence element integration into the regulatory region of the *flhD* operon. *J. Bacteriol.* 186, 7529–7537. <https://doi.org/10.1128/JB.186.22.7529-7537.2004>.
- Barker, M.M., Gaal, T., Josaitis, C.A., Gourse, R.L., 2001. Mechanism of regulation of transcription initiation by ppGpp. I. Effects of ppGpp on transcription initiation in vivo and in vitro. *J. Mol. Biol.* 305, 673–688. <https://doi.org/10.1006/jmbi.2000.4327>.
- Barrangou, R., Fremaux, C., Deveau, H., Richards, M., Boyaval, P., Moineau, S., Romero, D.A., Horvath, P., 2007. CRISPR provides acquired resistance against viruses in prokaryotes. *Science* 315, 1709–1712. <https://doi.org/10.1126/science.1138140>.

-
- Battesti, A., Bouveret, E., 2006. Acyl carrier protein/SpoT interaction, the switch linking SpoT-dependent stress response to fatty acid metabolism. *Mol. Microbiol.* 62, 1048–1063. <https://doi.org/10.1111/j.1365-2958.2006.05442.x>.
- Bekker, M., Vries, S. de, Beek, A. ter, Hellingwerf, K.J., Mattos, M.J.T. de, 2009. Respiration of *Escherichia coli* can be fully uncoupled via the nonelectrogenic terminal cytochrome bd-II oxidase. *Journal of bacteriology* 191, 5510–5517. <https://doi.org/10.1128/JB.00562-09>.
- Benjamini, Y., Hochberg, Y., 1995. Controlling the False Discovery Rate: A Practical and Powerful Approach to Multiple Testing. *Journal of the Royal Statistical Society: Series B (Methodological)* 57, 289–300. <https://doi.org/10.1111/j.2517-6161.1995.tb02031.x>.
- Bhattacharya, S.K., Dubey, A.K., 1995. Metabolic burden as reflected by maintenance coefficient of recombinant *Escherichia coli* overexpressing target gene. *Biotechnology Letters* 17, 1155–1160. <https://doi.org/10.1007/BF00128377>.
- Bi, E., Lutkenhaus, J., 1993. Cell division inhibitors SulA and MinCD prevent formation of the FtsZ ring. *Journal of bacteriology* 175, 1118–1125. <https://doi.org/10.1128/jb.175.4.1118-1125.1993>.
- Bikard, D., Jiang, W., Samai, P., Hochschild, A., Zhang, F., Marraffini, L.A., 2013. Programmable repression and activation of bacterial gene expression using an engineered CRISPR-Cas system. *Nucleic Acids Res.* 41, 7429–7437. <https://doi.org/10.1093/nar/gkt520>.
- Binder, D., Drepper, T., Jaeger, K.-E., Delvigne, F., Wiechert, W., Kohlheyer, D., Grünberger, A., 2017. Homogenizing bacterial cell factories: Analysis and engineering of phenotypic heterogeneity. *Metab. Eng.* 42, 145–156. <https://doi.org/10.1016/j.ymben.2017.06.009>.
- Biwer, A.P., Zuber, P.T., Zelic, B., Gerharz, T., Bellmann, K.J., Heinzle, E., 2005. Modeling and Analysis of a New Process for Pyruvate Production. *Ind. Eng. Chem. Res.* 44, 3124–3133. <https://doi.org/10.1021/ie0491138>.
- Blattner, F.R., Plunkett, G., Bloch, C.A., Perna, N.T., Burland, V., Riley, M., Collado-Vides, J., Glasner, J.D., Rode, C.K., Mayhew, G.F., Gregor, J., Davis, N.W., Kirkpatrick, H.A., Goeden, M.A., Rose, D.J., Mau, B., Shao, Y., 1997. The complete genome sequence of *Escherichia coli* K-12. *Science* 277, 1453–1462. <https://doi.org/10.1126/science.277.5331.1453>.

-
- Boecker, S., Zahoor, A., Schramm, T., Link, H., Klamt, S., 2019. Broadening the Scope of Enforced ATP Wasting as a Tool for Metabolic Engineering in *Escherichia coli*. *Biotechnology journal* 14, e1800438. <https://doi.org/10.1002/biot.201800438>.
- Bolger, A.M., Lohse, M., Usadel, B., 2014. Trimmomatic: a flexible trimmer for Illumina sequence data. *Bioinformatics (Oxford, England)* 30, 2114–2120. <https://doi.org/10.1093/bioinformatics/btu170>.
- Bolivar, F., Rodriguez, R.L., Greene, P.J., Betlach, M.C., Heyneker, H.L., Boyer, H.W., Crosa, J.H., Falkow, S., 1977. Construction and characterization of new cloning vehicle. II. A multipurpose cloning system. *Gene* 2, 95–113. [https://doi.org/10.1016/0378-1119\(77\)90000-2](https://doi.org/10.1016/0378-1119(77)90000-2).
- Bougdour, A., Gottesman, S., 2007. ppGpp regulation of RpoS degradation via anti-adaptor protein IraP. *Proceedings of the National Academy of Sciences of the United States of America* 104, 12896–12901. <https://doi.org/10.1073/pnas.0705561104>.
- Brockman, I.M., Prather, K.L.J., 2015. Dynamic knockdown of *E. coli* central metabolism for redirecting fluxes of primary metabolites. *Metab. Eng.* 28, 104–113. <https://doi.org/10.1016/j.ymben.2014.12.005>.
- Brons, H.J., Zehnder, A.J., 1990. Aerobic nitrate and nitrite reduction in continuous cultures of *Escherichia coli* E4. *Arch. Microbiol.* 153, 531–536. <https://doi.org/10.1007/BF00245261>.
- Brown, D.R., Barton, G., Pan, Z., Buck, M., Wigneshweraraj, S., 2014. Nitrogen stress response and stringent response are coupled in *Escherichia coli*. *Nat. Commun.* 5, 4115. <https://doi.org/10.1038/ncomms5115>.
- Buchholz, J., Graf, M., Freund, A., Busche, T., Kalinowski, J., Blombach, B., Takors, R., 2014. CO₂/HCO₃⁻ perturbations of simulated large scale gradients in a scale-down device cause fast transcriptional responses in *Corynebacterium glutamicum*. *Appl. Microbiol. Biotechnol.* 98, 8563–8572. <https://doi.org/10.1007/s00253-014-6014-y>.
- Butala, M., Klose, D., Hodnik, V., Rems, A., Podlesek, Z., Klare, J.P., Anderluh, G., Busby, S.J.W., Steinhoff, H.-J., Zgur-Bertok, D., 2011. Interconversion between bound and free conformations of LexA orchestrates the bacterial SOS response. *Nucleic Acids Res.* 39, 6546–6557. <https://doi.org/10.1093/nar/gkr265>.

-
- Bylund, F., Castan, A., Mikkola, R., Veide, A., Larsson, G., 2000. Influence of scale-up on the quality of recombinant human growth hormone. *Biotechnol. Bioeng.* 69, 119–128. [https://doi.org/10.1002/\(SICI\)1097-0290\(20000720\)69:2<119:AID-BIT1>3.0.CO;2-9](https://doi.org/10.1002/(SICI)1097-0290(20000720)69:2<119:AID-BIT1>3.0.CO;2-9).
- Bylund, F., Collet, E., Enfors, S.-O., Larsson, G., 1998. Substrate gradient formation in the large-scale bioreactor lowers cell yield and increases by-product formation. *Bioprocess Engineering* 18, 171. <https://doi.org/10.1007/s004490050427>.
- Bylund, F., Guillard, F., Enfors, S.-O., Trägårdh, C., Larsson, G., 1999. Scale down of recombinant protein production: a comparative study of scaling performance. *Bioprocess Engineering* 20, 377. <https://doi.org/10.1007/s004490050606>.
- Calvo-Villamañán, A., Ng, J.W., Planel, R., Ménager, H., Chen, A., Cui, L., Bikard, D., 2020. On-target activity predictions enable improved CRISPR-dCas9 screens in bacteria. *Nucleic Acids Res.* 48, e64. <https://doi.org/10.1093/nar/gkaa294>.
- Carneiro, S., Lourenço, A., Ferreira, E.C., Rocha, I., 2011. Stringent response of *Escherichia coli*: revisiting the bibliome using literature mining. *Microbial informatics and experimentation* 1, 14. <https://doi.org/10.1186/2042-5783-1-14>.
- Cassuto, E., Lash, T., Sriprakash, K.S., Radding, C.M., 1971. Role of exonuclease and beta protein of phage lambda in genetic recombination. V. Recombination of lambda DNA in vitro. *Proceedings of the National Academy of Sciences of the United States of America* 68, 1639–1643. <https://doi.org/10.1073/pnas.68.7.1639>.
- Cayley, S., Lewis, B.A., Guttman, H.J., Record, M., 1991. Characterization of the cytoplasm of *Escherichia coli* K-12 as a function of external osmolarity. *J. Mol. Biol.* 222, 281–300. [https://doi.org/10.1016/0022-2836\(91\)90212-O](https://doi.org/10.1016/0022-2836(91)90212-O).
- Chakiath, C., Esposito, D., 2007. Improved recombinational stability of lentiviral expression vectors using reduced-genome *Escherichia coli*. *Biotech.* 43, 466–470. <https://doi.org/10.2144/000112585>.
- Chang, D.-E., Smalley, D.J., Conway, T., 2002. Gene expression profiling of *Escherichia coli* growth transitions: an expanded stringent response model. *Molecular microbiology* 45, 289–306. <https://doi.org/10.1046/j.1365-2958.2002.03001.x>.
- Chang, Y., Su, T., Qi, Q., Liang, Q., 2016. Easy regulation of metabolic flux in *Escherichia coli* using an endogenous type I-E CRISPR-Cas system. *Microb. Cell Factories* 15, 195. <https://doi.org/10.1186/s12934-016-0594-4>.

-
- Chapman, A.G., Atkinson, D.E., 1977. Adenine Nucleotide Concentrations and Turnover Rates. Their Correlation with Biological Activity in Bacteria and Yeast, in: Rose, A.H., Tempest, D.W. (Eds.), *Advances in microbial physiology* 15, vol. 15. Academic, London, pp. 253–306.
- Chapman, A.G., Fall, L., Atkinson, D.E., 1971. Adenylate energy charge in *Escherichia coli* during growth and starvation. *Journal of bacteriology* 108, 1072–1086.
<https://doi.org/10.1128/jb.108.3.1072-1086.1971>.
- Chen, H., Boutros, P.C., 2011. VennDiagram: a package for the generation of highly-customizable Venn and Euler diagrams in R. *BMC bioinformatics* 12, 35.
<https://doi.org/10.1186/1471-2105-12-35>.
- Chowdhury, N., Kwan, B.W., Wood, T.K., 2016. Persistence Increases in the Absence of the Alarmone Guanosine Tetraphosphate by Reducing Cell Growth. *Scientific reports* 6, 20519. <https://doi.org/10.1038/srep20519>.
- Chubukov, V., Desmarais, J.J., Wang, G., Chan, L.J.G., Baidoo, E.E., Petzold, C.J., Keasling, J.D., Mukhopadhyay, A., 2017. Engineering glucose metabolism of *Escherichia coli* under nitrogen starvation. *NPJ Syst. Biol. Appl.* 3, 16035.
<https://doi.org/10.1038/npjbsa.2016.35>.
- Chubukov, V., Sauer, U., 2014. Environmental dependence of stationary-phase metabolism in *Bacillus subtilis* and *Escherichia coli*. *Appl. Environ. Microbiol.* 80, 2901–2909.
<https://doi.org/10.1128/AEM.00061-14>.
- Clark, D.P., 1989. The fermentation pathways of *Escherichia coli*. *FEMS Microbiol. Lett.* 63, 223–234. <https://doi.org/10.1111/j.1574-6968.1989.tb03398.x>.
- Cortés, J.T., Flores, N., Bolívar, F., Lara, A.R., Ramírez, O.T., 2016. Physiological effects of pH gradients on *Escherichia coli* during plasmid DNA production. *Biotechnol. Bioeng.* 113, 598–611. <https://doi.org/10.1002/bit.25817>.
- Court, D.L., Sawitzke, J.A., Thomason, L.C., 2002. Genetic engineering using homologous recombination. *Annual review of genetics* 36, 361–388.
<https://doi.org/10.1146/annurev.genet.36.061102.093104>.
- Cui, L., Vigouroux, A., Rousset, F., Varet, H., Khanna, V., Bikard, D., 2018. A CRISPRi screen in *E. coli* reveals sequence-specific toxicity of dCas9. *Nat. Commun.* 9, 1912.
<https://doi.org/10.1038/s41467-018-04209-5>.

-
- Dalebroux, Z.D., Swanson, M.S., 2012. ppGpp: magic beyond RNA polymerase. *Nature reviews. Microbiology* 10, 203–212. <https://doi.org/10.1038/nrmicro2720>.
- Darling, A.C.E., Mau, B., Blattner, F.R., Perna, N.T., 2004. Mauve: multiple alignment of conserved genomic sequence with rearrangements. *Genome research* 14, 1394–1403. <https://doi.org/10.1101/gr.2289704>.
- Dassler, T., Mitterweger, S., Wich, G., 2009. Process for the Fermentative Production of Heterologous Proteins by Means of Escherichia Coli. DE20081063900 C12P21/00.
- Datsenko, K.A., Wanner, B.L., 2000. One-step inactivation of chromosomal genes in Escherichia coli K-12 using PCR products. *Proceedings of the National Academy of Sciences of the United States of America* 97, 6640–6645. <https://doi.org/10.1073/pnas.120163297>.
- Datta, S., Costantino, N., Court, D.L., 2006. A set of recombineering plasmids for gram-negative bacteria. *Gene* 379, 109–115. <https://doi.org/10.1016/j.gene.2006.04.018>.
- Delvigne, F., Boxus, M., Ingels, S., Thonart, P., 2009. Bioreactor mixing efficiency modulates the activity of a prpoS:GFP reporter gene in E. coli. *Microb. Cell Factories* 8, 15. <https://doi.org/10.1186/1475-2859-8-15>.
- Delvigne, F., Destain, J., Thonart, P., 2006. A methodology for the design of scale-down bioreactors by the use of mixing and circulation stochastic models. *Biochemical Engineering Journal* 28, 256–268. <https://doi.org/10.1016/j.bej.2005.11.009>.
- Delvigne, F., Takors, R., Mudde, R., van Gulik, W., Noorman, H., 2017. Bioprocess scale-up/down as integrative enabling technology: from fluid mechanics to systems biology and beyond. *Microbial biotechnology* 10, 1267–1274. <https://doi.org/10.1111/1751-7915.12803>.
- Doniselli, N., Rodriguez-Aliaga, P., Amidani, D., Bardales, J.A., Bustamante, C., Guerra, D.G., Rivetti, C., 2015. New insights into the regulatory mechanisms of ppGpp and DksA on Escherichia coli RNA polymerase-promoter complex. *Nucleic Acids Res.* 43, 5249–5262. <https://doi.org/10.1093/nar/gkv391>.
- Doucette, C.D., Schwab, D.J., Wingreen, N.S., Rabinowitz, J.D., 2011. α -Ketoglutarate coordinates carbon and nitrogen utilization via enzyme I inhibition. *Nat. Chem. Biol.* 7, 894–901. <https://doi.org/10.1038/nchembio.685>.

- Durfee, T., Hansen, A.-M., Zhi, H., Blattner, F.R., Jin, D.J., 2008a. Transcription profiling of the stringent response in *Escherichia coli*. *Journal of bacteriology* 190, 1084–1096. <https://doi.org/10.1128/JB.01092-07>.
- Durfee, T., Nelson, R., Baldwin, S., Plunkett, G., Burland, V., Mau, B., Petrosino, J.F., Qin, X., Muzny, D.M., Ayele, M., Gibbs, R.A., Csörgo, B., Pósfai, G., Weinstock, G.M., Blattner, F.R., 2008b. The complete genome sequence of *Escherichia coli* DH10B: insights into the biology of a laboratory workhorse. *Journal of bacteriology* 190, 2597–2606. <https://doi.org/10.1128/JB.01695-07>.
- Edgar, R., Domrachev, M., Lash, A.E., 2002. Gene Expression Omnibus: NCBI gene expression and hybridization array data repository. *Nucleic Acids Res.* 30, 207–210. <https://doi.org/10.1093/nar/30.1.207>.
- Egan, S.M., Schleif, R.F., 1993. A regulatory cascade in the induction of rhaBAD. *J. Mol. Biol.* 234, 87–98. <https://doi.org/10.1006/jmbi.1993.1565>.
- Eiteman, M.A., Altman, E., 2006. Overcoming acetate in *Escherichia coli* recombinant protein fermentations. *Trends in Biotechnology* 24, 530–536. <https://doi.org/10.1016/j.tibtech.2006.09.001>.
- Enfors, S.-O., Jahic, M., Rozkov, A., Xu, B., Hecker, M., Jürgen, B., Krüger, E., Schweder, T., Hamer, G., O'Beirne, D., Noisommit-Rizzi, N., Reuss, M., Boone, L., Hewitt, C., McFarlane, C., Nienow, A., Kovacs, T., Trägårdh, C., Fuchs, L., Revstedt, J., Friberg, P.C., Hjertager, B., Blomsten, G., Skogman, H., Hjort, S., Hoeks, F., Lin, H.-Y., Neubauer, P., van der Lans, R., Luyben, K., Vrabel, P., Manelius, Å., 2001. Physiological responses to mixing in large scale bioreactors. *Journal of biotechnology* 85, 175–185. [https://doi.org/10.1016/S0168-1656\(00\)00365-5](https://doi.org/10.1016/S0168-1656(00)00365-5).
- Fang, X., Sastry, A., Mih, N., Kim, D., Tan, J., Yurkovich, J.T., Lloyd, C.J., Gao, Y., Yang, L., Palsson, B.O., 2017. Global transcriptional regulatory network for *Escherichia coli* robustly connects gene expression to transcription factor activities. *PNAS* 114, 10286–10291. <https://doi.org/10.1073/pnas.1702581114>.
- Ferenci, T., 2006. A cultural divide on the use of chemostats. *Microbiology (Reading, England)* 152, 1247–1248. <https://doi.org/10.1099/mic.0.28651-0>.
- Figueira, R., Brown, D.R., Ferreira, D., Eldridge, M.J.G., Burchell, L., Pan, Z., Helaine, S., Wigneshweraraj, S., 2015. Adaptation to sustained nitrogen starvation by *Escherichia coli*

-
- requires the eukaryote-like serine/threonine kinase YeaG. *Scientific reports* 5, 17524.
<https://doi.org/10.1038/srep17524>.
- Fischer, E., Sauer, U., 2005. Large-scale in vivo flux analysis shows rigidity and suboptimal performance of *Bacillus subtilis* metabolism. *Nature genetics* 37, 636–640.
<https://doi.org/10.1038/ng1555>.
- Fitzgerald, D.M., Bonocora, R.P., Wade, J.T., 2014. Comprehensive mapping of the *Escherichia coli* flagellar regulatory network. *PLoS genetics* 10, e1004649.
<https://doi.org/10.1371/journal.pgen.1004649>.
- Fonville, N.C., Bates, D., Hastings, P.J., Hanawalt, P.C., Rosenberg, S.M., 2010. Role of RecA and the SOS response in thymineless death in *Escherichia coli*. *PLoS genetics* 6, e1000865. <https://doi.org/10.1371/journal.pgen.1000865>.
- Gaca, A.O., Colomer-Winter, C., Lemos, J.A., 2015. Many means to a common end: the intricacies of (p)ppGpp metabolism and its control of bacterial homeostasis. *Journal of bacteriology* 197, 1146–1156. <https://doi.org/10.1128/JB.02577-14>.
- Gallant, J., Erlich, H., Hall, B., Laffler, T., 1970. Analysis of the RC Function. *Cold Spring Harbor Symposia on Quantitative Biology* 35, 397–405.
<https://doi.org/10.1101/SQB.1970.035.01.051>.
- Gao, C., Wang, S., Hu, G., Guo, L., Chen, X., Xu, P., Liu, L., 2018. Engineering *Escherichia coli* for malate production by integrating modular pathway characterization with CRISPRi-guided multiplexed metabolic tuning. *Biotechnol. Bioeng.* 115, 661–672.
<https://doi.org/10.1002/bit.26486>.
- Garneau, J.E., Dupuis, M.-È., Villion, M., Romero, D.A., Barrangou, R., Boyaval, P., Fremaux, C., Horvath, P., Magadán, A.H., Moineau, S., 2010. The CRISPR/Cas bacterial immune system cleaves bacteriophage and plasmid DNA. *Nature* 468, 67–71.
<https://doi.org/10.1038/nature09523>.
- Gentleman, R.C., Carey, V.J., Bates, D.M., Bolstad, B., Dettling, M., Dudoit, S., Ellis, B., Gautier, L., Ge, Y., Gentry, J., Hornik, K., Hothorn, T., Huber, W., Iacus, S., Irizarry, R., Leisch, F., Li, C., Maechler, M., Rossini, A.J., Sawitzki, G., Smith, C., Smyth, G., Tierney, L., Yang, J.Y.H., Zhang, J., 2004. Bioconductor: open software development for computational biology and bioinformatics. *Genome biology* 5, R80.
<https://doi.org/10.1186/gb-2004-5-10-r80>.

- Gentry, D.R., Hernandez, V.J., Nguyen, L.H., Jensen, D.B., Cashel, M., 1993. Synthesis of the stationary-phase sigma factor sigma s is positively regulated by ppGpp. *J. Bacteriol.* 175, 7982–7989. <https://doi.org/10.1128/jb.175.24.7982-7989.1993>.
- George, S., Larsson, G., Enfors, S.-O., 1993. A scale-down two-compartment reactor with controlled substrate oscillations: Metabolic response of *Saccharomyces cerevisiae*. *Bioprocess Engineering* 9, 249–257. <https://doi.org/10.1007/BF01061530>.
- Gerdes, K., Maisonneuve, E., 2012. Bacterial persistence and toxin-antitoxin loci. *Annu Rev Microbiol* 66, 103–123. <https://doi.org/10.1146/annurev-micro-092611-150159>.
- Gerding, M.A., Ogata, Y., Pecora, N.D., Niki, H., Boer, P.A.J. de, 2007. The trans-envelope Tol-Pal complex is part of the cell division machinery and required for proper outer-membrane invagination during cell constriction in *E. coli*. *Molecular microbiology* 63, 1008–1025. <https://doi.org/10.1111/j.1365-2958.2006.05571.x>.
- Gibson, D.G., 2011. Enzymatic assembly of overlapping DNA fragments. *Methods in enzymology* 498, 349–361. <https://doi.org/10.1016/B978-0-12-385120-8.00015-2>.
- Gibson, D.G., Young, L., Chuang, R.-Y., Venter, J.C., Hutchison, C.A., Smith, H.O., 2009. Enzymatic assembly of DNA molecules up to several hundred kilobases. *Nature methods* 6, 343–345. <https://doi.org/10.1038/nmeth.1318>.
- Glick, B.R., 1995. Metabolic load and heterologous gene expression. *Biotechnology advances* 13, 247–261. [https://doi.org/10.1016/0734-9750\(95\)00004-A](https://doi.org/10.1016/0734-9750(95)00004-A).
- González Barrios, A.F., Zuo, R., Hashimoto, Y., Yang, L., Bentley, W.E., Wood, T.K., 2006. Autoinducer 2 controls biofilm formation in *Escherichia coli* through a novel motility quorum-sensing regulator (MqsR, B3022). *Journal of bacteriology* 188, 305–316. <https://doi.org/10.1128/JB.188.1.305-316.2006>.
- Görke, B., Stülke, J., 2008. Carbon catabolite repression in bacteria: many ways to make the most out of nutrients. *Nature reviews. Microbiology* 6, 613–624. <https://doi.org/10.1038/nrmicro1932>.
- Gosset, G., Zhang, Z., Nayyar, S., Cuevas, W.A., Saier, M.H., 2004. Transcriptome analysis of Crp-dependent catabolite control of gene expression in *Escherichia coli*. *J. Bacteriol.* 186, 3516–3524. <https://doi.org/10.1128/JB.186.11.3516-3524.2004>.
- Gresham, D., Hong, J., 2015. The functional basis of adaptive evolution in chemostats. *FEMS microbiology reviews* 39, 2–16. <https://doi.org/10.1111/1574-6976.12082>.

- Grimbs, A., Klosik, D.F., Bornholdt, S., Hütt, M.-T., 2019. A system-wide network reconstruction of gene regulation and metabolism in *Escherichia coli*. *PLoS computational biology* 15, e1006962. <https://doi.org/10.1371/journal.pcbi.1006962>.
- Hanahan, D., 1983. Studies on transformation of *Escherichia coli* with plasmids. *J. Mol. Biol.* 166, 557–580. [https://doi.org/10.1016/S0022-2836\(83\)80284-8](https://doi.org/10.1016/S0022-2836(83)80284-8).
- Hardiman, T., Lemuth, K., Keller, M.A., Reuss, M., Siemann-Herzberg, M., 2007. Topology of the global regulatory network of carbon limitation in *Escherichia coli*. *Journal of biotechnology* 132, 359–374. <https://doi.org/10.1016/j.jbiotec.2007.08.029>.
- Haringa, C., Deshmukh, A.T., Mudde, R.F., Noorman, H.J., 2017. Euler-Lagrange analysis towards representative down-scaling of a 22 m³ aerobic *S. cerevisiae* fermentation. *Chemical Engineering Science* 170, 653–669. <https://doi.org/10.1016/j.ces.2017.01.014>.
- Haseltine, W.A., Block, R., 1973. Synthesis of guanosine tetra- and pentaphosphate requires the presence of a codon-specific, uncharged transfer ribonucleic acid in the acceptor site of ribosomes. *Proceedings of the National Academy of Sciences of the United States of America* 70, 1564–1568. <https://doi.org/10.1073/pnas.70.5.1564>.
- Haurlyuk, V., Atkinson, G.C., Murakami, K.S., Tenson, T., Gerdes, K., 2015. Recent functional insights into the role of (p)ppGpp in bacterial physiology. *Nature reviews. Microbiology* 13, 298–309. <https://doi.org/10.1038/nrmicro3448>.
- Hawkins, J.S., Wong, S., Peters, J.M., Almeida, R., Qi, L.S., 2015. Targeted Transcriptional Repression in Bacteria Using CRISPR Interference (CRISPRi). *Methods Mol. Biol.* 1311, 349–362. https://doi.org/10.1007/978-1-4939-2687-9_23.
- Hayashi, K., Morooka, N., Yamamoto, Y., Fujita, K., Isono, K., Choi, S., Ohtsubo, E., Baba, T., Wanner, B.L., Mori, H., Horiuchi, T., 2006. Highly accurate genome sequences of *Escherichia coli* K-12 strains MG1655 and W3110. *Molecular systems biology* 2, 2006.0007. <https://doi.org/10.1038/msb4100049>.
- Hewitt, C.J., Nebe-Von Caron, G., Axelsson, B., McFarlane, C.M., Nienow, A.W., 2000. Studies related to the scale-up of high-cell-density *E. coli* fed-batch fermentations using multiparameter flow cytometry: effect of a changing microenvironment with respect to glucose and dissolved oxygen concentration. *Biotechnol. Bioeng.* 70, 381–390. [https://doi.org/10.1002/1097-0290\(20001120\)70:4<381:AID-BIT3>3.0.CO;2-0](https://doi.org/10.1002/1097-0290(20001120)70:4<381:AID-BIT3>3.0.CO;2-0).

-
- Heyland, J., Blank, L.M., Schmid, A., 2011. Quantification of metabolic limitations during recombinant protein production in *Escherichia coli*. *Journal of biotechnology* 155, 178–184. <https://doi.org/10.1016/j.jbiotec.2011.06.016>.
- Hirokawa, Y., Kawano, H., Tanaka-Masuda, K., Nakamura, N., Nakagawa, A., Ito, M., Mori, H., Oshima, T., Ogasawara, N., 2013. Genetic manipulations restored the growth fitness of reduced-genome *Escherichia coli*. *Journal of bioscience and bioengineering* 116, 52–58. <https://doi.org/10.1016/j.jbiosc.2013.01.010>.
- Hochuli, E., Döbeli, H., Schacher, A., 1987. New metal chelate adsorbent selective for proteins and peptides containing neighbouring histidine residues. *Journal of Chromatography A* 411, 177–184. [https://doi.org/10.1016/S0021-9673\(00\)93969-4](https://doi.org/10.1016/S0021-9673(00)93969-4).
- Holms, W.H., Hamilton, I.D., Robertson, A.G., 1972. The rate of turnover of the adenosine triphosphate pool of *Escherichia coli* growing aerobically in simple defined media. *Archiv für Mikrobiologie* 83, 95–109. <https://doi.org/10.1007/BF00425016>.
- Hopkins, D.J., Betenbaugh, M.J., Dhurjati, P., 1987. Effects of dissolved oxygen shock on the stability of recombinant *Escherichia coli* containing plasmid pKN401. *Biotechnol. Bioeng.* 29, 85–91. <https://doi.org/10.1002/bit.260290113>.
- Hua, Q., Yang, C., Oshima, T., Mori, H., Shimizu, K., 2004. Analysis of Gene Expression in *Escherichia coli* in Response to Changes of Growth-Limiting Nutrient in Chemostat Cultures. *Appl. Environ. Microbiol.* 70, 2354–2366. <https://doi.org/10.1128/AEM.70.4.2354-2366.2004>.
- Huber, H., Weigl, G., Buchinger, W., 2009. FED-BATCH FERMENTATION PROCESS AND CULTURE MEDIUM FOR THE PRODUCTION OF PLASMID DNA IN *E. COLI* ON A MANUFACTURING SCALE. US20090388848;EP20040008556;US20050101764;US20040568857P C12P19/34;C12N1/20;C12N1/21;C12N9/88;C12N15/10;C12N15/74.
- Huergo, L.F., Dixon, R., 2015. The Emergence of 2-Oxoglutarate as a Master Regulator Metabolite. *Microbiol. Mol. Biol. Rev.* 79, 419–435. <https://doi.org/10.1128/MMBR.00038-15>.
- Huisman, O., D'Ari, R., Gottesman, S., 1984. Cell-division control in *Escherichia coli*: specific induction of the SOS function SfiA protein is sufficient to block septation. *Proceedings of the National Academy of Sciences of the United States of America* 81, 4490–4494. <https://doi.org/10.1073/pnas.81.14.4490>.

-
- Hunter, W.N., 2007. The non-mevalonate pathway of isoprenoid precursor biosynthesis. *The Journal of biological chemistry* 282, 21573–21577.
<https://doi.org/10.1074/jbc.R700005200>.
- Jarmander, J., Belotserkovsky, J., Sjöberg, G., Guevara-Martínez, M., Pérez-Zabaleta, M., Quillaguamán, J., Larsson, G., 2015. Cultivation strategies for production of (R)-3-hydroxybutyric acid from simultaneous consumption of glucose, xylose and arabinose by *Escherichia coli*. *Microb. Cell Factories* 14, 51. <https://doi.org/10.1186/s12934-015-0236-2>.
- Jinek, M., Chylinski, K., Fonfara, I., Hauer, M., Doudna, J.A., Charpentier, E., 2012. A programmable dual-RNA-guided DNA endonuclease in adaptive bacterial immunity. *Science* 337, 816–821. <https://doi.org/10.1126/science.1225829>.
- Jishage, M., Ishihama, A., 1998. A stationary phase protein in *Escherichia coli* with binding activity to the major sigma subunit of RNA polymerase. *Proceedings of the National Academy of Sciences of the United States of America* 95, 4953–4958.
<https://doi.org/10.1073/pnas.95.9.4953>.
- Jishage, M., Iwata, A., Ueda, S., Ishihama, A., 1996. Regulation of RNA polymerase sigma subunit synthesis in *Escherichia coli*: intracellular levels of four species of sigma subunit under various growth conditions. *Journal of bacteriology* 178, 5447–5451.
<https://doi.org/10.1128/jb.178.18.5447-5451.1996>.
- Jishage, M., Kvint, K., Shingler, V., Nyström, T., 2002. Regulation of sigma factor competition by the alarmone ppGpp. *Genes & development* 16, 1260–1270.
<https://doi.org/10.1101/gad.227902>.
- Johansson, J., Balsalobre, C., Wang, S.-Y., Urbonaviciene, J., Jin, D.J., Sondén, B., Uhlin, B.E., 2000. Nucleoid Proteins Stimulate Stringently Controlled Bacterial Promoters. *Cell* 102, 475–485. [https://doi.org/10.1016/S0092-8674\(00\)00052-0](https://doi.org/10.1016/S0092-8674(00)00052-0).
- Jonge, L.P. de, Buijs, N.A.A., Pierick, A. ten, Deshmukh, A., Zhao, Z., Kiel, J.A.K.W., Heijnen, J.J., van Gulik, W.M., 2011. Scale-down of penicillin production in *Penicillium chrysogenum*. *Biotechnology journal* 6, 944–958. <https://doi.org/10.1002/biot.201000409>.
- Joseleau-Petit, D., Vinella, D., D'Ari, R., 1999. Metabolic alarms and cell division in *Escherichia coli*. *Journal of bacteriology* 181, 9–14. <https://doi.org/10.1128/JB.181.1.9-14.1999>.

- Junker, B.H., 2004. Scale-up methodologies for *Escherichia coli* and yeast fermentation processes. *Journal of bioscience and bioengineering* 97, 347–364.
[https://doi.org/10.1016/S1389-1723\(04\)70218-2](https://doi.org/10.1016/S1389-1723(04)70218-2).
- Junne, S., Klingner, A., Kabisch, J., Schweder, T., Neubauer, P., 2011. A two-compartment bioreactor system made of commercial parts for bioprocess scale-down studies: impact of oscillations on *Bacillus subtilis* fed-batch cultivations. *Biotechnology journal* 6, 1009–1017. <https://doi.org/10.1002/biot.201100293>.
- Kanjee, U., Gutsche, I., Alexopoulos, E., Zhao, B., El Bakkouri, M., Thibault, G., Liu, K., Ramachandran, S., Snider, J., Pai, E.F., Houry, W.A., 2011. Linkage between the bacterial acid stress and stringent responses: the structure of the inducible lysine decarboxylase. *The EMBO journal* 30, 931–944. <https://doi.org/10.1038/emboj.2011.5>.
- Kanjee, U., Ogata, K., Houry, W.A., 2012. Direct binding targets of the stringent response alarmone (p)ppGpp. *Molecular microbiology* 85, 1029–1043.
<https://doi.org/10.1111/j.1365-2958.2012.08177.x>.
- Karcagi, I., Draskovits, G., Umenhoffer, K., Fekete, G., Kovács, K., Méhi, O., Balikó, G., Szappanos, B., Györfy, Z., Fehér, T., Bogos, B., Blattner, F.R., Pál, C., Pósfai, G., Papp, B., 2016. Indispensability of Horizontally Transferred Genes and Its Impact on Bacterial Genome Streamlining. *Molecular biology and evolution* 33, 1257–1269.
<https://doi.org/10.1093/molbev/msw009>.
- Kelly, W.J., 2008. Using computational fluid dynamics to characterize and improve bioreactor performance. *Biotechnol. Appl. Biochem.* 49, 225–238.
<https://doi.org/10.1042/BA20070177>.
- Khlebnikov, A., Risa, Ø., Skaug, T., Carrier, T.A., Keasling, J.D., 2000. Regulatable Arabinose-Inducible Gene Expression System with Consistent Control in All Cells of a Culture. *J. Bacteriol.* 182, 7029–7034. <https://doi.org/10.1128/JB.182.24.7029-7034.2000>.
- Kim, B., Kim, H.J., Lee, S.J., 2020. Regulation of Microbial Metabolic Rates Using CRISPR Interference With Expanded PAM Sequences. *Frontiers in microbiology* 11, 282.
<https://doi.org/10.3389/fmicb.2020.00282>.
- Kim, D., Seo, S.W., Gao, Y., Nam, H., Guzman, G.I., Cho, B.-K., Palsson, B.O., 2018. Systems assessment of transcriptional regulation on central carbon metabolism by Cra and CRP. *Nucleic Acids Res.* 46, 2901–2917. <https://doi.org/10.1093/nar/gky069>.

-
- Kjeldgaard, N.O., Maaloe, O., Schaechter, M., 1958. The transition between different physiological states during balanced growth of *Salmonella typhimurium*. *Journal of general microbiology* 19, 607–616. <https://doi.org/10.1099/00221287-19-3-607>.
- Kochanowski, K., Gerosa, L., Brunner, S.F., Christodoulou, D., Nikolaev, Y.V., Sauer, U., 2017. Few regulatory metabolites coordinate expression of central metabolic genes in *Escherichia coli*. *Molecular systems biology* 13, 903. <https://doi.org/10.15252/msb.20167402>.
- Koebmann, B.J., Westerhoff, H.V., Snoep, J.L., Nilsson, D., Jensen, P.R., 2002. The Glycolytic Flux in *Escherichia coli* Is Controlled by the Demand for ATP. *Journal of bacteriology* 184, 3909–3916. <https://doi.org/10.1128/JB.184.14.3909-3916.2002>.
- Kolisnychenko, V., Plunkett, G., Herring, C.D., Fehér, T., Pósfai, J., Blattner, F.R., Pósfai, G., 2002. Engineering a reduced *Escherichia coli* genome. *Genome research* 12, 640–647. <https://doi.org/10.1101/gr.217202>.
- Koob, M.D., Shaw, A.J., Cameron, D.C., 1994. Minimizing the Genome of *Escherichia coli*. *Annals of the New York Academy of Sciences* 745, 1–3. <https://doi.org/10.1111/j.1749-6632.1994.tb44359.x>.
- Korch, S.B., Malhotra, V., Contreras, H., Clark-Curtiss, J.E., 2015. The *Mycobacterium tuberculosis* relBE toxin:antitoxin genes are stress-responsive modules that regulate growth through translation inhibition. *Journal of microbiology (Seoul, Korea)* 53, 783–795. <https://doi.org/10.1007/s12275-015-5333-8>.
- Kriel, A., Brinsmade, S.R., Tse, J.L., Tehranchi, A.K., Bittner, A.N., Sonenshein, A.L., Wang, J.D., 2014. GTP dysregulation in *Bacillus subtilis* cells lacking (p)ppGpp results in phenotypic amino acid auxotrophy and failure to adapt to nutrient downshift and regulate biosynthesis genes. *Journal of bacteriology* 196, 189–201. <https://doi.org/10.1128/JB.00918-13>.
- Kulkarni, S.K., Stahl, F.W., 1989. Interaction between the *sbcC* gene of *Escherichia coli* and the *gam* gene of phage lambda. *Genetics* 123, 249–253. <https://doi.org/10.1093/genetics/123.2.249>.
- Kurokawa, M., Seno, S., Matsuda, H., Ying, B.-W., 2016. Correlation between genome reduction and bacterial growth. *DNA research : an international journal for rapid publication of reports on genes and genomes* 23, 517–525. <https://doi.org/10.1093/dnares/dsw035>.

-
- Kuschel, M., Siebler, F., Takors, R., 2017. Lagrangian Trajectories to Predict the Formation of Population Heterogeneity in Large-Scale Bioreactors. *Bioengineering* (Basel, Switzerland) 4. <https://doi.org/10.3390/bioengineering4020027>.
- Kuschel, M., Takors, R., 2020. Simulated oxygen and glucose gradients as a prerequisite for predicting industrial scale performance a priori. *Biotechnol. Bioeng.* 117, 2760–2770. <https://doi.org/10.1002/bit.27457>.
- Kvint, K., Farewell, A., Nyström, T., 2000. RpoS-dependent promoters require guanosine tetraphosphate for induction even in the presence of high levels of sigma(s). *The Journal of biological chemistry* 275, 14795–14798. <https://doi.org/10.1074/jbc.C000128200>.
- La Cruz, M. de, Ramírez, E.A., Sigala, J.-C., Utrilla, J., Lara, A.R., 2020. Plasmid DNA Production in Proteome-Reduced *Escherichia coli*. *Microorganisms* 8. <https://doi.org/10.3390/microorganisms8091444>.
- LaCroix, R.A., Sandberg, T.E., O'Brien, E.J., Utrilla, J., Ebrahim, A., Guzman, G.I., Szubin, R., Palsson, B.O., Feist, A.M., 2015. Use of adaptive laboratory evolution to discover key mutations enabling rapid growth of *Escherichia coli* K-12 MG1655 on glucose minimal medium. *Appl. Environ. Microbiol.* 81, 17–30. <https://doi.org/10.1128/AEM.02246-14>.
- Landberg, J., Wright, N.R., Wulff, T., Herrgård, M.J., Nielsen, A.T., 2020. CRISPR interference of nucleotide biosynthesis improves production of a single-domain antibody in *Escherichia coli*. *Biotechnol. Bioeng.* 117, 3835–3848. <https://doi.org/10.1002/bit.27536>.
- Landini, P., Egli, T., Wolf, J., Lacour, S., 2014. sigma_S, a major player in the response to environmental stresses in *Escherichia coli*: role, regulation and mechanisms of promoter recognition. *Environmental microbiology reports* 6, 1–13. <https://doi.org/10.1111/1758-2229.12112>.
- Lange, J., Takors, R., Blombach, B., 2017. Zero-growth bioprocesses: A challenge for microbial production strains and bioprocess engineering. *Eng. Life Sci.* 17, 27–35. <https://doi.org/10.1002/elsc.201600108>.
- Langmead, B., Salzberg, S.L., 2012. Fast gapped-read alignment with Bowtie 2. *Nature methods* 9, 357–359. <https://doi.org/10.1038/nmeth.1923>.
- Lapin, A., Schmid, J., Reuss, M., 2006. Modeling the dynamics of *E. coli* populations in the three-dimensional turbulent field of a stirred-tank bioreactor—A structured–segregated

-
- approach. *Chemical Engineering Science* 61, 4783–4797.
<https://doi.org/10.1016/j.ces.2006.03.003>.
- Lara, A.R., Galindo, E., Ramírez, O.T., Palomares, L.A., 2006a. Living With Heterogeneities in Bioreactors: Understanding the Effects of Environmental Gradients on Cells. *MB* 34, 355–382. <https://doi.org/10.1385/MB:34:3:355>.
- Lara, A.R., Leal, L., Flores, N., Gosset, G., Bolívar, F., Ramírez, O.T., 2006b. Transcriptional and metabolic response of recombinant *Escherichia coli* to spatial dissolved oxygen tension gradients simulated in a scale-down system. *Biotechnol. Bioeng.* 93, 372–385. <https://doi.org/10.1002/bit.20704>.
- Lara, A.R., Taymaz-Nikerel, H., Mashego, M.R., van Gulik, W.M., Heijnen, J.J., Ramírez, O.T., van Winden, W.A., 2009. Fast dynamic response of the fermentative metabolism of *Escherichia coli* to aerobic and anaerobic glucose pulses. *Biotechnol. Bioeng.* 104, 1153–1161. <https://doi.org/10.1002/bit.22503>.
- Lara, A.R., Vazquez-Limón, C., Gosset, G., Bolívar, F., López-Munguía, A., Ramírez, O.T., 2006c. Engineering *Escherichia coli* to improve culture performance and reduce formation of by-products during recombinant protein production under transient intermittent anaerobic conditions. *Biotechnol. Bioeng.* 94, 1164–1175. <https://doi.org/10.1002/bit.20954>.
- Larson, M.H., Gilbert, L.A., Wang, X., Lim, W.A., Weissman, J.S., Qi, L.S., 2013. CRISPR interference (CRISPRi) for sequence-specific control of gene expression. *Nat. Protoc.* 8, 2180–2196. <https://doi.org/10.1038/nprot.2013.132>.
- Larsson, G., Enfors, S.-O., 1988. Studies of insufficient mixing in bioreactors: Effects of limiting oxygen concentrations and short term oxygen starvation on *Penicillium chrysogenum*. *Bioprocess Engineering* 3, 123–127. <https://doi.org/10.1007/BF00373475>.
- Larsson, G., Trnkvist, M., Wernersson, E.S., Trgrdh, C., Noorman, H., Enfors, S.-O., 1996. Substrate gradients in bioreactors: origin and consequences. *Bioprocess Engineering* 14, 281–289. <https://doi.org/10.1007/BF00369471>.
- Laurie, A.D., Bernardo, L.M.D., Sze, C.C., Skarfstad, E., Szalewska-Palasz, A., Nyström, T., Shingler, V., 2003. The role of the alarmone (p)ppGpp in sigma N competition for core RNA polymerase. *The Journal of biological chemistry* 278, 1494–1503. <https://doi.org/10.1074/jbc.M209268200>.

-
- Lee, S., Kim, M.H., Kang, B.S., Kim, J.-S., Kim, G.-H., Kim, Y.-G., Kim, K.J., 2008. Crystal structure of *Escherichia coli* MazG, the regulator of nutritional stress response. *The Journal of biological chemistry* 283, 15232–15240. <https://doi.org/10.1074/jbc.M800479200>.
- Lee, S.Y., Kim, H.U., 2015. Systems strategies for developing industrial microbial strains. *Nature biotechnology* 33, 1061–1072. <https://doi.org/10.1038/nbt.3365>.
- Lempp, M., Farke, N., Kuntz, M., Freibert, S.A., Lill, R., Link, H., 2019. Systematic identification of metabolites controlling gene expression in *E. coli*. *Nat. Commun.* 10, 4463. <https://doi.org/10.1038/s41467-019-12474-1>.
- Li, Q., Zhao, P., Yin, H., Liu, Z., Zhao, H., Tian, P., 2020a. CRISPR interference-guided modulation of glucose pathways to boost aconitic acid production in *Escherichia coli*. *Microb. Cell Factories* 19, 174. <https://doi.org/10.1186/s12934-020-01435-9>.
- Li, S., Jendresen, C.B., Landberg, J., Pedersen, L.E., Sonnenschein, N., Jensen, S.I., Nielsen, A.T., 2020b. Genome-Wide CRISPRi-Based Identification of Targets for Decoupling Growth from Production. *ACS Synth. Biol.* 9, 1030–1040. <https://doi.org/10.1021/acssynbio.9b00143>.
- Li, X.-T., Thomason, L.C., Sawitzke, J.A., Costantino, N., Court, D.L., 2013. Positive and negative selection using the tetA-sacB cassette: recombineering and P1 transduction in *Escherichia coli*: Recombineering and P1 transduction in *Escherichia coli*. *Nucleic Acids Res.* 41, e204. <https://doi.org/10.1093/nar/gkt1075>.
- Li, Y., Chen, J., Lun, S.Y., 2001a. Biotechnological production of pyruvic acid. *Appl. Microbiol. Biotechnol.* 57, 451–459. <https://doi.org/10.1007/s002530100804>.
- Li, Y., Chen, J., Lun, S.Y., Rui, X.S., 2001b. Efficient pyruvate production by a multi-vitamin auxotroph of *Torulopsis glabrata*: key role and optimization of vitamin levels. *Appl. Microbiol. Biotechnol.* 55, 680–685. <https://doi.org/10.1007/s002530100598>.
- Li, Y., Wang, G., 2016. Strategies of isoprenoids production in engineered bacteria. *Journal of applied microbiology* 121, 932–940. <https://doi.org/10.1111/jam.13237>.
- Liaw, S.H., Eisenberg, D., 1994. Structural model for the reaction mechanism of glutamine synthetase, based on five crystal structures of enzyme-substrate complexes. *Biochemistry* 33, 675–681. <https://doi.org/10.1021/bi00169a007>.

-
- Lieder, S., Nikel, P.I., Lorenzo, V. de, Takors, R., 2015. Genome reduction boosts heterologous gene expression in *Pseudomonas putida*. *Microb. Cell Factories* 14, 23. <https://doi.org/10.1186/s12934-015-0207-7>.
- Linton, J.D., Musgrave, S.G., 1983. Product formation by a nitrogen limited culture of *Beneckea natriegens* in a chemostat in the presence of excess glucose. *Appl. Microbiol. Biotechnol.* 18, 24–28. <https://doi.org/10.1007/BF00508125>.
- Lo, T.-M., Chng, S.H., Teo, W.S., Cho, H.-S., Chang, M.W., 2016. A Two-Layer Gene Circuit for Decoupling Cell Growth from Metabolite Production. *Cell Syst.* 3, 133–143. <https://doi.org/10.1016/j.cels.2016.07.012>.
- Löffler, M., Simen, J.D., Jäger, G., Schäferhoff, K., Freund, A., Takors, R., 2016. Engineering *E. coli* for large-scale production - Strategies considering ATP expenses and transcriptional responses. *Metab. Eng.* 38, 73–85. <https://doi.org/10.1016/j.ymben.2016.06.008>.
- Löffler, M., Simen, J.D., Müller, J., Jäger, G., Laghrami, S., Schäferhoff, K., Freund, A., Takors, R., 2017. Switching between nitrogen and glucose limitation: Unraveling transcriptional dynamics in *Escherichia coli*. *Journal of biotechnology* 258, 2–12. <https://doi.org/10.1016/j.jbiotec.2017.04.011>.
- Love, M.I., Huber, W., Anders, S., 2014. Moderated estimation of fold change and dispersion for RNA-seq data with DESeq2. *Genome biology* 15, 550. <https://doi.org/10.1186/s13059-014-0550-8>.
- Luo, W., Friedman, M.S., Shedden, K., Hankenson, K.D., Woolf, P.J., 2009. GAGE: generally applicable gene set enrichment for pathway analysis. *BMC bioinformatics* 10, 161. <https://doi.org/10.1186/1471-2105-10-161>.
- Ma, Y., Cui, Y., Du, L., Liu, X., Xie, X., Chen, N., 2018. Identification and application of a growth-regulated promoter for improving L-valine production in *Corynebacterium glutamicum*. *Microb. Cell Factories* 17, 185. <https://doi.org/10.1186/s12934-018-1031-7>.
- Maciag, M., Kochanowska, M., Lyzeń, R., Wegrzyn, G., Szalewska-Pałasz, A., 2010. ppGpp inhibits the activity of *Escherichia coli* DnaG primase. *Plasmid* 63, 61–67. <https://doi.org/10.1016/j.plasmid.2009.11.002>.
- Maeda, H., Fujita, N., Ishihama, A., 2000. Competition among seven *Escherichia coli* sigma subunits: relative binding affinities to the core RNA polymerase. *Nucleic Acids Res.* 28, 3497–3503. <https://doi.org/10.1093/nar/28.18.3497>.

- Maeda, S., Shimizu, K., Kihira, C., Iwabu, Y., Kato, R., Sugimoto, M., Fukiya, S., Wada, M., Yokota, A., 2017. Pyruvate dehydrogenase complex regulator (PdhR) gene deletion boosts glucose metabolism in *Escherichia coli* under oxygen-limited culture conditions. *Journal of bioscience and bioengineering* 123, 437–443. <https://doi.org/10.1016/j.jbiosc.2016.11.004>.
- Magnusson, L.U., Farewell, A., Nyström, T., 2005. ppGpp: a global regulator in *Escherichia coli*. *Trends in microbiology* 13, 236–242. <https://doi.org/10.1016/j.tim.2005.03.008>.
- Maresca, M., Eler, A., Fu, J., Friedrich, A., Zhang, Y., Stewart, A.F., 2010. Single-stranded heteroduplex intermediates in lambda Red homologous recombination. *BMC molecular biology* 11, 54. <https://doi.org/10.1186/1471-2199-11-54>.
- Marsić, N., Roje, S., Stojiljković, I., Salaj-Smic, E., Trgovcević, Z., 1993. In vivo studies on the interaction of RecBCD enzyme and lambda Gam protein. *J. Bacteriol.* 175, 4738–4743. <https://doi.org/10.1128/jb.175.15.4738-4743.1993>.
- Martínez-Antonio, A., Collado-Vides, J., 2003. Identifying global regulators in transcriptional regulatory networks in bacteria. *Current opinion in microbiology* 6, 482–489. <https://doi.org/10.1016/j.mib.2003.09.002>.
- Martínez-García, E., Jatsenko, T., Kivisaar, M., Lorenzo, V. de, 2015. Freeing *Pseudomonas putida* KT2440 of its proviral load strengthens endurance to environmental stresses. *Environmental microbiology* 17, 76–90. <https://doi.org/10.1111/1462-2920.12492>.
- Martínez-García, E., Nikel, P.I., Aparicio, T., Lorenzo, V. de, 2014a. *Pseudomonas* 2.0: genetic upgrading of *P. putida* KT2440 as an enhanced host for heterologous gene expression. *Microb. Cell Factories* 13, 159. <https://doi.org/10.1186/s12934-014-0159-3>.
- Martínez-García, E., Nikel, P.I., Chavarría, M., Lorenzo, V. de, 2014b. The metabolic cost of flagellar motion in *Pseudomonas putida* KT2440. *Environmental microbiology* 16, 291–303. <https://doi.org/10.1111/1462-2920.12309>.
- Mazumder, A., Kapanidis, A.N., 2019. Recent Advances in Understanding σ^{70} -Dependent Transcription Initiation Mechanisms. *J. Mol. Biol.* 431, 3947–3959. <https://doi.org/10.1016/j.jmb.2019.04.046>.
- McMurry, L., Petrucci, R.E., Levy, S.B., 1980. Active efflux of tetracycline encoded by four genetically different tetracycline resistance determinants in *Escherichia coli*. *Proceedings of the National Academy of Sciences of the United States of America* 77, 3974–3977. <https://doi.org/10.1073/pnas.77.7.3974>.

- Mechold, U., Potrykus, K., Murphy, H., Murakami, K.S., Cashel, M., 2013. Differential regulation by ppGpp versus pppGpp in *Escherichia coli*. *Nucleic Acids Res.* 41, 6175–6189. <https://doi.org/10.1093/nar/gkt302>.
- Merrick, M.J., 1993. In a class of its own--the RNA polymerase sigma factor sigma 54 (sigma N). *Mol. Microbiol.* 10, 903–909. <https://doi.org/10.1111/j.1365-2958.1993.tb00961.x>.
- Meyer, H.-P., Leist, C., Fiechter, A., 1984. Acetate formation in continuous culture of *Escherichia coli* K12 D1 on defined and complex media. *Journal of biotechnology* 1, 355–358. [https://doi.org/10.1016/0168-1656\(84\)90027-0](https://doi.org/10.1016/0168-1656(84)90027-0).
- Michalowski, A., Siemann-Herzberg, M., Takors, R., 2017. *Escherichia coli* HGT: Engineered for high glucose throughput even under slowly growing or resting conditions. *Metab. Eng.* 40, 93–103. <https://doi.org/10.1016/j.ymben.2017.01.005>.
- Miller, J.H., 1972. *Experiments in molecular genetics*, 11th ed. Cold Spring Harbor Laboratory, Cold Spring Harbor, NY, 466 pp.
- Miller, R.E., Stadtman, E.R., 1972. Glutamate Synthase from *Escherichia coli*. *Journal of Biological Chemistry* 247, 7407–7419. [https://doi.org/10.1016/S0021-9258\(19\)44642-5](https://doi.org/10.1016/S0021-9258(19)44642-5).
- Miyake, Y., Inaba, T., Watanabe, H., Teramoto, J., Yamamoto, K., Ishihama, A., 2019. Regulatory roles of pyruvate-sensing two-component system PyrSR (YpdAB) in *Escherichia coli* K-12. *FEMS Microbiol. Lett.* 366. <https://doi.org/10.1093/femsle/fnz009>.
- Miyata, R., Yonehara, T., Yotsumoto, K., Tsutsui, H., 1987. Process for preparing pyruvic acid by fermentation. WO1987JP00621 C12P7/40;C12P7/40.
- Mizoguchi, H., Mori, H., Fujio, T., 2007. *Escherichia coli* minimum genome factory. *Biotechnol. Appl. Biochem.* 46, 157–167. <https://doi.org/10.1042/BA20060107>.
- Mizoguchi, H., Sawano, Y., Kato, J., Mori, H., 2008. Superpositioning of deletions promotes growth of *Escherichia coli* with a reduced genome. *DNA research : an international journal for rapid publication of reports on genes and genomes* 15, 277–284. <https://doi.org/10.1093/dnares/dsn019>.
- Mojica, F.J.M., Díez-Villaseñor, C., García-Martínez, J., Almendros, C., 2009. Short motif sequences determine the targets of the prokaryotic CRISPR defence system. *Microbiology (Reading, England)* 155, 733–740. <https://doi.org/10.1099/mic.0.023960-0>.
- Molodtsov, V., Sineva, E., Zhang, L., Huang, X., Cashel, M., Ades, S.E., Murakami, K.S., 2018. Allosteric Effector ppGpp Potentiates the Inhibition of Transcript Initiation by DksA. *Molecular cell* 69, 828-839.e5. <https://doi.org/10.1016/j.molcel.2018.01.035>.

- Monod, J., 1949. The Growth of Bacterial Cultures. *Annu Rev Microbiol* 3, 371–394.
<https://doi.org/10.1146/annurev.mi.03.100149.002103>.
- Monod, J., 1950. La technique de culture continue: théorie et applications. *Annales de l'Institut Pasteur*, 390–410.
- Monot, F., Engasser, J.M., 1983. Production of acetone and butanol by batch and continuous culture of *Clostridium acetobutylicum* under nitrogen limitation. *Biotechnology Letters* 5, 213–218. <https://doi.org/10.1007/BF00161117>.
- Montero, M., Rahimpour, M., Viale, A.M., Almagro, G., Eydallin, G., Sevilla, Á., Cánovas, M., Bernal, C., Lozano, A.B., Muñoz, F.J., Baroja-Fernández, E., Bahaji, A., Mori, H., Codoñer, F.M., Pozueta-Romero, J., 2014. Systematic production of inactivating and non-inactivating suppressor mutations at the *relA* locus that compensate the detrimental effects of complete spot loss and affect glycogen content in *Escherichia coli*. *PloS one* 9, e106938. <https://doi.org/10.1371/journal.pone.0106938>.
- Mosberg, J.A., Lajoie, M.J., Church, G.M., 2010. Lambda red recombineering in *Escherichia coli* occurs through a fully single-stranded intermediate. *Genetics* 186, 791–799.
<https://doi.org/10.1534/genetics.110.120782>.
- Mueller, E.A., Egan, A.J., Breukink, E., Vollmer, W., Levin, P.A., 2019. Plasticity of *Escherichia coli* cell wall metabolism promotes fitness and antibiotic resistance across environmental conditions. *eLife* 8. <https://doi.org/10.7554/eLife.40754>.
- Mueller, E.J., Oh, S., Kavalerchik, E., Kappock, T.J., Meyer, E., Li, C., Ealick, S.E., Stubbe, J., 1999. Investigation of the ATP binding site of *Escherichia coli* aminoimidazole ribonucleotide synthetase using affinity labeling and site-directed mutagenesis. *Biochemistry* 38, 9831–9839. <https://doi.org/10.1021/bi990638r>.
- Murakami, K.S., Masuda, S., Campbell, E.A., Muzzin, O., Darst, S.A., 2002. Structural basis of transcription initiation: an RNA polymerase holoenzyme-DNA complex. *Science* 296, 1285–1290. <https://doi.org/10.1126/science.1069595>.
- Murphy, K.C., 2016. λ Recombination and Recombineering. *EcoSal Plus* 7.
<https://doi.org/10.1128/ecosalplus.ESP-0011-2015>.
- Murray, K.D., Bremer, H., 1996. Control of *spoT*-dependent ppGpp synthesis and degradation in *Escherichia coli*. *J. Mol. Biol.* 259, 41–57.
<https://doi.org/10.1006/jmbi.1996.0300>.

-
- Muse, W.B., Bender, R.A., 1998. The *nac* (nitrogen assimilation control) gene from *Escherichia coli*. *J. Bacteriol.* 180, 1166–1173. <https://doi.org/10.1128/JB.180.5.1166-1173.1998>.
- Nakashima, N., Ohno, S., Yoshikawa, K., Shimizu, H., Tamura, T., 2014. A vector library for silencing central carbon metabolism genes with antisense RNAs in *Escherichia coli*. *Appl. Environ. Microbiol.* 80, 564–573. <https://doi.org/10.1128/AEM.02376-13>.
- Nanchen, A., Schicker, A., Revelles, O., Sauer, U., 2008. Cyclic AMP-dependent catabolite repression is the dominant control mechanism of metabolic fluxes under glucose limitation in *Escherichia coli*. *Journal of bacteriology* 190, 2323–2330. <https://doi.org/10.1128/JB.01353-07>.
- Neubauer, P., Åhman, M., Törnkvist, M., Larsson, G., Enfors, S.-O., 1995a. Response of guanosine tetraphosphate to glucose fluctuations in fed-batch cultivations of *Escherichia coli*. *Journal of biotechnology* 43, 195–204. [https://doi.org/10.1016/0168-1656\(95\)00130-1](https://doi.org/10.1016/0168-1656(95)00130-1).
- Neubauer, P., Häggström, L., Enfors, S.O., 1995b. Influence of substrate oscillations on acetate formation and growth yield in *Escherichia coli* glucose limited fed-batch cultivations. *Biotechnol. Bioeng.* 47, 139–146. <https://doi.org/10.1002/bit.260470204>.
- Neubauer, P., Junne, S., 2010. Scale-down simulators for metabolic analysis of large-scale bioprocesses. *Current opinion in biotechnology* 21, 114–121. <https://doi.org/10.1016/j.copbio.2010.02.001>.
- Nieß, A., Löffler, M., Simen, J.D., Takors, R., 2017. Repetitive Short-Term Stimuli Imposed in Poor Mixing Zones Induce Long-Term Adaptation of *E. coli* Cultures in Large-Scale Bioreactors: Experimental Evidence and Mathematical Model. *Frontiers in microbiology* 8, 1195. <https://doi.org/10.3389/fmicb.2017.01195>.
- Nishimura, I., Kurokawa, M., Liu, L., Ying, B.-W., 2017. Coordinated Changes in Mutation and Growth Rates Induced by Genome Reduction. *mBio* 8, e00676-17. <https://doi.org/10.1128/mBio.00676-17>.
- Noack, S., Baumgart, M., 2018. Communities of Niche-Optimized Strains: Small-Genome Organism Consortia in Bioproduction. *Trends in Biotechnology*. <https://doi.org/10.1016/j.tibtech.2018.07.011>.
- Noguchi, Y., Nakai, Y., Shimba, N., Toyosaki, H., Kawahara, Y., Sugimoto, S., Suzuki, E.-I., 2004. The energetic conversion competence of *Escherichia coli* during aerobic respiration

-
- studied by ³¹P NMR using a circulating fermentation system. *Journal of biochemistry* 136, 509–515. <https://doi.org/10.1093/jb/mvh147>.
- Noorman, H., 2011. An industrial perspective on bioreactor scale-down: what we can learn from combined large-scale bioprocess and model fluid studies. *Biotechnology journal* 6, 934–943. <https://doi.org/10.1002/biot.201000406>.
- Notley-McRobb, L., King, T., Ferenci, T., 2002. rpoS Mutations and Loss of General Stress Resistance in *Escherichia coli* Populations as a Consequence of Conflict between Competing Stress Responses. *Journal of bacteriology* 184, 806–811. <https://doi.org/10.1128/JB.184.3.806-811.2002>.
- Novick, A., Szilard, L., 1950. Description of the chemostat. *Science* 112, 715–716. <https://doi.org/10.1126/science.112.2920.715>.
- Ogasawara, H., Ishizuka, T., Yamaji, K., Kato, Y., Shimada, T., Ishihama, A., 2019. Regulatory role of pyruvate-sensing BtsSR in biofilm formation by *Escherichia coli* K-12. *FEMS Microbiol. Lett.* 366. <https://doi.org/10.1093/femsle/fnz251>.
- Oliveira-Filho, E.R., Silva, J.G.P., Macedo, M.A. de, Taciro, M.K., Gomez, J.G.C., Silva, L.F., 2019. Investigating Nutrient Limitation Role on Improvement of Growth and Poly(3-Hydroxybutyrate) Accumulation by *Burkholderia sacchari* LMG 19450 From Xylose as the Sole Carbon Source. *Frontiers in bioengineering and biotechnology* 7, 416. <https://doi.org/10.3389/fbioe.2019.00416>.
- Olughu, W., Deepika, G., Hewitt, C., Rielly, C., 2019. Insight into the large-scale upstream fermentation environment using scaled-down models. *J. Chem. Technol. Biotechnol.* 94, 647–657. <https://doi.org/10.1002/jctb.5804>.
- Olughu, W., Nienow, A., Hewitt, C., Rielly, C., 2020. Scale-down studies for the scale-up of a recombinant *Corynebacterium glutamicum* fed-batch fermentation: loss of homogeneity leads to lower levels of cadaverine production. *J. Chem. Technol. Biotechnol.* 95, 675–685. <https://doi.org/10.1002/jctb.6248>.
- Olvera, L., Mendoza-Vargas, A., Flores, N., Olvera, M., Sigala, J.C., Gosset, G., Morett, E., Bolívar, F., 2009. Transcription analysis of central metabolism genes in *Escherichia coli*. Possible roles of sigma38 in their expression, as a response to carbon limitation. *PloS one* 4, e7466. <https://doi.org/10.1371/journal.pone.0007466>.

- Onakpoya, I., Hunt, K., Wider, B., Ernst, E., 2014. Pyruvate supplementation for weight loss: a systematic review and meta-analysis of randomized clinical trials. *Crit. Rev. Food Sci. Nutr.* 54, 17–23. <https://doi.org/10.1080/10408398.2011.565890>.
- Oosterhuis, N.M.G., Groesbeek, N.M., Olivier, A.P.C., Kossen, N.W.F., 1983. Scale-down aspects of the gluconic acid fermentation. *Biotechnology Letters* 5, 141–146. <https://doi.org/10.1007/BF00131892>.
- Pablos, T.E., Sigala, J.C., Le Borgne, S., Lara, A.R., 2014. Aerobic expression of *Vitreoscilla* hemoglobin efficiently reduces overflow metabolism in *Escherichia coli*. *Biotechnology journal* 9, 791–799. <https://doi.org/10.1002/biot.201300388>.
- Papa, L.J., Shoulders, M.D., 2019. Genetic Engineering by DNA Recombineering. *Current protocols in chemical biology* 11, e70. <https://doi.org/10.1002/cpch.70>.
- Pardee, A.B., Jacob, F., Monod, J., 1959. The genetic control and cytoplasmic expression of “Inducibility” in the synthesis of β -galactosidase by *E. coli*. *J. Mol. Biol.* 1, 165–178. [https://doi.org/10.1016/S0022-2836\(59\)80045-0](https://doi.org/10.1016/S0022-2836(59)80045-0).
- Pastan, I., Adhya, S., 1976. Cyclic adenosine 5'-monophosphate in *Escherichia coli*. *Bacteriological Reviews* 40, 527–551. <https://doi.org/10.1128/br.40.3.527-551.1976>.
- Patil, V., Santos, C.N.S., Ajikumar, P.K., Sarria, S., Takors, R., 2021. Balancing glucose and oxygen uptake rates to enable high amorpha-4,11-diene production in *Escherichia coli* via the methylerythritol phosphate pathway. *Biotechnol. Bioeng.* 118, 1317–1329. <https://doi.org/10.1002/bit.27655>.
- Perez-Zabaleta, M., Guevara-Martínez, M., Gustavsson, M., Quillaguamán, J., Larsson, G., van Maris, A.J.A., 2019. Comparison of engineered *Escherichia coli* AF1000 and BL21 strains for (R)-3-hydroxybutyrate production in fed-batch cultivation. *Appl. Microbiol. Biotechnol.* 103, 5627–5639. <https://doi.org/10.1007/s00253-019-09876-y>.
- Perez-Zabaleta, M., Sjöberg, G., Guevara-Martínez, M., Jarmander, J., Gustavsson, M., Quillaguamán, J., Larsson, G., 2016. Increasing the production of (R)-3-hydroxybutyrate in recombinant *Escherichia coli* by improved cofactor supply. *Microb. Cell Factories* 15, 91. <https://doi.org/10.1186/s12934-016-0490-y>.
- Pirt, S.J., 1965. The maintenance energy of bacteria in growing cultures. *Proceedings of the Royal Society of London. Series B, Biological sciences* 163, 224–231. <https://doi.org/10.1098/rspb.1965.0069>.

- Polaris Market Research, 2020. Biotechnology Market Share, Size, Trends & Industry Analysis Report By Technology (Fermentation, Tissue Engineering and Regeneration, PCR Technology, Nanobiotechnology, Chromatography, DNA Sequencing, Cell Based Assays); By Application (BioPharmacy, BioServices, BioAgriculture, BioIndustrial, Bioinformatics); and By Regions: Segment Forecast, 2020 - 2026 Report ID: PM1011. <https://www.polarismarketresearch.com/industry-analysis/biotechnology-market>.
- Pósfai, G., Plunkett, G., Fehér, T., Frisch, D., Keil, G.M., Umenhoffer, K., Kolisnychenko, V., Stahl, B., Sharma, S.S., Arruda, M. de, Burland, V., Harcum, S.W., Blattner, F.R., 2006. Emergent properties of reduced-genome *Escherichia coli*. *Science (New York, N.Y.)* 312, 1044–1046. <https://doi.org/10.1126/science.1126439>.
- Potrykus, K., Murphy, H., Philippe, N., Cashel, M., 2011. ppGpp is the major source of growth rate control in *E. coli*. *Environmental microbiology* 13, 563–575. <https://doi.org/10.1111/j.1462-2920.2010.02357.x>.
- Qi, L.S., Larson, M.H., Gilbert, L.A., Doudna, J.A., Weissman, J.S., Arkin, A.P., Lim, W.A., 2013. Repurposing CRISPR as an RNA-guided platform for sequence-specific control of gene expression. *Cell* 152, 1173–1183. <https://doi.org/10.1016/j.cell.2013.02.022>.
- Quail, M.A., Haydon, D.J., Guest, J.R., 1994. The *pdhR-aceEF-lpd* operon of *Escherichia coli* expresses the pyruvate dehydrogenase complex. *Mol. Microbiol.* 12, 95–104. <https://doi.org/10.1111/j.1365-2958.1994.tb00998.x>.
- Ramseier, T.M., Nègre, D., Cortay, J.C., Scarabel, M., Cozzone, A.J., Saier, M.H., 1993. In vitro binding of the pleiotropic transcriptional regulatory protein, FruR, to the *fru*, *pps*, *ace*, *pts* and *icd* operons of *Escherichia coli* and *Salmonella typhimurium*. *J. Mol. Biol.* 234, 28–44. <https://doi.org/10.1006/jmbi.1993.1561>.
- Ran, F.A., Hsu, P.D., Lin, C.-Y., Gootenberg, J.S., Konermann, S., Trevino, A.E., Scott, D.A., Inoue, A., Matoba, S., Zhang, Y., Zhang, F., 2013. Double nicking by RNA-guided CRISPR Cas9 for enhanced genome editing specificity. *Cell* 154, 1380–1389. <https://doi.org/10.1016/j.cell.2013.08.021>.
- Rath, D., Amlinger, L., Hoekzema, M., Devulapally, P.R., Lundgren, M., 2015. Efficient programmable gene silencing by Cascade. *Nucleic Acids Res.* 43, 237–246. <https://doi.org/10.1093/nar/gku1257>.

- Record Jr, M., Courtenay, E.S., Cayley, D., Guttman, H.J., 1998. Responses of *E. coli* to osmotic stress: large changes in amounts of cytoplasmic solutes and water. *Trends in Biochemical Sciences* 23, 143–148. [https://doi.org/10.1016/S0968-0004\(98\)01196-7](https://doi.org/10.1016/S0968-0004(98)01196-7).
- Reddy, P., Kamireddi, M., 1998. Modulation of *Escherichia coli* adenyl cyclase activity by catalytic-site mutants of protein IIA(Glc) of the phosphoenolpyruvate:sugar phosphotransferase system. *J. Bacteriol.* 180, 732–736. <https://doi.org/10.1128/JB.180.3.732-736.1998>.
- Reitzer, L., 2003. Nitrogen assimilation and global regulation in *Escherichia coli*. *Annual review of microbiology* 57, 155–176. <https://doi.org/10.1146/annurev.micro.57.030502.090820>.
- Rohmer, M., Seemann, M., Horbach, S., Bringer-Meyer, S., Sahm, H., 1996. Glyceraldehyde 3-Phosphate and Pyruvate as Precursors of Isoprenic Units in an Alternative Non-mevalonate Pathway for Terpenoid Biosynthesis. *J. Am. Chem. Soc.* 118, 2564–2566. <https://doi.org/10.1021/ja9538344>.
- Ross, W., Sanchez-Vazquez, P., Chen, A.Y., Lee, J.-H., Burgos, H.L., Gourse, R.L., 2016. ppGpp Binding to a Site at the RNAP-DksA Interface Accounts for Its Dramatic Effects on Transcription Initiation during the Stringent Response. *Molecular cell* 62, 811–823. <https://doi.org/10.1016/j.molcel.2016.04.029>.
- Rubroder, F.J., Keller, R., Rubroeder, F.J., 2001. Process for obtaining insulin precursors having correctly bonded cystine bridges.
US20010947563;DE19971035711;US19990386303;US19980134836
C12N15/09;A61K38/28;A61P5/50;C07K1/02;C07K1/113;C07K1/12;C07K1/14;C07K14/575;C07K14/62;C12N1/21;C12N15/00;C12P21/02;A61K38/00;C12R1/19;C07K14/62.
- Rugbjerg, P., Myling-Petersen, N., Porse, A., Sarup-Lytzen, K., Sommer, M.O.A., 2018. Diverse genetic error modes constrain large-scale bio-based production. *Nat. Commun.* 9, 787. <https://doi.org/10.1038/s41467-018-03232-w>.
- Ruwe, M., Persicke, M., Busche, T., Müller, B., Kalinowski, J., 2019. Physiology and Transcriptional Analysis of (p)ppGpp-Related Regulatory Effects in *Corynebacterium glutamicum*. *Frontiers in microbiology* 10, 2769. <https://doi.org/10.3389/fmicb.2019.02769>.
- Saier, M.H., Crasnier, M., 1996. Inducer exclusion and the regulation of sugar transport. *Research in Microbiology* 147, 482–489. [https://doi.org/10.1016/S0923-2508\(96\)90150-3](https://doi.org/10.1016/S0923-2508(96)90150-3).

- Saier, M.H., Straud, H., Massman, L.S., Judice, J.J., Newman, M.J., Feucht, B.U., 1978. Permease-specific mutations in *Salmonella typhimurium* and *Escherichia coli* that release the glycerol, maltose, melibiose, and lactose transport systems from regulation by the phosphoenolpyruvate:sugar phosphotransferase system. *J. Bacteriol.* 133, 1358–1367. <https://doi.org/10.1128/jb.133.3.1358-1367.1978>.
- Sanchez-Vazquez, P., Dewey, C.N., Kitten, N., Ross, W., Gourse, R.L., 2019. Genome-wide effects on *Escherichia coli* transcription from ppGpp binding to its two sites on RNA polymerase. *PNAS* 116, 8310–8319. <https://doi.org/10.1073/pnas.1819682116>.
- Sander, T., Farke, N., Diehl, C., Kuntz, M., Glatter, T., Link, H., 2019a. Allosteric Feedback Inhibition Enables Robust Amino Acid Biosynthesis in *E. coli* by Enforcing Enzyme Overabundance. *Cell Syst.* 8, 66-75.e8. <https://doi.org/10.1016/j.cels.2018.12.005>.
- Sander, T., Wang, C.Y., Glatter, T., Link, H., 2019b. CRISPRi-Based Downregulation of Transcriptional Feedback Improves Growth and Metabolism of Arginine Overproducing *E. coli*. *ACS Synth. Biol.* 8, 1983–1990. <https://doi.org/10.1021/acssynbio.9b00183>.
- Sandoval-Basurto, E.A., Gosset, G., Bolívar, F., Ramírez, O.T., 2005. Culture of *Escherichia coli* under dissolved oxygen gradients simulated in a two-compartment scale-down system: metabolic response and production of recombinant protein. *Biotechnol. Bioeng.* 89, 453–463. <https://doi.org/10.1002/bit.20383>.
- Santos-Zavaleta, A., Salgado, H., Gama-Castro, S., Sánchez-Pérez, M., Gómez-Romero, L., Ledezma-Tejeida, D., García-Sotelo, J.S., Alquicira-Hernández, K., Muñoz-Rascado, L.J., Peña-Loredo, P., Ishida-Gutiérrez, C., Velázquez-Ramírez, D.A., Del Moral-Chávez, V., Bonavides-Martínez, C., Méndez-Cruz, C.-F., Galagan, J., 2019. RegulonDB v 10.5: tackling challenges to unify classic and high throughput knowledge of gene regulation in *E. coli* K-12. *Nucleic Acids Res.* 47, D212-D220. <https://doi.org/10.1093/nar/gky1077>.
- Sarkar, D., Siddiquee, K.A.Z., Araúzo-Bravo, M.J., Oba, T., Shimizu, K., 2008. Effect of *cra* gene knockout together with *edd* and *iclR* genes knockout on the metabolism in *Escherichia coli*. *Archives of microbiology* 190, 559–571. <https://doi.org/10.1007/s00203-008-0406-2>.
- Sawai, H., Mimitsuka, T., Minegishi, S.-I., Henmi, M., Yamada, K., Shimizu, S., Yonehara, T., 2011. A novel membrane-integrated fermentation reactor system: application to pyruvic acid production in continuous culture by *Torulopsis glabrata*. *Bioprocess Biosyst. Eng.* 34, 721–725. <https://doi.org/10.1007/s00449-011-0521-3>.

- Schilling, B.M., Pfefferle, W., Bachmann, B., Leuchtenberger, W., Deckwer, W.-D., 1999. A special reactor design for investigations of mixing time effects in a scaled-down industrial L-lysine fed-batch fermentation process. *Biotechnol. Bioeng.* 64, 599–606. [https://doi.org/10.1002/\(SICI\)1097-0290\(19990905\)64:5<599:AID-BIT10>3.0.CO;2-C](https://doi.org/10.1002/(SICI)1097-0290(19990905)64:5<599:AID-BIT10>3.0.CO;2-C).
- Schuhmacher, T., Löffler, M., Hurler, T., Takors, R., 2014. Phosphate limited fed-batch processes: impact on carbon usage and energy metabolism in *Escherichia coli*. *Journal of biotechnology* 190, 96–104. <https://doi.org/10.1016/j.jbiotec.2014.04.025>.
- Schultenkämper, K., Brito, L.F., Wendisch, V.F., 2020. Impact of CRISPR interference on strain development in biotechnology. *Biotechnol. Appl. Biochem.* 67, 7–21. <https://doi.org/10.1002/bab.1901>.
- Schweder, T., Krüger, E., Xu, B., Jrgen, B., Blomsten, G., Enfors, S.-O., Hecker, M., 1999. Monitoring of genes that respond to process-related stress in large-scale bioprocesses. *Biotechnol. Bioeng.* 65, 151–159. [https://doi.org/10.1002/\(SICI\)1097-0290\(19991020\)65:2<151:AID-BIT4>3.0.CO;2-V](https://doi.org/10.1002/(SICI)1097-0290(19991020)65:2<151:AID-BIT4>3.0.CO;2-V).
- Sharma, A.K., Shukla, E., Janoti, D.S., Mukherjee, K.J., Shiloach, J., 2020. A novel knock out strategy to enhance recombinant protein expression in *Escherichia coli*. *Microb. Cell Factories* 19. <https://doi.org/10.1186/s12934-020-01407-z>.
- Sharma, S.S., Blattner, F.R., Harcum, S.W., 2007a. Recombinant protein production in an *Escherichia coli* reduced genome strain. *Metab. Eng.* 9, 133–141. <https://doi.org/10.1016/j.ymben.2006.10.002>.
- Sharma, S.S., Campbell, J.W., Frisch, D., Blattner, F.R., Harcum, S.W., 2007b. Expression of two recombinant chloramphenicol acetyltransferase variants in highly reduced genome *Escherichia coli* strains. *Biotechnol. Bioeng.* 98, 1056–1070. <https://doi.org/10.1002/bit.21491>.
- Shetty, R.P., Endy, D., Knight, T.F., 2008. Engineering BioBrick vectors from BioBrick parts. *J. Biol. Eng.* 2, 5. <https://doi.org/10.1186/1754-1611-2-5>.
- Shiio, I., Otsuka, S.I., Katsuya, N., 1962. Effect of biotin on the bacterial formation of glutamic acid. II. Metabolism of glucose. *Journal of biochemistry* 52, 108–116. <https://doi.org/10.1093/oxfordjournals.jbchem.a127578>.
- Shimizu, K., 2013. Metabolic Regulation of a Bacterial Cell System with Emphasis on *Escherichia coli* Metabolism. *ISRN biochemistry* 2013, 645983. <https://doi.org/10.1155/2013/645983>.

- Simen, J.D., Löffler, M., Jäger, G., Schäferhoff, K., Freund, A., Matthes, J., Müller, J., Takors, R., 2017. Transcriptional response of *Escherichia coli* to ammonia and glucose fluctuations. *Microbial biotechnology* 10, 858–872. <https://doi.org/10.1111/1751-7915.12713>.
- Sleight, S.C., Sauro, H.M., 2013. Visualization of evolutionary stability dynamics and competitive fitness of *Escherichia coli* engineered with randomized multigene circuits. *ACS Synth. Biol.* 2, 519–528. <https://doi.org/10.1021/sb400055h>.
- Soini, J., Ukkonen, K., Neubauer, P., 2008. High cell density media for *Escherichia coli* are generally designed for aerobic cultivations - consequences for large-scale bioprocesses and shake flask cultures. *Microb. Cell Factories* 7, 26. <https://doi.org/10.1186/1475-2859-7-26>.
- Soma, Y., Tsuruno, K., Wada, M., Yokota, A., Hanai, T., 2014. Metabolic flux redirection from a central metabolic pathway toward a synthetic pathway using a metabolic toggle switch. *Metab. Eng.* 23, 175–184. <https://doi.org/10.1016/j.ymben.2014.02.008>.
- Somerville, C.R., Ahmed, A., 1979. Mutants of *Escherichia coli* defective in the degradation of guanosine 5'-triphosphate, 3'-diphosphate (pppGpp). *Molec. Gen. Genet.* 169, 315–323. <https://doi.org/10.1007/BF00382277>.
- Steinchen, W., Bange, G., 2016. The magic dance of the alarmones (p)ppGpp. *Mol. Microbiol.* 101, 531–544. <https://doi.org/10.1111/mmi.13412>.
- Steinchen, W., Zegarra, V., Bange, G., 2020. (p)ppGpp: Magic Modulators of Bacterial Physiology and Metabolism. *Frontiers in microbiology* 11, 2072. <https://doi.org/10.3389/fmicb.2020.02072>.
- Stephanopoulos, G., 1999. Metabolic fluxes and metabolic engineering. *Metab. Eng.* 1, 1–11. <https://doi.org/10.1006/mben.1998.0101>.
- Stephenson, A.L., Dennis, J.S., Howe, C.J., Scott, S.A., Smith, A.G., 2010. Influence of nitrogen-limitation regime on the production by *Chlorella vulgaris* of lipids for biodiesel feedstocks. *Biofuels* 1, 47–58. <https://doi.org/10.4155/bfs.09.1>.
- Stouthamer, A.H., 1973. A theoretical study on the amount of ATP required for synthesis of microbial cell material. *Antonie van Leeuwenhoek* 39, 545–565. <https://doi.org/10.1007/BF02578899>.
- Stouthamer, A.H., Bettenhausen, C., 1973. Utilization of energy for growth and maintenance in continuous and batch cultures of microorganisms. *Biochimica et Biophysica Acta*

- (BBA) - Reviews on Bioenergetics 301, 53–70. [https://doi.org/10.1016/0304-4173\(73\)90012-8](https://doi.org/10.1016/0304-4173(73)90012-8).
- Sun, C., Guo, Y., Tang, K., Wen, Z., Li, B., Zeng, Z., Wang, X., 2017. MqsR/MqsA Toxin/Antitoxin System Regulates Persistence and Biofilm Formation in *Pseudomonas putida* KT2440. *Frontiers in microbiology* 8, 840. <https://doi.org/10.3389/fmicb.2017.00840>.
- Sun, Y., Fukamachi, T., Saito, H., Kobayashi, H., 2011. ATP requirement for acidic resistance in *Escherichia coli*. *Journal of bacteriology* 193, 3072–3077. <https://doi.org/10.1128/JB.00091-11>.
- Sunya, S., Bideaux, C., Molina-Jouve, C., Gorret, N., 2013. Short-term dynamic behavior of *Escherichia coli* in response to successive glucose pulses on glucose-limited chemostat cultures. *Journal of biotechnology* 164, 531–542. <https://doi.org/10.1016/j.jbiotec.2013.01.014>.
- Sunya, S., Delvigne, F., Uribe Larrea, J.-L., Molina-Jouve, C., Gorret, N., 2012a. Comparison of the transient responses of *Escherichia coli* to a glucose pulse of various intensities. *Appl. Microbiol. Biotechnol.* 95, 1021–1034. <https://doi.org/10.1007/s00253-012-3938-y>.
- Sunya, S., Gorret, N., Delvigne, F., Uribe Larrea, J.-L., Molina-Jouve, C., 2012b. Real-time monitoring of metabolic shift and transcriptional induction of *yciG:luxCDABE* *E. coli* reporter strain to a glucose pulse of different concentrations. *Journal of biotechnology* 157, 379–390. <https://doi.org/10.1016/j.jbiotec.2011.12.009>.
- Szenk, M., Dill, K.A., Graff, A.M.R. de, 2017. Why Do Fast-Growing Bacteria Enter Overflow Metabolism? Testing the Membrane Real Estate Hypothesis. *Cell Syst.* 5, 95–104. <https://doi.org/10.1016/j.cels.2017.06.005>.
- Takors, R., 2012. Scale-up of microbial processes: impacts, tools and open questions. *Journal of biotechnology* 160, 3–9. <https://doi.org/10.1016/j.jbiotec.2011.12.010>.
- Tatusov, R.L., Fedorova, N.D., Jackson, J.D., Jacobs, A.R., Kiryutin, B., Koonin, E.V., Krylov, D.M., Mazumder, R., Mekhedov, S.L., Nikolskaya, A.N., Rao, B.S., Smirnov, S., Sverdlov, A.V., Vasudevan, S., Wolf, Y.I., Yin, J.J., Natale, D.A., 2003. The COG database: an updated version includes eukaryotes. *BMC bioinformatics* 4, 41. <https://doi.org/10.1186/1471-2105-4-41>.
- Taymaz-Nikerel, H., Borujeni, A.E., Verheijen, P.J.T., Heijnen, J.J., van Gulik, W.M., 2010. Genome-derived minimal metabolic models for *Escherichia coli* MG1655 with estimated

-
- in vivo respiratory ATP stoichiometry. *Biotechnol. Bioeng.* 107, 369–381.
<https://doi.org/10.1002/bit.22802>.
- Tian, T., Kang, J.W., Kang, A., Lee, T.S., 2019. Redirecting Metabolic Flux via Combinatorial Multiplex CRISPRi-Mediated Repression for Isopentenol Production in *Escherichia coli*. *ACS Synth. Biol.* 8, 391–402.
<https://doi.org/10.1021/acssynbio.8b00429>.
- Tomar, A., Eiteman, M.A., Altman, E., 2003. The effect of acetate pathway mutations on the production of pyruvate in *Escherichia coli*. *Appl. Microbiol. Biotechnol.* 62, 76–82.
<https://doi.org/10.1007/s00253-003-1234-6>.
- Tomasek, K., Bergmiller, T., Guet, C.C., 2018. Lack of cations in flow cytometry buffers affect fluorescence signals by reducing membrane stability and viability of *Escherichia coli* strains. *Journal of biotechnology* 268, 40–52.
<https://doi.org/10.1016/j.jbiotec.2018.01.008>.
- Travers, A.A., Burgess, R.R., 1969. Cyclic re-use of the RNA polymerase sigma factor. *Nature* 222, 537–540. <https://doi.org/10.1038/222537a0>.
- Traxler, M.F., Summers, S.M., Nguyen, H.-T., Zacharia, V.M., Hightower, G.A., Smith, J.T., Conway, T., 2008. The global, ppGpp-mediated stringent response to amino acid starvation in *Escherichia coli*. *Molecular microbiology* 68, 1128–1148.
<https://doi.org/10.1111/j.1365-2958.2008.06229.x>.
- Traxler, M.F., Zacharia, V.M., Marquardt, S., Summers, S.M., Nguyen, H.-T., Stark, S.E., Conway, T., 2011. Discretely calibrated regulatory loops controlled by ppGpp partition gene induction across the 'feast to famine' gradient in *Escherichia coli*. *Molecular microbiology* 79, 830–845. <https://doi.org/10.1111/j.1365-2958.2010.07498.x>.
- Treviño-Quintanilla, L.G., Freyre-González, J.A., Martínez-Flores, I., 2013. Anti-Sigma Factors in *E. coli*: Common Regulatory Mechanisms Controlling Sigma Factors Availability. *Current Genomics* 14, 378–387.
<https://doi.org/10.2174/1389202911314060007>.
- Tsukagoshi, N., Aono, R., 2000. Entry into and release of solvents by *Escherichia coli* in an organic-aqueous two-liquid-phase system and substrate specificity of the AcrAB-TolC solvent-extruding pump. *J. Bacteriol.* 182, 4803–4810.
<https://doi.org/10.1128/jb.182.17.4803-4810.2000>.

- Umenhoffer, K., Draskovits, G., Nyerges, Á., Karcagi, I., Bogos, B., Tímár, E., Csörgő, B., Herczeg, R., Nagy, I., Fehér, T., Pál, C., Pósfai, G., 2017. Genome-Wide Abolishment of Mobile Genetic Elements Using Genome Shuffling and CRISPR/Cas-Assisted MAGE Allows the Efficient Stabilization of a Bacterial Chassis. *ACS Synth. Biol.* 6, 1471–1483. <https://doi.org/10.1021/acssynbio.6b00378>.
- Umenhoffer, K., Feher, T., Baliko, G., Ayaydin, F., Posfai, J., Blattner, F.R., Posfai, G., 2010. Reduced evolvability of *Escherichia coli* MDS42, an IS-less cellular chassis for molecular and synthetic biology applications. *Microb. Cell Factories* 9, 38. <https://doi.org/10.1186/1475-2859-9-38>.
- Unthan, S., Baumgart, M., Radek, A., Herbst, M., Siebert, D., Brühl, N., Bartsch, A., Bott, M., Wiechert, W., Marin, K., Hans, S., Krämer, R., Seibold, G., Frunzke, J., Kalinowski, J., Rückert, C., Wendisch, V.F., Noack, S., 2015. Chassis organism from *Corynebacterium glutamicum*—a top-down approach to identify and delete irrelevant gene clusters. *Biotechnology journal* 10, 290–301. <https://doi.org/10.1002/biot.201400041>.
- Valgepea, K., Peebo, K., Adamberg, K., Vilu, R., 2015. Lean-proteome strains - next step in metabolic engineering. *Frontiers in bioengineering and biotechnology* 3, 11. <https://doi.org/10.3389/fbioe.2015.00011>.
- Van, D.S.J., Burgard, A.P., Haselbeck, R., Pujol, B.C.J., Niu, W., Trawick, J.D., Yim, H., Burk, M.J., Osterhout, R.E., Sun, J., 2010. MICROORGANISMS FOR THE PRODUCTION OF 1,4-BUTANEDIOL AND RELATED METHODS. US20100794700;US20090184311P C12N1/21;C12N1/00.
- van Heeswijk, W.C., Westerhoff, H.V., Boogerd, F.C., 2013. Nitrogen assimilation in *Escherichia coli*: putting molecular data into a systems perspective. *Microbiol. Mol. Biol. Rev.* 77, 628–695. <https://doi.org/10.1128/MMBR.00025-13>.
- Vasilakou, E., van Loosdrecht, Mark C. M., Wahl, S.A., 2020. *Escherichia coli* metabolism under short-term repetitive substrate dynamics: adaptation and trade-offs. *Microb. Cell Factories* 19, 116. <https://doi.org/10.1186/s12934-020-01379-0>.
- Veit, A., Polen, T., Wendisch, V.F., 2007. Global gene expression analysis of glucose overflow metabolism in *Escherichia coli* and reduction of aerobic acetate formation. *Appl. Microbiol. Biotechnol.* 74, 406–421. <https://doi.org/10.1007/s00253-006-0680-3>.

- Vinella, D., Albrecht, C., Cashel, M., D'Ari, R., 2005. Iron limitation induces SpoT-dependent accumulation of ppGpp in *Escherichia coli*. *Mol. Microbiol.* 56, 958–970. <https://doi.org/10.1111/j.1365-2958.2005.04601.x>.
- Visca, P., Leoni, L., Wilson, M.J., Lamont, I.L., 2002. Iron transport and regulation, cell signalling and genomics: lessons from *Escherichia coli* and *Pseudomonas*. *Mol. Microbiol.* 45, 1177–1190. <https://doi.org/10.1046/j.1365-2958.2002.03088.x>.
- Vrábel, P., van der Lans, R.G., Luyben, K.C., Boon, L., Nienow, A.W., 2000. Mixing in large-scale vessels stirred with multiple radial or radial and axial up-pumping impellers: modelling and measurements. *Chemical Engineering Science* 55, 5881–5896. [https://doi.org/10.1016/S0009-2509\(00\)00175-5](https://doi.org/10.1016/S0009-2509(00)00175-5).
- Wang, B., Dai, P., Ding, D., Del Rosario, A., Grant, R.A., Pentelute, B.L., Laub, M.T., 2019a. Affinity-based capture and identification of protein effectors of the growth regulator ppGpp. *Nat. Chem. Biol.* 15, 141–150. <https://doi.org/10.1038/s41589-018-0183-4>.
- Wang, J.D., Levin, P.A., 2009. Metabolism, cell growth and the bacterial cell cycle. *Nature reviews. Microbiology* 7, 822–827. <https://doi.org/10.1038/nrmicro2202>.
- Wang, Q., Yu, H., Xia, Y., Kang, Z., Qi, Q., 2009. Complete PHB mobilization in *Escherichia coli* enhances the stress tolerance: a potential biotechnological application. *Microb. Cell Factories* 8, 47. <https://doi.org/10.1186/1475-2859-8-47>.
- Wang, X., Xia, K., Yang, X., Tang, C., 2019b. Growth strategy of microbes on mixed carbon sources. *Nat. Commun.* 10, 1279. <https://doi.org/10.1038/s41467-019-09261-3>.
- Ward, V.C.A., Chatzivasileiou, A.O., Stephanopoulos, G., 2018. Metabolic engineering of *Escherichia coli* for the production of isoprenoids. *FEMS Microbiol. Lett.* 365. <https://doi.org/10.1093/femsle/fny079>.
- Weber, J., Hoffmann, F., Rinas, U., 2002. Metabolic adaptation of *Escherichia coli* during temperature-induced recombinant protein production: 2. Redirection of metabolic fluxes. *Biotechnol. Bioeng.* 80, 320–330. <https://doi.org/10.1002/bit.10380>.
- Wegerer, A., Sun, T., Altenbuchner, J., 2008. Optimization of an *E. coli* L-rhamnose-inducible expression vector: test of various genetic module combinations. *BMC biotechnology* 8, 2. <https://doi.org/10.1186/1472-6750-8-2>.
- Wehrs, M., Tanjore, D., Eng, T., Lievens, J., Pray, T.R., Mukhopadhyay, A., 2019. Engineering Robust Production Microbes for Large-Scale Cultivation. *Trends in microbiology* 27, 524–537. <https://doi.org/10.1016/j.tim.2019.01.006>.

- Weinstein-Fischer, D., Altuvia, S., 2007. Differential regulation of *Escherichia coli* topoisomerase I by Fis. *Mol. Microbiol.* 63, 1131–1144. <https://doi.org/10.1111/j.1365-2958.2006.05569.x>.
- Wen, Q., Chen, Z., Tian, T., Chen, W., 2010. Effects of phosphorus and nitrogen limitation on PHA production in activated sludge. *Journal of Environmental Sciences* 22, 1602–1607. [https://doi.org/10.1016/S1001-0742\(09\)60295-3](https://doi.org/10.1016/S1001-0742(09)60295-3).
- Wess, J., Brinek, M., Boles, E., 2019. Improving isobutanol production with the yeast *Saccharomyces cerevisiae* by successively blocking competing metabolic pathways as well as ethanol and glycerol formation. *Biotechnol. Biofuels* 12, 173. <https://doi.org/10.1186/s13068-019-1486-8>.
- Wick, R.R., Judd, L.M., Gorrie, C.L., Holt, K.E., 2017. Unicycler: Resolving bacterial genome assemblies from short and long sequencing reads. *PLoS computational biology* 13, e1005595. <https://doi.org/10.1371/journal.pcbi.1005595>.
- Wickstrum, J.R., Santangelo, T.J., Egan, S.M., 2005. Cyclic AMP receptor protein and RhaR synergistically activate transcription from the L-rhamnose-responsive rhaSR promoter in *Escherichia coli*. *J. Bacteriol.* 187, 6708–6718. <https://doi.org/10.1128/JB.187.19.6708-6718.2005>.
- Williamson, G., Tamburrino, G., Bizior, A., Boeckstaens, M., Dias Mirandela, G., Bage, M., Pisljakov, A., Ives, C.M., Terras, E., Hoskisson, P.A., Marini, A.-M., Zachariae, U., Javelle, A., 2020. A two-lane mechanism for selective biological ammonium transport. *eLife* 9. <https://doi.org/10.7554/eLife.57183>.
- Wilms, B., Hauck, A., Reuss, M., Syltatk, C., Mattes, R., Siemann, M., Altenbuchner, J., 2001. High-cell-density fermentation for production of L-N-carbamoylase using an expression system based on the *Escherichia coli* rhaBAD promoter. *Biotechnol. Bioeng.* 73, 95–103. <https://doi.org/10.1002/bit.1041>.
- Wu, J., Du, G., Chen, J., Zhou, J., 2015. Enhancing flavonoid production by systematically tuning the central metabolic pathways based on a CRISPR interference system in *Escherichia coli*. *Scientific reports* 5, 13477. <https://doi.org/10.1038/srep13477>.
- Wu, Y., Chen, T., Liu, Y., Tian, R., Lv, X., Li, J., Du, G., Chen, J., Ledesma-Amaro, R., Liu, L., 2020. Design of a programmable biosensor-CRISPRi genetic circuits for dynamic and autonomous dual-control of metabolic flux in *Bacillus subtilis*. *Nucleic Acids Res.* 48, 996–1009. <https://doi.org/10.1093/nar/gkz1123>.

- Xi, H., Schneider, B.L., Reitzer, L., 2000. Purine catabolism in *Escherichia coli* and function of xanthine dehydrogenase in purine salvage. *Journal of bacteriology* 182, 5332–5341. <https://doi.org/10.1128/JB.182.19.5332-5341.2000>.
- Xu, X., Li, X., Liu, Y., Zhu, Y., Li, J., Du, G., Chen, J., Ledesma-Amaro, R., Liu, L., 2020. Pyruvate-responsive genetic circuits for dynamic control of central metabolism. *Nat. Chem. Biol.* 16, 1261–1268. <https://doi.org/10.1038/s41589-020-0637-3>.
- Yang, J., Anderson, B.W., Turdiev, A., Turdiev, H., Stevenson, D.M., Amador-Noguez, D., Lee, V.T., Wang, J.D., 2020. Systemic characterization of pppGpp, ppGpp and pGpp targets in *Bacillus* reveals NahA converts (p)ppGpp to pGpp to regulate alarmone composition and signaling. *bioRxiv*, 2020.03.23.003749. <https://doi.org/10.1101/2020.03.23.003749>.
- Yu, B.J., Kang, K.H., Lee, J.H., Sung, B.H., Kim, M.S., Kim, S.C., 2008. Rapid and efficient construction of markerless deletions in the *Escherichia coli* genome. *Nucleic Acids Res.* 36, e84. <https://doi.org/10.1093/nar/gkn359>.
- Yu, D., Ellis, H.M., Lee, E.C., Jenkins, N.A., Copeland, N.G., Court, D.L., 2000. An efficient recombination system for chromosome engineering in *Escherichia coli*. *Proceedings of the National Academy of Sciences of the United States of America* 97, 5978–5983. <https://doi.org/10.1073/pnas.100127597>.
- Yuan, J., Fowler, W.U., Kimball, E., Lu, W., Rabinowitz, J.D., 2006. Kinetic flux profiling of nitrogen assimilation in *Escherichia coli*. *Nature chemical biology* 2, 529–530. <https://doi.org/10.1038/nchembio816>.
- Yuan, W., Zhong, S., Xiao, Y., Wang, Z., Sun, J., 2020. Efficient biocatalyst of L-DOPA with *Escherichia coli* expressing a tyrosine phenol-lyase mutant from *Kluyvera intermedia*. *Appl. Biochem. Biotechnol.* 190, 1187–1200. <https://doi.org/10.1007/s12010-019-03164-1>.
- Zelić, B., Gerharz, T., Bott, M., Vasić-Rački, Đ., Wandrey, C., Takors, R., 2003. Fed-Batch Process for Pyruvate Production by Recombinant *Escherichia coli* YYC202 Strain. *Eng. Life Sci.* 3, 299–305. <https://doi.org/10.1002/elsc.200301756>.
- Zelić, B., Gostović, S., Vuorilehto, K., Vasić-Racki, D., Takors, R., 2004. Process strategies to enhance pyruvate production with recombinant *Escherichia coli*: from repetitive fed-batch to in situ product recovery with fully integrated electrodialysis. *Biotechnol. Bioeng.* 85, 638–646. <https://doi.org/10.1002/bit.10820>.

-
- Zhang, G., Gurtu, V., Kain, S.R., 1996. An enhanced green fluorescent protein allows sensitive detection of gene transfer in mammalian cells. *Biochemical and biophysical research communications* 227, 707–711. <https://doi.org/10.1006/bbrc.1996.1573>.
- Zhang, J.-L., Peng, Y.-Z., Liu, D., Liu, H., Cao, Y.-X., Li, B.-Z., Li, C., Yuan, Y.-J., 2018a. Gene repression via multiplex gRNA strategy in *Y. lipolytica*. *Microb. Cell Factories* 17, 62. <https://doi.org/10.1186/s12934-018-0909-8>.
- Zhang, Q., Hou, Z., Ma, Q., Mo, X., Sun, Q., Tan, M., Xia, L., Lin, G., Yang, M., Zhang, Y., Xu, Q., Li, Y., Chen, N., Xie, X., 2020. CRISPRi-Based Dynamic Control of Carbon Flow for Efficient N-Acetyl Glucosamine Production and Its Metabolomic Effects in *Escherichia coli*. *Journal of agricultural and food chemistry* 68, 3203–3213. <https://doi.org/10.1021/acs.jafc.9b07896>.
- Zhang, Y., Zborníková, E., Rejman, D., Gerdes, K., 2018b. Novel (p)ppGpp Binding and Metabolizing Proteins of *Escherichia coli*. *mBio* 9. <https://doi.org/10.1128/mBio.02188-17>.
- Zhang, Z., Aboulwafa, M., Saier, M.H., 2014. Regulation of *crp* gene expression by the catabolite repressor/activator, Cra, in *Escherichia coli*. *Journal of molecular microbiology and biotechnology* 24, 135–141. <https://doi.org/10.1159/000362722>.
- Zheng, D., Constantinidou, C., Hobman, J.L., Minchin, S.D., 2004. Identification of the CRP regulon using in vitro and in vivo transcriptional profiling. *Nucleic Acids Res.* 32, 5874–5893. <https://doi.org/10.1093/nar/gkh908>.
- Zhu, M., Dai, X., 2019. Growth suppression by altered (p)ppGpp levels results from non-optimal resource allocation in *Escherichia coli*. *Nucleic Acids Res.* 47, 4684–4693. <https://doi.org/10.1093/nar/gkz211>.
- Zhu, Y., Eiteman, M.A., Altman, R., Altman, E., 2008. High glycolytic flux improves pyruvate production by a metabolically engineered *Escherichia coli* strain. *Appl. Environ. Microbiol.* 74, 6649–6655. <https://doi.org/10.1128/AEM.01610-08>.
- Ziegler, M., Takors, R., 2020. Reduced and Minimal Cell Factories in Bioprocesses: Towards a Streamlined Chassis, in: Lara, A.R., Gosset, G. (Eds.), *Minimal Cells: Design, Construction, Biotechnological Applications*. Springer International Publishing, Cham, pp. 1–44.

- Ziegler, M., Zieringer, J., Döring, C.-L., Paul, L., Schaal, C., Takors, R., 2021a. Engineering of a robust *Escherichia coli* chassis and exploitation for large-scale production processes. *Metab. Eng.* 67, 75–87. <https://doi.org/10.1016/j.ymben.2021.05.011>.
- Ziegler, M., Zieringer, J., Takors, R., 2021b. Transcriptional profiling of the stringent response mutant strain *E. coli* SR reveals enhanced robustness to large-scale conditions. *Microbial biotechnology* 14, 993–1010. <https://doi.org/10.1111/1751-7915.13738>.
- Zieringer, J., Wild, M., Takors, R., 2020. Data-driven in silico prediction of regulation heterogeneity and ATP demands of *Escherichia coli* in large-scale bioreactors. *Biotechnol. Bioeng.* <https://doi.org/10.1002/bit.27568>.
- Zimmer, D.P., Soupene, E., Lee, H.L., Wendisch, V.F., Khodursky, A.B., Peter, B.J., Bender, R.A., Kustu, S., 2000. Nitrogen regulatory protein C-controlled genes of *Escherichia coli*: scavenging as a defense against nitrogen limitation. *Proceedings of the National Academy of Sciences of the United States of America* 97, 14674–14679. <https://doi.org/10.1073/pnas.97.26.14674>.

Attachments

Pagination of the attachments is not consecutive to the main text of this thesis as pagination of the original documents was conserved.

Original publications and manuscripts are attached in the following order:


- Transcriptional profiling of the stringent response mutant strain *E. coli* SR reveals enhanced robustness to large-scale conditions
 - Original publication
 - Supplementary Tables S1 to S4, Supplementary Material A to E³

- Engineering of a robust *Escherichia coli* chassis and exploitation for large-scale processes
 - Original publication
 - Supplementary Material S1 to S10

- CRISPRi enables fast growth followed by stable aerobic pyruvate formation in *Escherichia coli* without auxotrophy
 - Submitted Manuscript
 - Supplementary Material S1 and S2

³Due to its large size Appendix S1 (containing the mapping statistics, normalized counts and log₂fold values) is not included. It is available in electronic form from the publisher's website or on demand from the author of this thesis.

Transcriptional profiling of the stringent response mutant strain *E. coli* SR reveals enhanced robustness to large-scale conditions

Martin Ziegler,  Julia Zieringer and Ralf Takors
Institute of Biochemical Engineering, University of Stuttgart, Stuttgart, Germany.

Summary

In large-scale fed-batch production processes, microbes are exposed to heterogeneous substrate availability caused by long mixing times. *Escherichia coli*, the most common industrial host for recombinant protein production, reacts by recurring accumulation of the alarmone ppGpp and energetically wasteful transcriptional strategies. Here, we compare the regulatory responses of the stringent response mutant strain *E. coli* SR and its parent strain *E. coli* MG1655 to repeated nutrient starvation in a two-compartment scale-down reactor. Our data show that *E. coli* SR can withstand these stress conditions without a ppGpp-mediated stress response maintaining fully functional ammonium uptake and biomass formation. Furthermore, *E. coli* SR exhibited a substantially reduced short-term transcriptional response compared to *E. coli* MG1655 (less than half as many differentially expressed genes). *E. coli* SR proceeded adaptation via more general SOS response pathways by initiating negative regulation of transcription, translation and cell division. Our results show that locally induced stress responses propagating through the bioreactor do not result in cyclical induction and repression of genes in *E. coli* SR, but in a reduced and coordinated response, which makes it potentially suitable for large-scale production processes.

Introduction

Heterogeneities in large-scale fed-batch bioprocesses have long been recognized as a cause for process

performance loss at industrial scale compared to homogeneous processes at laboratory scale (Bylund *et al.*, 1998). Due to physical, economical and engineering constraints, the generation of gradients in large-scale reactors is inevitable. Hydrostatic pressure influences the solubility and transfer of gasses, and the mixing time of large reactors can be orders of magnitude higher than that of laboratory reactors producing strong measurable chemical gradients (Larsson *et al.*, 1996; Enfors *et al.*, 2001; Junker, 2004; Delvigne *et al.*, 2006). Common consequences of spatial heterogeneities are loss of productivity, reduced biomass yield, increased byproduct formation and genetic or plasmid instability (Hopkins *et al.*, 1987; George *et al.*, 1993; Neubauer *et al.*, 1995b; Bylund *et al.*, 1998; Bylund *et al.*, 2000; Jonge *et al.*, 2011). Reduced process performance is not limited to a single species but can be observed for many industrial workhorse organisms like *Escherichia coli*, *Saccharomyces cerevisiae*, *Penicillium chrysogenum* and *Bacillus subtilis* (George *et al.*, 1993; Jonge *et al.*, 2011; Junne *et al.*, 2011; Larsson and Enfors, 1988).

Due to the enormous costs associated with using and maintaining large-scale equipment, few experiments in the context of academic research have been performed in industrial scale bioreactors (Bylund *et al.*, 1999; Bylund *et al.*, 2000; Enfors *et al.*, 2001). In consequence, researchers have relied on the use of computational fluid dynamics (CFD) to simulate reactor flow fields and on scale-down reactors to experimentally investigate selected scenarios (Kelly, 2008; Takors, 2012). Various designs of scale-down reactors exist and have been extensively reviewed elsewhere (Delvigne *et al.*, 2017; Delvigne *et al.*, 2006; Neubauer and Junne, 2010). One of the commonly used scale-down reactors follows a multi-compartment approach: A primary stirred tank reactor (STR) is coupled to a secondary plug flow reactor (PFR). The STR is operated as a well-mixed compartment under standard limited growth conditions and the PFR simulates a feeding, starvation or anaerobic zone providing the stimulus to be investigated (Lara *et al.*, 2006).

Many studies have focused on experimentally simulating the zone close to the feeding point which is usually characterized by substrate excess and potentially oxygen limitation (Enfors *et al.*, 2001; Lara *et al.*, 2009;

Received 12 October, 2020; revised 8 December, 2020; accepted 8 December, 2020.

*For correspondence. E-mail ralf.takors@ibvt.uni-stuttgart.de; Tel. +49 711 685-64535; Fax +49 711 685-55164.

Funding informationNo funding information provided.

Microbial Biotechnology (2021) 14(3), 993–1010
doi:10.1111/1751-7915.13738

© 2020 The Authors. *Microbial Biotechnology* published by Society for Applied Microbiology and John Wiley & Sons Ltd.

This is an open access article under the terms of the Creative Commons Attribution License, which permits use, distribution and reproduction in any medium, provided the original work is properly cited.

Junne *et al.*, 2011). For a variety of hosts, common observations in this scenario include the formation of small organic acids and solvents as overflow metabolites or as anaerobic fermentation products (George *et al.*, 1993; Neubauer *et al.*, 1995b). Ultimately, byproduct formation may lead to process performance loss even if reuptake of byproducts occurs in the well-mixed limited growth zone (Enfors *et al.*, 2001).

Occasionally, starvation zones have attracted attention as well (Neubauer *et al.*, 1995a; Neubauer *et al.*, 1995b). From CFD simulation and measured data, it is known that distant from the feeding point or close to the reactor walls poorly mixed zones with very low nutrient concentrations exist. An early scale-down study with *E. coli* employing oscillatory feeding protocols revealed the involvement of the stringent response in the cellular reaction to transient glucose starvation (Neubauer *et al.*, 1995a).

The stringent response is a global regulatory program usually preparing *E. coli* for entry into the stationary phase (Magnusson *et al.*, 2005; Gaca *et al.*, 2015; Hauryliuk *et al.*, 2015). Its hallmark is the synthesis of the alarmone (p)ppGpp on short time-scales by the ribosome-associated protein RelA or on longer time-scales by the bifunctional enzyme SpoT (Gallant *et al.*, 1970; Atherly, 1979; Murray and Bremer, 1996). ppGpp acts primarily as a transcription factor by binding to RNA polymerase and modulating its affinity to transcription initiation sites and alternative sigma factors. Additionally, ppGpp directly modulates the activity of certain proteins (Dalebroux and Swanson, 2012; Kanjee *et al.*, 2011).

The fast and reversible initiation of the stringent response to oscillatory substrate supply was later confirmed by measurements of ppGpp in continuous glucose chemostat cultivations in a two-compartment stirred tank-plug flow reactor (STR-PFR) setup (Löffler *et al.*, 2016). The feeding point was placed in the STR creating a starvation zone in the PFR, which allowed to resolve the timescale of cellular response. Moreover, it was shown that extensive transcriptional responses take place as cells move transiently through a nutrient poor zone. From theoretical calculations of ATP costs Löffler *et al.* estimated that an increase in maintenance energy demand of more than 30% was caused by the repeated exposure of cells to the nutrient gradient offering a new explanation for performance losses in large-scale bioprocesses (Löffler *et al.*, 2016). Analogous experiments with ammonium as the limiting nutrient revealed similar, yet less pronounced, regulation patterns affirming the importance of the stringent response for global regulation in *E. coli* in a scenario of oscillating starvation stimuli (Simen *et al.*, 2017). Fed-batch processes limited by ammonium or other nitrogen sources are interesting fermentation scenarios for the production of small

molecules which mainly consist of carbon such as fatty alcohols (Chubukov *et al.*, 2017). Nitrogen limitation is commonly used to enhance the accumulation of cellular carbon storage products such as polyhydroxyalkanoates used for bioplastic synthesis (Wen *et al.*, 2010; Oliveira-Filho *et al.*, 2019), including *E. coli* as a potential host (Wang *et al.*, 2009). As nitrogen forms a relatively large part of cells, nitrogen limitation can be easily explored during process development. During scale-up, such processes will likely suffer from similar issues as carbon-limited processes (Simen *et al.*, 2017).

Recently, the strains *E. coli* SR and *E. coli* HGT with modulated stringent response were constructed in our laboratory (Michalowski *et al.*, 2017). The strains lack *relA* which is primarily responsible for rapid ppGpp synthesis upon nutrient depletion and carry modifications in the bifunctional enzyme SpoT. It was shown that they do not react to the exhaustion of ammonium supply by ppGpp synthesis (Michalowski *et al.*, 2017). Strain *E. coli* SR displays no negative phenotypic differences in batch cultivations compared to its parent strain *E. coli* K-12 MG1655. However, under conditions of ammonium limitation, *E. coli* SR was found to have an elevated specific glucose consumption rate which is beneficial for two-stage processes involving product formation in the nitrogen limited phase (Jarmander *et al.*, 2015; Perez-Zabaleta *et al.*, 2016).

The combination of properties displayed by *E. coli* SR indicates that this strain can potentially be developed as a platform strain for robust scale-up from lab to production. In this work, we compared the phenotypic and transcriptional responses of *E. coli* SR and its parent strain *E. coli* MG1655 in a two-compartment scale-down reactor. We focused our investigation on the regulatory differences between these strains in the response to repeated short-term stimuli. The primary stirred tank reactor was operated as an ammonium-limited chemostat while a plug flow reactor simulated a nitrogen starvation zone.

Results

Continuous cultivation with periodic nutrient depletion

We cultivated *E. coli* SR and *E. coli* MG1655 in two independent continuous fermentations each in a previously described scale-down reactor consisting of a primary stirred tank reactor (STR) and a secondary plug-flow reactor (PFR), schematically shown in Fig. 1 (Löffler *et al.*, 2016; Simen *et al.*, 2017; Ankenbauer *et al.*, 2020). *E. coli* SR is a strain with modulated stringent response that was engineered to alleviate the induction of the stringent response and the general stress response upon nutrient depletion (Michalowski *et al.*, 2017). The chemostat was operated at a dilution rate of $D = 0.2 \text{ h}^{-1}$ and ammonium was chosen as the limiting

nutrient. After establishment of a steady state in the STR alone, a reference sample (S0, $t = 0$ h) was taken and the PFR connected. Periodic passage from the STR (average residence time $-\tau_{STR} = 6.2\text{min}$) through the PFR (average residence time $-\tau_{PFR} = 2.6\text{min}$) then created a repeated short nitrogen starvation stimulus. The average residence times represent worst-case scenarios that are still consistent with mixing studies (Vrábel *et al.*, 2000; Noorman, 2011) and the volume ratio STR to PFR was approximately 3:1 to represent existing simulation results (Lapin *et al.*, 2006; Haringa *et al.*, 2017). The long-term response of cells was investigated from additional samples taken from the STR shortly after connection of the PFR (S5, $t = 5$ min) and after establishment of a new steady-state (S28, $t = 28$ h) in the two-compartment cultivation. The short-term response of cells to the PFR stimulus was monitored by sampling from five ports along the primary axis of the PFR at identical timepoints. Transcript samples for the PFR were taken from port 5 (P5_5 and P5_28).

Basic growth and fermentation data confirmed earlier results that there are no detrimental differences in

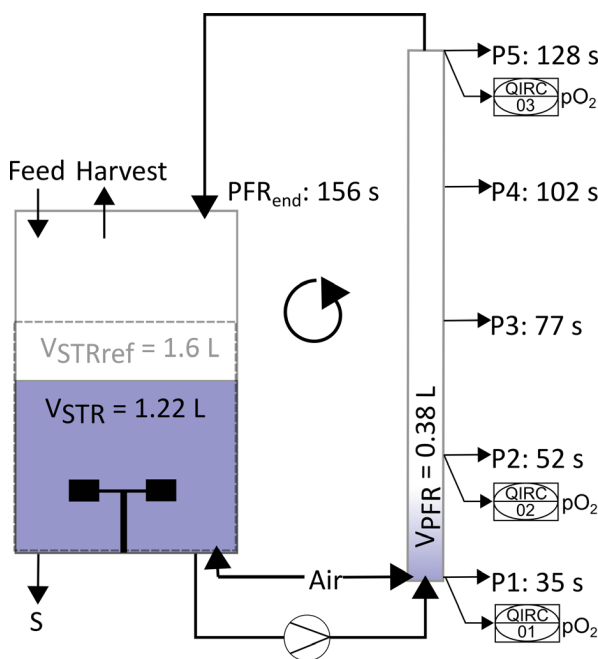


Fig. 1. Experimental design of the two-compartment system. The fermenter consists of a stirred tank reactor (STR) as the primary cultivation vessel and a plug-flow reactor (PFR) connected by an active pump. The ammonium-limited chemostat was operated at a dilution rate of $D = 0.2\text{ h}^{-1}$ with the feeding point placed in the STR. The STR served as a limitation zone and the PFR formed a starvation zone. The setup was designed to resolve different timescales of cellular response. Oxygen saturation was measured by three oxygen probes and recorded by the process control system (01, 02, 03). V_{STRref} : Reference Volume without connection of PFR (constant volume).

fundamental physiological parameters (Table 1) between *E. coli* MG1655 and *E. coli* SR under nitrogen-limited conditions (Michalowski *et al.*, 2017). There were no statistically significant differences in any parameter (two-tailed t-test, $p > 0.1$). Both strains reached practically identical biomass yields on ammonium and depleted ammonium to equally low levels regardless of process time and PFR action (Fig. 2). The most noteworthy difference between *E. coli* MG1655 and *E. coli* SR was a reduced concentration of excess glucose in the fermentation broth of *E. coli* SR. Consequently, we calculated a lower biomass yield on glucose for *E. coli* SR (Table 1). Under conditions of long-term nitrogen starvation in batch fermentations *E. coli* SR had previously displayed a relaxation in glucose and nitrogen uptake coupling and we thus suspected an increased specific glucose uptake rate (Michalowski *et al.*, 2017). The calculated specific glucose uptake rate was higher for *E. coli* SR, but the difference was not statistically significant in our experiments (two-tailed t-test, $P\text{-value} > 0.1$). Data from the fermentation broth supernatant showed that both strains converted comparable amounts of substrate into acetate as the primary byproduct. Carbon balancing revealed an increased fraction of unknown substances among the fermentation products of *E. coli* SR which were identified as dissolved organic substances in the fermentation supernatant by total dissolved carbon analysis. The elevated glucose uptake rate of *E. coli* SR likely leads to higher byproduct formation of typical overflow metabolites such as lactate, pyruvate, formate and the regulator 2-oxoglutarate, all of which are known to accumulate under nitrogen-limited conditions with glucose excess (Hua *et al.*, 2004). Apart from the primary byproduct acetate, individual small carbon byproducts were not measured as the overall total carbon efflux/influx balancing was in good agreement for both strains. Carbon recovery was $101 \pm 2\%$ for *E. coli* MG1655 and $102 \pm 1\%$ for *E. coli* SR indicating that in sum all relevant substances were detected.

In general, process time and the periodic PFR stimulus hardly affected global process parameters which is in accordance with former observations made in this reactor setup for nitrogen limitation and K-12 strains (Simen *et al.*, 2017). In sharp contrast, we found substantial regulatory differences between the two strains both in the short-term and in the long-term transcriptional responses to the periodic starvation stimulus.

Transcriptomic analysis: Overview

RNA-seq-based transcriptomic data to examine potentially important genes for the ammonium stress response of *E. coli* WT and *E. coli* SR was analysed. After filtering, 4037 predicted *E. coli* genes remained for further

Table 1. Physiological measurements.

E. coli MG1655	E. coli SR	
$Y_{XN} \left[\frac{g_{CDW}}{g_{NH_4^+}} \right]$	4.63 ± 0.12 ^a	4.62 ± 0.27
$Y_{XS} \left[\frac{g_{CDW}}{g_{Glucose}} \right]$	0.32 ± 0.01	0.28 ± 0.01
$C_{Glucose,STR} \left[\frac{g_{Glucose}}{g} \right]$	2.07 ± 0.25	1.49 ± 0.06
$C_{Acetate,STR} \left[\frac{g_{Acetate}}{g} \right]$	1.39 ± 0.11	1.29 ± 0.14
$q_{NH_4^+} \left[\frac{g_{NH_4^+}}{g_{CDW} \cdot h} \right]$	0.04 ± 0.01	0.05 ± 0.01
$q_S \left[\frac{g_{Glucose}}{g_{CDW} \cdot h} \right]$	0.63 ± 0.05	0.77 ± 0.14
$q_{Ac} \left[\frac{g_{Acetate}}{g_{CDW} \cdot h} \right]$	0.10 ± 0.01	0.10 ± 0.01
$q_{CO_2} \left[\frac{mmol_{CO_2}}{g_{CDW} \cdot h} \right]$	8.73 ± 1.06	9.98 ± 2.23
$q_{O_2} \left[\frac{mmol_{O_2}}{g_{CDW} \cdot h} \right]$	9.28 ± 0.47	10.9 ± 2.02
$RQ \left[\frac{mol_{CO_2}}{mol_{O_2}} \right]$	0.95 ± 0.16	0.91 ± 0.04
$q_{ATP} \left[\frac{mmol_{ATP}}{g_{CDW} \cdot h} \right]$	29.23 ± 0.62 ^b	34.73 ± 6.39
$D \left[\frac{1}{h} \right]$	0.20 ± 0.01	0.21 ± 0.03

a. Errors indicate SEM ($n = 2$). All rates were calculated from averaged values collected over the entire STR-PFR process time.

b. Estimated values assuming a P/O-Ratio of 1.2.

analysis (see Supporting information). The fast tactical transcriptional response to ammonia shortage was determined by comparing PFR port 5 samples to STR samples taken at the same process time points. Long-term responses were studied by comparing post-perturbation samples from the STR after 5 min (S5) and 28 h (S28)

to the reference sample (S0). The statistical threshold for significance was set for adjusted p-value < 0.01 and $\log_2FC > |1|$. 54 differentially expressed genes (DEGs) (UP: 14, DOWN: 40) formed the long-term response of *E. coli* MG1655. The short-term response was more pronounced comprising 837 DEGs (UP: 242, DOWN: 595). *E. coli* SR disclosed a similar number of 61 DEGs for the long term response (UP: 12, DOWN: 49), but substantially less DEGs as short term response (Total: 387, UP: 161, DOWN: 226) (Fig. 3). \log_2FC values range from -4.69 to 4.96 (WT) and -3.90 to 5.13 (SR). Fig. 3 depicts an overview of transcriptional dynamics outlining the halved response of *E. coli* SR 5 min after repeated nitrogen limited perturbation compared to WT.

Figure 4 shows that the multi-transcript response of each strain could be well described by 2-dimensional PCA covering 96% and 87% of total variance for *E. coli* WT and *E. coli* SR, respectively. Notably, biological duplicates were found in close proximity. PC1 accounts for the sample port location, PC2 for the time course. Unique and clearly distinguishable differences between STR and PFR transcript patterns were observed already after 5 min of repeated nitrogen starvation for both strains (Figure 4, A1). In particular, principal component 1 (PC1) disclosed major differences between the samples of each strain accounting for 88% and 67% regarding *E. coli* WT and *E. coli* SR, respectively. The PCA finding is in agreement with the reduced number of DEGs observed for *E. coli* SR. The impact of PC2 is more pronounced for *E. coli* SR although almost

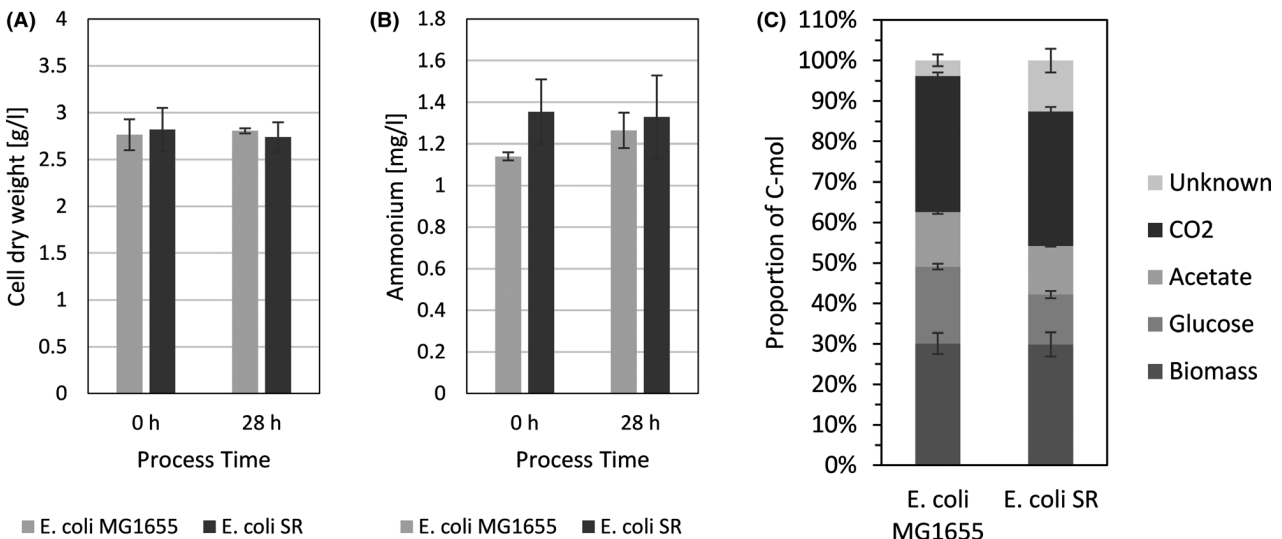


Fig. 2. Physiological measurements. A. Cell dry weight. Concentration of cell dry weight after at least 25 h chemostat process before connecting the plug-flow reactor (0 h) and after 28 h of chemostat process with connected PFR (28 h). B. Ammonium. Concentration of residual ammonium in the supernatant. C. Carbon Balance. Columns show efflux fractions of total C-mol based on carbon influx. The final fraction represents undetermined dissolved organic substances in the fermentation broth, as measured by the difference of all efflux carbon detected by exhaust gas or total carbon analysis and the sum of the individually measured efflux components. Error bars indicate SEM ($n = 2$) of individual components (A, B and C).

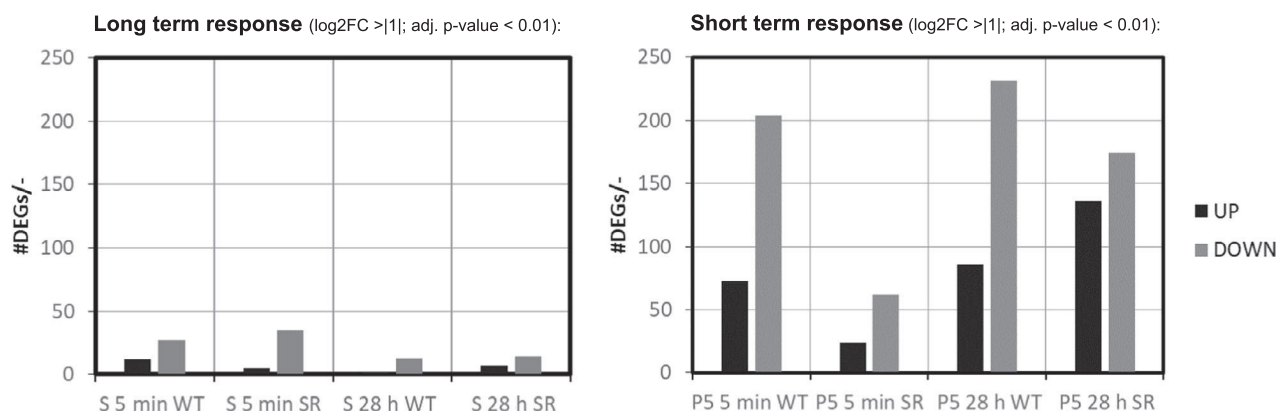


Fig. 3. Number of UP (black) and DOWN (gray) regulated genes (DEGs). Long-term (left) and short-term (right) response to repeated nitrogen starvation for *E. coli* MG1655 (WT) and *E. coli* SR (SR) and given process times.

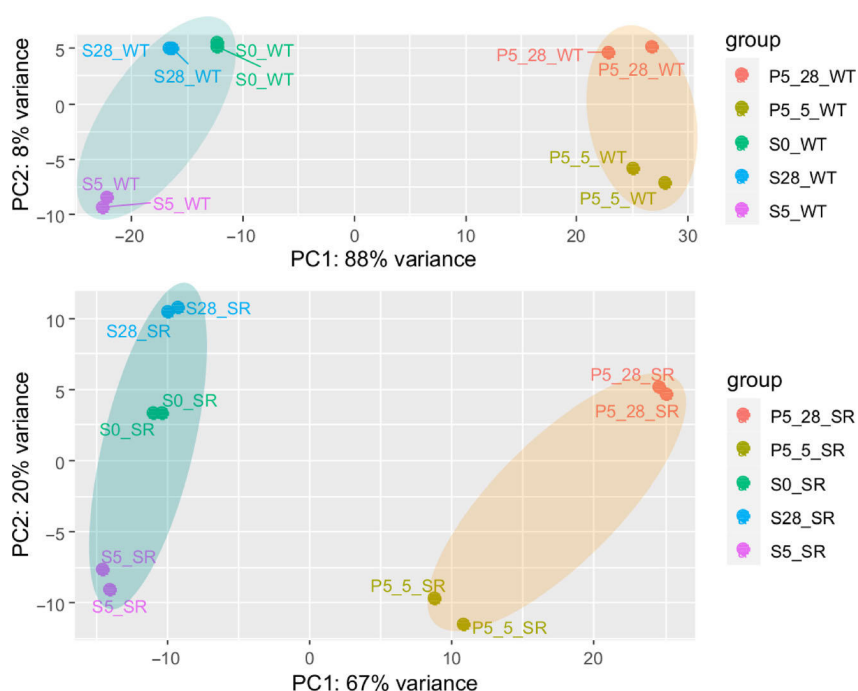


Fig. 4. Principal component analysis of transcript data of *E. coli* MG1655 (WT) (top) and *E. coli* SR (bottom) obtained from STR (S) and PFR (port 5, P5) at three process time points (0 h, 5 min, and 28 h). Covered measurement variance of each principal component (PC) is indicated. Ellipses cluster samples of STR and PFR. PC1 accounts for ‘sample port location’, PC2 for ‘process time’.

identical numbers of DEGs were found as long-term response in both strains. However, given the low impact of PC1 for *E. coli* SR, similar DEG values affect the relative principal component analysis stronger.

As long-term responses of both strains were similar (see Appendix: Supporting information) and weaker than short-term responses (Fig. 4) further analysis focused on short-term transcript patterns. Notably, changes between long- and short-term responses of both strains were dominated by counteracting transcript dynamics resetting perturbations after PFR passages (MG1655: 5 min and

28 h). Observations are in line with similar findings (Chang *et al.*, 2002). Additional differences were found in the upregulation of carbohydrate transport (SR: 5 min) and catabolic processes (SR: 28 h) (see Fig. A5 and A6).

Regulatory response to short-term ammonium limitation

Preceding investigations of *E. coli* K-12 strains in STR-PFR scale-down reactors revealed the rapid accumulation of the alarmone ppGpp upon entry into the nutrient

limited zone under both glucose and ammonium limitation (Löffler *et al.*, 2016; Simen *et al.*, 2017). Concomitantly, an extensive transcriptional reprogramming of cells occurred. In standard batch fermentations *E. coli* SR in turn did not react to ammonium depletion by ppGpp synthesis (Michalowski *et al.*, 2017). We therefore measured intracellular ppGpp levels from samples taken from the five ports of the PFR along its primary axis (Fig. 5). During the PFR passage *E. coli* MG1655 accumulated ppGpp to levels 2 – 3 fold higher than measured in the STR, displaying the same behaviour as previously observed for the closely related K-12 strain *E. coli* W3110 (Simen *et al.*, 2017). In contrast, *E. coli* SR had no elevated levels of ppGpp at any point during the PFR passage regardless of process time. These results complement previous findings for the case of repeated short stimuli and confirm the strain's resilience to ammonium exhaustion.

Based on these encouraging findings, we focused our investigation on the short-term transcriptional response of both strains along the PFR axis. We compared data from samples drawn from port 5 of the PFR to samples drawn from the STR at identical process time points. Short-term changes revealed a significantly different response of *E. coli* SR compared to *E. coli* MG1655 not only in the amount of DEGs (Fig. 3), but also in the function of these genes (Fig. 4, 6). To elucidate patterns in the transcriptional responses, we searched for common DEGs, investigated the behaviour of gene clusters of orthologous groups (COGs), and compared sigma factor (σ) activities. The gene expression patterns of each strain individually were assigned to 21 functional

categories based on the COG database (Tatusov *et al.*, 2003). In total 3532 of the 4037 genes (87.5%) could be annotated to COG. For each COG category, the resulting t-values are represented in a lollipop plot (Fig. 7). Significant changes were defined with a FDR-corrected p-value < 0.01. Furthermore, the activation and deactivation of sigma factors over time were investigated (Fig. 7). In this case, 3935 out of 4037 genes could be assigned to the sigma factor-gene interaction database from RegulonDB (Santos-Zavaleta *et al.*, 2019).

After the first 5 min of PFR action *E. coli* MG1655 and *E. coli* SR exhibited substantially different transcriptional responses. The strains had only 64 DEGs in common, split equally between up- and down regulation (Fig. 6 left). Hence, these genes mirror the transcriptional response to short-term starvation irrespective of a functional stringent response, in which 14 out of the 32 common upregulated genes are associated with the Ntr-reponse (e.g. *glnK*, *amtB*, *glnAHPQ*, *rutA*). Downregulated genes consist of genes responsible for amino acid biosynthesis (e.g. *argCF*, *metABFINR*) and other cellular functions such as DNA cleavage, transporters and oxidoreductases. The only oppositely regulated gene was *guaC* coding for the GMP reductase GuaC. Transcriptional control of the *guaC* promoter by the stringent response was proposed after its initial discovery and is clearly supported by our data (Andrews and Guest, 1988). Individual, strain-specific short-term regulation was observed for 398 (*E. coli* MG1655) and 32 (*E. coli* SR) specific DEGs after 5 min, clearly demonstrating the effect of the stringent response on the *E. coli* transcriptome.

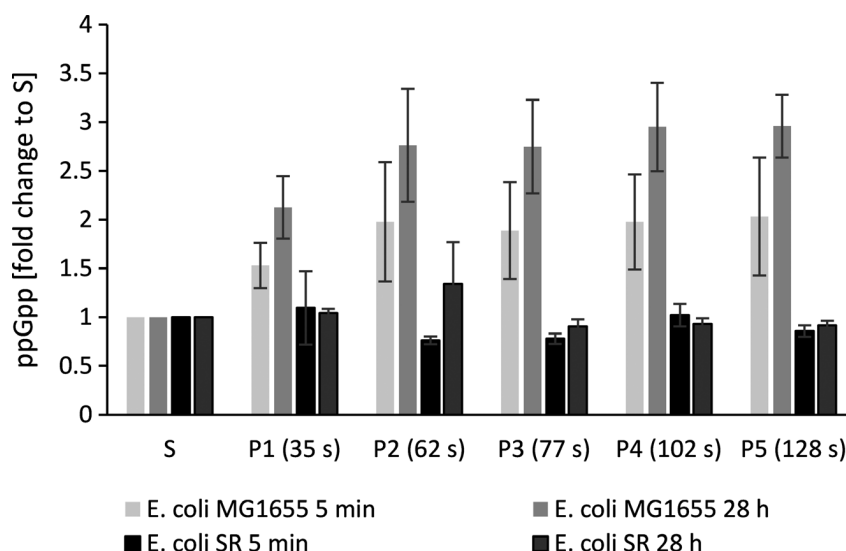


Fig. 5. Alarmone accumulation along the PFR. Concentration of ppGpp measured from samples drawn along the plug flow reactor (P1 to P5) relative to the concentration measured in the stirred tank reactor (S, all values set to 1) for *E. coli* MG1655 (WT) and *E. coli* SR (SR). Error Bars represent SEM ($n = 2$).

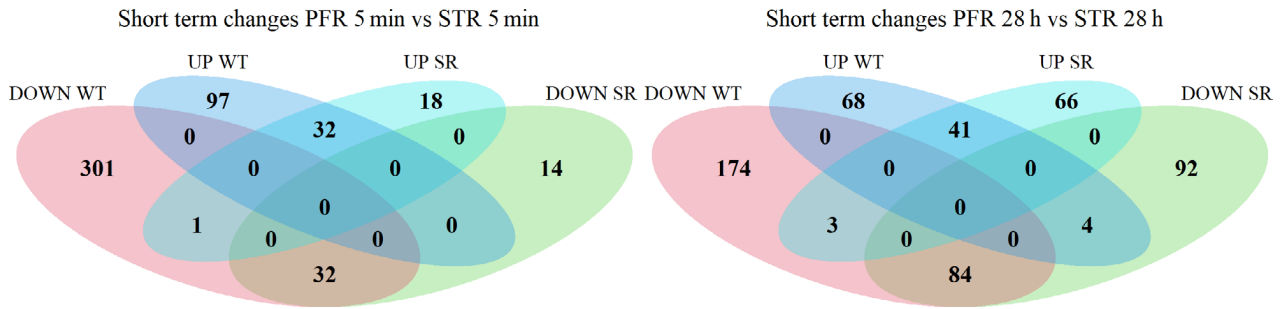


Fig. 6. Venn diagrams representing partially overlapping sets of DEGs of *E. coli* MG1655 (WT) and *E. coli* SR. The number of significantly up- (UP) and downregulated (DOWN) genes in each set is indicated by numbers. Left: Short-term responses 5 min after PFR connection. Right: Short-term responses 28 h after PFR connection. Complete gene lists of the Venn diagrams are available in the supplementary data.

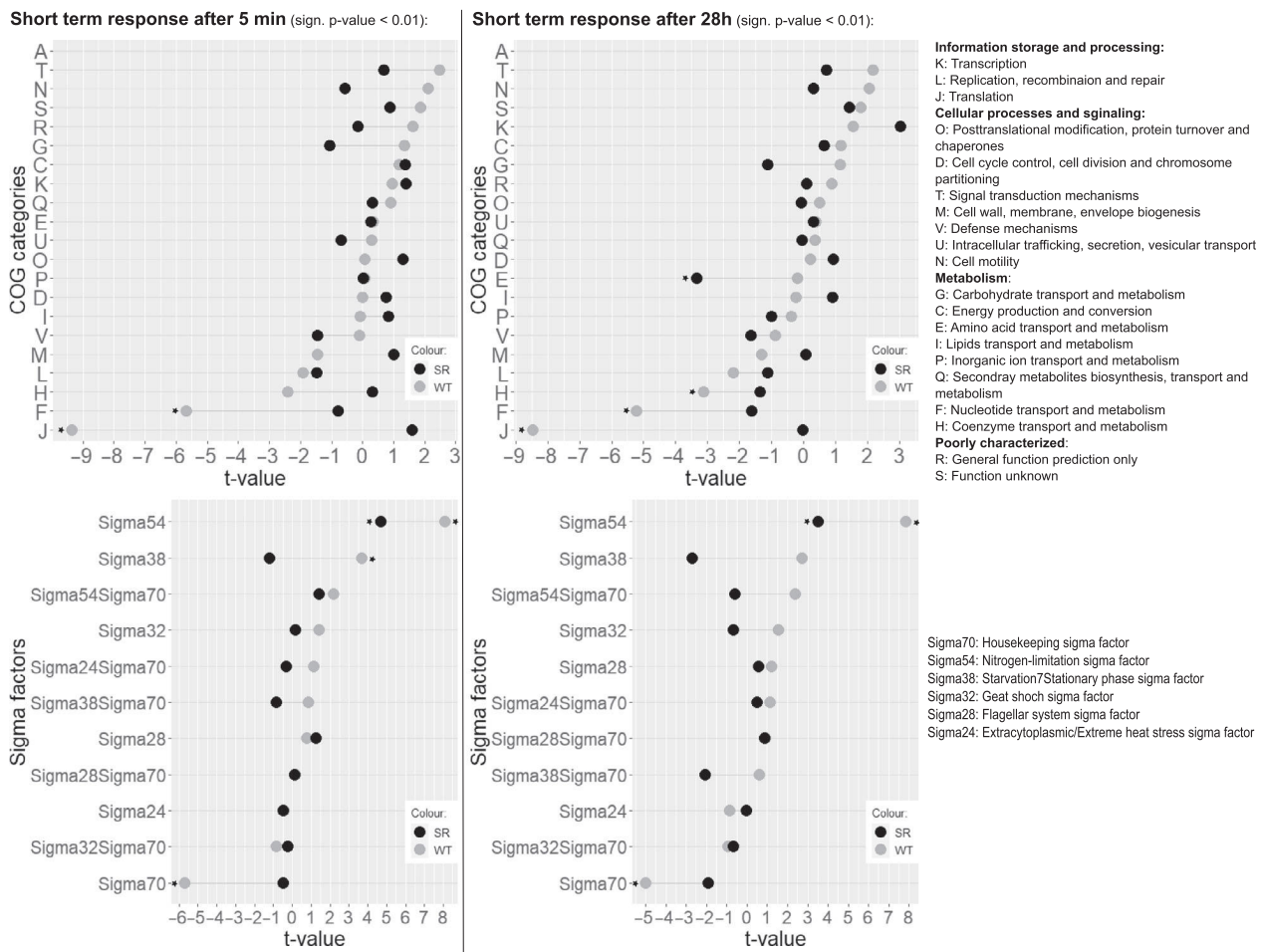


Fig. 7. Top: Transcriptional patterns grouped into COG categories of *E. coli* MG1655 (WT) and *E. coli* SR (SR). Left: short-term patterns to the PFR stimulus 5 min after PFR connection. Right: short-term patterns to the PFR stimulus 28 h after PFR connection. Bottom: Sigma factor activities of *E. coli* MG1655 (WT, grey) and *E. coli* SR (SR, black). Left: Short-term response to the PFR stimulus 5 min after PFR connection. Right: Short-term response to the PFR stimulus 28 h after PFR connection. Significant categories are indicated with an asterisk.

Gene expression along the PFR after 28 h of PFR action differs strongly from the early response. 125 DEGs, mostly downregulated, are shared by both strains and the number of individually regulated genes is similar

with 242 genes for *E. coli* MG1655 and 158 genes for *E. coli* SR (Fig. 6 right). Additionally, seven genes are oppositely regulated. Three of them (*tolQ*, *guaC*, *purM*) are upregulated in *E. coli* SR and downregulated in

E. coli MG1655. These genes correspond to cell envelope integrity during cell division (Gerding *et al.*, 2007), nucleotide metabolism (Kanjee *et al.*, 2012) and purine *de novo* biosynthesis (Mueller *et al.*, 1999). While purine *de novo* biosynthesis is actively inhibited by ppGpp via inhibition of GuaB, GTP synthesis solely originates from purine salvage pathways with *xdhA* significantly increased in *E. coli* MG1655 (Xi *et al.*, 2000). The residual four oppositely regulated DEGs (*csiD*, *glnL*, *lhgO*, *yeaH*) predominantly play a role in the adaptation to nitrogen starvation and except for *glnL* are known to be induced by ppGpp. NtrB encoded by *glnL* is an essential part of the Ntr response cascade to nitrogen starvation and *yeaG* positively impacts *rpoS* transcription and translation under prolonged nitrogen starvation (Brown *et al.*, 2014). Despite these differences in adaptation to nitrogen limitation, we observed no alterations in the uptake or utilization of ammonium which indicates that the additional regulatory adaptations of *E. coli* MG1655 are irrelevant in the context of a bioprocess.

Transcriptional patterns could be identified by functional enrichments of groups based on COG categories and sigma factor activities. COG groups J (Translation, ribosomal structure, and biogenesis) and F (nucleotide transport and metabolism) were significantly down regulated as part of the stringent response of *E. coli* MG1655 after both 5 min and 28 h (Fig. 7). For the 28 h sampling point group H (coenzyme transport and metabolism) was also significantly downregulated. As already indicated by the oppositely regulated genes (Fig. 7), σ 54-mediated genes responsible for the activation of the Ntr stress response including *yeaG/H* via NtrBC were induced in *E. coli* MG1655, as well as the σ 38 regulon as part of the general stress response (Brown *et al.*, 2014; Figueira *et al.*, 2015) (Fig. 7). Due to the limited amount of RNA-Polymerase (RNAP) core enzymes, σ 70 competes with σ 54, resulting in an antiproportional expression of their mediated genes (Jishage *et al.*, 1996). In contrast, *E. coli* SR only increased the expression of genes regulated by σ 54 after 5 min and no significant COG category was identified at this time-point. The absence of the stringent response in *E. coli* SR is clearly visible in an overall dampened regulatory response. The only significantly regulated group is E (amino acid transport and metabolism) after 28 h of PFR action, and the significantly downregulated genes in this group are predominantly ABC-transporters.

To unravel more detailed patterns in the transcriptional responses we assigned genes to the up-to-date gene ontology (GO) gene sets using GAGE (Luo *et al.*, 2009). 3345 out of 4037 genes (83%) could be mapped to GO Terms. As shown in Fig. 3 the majority of significant DEGs for *E. coli* MG1655 were downregulated. This is

mirrored by the results of the identified top 20 GO categories which were uniformly down-regulated (Fig. 8). *E. coli* MG1655 predominantly downregulated genes related to ribosomal biosynthesis and translation after 5 min and 28 h as expected for a stringent phenotype (Fig. 8). These transcriptional changes are counteracted in the long-term response observed from the STR (Fig. A3 to A6) which indicates looping induction and repression of the genes. Patterns from *E. coli* SR were less pronounced and grouped differently. After 5 min we observed decreasing gene expression of ATP-demanding processes such as ABC transporters and ATPase complexes (Fig. 8). After 28 h the PFR passage mainly induced an increased negative regulation of transcription and metabolic processes (Fig. 8). Care must be taken in the interpretation of this group though. General categories affecting transcription (GO:0006351, GO:0045892, GO:0097659, GO:1903507) or RNA processes (GO:0032774, GO:1902679, GO:0051253, GO:0051252) are represented as simultaneously negatively and positively regulated. Moreover, all negative regulators included in these terms, such as members of the CRP family, are also capable of positive regulation. Other negative regulation categories involve genes which actively inhibit translation and belong to SOS signals like DNA damage, prevention of cell division and programmed cell death (PCD). *E. coli* SR thereby focuses on σ 38 regulated genes, as well as toxin and antitoxin systems (*mazEF* and *mqsRA*) possibly resulting in arrested growth and a dormant cell state or even PCD. As growth arrest is usually a primary outcome of the stringent response, which is absent in *E. coli* SR, we hypothesize that this pattern might provide an alternative way for *E. coli* SR to achieve cell cycle arrest.

In summary, the short-term response transcriptional patterns of *E. coli* MG1655 were extensive and dominated by the stringent response and the Ntr regulon. The major activated sigma factors were σ 54 and σ 38. Overall, the transcription of ribosomal genes and other genes necessary for growth was inhibited, while genes involved in the transport and fixation of ammonia were induced. Our observations reflect well-known regulatory patterns exerted by *E. coli* K-12 when facing nitrogen starvation (Chang *et al.*, 2002; Traxler *et al.*, 2008; Traxler *et al.*, 2011; Simen *et al.*, 2017; Wang and Levin, 2009). In contrast, the transcriptional short-term response of *E. coli* SR is dampened both in the number of DEGs and the patterns observed, especially shortly after connection of the PFR. The only significantly activated sigma factor is σ 54 indicating a functional but attenuated Ntr response in the absence of ppGpp accumulation. Adaptation to ongoing starvation was possibly attempted via negative regulation of metabolic processes and SOS pathways.

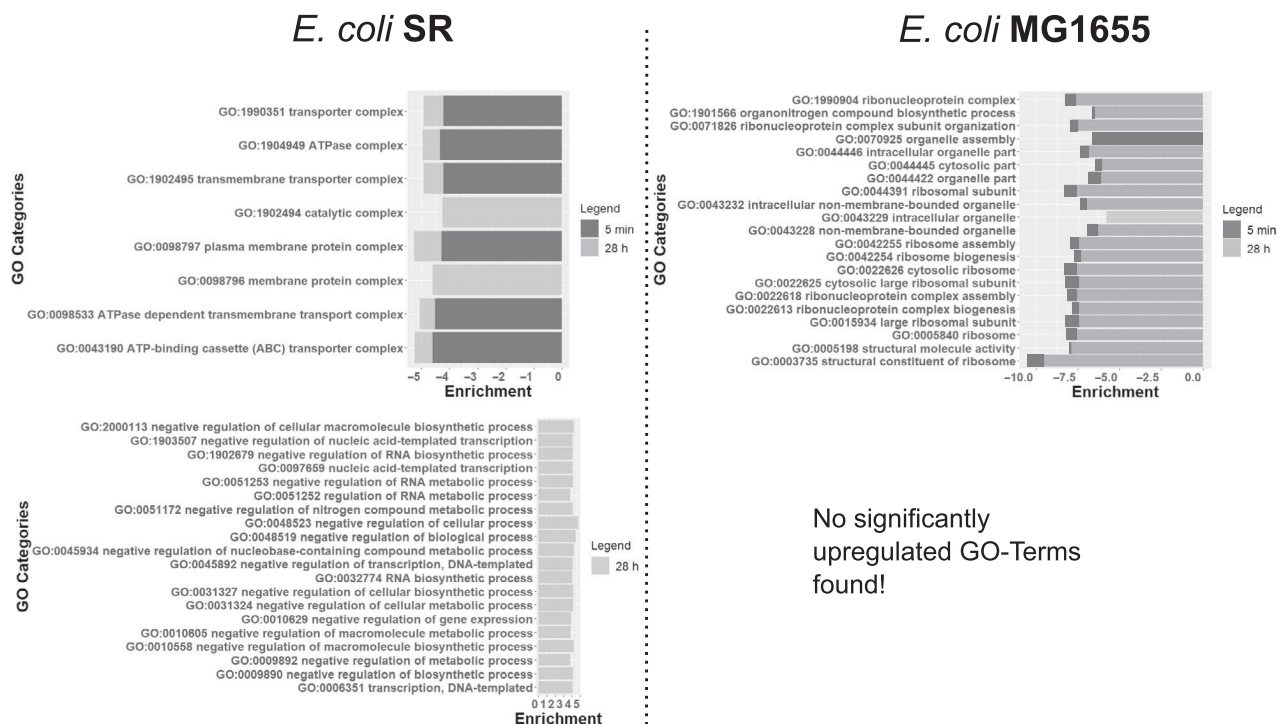


Fig. 8. Significant GO categories after 5 min and 28 h of both *E. coli* SR (left) and *E. coli* MG1655 (right). Downregulated categories are arranged at the top and upregulated GO terms at the bottom. 5 min: Short-term response of *E. coli* SR (left) and *E. coli* MG1655 (right) after 5 min of PFR action. Only the Top 20 out of 102 significantly downregulated categories are shown. Neither strain had significantly upregulated categories for this time-point. 28h : Short-term response of *E. coli* SR (left, light grey) and *E. coli* MG1655 (right, light grey) after 28 h of PFR action. For *E. coli* SR only the Top 20 out of 24 significantly upregulated categories are shown. For *E. coli* MG1655 only the Top 20 out of 95 significantly downregulated categories are shown. No significantly upregulated categories were found for this time-point.

Discussion

In the present study, we investigated the regulatory responses of the stringent response mutant strain *E. coli* SR when exposed to repeated short starvation stimuli in a scale-down reactor. The comparison with its wild-type parent *E. coli* MG1655 unravelled dampened regulatory patterns which are potentially beneficial for the application of *E. coli* SR in industrial large-scale reactors. The reduced regulatory patterns might be beneficial for heterologous protein expression as well as the production of small molecules as less interference with engineered metabolic pathways may occur and energy otherwise spent for adaptive responses is available for product formation.

An important finding of our study is that despite the regulatory differences *E. coli* SR displayed no dysfunctionalities in handling the shortage of ammonium. *E. coli* SR reached the same biomass yield on ammonium as *E. coli* MG1655 both with and without PFR action. Moreover, both strains depleted ammonium to comparable levels of about 1.2 mg l⁻¹ or 67 μmol l⁻¹, well in line with previously reported values for *E. coli* K-12 strains in nitrogen limited chemostats (Hua *et al.*, 2004). The low

remaining ammonium concentration indicates that uptake in both strains is mediated actively by AmtB with $K_m = 0.8$ mM (Williamson *et al.*, 2020) and incorporation is accomplished by the GS-GOGAT System with GS $K_m = 0.1$ mM (Alibhai and Villafranca, 1994). This is supported by our transcriptional data which revealed that *amtB*, *gltB* and *gltD* were significantly enriched for both strains over all time-points. Transcripts of *glnA* were also always significantly enriched except for the time point 28 h of *E. coli* SR. Concomitantly, we identified transcriptional patterns typical for the σ₅₄- and NtrBC-mediated responses to nitrogen starvation (Reitzer, 2003). 13 out of 21 known NtrC-regulated operons (Brown *et al.*, 2014) were induced at PFR port 5 in *E. coli* MG1655 at all time points (Table S2). For *E. coli* SR, the Ntr response was slightly reduced, with 9 out of 21 operons induced (Table S3) and lower overexpression of σ₅₄ transcribed genes. These findings lead to the conclusion of an active, but diminished Ntr response of *E. coli* SR that still allowed fully functional ammonium assimilation. Additionally, the energy consumption as maintenance add-on for both strains was calculated according to Löffler *et al.* (2016) assuming *de novo* synthesis of all upregulated DEGs over the whole process time (28 h).

The resulting energy savings of *E. coli* SR due to weaker transcriptional response added up to around 46.5%. In terms of microbial productivity, the reduced maintenance demand potentially increases the amount of available ATP for biomass-specific productivities and improves cell fitness.

In a previous study, a significantly elevated specific glucose consumption rate under ammonium limitation was observed in *E. coli* SR (Michalowski *et al.*, 2017). Similarly, we observed reduced excess glucose and the accompanying formation of dissolved byproducts in the fermentation supernatant. In *E. coli* K-12 strains, the consumption of glucose is usually tightly coupled to the availability of nitrogen on the level of metabolite control by the interaction of 2-oxoglutarate with PtsI (Doucette *et al.*, 2011). The exact mechanism by which coupling of nitrogen and glucose uptake rates are relaxed in *E. coli* SR is not clear as the strain is isogenic to *E. coli* MG1655 except for the deletion of *relA* and the modifications in *spoT*. However, we found an increased transcription of *ptsI*, *ptsH* and *ptsG* in *E. coli* SR compared to *E. coli* MG1655 (Table S6). Artificially increased expression of *ptsI* has been shown to increase specific glucose uptake rates in nitrogen limited conditions (Chubukov *et al.*, 2017). We presume that the increased glucose uptake rate in *E. coli* SR might be caused by deregulated expression of *ptsI*, potentially connected to the absence of the stringent response by the action of CRP whose transcription is negatively regulated by ppGpp (Johansson *et al.*, 2000). It remains to be clarified whether *E. coli* SR has altered cytoplasmic 2-oxoglutarate levels or the action of ppGpp influences the coupling of glucose consumption to nitrogen availability, potentially by the proposed mechanism. Increased specific glucose uptake rates in conjunction with higher respiratory activity have also been observed in *E. coli* MG1655 subjected to repeated glucose feast-famine cycles (Vasilakou *et al.*, 2020). Future studies should thus examine how *E. coli* SR reacts to varying availability of glucose or other carbon sources.

In view of these differences in carbon metabolism, we hypothesized that biological energy availability might be unequal for *E. coli* MG1655 and *E. coli* SR. From oxygen and glucose uptake rates the specific ATP production rate q_{ATP} was estimated (Table 1). q_{ATP} greatly depends on the effective P/O ratio and current scientific consensus estimates realistic P/O ratios between 1.0 and 1.5 for *E. coli* (Noguchi *et al.*, 2004; Szenk *et al.*, 2017). For our estimations of q_{ATP} we assumed a conservative P/O ratio of 1.2 and 2 moles of ATP per mol glucose from glycolysis. The result indicates that *E. coli* SR might have an increased availability of ATP compared to its wild-type parent under the applied experimental conditions. Given that the respiratory capability

and thus the ATP production capability of K-12 strains is not exhausted at a dilution rate of $D = 0.2 \text{ h}^{-1}$ it appears that the increased glycolytic flux to byproducts displayed by *E. coli* SR was also not a result of increased energy demand. Moreover, increased glucose uptake has been reported previously for *E. coli* SR under conditions of ammonia limitation despite high adenylate energy charge (Michalowski *et al.*, 2017). Carbon and redox homeostasis at elevated glycolytic flux would then be maintained by byproduct excretion and increased respiration, possibly involving the dissipation of surplus energy by uncoupling of the electron transport chain (Bekker *et al.*, 2009).

Nitrogen limitation inducing the stringent response is a well-documented phenomenon in *E. coli*. Multiple previous studies predominantly observed heavily increased gene expression corresponding to amino acid transport and metabolism (Barker *et al.*, 2001; Durfee *et al.*, 2008; Traxler *et al.*, 2008; Traxler *et al.*, 2011; Brown *et al.*, 2014; Simen *et al.*, 2017). Conversely, we observed almost equally distributed up- and downregulated genes for amino acid transport and metabolism (see Supporting information: Transcriptomics), which was only reported by few research groups (Chang *et al.*, 2002; Traxler *et al.*, 2008). As a result, no overall significant statistical trend was detectable for this category (Fig. 7). We suggest that the individual operons do not solely respond to ppGpp, but rather depend on other signals and regulatory networks which were not found to be significantly expressed in this study such as the Lrp regulon. Additionally, caution is advised when comparing transcriptomic analyses originating from different studies as they greatly depend on the transcriptional reference state and thus the details of the experimental design.

In general, the amount of DEGs of *E. coli* K-12 MG1655 was similar to the numbers found in the analogous study of Simen *et al.* (2017) who employed the closely related *E. coli* K-12 W3110 confirming the validity of our data. The amount of DEGs is also less than observed during the related study of glucose starvation by Löffler *et al.* (2016) which points towards significant potential of *E. coli* SR to preserve energy in glucose starvation conditions. An interesting difference to the former studies in this scale-down reactor setup is the absence of increased motility in the STR after PFR connection (Löffler *et al.*, 2016; Simen *et al.*, 2017). Our dataset contains no upregulated flagellar or sigma factor 28 mediated gene patterns from the STR at any timepoint (Fig. 7). We first hypothesized that the cause might be genetic differences affecting motility which are well documented between MG1655 and W3110 and even between different MG1655 isolates (Barker *et al.*, 2004; Hayashi *et al.*, 2006). However, sequencing of our MG1655 isolate revealed the presence of the canonical

IS-1 insertion upstream of *flhD* which confers motility and our MG1655 isolate displayed vivid spreading in motility agar (Supporting information, Fig. A7). An alternative explanation could be derived by the interplay of quorum sensing and flagellar regulation through the action of autoinducer-2 (AI-2) and the motility quorum sensing regulator MqsR. While transcript levels of *luxS* (*LuxS* synthesizes AI-2) remain unchanged, the expression of *mqsR* is significantly enriched at PFR port 5 and MqsR is known to induce the flagellar synthesis cascade (González Barrios *et al.*, 2006). However, cell dry weight (CDW) was always below 3 g l^{-1} in our experiments whereas Simen *et al.* worked with around 10 g l^{-1} CDW. Higher biomass should lead to increased AI-2 levels and may cause a preconditioned phenotype that rapidly initiates flagellar biosynthesis when encountering nutrient stress. Thus, rapid induction of motility genes might become more pronounced during high cell density processes in large-scale reactors and remains to be examined in further studies. Additionally, as introduced by Löffler *et al.* (2016) during glucose fluctuation, genes of the category cell motility were identified as one of the most prominent energy consumers and might therefore be candidates for genome reduction (Löffler *et al.*, 2016).

Analysis of gene expression patterns (Fig. 7 and 8) revealed that both strains individually adapted to repeated nitrogen starvation. *E. coli* MG1655 adjusted by utilizing the ppGpp-mediated general stress response including activation of toxin/antitoxin (TA) systems like *mqsRA* and *mazEF*. This strategy intends to arrest the cell cycle and form persister cells (Balaban *et al.*, 2004). Persister cell formation is not yet fully understood and usually only involves a small fraction of cells (Chowdhury *et al.*, 2016; Gerdes and Maisonneuve, 2012; Korch *et al.*, 2015). Thus, it seems to be only of minor importance for industrial processes but some persister genes affect persister level due to altered growth rates rather than contributing to a mechanism of cell cycle arrest and might have a significant impact on bioprocess performance (Allison *et al.*, 2011). Nonetheless two common dependencies affecting persister formation, ppGpp and TA systems, are known which is in line with our findings (Aizenman *et al.*, 1996; González Barrios *et al.*, 2006; Chowdhury *et al.*, 2016; Sun *et al.*, 2017; Wang and Levin, 2009). Persister formation benefits from increased ppGpp concentrations but is still possible at lower rates in the absence of ppGpp by proteins which simply reduce growth (Chowdhury *et al.*, 2016). The nucleotide pyrophosphohydrolase MazG which is negatively regulated by the *mazEF* system is able to initiate cell cycle arrest and was significantly upregulated in *E. coli* SR after 28 h (Lee *et al.*, 2008). Additionally, *E. coli* SR initiated negative regulation of transcription, translation and

cell division processes as part of the SOS response (Fig. 8). Most likely, the SOS pathways were activated due to ongoing DNA replication during starvation conditions which might ultimately result in DNA damage and inhibited cell division (Bi and Lutkenhaus, 1993; Joseleau-Petit *et al.*, 1999; Traxler *et al.*, 2008). As part of the SOS response and as a key gene involved in filamentation *sulA* was significantly upregulated in *E. coli* SR. *SulA* inhibits the initiation of cellular division by repressing the assembly of FtsZ into the Z ring (Huisman *et al.*, 1984; Fonville *et al.*, 2010). Simultaneously with the overexpression of *sulA*, *lexA* was significantly increased which acts as a major repressor of SOS signals. *LexA* regulates the response strength and is actively involved in the occurrence of persister cells in bacterial populations (Butala *et al.*, 2011). These results indicate a coordinated and rather complex SOS response in *E. coli* SR to form persister cells which is not yet fully understood.

The natural regulation of *E. coli* has evolved towards optimality in its lifestyle as a gut bacterium and is not honed for the demands of a large-scale bioprocess. The absence of the stringent response and the conservation of the ability to grow efficiently in minimal medium suggest that *E. coli* SR has the potential to become a platform strain for applications in large-scale reactors. Our transcriptional analysis shows that the short-term response of *E. coli* SR to ammonium depletion is dampened but a functional Ntr/σ54 response remains. Regarding glucose-limited fermentations, we hypothesize that *E. coli* SR has significant potential to preserve energy in such conditions since the regulatory responses are usually even more pronounced and centred around the stringent response (Hardiman *et al.*, 2007; Löffler *et al.*, 2016). We therefore propose to confirm the suitability of *E. coli* SR for large-scale applications in multi-compartment scale-down reactors employing exemplary small-molecule production scenarios. These should include standard glucose-limited fed-batches as well as ammonium limited fed-batches with a prolonged nitrogen-limited production phase to exploit its elevated glucose consumption.

Experimental procedures

Bacterial strains and media

Strains *E. coli* MG1655 or *E. coli* SR were used in all experiments (Table 2).

2xYT agar plates were prepared by autoclaving 16 g l^{-1} tryptone, 10 g l^{-1} yeast extract, 5 g l^{-1} NaCl and 18 g l^{-1} agar-agar dissolved in demineralized water. Minimal medium for precultures consisted of 4 g l^{-1} glucose, 0.96 g l^{-1} $\text{NaH}_2\text{PO}_4 \cdot 2\text{H}_2\text{O}$, 3.51 g l^{-1} K_2HPO_4 , 2.4 g l^{-1} $(\text{NH}_4)_2\text{SO}_4$, 0.01 g l^{-1} thiamine hydrochloride and 0.2%

Table 2. Bacterial Strains used in this study.

Strain	Genotype/strain information	Reference
<i>Escherichia coli</i> K-12 MG1655 (“wild type” strain, abbrev. WT)	F ⁻ , λ ⁻ , <i>ilvG</i> ⁻ , <i>rfb</i> -50, <i>rph</i> -1	Michalowski <i>et al.</i> (2017)
<i>Escherichia coli</i> SR	MG1655 Δ <i>relA</i> , <i>spoT</i> [R290E;K292D]	Michalowski <i>et al.</i> (2017)

(V/V) trace elements stock solution. Minimal medium for batch cultivation in the bioreactor consisted of 19 g l⁻¹ glucose, 1.50 g l⁻¹ NaH₂PO₄·2H₂O, 3.9 g l⁻¹ K₂HPO₄, 5.7 g l⁻¹ (NH₄)₂SO₄ and 0.2% (V/V) trace elements stock solution. 200 μl of antifoaming agent Struktol J647 (Schill + Seilacher, Hamburg, Germany) was added to the batch medium prior to inoculation. Minimal medium for continuous chemostat cultivation in the bioreactor consisted of 11.4 g l⁻¹ glucose, 1 g l⁻¹ NaH₂PO₄·2H₂O, 2.6 g l⁻¹ K₂HPO₄, 2.28 g l⁻¹ (NH₄)₂SO₄ and 0.2% (V/V) trace elements stock solution. Throughout the chemostat phase 50 μl/h of antifoaming agent Struktol J647 were added continuously to the fermentation medium. The composition of trace element stock solution was 4.175 FeCl₃·6H₂O, 0.045 g l⁻¹ ZnSO₄·7H₂O, 0.025 g l⁻¹ MnSO₄·H₂O, 0.4 g l⁻¹ CuSO₄·5H₂O, 0.045 CoCl₂·6H₂O, 2.2 g l⁻¹ CaCl₂·2H₂O, 50 g l⁻¹ MgSO₄·7H₂O and 55 g l⁻¹ sodium citrate dihydrate. Stock solutions of salts, trace elements and glucose were autoclaved separately, and stock solutions of thiamine hydrochloride were filter sterilized and stored at 4°C. All compounds were combined just before the experiments to prevent possible aging of media.

Bioreactor setup

Cultivations were carried out in a two-compartment scale-down reactor. The primary reactor was a stirred tank reactor (STR), and a plug flow reactor (PFR) was used as the secondary compartment mimicking a starvation zone. The plug flow reactor was connected to the stirred tank reactor after establishment and sampling of a steady state in the chemostat phase. The basic technical setup has been characterized previously (Löffler *et al.*, 2016; Simen *et al.*, 2017). Minor modifications to the original setup have been made and are described elsewhere (Ankenbauer *et al.*, 2020).

The primary reactor was a 3 l bioreactor (Bioengineering, Wald, Switzerland) equipped with flow baffles and two six-blade Rushton type impellers operated at 1000 rpm. A constant aeration rate of 2.0 standard litres of ambient pressurized air per minute was employed and the system operated at a total pressure of 1.5 bar.

Temperature was monitored by a platinum resistance thermometer and regulated by electrical heating or water cooling. Temperature was set to 28–30°C for the batch phase and to 37°C for the continuous chemostat phase. The reactor was equipped with a pH sensor (Mettler Toledo, Columbus, USA) to control pH and a pO₂ sensor for monitoring dissolved oxygen tension (PreSens, Regensburg, Germany). During all fermentation stages pH was set to 7.0 and regulated by automated addition of 3 M NaOH or 2.5 M H₃PO₄. Dissolved oxygen tension was not regulated but maintained values above 70% saturation to 1.5 bar ambient air throughout the entire cultivation. In the exhaust gas stream, the concentration of oxygen and carbon dioxide was measured by gas sensors (BlueSens, Herten, Germany). During the chemostat phase the feed was constantly added to the reactor by a peristaltic pump (Watson-Marlow, Falmouth, UK). The feed flow was monitored by a balance recording the weight of the stirred feed barrel and manually adjusted if necessary. The harvesting pump operated as a slave pump set to maintain a constant weight of the bioreactor. For this purpose, the stirred tank reactor was installed on a balance as well.

The secondary compartment was a plug-flow reactor with an inner tube diameter of 20 mm and a total volume of approximately 380 ml. Five ports along the primary axis were used to take samples throughout the cultivation. Oxygen saturation in the PFR was monitored close to ports P1, P2 and P5 and additional aeration of 0.15 standard litres per minute was provided next to port P1 to ensure levels above 30% saturation to ambient air conditions throughout the entire PFR passage. Temperature in the PFR was maintained at 36–37°C by water heating and isolation material. A diaphragm metering pump (Sigma/1, ProMinent, Heidelberg, Germany) was used to transfer biosuspension from the stirred tank reactor to the plug flow reactor after connection of the two reactors.

Preculture, batch cultivation and continuous cultivation

A small amount of glycerol stock seed culture was spread onto 2xYT agar plates and incubated at 37°C for 24 h. A single colony was picked to inoculate 500 ml baffled shaking flasks with 50 ml of preculture minimal media. Flasks were then incubated at 37°C on an orbital shaker set to 150 rpm for 16 h. In the next morning 500 μl of biosuspension were transferred to 1000 ml baffled shaking flasks containing 100 ml preculture minimal media and incubated at 37°C on an orbital shaker set to 150 rpm for 8 h. 50 ml of this culture were used to inoculate the bioreactor. Total volume in the bioreactor was 1.6 l after inoculation. Batch fermentation in the bioreactor ensued at 28–30°C overnight. In the next morning

feed and harvest trains were connected and a constant feed/harvest rate at 5.33 ml min⁻¹ corresponding to a dilution rate of 0.2 h⁻¹ established. After 25 h (five volumetric residence times) of STR cultivation a reference sample was taken. The plug-flow reactor was then connected to the primary reactor via a diaphragm metering pump effectively circulating about one-quarter of the total fermentation broth from the STR through the PFR and back into the STR. In the following 28 h samples were taken at predefined time points from the STR and the five PFR ports. After 28 h of STR-PFR cultivation the fermentation was aborted, and the final broth volume measured. This value was used for all volumetric calculations during data analysis.

Determination of optical density and biomass

In preliminary experiments with identical setup correlation factors of optical density and biomass as cell dry weight (CDW) were determined for *E. coli* MG1655 and *E. coli* SR (Supporting information, Table S1). The resulting correlation factors for converting OD_{600nm} values to g l⁻¹ cell dry weight were 0.324 for *E. coli* MG1655 and 0.321 for *E. coli* SR. In the main cultivations optical density was measured from appropriately diluted broth on a spectrophotometer at 600 nm and converted into biomass concentration.

Determination of acetic acid, ammonium and glucose concentrations

Five millilitres of biosuspension was directly sampled into a syringe connected to a single-use 0.45 µm sterile filter and immediately sterile filtered. The clear supernatant was flash frozen in liquid nitrogen and stored at -70°C until analysis. Glucose concentration was determined by D-Glucose UV-Test Kit (R-Biopharm, Darmstadt, Germany) and acetic acid concentration by Acetic acid UV-Test Kit (R-Biopharm, Darmstadt, Germany). Ammonium concentration was determined by Ammonium cuvette test LCK 304 (Hach Lange, Düsseldorf, Germany). At the end of the cultivation feed samples were taken and processed identically.

Analysis of total carbon, inorganic carbon and biomass composition

For total carbon and inorganic carbon analysis 0.5 ml biosuspension sample were mixed with 50 µl of 5 M KOH to prevent loss of dissolved carbonate. The suspension was then diluted 1:20 with demineralized water and stored at 4°C until analysis. Analysis was performed with a multi N/C 2100 S composition analyzer (Analytik Jena, Jena, Germany) to yield the total concentration of

carbon and inorganic carbon in the fermenter effluent stream. At the end of the cultivation feed samples were taken and processed identically.

To determine biomass composition 1.0 ml of biosuspension was centrifuged at 4°C and 14 000 rpm (20817 g) for 3 min. The supernatant was discarded, the pellet resuspended in 1.0 ml of freshly prepared 0.9% NaCl solution and centrifuged again. The pellet was resuspended in 5 ml 0.9% NaCl, flash frozen in liquid nitrogen and stored at -70°C until analysis. Analysis was performed with a multi N/C 2100 S composition analyzer (Analytik Jena, Jena, Germany) and the carbon content of the biomass calculated from these values.

Measurement of ppGpp

Two millilitres of biosuspension was sampled directly into 0.5 ml of precooled (< -20°C) quenching solution and incubated at 6°C on a shaker for 15 min. Quenching solution consisted of 80 µM EDTA dissolved in 35% (V/V) perchloric acid. 500 µl 1 M K₂HPO₄ was added and the sample briefly vortexed. 550 µl 5 M KOH was added and the sample vortexed again. To remove precipitating potassium perchlorate samples were then centrifuged at 4°C and 7830 rpm (7197 g) for 5 min. 1.5 ml of supernatant was carefully transferred to new tubes, flash frozen in liquid nitrogen and stored at -70°C. Prior to analysis samples were thawed and their pH adjusted to 6.95 – 7.05 with 5 M KOH or 35% (V/V) perchloric acid. Samples were centrifuged again to remove all potassium perchlorate precipitate. HPLC analysis was carried out as described previously (Löffler *et al.*, 2016). If necessary, quantification was conducted by ppGpp standard addition (TriLink, San Diego, CA, USA). Samples from one time-point were analysed directly in sequence and the data normalized to the sample drawn from the STR to eliminate differences caused by column aging.

Transcriptome analysis

0.5 ml broth was sampled from the bioreactor and directly flash-frozen in liquid nitrogen. Frozen broth was then stored at -70°C until the day of RNA isolation. Total RNA was isolated using RNeasy Mini Kit (Qiagen, Hilden, Germany) according to the manufacturer's instructions. Isolated RNA was DNase treated and shipped to commercial sequencing partner GENEWIZ® on dry ice. Samples were treated for rRNA depletion, sequencing libraries prepared and Illumina HiSeq 2x150 bp sequencing performed. Raw FASTQ files were obtained for bioinformatic analysis. Trimmomatic v. 0.32 (Bolger *et al.*, 2014) was used to remove adapters and low-quality reads (<Q20) checked by fastqc reports. Genes were aligned to the NCBI *E. coli* K-12 MG1655

reference genome (RefSeq: NC_000913.3) using the RNA-sequencing aligner Bowtie2 v. 2.3.2.2 (Langmead and Salzberg, 2012). On average the mapping of the reads covered 96.2%. Aligned reads were counted for each gene based on the corresponding annotation available from the NCBI database for the chosen reference sequence applying HTseq-count v. 0.6.1 in the union mode (Anders *et al.*, 2015). On average 86.4 % of the sequenced reads could be assigned uniquely to annotated features. Sequencing depth was around 27 million reads per sample on average with a mean quality phred score of 37.63.

Differential gene expression analysis was performed with the R-package DESeq2 v. 1.26.0 (Love *et al.*, 2014) available from Bioconductor (Gentleman *et al.*, 2004). Prior to statistical analysis, all residual non-protein encoding RNA molecules (tRNA, rRNA and sRNA) were removed from the HTseq-derived raw count data and a non-specific filter was applied to remove low coverage genes with fewer than two counts per million (54 reads on average). All filtering steps caused deviations from the raw data of less than 6 %. Samples were grouped by replicates and an experimental design was chosen that used sample time and location (STR or PFR port 5) as a combined environmental factor. To normalize read counts for the comparison of sequencing depth and RNA composition, DESeq2 uses the median of ratios method to derive a scaling factor. Dividing the original read counts by the scaling factor generated normalized count values. No outliers were observed in the two biological replicates using Pearson correlation. Resulting *p*-values were adjusted for multiple testing according to control the false discovery rate (FDR) (Benjamini and Hochberg, 1995). Genes were identified as significantly differentially expressed by applying FDR adjusted *P*-values < 0.01 and a log₂ fold change ≥ 11.

A principal component analysis was used to display the sample to sample distances calculated within the DESeq2 package (negative binomial distribution model). Principal component analysis was performed using plotPCA.san available on Github (<https://gist.github.com/sansense/3399064897f1252d31b23ea5178c033c>).

Gene set enrichment and overrepresentation analysis of up- and downregulated genes were performed using the Bioconductor's R-package GAGE v. 2.36.0 (Luo *et al.*, 2009). GAGE tests whether the mean fold-change of a gene subset is significantly different from the background using a two-tailed *t*-test. Genes were selected as significantly different with an FDR adjusted *P*-value < 0.01 (Benjamini and Hochberg, 1995). Functional annotation were derived from the Cluster of Orthologous Groups (COG) database (Tatusov *et al.*, 2003), the experimental sigma factor-gene interaction dataset from RegulonDB v. 10.6.3 (Santos-Zavaleta

et al., 2019) and the Gene Ontology (GO) Groups database with the function go.gsets from GAGE (Luo *et al.*, 2009). Furthermore, Venn diagrams were used to identify significant genes shared by both strains and differences in gene expression regulation (Chen and Boutros, 2011).

The RNA sequencing data derived from periodic ammonia starvation experiments have been deposited in NCBI's Gene Expression Omnibus (GEO) and are accessible through GEO series accession number GSE158198 (Edgar *et al.*, 2002). Raw counts and processed data can be found in the Supporting information. Data analysis was performed using the free statistical computing environment R v. 3.6.2.

Acknowledgements

The authors would like to thank the group of Computational Biology at the Institute of Biochemical Engineering for the use of the Galaxy-Server.

Conflict of interest

The authors declare that they have no conflicts of interest.

Author contributions

Prof. Dr.-Ing. Ralf Takors advised the study during the entire investigation. Martin Ziegler performed the experiments, and Julia Zieringer conducted the transcriptomic analysis. Evaluation and writing of the manuscript were equally accomplished by Martin Ziegler and Julia Zieringer.

References

- Aizenman, E., Engelberg-Kulka, H., and Glaser, G. (1996) An Escherichia coli chromosomal "addiction module" regulated by guanosine corrected 3',5'-bispyrophosphate: a model for programmed bacterial cell death. *Proc Natl Acad Sci USA* **93**: 6059–6063. <https://doi.org/10.1073/pnas.93.12.6059>
- Alibhai, M., and Villafranca, J.J. (1994) Kinetic and mutagenic studies of the role of the active site residues Asp-50 and Glu-327 of Escherichia coli glutamine synthetase. *Biochemistry* **33**: 682–686. <https://doi.org/10.1021/bi00169a008>
- Allison, K.R., Brynildsen, M.P., and Collins, J.J. (2011) Heterogeneous bacterial persisters and engineering approaches to eliminate them. *Curr Opin Microbiol* **14**: 593–598. <https://doi.org/10.1016/j.mib.2011.09.002>
- Anders, S., Pyl, P.T., and Huber, W. (2015) HTSeq—a Python framework to work with high-throughput sequencing data. *Bioinformatics (Oxford, England)* **31**: 166–169. <https://doi.org/10.1093/bioinformatics/btu638>

- Andrews, S.C., and Guest, J.R. (1988) Nucleotide sequence of the gene encoding the GMP reductase of *Escherichia coli* K12. *Biochem J* **255**: 35–43. <https://doi.org/10.1042/bj2550035>.
- Ankenbauer, A., Schäfer, R.A., Viegas, S.C., Pobre, V., Voß, B., Arraiano, C.M., and Takors, R. (2020) *Pseudomonas putida* KT2440 is naturally endowed to withstand industrial-scale stress conditions. *Microb Biotechnol* **13**: 1145–1161. <https://doi.org/10.1111/1751-7915.13571>
- Atherly, A.G. (1979) *Escherichia coli* mutant containing a large deletion from relA to argA. *J. Bacteriol.* **138**: 530–534.
- Balaban, N.Q., Merrin, J., Chait, R., Kowalik, L., and Leibler, S. (2004) Bacterial persistence as a phenotypic switch. *Science* **305**: 1622–1625. <https://doi.org/10.1126/science.1099390>
- Barker, M.M., Gaal, T., Josaitis, C.A., and Gourse, R.L. (2001) Mechanism of regulation of transcription initiation by ppGpp. I. Effects of ppGpp on transcription initiation in vivo and in vitro. *J Mol Biol* **305**: 673–688. <https://doi.org/10.1006/jmbi.2000.4327>
- Barker, C.S., Prüss, B.M., and Matsumura, P. (2004) Increased motility of *Escherichia coli* by insertion sequence element integration into the regulatory region of the flhD operon. *J. Bacteriol.* **186**: 7529–7537. <https://doi.org/10.1128/JB.186.22.7529-7537.2004>
- Bekker, M., de Vries, S., Ter Beek, A., Hellingwerf, K.J., and de Mattos, M.J.T. (2009) Respiration of *Escherichia coli* can be fully uncoupled via the nonelectrogenic terminal cytochrome bd-II oxidase. *J Bacteriol* **191**: 5510–5517. <https://doi.org/10.1128/JB.00562-09>
- Benjamini, Y., and Hochberg, Y. (1995) Controlling the false discovery rate: a practical and powerful approach to multiple testing. *J Roy Stat Soc: Ser B (Methodol)* **57**: 289–300. <https://doi.org/10.1111/j.2517-6161.1995.tb02031.x>
- Bi, E., and Lutkenhaus, J. (1993) Cell division inhibitors SulA and MinCD prevent formation of the FtsZ ring. *J Bacteriol* **175**: 1118–1125. <https://doi.org/10.1128/jb.175.4.1118-1125.1993>
- Bolger, A.M., Lohse, M., and Usadel, B. (2014) Trimmomatic: a flexible trimmer for Illumina sequence data. *Bioinformatics (Oxford, England)* **30**: 2114–2120. <https://doi.org/10.1093/bioinformatics/btu170>
- Brown, D.R., Barton, G., Pan, Z., Buck, M., and Wigneshw-
eraj, S. (2014) Nitrogen stress response and stringent response are coupled in *Escherichia coli*. *Nat Commun* **5**: 4115. <https://doi.org/10.1038/ncomms5115>
- Butala, M., Klose, D., Hodnik, V., Rems, A., Podlesek, Z., Klare, J.P., et al. (2011) Interconversion between bound and free conformations of LexA orchestrates the bacterial SOS response. *Nucleic Acids Res* **39**: 6546–6557. <https://doi.org/10.1093/nar/gkr265>
- Bylund, F., Castan, A., Mikkola, R., Veide, A., and Larsson, G. (2000) Influence of scale-up on the quality of recombinant human growth hormone. *Biotechnol Bioeng* **69**: 119–128. [https://doi.org/10.1002/\(SICI\)1097-0290\(20000720\)69:2<119::AID-BIT1>3.0.CO;2-9](https://doi.org/10.1002/(SICI)1097-0290(20000720)69:2<119::AID-BIT1>3.0.CO;2-9)
- Bylund, F., Collet, E., Enfors, S.-O., and Larsson, G. (1998) Substrate gradient formation in the large-scale bioreactor lowers cell yield and increases by-product formation. *Bioprocess Eng* **18**: 171. <https://doi.org/10.1007/s004490050427>
- Bylund, F., Guillard, F., Enfors, S.-O., Trägårdh, C., and Larsson, G. (1999) Scale down of recombinant protein production: a comparative study of scaling performance. *Bioprocess Eng* **20**: 377. <https://doi.org/10.1007/s004490050606>
- Chang, D.-E., Smalley, D.J., and Conway, T. (2002) Gene expression profiling of *Escherichia coli* growth transitions: an expanded stringent response model. *Mol Microbiol* **45**: 289–306. <https://doi.org/10.1046/j.1365-2958.2002.03001.x>
- Chen, H., and Boutros, P.C. (2011) VennDiagram: a package for the generation of highly-customizable Venn and Euler diagrams in R. *BMC Bioinformatics* **12**: 35. <https://doi.org/10.1186/1471-2105-12-35>
- Chowdhury, N., Kwan, B.W., and Wood, T.K. (2016) Persistence increases in the absence of the alarmone guanosine tetraphosphate by reducing cell growth. *Sci Rep* **6**: 20519. <https://doi.org/10.1038/srep20519>
- Chubukov, V., Desmarais, J.J., Wang, G., Chan, L.J.G., Baidoo, E.E., Petzold, C.J., et al. (2017) Engineering glucose metabolism of *Escherichia coli* under nitrogen starvation. *NPJ Syst Biol App* **3**: 16035. <https://doi.org/10.1038/npsba.2016.35>
- Dalebroux, Z.D., and Swanson, M.S. (2012) ppGpp: magic beyond RNA polymerase. *Nat Rev Microbiol* **10**: 203–212. <https://doi.org/10.1038/nrmicro2720>
- Delvigne, F., Destain, J., and Thonart, P. (2006) A methodology for the design of scale-down bioreactors by the use of mixing and circulation stochastic models. *Biochem Eng J* **28**: 256–268. <https://doi.org/10.1016/j.bej.2005.11.009>
- Delvigne, F., Takors, R., Mudde, R., van Gulik, W., and Noorman, H. (2017) Bioprocess scale-up/down as integrative enabling technology: from fluid mechanics to systems biology and beyond. *Microb Biotechnol* **10**: 1267–1274. <https://doi.org/10.1111/1751-7915.12803>
- Doucette, C.D., Schwab, D.J., Wingreen, N.S., and Rabinowitz, J.D. (2011) α -Ketoglutarate coordinates carbon and nitrogen utilization via enzyme I inhibition. *Nat Chem Biol* **7**: 894–901. <https://doi.org/10.1038/nchembio.685>
- Durfee, T., Hansen, A.-M., Zhi, H., Blattner, F.R., and Jin, D.J. (2008) Transcription profiling of the stringent response in *Escherichia coli*. *J Bacteriol* **190**: 1084–1096. <https://doi.org/10.1128/JB.01092-07>
- Edgar, R., Domrachev, M., and Lash, A.E. (2002) Gene Expression Omnibus: NCBI gene expression and hybridization array data repository. *Nucleic Acids Res* **30**: 207–210. <https://doi.org/10.1093/nar/30.1.207>
- Enfors, S.-O., Jahic, M., Rozkov, A., Xu, B., Hecker, M., Jürgen, B., et al. (2001) Physiological responses to mixing in large scale bioreactors. *J Biotechnol* **85**: 175–185. [https://doi.org/10.1016/S0168-1656\(00\)00365-5](https://doi.org/10.1016/S0168-1656(00)00365-5)
- Figueira, R., Brown, D.R., Ferreira, D., Eldridge, M.J.G., Burchell, L., Pan, Z., et al. (2015) Adaptation to sustained nitrogen starvation by *Escherichia coli* requires the eukaryote-like serine/threonine kinase YeaG. *Sci Rep* **5**: 17524. <https://doi.org/10.1038/srep17524>
- Fonville, N.C., Bates, D., Hastings, P.J., Hanawalt, P.C., and Rosenberg, S.M. (2010) Role of RecA and the SOS response in thymineless death in *Escherichia coli*. *PLoS*

- Genet* **6**: e1000865. <https://doi.org/10.1371/journal.pgen.1000865>
- Gaca, A.O., Colomer-Winter, C., and Lemos, J.A. (2015) Many means to a common end: the intricacies of (p)ppGpp metabolism and its control of bacterial homeostasis. *J Bacteriol* **197**: 1146–1156. <https://doi.org/10.1128/JB.02577-14>
- Gallant, J., Erlich, H., Hall, B., and Laffler, T. (1970) Analysis of the RC function. *Cold Spring Harb Symp Quant Biol* **35**: 397–405. <https://doi.org/10.1101/SQB.1970.035.01.051>
- Gentleman, R.C., Carey, V.J., Bates, D.M., Bolstad, B., Detting, M., Dudoit, S., *et al.* (2004) Bioconductor: open software development for computational biology and bioinformatics. *Genome Biol* **5**: R80. <https://doi.org/10.1186/gb-2004-5-10-r80>
- George, S., Larsson, G., and Enfors, S.-O. (1993) A scale-down two-compartment reactor with controlled substrate oscillations: metabolic response of *Saccharomyces cerevisiae*. *Bioprocess Eng* **9**: 249–257. <https://doi.org/10.1007/BF01061530>
- Gerdes, K., and Maisonneuve, E. (2012) Bacterial persistence and toxin-antitoxin loci. *Annu Rev Microbiol* **66**: 103–123. <https://doi.org/10.1146/annurev-micro-092611-150159>
- Gerding, M.A., Ogata, Y., Pecora, N.D., Niki, H., and de Boer, P.A.J. (2007) The trans-envelope Tol-Pal complex is part of the cell division machinery and required for proper outer-membrane invagination during cell constriction in *E. coli*. *Mol Microbiol* **63**: 1008–1025. <https://doi.org/10.1111/j.1365-2958.2006.05571.x>
- González Barrios, A.F., Zuo, R., Hashimoto, Y., Yang, L., Bentley, W.E., and Wood, T.K. (2006) Autoinducer 2 controls biofilm formation in *Escherichia coli* through a novel motility quorum-sensing regulator (MqsR, B3022). *J Bacteriol* **188**: 305–316. <https://doi.org/10.1128/JB.188.1.305-316.2006>
- Hardiman, T., Lemuth, K., Keller, M.A., Reuss, M., and Siemann-Herzberg, M. (2007) Topology of the global regulatory network of carbon limitation in *Escherichia coli*. *J Biotechnol* **132**: 359–374. <https://doi.org/10.1016/j.jbiotec.2007.08.029>
- Haringa, C., Deshmukh, A.T., Mudde, R.F., and Noorman, H.J. (2017) Euler-Lagrange analysis towards representative down-scaling of a 22 m³ aerobic *S. cerevisiae* fermentation. *Chem Eng Sci* **170**: 653–669. <https://doi.org/10.1016/j.ces.2017.01.014>
- Hauryluk, V., Atkinson, G.C., Murakami, K.S., Tenson, T., and Gerdes, K. (2015) Recent functional insights into the role of (p)ppGpp in bacterial physiology. *Nat Rev Microbiol* **13**: 298–309. <https://doi.org/10.1038/nrmicro3448>
- Hayashi, K., Morooka, N., Yamamoto, Y., Fujita, K., Isono, K., Choi, S., *et al.* (2006) Highly accurate genome sequences of *Escherichia coli* K-12 strains MG1655 and W3110. *Mol Syst Biol* **2**, 2006.007. <https://doi.org/10.1038/msb4100049>
- Hopkins, D.J., Betenbaugh, M.J., and Dhurjati, P. (1987) Effects of dissolved oxygen shock on the stability of recombinant *Escherichia coli* containing plasmid pKN401. *Biotechnol Bioeng* **29**: 85–91. <https://doi.org/10.1002/bit.260290113>
- Hua, Q., Yang, C., Oshima, T., Mori, H., and Shimizu, K. (2004) Analysis of gene expression in *Escherichia coli* in response to changes of growth-limiting nutrient in chemostat cultures. *Appl Environ Microbiol* **70**: 2354–2366. <https://doi.org/10.1128/AEM.70.4.2354-2366.2004>
- Huisman, O., D'Ari, R., and Gottesman, S. (1984) Cell-division control in *Escherichia coli*: specific induction of the SOS function SfiA protein is sufficient to block septation. *Proc Natl Acad Sci USA* **81**: 4490–4494. <https://doi.org/10.1073/pnas.81.14.4490>
- Jarmander, J., Belotserkovsky, J., Sjöberg, G., Guevara-Martínez, M., Pérez-Zabaleta, M., Quillaguamán, J., and Larsson, G. (2015) Cultivation strategies for production of (R)-3-hydroxybutyric acid from simultaneous consumption of glucose, xylose and arabinose by *Escherichia coli*. *Microb Cell Fact* **14**: 51. <https://doi.org/10.1186/s12934-015-0236-2>
- Jishage, M., Iwata, A., Ueda, S., and Ishihama, A. (1996) Regulation of RNA polymerase sigma subunit synthesis in *Escherichia coli*: intracellular levels of four species of sigma subunit under various growth conditions. *J Bacteriol* **178**: 5447–5451. <https://doi.org/10.1128/jb.178.18.5447-5451.1996>
- Johansson, J., Balsalobre, C., Wang, S.-Y., Urbonaviciene, J., Jin, D.J., Sondén, B., and Uhlin, B.E. (2000) Nucleoid proteins stimulate stringently controlled bacterial promoters. *Cell* **102**: 475–485. [https://doi.org/10.1016/S0092-8674\(00\)00052-0](https://doi.org/10.1016/S0092-8674(00)00052-0)
- de Jonge, L.P., Buijs, N.A.A., ten Pierick, A., Deshmukh, A., Zhao, Z., Kiel, J.A.K.W., *et al.* (2011) Scale-down of penicillin production in *Penicillium chrysogenum*. *Biotechnol J* **6**: 944–958. <https://doi.org/10.1002/biot.201000409>
- Joseleau-Petit, D., Vinella, D., and D'Ari, R. (1999) Metabolic alarms and cell division in *Escherichia coli*. *J Bacteriol* **181**: 9–14. <https://doi.org/10.1128/JB.181.1.9-14.1999>
- Junker, B.H. (2004) Scale-up methodologies for *Escherichia coli* and yeast fermentation processes. *J Biosci Bioeng* **97**: 347–364. [https://doi.org/10.1016/S1389-1723\(04\)70218-2](https://doi.org/10.1016/S1389-1723(04)70218-2)
- Junne, S., Klingner, A., Kabisch, J., Schweder, T., and Neubauer, P. (2011) A two-compartment bioreactor system made of commercial parts for bioprocess scale-down studies: impact of oscillations on *Bacillus subtilis* fed-batch cultivations. *Biotechnol J* **6**: 1009–1017. <https://doi.org/10.1002/biot.201100293>
- Kanjee, U., Gutsche, I., Alexopoulos, E., Zhao, B., El Bakouri, M., Thibault, G., *et al.* (2011) Linkage between the bacterial acid stress and stringent responses: the structure of the inducible lysine decarboxylase. *EMBO J* **30**: 931–944. <https://doi.org/10.1038/emboj.2011.5>
- Kanjee, U., Ogata, K., and Houry, W.A. (2012) Direct binding targets of the stringent response alarmone (p)ppGpp. *Mol Microbiol* **85**: 1029–1043. <https://doi.org/10.1111/j.1365-2958.2012.08177.x>
- Kelly, W.J. (2008) Using computational fluid dynamics to characterize and improve bioreactor performance. *Biotechnol Appl Biochem* **49(Pt 4)**: 225–238. <https://doi.org/10.1042/BA20070177>
- Korch, S.B., Malhotra, V., Contreras, H., and Clark-Curtiss, J.E. (2015) The *Mycobacterium tuberculosis* relBE toxin: antitoxin genes are stress-responsive modules that

- regulate growth through translation inhibition. *J Microbiol (Seoul, Korea)* **53(11)**: 783–795. <https://doi.org/10.1007/s12275-015-5333-8>
- Langmead, B., and Salzberg, S.L. (2012) Fast gapped-read alignment with Bowtie 2. *Nat Methods* **9**: 357–359. <https://doi.org/10.1038/nmeth.1923>
- Lapin, A., Schmid, J., and Reuss, M. (2006) Modeling the dynamics of *E. coli* populations in the three-dimensional turbulent field of a stirred-tank bioreactor—A structured—segregated approach. *Chem Eng Sci* **61**:4783–4797. <https://doi.org/10.1016/j.ces.2006.03.003>
- Lara, A.R., Galindo, E., Ramírez, O.T., and Palomares, L.A. (2006) Living with heterogeneities in bioreactors: understanding the effects of environmental gradients on cells. *Mol Biotechnol* **34**: 355–382. <https://doi.org/10.1385/MB:34:3:355>
- Lara, A.R., Taymaz-Nikerel, H., Mashego, M.R., van Gulik, W.M., Heijnen, J.J., Ramírez, O.T., and van Winden, W.A. (2009) Fast dynamic response of the fermentative metabolism of *Escherichia coli* to aerobic and anaerobic glucose pulses. *Biotechnol Bioeng* **104**: 1153–1161. <https://doi.org/10.1002/bit.22503>
- Larsson, G., and Enfors, S.-O. (1988) Studies of insufficient mixing in bioreactors: effects of limiting oxygen concentrations and short term oxygen starvation on *Penicillium chrysogenum*. *Bioprocess Eng* **3**: 123–127. <https://doi.org/10.1007/BF00373475>
- Larsson, G., Trnkvist, M., Wernersson, E.S., Trgrdh, C., Noorman, H., and Enfors, S.-O. (1996) Substrate gradients in bioreactors: origin and consequences. *Bioprocess Eng* **14**: 281–289. <https://doi.org/10.1007/BF00369471>
- Lee, S., Kim, M.H., Kang, B.S., Kim, J.-S., Kim, G.-H., Kim, Y.-G., and Kim, K.J. (2008) Crystal structure of *Escherichia coli* MazG, the regulator of nutritional stress response. *J Biol Chem* **283**: 15232–15240. <https://doi.org/10.1074/jbc.M800479200>
- Löffler, M., Simen, J.D., Jäger, G., Schäferhoff, K., Freund, A., and Takors, R. (2016) Engineering *E. coli* for large-scale production - Strategies considering ATP expenses and transcriptional responses. *Metab Eng* **38**: 73–85. <https://doi.org/10.1016/j.ymben.2016.06.008>
- Love, M.I., Huber, W., and Anders, S. (2014) Moderated estimation of fold change and dispersion for RNA-seq data with DESeq2. *Genome Biol* **15**: 550. <https://doi.org/10.1186/s13059-014-0550-8>
- Luo, W., Friedman, M.S., Shedden, K., Hankenson, K.D., and Woolf, P.J. (2009) GAGE: generally applicable gene set enrichment for pathway analysis. *BMC Bioinform* **10**: 161. <https://doi.org/10.1186/1471-2105-10-161>
- Magnusson, L.U., Farewell, A., and Nyström, T. (2005) ppGpp: a global regulator in *Escherichia coli*. *Trends Microbiol* **13**: 236–242. <https://doi.org/10.1016/j.tim.2005.03.008>
- Michalowski, A., Siemann-Herzberg, M., and Takors, R. (2017) *Escherichia coli* HGT: engineered for high glucose throughput even under slowly growing or resting conditions. *Metab Eng* **40**: 93–103. <https://doi.org/10.1016/j.ymben.2017.01.005>
- Mueller, E.J., Oh, S., Kavalerchik, E., Kappock, T.J., Meyer, E., Li, C., et al. (1999) Investigation of the ATP binding site of *Escherichia coli* aminoimidazole ribonucleotide synthetase using affinity labeling and site-directed mutagenesis. *Biochemistry* **38**: 9831–9839. <https://doi.org/10.1021/bi990638r>
- Murray, K.D., and Bremer, H. (1996) Control of spoT-dependent ppGpp synthesis and degradation in *Escherichia coli*. *J Mol Biol* **259**: 41–57.
- Neubauer, P., Åhman, M., Törnkqvist, M., Larsson, G., and Enfors, S.-O. (1995a) Response of guanosine tetraphosphate to glucose fluctuations in fed-batch cultivations of *Escherichia coli*. *J Biotechnol* **43**: 195–204. [https://doi.org/10.1016/0168-1656\(95\)00130-1](https://doi.org/10.1016/0168-1656(95)00130-1)
- Neubauer, P., Häggström, L., and Enfors, S.O. (1995b) Influence of substrate oscillations on acetate formation and growth yield in *Escherichia coli* glucose limited fed-batch cultivations. *Biotechnol Bioeng* **47**: 139–146. <https://doi.org/10.1002/bit.260470204>
- Neubauer, P., and Junne, S. (2010) Scale-down simulators for metabolic analysis of large-scale bioprocesses. *Curr Opin Biotechnol* **21**: 114–121. <https://doi.org/10.1016/j.copbio.2010.02.001>
- Noguchi, Y., Nakai, Y., Shimba, N., Toyosaki, H., Kawahara, Y., Sugimoto, S., and Suzuki, E.-I. (2004) The energetic conversion competence of *Escherichia coli* during aerobic respiration studied by ³¹P NMR using a circulating fermentation system. *J Biochem* **136**: 509–515. <https://doi.org/10.1093/jb/mvh147>
- Noorman, H. (2011) An industrial perspective on bioreactor scale-down: what we can learn from combined large-scale bioprocess and model fluid studies. *Biotechnol J* **6**: 934–943. <https://doi.org/10.1002/biot.201000406>
- Oliveira-Filho, E.R., Silva, J.G.P., de Macedo, M.A., Taciro, M.K., Gomez, J.G.C., and Silva, L.F. (2019) Investigating nutrient limitation role on improvement of growth and Poly (3-Hydroxybutyrate) accumulation by *Burkholderia sacchari* LMG 19450 from xylose as the sole carbon source. *Front Bioeng Biotechnol* **7**: 416. <https://doi.org/10.3389/fbioe.2019.00416>
- Perez-Zabaleta, M., Sjöberg, G., Guevara-Martínez, M., Jarmander, J., Gustavsson, M., Quillaguamán, J., and Larsson, G. (2016) Increasing the production of (R)-3-hydroxybutyrate in recombinant *Escherichia coli* by improved cofactor supply. *Microb Cell Fact* **15**: 91. <https://doi.org/10.1186/s12934-016-0490-y>
- Reitzer, L. (2003) Nitrogen assimilation and global regulation in *Escherichia coli*. *Annu Rev Microbiol* **57**: 155–176. <https://doi.org/10.1146/annurev.micro.57.030502.090820>
- Santos-Zavaleta, A., Salgado, H., Gama-Castro, S., Sánchez-Pérez, M., Gómez-Romero, L., Ledezma-Tejeda, D., et al. (2019) RegulonDB v 10.5: tackling challenges to unify classic and high throughput knowledge of gene regulation in *E. coli* K-12. *Nucleic Acids Res* **47**: D212–D220. <https://doi.org/10.1093/nar/gky1077>
- Simen, J.D., Löffler, M., Jäger, G., Schäferhoff, K., Freund, A., Matthes, J., et al. (2017) Transcriptional response of *Escherichia coli* to ammonia and glucose fluctuations. *Microb Biotechnol* **10**: 858–872. <https://doi.org/10.1111/1751-7915.12713>
- Sun, C., Guo, Y., Tang, K., Wen, Z., Li, B., Zeng, Z., and Wang, X. (2017) MqsR/MqsA toxin/antitoxin system regulates persistence and biofilm formation in *Pseudomonas*

- putida* KT2440. *Front Microbiol* **8**: 840. <https://doi.org/10.3389/fmicb.2017.00840>
- Szenk, M., Dill, K.A., and de Graff, A.M.R. (2017) Why do fast-growing bacteria enter overflow metabolism? Testing the membrane real estate hypothesis. *Cell systems* **5**: 95–104. <https://doi.org/10.1016/j.cels.2017.06.005>
- Takors, R. (2012) Scale-up of microbial processes: impacts, tools and open questions. *J Biotechnol* **160**: 3–9. <https://doi.org/10.1016/j.jbiotec.2011.12.010>
- Tatusov, R.L., Fedorova, N.D., Jackson, J.D., Jacobs, A.R., Kiryutin, B., Koonin, E.V., *et al.* (2003) The COG database: an updated version includes eukaryotes. *BMC Bioinform* **4**: 41. <https://doi.org/10.1186/1471-2105-4-41>
- Traxler, M.F., Summers, S.M., Nguyen, H.-T., Zacharia, V.M., Hightower, G.A., Smith, J.T., and Conway, T. (2008) The global, ppGpp-mediated stringent response to amino acid starvation in *Escherichia coli*. *Mol Microbiol* **68**: 1128–1148. <https://doi.org/10.1111/j.1365-2958.2008.06229.x>
- Traxler, M.F., Zacharia, V.M., Marquardt, S., Summers, S.M., Nguyen, H.-T., Stark, S.E., and Conway, T. (2011) Discretely calibrated regulatory loops controlled by ppGpp partition gene induction across the 'feast to famine' gradient in *Escherichia coli*. *Mol Microbiol* **79**: 830–845. <https://doi.org/10.1111/j.1365-2958.2010.07498.x>
- Vasilakou, E., van Loosdrecht, M.C.M., and Wahl, S.A. (2020) *Escherichia coli* metabolism under short-term repetitive substrate dynamics: adaptation and trade-offs. *Microb Cell Fact* **19**: 116. <https://doi.org/10.1186/s12934-020-01379-0>
- Vrábel, P., van der Lans, R.G., Luyben, K.C., Boon, L., and Nienow, A.W. (2000) Mixing in large-scale vessels stirred with multiple radial or radial and axial up-pumping impellers: modelling and measurements. *Chem Eng Sci* **55**: 5881–5896. [https://doi.org/10.1016/S0009-2509\(00\)00175-5](https://doi.org/10.1016/S0009-2509(00)00175-5)
- Wang, J.D., and Levin, P.A. (2009) Metabolism, cell growth and the bacterial cell cycle. *Nat Rev Microbiol* **7**: 822–827. <https://doi.org/10.1038/nrmicro2202>
- Wang, Q., Yu, H., Xia, Y., Kang, Z., and Qi, Q. (2009) Complete PHB mobilization in *Escherichia coli* enhances the stress tolerance: a potential biotechnological application. *Microb Cell Fact* **8**: 47. <https://doi.org/10.1186/1475-2859-8-47>
- Wen, Q., Chen, Z., Tian, T., and Chen, W. (2010) Effects of phosphorus and nitrogen limitation on PHA production in activated sludge. *J Environ Sci* **22**: 1602–1607. [https://doi.org/10.1016/S1001-0742\(09\)60295-3](https://doi.org/10.1016/S1001-0742(09)60295-3)
- Williamson, G., Tamburrino, G., Bizior, A., Boeckstaens, M., Dias Mirandela, G., Bage, M., *et al.* (2020) A two-lane mechanism for selective biological ammonium transport. *eLife* **9**: <https://doi.org/10.7554/eLife.57183>
- Xi, H., Schneider, B.L., and Reitzer, L. (2000) Purine catabolism in *Escherichia coli* and function of xanthine dehydrogenase in purine salvage. *J Bacteriol* **182**: 5332–5341. <https://doi.org/10.1128/JB.182.19.5332-5341.2000>

Supporting information

Additional supporting information may be found online in the Supporting Information section at the end of the article.

Table S1. Long term changes STR 5min vs STR 0h.

Table S2. Long term changes STR 28h vs STR 0h.

Table S3. Short term changes PFR28h vs STR28h.

Table S4. Short term changes PFR5min vs STR5min.

Appendix S1. Supplementary Information.

Table S1: Long term changes STR 5min vs STR 0h

DOWN WT	UP WT	UP SR	DOWN SR
argT cbl	argF argI caiF	cspA gatA	argT asnB cbl
copA cueO	carB gatA	gatB mdtJ	csiD cueO
ddpA ddpB	gatB gatD	zntA	dapB ddpA
ddpC ddpD	gatZ mglA		ddpB ddpC
ddpF ddpX	ptsG sbp		ddpD ddpF
glnA glnG	zntA		ddpX gdhA
glnH glnK			glnA glnG
glnL mepM			glnK glnL lysC
nac pheL			mepM mgtA
pliG yhdX			nac pliG
ykgL ykgM			pmrD psiE
ykgO yodB			rutA rutB
zinT znuA			trpL yhdY
znuC			ykgM ykgO
			yneM ynfM
			zinT znuA
			znuC

Table S2: Long term changes STR 28h vs STR 0h

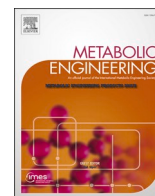
DOWN WT	UP WT	UP SR	DOWN SR
cbl cycA	serA yhjE	asnA gatA	cycA guaD
ddpA ddpB		gatB gltB	ibpB rcsA tisB
ddpC ddpD		serA yhjE yjiY	wcaD wcaE
ddpX feaR			wcaF wza
nac ydcS			ydcS ydcT
ydcT ydcV			ydcV ygiL
ynfM			yjbE

Table S3: Short term changes PFR28h vs STR28h

DOWN WT	UP WT	UP SR	DOWN SR
accC adeP adk aldA	amtB argT	amtB argT	adeP amn ampG
ampG apt argA argC	asnA asnB	aroH aroL	argC argF aroA artJ
argD argF argI aroA	astA astB	asnA astA	astE bcp bcsG beta
artJ artM asnS atpB	astC astD	astC bamC	carA chaA chbR
atpE atpF atpH borD	bhsA bolA	bamE bhsA	codB csgE csgF csiD
carA codB csgF cysC	bsmA bssR	blr bsmA	cysC cysD cysJ cysK
cysD cysI cysJ cysK	bssS cbl	chaC cnu	cysP cysU cysW
cysP cysU cysW dppB	chaC csiD	cohE cpxP	dapB dctR ddpB
dusB efeO efp epmC	csrA cydA	crp ddpX	ddpC ddpD dosC
evgS fhuD fimC fimD	cydX cysQ	dnaT dut	dppB dusB envZ
fis flhD folC folD folK	ddpA ddpX	endA fabA	evgS fecC fimD flhC
fruB fusA gatA gatB	dps fdhF fic	fdhF ftnB fur	folK gadW gdhA
gatY gatZ ghrB ghxP	glgS glnA	glcC glmU	glgB glnL glrR glyA
glnB glyA gpt gsiD gsk	glnG glnH	glnH glnK	groS gsiA gsiB gsiD
gtrB gtrS guaB guaC	glnK glnL	glnP glnQ	gspC gtrS hisF hisI
hflD hsdS ilvC infA	glnP glnQ	glpA greB	hsdS ilvB ilvC ilvX
ispA ispE lpxH lpxT	hisJ hspQ	guaC higA	katE leuA leuB lhgO

Table S4: Short term changes PFR5min vs STR5min

DOWN WT	UP WT	UP SR	DOWN SR
aceE adeP	asnA asnB	aroH asnA	argC argF
adk ampG	astA astB	asnB astA	csgE cysU
ansA apt	astC astD	astC bameE	dctA evgS
argA argB	bhsA blc bolA	bhsA chaC	folK groS
argC argD	bssR bssS cbl	crp csiD	hsdS maa
argF argG	chaC clpA	cydA cydB	mcrB mcrC
argI argR artJ	csiD cutC	ddpX fdhF	metA metB
artM artQ	cysQ ddpA	glnA glnH	metF metI
asnS atpA	ddpB ddpX	glnK glnP	metN metR
atpB atpE	dkgA dps	glnQ guaC	mmuP nagC
atpF atpH	dtpB fdhF	hycA hypA	opgC rbsA
atpI borD	gabD gcd gcl	hypB insH1	recG rpsU
caiF carA	glgA glgP glgS	iraP mazF	sdhC sdhD
carB codA	glnA glnG	mtr nac	tnaC udk
codB cvpA	glnH glnK	patA proP	waaL ybdL
cyoA cyoB	glnL glnP	prpB psiE	ybgA yciW
cysC cysD	glnQ glpD	rlmD rpoH	ydiH ydjO



Engineering of a robust *Escherichia coli* chassis and exploitation for large-scale production processes

Martin Ziegler, Julia Zieringer, Clarissa-Laura Döring, Liv Paul, Christoph Schaal, Ralf Takors*

University of Stuttgart - Institute of Biochemical Engineering, Allmandring 31, 70569, Stuttgart, Germany

ARTICLE INFO

Keywords:

Large-scale
Fermentation
E. coli
Protein production
Deletions
Heterogeneities

ABSTRACT

In large-scale bioprocesses microbes are exposed to heterogeneous substrate availability reducing the overall process performance. A series of deletion strains was constructed from *E. coli* MG1655 aiming for a robust phenotype in heterogeneous fermentations with transient starvation. Deletion targets were hand-picked based on a list of genes derived from previous large-scale simulation runs. Each gene deletion was conducted on the premise of strict neutrality towards growth parameters in glucose minimal medium. The final strain of the series, named *E. coli* RM214, was cultivated continuously in an STR-PFR (stirred tank reactor – plug flow reactor) scale-down reactor. The scale-down reactor system simulated repeated passages through a glucose starvation zone. When exposed to nutrient gradients, *E. coli* RM214 had a significantly lower maintenance coefficient than *E. coli* MG1655 ($\Delta m_s = 0.038 \text{ g}_{\text{Glucose}}/\text{g}_{\text{CDW}}/\text{h}$, $p < 0.05$). In an exemplary protein production scenario *E. coli* RM214 remained significantly more productive than *E. coli* MG1655 reaching 44% higher eGFP yield after 28 h of STR-PFR cultivation. This study developed *E. coli* RM214 as a robust chassis strain and demonstrated the feasibility of engineering microbial hosts for large-scale applications.

1. Introduction

Large-scale fed-batch bioprocesses often suffer from reduced process performance compared to lab-scale experiments conducted during process development (Bylund et al., 2000; Enfors et al., 2001). The physical and engineering constraints in large-scale reactors inevitably lead to the formation of spatial heterogeneities of relevant process parameters such as nutrient availability, concentrations of dissolved oxygen, carbon dioxide, and pH (Bylund et al., 1998; Cortés et al., 2016). Heterogeneities of nutrient availability are caused by long mixing times of large-scale reactors (Delvigne et al., 2006; Noorman, 2011). Studies employing computational fluid dynamics (CFD) have revealed that in fed-batch processes this typically results in the formation of zones with high nutrient concentrations close to the feeding point and zones depleted of nutrients at the far end of the reactor (Haringa et al., 2017; Kuschel and Takors, 2020). Depending on the mixing time and their position in the reactor cells frequently move through different zones on a timescale of seconds to minutes and cellular regulatory programs ranging from overflow metabolism to starvation responses are repeatedly triggered

and shut down (Kuschel et al., 2017). Due to the delay of transcriptional responses, regulatory consequences of stress stimuli may be effective distant from the spot of stress induction which finally creates a heterogeneous population status (Nieß et al., 2017; Zieringer et al., 2020). There is evidence from an increasing number of studies that the performance of many industrial workhorse organisms such as *Escherichia coli*, *Bacillus subtilis*, *Corynebacterium glutamicum*, *Saccharomyces cerevisiae* and *Penicillium chrysogenum* is negatively affected when facing process heterogeneities (George et al., 1993; Jonge et al., 2011; Junne et al., 2011; Larsson and Enfors, 1988; Olughu et al., 2020; Vasilakou et al., 2020).

Substantial effort has been made by the scientific community to understand microbial responses to the different zones occurring in large-scale reactors (Lara et al., 2006a, 2006b; Löffler et al., 2016; Olughu et al., 2019). In academic laboratories, the conditions of industrial reactors are commonly simulated using multi-compartment scale-down reactors (Delvigne et al., 2017; Neubauer and Junne, 2010; Takors, 2012). Typically, nutrient pulsing or secondary vessels are employed to deliver a stimulus representative for the conditions under investigation

* Corresponding author. University of Stuttgart - Institute of Biochemical Engineering, Allmandring 31, 70569, Stuttgart, Germany.

E-mail addresses: martin.ziegler@ibvt.uni-stuttgart.de (M. Ziegler), julia.zieringer@ibvt.uni-stuttgart.de (J. Zieringer), clarissa-laura.doering@uniklinik-freiburg.de (C.-L. Döring), liv.paul@gmx.de (L. Paul), christoph.schaal@ibvt.uni-stuttgart.de (C. Schaal), takors@ibvt.uni-stuttgart.de, ralf.takors@ibvt.uni-stuttgart.de (R. Takors).

<https://doi.org/10.1016/j.ymben.2021.05.011>

Received 8 December 2020; Received in revised form 30 May 2021; Accepted 31 May 2021

Available online 4 June 2021

1096-7176/© 2021 International Metabolic Engineering Society. Published by Elsevier Inc. All rights reserved.

(Bylund et al., 1999). The design of a scale-down reactor also serves to control the circulation of the microbial population and its residence time in stimulus zones. A commonly used design follows the two-compartment approach comprising a primary stirred tank reactor (STR) coupled to a secondary plug-flow reactor (PFR). While the STR represents the bulk of the fermentation broth, the plug-flow compartment represents a stimulus zone with a defined residence time. Together, the STR-PFR two-compartment reactor enables the study of cellular behavior in heterogeneous environments.

Zones with low nutrient concentration but high oxygen availability occur in reactor segments far away from the feeding point. The effects of such transient starvation conditions on the performance and intracellular regulation of microbial populations can be studied in C-limited scale-down reactors. In the case of *Escherichia coli* K-12 repeated passages of cells through starvation zones were found to negatively impact process performance which could be observed as a reduced biomass yield (Neubauer et al., 1995b). In parallel, regulatory responses such as the stringent response and the general stress response are rapidly initiated (Delvigne et al., 2009; Löffler et al., 2016; Neubauer et al., 1995a; Simen et al., 2017; Sunya et al., 2012). Noteworthy, these cellular responses serve rather long-term than short-term needs and appear to be futile if cells enter zones of nutrient access shortly after the induction of the strategic precaution measure. Transcriptional investigations in a carbon-limited STR-PFR system offered a potential link between futile regulation and reduced process performance: Frequent transcriptional reprogramming was proposed to cause high secondary metabolic costs from aberrant transcription and translation (Löffler et al., 2016). It was estimated that an increased maintenance of up to 30–40% was caused by the transcriptional oscillations and a substantial fraction of this originated from the expression of open reading frames whose products appeared to bestow no apparent benefit in a controlled bioprocess employing standard glucose minimal medium.

The data collected by Löffler et al. (2016) led us to propose a novel design approach for production strains: We reasoned that an intelligently engineered deletion strain might have advantages in conditions that repeatedly induce wasteful expression of process-irrelevant genes. A heterogeneous fermentation with repeated transient starvation could then be a suitable testing environment. The choice of deletion targets would have to be based on the estimated effect of the deletion and be restricted by the requirements of neutrality towards growth and global regulation. The design process differs from previous considerations on the creation of lean-proteome strains in the regard that savings only become apparent due to fluctuating induction (Valgepea et al., 2015). Secondary metabolic costs can traditionally be assessed through Pirt's maintenance coefficient (Pirt, 1965). We hypothesized that the deletion of a suitable set of genes should lead to a reduced maintenance coefficient under scale-down conditions representing starvation zones. The resulting strain could then serve as a base strain for the construction of robust production strains.

We identified deletion candidates matching the defined criteria and constructed a series of deletion strains from *E. coli* MG1655. The final strain of the series, named *E. coli* RM214, was fermented in continuous cultivations in an STR-PFR system simulating starvation zones. *E. coli* RM214 had a significantly lower maintenance coefficient than *E. coli* MG1655 under simulated large-scale conditions. We then characterized *E. coli* RM214 in an exemplary protein production scenario using eGFP as a model product. Compared to *E. coli* MG1655, the deletion strain showed an increased resilience towards the scale-down conditions as evidenced by reduced productivity losses and a higher fraction of producing cells.

2. Materials and methods

2.1. Bacterial strains, media, and buffer solutions

All strains used in this study are listed in Table 1.

Table 1
Bacterial Strains used in this study.

Strain	Genotype/Strain Information	Reference/Source
<i>Escherichia coli</i> K-12 MG1655	F ⁻ , λ ⁻ , <i>ilvG</i> ⁻ , <i>rfb</i> -50, <i>rph</i> -1 ("wild type" strain, abbrev. WT)	Michalowski et al., (2017)
<i>Escherichia coli</i> DH5α λpir	<i>supE44</i> , Δ <i>lacU169</i> (Φ80 <i>lacZ</i> Δ <i>M15</i>), <i>recA1</i> , <i>endA1</i> , <i>hsdR17</i> , <i>thi</i> -1, <i>gyrA96</i> , <i>relA1</i> , λpir phage lysogen	Michalowski et al., (2017)
<i>Escherichia coli</i> DH10B pSIM5	F ⁻ <i>mcrA</i> Δ(<i>mrr</i> - <i>hsdRMS</i> - <i>mcrBC</i>) φ80 <i>lacZ</i> Δ <i>M15</i> Δ <i>lacX74</i> <i>recA1</i> <i>endA1</i> <i>araD139</i> Δ(<i>ara-leu</i>)7697 <i>galU</i> <i>galK</i> λ ⁻ <i>rpsL</i> (Str ^R) <i>nupG</i>	Datta et al., (2006)
T-SACK	W3110 <i>araD</i> <> <i>tetA</i> - <i>sacB</i> - <i>amp</i> <i>fliC</i> <> <i>cat</i> <i>argG</i> :: <i>Tn5</i>	Li et al., (2013)
<i>Escherichia coli</i> CD101	MG1655 Δ <i>fliC</i>	This study
<i>Escherichia coli</i> CD201	MG1655 Δ <i>fliA</i> Δ <i>fliA</i>	This study
<i>Escherichia coli</i> CD202	MG1655 Δ <i>fliK</i> Δ <i>fliA</i> Δ <i>fliC</i>	This study
<i>Escherichia coli</i> CD203	MG1655 Δ <i>fliK</i> Δ <i>fliA</i> Δ <i>fliC</i> Δ <i>fliG</i> Δ <i>fliH</i> Δ <i>fliJ</i> Δ <i>fliK</i> Δ <i>fliL</i> Δ <i>fliM</i> Δ <i>fliN</i> Δ <i>fliO</i> Δ <i>fliP</i> Δ <i>fliQ</i> Δ <i>fliR</i> Δ <i>fliS</i> Δ <i>fliT</i> Δ <i>fliU</i> Δ <i>fliV</i> Δ <i>fliW</i> Δ <i>fliX</i> Δ <i>fliY</i> Δ <i>fliZ</i>	This study
<i>Escherichia coli</i> CD204	MG1655 Δ <i>fliK</i> Δ <i>fliA</i> Δ <i>fliC</i> Δ <i>fliG</i> Δ <i>fliH</i> Δ <i>fliJ</i> Δ <i>fliK</i> Δ <i>fliL</i> Δ <i>fliM</i> Δ <i>fliN</i> Δ <i>fliO</i> Δ <i>fliP</i> Δ <i>fliQ</i> Δ <i>fliR</i> Δ <i>fliS</i> Δ <i>fliT</i> Δ <i>fliU</i> Δ <i>fliV</i> Δ <i>fliW</i> Δ <i>fliX</i> Δ <i>fliY</i> Δ <i>fliZ</i>	This study
<i>Escherichia coli</i> CD205	MG1655 Δ <i>fliK</i> Δ <i>fliA</i> Δ <i>fliC</i> Δ <i>fliG</i> Δ <i>fliH</i> Δ <i>fliJ</i> Δ <i>fliK</i> Δ <i>fliL</i> Δ <i>fliM</i> Δ <i>fliN</i> Δ <i>fliO</i> Δ <i>fliP</i> Δ <i>fliQ</i> Δ <i>fliR</i> Δ <i>fliS</i> Δ <i>fliT</i> Δ <i>fliU</i> Δ <i>fliV</i> Δ <i>fliW</i> Δ <i>fliX</i> Δ <i>fliY</i> Δ <i>fliZ</i>	This study
<i>Escherichia coli</i> RM206	MG1655 Δ <i>fliK</i> Δ <i>fliA</i> Δ <i>fliC</i> Δ <i>fliG</i> Δ <i>fliH</i> Δ <i>fliJ</i> Δ <i>fliK</i> Δ <i>fliL</i> Δ <i>fliM</i> Δ <i>fliN</i> Δ <i>fliO</i> Δ <i>fliP</i> Δ <i>fliQ</i> Δ <i>fliR</i> Δ <i>fliS</i> Δ <i>fliT</i> Δ <i>fliU</i> Δ <i>fliV</i> Δ <i>fliW</i> Δ <i>fliX</i> Δ <i>fliY</i> Δ <i>fliZ</i> Δ <i>fliE</i> Δ <i>fliF</i> Δ <i>fliG</i> Δ <i>fliH</i> Δ <i>fliI</i> Δ <i>fliJ</i> Δ <i>fliK</i> Δ <i>fliL</i> Δ <i>fliM</i> Δ <i>fliN</i> Δ <i>fliO</i> Δ <i>fliP</i> Δ <i>fliQ</i> Δ <i>fliR</i> Δ <i>fliS</i> Δ <i>fliT</i> Δ <i>fliU</i> Δ <i>fliV</i> Δ <i>fliW</i> Δ <i>fliX</i> Δ <i>fliY</i> Δ <i>fliZ</i>	This study
<i>Escherichia coli</i> RM207	MG1655 Δ <i>fliK</i> Δ <i>fliA</i> Δ <i>fliC</i> Δ <i>fliG</i> Δ <i>fliH</i> Δ <i>fliJ</i> Δ <i>fliK</i> Δ <i>fliL</i> Δ <i>fliM</i> Δ <i>fliN</i> Δ <i>fliO</i> Δ <i>fliP</i> Δ <i>fliQ</i> Δ <i>fliR</i> Δ <i>fliS</i> Δ <i>fliT</i> Δ <i>fliU</i> Δ <i>fliV</i> Δ <i>fliW</i> Δ <i>fliX</i> Δ <i>fliY</i> Δ <i>fliZ</i> Δ <i>fliE</i> Δ <i>fliF</i> Δ <i>fliG</i> Δ <i>fliH</i> Δ <i>fliI</i> Δ <i>fliJ</i> Δ <i>fliK</i> Δ <i>fliL</i> Δ <i>fliM</i> Δ <i>fliN</i> Δ <i>fliO</i> Δ <i>fliP</i> Δ <i>fliQ</i> Δ <i>fliR</i> Δ <i>fliS</i> Δ <i>fliT</i> Δ <i>fliU</i> Δ <i>fliV</i> Δ <i>fliW</i> Δ <i>fliX</i> Δ <i>fliY</i> Δ <i>fliZ</i> Δ <i>cspD</i>	This study
<i>Escherichia coli</i> RM208	MG1655 Δ <i>fliK</i> Δ <i>fliA</i> Δ <i>fliC</i> Δ <i>fliG</i> Δ <i>fliH</i> Δ <i>fliJ</i> Δ <i>fliK</i> Δ <i>fliL</i> Δ <i>fliM</i> Δ <i>fliN</i> Δ <i>fliO</i> Δ <i>fliP</i> Δ <i>fliQ</i> Δ <i>fliR</i> Δ <i>fliS</i> Δ <i>fliT</i> Δ <i>fliU</i> Δ <i>fliV</i> Δ <i>fliW</i> Δ <i>fliX</i> Δ <i>fliY</i> Δ <i>fliZ</i> Δ <i>fliE</i> Δ <i>fliF</i> Δ <i>fliG</i> Δ <i>fliH</i> Δ <i>fliI</i> Δ <i>fliJ</i> Δ <i>fliK</i> Δ <i>fliL</i> Δ <i>fliM</i> Δ <i>fliN</i> Δ <i>fliO</i> Δ <i>fliP</i> Δ <i>fliQ</i> Δ <i>fliR</i> Δ <i>fliS</i> Δ <i>fliT</i> Δ <i>fliU</i> Δ <i>fliV</i> Δ <i>fliW</i> Δ <i>fliX</i> Δ <i>fliY</i> Δ <i>fliZ</i> Δ <i>cspD</i> Δ <i>aldA</i> Δ <i>gatA</i> Δ <i>BCDR</i>	This study
<i>Escherichia coli</i> RM209	MG1655 Δ <i>fliK</i> Δ <i>fliA</i> Δ <i>fliC</i> Δ <i>fliG</i> Δ <i>fliH</i> Δ <i>fliJ</i> Δ <i>fliK</i> Δ <i>fliL</i> Δ <i>fliM</i> Δ <i>fliN</i> Δ <i>fliO</i> Δ <i>fliP</i> Δ <i>fliQ</i> Δ <i>fliR</i> Δ <i>fliS</i> Δ <i>fliT</i> Δ <i>fliU</i> Δ <i>fliV</i> Δ <i>fliW</i> Δ <i>fliX</i> Δ <i>fliY</i> Δ <i>fliZ</i> Δ <i>fliE</i> Δ <i>fliF</i> Δ <i>fliG</i> Δ <i>fliH</i> Δ <i>fliI</i> Δ <i>fliJ</i> Δ <i>fliK</i> Δ <i>fliL</i> Δ <i>fliM</i> Δ <i>fliN</i> Δ <i>fliO</i> Δ <i>fliP</i> Δ <i>fliQ</i> Δ <i>fliR</i> Δ <i>fliS</i> Δ <i>fliT</i> Δ <i>fliU</i> Δ <i>fliV</i> Δ <i>fliW</i> Δ <i>fliX</i> Δ <i>fliY</i> Δ <i>fliZ</i> Δ <i>cspD</i> Δ <i>aldA</i> Δ <i>gatA</i> Δ <i>BCDR</i> Δ <i>uhpT</i> Δ <i>CBA</i>	This study
<i>Escherichia coli</i> RM210	MG1655 Δ <i>fliK</i> Δ <i>fliA</i> Δ <i>fliC</i> Δ <i>fliG</i> Δ <i>fliH</i> Δ <i>fliJ</i> Δ <i>fliK</i> Δ <i>fliL</i> Δ <i>fliM</i> Δ <i>fliN</i> Δ <i>fliO</i> Δ <i>fliP</i> Δ <i>fliQ</i> Δ <i>fliR</i> Δ <i>fliS</i> Δ <i>fliT</i> Δ <i>fliU</i> Δ <i>fliV</i> Δ <i>fliW</i> Δ <i>fliX</i> Δ <i>fliY</i> Δ <i>fliZ</i> Δ <i>fliE</i> Δ <i>fliF</i> Δ <i>fliG</i> Δ <i>fliH</i> Δ <i>fliI</i> Δ <i>fliJ</i> Δ <i>fliK</i> Δ <i>fliL</i> Δ <i>fliM</i> Δ <i>fliN</i> Δ <i>fliO</i> Δ <i>fliP</i> Δ <i>fliQ</i> Δ <i>fliR</i> Δ <i>fliS</i> Δ <i>fliT</i> Δ <i>fliU</i> Δ <i>fliV</i> Δ <i>fliW</i> Δ <i>fliX</i> Δ <i>fliY</i> Δ <i>fliZ</i> Δ <i>cspD</i> Δ <i>aldA</i> Δ <i>gatA</i> Δ <i>BCDR</i> Δ <i>uhpT</i> Δ <i>CBA</i> Δ <i>yeeL</i>	This study
<i>Escherichia coli</i> RM214	MG1655 Δ <i>fliK</i> Δ <i>fliA</i> Δ <i>fliC</i> Δ <i>fliG</i> Δ <i>fliH</i> Δ <i>fliJ</i> Δ <i>fliK</i> Δ <i>fliL</i> Δ <i>fliM</i> Δ <i>fliN</i> Δ <i>fliO</i> Δ <i>fliP</i> Δ <i>fliQ</i> Δ <i>fliR</i> Δ <i>fliS</i> Δ <i>fliT</i> Δ <i>fliU</i> Δ <i>fliV</i> Δ <i>fliW</i> Δ <i>fliX</i> Δ <i>fliY</i> Δ <i>fliZ</i> Δ <i>fliE</i> Δ <i>fliF</i> Δ <i>fliG</i> Δ <i>fliH</i> Δ <i>fliI</i> Δ <i>fliJ</i> Δ <i>fliK</i> Δ <i>fliL</i> Δ <i>fliM</i> Δ <i>fliN</i> Δ <i>fliO</i> Δ <i>fliP</i> Δ <i>fliQ</i> Δ <i>fliR</i> Δ <i>fliS</i> Δ <i>fliT</i> Δ <i>fliU</i> Δ <i>fliV</i> Δ <i>fliW</i> Δ <i>fliX</i> Δ <i>fliY</i> Δ <i>fliZ</i> Δ <i>cspD</i> Δ <i>aldA</i> Δ <i>gatA</i> Δ <i>BCDR</i> Δ <i>uhpT</i> Δ <i>CBA</i> Δ <i>yeeL</i> Δ <i>fliA</i>	This study
<i>Escherichia coli</i> BW3110 pJOE4056.2	W3110 <i>rhaB</i> ⁻	Wegerer et al., (2008)
<i>Escherichia coli</i> DH5α λpir pJOE4056.2_tetA	<i>supE44</i> , Δ <i>lacU169</i> (Φ80 <i>lacZ</i> Δ <i>M15</i>), <i>recA1</i> , <i>endA1</i> , <i>hsdR17</i> , <i>thi</i> -1, <i>gyrA96</i> , <i>relA1</i> , λpir phage lysogen	This study
<i>Escherichia coli</i> K-12 MG1655 <i>rhaB</i> ⁻	F ⁻ , λ ⁻ , <i>ilvG</i> ⁻ , <i>rfb</i> -50, <i>rph</i> -1, <i>rhaB</i> ⁻	This study
<i>Escherichia coli</i> RM214 <i>rhaB</i> ⁻	MG1655 Δ <i>fliK</i> Δ <i>fliA</i> Δ <i>fliC</i> Δ <i>fliG</i> Δ <i>fliH</i> Δ <i>fliJ</i> Δ <i>fliK</i> Δ <i>fliL</i> Δ <i>fliM</i> Δ <i>fliN</i> Δ <i>fliO</i> Δ <i>fliP</i> Δ <i>fliQ</i> Δ <i>fliR</i> Δ <i>fliS</i> Δ <i>fliT</i> Δ <i>fliU</i> Δ <i>fliV</i> Δ <i>fliW</i> Δ <i>fliX</i> Δ <i>fliY</i> Δ <i>fliZ</i> Δ <i>fliE</i> Δ <i>fliF</i> Δ <i>fliG</i> Δ <i>fliH</i> Δ <i>fliI</i> Δ <i>fliJ</i> Δ <i>fliK</i> Δ <i>fliL</i> Δ <i>fliM</i> Δ <i>fliN</i> Δ <i>fliO</i> Δ <i>fliP</i> Δ <i>fliQ</i> Δ <i>fliR</i> Δ <i>fliS</i> Δ <i>fliT</i> Δ <i>fliU</i> Δ <i>fliV</i> Δ <i>fliW</i> Δ <i>fliX</i> Δ <i>fliY</i> Δ <i>fliZ</i> Δ <i>cspD</i> Δ <i>aldA</i> Δ <i>gatA</i> Δ <i>BCDR</i> Δ <i>uhpT</i> Δ <i>yeeL</i> Δ <i>fliA</i> <i>rhaB</i> ⁻	This study

(continued on next page)

Table 1 (continued)

Strain	Genotype/Strain Information	Reference/ Source
<i>Escherichia coli</i> K-12 MG1655 rhaB ⁻ pJOE4056.2_tetA	F ⁻ , λ ⁻ , <i>ilvG</i> ⁻ , <i>rfb</i> -50, <i>rph</i> -1, <i>rhaB</i> ⁻	This study
<i>Escherichia coli</i> RM214 rhaB ⁻ pJOE4056.2_tetA	MG1655 Δ <i>flk</i> Δ <i>fljA</i> Δ <i>fljC</i> Δ <i>flg</i> NMABCDEFGHIJKL Δ <i>flj</i> EFGHIJKLMNOPQR Δ <i>flh</i> EABcheZYBRtaptarcheWAmotBA Δ <i>cspD</i> Δ <i>aldA</i> Δ <i>gat</i> ABCD R Δ <i>uhpT</i> Δ <i>yeel</i> Δ <i>flxA</i> rhaB	This study

2xYT medium was prepared by autoclaving 16 g/l tryptone, 10 g/l yeast extract, 5 g/l NaCl dissolved in demineralized water. For agar plates 18 g/l agar-agar was added prior to autoclaving. For pH indicator plates 0.03 g/l of neutral red and 10 g/l Rhamnose were supplemented from sterile stock solutions directly before pouring. SOC medium was prepared as described previously (Hanahan, 1983). Agar plates for *tetA-sacB* counterselection were prepared as described previously (Li et al., 2013). If strains with antibiotic resistance markers were cultivated, antibiotics were added to media after autoclaving in the following concentrations: Chloramphenicol 20 µg/ml, Tetracycline hydrochloride 10 µg/ml, disodium Carbenicillin 100 µg/ml.

Minimal media for shaking flask experiments and the precultures for bioreactor experiments consisted of 4 g/l glucose, 3.2 g/l NaH₂PO₄·2H₂O, 11.7 g/l K₂HPO₄, 8 g/l (NH₄)₂SO₄, 0.01 g/l thiamine hydrochloride and 0.2% (V/V) trace elements stock solution. Minimal media for batch cultivation in the bioreactor consisted of 13.4 g/l glucose, 1 g/l NaH₂PO₄·2H₂O, 2.6 g/l K₂HPO₄, 9 g/l (NH₄)₂SO₄ and 0.2% (V/V) trace elements stock solution. In the experiments with strains carrying pJOE4056.2_tetA for GFP production 10 µg/ml Tetracycline hydrochloride and 1 g/l Rhamnose were supplemented. Towards the end of the batch phase about 100 µl of antifoaming agent Struktol J647 was added to prevent foaming upon glucose depletion. Minimal media for continuous chemostat cultivation in the bioreactor consisted of 13.14 g/l glucose, 1 g/l NaH₂PO₄·2H₂O, 2.6 g/l K₂HPO₄, 9 g/l (NH₄)₂SO₄ and 0.2% (V/V) trace elements stock solution. In the experiments with strains carrying pJOE4056.2_tetA for GFP production 10 µg/ml Tetracycline hydrochloride and 1 g/l Rhamnose were supplemented. Throughout the chemostat phase 50 µl/h of antifoaming agent Struktol J647 were added continuously to the fermentation medium.

The composition of trace element stock solution was 4.175 g/l FeCl₃·6H₂O, 0.045 g/l ZnSO₄·7H₂O, 0.025 g/l MnSO₄·H₂O, 0.4 g/l CuSO₄·5H₂O, 0.045 g/l CoCl₂·6H₂O, 2.2 g/l CaCl₂·2H₂O, 50 g/l MgSO₄·7H₂O and 55 g/l sodium citrate dihydrate. Stock solutions of salts, trace elements and sugars were autoclaved separately, and stock solutions of thiamine hydrochloride and the antibiotics were filter sterilized and stored at 4 °C. All compounds were combined just before the experiments to prevent potential aging of media.

PBS-MgCa for the measurement of eGFP fluorescence and flow cytometry analysis contained 8 g/l NaCl, 0.2 g/l KCl, 1.44 g/l Na₂HPO₄, 0.24 g/l KH₂PO₄, 1 mM MgSO₄ and 0.1 mM CaCl₂. Prior to use PBS-MgCa was filtered with a sterile filter (pore size < 0.2 µm) to reduce particle load (Tomasek et al., 2018).

2.2. Construction of deletion strains

Chromosomal modifications were conducted using recombineering methods that have been comprehensively described and reviewed previously (Murphy, 2016). The *tetA-sacB* cassette and lambda recombineering functions provided by pSIM5 were used to perform chromosomal modifications with base-pair precision (Datta et al., 2006; Li et al., 2013). Deletions of single genes were designed to span the coding sequence only and deletions of operons or larger genomic regions were designed to begin with the coding sequence of the first gene and end

with the coding sequence of the final gene. All deletions were verified by sequencing. Table S1 contains an annotated list of primers used in this study and Supplementary Information S2 a more detailed description of the recombineering method used.

2.3. Construction of GFP production strains

The protein expression system used for the bioreactor fermentations closely resembles previously described systems based on pJOE4056.2 (Wegerer et al., 2008; Wilms et al., 2001). For additional stability, the *bla* resistance cassette from plasmid pJOE4056.2 was exchanged for a *tetA* resistance cassette yielding pJOE4056.2_tetA to enable continuous selective pressure under the conditions of a chemostat. Use of pJOE4056.2_tetA requires induction with the rare sugar rhamnose at low glucose concentrations. Prior to plasmid transformation, we thus inactivated the chromosomal copy of *rhaB* encoding rhamnulokinase in *E. coli* MG1655 and *E. coli* RM214 to yield *rhaB*⁻ strains incapable of utilizing the rare sugar rhamnose. Supplementary Information S2 contains a more detailed description of the procedure.

2.4. Shaking flask cultivations

For growth experiments glycerol stock cultures strains were streaked on 2xTY agar plates and incubated overnight at 37 °C. For precultures, a single colony was picked to inoculate 15 ml minimal medium in a 50 ml baffled shaking flask and incubated at 37 °C on an orbital shaker set to 130 rpm overnight. On the following morning, an inoculum of the preculture was transferred into 50 ml minimal medium in a 500 ml baffled shaking flask to reach a starting OD of 0.2 and the culture incubated at 37 °C on an orbital shaker set to 130 rpm. Samples were drawn hourly using a fixed needle reaching through the attached cotton plug and a syringe. In all shaking flask experiments the wild type strain *E. coli* MG1655 was cultivated in parallel as a reference and data collected from other strains was normalized to this reference data.

2.5. Bioreactor setup

Bioreactor fermentations were carried out in a two-compartment scale-down reactor. The primary reactor was a stirred tank reactor, and a plug flow reactor was used as the secondary compartment mimicking a starvation zone. The plug flow reactor was connected to the stirred tank reactor only after establishment and sampling of a steady state in the chemostat phase. The technical setup has been characterized previously and includes the modifications described by Ankenbauer et al. (Ankenbauer et al., 2020; Löffler et al., 2016). A schematic overview of the two-compartment reactor is shown in Fig. 1 and Supplementary Information S2 contains a comprehensive description of the setup.

2.6. Preculture, batch cultivation and continuous cultivation

100 µl of glycerol stock seed culture were directly used to inoculate 300 ml of preculture minimal medium in a 3 l baffled shaking flasks and incubated at 37 °C on an orbital shaker set to 130 rpm overnight. The next morning 160 ml of preculture were used to inoculate the bioreactor complementing the total volume in the bioreactor to 1.6 l fermentation broth. Batch fermentation in the bioreactor ensued at 37 °C. Upon depletion of glucose, indicated by a sharp increase in dissolved oxygen tension, feed and harvest lines were connected. The reactor was refilled with feed medium to 1.6 l broth and a constant feed/harvest rate was established. For GFP production experiments with strains carrying pJOE4056.2_tetA the feed rate was set to 5.33 ml/min corresponding to a dilution rate of 0.2 h⁻¹. For bioreactor cultivations aimed at investigating genomic stability and determining the maintenance coefficient of *E. coli* MG1655 and *E. coli* RM214 the batch phase was shortened, and feed rates were set to 8.00 ml/min, 5.33 ml/min, 2.67 ml/min or 1.33

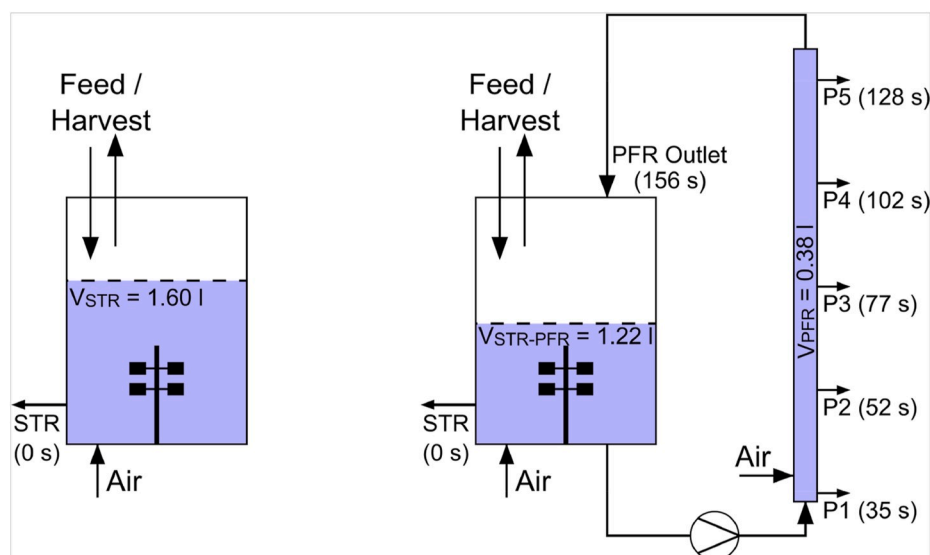


Fig. 1. Reactor Setup. The primary reactor was a standard laboratory reactor operated as a fully aerobic glucose limited chemostat at 37 °C (left scheme). For measurements of the well mixed STR reference state the entire biosuspension was in the primary reactor ($V_{STR} = 1.60$ l). Scale-down conditions were installed by connecting a secondary plug-flow reactor (PFR). An active pump then constantly circulated $V_{PFR} = 0.38$ l fermentation broth between STR and PFR reducing the volume fraction in the STR to $V_{STR-PFR} = 1.22$ l (right scheme). Labels STR and P1 to P5 designate sampling ports with the respective average residence time of biosuspension after leaving the STR. Fermentations were carried out in two phases each lasting for at least five volumetric residence times: First, a homogenous STR reference state was established, followed by a subsequent heterogeneous STR-PFR phase.

ml/min corresponding to dilution rates of 0.3 h^{-1} , 0.2 h^{-1} , 0.1 h^{-1} or 0.05 h^{-1} . After cultivation for at least five volumetric residence times a reference sample was taken. Then, the plug-flow reactor was connected to the primary reactor via a diaphragm metering pump effectively circulating about one-quarter (380 ml) of the total fermentation broth from the primary reactor through the plug-flow reactor and back into the stirred tank reactor. In the following five to six volumetric residence times samples were taken at predefined time points from the STR and the five PFR ports. Afterwards the fermentation was aborted, and the actual final broth volume measured. This value was used for all volumetric calculations during data analysis.

2.7. Determination of optical density and biomass dry weight

Optical density of fermentation broth appropriately diluted with 0.9% NaCl from the primary reactor was measured in triplicates at 600 nm on a spectrophotometer (Amersham Biosciences/GE Healthcare, Amersham, United Kingdom). For measurement of biomass dry weight quadruplicates of 5 ml broth were centrifuged in weighted glass tubes at 2500 g and 4 °C for 7.5 min. Supernatant was immediately decanted and the pellet washed by resuspending in 5 ml of freshly prepared 150 mM NH_4HCO_3 held at 4 °C. The suspension was centrifuged again, and the washing repeated once. After a final centrifugation, the remaining liquid was decanted carefully, the pellet dried at 105 °C and glass tubes containing dried pellets were weighed again.

2.8. Determination of acetic acid, ammonium and glucose concentrations in fermentation supernatant and feed

5 ml of biosuspension was directly sampled into a syringe connected to a single-use 0.45 μm sterile filter and immediately filtered. The clear supernatant was flash frozen in liquid nitrogen and stored at -70 °C until analysis. Glucose concentration was determined by D-Glucose UV-Test Kit (R-Biopharm, Darmstadt, Germany) and acetic acid concentration by Acetic acid UV-Test Kit (R-Biopharm, Darmstadt, Germany). Ammonium concentration was determined by Ammonium cuvette test LCK 303 or LCK 304 (Hach Lange, Düsseldorf, Germany). At the end of the cultivation feed samples were taken directly from the feed line, flash frozen in liquid nitrogen and processed as described.

2.9. Analysis of total carbon, inorganic carbon and biomass composition

For total carbon and inorganic carbon analysis 0.5 ml biosuspension

sample were mixed with 50 μl of 5 M KOH to prevent loss of dissolved carbonate. Then, the suspension was diluted 1:20 with demineralized water, flash frozen in liquid nitrogen, and stored at -70 °C until analysis. Analysis was performed with a multi N/C 2100 S composition analyzer (Analytik Jena, Jena, Germany) to yield the total concentration of carbon and inorganic carbon in the fermenter effluent stream.

To determine biomass composition 1.0 ml of biosuspension was centrifuged at 4 °C and 14000 rpm (20817 g) for 3 min. The supernatant was discarded, the pellet resuspended in 1.0 ml of 0.9% NaCl solution and centrifuged again. The pellet was resuspended in 5 ml 0.9% NaCl, flash frozen in liquid nitrogen and stored at -70 °C until analysis. Analysis was performed with a multi N/C 2100 S composition analyzer (Analytik Jena, Jena, Germany) and the carbon and nitrogen content of the biomass calculated from these values.

2.10. Measurement of nucleotides

2 ml of biosuspension was sampled directly into 0.5 ml of precooled (<-20 °C) quenching solution and incubated at 6 °C on a shaker for 15 min. Quenching solution consisted of 80 μM EDTA dissolved in 35% (V/V) perchloric acid. 500 μl 1 M K_2HPO_4 was added, and the sample was briefly vortexed. 550 μl 5 M KOH was added and the sample was vortexed again. To remove precipitating potassium perchlorate samples were then centrifuged at 4 °C and 7830 rpm (7197 g) for 5 min. 1.5 ml of supernatant was carefully transferred to new tubes, flash frozen in liquid nitrogen, and stored at -70 °C. Prior to analysis samples were thawed and centrifuged for 10 min at 4 °C and 7197 g. 1 ml of supernatant was transferred to new tubes and their pH adjusted to 6.95–7.05 with 5 M KOH or 35% (V/V) perchloric acid. Samples were centrifuged again for 30 min at 4 °C at 18000 g to remove potassium perchlorate precipitate from neutralization. 500 μl of supernatant were then transferred into RotiSpin Mini 3 kDa MWCO tubes and centrifuged again for 30 min at 4 °C at 18000 g. HPLC analysis was carried out as described previously (Löffler et al., 2016).

2.11. Measurement of eGFP fluorescence

Freshly sampled biosuspension was flash-frozen in liquid nitrogen and stored at -70 °C until analysis. On the day of analysis all samples were thawed and diluted 1:100 with ice-cold PBS-MgCa. 200 μl of diluted sample were transferred into a black 96 well-plate with transparent bottom and lid and the fluorescence (excitation 485 nm, emission 535 nm) was quantified in a SLT SpectraFluor plate-reader (Tecan,

Switzerland). Then, the measured fluorescence values were converted into absolute eGFP concentrations using a calibration curve recorded with purified protein (see **Supplementary Information S2**).

2.12. Flow cytometry analysis

Freshly sampled biosuspension was diluted with PBS-MgCa to yield an OD of approximately 0.04. Diluted biosuspension was passed through a 30 μ M CellTrics® filter to reduce particle content and analyzed in a BD Accuri™ C6 Plus Flow Cytometer. The excitation laser had a wavelength of 488 nm and a 533/30 nm emission filter was used to capture GFP fluorescence. Particle signals with a forward scatter height (FSC-H) signal less than 2500 were ignored and 250000 events collected. Events with an eGFP area signal less than 10 were excluded from the analysis to remove dust and cell debris, usually resulting in 235000–249000 remaining events. Cells from events with an eGFP area less than 2000 were defined to form the non-producing population, while cells from events with an eGFP area equal or greater than 2000 were defined to form the producing population. Histograms of all samples can be found in **Supplementary Fig. S3**.

2.13. Genomic DNA sequencing

1 ml of biosuspension was sampled, flash-frozen in liquid nitrogen and stored at -70°C . On the day of extraction samples were thawed and total DNA extracted with DNeasy Blood and Tissue Kit (Qiagen). Isolated DNA was shipped to and sequenced by the commercial sequencing partner Eurofins Genomics resulting in approximately 5–6 million paired end reads (150 bp) per sample. Data was delivered as fastq files and assembly of the reads conducted with Unicycler 0.4.8 with the following settings: min contig length 300 bp, min contig coverage 5 (Wick et al., 2017). The obtained contigs were processed with Mauve version 20150226 build 10 using the reference sequence NC_0000913.3 from the NCBI database (Darling et al., 2004). Finally, small nucleotide polymorphisms were detected using snippy (<https://github.com/tseemann/snippy>) and the output manually examined using Geneious Prime 2020.2.3 (<https://www.geneious.com>). Supplementary Data S9 contains lists of all SNPs found.

2.14. RT-qPCR

1.5 ml of freshly drawn biosuspension were immediately flash frozen in liquid nitrogen and stored at -70°C . Frozen liquid cell suspensions were thawed on ice and 200 μ l each were transferred into bead bashing tubes pre-filled with 700 μ l Lysis buffer. Cells were disrupted with a Precellys® homogenisator for 2×20 s. RNA was extracted using the Quick-RNA Fungal/Bacterial Kit (Zymo Research) following the manufacturer's instructions. The RNA concentrations were measured by Nanodrop. 10 μ g RNA each was treated with 2 units TURBO DNase (Thermo Fisher Scientific) in 50 μ l reactions for 60 min, with additional 2 units enzyme after 20 and 40 min, respectively. RNA from the DNase reactions were purified with Zymo Clean & Concentrator™-5 (Zymo Research) according to the manufacturer's protocol and were then measured by Nanodrop. cDNA synthesis with SuperScript® IV reverse transcriptase (Invitrogen) was carried out according to the protocol for random hexamers as primers. 1 μ g RNA was used as starting input for 20 μ l reactions, but no RNase inhibitor was added. A no reverse transcriptase control was included. For the qPCR reactions, the cDNA reaction mixes were diluted with 100 μ l nuclease free water. 2 μ l from all cDNA reactions were pooled together and a dilution series was prepared (1, 1:10, 1:100, 1:1000) for determination of PCR efficiency for each primer pair during each PCR run. For 15 μ l reactions 7.5 μ l ORA™ qPCR Green ROX L Mix (highQu), 0.4 μ l forward primer, 0.4 μ l reverse primer (f.c. 266 nM, each), 4.7 μ l H₂O and 2 μ l of diluted cDNA reactions were mixed. eGFP was amplified using primers eGFP2-forward and eGFP2-reverse (amplicon length: 248 bp), for cysG primers

cysG_housekeeping_fwd and cysG_housekeeping_reverse (amplicon length: 197 bp) were used. All reactions were performed as triplicates. Reactions were carried out on a Biorad CFX96 in 96 well plates. Program parameters were 95°C , 3 min; $39 \times (95^{\circ}\text{C}, 5 \text{ s}; 59^{\circ}\text{C}, 15 \text{ s}; 72^{\circ}\text{C}, 15 \text{ s})$; 65°C – 95°C (0,5 $^{\circ}\text{C}$ increment). Data was analyzed with Biorad CFX Manager 3.1. Relative expression of eGFP to cysG was calculated from the c_q numbers measured by the instrument adjusted for amplification efficiency. Relative expressions from time points STR-PFR 25 h and STR-PFR 28 h were normalized to the corresponding STR sample.

3. Results

3.1. Engineering of E. coli deletion strains

Our primary goal was to engineer a series of deletion strains based on *E. coli* MG1655 with physiological advantages under heterogeneous conditions with nutrient depleted zones. Strains would ultimately be assayed in a scale-down reactor consisting of a primary stirred tank reactor (STR) and a secondary plug-flow reactor (PFR) mimicking a starvation zone (Fig. 1).

We began with defining criteria for the choice of handpicked deletion targets: First, only genes that cause relevant metabolic burden in the context of a large-scale bioprocess should be chosen. We thus based our choice of targets primarily on the list of genes with high add-on maintenance under repeated transient starvation published by Löffler et al. (2016) and selected genes with an estimated add-on maintenance $> 0.05\%$. Except for *fliC* none of the chosen genes had an estimated maintenance add-on $> 1\%$, so we expected very little contribution of most single deletions. It was thus clear that multiple deletions would be necessary to achieve reasonably measurable effects. To maximize potential savings, we removed the entire operon if a candidate gene was part of a functionally connected operon. Second, any deletion must not be detrimental to basic growth parameters in glucose minimal medium. In the past, *E. coli* deletion strain series such as the MDS or the MGF series, had suffered from biological fitness losses (Karcagi et al., 2016; Kurokawa et al., 2016). Learning from these studies, any genes involved in primary carbon metabolism or basic cellular functions were outright excluded and we aimed for a highly selective approach with a strictly limited scope. Third, global regulatory programs must be left intact to avoid potential side effects. This included the general stress response, SOS responses and the stringent response. The stringent response had previously been identified as the major repeatedly induced regulatory program but strains with modulated ppGpp availability already exist and have dampened regulatory patterns in nutrient-limited conditions (Michalowski et al., 2017; Ziegler et al., 2020). In this study, one of our goals was to work orthogonally to cellular regulation.

With these criteria in mind, we developed a set of planned deletions containing most parts of the flagellar apparatus, the chemotaxis systems, and multiple other handpicked genes (with add-on to maintenance $> 0.05\%$): *cspD*, *aldA*, *flxA*. CspD is a toxin of dispensable function, AldA is irrelevant in glucose-limited medium as its essential function is complemented by PrpC and FlxA is a protein from the Qin prophage. All of these genes are non-essential (Baba et al., 2006). Using lambda recombineering with the *tetA-sacB* cassette we sequentially engineered the strains starting from *E. coli* MG1655 until completion of the final strain *E. coli* RM214 (Table 1). We assayed any new deletion strain from the series for its basic growth parameters in shaking flask fermentations cultivating *E. coli* MG1655 as a benchmark in parallel. None of the deletion strains had major advantages or deficits in maximum specific growth rate or biomass yield in glucose minimal medium affirming our choice of deletion targets (Fig. 2). Conducting the genomic deletions required a high number of total passages until *E. coli* RM214 was completed. We sequenced both the genome of *E. coli* MG1655 and *E. coli* RM214 and identified no problematic mutations (Supplementary Information S2, Supplementary Data S9). As we expected little impact of single deletions, we decided to focus our characterization only on the

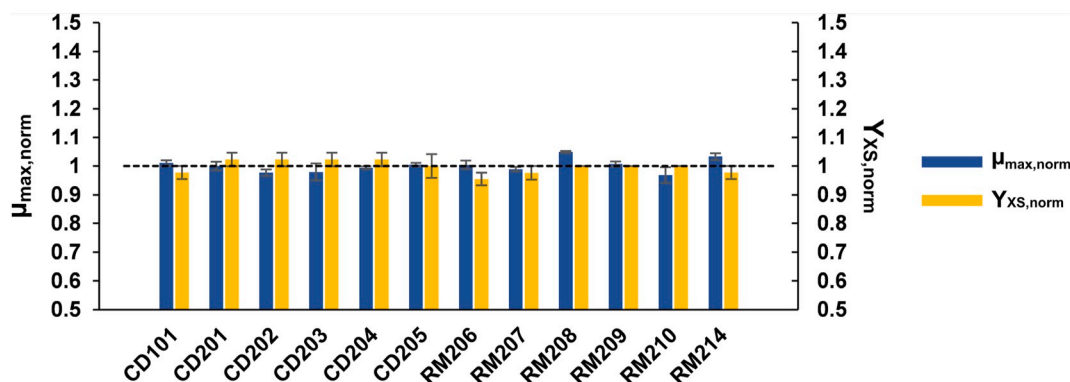


Fig. 2. Basic growth parameters of deletion strains. Deletion strains CD101 to RM214 were cultivated in minimal glucose medium in shaking flask fermentations. The maximum specific growth rate (blue) and biomass yield (yellow) were determined. The parent strain *E. coli* MG1655 was cultivated in parallel, and all data collected normalized to its growth parameters. Error bars indicate SEM ($n = 3$). The dashed line is a visual aid indicating reference values of 1. (For interpretation of the references to colour in this figure legend, the reader is referred to the Web version of this article.)

final strain of the series, *E. coli* RM214, and compared it to its parent wild-type strain *E. coli* MG1655.

3.2. Maintenance coefficient and genomic stability in scale-down fermentations

To test the initial hypothesis of a reduced maintenance coefficient in heterogeneous conditions and unravel potential benefits of *E. coli* RM214, we cultivated *E. coli* MG1655 and *E. coli* RM214 in two-compartment scale-down fermentations. Continuous chemostat cultivations with two phases were used to enable accurate assessment of fermentation parameters. In the first phase, strains were cultivated in standard well-mixed conditions employing only a STR (Fig. 1, left scheme). After five volumetric residence times this reference state was sampled and the secondary PFR compartment connected to the STR. A diaphragm metering pump then continuously circulated about one-fourth of the fermentation broth from the STR through the PFR and back into the STR. As feeding occurred only in the STR, the PFR simulated repeated passages of fractions of the population through a starvation zone (Fig. 1, right scheme). After continued cultivation for another five volumetric residence times the new STR-PFR steady state was sampled. Therefore, the total process time always exceeded ten volumetric residence times.

We cultivated *E. coli* MG1655 and *E. coli* RM214 at four different dilution rates (0.05 h^{-1} , 0.1 h^{-1} , 0.2 h^{-1} , 0.3 h^{-1}) each. We measured biomass concentrations in the well mixed STR reference state and during the heterogeneous STR-PFR phase. *E. coli* RM214 had a slightly increased biomass yield on substrate, especially under STR-PFR conditions and at $D = 0.05 \text{ h}^{-1}$. We estimated Pirt's maintenance coefficient m_s of both strains by linear regression of Y_{XS}^{-1} vs D^{-1} (Fig. 3). We found no statistically significant differences under well mixed STR conditions, but the maintenance coefficient of *E. coli* RM214 was significantly lower than that of *E. coli* MG1655 under STR-PFR conditions ($\Delta m_s = -0.038 \text{ g}_{\text{Glucose}} \cdot \text{g}_{\text{CDW}}^{-1} \cdot \text{h}^{-1}$, $p < 0.05$). Differences in the true biomass yield Y_{XS}^{true} were not significant under any conditions ($p > 0.05$). The results confirm the initial hypothesis and the effectiveness of our tailored deletion strategy for the targeted environment.

We sequenced the strains' genomes from the STR-PFR samples from all fermentations to investigate potential genomic instability that may have influenced the observations due to the long fermentation time ($>200 \text{ h}$ at $D = 0.05 \text{ h}^{-1}$). In *E. coli* MG1655, we found SNPs in *insH5* in samples from all dilution rates but no other mutations. We also found SNPs in *insH5* in all samples from *E. coli* RM214 and additional mutations in *ycfK* and *stfE* of the inactive e14 prophage (Supplementary Data S9). Apart from these minor alterations, the strains were remarkably stable. They showed no accumulation of mutations in any

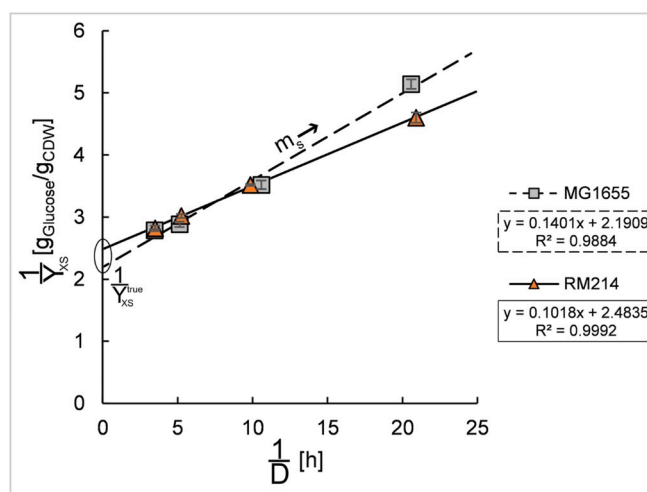


Fig. 3. Determination of maintenance coefficients under heterogeneous STR-PFR conditions. *E. coli* MG1655 (grey squares, dashed line) and *E. coli* RM214 (orange triangles, solid line) were cultivated in the STR-PFR system (glucose limited chemostats, $D = 0.05 \text{ h}^{-1}$, 0.1 h^{-1} , 0.2 h^{-1} , 0.3 h^{-1}). Maintenance coefficients m_s (slope) and true biomass yields Y_{XS}^{true} (intersection) were determined from the linear regression of data points. The difference of the maintenance coefficients is statistically significant ($\Delta m_s = -0.038 \text{ g}_{\text{Glucose}} \cdot \text{g}_{\text{CDW}}^{-1} \cdot \text{h}^{-1}$, $p < 0.05$). Error bars indicate technical standard deviation. (For interpretation of the references to colour in this figure legend, the reader is referred to the Web version of this article.)

regulatory genes or genes involved in central metabolism confirming that the engineered deletions bestowed the reduced maintenance coefficient to *E. coli* RM214.

3.3. Construction of eGFP production strains

Based on these encouraging findings we hypothesized that *E. coli* RM214 should better withstand the stressful conditions of an exemplary heterogeneous production scenario including transient starvation than its ancestor strain *E. coli* MG1655. We chose to produce eGFP as an easily measurable proxy for industrially relevant intracellularly accumulated proteins such as insulin varieties or other biopharmaceuticals commonly produced in *E. coli* (Baeshen et al., 2014, 2015).

A suitable expression system to produce proteins in glucose-limited fermentations is the rhamnose-inducible expression system from pJOE4056.2 (Wegerer et al., 2008). Expression from the rhamnose promoter occurs in the presence of non-toxic rhamnose and is enhanced

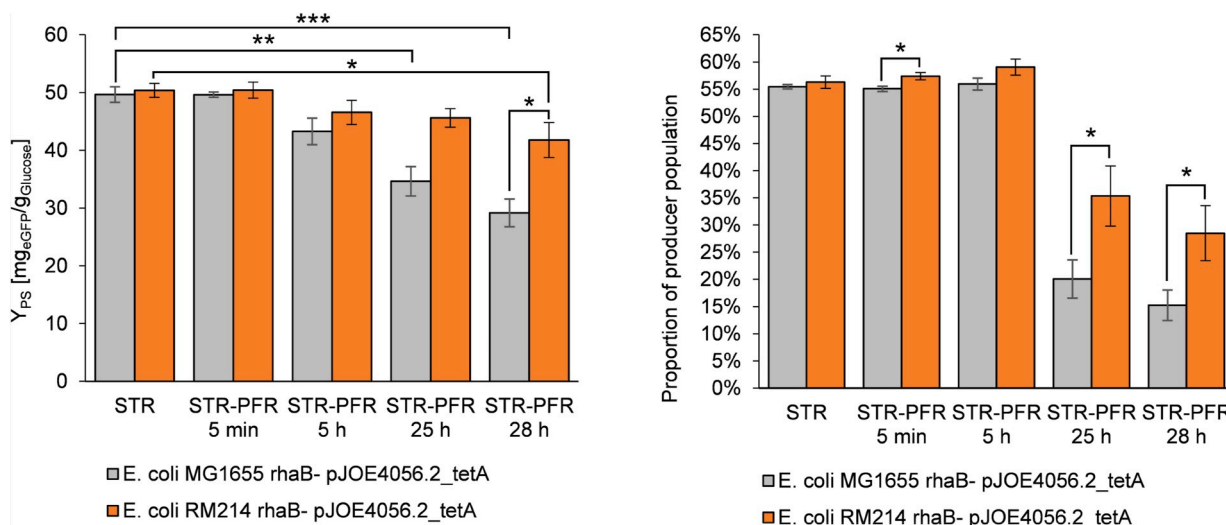


Fig. 4. EGFP yield on substrate and proportion of cells with high eGFP content. *E. coli* MG1655 rhaB⁻ pJOE4056.2_tetA (grey) and *E. coli* RM214 rhaB⁻ pJOE4056.2_tetA (orange) were cultivated in the STR-PFR system (glucose limited chemostat, $D = 0.2 \text{ h}^{-1}$). Samples were collected from the primary vessel. Error bars indicate SEM ($n = 4$), statistical indicators: * $p < 0.05$, ** $p < 0.01$, *** $p < 0.001$. **Left:** eGFP yield on substrate declines for both strains after PFR connection. Simultaneously, the difference between the strains gradually increases. Statistics: two-tailed t -tests comparing means of a single strain at later time points to the STR mean of the strain; and comparing the means of both strains at each time point to each other. **Right:** The proportion of cells with high eGFP content declines towards the end of the fermentation and is lower for *E. coli* MG1655 rhaB⁻ pJOE4056.2_tetA than for *E. coli* RM214 rhaB⁻ pJOE4056.2_tetA. Statistics: one-tailed t -tests comparing the presumably lower mean of *E. coli* MG1655 rhaB⁻ pJOE4056.2_tetA to that of *E. coli* RM214 rhaB⁻ pJOE4056.2_tetA at each time point. (For interpretation of the references to colour in this figure legend, the reader is referred to the Web version of this article.)

by low levels of glucose sensed by cAMP-CRP signaling. However, the use of rhamnose as a stable inducer requires the absence of rhamnose catabolism (Wilms et al., 2001). We therefore inactivated the chromosomal copy of *rhaB* by replacing the original gene in *E. coli* MG1655 and *E. coli* RM214 with an inactive frameshift copy from *E. coli* BW3110 by recombineering with the *tetA-sacB* cassette. The resulting strains were termed *E. coli* MG1655 rhaB⁻ and *E. coli* RM214 rhaB⁻. The absence of rhamnose catabolism was additionally confirmed by streaking the strains on 2xTY pH indicator agar plates containing Rhamnose. *E. coli* MG1655 rhaB⁻ and *E. coli* RM214 rhaB⁻ formed white colonies meaning that no acidification of the medium caused by rhamnose degradation occurred.

We then exchanged the *bla* resistance gene from pJOE4056.2 for the *tetA* resistance gene from *E. coli* T-SACK generating pJOE4056.2_tetA (Supplementary Fig. S2A). TetA is a tetracycline exporter and thus enables continuous selective pressure in the presence of tetracycline during prolonged cultivations. Transformation of the rhaB⁻ strains with pJOE4056.2_tetA yielded *E. coli* MG1655 rhaB⁻ pJOE4056.2_tetA and *E. coli* RM214 rhaB⁻ pJOE4056.2_tetA (Table 1).

3.4. Scale-down fermentations with eGFP production

E. coli MG1655 rhaB⁻ pJOE4056.2_tetA and *E. coli* RM214 rhaB⁻ pJOE4056.2_tetA were then fermented in quadruplicates each in the STR-PFR scale-down reactor in continuous chemostat cultivations at a dilution rate of $D = 0.2 \text{ h}^{-1}$. Heterogeneities were introduced by using the two-compartment STR-PFR reactor in the same setting as described above (Fig. 1). Again, this included a well-mixed STR only chemostat phase, and a subsequent STR-PFR chemostat phase to enable direct observation of the short-term and long-term influence of the nutrient-limited zone.

Under well-mixed STR conditions, we observed no substantial differences between the fermentations of *E. coli* MG1655 rhaB⁻ pJOE4056.2_tetA and *E. coli* RM214 rhaB⁻ pJOE4056.2_tetA. They reached comparable cell dry weight and eGFP yield on glucose (Fig. 4). In fact, the strains had virtually identical fermentation and production parameters in any parameter measured (Table 2). The primary product eGFP formed a considerable fraction of the total biomass and we

detected only trace amounts of acetate byproduct as expected for glucose-limited fermentations. We also determined the proportion of cells with high eGFP content by flow cytometry and found these to be practically identical for both strains in the STR reference steady-state (Fig. 4). As *E. coli* RM214 was specifically engineered to have advantageous traits in heterogenous fermentations including starvation zones these findings were not surprising and instead proved that our genomic deletions did not interfere with the basic fermentation traits of *E. coli* K-12 strains.

Upon connecting the PFR the process performance of both strains started to decline, but this phenomenon occurred remarkably slower and much less pronounced in *E. coli* RM214 rhaB⁻ pJOE4056.2_tetA than in *E. coli* MG1655 rhaB⁻ pJOE4056.2_tetA. Five hours after connection of the PFR both strains still had similar fractions of producing cells and reached comparable biomass concentration. However, first differences in cellular eGFP content and product yield already became apparent. Over the remaining process time production parameters we observed a 43% higher product yield for *E. coli* RM214 rhaB⁻ pJOE4056.2_tetA than for *E. coli* MG1655 rhaB⁻ pJOE4056.2_tetA ($\Delta Y_{ps} = 13 \text{ mg}_{eGFP}/\text{g}_{Glucose}$, two-tailed t -test, $p < 0.05$). Instead, biomass concentration increased in *E. coli* MG1655 rhaB⁻ pJOE4056.2_tetA indicating a shift from production to biomass formation (Supplementary Fig. S7A). Noteworthy, we found a linear correlation describing the tradeoff between eGFP production and biomass formation using data from both *E. coli* MG1655 rhaB⁻ pJOE4056.2_tetA and *E. coli* RM214 rhaB⁻ pJOE4056.2_tetA (Supplementary Fig. S7C and Supplementary Fig. S7D). We suspected that the divergence may be caused by a reduced fraction of producing cells for *E. coli* MG1655 rhaB⁻ pJOE4056.2_tetA compared to *E. coli* RM214 rhaB⁻ pJOE4056.2_tetA and measured the fluorescence of individual cells by flow cytometry. Similar to the eGFP yield, the proportion of actively producing cells shrank rapidly in *E. coli* MG1655 rhaB⁻ pJOE4056.2_tetA and more slowly in *E. coli* RM214 rhaB⁻ pJOE4056.2_tetA. At the final time point the fraction of producing cells was significantly higher for *E. coli* RM214 rhaB⁻ pJOE4056.2_tetA than for *E. coli* MG1655 rhaB⁻ pJOE4056.2_tetA (one-tailed t -test, $p > 0.05$). To check whether differential expression of eGFP might be responsible for the reduction of eGFP yield in the heterogeneous

Table 2
Fermentation parameters^a of the eGFP production chemostat processes.

	<i>E. coli</i> MG1655 rhaB ⁻ pJOE4056.2_tetA		<i>E. coli</i> RM214 rhaB ⁻ pJOE4056.2_tetA	
	STR	STR-PFR 28 h	STR	STR-PFR 28 h
$c_x \left[\frac{g_{CDW}}{l} \right]$	4.02 ± 0.066	4.28 ± 0.024	4.02 ± 0.053	4.13 ± 0.024
$c_P \left[\frac{mg_{eGFP}}{l} \right]$	630 ± 20	370 ± 32	650 ± 11	540 ± 41
$Y_{XS} \left[\frac{g_{CDW}}{g_{Glucose}} \right]$	0.315 ± 0.0048	0.3360 ± 0.00075	0.314 ± 0.0032	0.322 ± 0.0034
$Y_{PS} \left[\frac{mg_{eGFP}}{g_{Glucose}} \right]$	50 ± 1.3	29 ± 2.4	50 ± 1.2	42 ± 3.0
$c_{Acetate, STR} \left[\frac{g_{Acetate}}{l} \right]$	0.14 ± 0.040	0.017 ± 0.0072	0.010 ± 0.0061	0.07 ± 0.030
$c_{NH_4^+} \left[\frac{g_{NH_4^+}}{l} \right]$	1.64 ± 0.025	1.6 ± 0.12	1.57 ± 0.058	1.52 ± 0.033
$q_S \left[\frac{g_{Glucose}}{g_{CDW} \cdot h} \right]$	0.64 ± 0.013	0.60 ± 0.012	0.62 ± 0.020	0.60 ± 0.018
$q_P \left[\frac{mg_{eGFP}}{g_{CDW} \cdot h} \right]$	32 ± 1.4	18 ± 1.7	31 ± 1.2	25 ± 2.0
$Q_{CO_2} \left[\frac{mmol_{CO_2}}{h} \right]$	73.5 ± 0.70	70.6 ± 0.54	72.6 ± 0.49	69.8 ± 0.64
$Q_{O_2} \left[\frac{mmol_{O_2}}{h} \right]$	69.9 ± 0.90	67 ± 1.2	69.8 ± 0.90	65.6 ± 0.44
$RQ \left[\frac{mol_{CO_2}}{mol_{O_2}} \right]$	1.05 ± 0.019	1.06 ± 0.013	1.04 ± 0.011	1.06 ± 0.010
$eGFP \text{ content} \left[\frac{mg_{eGFP}}{g_{CDW}} \right]$	158 ± 6.5	87 ± 7.3	161 ± 4.6	130 ± 10
Proportion of producing population [%]	55.4 ± 0.43	15 ± 2.8	56 ± 1.2	28 ± 5.1
$D \left[\frac{1}{h} \right]$	0.201 ± 0.0026		0.194 ± 0.0028	

^a Errors indicate SEM (n = 4).

conditions in general or for the differences between the two strains, we conducted RT-qPCR using the housekeeping gene *cysG* as a reference. However, we found no clear indication for differential expression of eGFP towards the end of the fermentation or between the two strains (Supplementary information S10).

After connection of the PFR we observed alterations in the respiratory parameters of both strains. Initially, cells reacted with a short spike of increased respiratory activity which then dropped rapidly in the following hour. The oxygen uptake rate Q_{O_2} and the carbon dioxide formation rate Q_{CO_2} recovered over the next two volumetric residence times and then slowly drifted towards new steady states but never reached the initial STR only values (Supplementary Fig. S6). We calculated total carbon balances but the deviations in the respiratory rates caused only minor redistributions between the STR reference status and the STR-PFR 28 h sample (Fig. 5, Table S5A and Table S5B). Apart from small gains in the biomass (CDW) fraction and small reductions in the carbon dioxide formation no major differences occurred. Declining

productivity was hence accompanied by slightly declining respiration and increased biomass formation. From all collected indications we conclude that the primary factor for loss of productivity of both strains was a restructuring of the biomass composition towards lower eGFP content (Fig. S7B). This is supported by our observations using flow cytometry. The proportion of cells with high eGFP content dropped substantially in the late fermentation stages (Fig. 4). We presume that the reduced cellular eGFP content then led to lower metabolic burden and thus enabled slightly higher biomass yields. In all parameters measured, *E. coli* RM214 rhaB⁻ pJOE4056.2_tetA proved to be more robust to the STR-PFR conditions and maintained productive for a longer period than *E. coli* MG1655 rhaB⁻ pJOE4056.2_tetA. Since the only clearly different parameter between the two strains is the maintenance coefficient, we propose that *E. coli* RM214 rhaB⁻ pJOE4056.2_tetA benefits from a small surplus of substrate that can be used to meet the high precursor and ATP demand of heterologous protein synthesis.

The energetic state of cells during cultivations can be assessed by calculating the Adenylate Energy Charge (AEC) from measured nucleotide concentrations (Chapman et al., 1971). Initially, in the well-mixed STR only phase, the concentration of all nucleotides and the AEC was comparable for both strains (Supplementary Fig. S4A). After connection of the PFR, we then simultaneously sampled cells from the STR and the five ports along the primary axis of the PFR to obtain a time-resolved profile of the short-term AEC changes during PFR passage (Fig. 6). As expected during passage through a nutrient starvation zone, the AEC of cells dropped rapidly after leaving the STR and continued to decline towards a plateau. Shortly after PFR connection, the pattern was highly similar for both strains (Fig. 6, upper panel). After 25 h of cultivation under scale-down conditions, the AEC of both strains in the STR and at all sampling ports of the PFR was higher than before (Fig. 6, lower panel). Here, differences between the strains also became apparent as the AEC of *E. coli* MG1655 rhaB⁻ pJOE4056.2_tetA was higher than that of *E. coli* RM214 rhaB⁻ pJOE4056.2_tetA at all sampling points. We then compared the AEC of samples drawn from the primary vessel at different time points to unravel long-term effects of the heterogeneous conditions. Both strains individually showed statistically significant increases in the AEC between time points STR and STR-PFR 25 h (two-tailed t-tests, p <

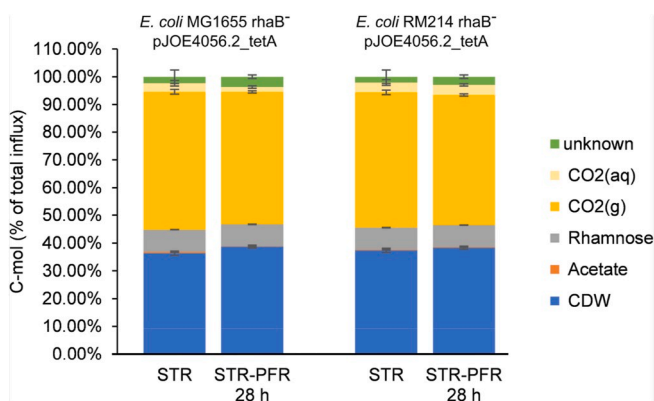


Fig. 5. Carbon Balance. *E. coli* MG1655 rhaB⁻ pJOE4056.2_tetA (grey) and *E. coli* RM214 rhaB⁻ pJOE4056.2_tetA (orange) were cultivated in the STR-PFR system (glucose limited chemostat, D = 0.2 h⁻¹). Columns show efflux fractions of individual substances. Error bars indicate SEM (n = 4). For raw data see Supplementary Tables S5A and S5B.

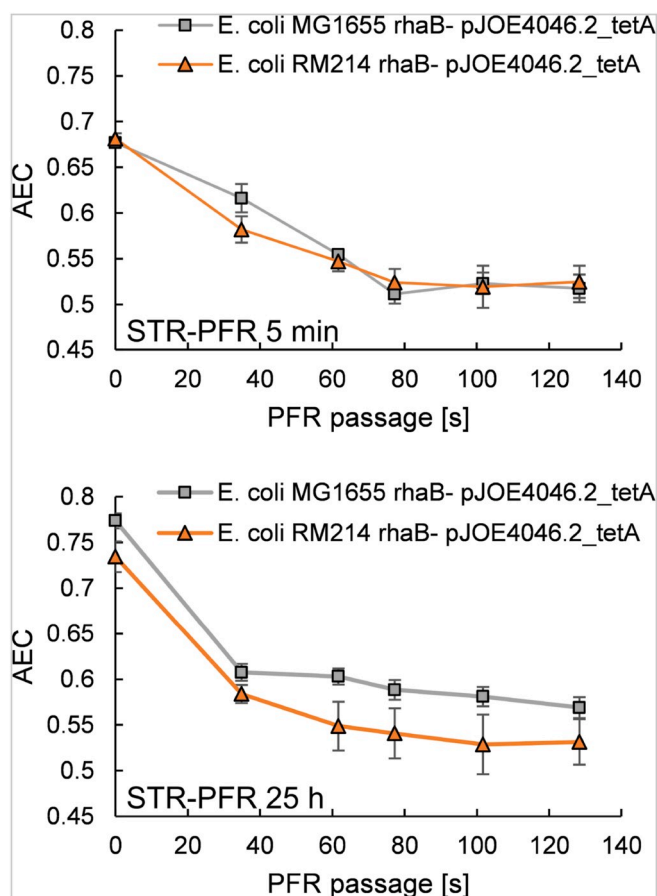


Fig. 6. Adenylate Energy Charge in the STR and during PFR passage. *E. coli* MG1655 rhaB⁻ pJOE4056.2.tetA and *E. coli* RM214 rhaB⁻ pJOE4056.2.tetA were cultivated in the STR-PFR system (glucose limited chemostat, $D = 0.2 \text{ h}^{-1}$). The adenylate energy charge of cultures was determined shortly after PFR connection (STR-PFR 5 min, upper panel) and after five volumetric residence times (STR-PFR 25 h, lower panel). Samples were drawn from the primary reactor (0 s) and the five sampling ports along the axis of the PFR (35 s, 52 s, 77 s, 102 s, 128 s). Error bars indicate SEM ($n = 4$).

0.05; see [Supplementary Table S4B](#)). In fact, the AEC of *E. coli* MG1655 rhaB⁻ pJOE4056.2.tetA sampled from the primary fermentation vessel ([Fig. 6](#) and 0 s) at time point STR-PFR 25 h was the highest recorded value from all samples indicating that the strain was possibly trying to adapt to the unfavorable conditions. The coincidence with its reduced productivity and slightly increased biomass yield at the late fermentation stages points towards the preservation of cellular energy at the expense of heterologous protein productivity. The data from *E. coli* RM214 rhaB⁻ pJOE4056.2.tetA indicates a similar but less pronounced trend. Comparing the two strains to each other reveals a marginally significant difference ($p = 0.077$; see [Supplementary Table S4B](#)) of the AEC values measured in samples from the STR at STR-PFR 25 h which is reflected by the generally slightly lower AEC values of the deletion strain at this time point ([Fig. 6](#), lower panel). It is noteworthy that the total AxP levels of both strains were comparable for all samples and only the distribution among ATP, ADP and AMP varied ([Supplementary Fig. S4A](#)).

4. Discussion

In this study, we created a series of deletion strains lacking genes with high add-on maintenance under heterogeneous conditions with repeated starvation. The final strain of the series, *E. coli* RM214 had a significantly lower maintenance coefficient than its parent *E. coli*

MG1655 in an STR-PFR scale-down reactor. Moreover, *E. coli* RM214 rhaB⁻ pJOE4056.2.tetA proved to be more robust to the influence of heterogeneities in an exemplary protein production scenario reaching a significantly higher product yield in the STR-PFR phase.

The core concept of our deletion approach was to remove genes that are wastefully expressed under transient starvation conditions. The expected individual contribution of each single gene was very low ([Löffler et al., 2016](#)). The only remarkable exception was *flhC* whose expression alone was estimated to cause add-on maintenance of 3.10%, by far exceeding the expected add-on maintenance of 0.55% for the second-in-line *aldA* ([Löffler et al., 2016](#)). Multiple other flagellar and chemotaxis genes were also candidates, so the removal of these systems formed a major fraction of the deletions conducted in the creation of *E. coli* RM214. As the goal of this study was to investigate the fundamental usefulness of the whole design approach and each individual deletion had likely little effect, we did not attempt to experimentally assess the individual contributions or potential interactions. The data collected in this study thus serves to prove the general applicability of the approach but is insufficient to test the quantitative reliability of the individual metabolic cost predictions by [Löffler et al. \(2016\)](#). An in-depth study focusing on the effects of subsets or individual deletions would allow judging the predictions and the parallel investigation of fundamental effects and potential interactions. This is particularly interesting as the magnitude of effects observed by us exceeds the sum of all individual contributions from transcriptional and translational metabolic costs as estimated by [Löffler et al. \(2016\)](#). The calculations by [Löffler et al. \(2016\)](#) were thus either very conservative or other effects such as the actual absence of the expressed proteins provided additional secondary benefits. Investigating such secondary benefits could be helpful in refining the target selection among transiently expressed process-irrelevant genes. A potential secondary benefit enjoyed by *E. coli* RM214 could for example arise from the absence of the motility system which could save proton motive force otherwise used for flagellar rotation. On the other hand, we can confidently exclude the possibility that the slightly reduced genome of *E. coli* RM214 had a major impact due to reduced replication cost. The combined size of the deletions in *E. coli* RM214 was only about 50 kb, just slightly more than 1% of the *E. coli* K-12 genome, and the metabolic demand of DNA replication is per se very low ([Stouthamer, 1973](#)).

Key findings of our study are the reduced maintenance demand of *E. coli* RM214 compared to its parent strain and the slower product yield decline of *E. coli* RM214 rhaB⁻ pJOE4056.2.tetA under STR-PFR conditions. Both differences must be caused by the genotype of *E. coli* RM214 but do these findings relate to each other by a causative link or did we observe correlated phenomena? The overall eGFP transcript levels in the production scenario were fairly stable ([Supplementary Information S10](#)), so it appears unlikely that differential expression of eGFP from pJOE4056.2.tetA causes the different yields. The flow cytometry data indicate that microbial individuality may play a role, but without a plausible mechanism we must assume that this is a correlated observation. Instead, we opine that a connecting mechanism can be drawn from the overall balances and the strains' cultivation parameters. Substrate consumed for maintenance demand is, by definition, not available for biomass formation. It is commonly assumed that it is fully converted into terminal products and the energy available from this conversion harnessed by the cells as ATP to meet their maintenance demand ([Stouthamer and Bettenhausen, 1973](#)). Thus, a logical link between maintenance coefficient and protein yield exists: A reduced maintenance coefficient means that more substrate is available for biomass or product formation including potential secondary ATP costs that may arise from a high foreign protein content. A simple estimation allows us to test the quantitative feasibility of a causative relation by comparing the magnitude of the reduced maintenance coefficient to the difference in protein yield: Given that there were no significant differences in Y_{XS}^{true} we can assume that Δm_s is entirely available for the additional production of eGFP in *E. coli* RM214 rhaB⁻ pJOE4056.2.tetA.

Using Y_{XS} from STR-PFR 28 h and an assumed protein content of roughly 65% (Taymaz-Nikerel et al., 2010) the difference in maintenance demand could sustain an additional eGFP production rate of no more than $\Delta q_{p,ms} = 9.3 \text{ mg}_{eGFP}/\text{g}_{CDW}/\text{h}$. The experimental difference of $\Delta q_{p,ms} = 7 \text{ mg}_{eGFP}/\text{g}_{CDW}/\text{h}$ falls well within that range. A causative relation between the two observations is thus quantitatively feasible, and in our opinion likely. In this case up to 82% of the saved substrate due to lower m_s could have been used for the formation of additional eGFP in *E. coli* RM214 rhaB⁻ pJOE4056.2_tetA.

The connection between maintenance demand, energy availability and eGFP production is also supported by the AEC data collected. We found a declining AEC during PFR passage for both *E. coli* RM214 rhaB⁻ pJOE4056.2_tetA and *E. coli* MG1655 rhaB⁻ pJOE4056.2_tetA at all time points, which is similar to the pattern observed in a preceding study with non-producing *E. coli* K-12 (Löffler et al., 2016). However, it is important to note that we measured lower AEC values in the STR and a steeper decline in the PFR, putatively due to heterologous protein production. In the heterogeneous fermentation phase, when productivity declined, we measured increased AEC values, especially in samples of the less productive *E. coli* MG1655 rhaB⁻ pJOE4056.2_tetA (Supplementary Information S4). The AEC is a measurement of the energetic state of cells and usually tightly balanced in a range between 0.7 and 0.9 (Chapman et al., 1971). The activity of many cellular processes is connected to the AEC and a lower AEC is associated with the activation of catabolic enzymes to meet cellular energy demands (Atkinson, 1968). Substrate depletion generally causes a reduction of the AEC (Chapman and Atkinson, 1977). Conversely, reduced AEC values have been reported in conditions when cells experienced high anabolic demand or high secondary metabolic costs, for instance caused by cultivation at their maximum specific growth rate, or induction of motility (Lieder et al., 2015; Martinez-Garcia et al., 2014). Heterologous protein induction is known to cause increased ATP maintenance demand (Weber et al., 2002). We thus propose that the AEC values measured from samples drawn from the primary reactor at different time points of the fermentations can be explained by the ATP demands associated with eGFP productivity. It appears likely that the generally lower AEC measured in this study compared to data from non-producing *E. coli* K-12 cultivated under similar conditions is caused by the production of eGFP. The significant increases of the AEC values of both strains towards the end of the fermentations are then a consequence of their diminishing eGFP productivity. This also explains the more pronounced AEC increase and concomitant eGFP yield decrease of *E. coli* MG1655 rhaB⁻ pJOE4056.2_tetA compared to the deletion strain. The question then arises to what extent the lower maintenance coefficient of *E. coli* RM214 rhaB⁻ pJOE4056.2_tetA under scale-down conditions influences the AEC values. From data collected in the maintenance study (Fig. 3) and the eGFP production fermentations we can roughly estimate the ATP demand for eGFP production of both strains at time point STR-PFR 25 h (Supplementary Data S8). About 13% of the total ATP demand of *E. coli* MG1655 rhaB⁻ pJOE4056.2_tetA and 22% of the total ATP demand of *E. coli* RM214 rhaB⁻ pJOE4056.2_tetA can be attributed to eGFP production. Despite its lower maintenance coefficient the combined ATP demand for maintenance plus eGFP production of the highly productive *E. coli* RM214 rhaB⁻ pJOE4056.2_tetA then still exceeds the respective values of *E. coli* MG1655 rhaB⁻ pJOE4056.2_tetA which is reflected by its lower AEC at this time point.

A secondary observation made in this study was that loss of productivity in the STR-PFR condition was accompanied by a decline in the proportion of highly productive cells (Fig. 4). Microbial population heterogeneity is a subject of intense research (Binder et al., 2017) and our data provides no clear explanation why this shift occurs. Two things should be noted: First, the population heterogeneity for both *E. coli* MG1655 rhaB⁻ pJOE4056.2_tetA and *E. coli* RM214 rhaB⁻ pJOE4056.2_tetA is of the bimodal kind (Supplementary Fig. S3) and the fractions of producing cells in the homogeneous STR cultivation phase are practically identical for both strains. Second, once the PFR is

activated, we saw a decrease in the fraction of highly productive cells in all fermentations (Fig. 4, Supplementary Fig. S3) but the decrease was faster and more consistent for *E. coli* MG1655 rhaB⁻ pJOE4056.2_tetA. The overall level of population heterogeneity is generally high since only slightly more than half of all cells are strongly accumulating eGFP. We presume this is caused by the interplay of our expression system and the fermentation conditions. The regulation of rhamnose catabolism is autocatalytic and thus bimodality might be caused by a similar mechanism as in the case of expression from the arabinose promoter P_{BAD} (Khlebnikov et al., 2000). However, transcript measurements by RT-qPCR did not lead to a concise pattern that would explain both the differences between the two strains and the declining eGFP yield of each individual strain over the course of the heterogeneous fermentation phase. Given the fairly stable expression of eGFP and the continuous selective advantage provided by tetA, it also appears unlikely that plasmid loss or mutations were the underlying cause. Moreover, the general stability of eGFP expression from pJOE4056.2 has been determined to be perfect for over 50 generations in earlier studies (Wegeber et al., 2008).

The deletion approach in this study differs from previous works because target selection was based on existing expression data and limited to candidates that imposed a high metabolic burden but were irrelevant under the specified conditions (Valgepea et al., 2015). Large-scale genomic deletions, the contrary approach, have been conducted before in *E. coli* K-12, for instance as part of the construction of the MDS strains (Posfai et al., 2006). These strains had little benefits in standard protein production scenarios over their wild-type parent and were even inferior in basic process parameters, potentially caused by disrupted regulation (Karcagi et al., 2016; Sharma et al., 2007a, 2007b). It needs to be emphasized that our deletion strategy only provided advantages in the specified conditions of a heterogeneous bioprocess with transient starvation as *E. coli* RM214 had no benefit compared to *E. coli* MG1655 under well-mixed conditions. In this regard, it also appears clear that the deletion targets chosen by us cannot be directly transferred to other hosts or conditions since the naturally evolved regulation might be divergent. This is exemplified by an interesting comparison of our results to existing data from *Pseudomonas putida*. The exposure of *P. putida* KT2440 to heterogeneous STR-PFR conditions led to an increased and potentially wasteful expression of *fliC* similarly as in the case of *E. coli* (Ankenbauer et al., 2020). However, the deletion of the flagellar apparatus in *P. putida* EM329 led to significant improvements of basic fermentation and protein production parameters already under well mixed conditions (Lieder et al., 2015; Martinez-Garcia et al., 2014). This demonstrates not only the diverging regulation of motility between different microbes, but also implies that a strain like *P. putida* EM329 might unintentionally display additional beneficial traits in heterogeneous fermentations with starvation zones.

A premise of our study was to work orthogonally to global cellular regulation. The general stress response, stringent response and SOS responses were not modified as they might provide important functions for cellular adaptation and some expression systems depend on intracellular signaling molecules of global regulatory circuits. Examples include not only the CRP-cAMP dependent system used in this study but also novel adaptive expression systems that autoregulate cellular stress (Lo et al., 2016). Interestingly, in a former study, the rapid inactivation of *rpoS* in homogeneous chemostat cultivations was reported, which pointed to a large selective advantage of mutants (Notley-McRobb et al., 2002). In contrast, we did not find any mutations in genes involved in the stringent response or the general stress response for neither *E. coli* MG1655 nor *E. coli* RM214 at any growth rate. We conclude that under heterogeneous conditions the selective pressure on inactivating global regulatory programs is either very low or their activation may even be favorable for cellular viability which affirms our neutral approach to cellular regulation. However, this does not mean that modulating cellular regulation could not be beneficial for process or production parameters. Recently, several *E. coli* knock out strains lacking

hand-picked genes that are connected to post-induction stress responses were presented (Sharma et al., 2020). These strains have advantageous traits for protein production which could be integrated into *E. coli* RM214.

Our study design focused on the influence of starvation zones on microbial culture performance. The carbon limited STR contained a substrate-limited growth and production zone representing the bulk of large-scale fermentations. The PFR served to introduce a transient starvation stimulus representative of repeated passages through a hunger zone as predicted to occur in large-scale reactors (Haringa et al., 2017; Kuschel and Takors, 2020). Since our experimental setup was specifically chosen for the study of transient starvation, it does not capture the effects of other heterogeneities, in particular transient substrate excess. It is well-known that close to the feeding point, substrate excess and concomitant oxygen limitation dominate the environment in large-scale fed-batch processes. *E. coli* typically reacts to such conditions with the production of solvents or small organic acids caused by overflow metabolism or anaerobic fermentation (Lara et al., 2009). The formation of byproducts then results in process performance losses even if reuptake in zones with lower nutrient concentration is possible (Enfors et al., 2001; Neubauer et al., 1995b). Since our deletion approach was only aimed at reducing the additional metabolic costs of transient starvation, *E. coli* RM214 probably responds to glucose excess like other *E. coli* K-12 strains. In principle, copying the design approach to construct an *E. coli* strain with reduced additional maintenance in excess zones appears to be feasible as the transcriptional response of *E. coli* MG1655 to glucose excess is large and involves many potentially process-irrelevant genes (Veit et al., 2007). However, the resulting genetic modifications would not reduce process performance loss from byproduct formation which is likely the dominating issue in substrate excess conditions. Various strategies to alleviate byproduct metabolism have been developed by other research groups, such as the use of alternative substrate transporters, knock-outs or the expression of recombinant *Vitreoscilla* hemoglobin (Anda et al., 2006; Eiteman and Altman, 2006; Pablos et al., 2014). Given that our strain design approach avoids modifications to global regulation or central carbon metabolism, we are confident that it is compatible with these existing strategies and their combination could result in chassis strains for generally robust scale-up. A limitation of our study originates from the focus on the model protein eGFP. However, recombinant protein production is frequently limited by the availability of cellular precursors and ATP, so it is not far-fetched to expect similar effects with other protein products (Glick, 1995; Heyland et al., 2011). The reduced maintenance coefficient of *E. coli* RM214 should also be helpful to produce molecules formed in ATP-intensive pathways such as terpenoids (Li and Wang, 2016; Ward et al., 2018). Potential advantages could also occur when the accumulation of toxic products causes increased ATP demand for product export, membrane maintenance or pH homeostasis (Sun et al., 2011; Tsukagoshi and Aono, 2000). On the other hand, it may be less helpful when the formation of a small molecule product is connected to net ATP synthesis. Glycolytic flux depends on the ATP requirements of cells and in such cases enforced ATP wasting can even increase the production rate (Boecker et al., 2019; Koebmann et al., 2002).

With the increasing knowledge about cellular metabolism and its interplay with the heterogeneous conditions of large-scale processes new possibilities to improve process performance arise. In a recent review Wehrs et al. (2019) emphasized that strains should be engineered specifically for the demands of large-scale production (Wehrs et al., 2019). In this context, our series of deletion strains is the first step towards host strains robust against the repeated exposure to starvation zones.

5. Conclusion

Large-scale fermentations often suffer from process performance loss

due to heterogeneous environments. *E. coli* RM214 was engineered to obtain a deletion strain with reduced maintenance and superior production properties in fermentations with starvation zones. Our study is the first that aimed to improve a microbe by repeated genomic deletions for enhanced robustness towards heterogeneous conditions. The exemplified application of *E. coli* RM214 for eGFP production demonstrates the cellular capacity to exploit the maintenance advantage for preventing non-wanted performance loss in heterogeneously mixed industrial production scenarios. Although only showcased for eGFP, the strain offers the capacity to serve as a platform for a variety of different products. Notably, this complements classical scale-up engineering and should be a highly valuable tool to prevent non-wanted performance of essential Titer-Rate-Yield values under industrial production conditions.

Funding

This research was funded from discretionary funds provided by the University of Stuttgart.

CRediT authorship contribution statement

Martin Ziegler: Conceptualization, Methodology, Investigation, Writing – original draft, Visualization. **Julia Zieringer:** Software, Formal analysis. **Clarissa-Laura Döring:** Methodology, Investigation. **Liv Paul:** Investigation. **Christoph Schaal:** Investigation. **Ralf Takors:** Conceptualization, Writing – review & editing, Supervision.

Declaration of competing interest

Authors Martin Ziegler and Ralf Takors declare that findings of this manuscript contents are part of a patent application submitted by the privately owned company Manus Bio (Massachusetts, USA). The authors Martin Ziegler and Ralf Takors are listed as inventors.

Acknowledgements

The authors acknowledge the support of the Computational Biology Group at IBVT Stuttgart: Richard Schäfer and Prof. Björn Voß for providing access to a Galaxy Server.

The authors acknowledge the support of Dr. rer. nat. habil. Jürgen Dippon for assistance with statistical analysis.

The authors acknowledge the support of Florian Hiering and apl. Prof. Martin Siemann-Herzberg for assistance with the purification and quantification of eGFP.

The authors acknowledge the support of Andreas Freund for technical assistance.

The authors would like to thank the staff of the Court laboratory at the National Cancer Institute in Frederick, MD USA for providing the strains *T-SACK* and *E. coli* DH10B pSIM5.

The authors would like to thank apl. Prof. Martin Siemann-Herzberg and Dr. Josef Altenbuchner for providing the strain *E. coli* BW3110 pJOE4056.2.

Appendix A. Supplementary data

Supplementary data to this article can be found online at <https://doi.org/10.1016/j.ymben.2021.05.011>.

References

- Anda, R. de, Lara, A.R., Hernández, V., Hernández-Montalvo, V., Gosset, G., Bolívar, F., Ramírez, O.T., 2006. Replacement of the glucose phosphotransferase transport system by galactose permease reduces acetate accumulation and improves process performance of *Escherichia coli* for recombinant protein production without impairment of growth rate. *Metab. Eng.* 8, 281–290. <https://doi.org/10.1016/j.ymben.2006.01.002>.

- Ankenbauer, A., Schäfer, R.A., Viegas, S.C., Pobre, V., Voß, B., Arraiano, C.M., Takors, R., 2020. *Pseudomonas putida* KT2440 is naturally endowed to withstand industrial-scale stress conditions. *Microbial biotechnology* 13, 1145–1161. <https://doi.org/10.1111/1751-7915.13571>.
- Atkinson, D.E., 1968. The energy charge of the adenylate pool as a regulatory parameter. Interaction with feedback modifiers. *Biochemistry* 7, 4030–4034. <https://doi.org/10.1021/bi00851a033>.
- Baba, T., Ara, T., Hasegawa, M., Takai, Y., Okumura, Y., Baba, M., Datsenko, K.A., Tomita, M., Wanner, B.L., Mori, H., 2006. Construction of *Escherichia coli* K-12 in-frame, single-gene knockout mutants: the Keio collection. *Mol. Syst. Biol.* 2 <https://doi.org/10.1038/msb4100050>.
- Baeshen, M.N., Al-Hejin, A.M., Bora, R.S., Ahmed, M.M.M., Ramadan, H.A.I., Saini, K.S., Baeshen, N.A., Redwan, E.M., 2015. Production of biopharmaceuticals in *E. coli*: current scenario and future perspectives. *J. Microbiol. Biotechnol.* 25, 953–962. <https://doi.org/10.4014/jmb.1412.12079>.
- Baeshen, N.A., Baeshen, M.N., Sheikh, A., Bora, R.S., Ahmed, M.M.M., Ramadan, H.A.I., Saini, K.S., Redwan, E.M., 2014. Cell factories for insulin production. *Microb. Cell Factories* 13, 141. <https://doi.org/10.1186/s12934-014-0141-0>.
- Binder, D., Drepper, T., Jaeger, K.-E., Delvigne, F., Wiechert, W., Kohlheyder, D., Grünberger, A., 2017. Homogenizing bacterial cell factories: analysis and engineering of phenotypic heterogeneity. *Metab. Eng.* 42, 145–156. <https://doi.org/10.1016/j.ymben.2017.06.009>.
- Boecker, S., Zahoor, A., Schramm, T., Link, H., Klamt, S., 2019. Broadening the scope of enforced ATP wasting as a tool for metabolic engineering in *Escherichia coli*. *Biotechnol. J.* 14, e1800438 <https://doi.org/10.1002/biot.201800438>.
- Bylund, F., Castan, A., Mikkola, R., Veide, A., Larsson, G., 2000. Influence of scale-up on the quality of recombinant human growth hormone. *Biotechnol. Bioeng.* 69, 119–128. [https://doi.org/10.1002/\(SICI\)1097-0290\(20000720\)69:2<119::AID-BIT1>3.0.CO;2-9](https://doi.org/10.1002/(SICI)1097-0290(20000720)69:2<119::AID-BIT1>3.0.CO;2-9).
- Bylund, F., Collet, E., Enfors, S.-O., Larsson, G., 1998. Substrate gradient formation in the large-scale bioreactor lowers cell yield and increases by-product formation. *Bioprocess Eng.* 18, 171. <https://doi.org/10.1007/s004490050427>.
- Bylund, F., Guillard, F., Enfors, S.-O., Trägårdh, C., Larsson, G., 1999. Scale down of recombinant protein production: a comparative study of scaling performance. *Bioprocess Eng.* 20, 377. <https://doi.org/10.1007/s004490050606>.
- Chapman, A.G., Atkinson, D.E., 1977. Adenine nucleotide concentrations and turnover rates. Their correlation with biological activity in bacteria and yeast. In: Rose, A.H., Tempest, D.W. (Eds.), *Advances in Microbial Physiology*, vol. 15. Academic, London, pp. 253–306.
- Chapman, A.G., Fall, L., Atkinson, D.E., 1971. Adenylate energy charge in *Escherichia coli* during growth and starvation. *J. Bacteriol.* 108, 1072–1086.
- Cortés, J.T., Flores, N., Bolívar, F., Lara, A.R., Ramírez, O.T., 2016. Physiological effects of pH gradients on *Escherichia coli* during plasmid DNA production. *Biotechnol. Bioeng.* 113, 598–611. <https://doi.org/10.1002/bit.25817>.
- Darling, A.C.E., Mau, B., Blattner, F.R., Perna, N.T., 2004. Mauve: multiple alignment of conserved genomic sequence with rearrangements. *Genome Res.* 14, 1394–1403. <https://doi.org/10.1101/gr.2289704>.
- Datta, S., Costantino, N., Court, D.L., 2006. A set of recombinering plasmids for gram-negative bacteria. *Gene* 379, 109–115. <https://doi.org/10.1016/j.gene.2006.04.018>.
- Delvigne, F., Boxus, M., Ingels, S., Thonart, P., 2009. Bioreactor mixing efficiency modulates the activity of a prpoS:GFP reporter gene in *E. coli*. *Microb. Cell Factories* 8, 15. <https://doi.org/10.1186/1475-2859-8-15>.
- Delvigne, F., Destain, J., Thonart, P., 2006. A methodology for the design of scale-down bioreactors by the use of mixing and circulation stochastic models. *Biochem. Eng. J.* 28, 256–268. <https://doi.org/10.1016/j.bej.2005.11.009>.
- Delvigne, F., Takors, R., Mudde, R., van Gulik, W., Noorman, H., 2017. Bioprocess scale-up/down: an integrative enabling technology: from fluid mechanics to systems biology and beyond. *Microbial biotechnology* 10, 1267–1274. <https://doi.org/10.1111/1751-7915.12803>.
- Eiteman, M.A., Altman, E., 2006. Overcoming acetate in *Escherichia coli* recombinant protein fermentations. *Trends Biotechnol.* 24, 530–536. <https://doi.org/10.1016/j.tibtech.2006.09.001>.
- Enfors, S.-O., Jahic, M., Rozkov, A., Xu, B., Hecker, M., Jürgen, B., Krüger, E., Schweder, T., Hamer, G., O'Beirne, D., Noisommit-Rizzi, N., Reuss, M., Boone, L., Hewitt, C., McFarlane, C., Nienow, A., Kovacs, T., Trägårdh, C., Fuchs, L., Revstedt, J., Friberg, P.C., Hjertager, B., Blomsten, G., Skogman, H., Hjort, S., Hoeks, F., Lin, H.-Y., Neubauer, P., van der Lans, R., Luyben, K., Vrabel, P., Manelius, Å., 2001. Physiological responses to mixing in large scale bioreactors. *J. Biotechnol.* 85, 175–185. [https://doi.org/10.1016/S0168-1656\(00\)00365-5](https://doi.org/10.1016/S0168-1656(00)00365-5).
- George, S., Larsson, G., Enfors, S.-O., 1993. A scale-down two-compartment reactor with controlled substrate oscillations: metabolic response of *Saccharomyces cerevisiae*. *Bioprocess Eng.* 9, 249–257. <https://doi.org/10.1007/BF01061530>.
- Glick, B.R., 1995. Metabolic load and heterologous gene expression. *Biotechnol. Adv.* 13, 247–261. [https://doi.org/10.1016/0734-9750\(95\)00004-A](https://doi.org/10.1016/0734-9750(95)00004-A).
- Hanahan, D., 1983. Studies on transformation of *Escherichia coli* with plasmids. *J. Mol. Biol.* 166, 557–580. [https://doi.org/10.1016/S0022-2836\(83\)80284-8](https://doi.org/10.1016/S0022-2836(83)80284-8).
- Haringa, C., Deshmukh, A.T., Mudde, R.F., Noorman, H.J., 2017. Euler-Lagrange analysis towards representative down-scaling of a 22 m³ aerobic *S. cerevisiae* fermentation. *Chem. Eng. Sci.* 170, 653–669. <https://doi.org/10.1016/j.ces.2017.01.014>.
- Heyland, J., Blank, L.M., Schmid, A., 2011. Quantification of metabolic limitations during recombinant protein production in *Escherichia coli*. *J. Biotechnol.* 155, 178–184. <https://doi.org/10.1016/j.biotech.2011.06.016>.
- Jonge, L.P. de, Buijs, N.A.A., Pierick, A. ten, Deshmukh, A., Zhao, Z., Kiel, J.A.K.W., Heijnen, J.J., van Gulik, W.M., 2011. Scale-down of penicillin production in *Penicillium chrysogenum*. *Biotechnol. J.* 6, 944–958. <https://doi.org/10.1002/biot.201000409>.
- Junne, S., Klingner, A., Kabisch, J., Schweder, T., Neubauer, P., 2011. A two-compartment bioreactor system made of commercial parts for bioprocess scale-down studies: impact of oscillations on *Bacillus subtilis* fed-batch cultivations. *Biotechnol. J.* 6, 1009–1017. <https://doi.org/10.1002/biot.201100293>.
- Karcagi, I., Draskovits, G., Umenhoffer, K., Fekete, G., Kovács, K., Méhi, O., Balikó, G., Szappanos, B., Györfy, Z., Fehér, T., Bogos, B., Blattner, F.R., Pál, C., Pósfai, G., Papp, B., 2016. Indispensability of horizontally transferred genes and its impact on bacterial genome streamlining. *Mol. Biol. Evol.* 33, 1257–1269. <https://doi.org/10.1093/molbev/msw009>.
- Khlebnikov, A., Risa, Ø., Skaug, T., Carrier, T.A., Keasling, J.D., 2000. Regulatable Arabinose-inducible gene expression system with consistent control in all cells of a culture. *J. Bacteriol.* 182, 7029–7034. <https://doi.org/10.1128/JB.182.24.7029-7034.2000>.
- Koebmann, B.J., Westerhoff, H.V., Snoep, J.L., Nilsson, D., Jensen, P.R., 2002. The glycolytic flux in *Escherichia coli* is controlled by the demand for ATP. *J. Bacteriol.* 184, 3909–3916. <https://doi.org/10.1128/JB.184.14.3909-3916.2002>.
- Kurokawa, M., Seno, S., Matsuda, H., Ying, B.-W., 2016. Correlation between genome reduction and bacterial growth. *DNA Res. : an international journal for rapid publication of reports on genes and genomes* 23, 517–525. <https://doi.org/10.1093/dnares/dsw035>.
- Kuschel, M., Siebler, F., Takors, R., 2017. Lagrangian Trajectories to Predict the Formation of Population Heterogeneity in Large-Scale Bioreactors, vol. 4. Bioengineering, Basel, Switzerland. <https://doi.org/10.3390/bioengineering4020027>.
- Kuschel, M., Takors, R., 2020. Simulated oxygen and glucose gradients as a prerequisite for predicting industrial scale performance a priori. *Biotechnol. Bioeng.* 117, 2760–2770. <https://doi.org/10.1002/bit.27457>.
- Lara, A.R., Galindo, E., Ramírez, O.T., Palomares, L.A., 2006a. Living with heterogeneities in bioreactors: understanding the effects of environmental gradients on cells. *MB* 34, 355–382. <https://doi.org/10.1385/MB:34:3:355>.
- Lara, A.R., Leal, L., Flores, N., Gosset, G., Bolívar, F., Ramírez, O.T., 2006b. Transcriptional and metabolic response of recombinant *Escherichia coli* to spatial dissolved oxygen tension gradients simulated in a scale-down system. *Biotechnol. Bioeng.* 93, 372–385. <https://doi.org/10.1002/bit.20704>.
- Lara, A.R., Taymaz-Nikerel, H., Mashego, M.R., van Gulik, W.M., Heijnen, J.J., Ramírez, O.T., van Winden, W.A., 2009. Fast dynamic response of the fermentative metabolism of *Escherichia coli* to aerobic and anaerobic glucose pulses. *Biotechnol. Bioeng.* 104, 1153–1161. <https://doi.org/10.1002/bit.22503>.
- Larsson, G., Enfors, S.-O., 1988. Studies of insufficient mixing in bioreactors: effects of limiting oxygen concentrations and short term oxygen starvation on *Penicillium chrysogenum*. *Bioprocess Eng.* 3, 123–127. <https://doi.org/10.1007/BF00373475>.
- Li, X.-T., Thomason, L.C., Sawitzke, J.A., Costantino, N., Court, D.L., 2013. Positive and negative selection using the tetA-sacB cassette: recombinering and P1 transduction in *Escherichia coli*. *Nucleic Acids Res.* 41, e204 <https://doi.org/10.1093/nar/gkt1075>.
- Li, Y., Wang, G., 2016. Strategies of isoprenoids production in engineered bacteria. *J. Appl. Microbiol.* 121, 932–940. <https://doi.org/10.1111/jam.13237>.
- Lieder, S., Nikel, P.I., Lorenzo, V. de, Takors, R., 2015. Genome reduction boosts heterologous gene expression in *Pseudomonas putida*. *Microb. Cell Factories* 14, 23. <https://doi.org/10.1186/s12934-015-0207-7>.
- Lo, T.-M., Chng, S.H., Teo, W.S., Cho, H.-S., Chang, M.W., 2016. A two-layer gene circuit for decoupling cell growth from metabolite production. *Cell Syst* 3, 133–143. <https://doi.org/10.1016/j.cels.2016.07.012>.
- Löffler, M., Simen, J.D., Jager, G., Schaeferhoff, K., Freund, A., Takors, R., 2016. Engineering *E. coli* for large-scale production - strategies considering ATP expenses and transcriptional responses. *Metab. Eng.* 38, 73–85. <https://doi.org/10.1016/j.ymben.2016.06.008>.
- Martinez-García, E., Nikel, P.I., Chavarria, M., Lorenzo, V. de, 2014. The metabolic cost of flagellar motion in *Pseudomonas putida* KT2440. *Environ. Microbiol.* 16, 291–303. <https://doi.org/10.1111/1462-2920.12309>.
- Michalowski, A., Siemann-Herzberg, M., Takors, R., 2017. *Escherichia coli* HGT: engineered for high glucose throughput even under slowly growing or resting conditions. *Metab. Eng.* 40, 93–103. <https://doi.org/10.1016/j.ymben.2017.01.005>.
- Murphy, K.C., 2016. λ recombination and recombinering. *EcoSal Plus* 7. <https://doi.org/10.1128/ecosalplus.ESP-0011-2015>.
- Neubauer, P., Åhman, M., Törnkvist, M., Larsson, G., Enfors, S.-O., 1995a. Response of guanosine tetraphosphate to glucose fluctuations in fed-batch cultivations of *Escherichia coli*. *J. Biotechnol.* 43, 195–204. [https://doi.org/10.1016/0168-1656\(95\)00130-1](https://doi.org/10.1016/0168-1656(95)00130-1).
- Neubauer, P., Håggström, L., Enfors, S.O., 1995b. Influence of substrate oscillations on acetate formation and growth yield in *Escherichia coli* glucose limited fed-batch cultivations. *Biotechnol. Bioeng.* 47, 139–146. <https://doi.org/10.1002/bit.260470204>.
- Neubauer, P., Junne, S., 2010. Scale-down simulators for metabolic analysis of large-scale bioprocesses. *Curr. Opin. Biotechnol.* 21, 114–121. <https://doi.org/10.1016/j.copbio.2010.02.001>.
- Nieß, A., Löffler, M., Simen, J.D., Takors, R., 2017. Repetitive short-term stimuli imposed in poor mixing zones induce long-term adaptation of *E. coli* cultures in large-scale bioreactors: experimental evidence and mathematical model. *Front. Microbiol.* 8, 1195. <https://doi.org/10.3389/fmicb.2017.01195>.
- Noorman, H., 2011. An industrial perspective on bioreactor scale-down: what we can learn from combined large-scale bioprocess and model fluid studies. *Biotechnol. J.* 6, 934–943. <https://doi.org/10.1002/biot.201000406>.

- Notley-McRobb, L., King, T., Ferenci, T., 2002. rpoS mutations and loss of general stress resistance in *Escherichia coli* populations as a consequence of conflict between competing stress responses. *J. Bacteriol.* 184, 806–811. <https://doi.org/10.1128/JB.184.3.806-811.2002>.
- Olughu, W., Deepika, G., Hewitt, C., Rielly, C., 2019. Insight into the large-scale upstream fermentation environment using scaled-down models. *J. Chem. Technol. Biotechnol.* 94, 647–657. <https://doi.org/10.1002/jctb.5804>.
- Olughu, W., Nienow, A., Hewitt, C., Rielly, C., 2020. Scale-down studies for the scale-up of a recombinant *Corynebacterium glutamicum* fed-batch fermentation: loss of homogeneity leads to lower levels of cadaverine production. *J. Chem. Technol. Biotechnol.* 95, 675–685. <https://doi.org/10.1002/jctb.6248>.
- Pablos, T.E., Sigala, J.C., Le Borgne, S., Lara, A.R., 2014. Aerobic expression of Vitreoscilla hemoglobin efficiently reduces overflow metabolism in *Escherichia coli*. *Biotechnol. J.* 9, 791–799. <https://doi.org/10.1002/biot.201300388>.
- Pirt, S.J., 1965. The maintenance energy of bacteria in growing cultures. *Proc. Roy. Soc. Lond. B Biol. Sci.* 163, 224–231. <https://doi.org/10.1098/rspb.1965.0069>.
- Posfai, G., Plunkett, G.3., Feher, T., Frisch, D., Keil, G.M., Umenhoffer, K., Kolisnychenko, V., Stahl, B., Sharma, S.S., Arruda, M. de, Burland, V., Harcum, S.W., Blattner, F.R., 2006. Emergent properties of reduced-genome *Escherichia coli*. *Science* 312, 1044–1046. <https://doi.org/10.1126/science.1126439>.
- Sharma, A.K., Shukla, E., Janoti, D.S., Mukherjee, K.J., Shiloach, J., 2020. A novel knock out strategy to enhance recombinant protein expression in *Escherichia coli*. *Microb. Cell Factories* 19. <https://doi.org/10.1186/s12934-020-01407-z>.
- Sharma, S.S., Blattner, F.R., Harcum, S.W., 2007a. Recombinant protein production in an *Escherichia coli* reduced genome strain. *Metab. Eng.* 9, 133–141. <https://doi.org/10.1016/j.ymben.2006.10.002>.
- Sharma, S.S., Campbell, J.W., Frisch, D., Blattner, F.R., Harcum, S.W., 2007b. Expression of two recombinant chloramphenicol acetyltransferase variants in highly reduced genome *Escherichia coli* strains. *Biotechnol. Bioeng.* 98, 1056–1070. <https://doi.org/10.1002/bit.21491>.
- Simen, J.D., Löffler, M., Jäger, G., Schäferhoff, K., Freund, A., Matthes, J., Müller, J., Takors, R., 2017. Transcriptional response of *Escherichia coli* to ammonia and glucose fluctuations. *Microbial biotechnology* 10, 858–872. <https://doi.org/10.1111/1751-7915.12713>.
- Stouthamer, A.H., 1973. A theoretical study on the amount of ATP required for synthesis of microbial cell material. *Antonie Leeuwenhoek* 39, 545–565. <https://doi.org/10.1007/BF02578899>.
- Stouthamer, A.H., Bettenhausen, C., 1973. Utilization of energy for growth and maintenance in continuous and batch cultures of microorganisms. *Biochim. Biophys. Acta Rev. Bioenerg.* 301, 53–70. [https://doi.org/10.1016/0304-4173\(73\)90012-8](https://doi.org/10.1016/0304-4173(73)90012-8).
- Sun, Y., Fukamachi, T., Saito, H., Kobayashi, H., 2011. ATP requirement for acidic resistance in *Escherichia coli*. *J. Bacteriol.* 193, 3072–3077. <https://doi.org/10.1128/JB.00091-11>.
- Sunya, S., Gorret, N., Delvigne, F., Uribelarra, J.-L., Molina-Jouve, C., 2012. Real-time monitoring of metabolic shift and transcriptional induction of yciG:lucDABE *E. coli* reporter strain to a glucose pulse of different concentrations. *J. Biotechnol.* 157, 379–390. <https://doi.org/10.1016/j.jbiotec.2011.12.009>.
- Takors, R., 2012. Scale-up of microbial processes: impacts, tools and open questions. *J. Biotechnol.* 160, 3–9. <https://doi.org/10.1016/j.jbiotec.2011.12.010>.
- Taymaz-Nikerel, H., Borujeni, A.E., Verheijen, P.J.T., Heijnen, J.J., van Gulik, W.M., 2010. Genome-derived minimal metabolic models for *Escherichia coli* MG1655 with estimated in vivo respiratory ATP stoichiometry. *Biotechnol. Bioeng.* 107, 369–381. <https://doi.org/10.1002/bit.22802>.
- Tomasek, K., Bergmiller, T., Guet, C.C., 2018. Lack of cations in flow cytometry buffers affect fluorescence signals by reducing membrane stability and viability of *Escherichia coli* strains. *J. Biotechnol.* 268, 40–52. <https://doi.org/10.1016/j.jbiotec.2018.01.008>.
- Tsukagoshi, N., Aono, R., 2000. Entry into and release of solvents by *Escherichia coli* in an organic-aqueous two-liquid-phase system and substrate specificity of the AcrAB-TolC solvent-extruding pump. *J. Bacteriol.* 182, 4803–4810. <https://doi.org/10.1128/jb.182.17.4803-4810.2000>.
- Valgepea, K., Peebo, K., Adamberg, K., Vilu, R., 2015. Lean-proteome strains - next step in metabolic engineering. *Frontiers in bioengineering and biotechnology* 3, 11. <https://doi.org/10.3389/fbioe.2015.00011>.
- Vasilakou, E., Loosdrecht, van, Mark, C.M., Wahl, S.A., 2020. *Escherichia coli* metabolism under short-term repetitive substrate dynamics: adaptation and trade-offs. *Microb. Cell Factories* 19, 116. <https://doi.org/10.1186/s12934-020-01379-0>.
- Veit, A., Polen, T., Wendisch, V.F., 2007. Global gene expression analysis of glucose overflow metabolism in *Escherichia coli* and reduction of aerobic acetate formation. *Appl. Microbiol. Biotechnol.* 74, 406–421. <https://doi.org/10.1007/s00253-006-0680-3>.
- Ward, V.C.A., Chatzivasileiou, A.O., Stephanopoulos, G., 2018. Metabolic engineering of *Escherichia coli* for the production of isoprenoids. *FEMS Microbiol. Lett.* 365 <https://doi.org/10.1093/femsle/fny079>.
- Weber, J., Hoffmann, F., Rinas, U., 2002. Metabolic adaptation of *Escherichia coli* during temperature-induced recombinant protein production: 2. Redirection of metabolic fluxes. *Biotechnol. Bioeng.* 80, 320–330. <https://doi.org/10.1002/bit.10380>.
- Wegerer, A., Sun, T., Altenbuchner, J., 2008. Optimization of an *E. coli* L-rhamnose-inducible expression vector: test of various genetic module combinations. *BMC Biotechnol.* 8, 2. <https://doi.org/10.1186/1472-6750-8-2>.
- Wehrs, M., Tanjore, D., Eng, T., Lievense, J., Pray, T.R., Mukhopadhyay, A., 2019. Engineering robust production microbes for large-scale cultivation. *Trends Microbiol.* 27, 524–537. <https://doi.org/10.1016/j.tim.2019.01.006>.
- Wick, R.R., Judd, L.M., Gorrie, C.L., Holt, K.E., 2017. Unicycler: resolving bacterial genome assemblies from short and long sequencing reads. *PLoS Comput. Biol.* 13, e1005595 <https://doi.org/10.1371/journal.pcbi.1005595>.
- Wilms, B., Hauck, A., Reuss, M., Sylđatk, C., Mattes, R., Siemann, M., Altenbuchner, J., 2001. High-cell-density fermentation for production of L-N-carbamoylase using an expression system based on the *Escherichia coli* rhaBAD promoter. *Biotechnol. Bioeng.* 73, 95–103. <https://doi.org/10.1002/bit.1041>.
- Ziegler, M., Zieringer, J., Takors, R., 2020. Transcriptional profiling of the stringent response mutant strain *E. coli* SR reveals enhanced robustness to large-scale conditions. *Microbial biotechnology*. <https://doi.org/10.1111/1751-7915.13738>.
- Zieringer, J., Wild, M., Takors, R., 2020. Data-driven in silico prediction of regulation heterogeneity and ATP demands of *Escherichia coli* in large-scale bioreactors. *Biotechnol. Bioeng.* <https://doi.org/10.1002/bit.27568>.

Table S1: Primer oligos used in this study

No.	Name	Function	Sequence 5'->3'
MZ_013	delta_fliR_downstream_fwd_(TS2f)	genomic deletion from flIE to flIR	TCCGTAACGGTTTATCATGTTAT
MZ_014	delta_fliR_downstream_rev_(TS2r)	genomic deletion from flIE to flIR	ATTTGAATGGTCCCTGACCT
MZ_015	delta_fliE_downstream_fwd_(TS1f)	genomic deletion from flIE to flIR	AATTAGCCAGTCGCTGAAA
MZ_016	delta_fliE_downstream_fwd_(TS1r)	genomic deletion from flIE to flIR	ATAACATGATAAACGTTACGGAAGTTTTGTAACCTGTTGTTAATTACA
MZ_033	delta_fliK_fwd_TS1f	genomic deletion of flk	CGCCAGATGTAGCGTTTTGT
MZ_034	delta_fliK_fwd_TS1r	genomic deletion of flk	GATACTGCAATTTCTCGGGTACGTATCCTTATACCTGAAATCTTC
MZ_035	delta_fliK_fwd_TS2f	genomic deletion of flk	CCCCGACGAAATGACAGTATC
MZ_036	delta_fliK_fwd_TS2r	genomic deletion of flk	GAATGGCGATTTACGGTGCC
MZ_055	flk_Deletionsanalyse_fwd	seq. of Δ flk strains	GGTCAGCAACGCCAGTATTATCG
MZ_056	flk_Deletionsanalyse_rev	seq. of Δ flk strains	CTCTGGCAAAAGTGATGTCATGG
MZ_083	fliA_Deletionsanalyse_fwd	seq. of Δ fliA strains	GCCATCACACCCATCAATGC
MZ_084	fliA_Deletionsanalyse_rev	seq. of Δ fliA strains	GTCAAACTGGGGGAGATGA
MZ_085	deltafliA_TS1f	genomic deletion of flIA	CTGGAGGATTTCTGCACAAG
MZ_086	deltafliA_TS1r	genomic deletion of flIA	CGTCAGTAAATGCCGCAC
MZ_087	deltafliA_TS2	genomic deletion of flIA	GTGGGCATTTACTGACGGATAAACAGCCCTGCGTTATATG
MZ_088	deltafliA_TS2r	genomic deletion of flIA	CTGACTGCTGTGCAAAATGG
MZ_089	Tet-SacB deltaxfiA 1	genomic deletion of flIA	ATCATTAAAGAACTCCTGGTAGTCAAAGTTAAAGTGGGGCATTACTGACGTCCTA
MZ_090	Tet-SacB deltaxfiA 2	genomic deletion of flIA	ATTTTTGTTGACACTCTATC
MZ_091	Tet-SacB fwd	amplifies tetA-sacB or fragments for SOEing PCR	CAGAAACGGATAATCATGCCGATAACTCATATAACGCAGGGCTGTTTATCATCAA
MZ_092	Tet-SacB rev	amplifies tetA-sacB or fragments for SOEing PCR	AGGAAAACTGTCCATATGC
MZ_093	Tet-SacB deltaxflk korrigiert fwd	genomic deletion of flk	TCCTAATTTTTGTTGACACTCTATC
MZ_094	Tet-SacB deltaxflk korrigiert rev	genomic deletion of flk	ATCAAAAGGGAAAACTGTCCATATGC
MZ_095	Tet-SacB Soeing rev (Tet)	amplifies tetA-sacB or fragments for SOEing PCR	AATCTCGGGCCAGGCATACCTTCCGAAAGATTTCCAGGTATAAGGATACGTATCCT
MZ_096	Tet-SacB Soeing fwd (SacB)	amplifies tetA-sacB or fragments for SOEing PCR	AATTTTTGTTGACACTCTATC
MZ_098	Tet-SacB deltaxfiC 2	genomic deletion of flIC	ATCTCTCGGTGCTGGGTATTATTGTCCAGTACTGTCAATTCCTCGGGGGATCA
MZ_099	deltafliC_dflia_TS1f	genomic deletion of flIC (in a Δ fliA context)	AAGGGAAAACTGTCCATATGC
MZ_100	deltafliC_dflia_TS1r	genomic deletion of flIC (in a Δ fliA context)	AACGACATATTCACGCACC
MZ_101	deltafliC_TS1f	genomic deletion of flIC	TCGTTGTAACCTGATTAACCTGAG
			GGCTGTTATTGGTGTCCGAG

No.	Name	Function	Sequence 5'→3'
MZ_102	deltafliC_TS2f	genomic deletion of flfC	CTCAGTTAATCAGGTTACAACGAGATTTCGTTATCCTATATCTTATGCAAGTTC
MZ_103	deltafliC_TS2r	genomic deletion of flfC	CCACGTTAATGATGCTTTGC
MZ_104	Deletionsanalyse flfC fwd	seq. of ΔflfC strains	GCCACTCATCGTAGGAGAAG
MZ_105	Deletionsanalyse flfC rev	seq. of ΔflfC strains	GATGTGACTGACAGACGATATTC
MZ_106	Deletionsanalyse flfC_fliA fwd	seq. of ΔflfC strains (in a ΔfliA context)	TTGCTCGTGTAGATGATTC
MZ_107	Tet-SacB_Kassettenweiterung fwd	amplifies tetA-sacB or fragments for SOEing PCR	CACATGGAAGTTGGAAGTCCTCTAAATTTTTGTTGACACTCTATC
MZ_108	Tet-SacB delatflic fwd_neu	genomic deletion of flfC	ATCAGGCAATTTGGCGTTGCCGTCAGTCTCAGTTAATCAGGTTACAACGACACA TGGAAAGTTGGAAGTCC
MZ_109	TetA-sacB delatcspD_1	genomic deletion of cspD	CGATCGGCTGGCATTTTGCCTTTAGGATGTACACAATGAGACAGAAGAGCACA TGGAAAGTTGGAAGTCC
MZ_110	TetA-sacB delatcspD_2	genomic deletion of cspD	CCCGTTTATCCATCTTACTTGTATAAGATTTGCCGAAGGATGTCGAAGCATCAA AGGAAAACCTGCCATATGC
MZ_111	deltacspD_TS1f	genomic deletion of cspD	GCAGTAAAGTGCTGCGTG
MZ_112	deltacspD_TS1r	genomic deletion of cspD	ATGTCGAAAGCCCTCTCTGTCTCATTGTGTACATC
MZ_113	deltacspD_TS2f	genomic deletion of cspD	GACAGAAAGAGGCTTCGACATCCTTCGC
MZ_114	deltacspD_TS2r	genomic deletion of cspD	CTTGTTCACCATCGCCACTT
MZ_115	Deletionsanalyse cspD fwd	seq. of ΔcspD strains	AACAGTCGATGTTTGGTAGC
MZ_116	Deletionsanalyse cspD rev	seq. of ΔcspD strains	AGCAATGGATGCTCATTCTC
MZ_119	deltafig_TS1f	genomic deletion from flgN to flgL	GCGTTGGGCATCTTTCC
MZ_120	deltafig_TS1r	genomic deletion from flgN to flgL	AGATTATCTCCGGCCTGCAC
MZ_121	deltafig_TS2f	genomic deletion from flgN to flgL	GTGCAGGCCGGAGATAAATCTTTTCGCTTTAAAAACATATCATGAA
MZ_122	deltafig_TS2r	genomic deletion from flgN to flgL	GTCTGATGTTGCCGTAGC
MZ_123	Deletionsanalyse flg fwd	seq. of ΔflgNMABCDEFHGHIJKL strains	GTCTTGGATGTATTACGCCG
MZ_124	Deletionsanalyse flg rev	seq. of ΔflgNMABCDEFHGHIJKL strains	CAAAGTCTGGATCCGCTATC
MZ_125	Deletionsanalyse flg WT rev	seq. of ΔflgNMABCDEFHGHIJKL strains (WT var)	CTGGCGACGCTGGATTA
MZ_132	TetA-sacB delatfig_1_neu	genomic deletion from flgN to flgL	GGACGGTGAACAATGCATTCGGCCTGCAGTGCAGGCCGGAGATAATCTCAC ATGGAAGTTGGAAGTCC
MZ_133	TetA-sacB delatfig_2_neu	genomic deletion from flgN to flgL	GAGCAGGCAGACAAAAACATACCCAGTTTCATGATATGTTTTAAAGCGAAAAATCAA AGGAAAACCTGCCATATGC
MZ_134	TetA-sacB delatfliE_1	genomic deletion from flfE to flfR	CCATGCCACCGCGTGGATCGGATGTAATAAACACAGGTTACAAAACCCACA TGGAAAGTTGGAAGTCC
MZ_135	TetA-sacB delatfliR_2	genomic deletion from flfE to flfR	GGTATTAATTTTCGGATAATCCCTTAGGATAACATGATAAACCGTTACGGAAATCAA AGGAAAACCTGCCATATGC
MZ_136	TetA-sacB delatfliH_1	genomic deletion from flhE to motA	TTTTCACTGAGTTATTAACATACTCGCGAGCGGTAATTTTTTTTGTCTCACATG GAAGTTGGAAGTCC

No.	Name	Function	Sequence 5'->3'
MZ_137	TetA-sacB delatflh_2	genomic deletion from flhE to motA	CGCTGACGACTGAACATCCTGTGCATGGTCAACAGTGGAAAGGATGATGTCAATCA AAGGGAAAACGTCCATATGC ACCATGACATTTTCAGCCATC AGGACAAAAAATAACGGCGC GCGCGTAAATTTTTTGTCTCTGACATCATCTCCCTTCCACTGTGTG GCTGGAAAGCGGAAACACA GTGAGAGTGAAGCCTGATCA CATCATGCTCTCAACACGCT CGGCGGAAAGTTATACGCTA ATTAACAATGTATTCACCGGAAACAAACATATAAATCACAGGAGTCCGCCCCACAT GGAAGTTGGAAGTCC AAACTGACGCGCACAGCGGGAGGAAAAAACCTCCGCCTCTTTCACTCAATCA AAGGGAAAACGTCCATATGC GTTGTTTCAGGACCCACCAT GGGCGACTCTGTGATTTAT ATAAATCACAGGAGTCCCTGAGTGAAGAGGGGGGAG TCATGCCATACTGGCACCC CTGATTAGTGGTGGTATCGG GTGCAGAAATCATTGTCGAA GTCATTGCGATGCGCCTTC GCGATGAAACGGTCTTGG ACATTTACGGATAACGCTG ACTACACCGTAATTAATTTTACCCGGCTCTTCTGCAATGCCAGTTTATCCCACAT GGAAGTTGGAAGTCC ATGATGTTTTGCGCGCCTATCGCTACGGCTGTGCGGAAATAAGGACGGTATATCA AAGGGAAAACGTCCATATGC GAAAACCTTTCACCTGGCAAGGT AGGACGGTAAATTAATACGGGTGAGTATTGTTCTG ACCGTAATTAATACCGTCCCTTATTCGGCAC CGTCCCGCATTAACCTTTG TACCACAGAAAACGGCCGGA GCAACGTCAAACCCAGGTC AATAATAAAAAAGCCCGGCTCATGCCGGGCAAAAAGTACCAGTTACGTCACA TGGAAAGTTGGAAGTCC
MZ_138	delatflh_TS1f	genomic deletion from flhE to motA	
MZ_139	delatflh_TS1r	genomic deletion from flhE to motA	
MZ_140	delatflh_TS2f	genomic deletion from flhE to motA	
MZ_141	delatflh_TS2r	genomic deletion from flhE to motA	
MZ_142	Deletionsanalyse flh fwd	seq. of Δ flhEABcheZYBRtaptarcheWAmotBA strains	
MZ_143	Deletionsanalyse flh rev	seq. of Δ flhEABcheZYBRtaptarcheWAmotBA strains	
MZ_144	Deletionsanalyse flh WT rev	seq. of Δ flhEABcheZYBRtaptarcheWAmotBA strains (WT)	
MZ_145	TetA-sacB delta_aldA_1	genomic deletion of aldA	
MZ_146	TetA-sacB delta_aldA_2	genomic deletion of aldA	
MZ_147	delta_aldA_TS1f	genomic deletion of aldA	
MZ_148	delta_aldA_TS1r	genomic deletion of aldA	
MZ_149	delta_aldA_TS2f	genomic deletion of aldA	
MZ_150	delta_aldA_TS2r	genomic deletion of aldA	
MZ_151	Deletionsanalyse aldA fwd	seq. of Δ aldA strains	
MZ_152	Deletionsanalyse aldA rev	seq. of Δ aldA strains	
MZ_164	Deletionsanalyse flIE-R fwd	seq. of Δ flIEFGHIJMLNQPQR strains	
MZ_165	Deletionsanalyse flIE-R rev	seq. of Δ flIEFGHIJMLNQPQR strains	
MZ_166	Deletionsanalyse flIE-R WT rev	seq. of Δ flIEFGHIJMLNQPQR strains (WT variant)	
MZ_167	TetA-SacB delta gatRDCBA fwd	genomic deletion from gatR to gata	
MZ_168	TetA-SacB delta gatRDCBA rev	genomic deletion from gatR to gata	
MZ_169	delta_gtc_TS1 fwd	genomic deletion from gatR to gata	
MZ_170	delta_gtc_TS1 rev	genomic deletion from gatR to gata	
MZ_171	delta_gtc_TS2 fwd	genomic deletion from gatR to gata	
MZ_172	delta_gtc_TS2 rev	genomic deletion from gatR to gata	
MZ_173	Deletionsanalyse gat fwd	seq. of Δ gatABCDR strains	
MZ_174	Deletionsanalyse gat rev	seq. of Δ gatABCDR strains	
MZ_184	TetA-SacB delta uhpTCBA fwd	genomic deletion from uhpT to ohpA	

No.	Name	Function	Sequence 5'→3'
MZ_185	TetA-SacB delta uhp TCBA rev	genomic deletion from uhpT to ohpA	GCTTATCGTTAAGGTAAGGGCGGTATTTTTTTACCCGGCCAGGACAAGACCATCAA AGGAAAAACTGTCCATATGC
MZ_186	delta_uhp_TS1 fwd	genomic deletion from uhpT to ohpA	CGGCTTTGGACTGAATG
MZ_187	delta_uhp_TS1 rev	genomic deletion from uhpT to ohpA	AGGACAAAGACACGTAACCTGGTACTTTTTG
MZ_188	delta_uhp_TS2 fwd	genomic deletion from uhpT to ohpA	CCAGTTACGTGTCTTGTCCCTGGCGGGTAA
MZ_189	delta_uhp_TS2 rev	genomic deletion from uhpT to ohpA	CGATCCGCAGGCTTCATTG
MZ_190	Deletionsanalyse uhp fwd	seq. of ΔuhpTCBA strains	TTGAGCGTTACGGGCAACGG
MZ_191	Deletionsanalyse uhp rev	seq. of ΔuhpTCBA strains	GGATTCGGCCTCGAAACCTG
MZ_192	TetA-SacB delta yeel. fwd	genomic deletion of yeel	ATGACACCACCGTTTATAACAGATCGGCATTACTATGCATAAGTACTGTCCACAT GGAAGTTGGAAGTCC
MZ_193	TetA-SacB delta yeel. rev	genomic deletion of yeel	AGTCTGATAGACTGCATTGCATTATAACCAGTAGGGAGGGGAGGTTAGGTATCA AAGGGAAAACTGCCATATGC
MZ_194	delta_yeel_TS1 fwd	genomic deletion of yeel	TGAAGAGTTGGTGGGTG
MZ_195	delta_yeel_TS1 rev	genomic deletion of yeel	GAGGTTAGGTGACAGTACTTATGCATAGTAATGC
MZ_196	delta_yeel_TS2 fwd	genomic deletion of yeel	AAGTACTGTCACCTAACCTCGCCTCC
MZ_197	delta_yeel_TS2 rev	genomic deletion of yeel	GACGGAAAAAGAAAATCCGACG
MZ_200	TetA-SacB delta fixA fwd	genomic deletion of fixA	TAAAGATTTTTTGTGCATGCCGATAGTGCTTTTTTAAAAAGGAGAAATCTCACAT GGAAGTTGGAAGTCC
MZ_202	delta_fixA_TS1 fwd	genomic deletion of fixA	GGCAAGTCACGAAAGGAA
MZ_203	delta_fixA_TS1 rev	genomic deletion of fixA	GGCTGTACAGATTTCTCCTTTTAAAAAAGCACACT
MZ_204	delta_fixA_TS2 fwd	genomic deletion of fixA	GGAGAAATCTGTGACAGCCGGTATTGTGG
MZ_205	delta_fixA_TS2 rev	genomic deletion of fixA	ACGCAAAAGTCATCAGCAAGT
MZ_208	Deletionsanalyse fixA fwd neu	seq. of ΔfixA strains	TATCGCACTACAACATGC
MZ_209	Deletionsanalyse fixA rev neu	seq. of ΔfixA strains	GTTAAACCTAAAAGCTGACC
MZ_210	Deletionsanalyse yeel fwd neu	seq. of ΔyeelL strains	GCCAAAATCAGGAGGC
MZ_211	Deletionsanalyse yeel rev neu	seq. of ΔyeelL strains	GTCAGCATTAAACATGGC
MZ_228	TetA-SacB delta fixA rev neu	genomic deletion of fixA	AAGGCTGATGGCGAAAAGTGGCCCGATGAGGGCCACAATACGGCTGTACACATC AAAGGGAAAACTGCCATATGC
MZ_425	rhaB*_BW3110_fwd	creation of rhaB- strains	CGATAACTGAAGTAATCCGG
MZ_426	rhaB*_BW3110_rev	creation of rhaB- strains	ATGACCTTTCGCAATTGTGTC
MZ_427	tetA*_fwd_rhaB	creation of rhaB- strains	AGGGCAGAAAACCTGGATGCCGCTACGTTTGATAAATATCGCGGTTTGGCCGAGTCACA TGGAAGTTGGAAGTCC
MZ_428	SacB_rev_rhaB	creation of rhaB- strains	AAATCCATCGTTTTTAAACAATGGGCTGCATAGTCAGAACGGGCTATGTCCACCATCAA AGGAAAAACTGCCATATGC
MZ_429	rhaB*_Seq_fwd	seq. of rhaB- allele	CAAAACCAGGCTTTGTGG

No.	Name	Function	Sequence 5'->3'
MZ_430	rhaB*_Seq_rev	seq. of rhaB- allele	GTGAGCATCACATCACCAC
MZ_431	TetA*_rev	ampl. tetA* with 107 for Gibson Ass. of pJOE 4056.2_tetA	CTCTTGGGTTATCAAGAGGG
MZ_432	pJOE_backbone_rev_tetA	Gibson Assembly of pJOE4056.2_tetA	GGACTTCCAACTTCCATGTGAAGAGTTTGTAGAAAACGCCAAAAAAG
MZ_433	pJOE_backbone_fwd_tetA	Gibson Assembly of pJOE4056.2_tetA	CCCTCTTGATAACCCCAAGAGGTCAGACCCCGTAGAAAAAG
MZ_434	pJOE_Seq1	seq. of pJOE4056.2 and pJOE4056.2_tetA	GTGACCACCCTGACCTACCG
MZ_435	pJOE_Seq2	seq. of pJOE4056.2 and pJOE4056.2_tetA	GGATCACTCTCGGCATGGA
MZ_436	pJOE_Seq3	seq. of pJOE4056.2 and pJOE4056.2_tetA	CTTGGTTTAATAGCGGGGCC
MZ_437	pJOE_Seq4	seq. of pJOE4056.2 and pJOE4056.2_tetA	TTATTGGCTGGTGGGGAT
MZ_438	pJOE_Seq5	seq. of pJOE4056.2 and pJOE4056.2_tetA	CTGTCCCTTCTAGTGTAGCCGT
MZ_439	pJOE_Seq6	seq. of pJOE4056.2 and pJOE4056.2_tetA	TTTCCTGCGTTATCCCCTGA
MZ_440	pJOE_Seq7	seq. of pJOE4056.2 and pJOE4056.2_tetA	GCGTTAATGTCTGGCTTCTGA
MZ_441	pJOE_Seq8	seq. of pJOE4056.2 and pJOE4056.2_tetA	AACGACAGGAGCACGATCAT
MZ_442	pJOE_Seq9	seq. of pJOE4056.2 and pJOE4056.2_tetA	AGAATCATAATGGGAAGGCC
MZ_443	pJOE_Seq10	seq. of pJOE4056.2 and pJOE4056.2_tetA	TTGTACGACCCGCTAAAAACG
MZ_450	pJOE_Seq_r1	seq. of pJOE4056.2 and pJOE4056.2_tetA	GAAC TTGTGGCCGTTTACG
MZ_451	pJOE_Seq_r2	seq. of pJOE4056.2 and pJOE4056.2_tetA	CTTGCTGGATCCCATGATGATG
qPCR Primer pairs			
	cysG_housekeeping_forward	qPCR analysis: cysG	CCCCAGGAAGAGATTAACCAG
	cysG_housekeeping_reverse	qPCR analysis: cysG	GGAATACCCCGAATAGGCAGAG
	egfp_2_forward	qPCR analysis: eGFP	TTCTTCAAGTCCGCCCATGCC
	egfp_2_reverse	qPCR analysis: eGFP	AAGTTCACCTTGATGCCCGTTC

Supplementary Information S2: Experimental procedures (additional information)

Construction of Deletion Strains

For each deletion locus, two cycles of recombination were used to first insert the dual-selectable *tetA-sacB* cassette and second to replace it with a fused DNA construct of sequences adjacent to the deletion locus. Successful recombination with the construct effectively resulted in the deletion of the target locus. Initially, the original strain was transformed with pSIM5. pSIM5 contains the *exo*, *bet*, and *gam* genes of bacteriophage lambda under transcriptional control of a temperature inducible system allowing induction at 42 °C and normal growth at 30 °C. Moreover, pSIM5 has a temperature-sensitive origin of replication that enables curing of the plasmid upon cultivation in non-selective media at 37 °C.

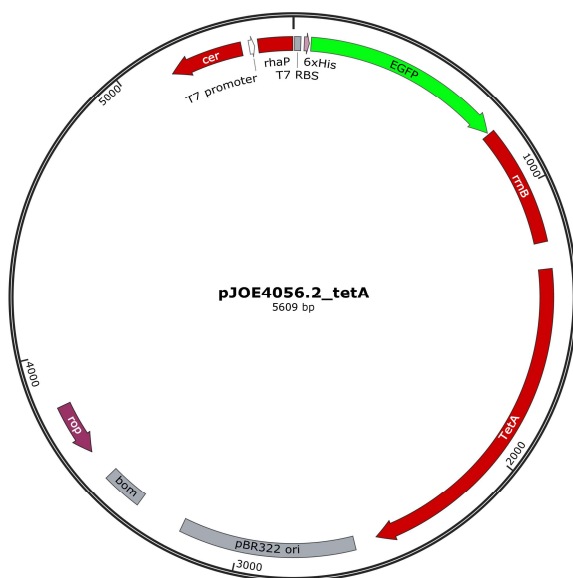
For the first recombineering cycle, the *tetA-sacB* cassette was amplified from the genome of T-SACK and used as a template for amplifying DNA fragments carrying about 50 bp of homologous arms for chromosomal recombination. If necessary, homologous arms were added separately to *tetA* and *sacB* and the fragments joined by overlap PCR. A strain carrying pSIM5 was then cultivated in 10 ml 2xTY medium in a 50 ml baffled shaking flask at 30 °C on a rotary shaker set to 130 rpm until an OD of 0.2 was reached. The culture was transferred into a 42 °C water bath and agitated for 15 min to induce recombineering proteins from pSIM5. Cells were then chilled on ice and electro-competent cells were prepared following standard protocols. Cells were transformed with about 100 ng of the *tetA-sacB* PCR product carrying homologous arms and regenerated in SOC medium at 37 °C for 3 – 4 hours. Regenerated cells were plated on 2xTY agar plates containing tetracycline. A single colony was picked and again transformed with pSIM5 to yield a recombineering competent intermediate strain carrying a chromosomal copy of the *tetA-sacB* cassette in the target locus.

For the second cycle of recombination, first the recombineering template was constructed by amplification of DNA sequences from the genome of *E. coli* MG1655 adjacent to the deletion locus and joining of these sequences by overlap PCR to create a fused construct of the neighboring regions. The homologous arms created in this step ranged from about 200 to 500 bp. The intermediate strain was subjected to the same procedure as described for the first recombination cycle. Cells were then transformed with about 100 ng of the target DNA sequence, regenerated in SOC medium at 37 °C for 3 – 4 hours and plated on counterselection agar. After incubation for 2 days at 42 °C large colonies were picked and tested for the absence of tetracycline resistance by streaking onto 2xTY agar plates containing tetracycline. Colonies showing no growth on tetracycline agar plates were cultivated in 2xTY at 37 °C, their DNA isolated and the presence of the deletion locus verified by sequencing.

Construction of eGFP production strains

Recombineering of *E. coli* MG1655 and *E. coli* RM214 was conducted as described in the previous section. For the first cycle of recombineering a *tetA-sacB* cassette with homology to the *rhaB* gene was created by amplifying the *tetA-sacB* cassette from the genome of T-SACK with primers 427 and 428. The resulting intermediate strain was then subjected to a second cycle of recombineering with a copy of the inactive *rhaB* gene amplified from the genome of *E. coli* BW3110 pJOE4056.2 with primers 425 and 426. After counter-selection and testing for the absence of tetracycline resistance the presence of the frameshift mutation was verified by sequencing and the inability of the strains to ferment rhamnose confirmed by streaking on 2xTY indicator agar plates containing rhamnose.

The backbone of pJOE4056.2 was amplified with primers 432 and 433. The *tetA* cassette was amplified from the genome of T-SACK with primers 107 and 431. The two fragments were joined and circularized in a Gibson assembly reaction (Gibson et al., 2009) to yield pJOE4056.2_ tetA and *E. coli* DH5 α λ pir was transformed with the reaction product by electroporation. After verification of the plasmid by partial sequencing, *E. coli* MG1655 *rhaB*⁻ and *E. coli* RM214 *rhaB*⁻ were transformed with pJOE4056.2_ tetA. Finally, the resulting strains were streaked on 2xTY indicator plates with rhamnose to confirm both the absence of rhamnose catabolism as well as the induction of eGFP production in presence of rhamnose and absence of glucose.



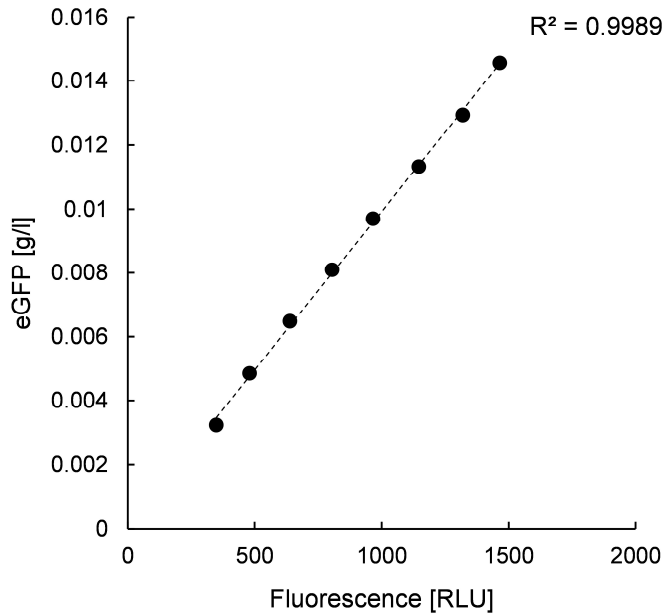
Supplementary Figure S2A. Plasmid map of pJOE4056.2_tetA.

Purification and Quantification of eGFP

E. coli BW3110 pJOE4056.2 was cultivated in glucose-limited minimal medium in preliminary experiments. Cells were harvested by centrifugation, resuspended in homogenization buffer (14 mM magnesium acetate, 60 mM potassium acetate, 10 mM Tris pH 8.0, 2 mM dithiothreitol) using approximately 1 ml buffer per 1 g of cell mass and passed twice through a high pressure homogenizer at 15 – 20 kPa. Homogenized cell suspension was cleared by centrifugation at 15.000 g for 15 min. Purification of his-tagged eGFP was conducted using nickel affinity chromatography (running buffer: 50 mM Tris-HCl pH 7.0, elution buffer: 50 mM tris-HCl pH 7.6, 15 mM Imidazol).

The concentration of purified eGFP stock solution was determined to be 3.236 g/l by Bradford Assay. The stock solution was diluted with ice-cold PBS-MgCa to measure an eGFP calibration curve. 200 μ l of diluted stock were transferred into a black 96 well-plate with transparent bottom and lid and the fluorescence (excitation 485 nm, emission 535 nm) quantified in a SLT SpectraFluor plate-reader (Tecan, Switzerland). The resulting calibration curve was used to convert the fluorescent values of bioprocess samples to eGFP concentrations [g/l]:

$$C_{eGFP} = RLU_{sample} * 9.9135 * 10^{-6} + 9.6462 * 10^{-6}$$



Supplementary Figure **S2B**. Calibration curve for the conversion of fluorescence units to eGFP concentration.

Bioreactor Setup

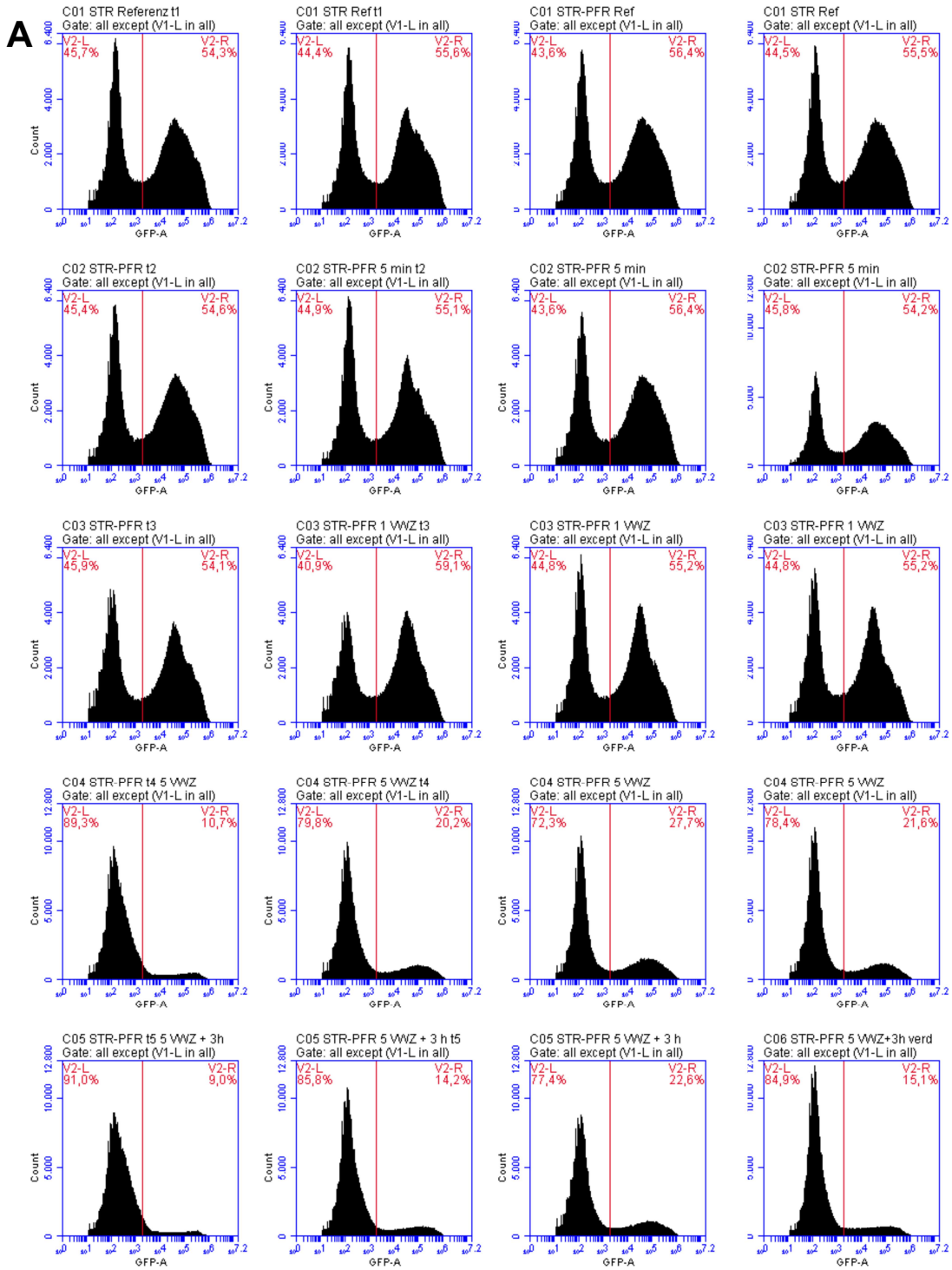
The primary reactor was a 3 l bioreactor (Bioengineering, Wald, Switzerland) equipped with flow baffles and two six-blade Rushton type impellers operated at 1000 rpm. A constant aeration rate of 2.0 standard liters of ambient pressurized air per minute was employed and the system operated at a total pressure of 1.5 bar. Temperature was monitored by a platinum resistance thermometer and regulated by electrical heating or water cooling. Temperature was set to 37 °C. The reactor was equipped with a pH sensor (Mettler Toledo, Columbus, USA) to control pH and a pO₂ sensor for monitoring dissolved oxygen tension (PreSens, Regensburg, Germany). During all fermentation stages pH was set to 7.0 and regulated by automated addition of 3 M NaOH or 2.5 M H₃PO₄. Dissolved oxygen tension was not regulated but maintained values above 50% saturation to 1.5 bar ambient air at all times. In the exhaust gas stream, the concentration of oxygen and carbon dioxide was measured by gas sensors (BlueSens, Herten, Germany). During the chemostat phase the feed was constantly added to the reactor by a peristaltic pump (Watson-Marlow, Falmouth, United Kingdom). The feed flow was monitored by a balance recording the weight of the stirred feed barrel and manually adjusted if necessary. The harvesting pump operated as a slave pump set to maintain a constant weight of the bioreactor. For this purpose, the stirred tank reactor was installed on a balance as well.

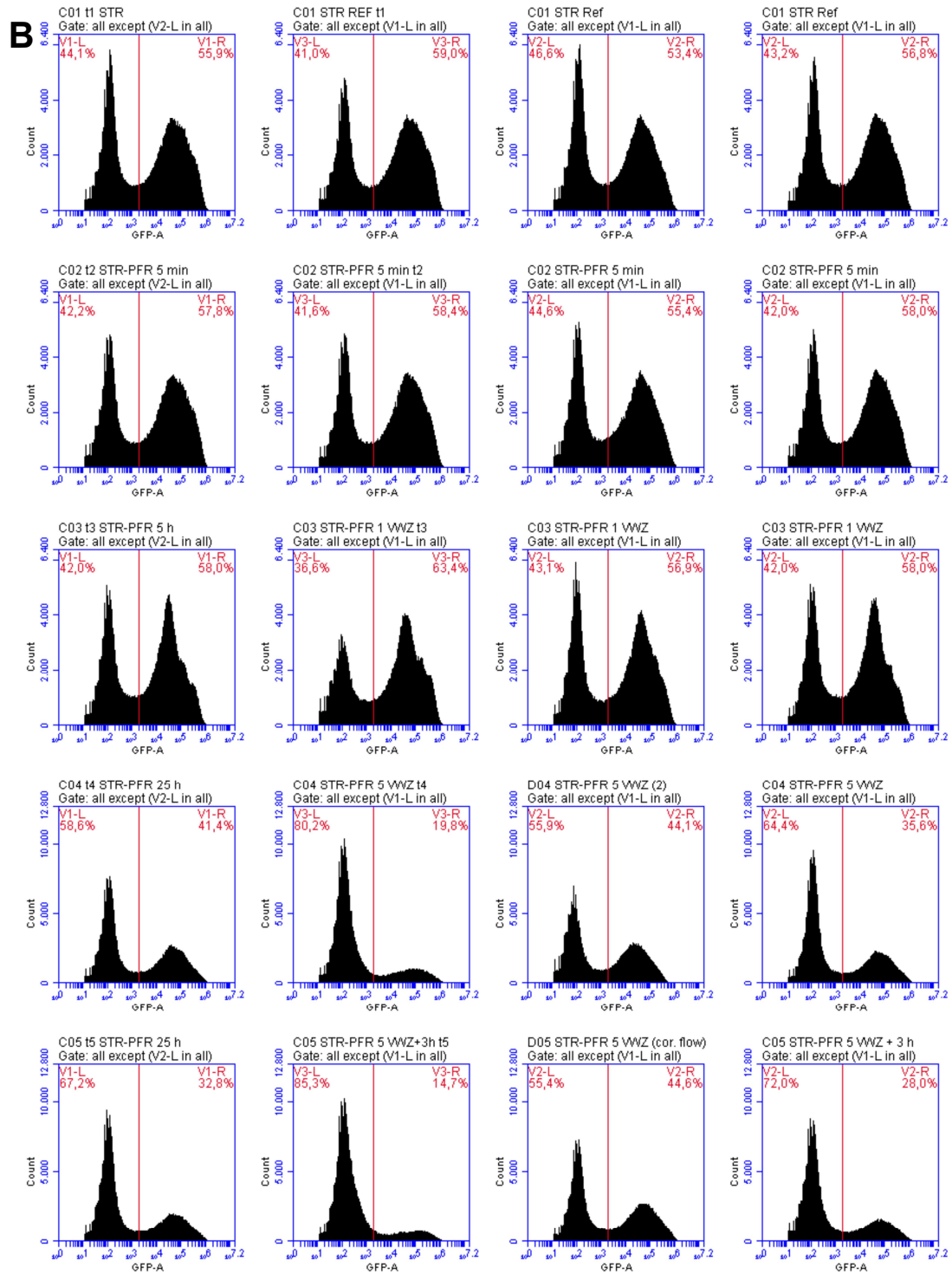
The secondary compartment was a plug-flow reactor with an inner tube diameter of 20 mm and a total volume of approximately 380 ml. Five ports along the primary axis were used to take samples throughout the cultivation. Next to the first port P1 additional constant aeration was provided at 0.15 standard liters per minute. In the PFR, oxygen saturation was monitored close to ports P1 and P5 and maintained levels above 30% saturation of ambient air conditions throughout the cultivation. Temperature in the PFR was maintained at 36 – 37 °C by water heating and isolation material. A diaphragm metering pump (Sigma/1, ProMinent, Heidelberg, Germany) was used to transfer biosuspension from the stirred tank reactor the plug flow reactor after connection of the two reactors.

Sequence analysis of *E. coli* RM214

Conducting the genomic deletions required a high number of total passages until *E. coli* RM214 was completed. We sequenced both the genome of *E. coli* MG1655 and *E. coli* RM214 to ensure no detrimental mutations or rearrangements had occurred (see also Supplementary Information S8). We first compared the sequence of our *E. coli* MG1655 isolate to the reference sequence NC_000913.3 which revealed the presence of two known sequence variations in different isolates of *E. coli* MG1655 affecting *gatC* and *glpR* (Freddolino et al., 2012). We found additional SNPs in *gfcD*, *yciG*, *wbbI* and an insertion in an intergenic region, none of which appear to confer a detrimental phenotype in standard cultivations. Sequence analysis of *E. coli* RM214 revealed additional SNPs in *elfC*, *trmD*, *dcuD*, the reversion of the SNP in *gfcD* and multiple SNPs in *insH5* in the *rac* prophage region. All these mutations are irrelevant as *elfC* is only involved in pathogenicity, *dcuD* encodes a weakly expressed C4-carboxylate transporter not beneficial in glucose minimal medium and *insH5* is known to be a mutational hotspot. TrmD is an essential tRNA-methyltransferase and the mutation confers an amino acid exchange [H78N]. However, inspection of the structure of TrmD revealed that the exchange had happened far away from the catalytically active center thus presumably not affecting the biological function. Our considerations are supported by the normal growth phenotype exhibited by all strains of the deletion series.

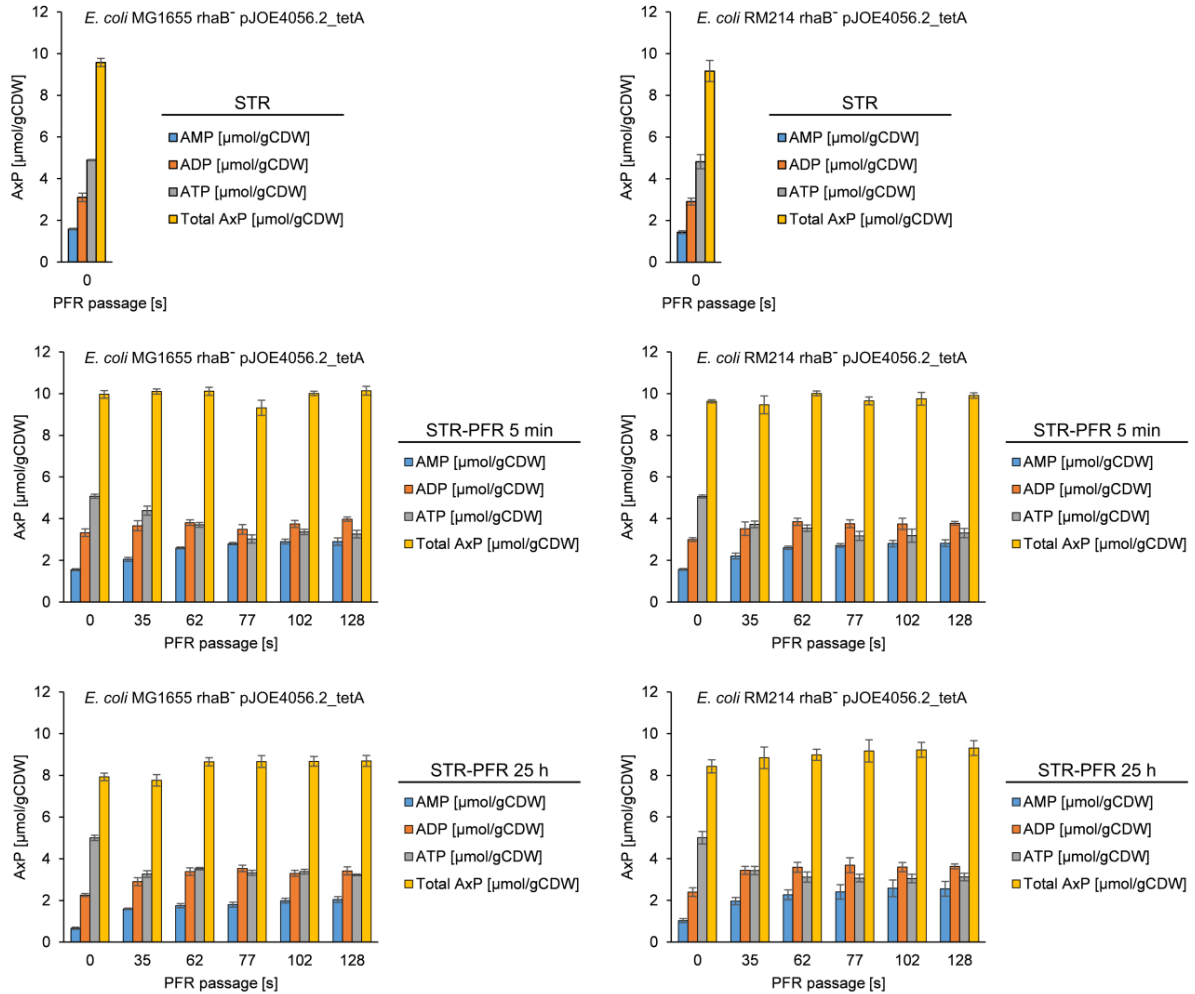
Supplementary Figure S3: Flow cytometry histograms





Supplementary Figure S3. Flow cytometry histograms of green fluorescence signals. The vertical red line (2000 RLU in signal GFP-A) indicates the division line used to separate non-producer cells (V1-L) from producer cells (V1-R). Each column of histograms was recorded from a single fermentation ($n = 4$ for each strain). Rows indicate the time-point of sampling (1st: STR reference sample, 2nd: STR-PFR 5 min, 3rd: STR-PFR 5 h, 4th: STR-PFR 25 h, 5th: STR-PFR 28 h). **A**: *E. coli* MG1655 *rhaB*⁻ pJOE4056.2_tetA. **B**: *E. coli* RM214 *rhaB*⁻ pJOE4056.2_tetA.

Supplementary Information S4: AxP concentrations and statistical evaluation.



Supplementary Figure **S4A**. AxP concentrations. Individual cellular levels of AMP, ADP, ATP and the total of all three substances along the PFR passage. The STR sample is indicated at 0 s, the following five samples correspond to the five ports along the primary axis of the PFR and are indicated at the respective mean residence time. The figures show samples from different time-points of the cultivations as given in the figure legend (STR, STR-PFR 5 min, STR-PFR 25 h). **Left:** *E. coli* MG1655 rhaB⁻ pJOE4056.2_tetA. **Right:** *E. coli* MG1655 rhaB⁻ pJOE4056.2_tetA. Error bars represent SEM (n = 4).

Table S4B: Statistical evaluation of AEC values from the primary reactor (STR)

Time point	intra-strain comparison								inter-strain comparison	
	<i>E. coli</i> MG1655 rhaB ⁻ pJOE4045.2_tetA				<i>E. coli</i> RM214 rhaB ⁻ pJOE4045.2_tetA				p	
	Mean AEC	SEM	p		Mean AEC	SEM	p			
STR	0.673	0.0032	-	n. s.	0.684	0.0056	-	n. s.	0.15	n. s.
STR-PFR 5 min	0.677	0.0038	0.46	n. s.	0.681	0.0060	0.77	n. s.	0.57	n. s.
STR-PFR 25 h	0.774	0.0080	2.4*10 ⁻⁵	***	0.734	0.017	0.028	*	0.077	n. s.

Statistics were calculated from n = 4 biological replicates. Significance indicators (two-tailed t-test): *** p < 0.001, ** p < 0.01, * p < 0.05. For the intra-strain comparison mean AEC values of a single strain at STR-PFR 5 min or STR-PFR 25 h were compared to its STR value. For the inter-strain comparison mean AEC values of the two strains at a single time point were compared.

Table S5.A: Carbon balance of *E. coli* MG1655 rhaB⁻ pJOE4056.2_tetA.

Process stage	CDW [%]	Acetate [%]	Rhamnose [%]	CO ₂ (g) [%]	CO ₂ (aq) [%]	Total [%]
STR	36.3 ± 0.8 ^a	0.5 ± 0.1	7.9 ± 0.1	49.9 ± 0.8	3.1 ± 1.0	97.7 ± 2.4
STR-PFR 5 min	34.6 ± 0.6	0.4 ± 0.1	7.9 ± 0.1	53.2 ± 0.5	1.5 ± 0.6	97.7 ± 0.8
STR-PFR 5 h	35.8 ± 0.3	0.7 ± 0.1	7.9 ± 0.1	47.9 ± 0.8	1.7 ± 0.4	94.0 ± 0.9
STR-PFR 25 h	38.1 ± 0.7	0.2 ± 0.1	7.9 ± 0.1	48.1 ± 0.3	1.8 ± 0.5	96.0 ± 1.0
STR-PFR 28 h	38.7 ± 0.5	0.1 ± 0.1	7.9 ± 0.1	47.9 ± 0.4	1.8 ± 0.4	96.3 ± 0.6

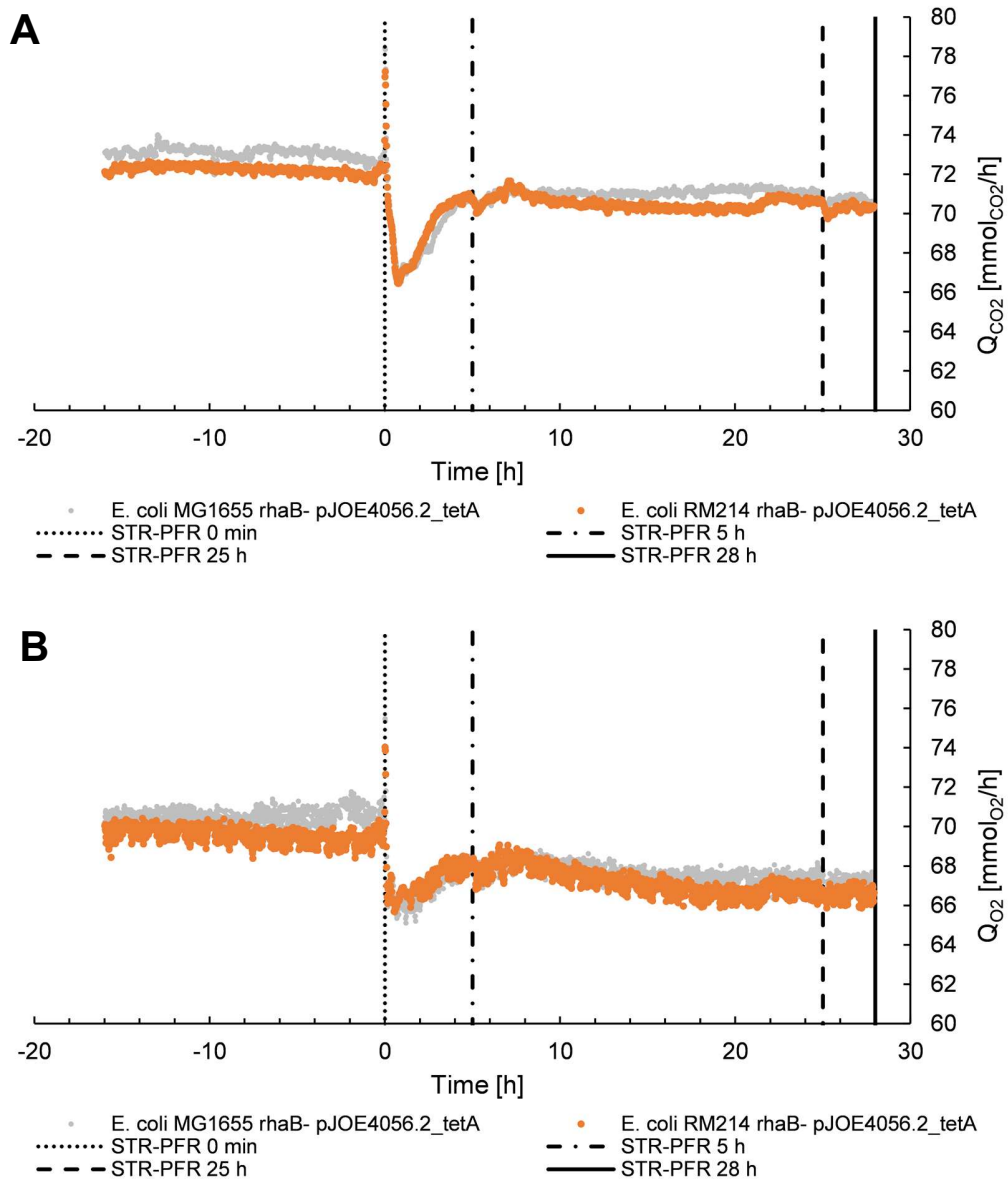
^a: Errors indicate SEM (n = 4).

Table S5.B: Carbon balance of *E. coli* RM214 rhaB⁻ pJOE4056.2_tetA.

Process stage	CDW [%]	Acetate [%]	Rhamnose [%]	CO ₂ (g) [%]	CO ₂ (aq) [%]	Total [%]
STR	37.3 ± 0.6	0.3 ± 0.1	7.9 ± 0.1	48.9 ± 0.3	3.5 ± 0.7	97.9 ± 1.1
STR-PFR 5 min	35.5 ± 0.7	0.3 ± 0.1	7.9 ± 0.1	52.5 ± 1.1	3.4 ± 0.7	99.6 ± 2.0
STR-PFR 5 h	36.2 ± 0.3	0.7 ± 0.2	7.9 ± 0.1	48.0 ± 1.0	3.3 ± 0.6	96.1 ± 1.4
STR-PFR 25 h	37.8 ± 0.7	0.3 ± 0.1	7.9 ± 0.1	47.3 ± 0.3	3.3 ± 0.7	96.7 ± 0.9
STR-PFR 28 h	38.3 ± 0.5	0.2 ± 0.1	7.9 ± 0.1	47.1 ± 0.2	3.6 ± 0.8	97.1 ± 0.7

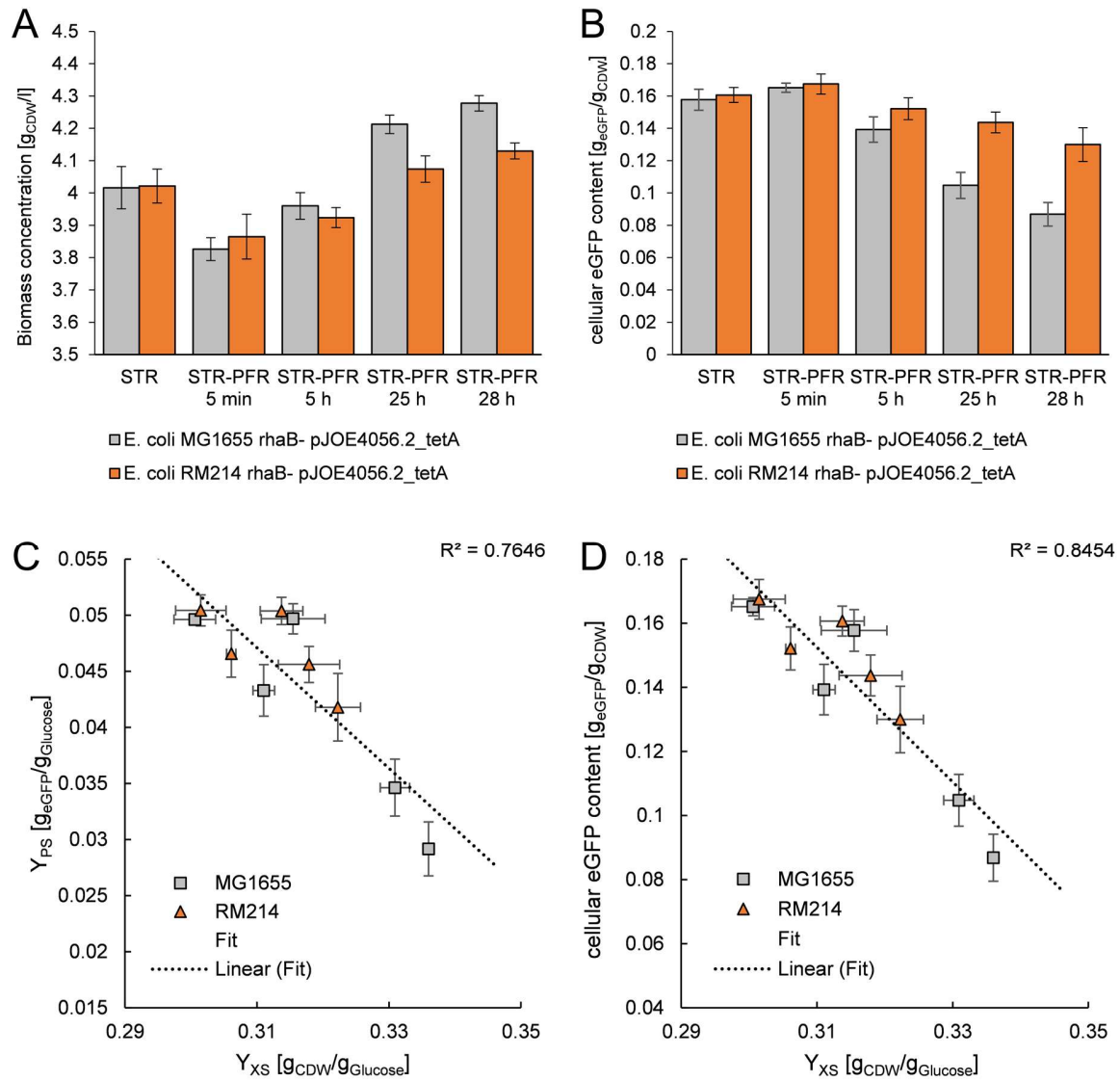
^a: Errors indicate SEM (n = 4).

Supplementary Figure S6: Exhaust Gas Parameters



Supplementary Figure S6. Exhaust Gas Parameters. **A**: Oxygen uptake rate Q_{O_2} . **B**: Carbon Dioxide formation rate Q_{CO_2} . Values represent means of four fermentations with data synchronized to $t = 0$ h. Technical measurement artifacts were eliminated prior to data analysis. Vertical lines indicate relevant process timepoints: PFR connection (STR-PFR 0 min) and sampling points after 1 volumetric residence time (STR-PFR 5 h), after 5 volumetric residence times (STR-PFR 25 h) and prior to abortion of the fermentation (STR-PFR 28 h).

Supplementary Figure S7: Cell Dry Weight and eGFP production



Supplementary Figure S7. Cell Dry Weight and eGFP production. **A**: Biomass concentration. **B**: Cellular eGFP content. **C**: Correlation of declining product yield and increasing biomass yield. **D**: Correlation of declining cellular eGFP content and increasing biomass yield. Correlations were calculated from all data points. Error bars represent SEM (n = 4).

Supplementary Data S8: Estimation of ATP demand for eGFP production

The maintenance model by Pirt describes the partition of substrate uptake for growth or maintenance demand (Pirt, 1965). See below for parameter explanations.

$$(1) \quad q_S = q_{S,\mu} + m_S$$

In analogy, we can differentiate between ATP demand for growth and ATP demand for maintenance.

$$(2) \quad q_{ATP} = q_{ATP,X} + m_{ATP}$$

Assuming complete oxidation of substrate used for maintenance requirements and an ATP formation of $Y_{ATP,S} = 16.4 \text{ mmol}_{ATP} * \text{mmol}_{Glucose}^{-1}$ (2 mol ATP from glycolysis, P/O-Ratio of 1.2 in the respiratory chain), we can estimate m_{ATP} from m_S .

$$(3) \quad m_{ATP} = m_S * Y_{ATP,S}$$

Inserting data from the heterogeneous STR-PFR conditions yields:

$$E. coli \text{ MG1655:} \quad m_{ATP} = m_S * Y_{ATP,S} = 0.14 \frac{g_{Glucose}}{g_{CDW} * h} * 16.4 \frac{mol_{ATP}}{mol_{Glucose} * h} = 12.74 \frac{mmol_{ATP}}{g_{CDW} * h}$$

$$E. coli \text{ RM214:} \quad m_{ATP} = m_S * Y_{ATP,S} = 0.10 \frac{g_{Glucose}}{g_{CDW} * h} * 16.4 \frac{mol_{ATP}}{mol_{Glucose} * h} = 9.10 \frac{mmol_{ATP}}{g_{CDW} * h}$$

With the same assumptions as before (2 mol ATP from glycolysis, P/O-Ratio of 1.2 in the respiratory chain), we can calculate the total ATP generation of *E. coli* MG1655 at $\mu = 0.2 \text{ h}^{-1}$ from measured glucose and oxygen uptake rates during the maintenance process at $D = 0.2 \text{ h}^{-1}$ at the STR-PFR 25 h time-point (data not shown). This yields an ATP generation of $q_{ATP} = 39.39 \text{ mmol}_{ATP} * g_{CDW}^{-1} * h^{-1}$. In balanced growth ATP generation equals ATP consumption.

Using equation (2) we can now calculate the ATP demand of *E. coli* MG1655 for growth at $\mu = 0.2 \text{ h}^{-1}$:

$$q_{ATP,X} = q_{ATP} - m_{ATP} = 26.65 \frac{mmol_{ATP}}{g_{CDW} * h}$$

Since $Y_{X,S,true}$ is not significantly different, we know that the true biomass yield for both strains is identical. Since the metabolic pathways are identical in both strains, the ATP demand for growth $q_{ATP,X}$ can then be assumed to be identical for both strains as well.

In order to calculate the ATP demand for eGFP production we need to introduce a parameter describing ATP demand for eGFP synthesis into equation (2). This parameter, $q_{ATP,eGFP}$, includes any additional cellular ATP expenses due to heterologous protein expression:

$$(4) \quad q_{ATP} = q_{ATP,X} + m_{ATP} + q_{ATP,eGFP}$$

We can calculate the total ATP generation of both production strains at $\mu = 0.2 \text{ h}^{-1}$ from measured glucose and oxygen uptake rates during the eGFP production processes at time-point STR-PFR 25 h (data not shown). This estimation yields an ATP generation of $q_{ATP} = 45.37 \text{ mmol}_{ATP} * \text{g}_{CDW}^{-1} * \text{h}^{-1}$ for *E. coli* MG1655 rhaB⁻ pJOE4056.2_tetA and $q_{ATP} = 45.95 \text{ mmol}_{ATP} * \text{g}_{CDW}^{-1} * \text{h}^{-1}$ for *E. coli* RM214 rhaB⁻ pJOE4056.2_tetA.

Using these values for total ATP generation and the estimated values of the base strains for m_{ATP} and $q_{ATP,X}$ at $\mu = 0.2 \text{ h}^{-1}$ from the maintenance processes, we can finally estimate the ATP demand of eGFP formation by inserting all values into equation (4):

$$q_{ATP,eGFP} = q_{ATP} - q_{ATP,X} - m_{ATP}$$

The results are documented in **Table S8**, and the proportion of ATP used for eGFP production is given.

Table S8: Estimated ATP demand of eGFP synthesis at STR-PFR 25 h

Strain	$q_{ATP,eGFP} [\text{mmol}_{ATP}/(\text{g}_{CDW} * \text{h})]$	$q_{ATP,eGFP}/q_{ATP} [\%]$
<i>E. coli</i> MG1655 rhaB ⁻ pJOE4056.2_tetA	6.0 ± 0.59^a	13 ± 1.3
<i>E. coli</i> RM214 rhaB ⁻ pJOE4056.2_tetA	10.2 ± 0.58	22 ± 1.7

^a: Errors indicate SEM (n = 4).

Parameter	Designation	Dimension
q_S	total cellular substrate consumption rate	$\text{g}_{Glucose} * \text{g}_{CDW}^{-1} * \text{h}^{-1}$
$q_{S,\mu}$	substrate consumption rate for growth	$\text{g}_{Glucose} * \text{g}_{CDW}^{-1} * \text{h}^{-1}$
m_S	Pirt's maintenance coefficient	$\text{g}_{Glucose} * \text{g}_{CDW}^{-1} * \text{h}^{-1}$
q_{ATP}	total cellular ATP consumption rate	$\text{mmol}_{ATP} * \text{g}_{CDW}^{-1} * \text{h}^{-1}$
$q_{ATP,X}$	ATP consumption rate for growth	$\text{mmol}_{ATP} * \text{g}_{CDW}^{-1} * \text{h}^{-1}$
m_{ATP}	ATP consumption rate for maintenance demand	$\text{mmol}_{ATP} * \text{g}_{CDW}^{-1} * \text{h}^{-1}$
$Y_{ATP,S}$	ATP produced per fully oxidized substrate	$\text{mmol}_{ATP} * \text{mmol}_{Glucose}^{-1}$
$q_{ATP,eGFP}$	ATP consumption rate for eGFP production	$\text{mmol}_{ATP} * \text{g}_{CDW}^{-1} * \text{h}^{-1}$
$Y_{XS,true}$	true biomass yield	$\text{g}_{CDW} * \text{g}_{Glucose}^{-1}$
μ	specific growth rate	h^{-1}
D	dilution rate	h^{-1}

Supplementary Data S9: SNPs found after continuous cultivation

Each tab contains the results of a genomic SNP analysis performed.

Cryo MG1655 VS NC_000913.3 compares our isolate (cryostock) of MG1655 to the refseq.

Cryo RM214 VS Cryo MG1655 shows SNPs accumulated during strain construction of RM214.

The remaining tabs compare sequenced samples from the end of continuous chemostat cultivations to the respective cryostock sample. The numbers indicate the dilution rate used during the chemostat phases (D005 means $D = 0.05$ 1/h and so on).

Cryo MG1655 VS NC_000913.3

CHROM	POS	TYPE	REF	ALT	EVIDENCE	Gene	Comment
NC_000913.3	1047882	snp	C	A	A:336 C:0	gfcD	Irrelevant, gfcD is not transcribed in E. coli K-12.
NC_000913.3	1315865	snp	G	T	T:300 G:0	yciG	Silent mutation
NC_000913.3	2105253	snp	T	A	A:310 T:0	wbbI	[I269F] of WbbI (beta-1,6-galactofuranosyltransferase)
NC_000913.3	2173360	del	ACC	A	A:225 ACC:0	gatC	Sequence variation in different MG1655 isolates has been documented previously.
NC_000913.3	3560455	ins	C	CG	CG:335 C:0	glpR	Sequence variation in different MG1655 isolates has been documented previously.
NC_000913.3	4296380	ins	A	ACG	ACG:169 A:0		Intergenic Repeat Region

Cryo RM214 VS Cryo MG1655

CHROM	POS	TYPE	REF	ALT	EVIDENCE	Gene	Comment
2:4504256-4522705	290658	snp	G	C	C:11 G:0		Low Coverage
2:4504256-4522705	566050	snp	N	T	T:30 N:0		Assembly Gap
2:4504256-4522705	998716	snp	T	G	G:325 T:0	elfc	V -> G at amino acid position 67 of ElfC. Cryptic operon that is involved in pathogenicity.
2:4504256-4522705	1047183	snp	A	C	C:306 A:0	gfcD	Identical to NC_000913.3 MG1655 Refseq, potentially a true polymorphism or reversion.
2:4504256-4522705	1128700	snp	G	T	T:51 G:0		Intergenic region downstream of murJ
2:4504256-4522705	1392292	snp	T	C	C:314 T:0		Intergenic region between pgrR and mppa
2:4504256-4522705	1396700	mnp	NNN	ACA	ACA:14 NNN:0		Assembly Gap
2:4504256-4522705	1427166	snp	A	G	G:118 A:0	ins-H5	ins-H5, rac Prophage
2:4504256-4522705	1427200	snp	T	C	C:55 T:0		
2:4504256-4522705	1427218	snp	T	C	C:33 T:0		
2:4504256-4522705	1427749	snp	G	A	A:55 G:1		
2:4504256-4522705	1427757	snp	A	G	G:83 A:1		
2:4504256-4522705	1427776	snp	C	T	T:115 C:1		
2:4504256-4522705	1427788	snp	A	G	G:146 A:1		
2:4504256-4522705	1427812	snp	A	G	G:189 A:0		
2:4504256-4522705	1427824	complex	CGCG	GGCA	GGCA:210 CGCG:0		
2:4504256-4522705	1527658	complex	NN	AA	AA:16 NN:0		Assembly Gap
2:4504256-4522705	1978629	snp	N	T	T:18 N:0		Assembly Gap
2:4504256-4522705	2304179	mnp	NNN	AAC	AAC:19 NNN:0		Assembly Gap
2:4504256-4522705	2725454	complex	NN	AT	AT:11 NN:0		Assembly Gap
2:4504256-4522705	2744523	snp	G	T	T:295 G:0	trmD	[H78N] of TrmD (tRNA-methyltransferase), TrmD is essential, the exchange is located in an alpha-helix on the surface of the protein and likely does not interfere with the active center.
2:4504256-4522705	3375243	snp	T	C	C:277 T:0	dcuD	[V321A] of DcuD (C4-dicarboxylate transporter), dcuD is a weakly transcribed gene and may be involved in glycerol metabolism.

MG1655 D005 VS MG1655 Cryo

CHROM	POS	TYPE	REF	ALT	EVIDENCE	Gene	Comment
2:4504256-4522705	390972	snp	N	A	A:32 N:0		Assembly Gap
2:4504256-4522705	566050	snp	N	T	T:19 N:0		Assembly Gap
2:4504256-4522705	729093	snp	N	T	T:11 N:0		Assembly Gap
2:4504256-4522705	1396700	mnp	NNN	ACA	ACA:14 NNN:0		Assembly Gap
2:4504256-4522705	1427166	snp	A	G	G:98 A:0	ins-H5	ins-H5, rac Prophage
2:4504256-4522705	1427200	snp	T	C	C:50 T:0		
2:4504256-4522705	1427218	snp	T	C	C:25 T:0		
2:4504256-4522705	1427749	snp	G	A	A:52 G:1		
2:4504256-4522705	1427757	snp	A	G	G:65 A:1		
2:4504256-4522705	1427776	snp	C	T	T:100 C:0		
2:4504256-4522705	1427788	snp	A	G	G:121 A:0		
2:4504256-4522705	1427812	snp	A	G	G:155 A:0		
2:4504256-4522705	1427824	complex	CGCG	GGCA	GGCA:176 CGCG:0		
2:4504256-4522705	1978629	snp	N	T	T:23 N:0		Assembly Gap
2:4504256-4522705	2725454	complex	NN	AT	AT:22 NN:0		Assembly Gap
2:4504256-4522705	3364958	snp	N	C	C:26 N:0		Assembly Gap
2:4504256-4522705	3423073	mnp	NN	TA	TA:14 NN:0		Assembly Gap
2:4504256-4522705	4497653	snp	N	T	T:33 N:0		Assembly Gap
2:4504256-4522705	4661603	snp	T	C	C:11 T:0		Assembly Gap

MG1655 D01 VS MG1655 Cryo

CHROM	POS	TYPE	REF	ALT	EVIDENCE	Gene	Comment
2:4504256-4522705	390972	snp	N	A	A:14 N:0		Assembly Gap
2:4504256-4522705	566050	snp	N	T	T:12 N:0		Assembly Gap
2:4504256-4522705	1427166	snp	A	G	G:32 A:0	ins-H5	ins-H5, rac Prophage
2:4504256-4522705	1427776	snp	C	T	T:30 C:0		
2:4504256-4522705	1427788	snp	A	G	G:46 A:0		
2:4504256-4522705	1427812	snp	A	G	G:68 A:0		
2:4504256-4522705	1427824	complex	CGCG	GGCA	GGCA:80 CGCG:0		
2:4504256-4522705	2725454	snp	N	A	A:10 N:0		Assembly Gap
2:4504256-4522705	2725455	snp	N	T	T:10 N:0		Assembly Gap
2:4504256-4522705	3364958	snp	N	C	C:12 N:0		Assembly Gap
2:4504256-4522705	3423073	mnp	NN	TA	TA:14 NN:0		Assembly Gap
2:4504256-4522705	4497653	snp	N	T	T:16 N:0		Assembly Gap

MG1655 D02 VS MG1655 Cryo

CHROM	POS	TYPE	REF	ALT	EVIDENCE	Gene	Comment
2:4504256-4522705	278410	snp	N	C	C:10 N:0		Assembly Gap
2:4504256-4522705	390972	snp	N	A	A:32 N:0		Assembly Gap
2:4504256-4522705	566050	snp	N	T	T:24 N:0		Assembly Gap
2:4504256-4522705	729093	snp	N	T	T:12 N:0		Assembly Gap
2:4504256-4522705	1396700	snp	N	A	A:11 N:0		Assembly Gap
2:4504256-4522705	1396701	snp	N	C	C:11 N:0		Assembly Gap
2:4504256-4522705	1396702	snp	N	A	A:11 N:0		Assembly Gap
2:4504256-4522705	1427166	snp	A	G	G:107 A:0	ins-H5	ins-H5, rac Prophage
2:4504256-4522705	1427200	snp	T	C	C:55 T:0		
2:4504256-4522705	1427218	snp	T	C	C:25 T:0		
2:4504256-4522705	1427749	snp	G	A	A:64 G:0		
2:4504256-4522705	1427757	snp	A	G	G:78 A:0		
2:4504256-4522705	1427776	snp	C	T	T:115 C:0		
2:4504256-4522705	1427788	snp	A	G	G:131 A:0		
2:4504256-4522705	1427812	snp	A	G	G:182 A:0		
2:4504256-4522705	1427824	complex	CGCG	GGCA	GGCA:198 CGCG:0		
2:4504256-4522705	1978629	snp	N	T	T:22 N:0		Assembly Gap
2:4504256-4522705	2304179	mnp	NNN	AAC	AAC:12 NNN:0		Assembly Gap
2:4504256-4522705	2725454	mnp	NN	AT	AT:15 NN:0		Assembly Gap
2:4504256-4522705	3364958	snp	N	C	C:18 N:0		Assembly Gap
2:4504256-4522705	3423073	mnp	NN	TA	TA:22 NN:0		Assembly Gap
2:4504256-4522705	4497653	snp	N	T	T:30 N:0		Assembly Gap

MG1655 D03 VS MG1655 Cryo

CHROM	POS	TYPE	REF	ALT	EVIDENCE	Gene	Comment
2:4504256-4522705	390972	snp	N	A	A:27 N:0		Assembly Gap
2:4504256-4522705	566050	snp	N	T	T:13 N:0		Assembly Gap
2:4504256-4522705	1427166	snp	A	G	G:80 A:0	ins-H5	ins-H5, rac Prophage
2:4504256-4522705	1427200	snp	T	C	C:38 T:0		
2:4504256-4522705	1427218	snp	T	C	C:17 T:0		
2:4504256-4522705	1427749	snp	G	A	A:46 G:0		
2:4504256-4522705	1427757	snp	A	G	G:67 A:0		
2:4504256-4522705	1427776	snp	C	T	T:95 C:0		
2:4504256-4522705	1427788	snp	A	G	G:113 A:0		
2:4504256-4522705	1427812	snp	A	G	G:158 A:0		
2:4504256-4522705	1427824	complex	CGCG	GGCA	GGCA:174 CGCG:0		
2:4504256-4522705	1527658	snp	N	A	A:10 N:0		Assembly Gap
2:4504256-4522705	1978629	snp	N	T	T:18 N:0		Assembly Gap
2:4504256-4522705	2304179	mnp	NNN	AAC	AAC:16 NNN:0		Assembly Gap
2:4504256-4522705	2725454	mnp	NN	AT	AT:15 NN:0		Assembly Gap
2:4504256-4522705	3364958	snp	N	C	C:12 N:0		Assembly Gap
2:4504256-4522705	3423073	mnp	NN	TA	TA:18 NN:0		Assembly Gap
2:4504256-4522705	4497653	snp	N	T	T:30 N:0		Assembly Gap

RM214 D005 VS RM214 Cryo

CHROM	POS	TYPE	REF	ALT	EVIDENCE	Gene	Comment
2:4455130-4470514	15384	del	CA	C	C:14 CA:0		Low Coverage
2:4455130-4470514	290081	snp	G	C	C:10 G:0		Assembly Gap
2:4455130-4470514	524561	complex	NN	GG	GG:17 NN:0		Assembly Gap
2:4455130-4470514	566734	snp	G	C	C:14 G:0		Assembly Gap
2:4455130-4470514	1206538	ins	G	GT	GT:246 G:2	ycfk (e14 prophage)	Identical to NC_000913.3 MG1655 Refseq, potentially true polymorphism
2:4455130-4470514	1208356	complex	AN	A	A:233 AN:0	stfE (e14 prophage)	Identical to NC_000913.3 MG1655 Refseq, potentially true polymorphism
2:4455130-4470514	1394788	mnp	NN	GC	GC:14 NN:0		Assembly Gap
2:4455130-4470514	1426598	snp	A	G	G:116 A:0	ins-H5	ins-H5, rac Prophage
2:4455130-4470514	1426632	snp	T	C	C:57 T:0		
2:4455130-4470514	1426650	snp	T	C	C:27 T:0		
2:4455130-4470514	1427181	snp	G	A	A:143 G:0		
2:4455130-4470514	1427189	snp	A	G	G:163 A:0		
2:4455130-4470514	1427208	snp	C	T	T:192 C:0		
2:4455130-4470514	1427220	snp	A	G	G:219 A:0		
2:4455130-4470514	2022495	snp	N	C	C:17 N:0		Assembly Gap
2:4455130-4470514	2065039	snp	N	T	T:21 N:0		Assembly Gap
2:4455130-4470514	2173885	mnp	NN	TA	TA:24 NN:0		Assembly Gap
2:4455130-4470514	2437787	snp	N	C	C:16 N:0		Assembly Gap
2:4455130-4470514	3650924	snp	N	A	A:20 N:0		Assembly Gap
2:4455130-4470514	3665101	snp	N	G	G:14 N:0		Assembly Gap

RM214 D01 VS RM214 Cryo

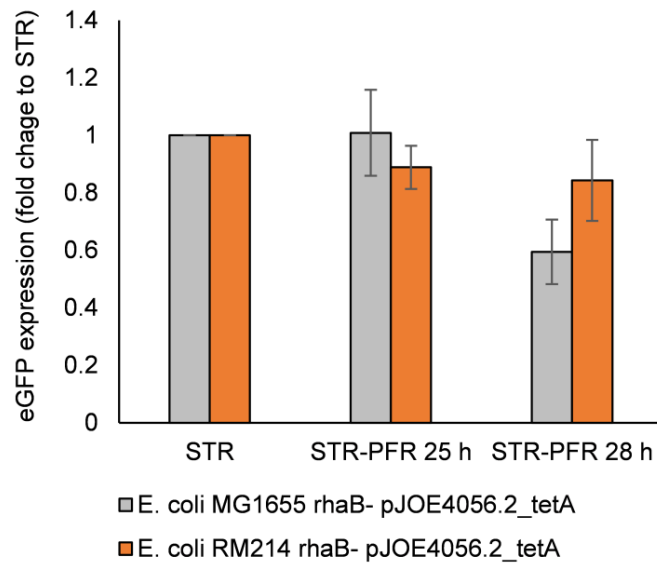
CHROM	POS	TYPE	REF	ALT	EVIDENCE	Gene	Comment
2:4455130-4470514	15384	del	CA	C	C:12 CA:0		Low Coverage
2:4455130-4470514	269203	snp	N	A	A:11 N:0		Assembly Gap
2:4455130-4470514	278787	snp	C	A	A:10 C:0		Assembly Gap
2:4455130-4470514	290081	snp	G	C	C:14 G:0		Assembly Gap
2:4455130-4470514	524561	mnp	NN	GG	GG:23 NN:0		Assembly Gap
2:4455130-4470514	573286	mnp	NNN	CTT	CTT:26 NNN:0		Assembly Gap
2:4455130-4470514	921089	snp	N	A	A:22 N:0		Assembly Gap
2:4455130-4470514	1206538	ins	G	GT	GT:201 G:1	ycfk (e14 prophage)	Identical to NC_000913.3 MG1655 Refseq, potentially true polymorphism
2:4455130-4470514	1208356	complex	AN	A	A:214 AN:0	stfE (e14 prophage)	Identical to NC_000913.3 MG1655 Refseq, potentially true polymorphism
2:4455130-4470514	1426598	snp	A	G	G:118 A:0	ins-H5	ins-H5, rac Prophage
2:4455130-4470514	1426632	snp	T	C	C:66 T:0		
2:4455130-4470514	1426650	snp	T	C	C:36 T:0		
2:4455130-4470514	1427181	snp	G	A	A:132 G:1		
2:4455130-4470514	1427189	snp	A	G	G:154 A:1		
2:4455130-4470514	1427208	snp	C	T	T:194 C:1		
2:4455130-4470514	1427220	snp	A	G	G:209 A:1		
2:4455130-4470514	2022495	snp	N	C	C:21 N:0		Assembly Gap
2:4455130-4470514	2173885	mnp	NN	TA	TA:15 NN:0		Assembly Gap
2:4455130-4470514	2437787	snp	N	C	C:17 N:0		Assembly Gap
2:4455130-4470514	3364418	mnp	NN	CA	CA:26 NN:0		Assembly Gap
2:4455130-4470514	3650924	snp	N	A	A:18 N:0		Assembly Gap

CHROM	POS	TYPE	REF	ALT	EVIDENCE	Gene	Comment
2:4455130-4470514	15384	del	CA	C	C:18 CA:0		low coverage
2:4455130-4470514	256558	snp	N	C	C:17 N:0		Assembly Gap
2:4455130-4470514	269203	snp	N	A	A:10 N:0		Assembly Gap
2:4455130-4470514	277833	snp	N	C	C:11 N:0		Assembly Gap
2:4455130-4470514	290081	snp	G	C	C:10 G:0		Assembly Gap
2:4455130-4470514	573286	complex	NNN	CTT	CTT:14 NNN:0		Assembly Gap
2:4455130-4470514	728517	snp	N	T	T:10 N:0		Assembly Gap
2:4455130-4470514	921089	snp	N	A	A:16 N:0		Assembly Gap
2:4455130-4470514	1092976	snp	N	T	T:20 N:0		Assembly Gap
2:4455130-4470514	1206538	ins	G	GT	GT:173 G:0	yckf (e14 prophage)	Identical to NC_000913.3 MG1655 Refseq, potentially true polymorphism
2:4455130-4470514	1394788	mnp	NN	GC	GC:21 NN:0		Assembly Gap
2:4455130-4470514	1426598	snp	A	G	G:81 A:1	ins-H5	ins-H5, rac Prophage
2:4455130-4470514	1426632	snp	T	C	C:48 T:0		
2:4455130-4470514	1426650	snp	T	C	C:27 T:0		
2:4455130-4470514	1427181	snp	G	A	A:93 G:0		
2:4455130-4470514	1427189	snp	A	G	G:111 A:0		
2:4455130-4470514	1427208	snp	C	T	T:148 C:0		
2:4455130-4470514	1427220	snp	A	G	G:166 A:0		
2:4455130-4470514	2022495	snp	N	C	C:24 N:0		Assembly Gap
2:4455130-4470514	2051091	snp	N	T	T:17 N:0		Assembly Gap
2:4455130-4470514	2065039	snp	N	T	T:23 N:0		Assembly Gap
2:4455130-4470514	2173885	mnp	NN	TA	TA:11 NN:0		Assembly Gap
2:4455130-4470514	2437787	snp	N	C	C:13 N:0		Assembly Gap
2:4455130-4470514	2661199	snp	N	T	T:14 N:0		Assembly Gap
2:4455130-4470514	3364418	mnp	NN	CA	CA:17 NN:0		Assembly Gap
2:4455130-4470514	3650924	snp	N	A	A:19 N:0		Assembly Gap
2:4455130-4470514	3665101	snp	N	G	G:26 N:0		Assembly Gap
2:4455130-4470514	3766292	snp	N	C	C:74 N:0		Assembly Gap
2:4455130-4470514	4497117	snp	N	T	T:24 N:0		Assembly Gap

RM214 D03 VS RM214 Cryo

CHROM	POS	TYPE	REF	ALT	EVIDENCE	Gene	Comment
2:4455130-4470514	15384	del	CA	C	C:12 CA:0		Assembly Gap
2:4455130-4470514	269203	snp	N	A	A:10 N:0		Assembly Gap
2:4455130-4470514	1206538	ins	G	GT	GT:124 G:0	ycfk (e14 prophage)	Identical to NC_000913.3 MG1655 Refseq, potentially true polymorphism
2:4455130-4470514	1208356	complex	AN	A	A:146 AN:0	stfE (e14 prophage)	Identical to NC_000913.3 MG1655 Refseq, potentially true polymorphism
2:4455130-4470514	1426598	snp	A	G	G:26 A:0	ins-H5	ins-H5, rac Prophage
2:4455130-4470514	1427181	snp	G	A	A:28 G:0		
2:4455130-4470514	1427189	snp	A	G	G:36 A:0		
2:4455130-4470514	1427208	snp	C	T	T:58 C:0		
2:4455130-4470514	1427220	snp	A	G	G:74 A:0		
2:4455130-4470514	2051091	snp	N	T	T:12 N:0		Assembly Gap
2:4455130-4470514	2065039	snp	N	T	T:12 N:0		Assembly Gap
2:4455130-4470514	2437787	snp	N	C	C:16 N:0		Assembly Gap

Supplementary Information S10: RT-qPCR measurements



Supplementary Figure **S10**. Expression of eGFP. RT-qPCR was used to quantify the expression of *egfp* relative to the housekeeping gene *cysG*. The relative expression at time points STR-PFR 25 h and STR-PFR 28 h was then normalized to the STR sample to yield the fold change in expression compared to the well mixed STR conditions. Mean values from four biological replicates for each strain are shown. Error bars indicate SEM (n = 4).



CRISPRi enables fast growth followed by stable aerobic pyruvate formation in *Escherichia coli* without auxotrophy

Journal:	<i>Engineering in Life Sciences</i>
Manuscript ID	Draft
Wiley - Manuscript type:	Research Article
Date Submitted by the Author:	n/a
Complete List of Authors:	Ziegler, Martin; University of Stuttgart, Institute of Biochemical Engineering Gäbele, Teresa; University of Stuttgart, Institute of Biochemical Engineering Takors, Ralf; University of Stuttgart, Institute of Biochemical Engineering
Keywords:	CRISPRi, fermentation, metabolic engineering, nitrogen limitation, pyruvate

SCHOLARONE™
Manuscripts

1
2
3 Research Article
4

5
6 **CRISPRi enables fast growth followed by stable aerobic**
7 **pyruvate formation in *Escherichia coli* without**
8 **auxotrophy**
9
10

11
12
13
14 Martin Ziegler¹

15 Teresa Gäbele¹

16
17 Ralf Takors¹
18
19
20

21 ¹Institute of Biochemical Engineering, University of Stuttgart, Stuttgart, Germany
22
23

24
25 **Correspondence:** Prof. Dr.-Ing. Ralf Takors (ralf.takors@ibvt.uni-stuttgart.de). Institute of Biochemical Engineering,
26 University of Stuttgart, Allmandring 31, 70569 Stuttgart, Germany.
27
28

29
30 **Keywords:** CRISPRi; fermentation; metabolic engineering; nitrogen limitation; pyruvate
31
32

33 **Abbreviations:** TCA, tricarboxylic acid; sgRNA, single-guide RNA; CRISPR, Clustered Regularly Interspaced Short
34 Palindromic Repeats; CRISPRi, CRISPR interference; Atc, anhydrotetracycline; *E. coli*, *Escherichia coli*;
35
36
37
38
39
40
41
42
43
44
45
46
47
48
49
50
51
52
53
54
55
56
57
58
59
60

Practical Application

Pyruvate is an important cellular precursor at the intersection of glycolysis and tricarboxylic acid cycle (TCA). Reduced pyruvate flux into the TCA improves its availability for the formation of pyruvate-derived products such as terpenoids synthesized via the methylerythritol-4-phosphate (MEP) pathway in *E. coli*. In this study, balanced reduction of pyruvate dehydrogenase activity by CRISPR interference was explored to trigger the accumulation of pyruvate while maintaining robust cellular growth and avoiding acetate auxotrophy. We demonstrate the applicability of the approach in exemplary aerobic fermentations including an extended nitrogen-limited production phase. The strategy has the potential to improve titer and carbon conversion in the biotechnical production of pyruvate-derived products.

For Peer Review

Abstract

CRISPR interference (CRISPRi) was applied to enable the aerobic production of pyruvate in *Escherichia coli* MG1655 under glucose excess conditions by targeting the promoter regions of *aceE* or *pdhR*. Knockdown strains were cultivated in aerobic shaking flasks and the influence of inducer concentration and different sgRNA binding sites on the production of pyruvate was measured. Targeting the promoter region of *aceE* triggered pyruvate production during the exponential phase. In lab-scale bioreactor fermentations, an *aceE* silenced strain successfully produced pyruvate under fully aerobic conditions during the exponential phase, but loss of productivity occurred during a subsequent nitrogen-limited phase. Combinatorial use of two sgRNAs targeting *aceE* did not improve the production phenotype. However, simultaneous silencing of *aceE* and *pdhR* in *E. coli* MG1655 pdCas9 psgRNA_aceE_234_pdhR_329 enabled the stable aerobic production of pyruvate with non-growing cells at $Y_{P/S} = 0.36 \pm 0.029 \text{ g}_{\text{Pyruvate}}/\text{g}_{\text{Glucose}}$ in lab-scale bioreactors throughout an extended nitrogen-limited production phase. Further experiments revealed that targeting *pdhR* alone was sufficient to enable strong pyruvate production in shaking flasks.

For Peer Review

1 Introduction

Pyruvate is a small metabolite at the intersection of glycolysis and the tricarboxylic acid (TCA) cycle. The production of pyruvate by biotechnical means is well established, for example by Toray Industries using *Torulopsis glabrata* [1, 2]. Processes with high titer, yield and productivity have been described not only for *T. glabrata* but also for *E. coli* [3–5]. The economic feasibility of *E. coli* as a pyruvic acid producer from glucose has been examined in a case study [6]. However, applications of pyruvate are relatively few compared to other small organic acids: Pyruvate primarily serves as an additive for the synthesis of small-volume specialty chemicals or pharmaceuticals such as L-DOPA and is sold as a food additive [7, 8]. Potential medical dietary benefits have been scientifically investigated but so far could not be confirmed beyond doubt [9]. The importance of pyruvate for biotechnological applications therefore originates from its position in the central carbon metabolism serving as a precursor for other small molecule compounds. Bioproducts derived from pyruvate include the amino acids alanine, isoleucine, leucine and valine [10], small carbon molecules such as lactate or isobutanol [11] and isoprenoids synthesized by the methylerythritol-4-phosphate (MEP) pathway [12]. The production of isoprenoids in *E. coli* by the native MEP pathway has received considerable attention in the past years [13, 14].

An important factor in engineering the productivity of heterologous pathways branching from pyruvate is the balance of precursor availability for growth and production. Pyruvate is usually produced from glucose and gene deletions or mutations with high impact on the catalytic activity of the pyruvate dehydrogenase complex result in acetate auxotrophy in aerobic conditions [15]. Whereas this enables decoupling of growth and pyruvate production, it also implies that any demand for reducing power and ATP exceeding the supply provided from glycolysis must be met by the co-consumption of acetate which is a more expensive substrate than glucose [6]. Several studies have thus explored the possibility of throttling the flux from pyruvate to acetyl-CoA to trigger the accumulation of pyruvate while maintaining a low level of flux through the TCA cycle to avoid acetate auxotrophy. The regulation of pyruvate dehydrogenase complex activity could be achieved by point mutations modulating catalytic activity [16]. Alternatively, gene expression was controlled by promoter engineering [10] or by regulated expression of antisense RNA [17]. Strains accumulating pyruvate while maintaining an acceptable growth phenotype have the potential to serve as chassis for pyruvate-derived products.

Another possibility to reduce the expression of genes is through steric hindrance by a DNA binding protein. In recent years targeted binding of DNA sequences has become readily available in *E. coli* K-12 by using CRISPR-Cas derived systems. The endogenous CRISPR system of *E. coli* K-12 can be repurposed by deletion of *cas3* to yield a DNA binding system lacking nuclease activity [18, 19]. Alternatively, CRISPRi which uses the exogenous catalytically inactive protein dCas9 from *S. pyogenes* can be introduced in conjunction with single-guide RNAs [20, 21]. A single-guide RNA (sgRNA) forms a stable complex with dCas9 which can then bind to a DNA region with complementarity to the targeting sequence and a protospacer adjacent motif (PAM). If the complex targets a region close to the transcription start of a single gene or operon, it may prevent binding of RNA polymerase which effectively represses the expression of the downstream genes. The repression strength in CRISPRi may vary over several orders of magnitude and depends primarily on the distance of the binding site to the transcription start, the target strand, and mismatches in the targeting sgRNA [20, 22]. CRISPRi has already been applied successfully to improve the microbial production of a plethora of small compounds [23]. The technique is of particular interest for metabolic engineers because it facilitates the fine-tuning of gene expression which is helpful to find an optimal balance between competing processes such as growth and production [24].

Fed-batch processes are the standard fermentation mode in white biotechnology. To further improve process performance complementary techniques such as the possibility to decouple growth and production phases or *in situ* product removal are actively investigated [3, 25]. These techniques include dual-phase fermentations, extended production phases with resting cells, or processes limited by other compounds than the primary carbon source [26, 27]. Nitrogen-limited processes are particularly attractive as nitrogen is a major component of biomass, nitrogen sources such as ammonia are usually cheap and easy to measure and the interplay of glucose and nitrogen metabolism in industrial hosts such as *E. coli* and *S. cerevisiae* is well characterized [28, 29]. In the case of a small

1
2
3 molecule carbon-based product nitrogen is not required for product formation and nitrogen limitation thus enables
4 the decoupling of growth and production.
5

6 In this study, we designed sgRNAs for the silencing of *aceE* in aerobic fermentations of *E. coli* MG1655 by targeting
7 the promoters *aceEp* and *pdhRp*. The repression of *aceEp* alone enabled the production of pyruvate in aerobic
8 pH-controlled fermentations during the exponential phase. However, it was not sufficient to create a stable
9 production phenotype throughout an extended nitrogen-limited production phase. The simultaneous repression of
10 both *aceEp* and *pdhRp* overcame this limitation and allowed the production of pyruvate during the batch phase and
11 a consecutive nitrogen-limited production phase. Repression of *pdhR* alone also triggered the accumulation of
12 pyruvate in shaking flask experiments.
13
14
15
16
17
18
19
20
21
22
23
24
25
26
27
28
29
30
31
32
33
34
35
36
37
38
39
40
41
42
43
44
45
46
47
48
49
50
51
52
53
54
55
56
57
58
59
60

For Peer Review

2 Materials and Methods

2.1 Media and Buffer Solutions

2xTY medium was prepared by autoclaving 16 g/l tryptone, 10 g/l yeast extract, 5 g/l NaCl dissolved in demineralized water. For agar plates 18 g/l agar-agar were added prior to autoclavation. SOC medium was prepared as described previously [30]. All cultivations were performed at 37 °C.

Minimal medium for shaking flask experiments consisted of 20 g/l glucose, 2.0 g/l NaH₂PO₄·2H₂O, 5.2 g/l K₂HPO₄, 4.56 g/l (NH₄)₂SO₄, 15 g/l 3-(*N*-morpholino)propanesulfonic acid (MOPS) and 0.4 % (V/V) trace elements stock solution.

N-lim minimal medium for precultures of bioreactor experiments consisted of 10 g/l glucose, 1.0 g/l NaH₂PO₄·2H₂O, 2.6 g/l K₂HPO₄, 2.2 g/l (NH₄)₂SO₄, 15 g/l 3-(*N*-morpholino)propanesulfonic acid (MOPS) and 0.2 % (V/V) trace elements stock solution. N-lim minimal medium for bioreactor experiments consisted of 70 g/l glucose, 1.0 g/l NaH₂PO₄·2H₂O, 2.6 g/l K₂HPO₄, 2.2 g/l (NH₄)₂SO₄ and 0.2 % (V/V) trace elements stock solution.

If strains with antibiotic resistance markers were cultivated in any liquid media or on 2xTY agar plates, appropriate antibiotics were added to media in the following concentrations: Chloramphenicol 25 µg/ml, disodium Carbenicillin 100 µg/ml. If necessary, inducers were added to minimal media in the following concentrations unless stated otherwise: Isopropyl β-d-1-thiogalactopyranoside (IPTG) 1 mM, Anhydrotetracycline (Atc) 0.1 µg/ml.

The composition of trace element stock solution was 4.175 g/l FeCl₃·6H₂O, 0.045 g/l ZnSO₄·7H₂O, 0.025 g/l MnSO₄·H₂O, 0.4 g/l CuSO₄·5H₂O, 0.045 g/l CoCl₂·6H₂O, 2.2 g/l CaCl₂·2H₂O, 50 g/l MgSO₄·7H₂O and 55 g/l sodium citrate dihydrate. Stock solutions of salts, trace elements and sugars were autoclaved separately, and stock solutions of antibiotics were filter sterilized and stored at -20 °C. All compounds were combined just before the experiments to prevent potential aging of media.

2.2 Bacterial Strains and Cloning of Plasmids for CRISPR interference

All strains used in this study are listed in Table 1 and all primers used in this study are listed in Table 2.

Cloning of psgRNA plasmids was conducted as described previously [31]. Briefly, primers were 5' phosphorylated using T4 polynucleotide kinase. Next, psgRNA-bacteria or a psgRNA plasmid was amplified by inverse PCR (iPCR) using a reverse primer binding the plasmid in the promoter region of the sgRNA expression cassette and a forward primer containing the complementary 20 nucleotide target binding sequence for CRISPR interference to be introduced flanked by an annealing region to the plasmid. After purification of the PCR reaction, DpnI degradation of the plasmid template, and separation of products on an agarose gel, bands at 2.6 kb were extracted and the purified DNA fragments circularized by blunt-end ligation using T4 DNA ligase. *E. coli* DH5α λ *pir* was transformed with 2 µl of the ligation reaction by electroporation and regenerated in SOC medium. Cells were then plated on 2xTY agar plates and incubated at 37 °C overnight. Cells from a single colony were grown in 2xTY, the plasmids extracted using E.Z.N.A.® Plasmid DNA mini Kit I (omega BIO-TEK) according to the manufacturer's instructions and the insert coding for the sgRNA verified by sequencing.

Cloning of psgRNA plasmids containing more than one sgRNA was performed using iPCR and BioBrick assembly cloning as described elsewhere [22, 32]. In short, the donor sgRNA plasmid was digested using EcoRI and BamHI and the recipient plasmid digested with EcoRI and BgIII. Fragments were separated on agarose gels, extracted, purified, and ligated using T4 DNA ligase. *E. coli* DH5α λ *pir* was transformed with 5 µl of the ligation reaction by electroporation and regenerated in SOC medium. Cells were then plated on 2xTY agar plates and incubated at 37 °C overnight. Cells from a single colony were grown in 2xTY, the plasmids extracted using E.Z.N.A.® Plasmid DNA mini Kit I (omega BIO-TEK) according to the manufacturer's instructions and the insert coding for the sgRNA verified by sequencing.

To construct the actual production strains, *E. coli* MG1655 was transformed with 1 μ l of purified psgRNA plasmid by electroporation, regenerated in SOC medium, plated on 2xTY agar plates, and incubated at 37 °C overnight. Electrocompetent cells were prepared from a single colony and transformed with 5 μ l of pdCas9 using identical procedures. The resulting strains carrying two plasmids were grown in 2xTY and stored as glycerol stocks at -70 °C.

2.3 β -Galactosidase Assay

The activity of β -galactosidase, the product of *lacZ*, was assayed according to Jeffrey Miller's protocol with minor adaptations [33]. Baffled 100 ml shaking flasks containing 10 ml 2xTY medium were inoculated with a single colony from an agar plate streak and incubated with appropriate antibiotics at 37 °C and 130 rpm. After 30 min, isopropyl- β -D-thiogalactopyranosid (IPTG) was added to a final concentration of 1 mM. Cells were grown to mid-log phase and the optical density at 600 nm measured. 2 ml of biosuspension were harvested by centrifugation for 2 min at 12000 g, the supernatant discarded, and the cell pellet resuspended in 2 ml of Z-buffer (60 mM Na₂HPO₄·2H₂O, 40 mM NaH₂PO₄·H₂O, 10 mM KCl, 1 mM MgSO₄, 50 mM β -mercaptoethanol, pH adjusted to 7.0 with NaOH / H₃PO₄ prior to addition of β -mercaptoethanol). An appropriate volume of resuspended cell suspension was further diluted in Z-buffer to yield 1 ml of assay sample solution. 1 ml of diluted cells were lysed with 50 μ l of chloroform and 25 μ l of 0.1 % sodium dodecyl sulfate (SDS) solution. After incubation for 5 min, 200 μ l of substrate solution (4 g/l o-Nitrophenyl- β -D-galactopyranoside (OPNG) dissolved in Z-buffer) were added and the time until the sample turned yellow was recorded. The reaction was stopped by adding 500 μ l stop solution (1 M Na₂CO₃ in deionized water) and the samples centrifuged for 7 min at 12000 g. The supernatant was transferred into PMMA semi-micro cuvettes and the absorption at 420 nm was measured. Miller units were calculated according to the following equation, where t is the time of reaction in minutes and V the volume of cell suspension used to correct for dilution of samples in Z-buffer:

$$\beta\text{-galactosidase activity [miller units]} = (\text{OD}_{420} \times 1000) / (\text{OD}_{600} \times t \times V)$$

2.4 Shaking flask cultivations

Strains were streaked from glycerol stock cultures on 2xTY agar plates and grown overnight at 37 °C. For precultures, a 100 ml baffled shaking flask containing 20 ml minimal medium was inoculated with a single colony and incubated at 37 °C on a rotary shaker set to 130 rpm for 16 – 40 h. For main cultures, a 500 ml baffled shaking flask containing 55 ml of minimal medium was inoculated with preculture to a starting OD of 0.2 and cultivated at 37 °C on a rotary shaker set to 130 rpm.

2.5 Bioreactor cultivations

Precultures for bioreactor experiments were inoculated from glycerol stock cultures by transferring 333 μ l of glycerol stock culture into a 100 ml baffled shaking flask containing 20 ml N-lim minimal medium. Precultures were incubated at 37 °C on a rotary shaker set to 130 rpm overnight. On the next morning, a glass bioreactor containing 200 ml of N-lim minimal medium was inoculated with preculture to a starting OD of 0.2. Glass bioreactors were equipped with a temperature control set to 37 °C and magnetic stirrers set to 500 rpm. Throughout the cultivation stirring speed and gassing were kept constant at 500 rpm and 300 ml/min. DO tension was monitored and never dropped below 30 % saturation to ambient air partial oxygen pressure. The pH was kept constant at 7.0 by automated addition of 3 M NaOH. Prior to fermentation start a single droplet (about 10 μ l) of Struktol J647 antifoaming agent was added to the vessel to prevent potential foaming.

2.6 Analytical Procedures

Bacterial growth was monitored by measurements of optical density at 600 nm. Biosuspension samples were appropriately diluted with 0.9 % NaCl solution and cell dry weight calculated from these values assuming a correlation factor of 0.3 [16].

2 ml of freshly sampled biosuspension were centrifuged at 12000 g for 2 min and aliquots of the resulting supernatant frozen until further analysis. Isocratic HPLC using a RI detector (1200Series, Agilent) with a Rezex ROA-Organic acid H⁺ column (Phenomenex) for separation was used to measure glucose, acetic acid, lactate, 2-oxoglutarate, ethanol, formate and succinate as described previously [16]. Glucose concentration was alternatively determined by D-Glucose UV-Test Kit (R-Biopharm, Darmstadt, Germany) and acetic acid concentration by Acetic acid UV-Test Kit (R-Biopharm, Darmstadt, Germany). Ammonium concentration was determined by Ammonium cuvette test LCK 303 or LCK 304 (Hach Lange, Düsseldorf, Germany). Pyruvate was determined by an enzymatic assay measuring the consumption of NADH upon conversion of pyruvate to lactate by L-lactate dehydrogenase (LDH). L-lactate dehydrogenase suspension (L2500, Merck) was diluted 1:10 in 2.5 M (NH₄)₂SO₄ solution. 500 µl of 100 mM tris (pH 7.4), 100 µl of 2 mM NADH and 290 µl deionized water were mixed in an acryl cuvette and 100 µl of appropriately diluted sample was added. The absorbance at 365 nm was measured and 10 µl of LDH suspension was added to initiate the reaction. After incubation for 10 min at room temperature the absorbance at 365 nm was measured again and the resulting difference in absorbance used to calculate the pyruvate content of the sample.

3 Results

Our goal was to apply CRISPRi to throttle the flux from pyruvate to the TCA cycle. We aimed for a strain that accumulated pyruvate aerobically while maintaining an acceptable growth phenotype without acetate auxotrophy. The target phenotype can be obtained by balanced reduction of the activity of the pyruvate dehydrogenase complex [16]. Therefore, our primary knockdown target was *aceE* which encodes a subunit of the pyruvate dehydrogenase complex. Additionally, we planned on using the strain in two-phase fermentations with an initial growth phase and a subsequent nitrogen-limited production phase. To achieve these goals, we created in total four series of knockdown strains each based on different silencing strategies. In the first series, single silencing of *aceE* was tested. Knockdown strains of the second series were subject to combinatorial silencing of *aceE*. The third series was engineered for simultaneous silencing of *aceE* and *pdhR*. For the fourth and final series, we tested single silencing of *pdhR*. Strains of all four series were tested in aerobic shaking flasks. One knockdown strain from the first and third series each was characterized in lab-scale reactors including a nitrogen-limited production phase.

3.1 Identification of binding sites for CRISPR interference

For CRISPRi, we used the two-plasmid system described by Qi et al. (2013) employing pCas9 with an anhydrotetracycline inducible dCas9 and psgRNA containing constitutively expressed sgRNA templates [20]. The crucial factor for gene silencing by CRISPRi is the design of sgRNAs. As the scope of our experiments was limited, we manually examined the DNA sequence around the transcription start site of promoters for suitable target sites and used BLAST to exclude candidates with potential off-target effects based on sequence similarity. To verify this simplistic approach, we designed three sgRNAs targeting *lacZp* and conducted beta-galactosidase assays to gain an estimate of repression efficiencies in induced or non-induced state. All sgRNAs targeting *lacZp* lead to strong reduction of β -galactosidase activity and thus were sufficient to knock-down *lacZ* (Supporting Information S1).

We then designed sgRNAs for the silencing of *aceE*. The *E. coli* gene *aceE* is part of the *pdhR-aceEF-lpd* operon which is primarily transcribed from *pdhRp* with minor contributions from the internal promoter *aceEp*, potentially involving σ^S [34, 35]. PdhR represses the entire operon and autoregulates its own synthesis by binding to the *pdhR* promoter region. Repression by PdhR is relieved by pyruvate and PdhR controls an additional small regulon of about 20 genes [36]. CRISPRi can inhibit transcription by blocking initiation or elongation. When inhibiting transcriptional elongation, targeting the non-template strand is in general more effective than targeting the template strand [20]. We drafted two potential approaches: First, CRISPRi targeting *aceEp* should block both initiation from *aceEp* as well as hinder elongation of transcripts originating from *pdhRp*. Second, CRISPRi targeting *pdhRp* should effectively block initiation for the entire *pdhR-aceEF-lpd* operon while mimicking the regulatory effects of a *pdhR* deletion [37]. To explore diverse target sites, we chose three sites around *aceEp* (232, 233 and 234), one on the template-strand and two on the non-template strand, and an additional target site close to the start of the coding region of *aceE* (235) on the non-template strand (Fig. 1). We then identified three target sites around *pdhRp* (327, 328 and 329) which we deemed suitable for blocking transcriptional initiation from this promoter. We opted to test CRISPRi against *aceEp* first to avoid potential side-effects of *pdhR* repression.

3.2 Silencing of *aceE*

The four sgRNAs (232, 233, 234 and 235) targeting *aceE* were individually cloned into psgRNA and transformed into *E. coli* MG1655. Transformation with pCas9 yielded the first series of knockdown strains. The strains were cultivated in aerobic shaking flasks in minimal medium with 0.1 $\mu\text{g/ml}$ anhydrotetracycline. Over the course of the fermentations the accumulation of pyruvate, the concomitant consumption of glucose, and the acidification of the medium were regularly measured. Cell growth was monitored by optical density. All four sgRNAs triggered the accumulation of pyruvate, but pyruvate yield from glucose varied considerably (Fig. 2 A). *E. coli* MG1655 pCas9 psgRNA_aceE_234 showed the strongest pyruvate production among strains of the first series (Fig. 3 left panel). As we had observed leakiness of the expression system before (Supporting Information S1) we also performed shaking

1
2
3 flask fermentations of *E. coli* MG1655 pdCas9 psgRNA_aceE_234 without addition of anhydrotetracycline but
4 observed only minor accumulation of pyruvate (Fig. 3 right panel).
5

6 To clarify the influence of anhydrotetracycline concentration on the silencing efficacy we cultivated another strain of
7 the first series, *E. coli* MG1655 pdCas9 psgRNA_aceE_233, with varying anhydrotetracycline concentrations. The
8 addition of as little as 0.01 µg/ml anhydrotetracycline was sufficient to induce the system and trigger the
9 accumulation of pyruvate at the expense of biomass formation (Supporting Information S2). Concentrations up to
10 0.5 µg/ml of anhydrotetracycline were well tolerated, but at 1.0 µg/ml anhydrotetracycline growth inhibition without
11 additional pyruvate production occurred. Small amounts of pyruvate were produced even in the absence of inducer.
12 We concluded that the initially chosen 0.1 µg/ml anhydrotetracycline was well within the working range and
13 continued to use this concentration.
14
15

17 **3.3 Loss of productivity in bioreactor cultivations of *E. coli* MG1655 pdCas9 18 psgRNA_aceE_234**

19 One of our goals was to enable the production of pyruvate during an extended nitrogen-limited production phase.
20 As *E. coli* MG1655 pdCas9 psgRNA_aceE_234 had achieved the highest specific pyruvate production in the shaking
21 flask experiments of the first series, we chose to characterize the strain in aerobic lab-scale fermentations with
22 controlled pH. The composition of the minimal medium included excessive glucose and trace elements, with
23 ammonium as the limiting nutrient. During the initial exponential batch-phase *E. coli* MG1655 pdCas9
24 psgRNA_aceE_234 grew fast and accumulated a maximum of 2.91 g/l pyruvate (Fig. 4 left panel). However, upon
25 depletion of ammonium the production of pyruvate stopped, and slow reuptake and consumption occurred over the
26 remaining course of the fermentation (Table 3). In parallel *E. coli* MG1655 pdCas9 psgRNA_aceE_234 produced
27 2-oxoglutarate to a final concentration of 3.6 g/l and formed small amounts of lactate and acetate as further
28 byproducts. We concluded that the CRISPRi silencing efficacy by single targeting of *aceE* was insufficient to maintain
29 pyruvate production and prevent its consumption at low metabolic rates.
30
31
32
33
34
35

36 **3.4 Combinatorial silencing of *aceE***

37 We hypothesized that stronger repression of *aceE* might be sufficient to prevent the complete decarboxylation of
38 pyruvate in the TCA cycle at low metabolic rates. In shaking flask experiments of the first series of knockdown strains
39 each sgRNA alone was sufficient to enable the production of pyruvate (Fig. 2 A), so we presumed that a combinatorial
40 repression of *aceE* by CRISPRi with two sgRNAs might be beneficial for the stabilization of pyruvate production.
41 Multiplex CRISPRi against a single gene or multiple genes was successfully applied in other studies to obtain desired
42 phenotypes [38, 39]. We thus constructed a second series of strains with four different combinations of sgRNAs
43 targeting *aceE* (232+234, 232+235, 233+234 and 233+235). However, cultivation in shaking flask fermentations
44 revealed that none of the strains showed beneficial properties surpassing those of the first series (Fig. 2 B). On the
45 contrary, the combinatorial silencing approach appeared to be detrimental in general. Except for *E. coli* MG1655
46 pdCas9 psgRNA_aceE_232_aceE_235 (Fig. 5) none of the combinatorial knockdown strains could reach the pyruvate
47 yield of the respective single knockdown strains. We suspected that close binding of multiple sgRNA-dCas9 complexes
48 to *aceE* could cause the declining pyruvate yield, so targeting multiple more distant sites might be a feasible
49 alternative. As the promoter of *pdhR* strongly drives expression of *aceE* in presence of pyruvate, we hypothesized
50 that simultaneously targeting *pdhRp* and *aceEp* might lead to effective repression of *aceE*.
51
52
53
54
55
56
57
58
59
60

3.5 Simultaneous silencing of *aceE* and *pdhR* enables stable pyruvate production in extended bioreactor cultivations

We tested six different combinations of sgRNAs targeting *aceEp* and *pdhRp* (233+327, 233+328, 233+329, 234+327, 234+328 and 234+329) in a third series of knockdown strains in shaking flask experiments (Fig. 2 C). Surprisingly, most of the double knockdown strains were clearly inferior to the single *aceE* knockdown variants from the first series. However, one strain, *E. coli* MG1655 pdCas9 psgRNA_aceE_234_pdhR_329, retained the ability to strongly produce pyruvate while benefitting from a high maximum specific growth rate. We therefore decided to characterize the strain in lab-scale bioreactors to determine its ability to produce pyruvate in an extended nitrogen-limited production phase using identical conditions as described before: excessive glucose was provided, and ammonium was used as the limiting nutrient (Fig. 4 right panel, Table 3). During the exponential batch phase *E. coli* MG1655 pdCas9 psgRNA_aceE_234_pdhR_329 accumulated about 4 g/l pyruvate. When the nitrogen supply was exhausted and growth ceased, the strain continued to produce pyruvate constantly over the entire remaining process time for more than 15 h. After 28 h the final fermentation sample was drawn, and a pyruvate content of 11.28 g/l was measured. Despite the accumulation of 2-oxoglutarate as the primary byproduct the specific pyruvate production rate was stable during the nitrogen-limited phase, albeit much lower than during the exponential phase. 2-oxoglutarate accumulated to a final concentration of 3.34 g/l. Other organic acids were produced in much smaller amounts: The final titer for lactate was 0.40 g/l and the final titer for acetate 0.37 g/l. No ethanol or formate were detected in the final fermentation sample.

Compared to the performance of *E. coli* MG1655 pdCas9 psgRNA_aceE_234 the double knockdown strain *E. coli* MG1655 pdCas9 psgRNA_aceE_234_pdhR_329 was clearly superior. Not only did it achieve the stable production of pyruvate during the nitrogen-limited phase but also had significantly higher maximum specific growth rate (two-tailed t-test, $p < 0.01$) and biomass specific pyruvate productivity (two-tailed t-test, $p < 0.01$) during the exponential phase. Probably owing to constant pyruvate production it also had a significantly higher specific glucose consumption rate during the nitrogen limited phase (two-tailed t-test, $p < 0.01$).

3.6 Silencing of *pdhR*

Based on our observations with strains from the third series, we were intrigued whether targeting only the promoter region of *pdhR* would be sufficient to trigger strong accumulation of pyruvate. We thus tested a fourth series of knockdown strains with the three different sgRNAs (327, 328 and 329) targeting the promoter region of *pdhR* (Fig. 1). Exemplary shaking flask fermentation data from *E. coli* MG1655 pdCas9 psgRNA_pdhR_329 is shown in Fig. 6. All three strains carrying a sgRNA targeting *pdhRp* exhibited a similar phenotype and strongly produced pyruvate (Fig. 2 D). In fact, pyruvate yield was higher than for most strains from the third series and comparable to that of *E. coli* MG1655 pdCas9 psgRNA_aceE_234 and *E. coli* MG1655 pdCas9 psgRNA_aceE_234_pdhR_329 in the shaking flask experiments. Future studies may reveal whether the strains from the fourth series share the stable pyruvate production phenotype of *E. coli* MG1655 pdCas9 psgRNA_aceE_234_pdhR_329 during a nitrogen-limited production phase.

4 Discussion

CRISPRi enables the rapid targeted silencing of virtually any non-essential gene for the purpose of metabolic engineering. In this study, we applied CRISPRi to reduce the expression of *aceE* resulting in the accumulation of pyruvate in aerobic fermentations. All sgRNAs tested enabled pyruvate production in shaking flasks, but at substantially differing yields. The simultaneous targeting of *aceEp* and *pdhRp* in *E. coli* MG1655 pdCas9 psgRNA_aceE_234_pdhR_329 lead to the stable production of pyruvate at low metabolic rates during a nitrogen-limited production phase.

The sgRNAs targeting *aceE* were designed to block transcript elongation originating from *pdhRp* and initiation from *aceEp*. Given that construct psgRNA_aceE_235, designed to only block elongation, showed the poorest performance we conclude that effective silencing is most easily accomplished by targeting promoter regions. Construct psgRNA_aceE_232 was clearly less effective than psgRNA_aceE_233 and psgRNA_aceE_234 confirming the importance of targeting the non-template strand. In the case of *pdhRp* all target sites were located close to the transcription initiation site and appeared well suited. These observations are well in line with previously published findings concerning the choice of CRISPRi targets [20]. Besides the good silencing efficacy, we observed substantial repression in the absence of inducer and even the lowest tested anhydrotetracycline concentration of 0.01 µg/ml was sufficient to exert repression (Supporting Information S2). We conclude that silencing efficacy should be fine-tuned by sgRNA design rather than by expression level of dCas9 if a specific level of activity is desired. Low cellular dCas9 levels are in principle desirable anyway, as toxic effects can occur if sgRNAs with certain seed sequences are used in conjunction with high dCas9 concentration [40].

Attempts to improve silencing of *aceE* by combinatorial CRISPRi against multiple target sites in *aceEp* were largely unsuccessful. In fact, there were detrimental effects, and except for *E. coli* MG1655 pdCas9 psgRNA_aceE_232_aceE_235 we could not achieve relevant improvements in any of the *aceE* double knockdown strains. Targeting the coding region of a gene with multiple sgRNAs was successful in other studies if the two target sites were sufficiently apart [20, 39]. It appears that these observations cannot be generally transferred to multiple targets within promoter regions. Regarding the distance between multiple target sites, data collected with Cas9 nickase showed that an offset of 8 base pairs was sufficient to allow the binding of multiple Cas9 complexes [41]. This condition was fulfilled by all double knockdown strains except *E. coli* MG1655 pdCas9 psgRNA_aceE_233_aceE_234. The inefficacy of most silencing combinations targeting *aceEp* and *pdhRp* was even more puzzling. While *E. coli* MG1655 pdCas9 psgRNA_aceE_234_pdhR_329 achieved the phenotype we were aiming for, mechanistic investigations, which were out of the scope of this study, are necessary to unravel why only this specific combination worked. A first approach could be to measure transcript levels of *aceE* and *pdhR* and investigate plasmid stability and integrity to exclude inactivation of the system. In-depth studies could then unravel interactions between the individual sgRNAs.

The stable production of pyruvate by *E. coli* MG1655 pdCas9 psgRNA_aceE_234_pdhR_329 during the nitrogen-limited production phase in the bioreactor fermentations was achieved by simultaneously targeting both *aceEp* and *pdhRp*. Pyruvate accumulation and the repression of *pdhR* can potentially influence cellular regulatory cascades. In wild-type *E. coli* PdhR autoregulates its own synthesis and serves as a regulator to 16 – 23 other genes [36]. Its central function is to relieve the repression of *pdhRp* at high pyruvate concentrations, thereby enhancing the expression of *pdhR*, *aceE* and *aceF* which accelerates pyruvate degradation to acetyl-CoA. Moreover, the PyrSR and BtsSR systems also sense pyruvate and each alters the expression of a small set of regulated genes [42, 43]. Despite the repression of *pdhR* in several knockdown strains and the concomitantly high pyruvate concentration, we did not observe detrimental effects due to altered regulation in any strain. Given the binary outer circumstances – glucose excess and complete nitrogen starvation – during the nitrogen-limited phase in the bioreactor fermentations of *E. coli* MG1655 pdCas9 psgRNA_aceE_234_pdhR_329 we presume that other regulatory responses such as the Ntr regulon dominated cellular adaptation. On the level of metabolite control, the concentration of 2-oxoglutarate controls glucose uptake by competition with phosphoenolpyruvate for its binding site at the phosphotransferase system and limits the metabolic rates in prolonged nitrogen starvation [29]. Glucose uptake was strongly reduced in the fermentations of both *E. coli* MG1655 pdCas9 psgRNA_aceE_234 and *E. coli* MG1655 pdCas9

1
2
3 psgRNA_aceE_234_pdhR_329 during the extended production phase compared to the exponential phase. However,
4 despite the continued accumulation of 2-oxoglutarate in the fermentation broth during the entire nitrogen-limited
5 phase, the specific glucose uptake rates were constant. Glucose uptake was thus either enabled by continued
6 2-oxoglutarate export or through the activation of other mechanisms. In another study, glucose uptake reduction in
7 nitrogen-limited conditions was alleviated by moderate overexpression of *ptsI* which indicates that the cellular levels
8 of 2-oxoglutarate, PtsI and phosphoenolpyruvate are naturally tightly balanced [44].
9

10 Even though *E. coli* MG1655 pdCas9 psgRNA_aceE_234_pdhR_329 accumulated less 2-oxoglutarate than *E. coli*
11 MG1655 pdCas9 psgRNA_aceE_234 during the nitrogen-limited production phase, a substantial flux into the TCA
12 cycle remained as proven by the continued formation of 2-oxoglutarate. Additional repression of pyruvate
13 dehydrogenase activity and subsequently increased pyruvate yield from glucose could potentially be achieved by
14 CRISPRi targeting the coding sequence of *aceF*. Deletions or repression of *poxB* and *ldhA* would likely further increase
15 pyruvate yield from glucose and reduce the accumulation of lactate. Since the experimental yields observed during
16 the fermentations of *E. coli* MG1655 pdCas9 psgRNA_aceE_234_pdhR_329 were lower in the nitrogen-limited
17 fermentation phase, pyruvate yield appeared to be dependent on the specific glucose uptake rate. We suggest that
18 pyruvate productivity could be indirectly improved by increasing specific glucose uptake, for instance by engineering
19 *ptsI* overexpression from a promoter induced in nitrogen-limited conditions.
20
21

22 The use case and metabolic behavior of our strains are similar to those from the studies of Michalowski et al. (2017),
23 so direct comparison of our strains with *E. coli* HGT is feasible. During the exponential phase pyruvate yield and
24 biomass specific pyruvate production rate of *E. coli* MG1655 pdCas9 psgRNA_aceE_234_pdhR_329 were comparable
25 to values reported for *E. coli* HGT and *E. coli* MG1655 pdCas9 psgRNA_aceE_234_pdhR_329 achieved a higher
26 maximum specific growth rate [16]. However, specific pyruvate productivity was lower during the second production
27 phase with resting cells which indicates that stronger repression of pyruvate dehydrogenase or higher glucose uptake
28 rates on the level of *E. coli* HGT may be necessary to improve the production phenotype of *E. coli* MG1655 pdCas9
29 psgRNA_aceE_234_pdhR_329. Extending the comparison to acetate auxotrophic strains, *E. coli* MG1655 pdCas9
30 psgRNA_aceE_234_pdhR_329 has clearly lower metabolic rates, but does not suffer from the disadvantage of
31 dependence on acetate addition [4]. Limiting the supply of acetate may lead to reduced productivity and even
32 pyruvate reuptake in auxotrophic strains [45].
33

34 A potential advantage of CRISPRi compared to other genetic modifications to lower gene expression or enzymatic
35 activity is its inherent flexibility to switch off or tune metabolic pathways during a process. A promising strategy for
36 regulating access of different metabolic pathways to the pyruvate pool is the addition of dynamic control circuits
37 [46]. Both a circuit based on PdhR and a dynamic CRISPRi silencing strategy have been applied successfully in *Bacillus*
38 *subtilis* and the principle can likely be transferred to *E. coli* [47, 48]. Integration of a pyruvate-sensing circuit based
39 on PdhR would require initial modifications of the genomic elements of the *pdhR*, *aceE* and *aceF* loci but would then
40 enable rapid phenotyping of dynamic control strategies by modulated transcription of dCas9 or sgRNAs targeting key
41 genes of competing pathways.
42
43

44 In conclusion, we successfully engineered CRISPRi knockdown strains for the stable production of pyruvate during
45 two-phase bioreactor fermentations. An important finding is that targeting *aceEp* with multiple sgRNAs was not
46 successful despite sufficient distance between the target sites. Simultaneously repressing *aceEp* and *pdhRp* improved
47 pyruvate accumulation during the exponential phase and was sufficient to enable constant pyruvate production
48 during a nitrogen-limited phase. Furthermore, targeting *pdhR* alone was sufficient to enable strong pyruvate
49 production in shaking flasks. Our study provides a foundation for controlled production of pyruvate and
50 pyruvate-derived products in *E. coli*, and *E. coli* MG1655 pdCas9 psgRNA_aceE_234_pdhR_329 may serve as a chassis
51 in future investigations.
52
53
54
55
56
57
58
59
60

Acknowledgements

The authors acknowledge the support of Prasika Arulrajah for assistance with sample analysis.

Conflict of Interest

The authors declare no conflicts of interest.

For Peer Review

References

- [1] Miyata, R., Yonehara, T., Yotsumoto, K., Tsutsui, H., *Process for preparing pyruvic acid by fermentation*. EP0389620 (A1), 1987.
- [2] Sawai, H., Mimitsuka, T., Minegishi, S.-I., Henmi, M. et al., A novel membrane-integrated fermentation reactor system: application to pyruvic acid production in continuous culture by *Torulopsis glabrata*. *Bioprocess Biosyst. Eng.* 2011, *34*, 721–725.
- [3] Zelić, B., Gostović, S., Vuorilehto, K., Vasić-Racki, D. et al., Process strategies to enhance pyruvate production with recombinant *Escherichia coli*: from repetitive fed-batch to in situ product recovery with fully integrated electrodialysis. *Biotechnol. Bioeng.* 2004, *85*, 638–646.
- [4] Zhu, Y., Eiteman, M. A., Altman, R., Altman, E., High glycolytic flux improves pyruvate production by a metabolically engineered *Escherichia coli* strain. *Appl. Environ. Microbiol.* 2008, *74*, 6649–6655.
- [5] Li, Y., Chen, J., Lun, S. Y., Rui, X. S., Efficient pyruvate production by a multi-vitamin auxotroph of *Torulopsis glabrata*: key role and optimization of vitamin levels. *Appl. Microbiol. Biotechnol.* 2001, *55*, 680–685.
- [6] Biver, A. P., Zuber, P. T., Zelic, B., Gerharz, T. et al., Modeling and Analysis of a New Process for Pyruvate Production. *Ind. Eng. Chem. Res.* 2005, *44*, 3124–3133.
- [7] Li, Y., Chen, J., Lun, S. Y., Biotechnological production of pyruvic acid. *Appl. Microbiol. Biotechnol.* 2001, *57*, 451–459.
- [8] Yuan, W., Zhong, S., Xiao, Y., Wang, Z. et al., Efficient biocatalyst of L-DOPA with *Escherichia coli* expressing a tyrosine phenol-lyase mutant from *Kluyvera intermedia*. *Appl. Biochem. Biotechnol.* 2020, *190*, 1187–1200.
- [9] Onakpoya, I., Hunt, K., Wider, B., Ernst, E., Pyruvate supplementation for weight loss: a systematic review and meta-analysis of randomized clinical trials. *Crit. Rev. Food Sci. Nutr.* 2014, *54*, 17–23.
- [10] Ma, Y., Cui, Y., Du, L., Liu, X. et al., Identification and application of a growth-regulated promoter for improving L-valine production in *Corynebacterium glutamicum*. *Microb. Cell Factories* 2018, *17*, 185.
- [11] Wess, J., Brinek, M., Boles, E., Improving isobutanol production with the yeast *Saccharomyces cerevisiae* by successively blocking competing metabolic pathways as well as ethanol and glycerol formation. *Biotechnol. Biofuels* 2019, *12*, 173.
- [12] Rohmer, M., Seemann, M., Horbach, S., Bringer-Meyer, S. et al., Glyceraldehyde 3-Phosphate and Pyruvate as Precursors of Isoprenic Units in an Alternative Non-mevalonate Pathway for Terpenoid Biosynthesis. *J. Am. Chem. Soc.* 1996, *118*, 2564–2566.
- [13] Ward, V. C. A., Chatzivasileiou, A. O., Stephanopoulos, G., Metabolic engineering of *Escherichia coli* for the production of isoprenoids. *FEMS Microbiol. Lett.* 2018, *365*.
- [14] Patil, V., Santos, C. N. S., Ajikumar, P. K., Sarria, S. et al., Balancing glucose and oxygen uptake rates to enable high amorpha-4,11-diene production in *Escherichia coli* via the methylerythritol phosphate (MEP) pathway. *Biotechnol. Bioeng.* 2020.
- [15] Tomar, A., Eiteman, M. A., Altman, E., The effect of acetate pathway mutations on the production of pyruvate in *Escherichia coli*. *Appl. Microbiol. Biotechnol.* 2003, *62*, 76–82.
- [16] Michalowski, A., Siemann-Herzberg, M., Takors, R., *Escherichia coli* HGT: Engineered for high glucose throughput even under slowly growing or resting conditions. *Metab. Eng.* 2017, *40*, 93–103.
- [17] Nakashima, N., Ohno, S., Yoshikawa, K., Shimizu, H. et al., A vector library for silencing central carbon metabolism genes with antisense RNAs in *Escherichia coli*. *Appl. Environ. Microbiol.* 2014, *80*, 564–573.
- [18] Chang, Y., Su, T., Qi, Q., Liang, Q., Easy regulation of metabolic flux in *Escherichia coli* using an endogenous type I-E CRISPR-Cas system. *Microb. Cell Factories* 2016, *15*, 195.
- [19] Rath, D., Amlinger, L., Hoekzema, M., Devulapally, P. R. et al., Efficient programmable gene silencing by Cascade. *Nucleic Acids Res.* 2015, *43*, 237–246.
- [20] Qi, L. S., Larson, M. H., Gilbert, L. A., Doudna, J. A. et al., Repurposing CRISPR as an RNA-guided platform for sequence-specific control of gene expression. *Cell* 2013, *152*, 1173–1183.
- [21] Bikard, D., Jiang, W., Samai, P., Hochschild, A. et al., Programmable repression and activation of bacterial gene expression using an engineered CRISPR-Cas system. *Nucleic Acids Res.* 2013, *41*, 7429–7437.

- 1
2
3 [22] Larson, M. H., Gilbert, L. A., Wang, X., Lim, W. A. et al., CRISPR interference (CRISPRi) for sequence-specific
4 control of gene expression. *Nat. Protoc.* 2013, 8, 2180–2196.
- 5 [23] Schultenkämper, K., Brito, L. F., Wendisch, V. F., Impact of CRISPR interference on strain development in
6 biotechnology. *Biotechnol. Appl. Biochem.* 2020, 67, 7–21.
- 7 [24] Sander, T., Wang, C. Y., Glatter, T., Link, H., CRISPRi-Based Downregulation of Transcriptional Feedback Improves
8 Growth and Metabolism of Arginine Overproducing *E. coli*. *ACS Synth. Biol.* 2019, 8, 1983–1990.
- 9 [25] Lo, T.-M., Chng, S. H., Teo, W. S., Cho, H.-S. et al., A Two-Layer Gene Circuit for Decoupling Cell Growth from
10 Metabolite Production. *Cell Syst.* 2016, 3, 133–143.
- 11 [26] Lange, J., Takors, R., Blombach, B., Zero-growth bioprocesses: A challenge for microbial production strains and
12 bioprocess engineering. *Eng. Life Sci.* 2017, 17, 27–35.
- 13 [27] Perez-Zabaleta, M., Guevara-Martínez, M., Gustavsson, M., Quillaguamán, J. et al., Comparison of engineered
14 *Escherichia coli* AF1000 and BL21 strains for (R)-3-hydroxybutyrate production in fed-batch cultivation. *Appl.*
15 *Microbiol. Biotechnol.* 2019, 103, 5627–5639.
- 16 [28] Aon, J. C., Cortassa, S., Involvement of nitrogen metabolism in the triggering of ethanol fermentation in aerobic
17 chemostat cultures of *Saccharomyces cerevisiae*. *Metab. Eng.* 2001, 3, 250–264.
- 18 [29] Huergo, L. F., Dixon, R., The Emergence of 2-Oxoglutarate as a Master Regulator Metabolite. *Microbiol. Mol.*
19 *Biol. Rev.* 2015, 79, 419–435.
- 20 [30] Hanahan, D., Studies on transformation of *Escherichia coli* with plasmids. *J. Mol. Biol.* 1983, 166, 557–580.
- 21 [31] Hawkins, J. S., Wong, S., Peters, J. M., Almeida, R. et al., Targeted Transcriptional Repression in Bacteria Using
22 CRISPR Interference (CRISPRi). *Methods Mol. Biol.* 2015, 1311, 349–362.
- 23 [32] Shetty, R. P., Endy, D., Knight, T. F., Engineering BioBrick vectors from BioBrick parts. *J. Biol. Eng.* 2008, 2, 5.
- 24 [33] Miller, J. H., *Experiments in molecular genetics*, 11th Ed., Cold Spring Harbor Laboratory, Cold Spring Harbor, NY
25 1972.
- 26 [34] Quail, M. A., Haydon, D. J., Guest, J. R., The *pdhR-aceEF-lpd* operon of *Escherichia coli* expresses the pyruvate
27 dehydrogenase complex. *Mol. Microbiol.* 1994, 12, 95–104.
- 28 [35] Olvera, L., Mendoza-Vargas, A., Flores, N., Olvera, M. et al., Transcription analysis of central metabolism genes
29 in *Escherichia coli*. Possible roles of sigma38 in their expression, as a response to carbon limitation. *PLoS one*
30 2009, 4, e7466.
- 31 [36] Anzai, T., Imamura, S., Ishihama, A., Shimada, T., Expanded roles of pyruvate-sensing PdhR in transcription
32 regulation of the *Escherichia coli* K-12 genome: fatty acid catabolism and cell motility. *Microb. Genom.* 2020, 6,
33 e000442.
- 34 [37] Maeda, S., Shimizu, K., Kihira, C., Iwabu, Y. et al., Pyruvate dehydrogenase complex regulator (PdhR) gene
35 deletion boosts glucose metabolism in *Escherichia coli* under oxygen-limited culture conditions. *Journal of*
36 *bioscience and bioengineering* 2017, 123, 437–443.
- 37 [38] Gao, C., Wang, S., Hu, G., Guo, L. et al., Engineering *Escherichia coli* for malate production by integrating modular
38 pathway characterization with CRISPRi-guided multiplexed metabolic tuning. *Biotechnol. Bioeng.* 2018, 115,
39 661–672.
- 40 [39] Zhang, J.-L., Peng, Y.-Z., Liu, D., Liu, H. et al., Gene repression via multiplex gRNA strategy in *Y. lipolytica*. *Microb.*
41 *Cell Factories* 2018, 17, 62.
- 42 [40] Cui, L., Vigouroux, A., Rousset, F., Varet, H. et al., A CRISPRi screen in *E. coli* reveals sequence-specific toxicity of
43 dCas9. *Nat. Commun.* 2018, 9, 1912.
- 44 [41] Ran, F. A., Hsu, P. D., Lin, C.-Y., Gootenberg, J. S. et al., Double nicking by RNA-guided CRISPR Cas9 for enhanced
45 genome editing specificity. *Cell* 2013, 154, 1380–1389.
- 46 [42] Ogasawara, H., Ishizuka, T., Yamaji, K., Kato, Y. et al., Regulatory role of pyruvate-sensing BtsSR in biofilm
47 formation by *Escherichia coli* K-12. *FEMS Microbiol. Lett.* 2019, 366.
- 48 [43] Miyake, Y., Inaba, T., Watanabe, H., Teramoto, J. et al., Regulatory roles of pyruvate-sensing two-component
49 system PyrSR (YpdAB) in *Escherichia coli* K-12. *FEMS Microbiol. Lett.* 2019, 366.
- 50 [44] Chubukov, V., Desmarais, J. J., Wang, G., Chan, L. J. G. et al., Engineering glucose metabolism of *Escherichia coli*
51 under nitrogen starvation. *NPJ Syst. Biol. Appl.* 2017, 3, 16035.
- 52
53
54
55
56
57
58
59
60

- 1
2
3 [45] Zelić, B., Gerharz, T., Bott, M., Vasić-Rački, Đ. et al., Fed-Batch Process for Pyruvate Production by Recombinant
4 Escherichia coli YYC202 Strain. *Eng. Life Sci.* 2003, 3, 299–305.
5 [46] Brockman, I. M., Prather, K. L. J., Dynamic knockdown of E. coli central metabolism for redirecting fluxes of
6 primary metabolites. *Metab. Eng.* 2015, 28, 104–113.
7 [47] Xu, X., Li, X., Liu, Y., Zhu, Y. et al., Pyruvate-responsive genetic circuits for dynamic control of central metabolism.
8 *Nat. Chem. Biol.* 2020, 16, 1261–1268.
9 [48] Wu, Y., Chen, T., Liu, Y., Tian, R. et al., Design of a programmable biosensor-CRISPRi genetic circuits for dynamic
10 and autonomous dual-control of metabolic flux in Bacillus subtilis. *Nucleic Acids Res.* 2020, 48, 996–1009.
11
12
13
14
15
16
17
18
19
20
21
22
23
24
25
26
27
28
29
30
31
32
33
34
35
36
37
38
39
40
41
42
43
44
45
46
47
48
49
50
51
52
53
54
55
56
57
58
59
60

For Peer Review

Tables

Table 1: Strains used in this study

Strains	Strain Information / CRISPRi targets	Reference
<i>Escherichia coli</i> DH5 α λ pir	cloning strain	[16]
<i>E. coli</i> MG1655	wild-type strain	[16]
<i>E. coli</i> Top10 pdCas9	contains dCas9 inducible by anhydrotetracycline	[20] ^a
<i>E. coli</i> Top10 pgRNA-bacteria	empty guideRNA plasmid	[20] ^b
<i>E. coli</i> MG1655 psgRNA_lacZ_236 pdCas9	<i>lacZ</i> (TTGGGAAGGGCGATCGGTGC)	[20] ^c
<i>E. coli</i> MG1655 psgRNA_lacZ_237 pdCas9	<i>lacZ</i> (GGCCAGTGAATCCGTAATCA)	This study
<i>E. coli</i> MG1655 psgRNA_lacZ_238 pdCas9	<i>lacZ</i> (AAGCATAAAGTGTAAGCCT)	This study
<i>E. coli</i> MG1655 psgRNA_lacZ_239 pdCas9	<i>lacZ</i> (AGCGGATAACAATTTACAC)	This study
<i>E. coli</i> MG1655 psgRNA_neg_241 pdCas9	-	This study
<i>E. coli</i> MG1655 psgRNA_aceE_232 pdCas9	<i>aceE</i> (ACCTGTCTTATTGAGCTTTC)	This study
<i>E. coli</i> MG1655 psgRNA_aceE_233 pdCas9	<i>aceE</i> (CTGTCCCATTGAACTCTCGC)	This study
<i>E. coli</i> MG1655 psgRNA_aceE_234 pdCas9	<i>aceE</i> (TCTAATAACGTTGAGTTTTTC)	This study
<i>E. coli</i> MG1655 psgRNA_aceE_235 pdCas9	<i>aceE</i> (AGCCAGTCGCGAGTTTCGAT)	This study
<i>E. coli</i> MG1655 psgRNA_aceE_232_aceE_234 pdCas9	<i>aceE</i> (ACCTGTCTTATTGAGCTTTC, TCTAATAACGTTGAGTTTTTC)	This study
<i>E. coli</i> MG1655 psgRNA_aceE_232_aceE_235 pdCas9	<i>aceE</i> (ACCTGTCTTATTGAGCTTTC, AGCCAGTCGCGAGTTTCGAT)	This study
<i>E. coli</i> MG1655 psgRNA_aceE_233_aceE_234 pdCas9	<i>aceE</i> (CTGTCCCATTGAACTCTCGC, TCTAATAACGTTGAGTTTTTC)	This study
<i>E. coli</i> MG1655 psgRNA_aceE_233_aceE_235 pdCas9	<i>aceE</i> (CTGTCCCATTGAACTCTCGC, AGCCAGTCGCGAGTTTCGAT)	This study
<i>E. coli</i> MG1655 psgRNA_pdhR_327 pdCas9	<i>pdhR</i> (TCAAAACCTGTATGGACATA)	This study
<i>E. coli</i> MG1655 psgRNA_pdhR_328 pdCas9	<i>pdhR</i> (TATTCACCTTATGTCCATAC)	This study
<i>E. coli</i> MG1655 psgRNA_pdhR_329 pdCas9	<i>pdhR</i> (AGCCACTTGCCGAAGTCAAT)	This study
<i>E. coli</i> MG1655 psgRNA_aceE_233_pdhR_327 pdCas9	<i>aceE + pdhR</i> (CTGTCCCATTGAACTCTCGC, TCAAAACCTGTATGGACATA)	This study
<i>E. coli</i> MG1655 psgRNA_aceE_233_pdhR_328 pdCas9	<i>aceE + pdhR</i> (CTGTCCCATTGAACTCTCGC, TATTCACCTTATGTCCATAC)	This study
<i>E. coli</i> MG1655 psgRNA_aceE_233_pdhR_329 pdCas9	<i>aceE + pdhR</i> (TCTAATAACGTTGAGTTTTTC, AGCCACTTGCCGAAGTCAAT)	This study
<i>E. coli</i> MG1655 psgRNA_aceE_234_pdhR_327 pdCas9	<i>aceE + pdhR</i> (TCTAATAACGTTGAGTTTTTC, TCAAAACCTGTATGGACATA)	This study
<i>E. coli</i> MG1655 psgRNA_aceE_234_pdhR_328 pdCas9	<i>aceE + pdhR</i> (TCTAATAACGTTGAGTTTTTC, TATTCACCTTATGTCCATAC)	This study
<i>E. coli</i> MG1655 psgRNA_aceE_234_pdhR_329 pdCas9	<i>aceE + pdhR</i> (TCTAATAACGTTGAGTTTTTC, AGCCACTTGCCGAAGTCAAT)	This study

a: pdCas9-bacteria was a gift from Stanley Qi (Addgene plasmid # 44249; <http://n2t.net/addgene:44249>; RRID: Addgene_44249)

b: pgRNA-bacteria was a gift from Stanley Qi (Addgene plasmid # 44251; <http://n2t.net/addgene:44251>; RRID: Addgene_44251)

c: Strain was constructed in this study according to information provided in the given reference.

Table 2: Primers used in this study

No.	Primer name	Sequence 5' → 3' (<u>binding sequence</u>)	Function
236	lacZ_236	TTGGGAAGGGCGATCGGTGCGTTTTAGAGCTAGAAAT AGCAAGTAAAATAAGGC	fwd primer for iPCR [20]
237	lacZ_237	GGCCAGTGAATCCGTAATCAGTTTTAGAGCTAGAAATA GCAAGTAAAATAAGGC	fwd primer for iPCR
238	lacZ_238	AAGCATAAAGTGTAAGCCTGTTTTAGAGCTAGAAATA GCAAGTAAAATAAGGC	fwd primer for iPCR
239	lacZ_239	AGCGGATAACAATTTACACGTTTTAGAGCTAGAAATA GCAAGTAAAATAAGGC	fwd primer for iPCR
232	aceE_232	ACCTGTCTTATTGAGCTTTCGTTTTAGAGCTAGAAATAG CAAGTAAAATAAGGC	fwd primer for iPCR
233	aceE_233	CTGTCCATTGAACTCTCGCGTTTTAGAGCTAGAAATAG CAAGTAAAATAAGGC	fwd primer for iPCR
234	aceE_234	TCTAATAACGTTGAGTTTTCGTTTTAGAGCTAGAAATAG CAAGTAAAATAAGGC	fwd primer for iPCR
235	aceE_235	AGCCAGTCGCGAGTTTCGATGTTTTAGAGCTAGAAATA GCAAGTAAAATAAGGC	fwd primer for iPCR
327	pdhR_327	TCAAAACCTGTATGGACATAGTTTTAGAGCTAGAAATA GCAAGTAAAATAAGGC	fwd primer for iPCR
328	pdhR_328	TATTCACCTTATGTCCATACGTTTTAGAGCTAGAAATAG CAAGTAAAATAAGGC	fwd primer for iPCR
329	pdhR_329	AGCCACTTGCCGAAGTCAATGTTTTAGAGCTAGAAATA GCAAGTAAAATAAGGC	fwd primer for iPCR
240	sgRNA_r	ACTAGTATTATACCTAGGACTGAGCTAGC	rev primer for iPCR [22]
241	sgRNA_neg	GTTTTAGAGCTAGAAATAGCAAGTAAAATAAGGC	fwd primer for iPCR [22]
242	sgRNA_seq_col_f	GGGTTATTGTCTCATGAGCGGATACATATTTG	sequencing of psgRNA [22]

Table 3: Yield coefficients and fermentation parameters of bioreactor fermentations with extended nitrogen-limited production phase.

		<i>E. coli</i> MG1655 pdCas9 psgRNA_aceE_234		<i>E. coli</i> MG1655 pdCas9 psgRNA_aceE_234_pdhR_329	
symbol	unit	exp. phase	N-lim. phase	exp. phase	N-lim. phase
μ	[h ⁻¹]	0.414 ± 0.0042 ^a	-	0.472 ± 0.0078	-
$Y_{X/S}$	[g _{CDW} /g _{Glucose}]	0.270 ± 0.0072	-	0.29 ± 0.036	-
q_s	[g _{Glucose} /g _{CDW} /h]	1.53 ± 0.046	0.30 ± 0.011	1.8 ± 0.24	0.38 ± 0.013
$Y_{P/S}$	[g _{Pyruvate} /g _{Glucose}]	0.40 ± 0.018	-	0.50 ± 0.065	0.36 ± 0.029
q_p	[g _{Pyruvate} /g _{CDW} /h]	0.61 ± 0.012	-0.021 ± 0.0026	0.83 ± 0.023	0.135 ± 0.0095
$Y_{2-Oxo/S}$	[g _{2-Oxoglutarate} /g _{Glucose}]	0.010 ± 0.0018	0.332 ± 0.0073	0.0390 ± 0.0065	0.16 ± 0.012
q_{2-Oxo}	[g _{2-Oxoglutarate} /g _{CDW} /h]	0.016 ± 0.0029	0.010 ± 0.0016	0.063 ± 0.0022	0.062 ± 0.0054

a: Errors indicate SEM, *E. coli* MG1655 pdCas9 psgRNA_aceE_234 (n = 3), *E. coli* MG1655 pdCas9 psgRNA_aceE_234_pdhR_329 (n = 5).

Figure Legends

Figure 1: sgRNA binding sites. Four binding sites (232, 233, 234 and 235) were chosen for CRISPRi targeting *aceE* and three binding sites (327,328 and 329) for CRISPRi against *pdhR*.

Figure 2: Pyruvate yield in shaking flask fermentations of *E. coli* MG1655 pdCas9 with different psgRNAs. Data is grouped into four series. Error bars indicate SEM (n = 3; *n = 2). **A:** wild-type reference (no plasmids) and first series, silencing of *aceE*. **B:** second series, combinatorial silencing of *aceE*. **C:** third series, simultaneous silencing of *aceE* and *pdhR*. **D:** fourth series, silencing of *pdhR*.

Figure 3: Shaking flask fermentations of the single knockdown strain *E. coli* pdCas9 psgRNA_aceE_234. The experiments were conducted with addition of the inducer anhydrotetracycline (left) or without anhydrotetracycline (right). Error bars indicate SEM (n = 3).

Figure 4: Bioreactor cultivations of knockdown strains. The aerobic lab-scale fermentations were carried out with excessive glucose. Depletion of ammonia initiates the nitrogen-limited second process phase. Error bars indicate SEM. Left: The best single knockdown strain from the 1st series *E. coli* MG1655 pdCas9 psgRNA_aceE_234 (n = 3). Right: The best double knockdown strain from the 3rd series *E. coli* MG1655 pdCas9 psgRNA_aceE_234_pdhR_329 (n = 5).

Figure 5: Shaking flask fermentations of the double knockdown strain *E. coli* MG1655 pdCas9 psgRNA_aceE_232_aceE_235. Error bars indicate SEM (n = 3).

Figure 6: Shaking flask fermentations of the single knockdown strain *E. coli* MG1655 pdCas9 psgRNA_aceE_pdhR_329. Error bars indicate SEM (n = 3).

Supporting Information Captions

Supporting Information S1: Knockdown of *lacZ*

Supporting Information S2: Inducer Concentration

For Peer Review

1
2
3
4
5
6
7
8
9
10
11
12
13
14
15
16
17
18
19
20
21
22
23
24
25
26
27
28
29
30
31
32
33
34
35
36
37
38
39
40
41
42
43
44
45
46
47
48
49
50
51
52
53
54
55
56
57
58
59
60

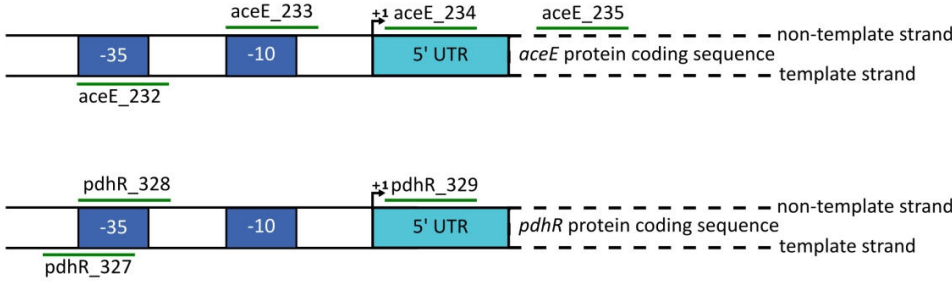


Figure 1: sgRNA binding sites. Four binding sites (232, 233, 234 and 235) were chosen for CRISPRi targeting *aceE* and three binding sites (327,328 and 329) for CRISPRi against *pdhRp*.

555x166mm (96 x 96 DPI)

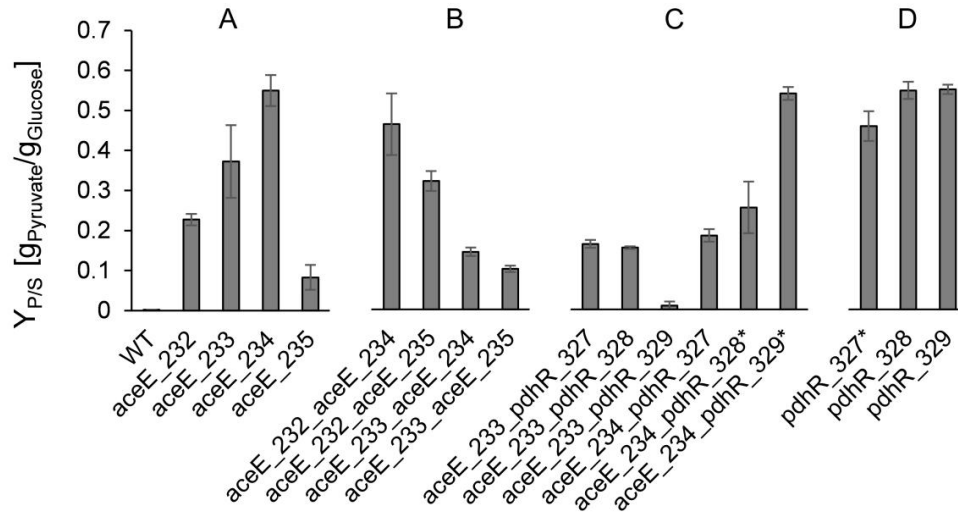


Figure 2: Pyruvate yield in shaking flask fermentations of *E. coli* MG1655 pdCas9 with different psgRNAs. Data is grouped into four series. Error bars indicate SEM ($n = 3$; * $n = 2$). **A**: wild type reference (no plasmids) and first series, silencing of *aceE*. **B**: second series, combinatorial silencing of *aceE*. **C**: third series, simultaneous silencing of *aceE* and *pdhR*. **D**: fourth series, silencing of *pdhR*.

1525x808mm (96 x 96 DPI)

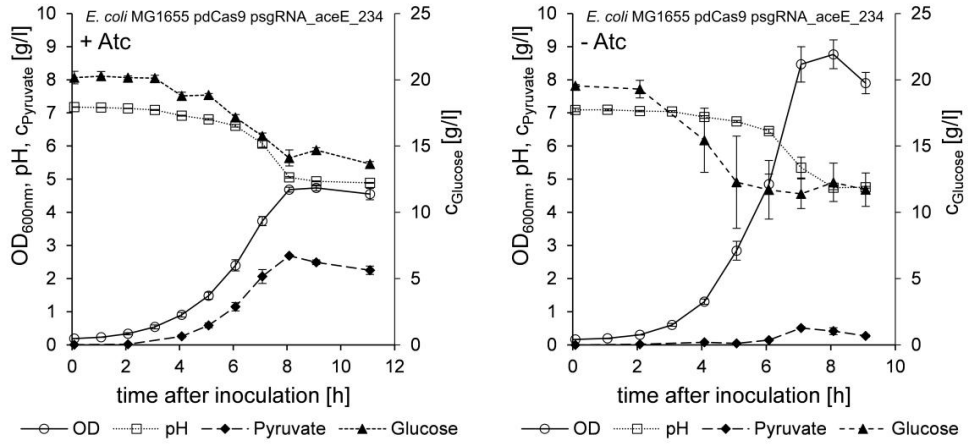


Figure 3: Shaking flask fermentations of the single knockdown strain *E. coli* pdCas9 psgRNA_aceE_234. The experiments were conducted with addition of the inducer anhydrotetracycline (left) or without anhydrotetracycline (right). Error bars indicate SEM (n = 3).

1875x906mm (96 x 96 DPI)

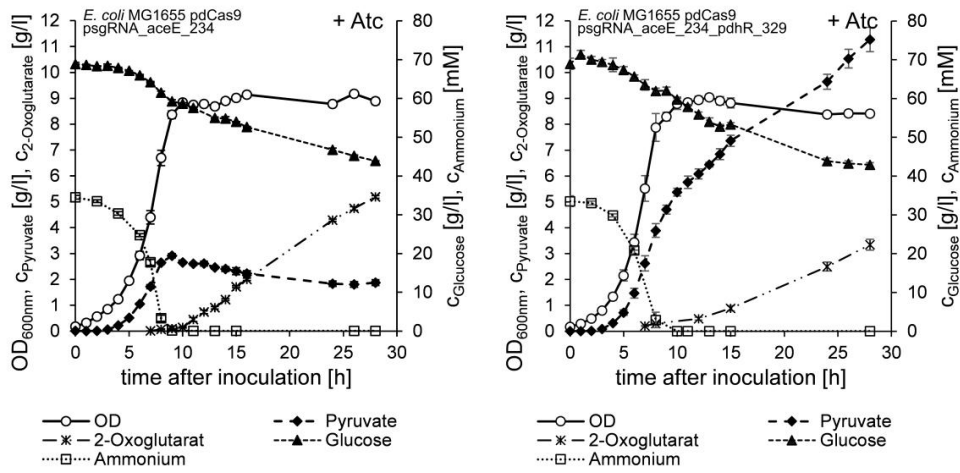


Figure 4: Bioreactor cultivations of knockdown strains. The aerobic lab scale fermentations were carried out with excessive glucose. Depletion of ammonia initiates the nitrogen limited second process phase. Error bars indicate SEM. Left: The best single knockdown strain from the 1st series *E. coli* MG1655 pdCas9 psgRNA_aceE_234 (n = 3). Right: The best double knockdown strain from the 3rd series *E. coli* MG1655 pdCas9 psgRNA_aceE_234_pdhR_329 (n = 5).

1897x940mm (96 x 96 DPI)

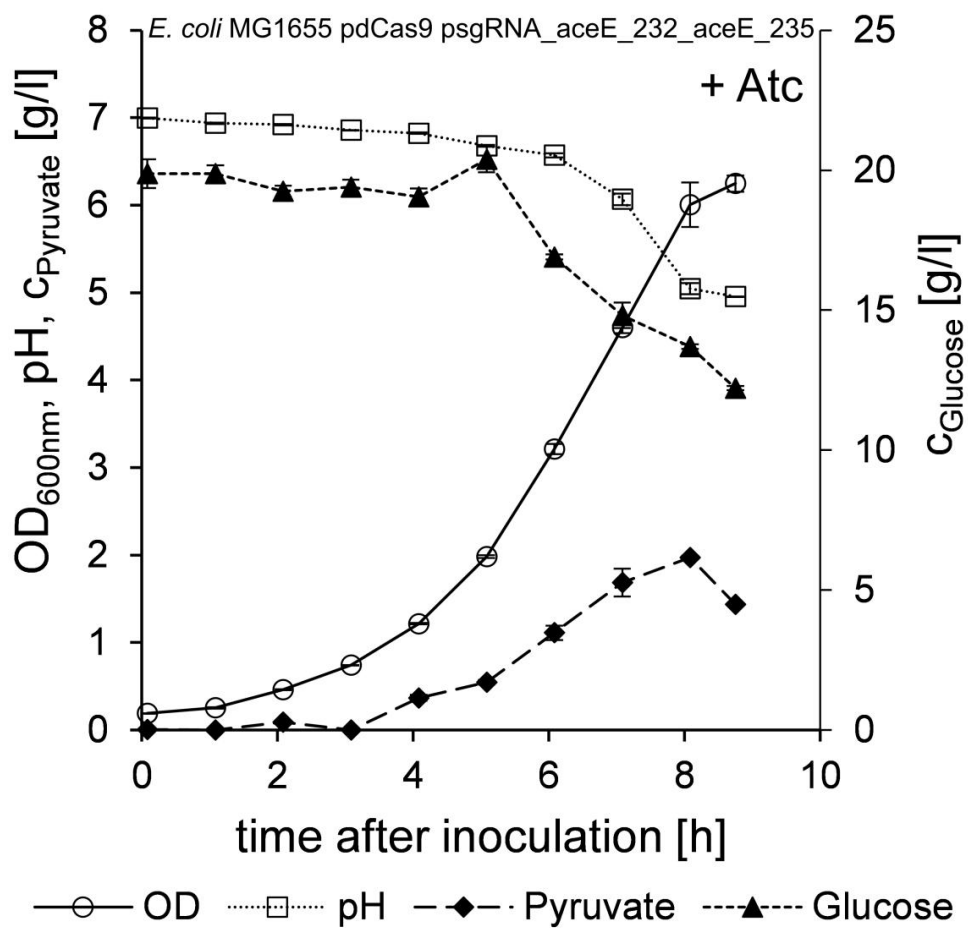


Figure 5: Shaking flask fermentations of the double knockdown strain *E. coli* MG1655 pdCas9 psgRNA_aceE_232_aceE_235. Error bars indicate SEM (n = 3).

922x884mm (96 x 96 DPI)

1
2
3
4
5
6
7
8
9
10
11
12
13
14
15
16
17
18
19
20
21
22
23
24
25
26
27
28
29
30
31
32
33
34
35
36
37
38
39
40
41
42
43
44
45
46
47
48
49
50
51
52
53
54
55
56
57
58
59
60

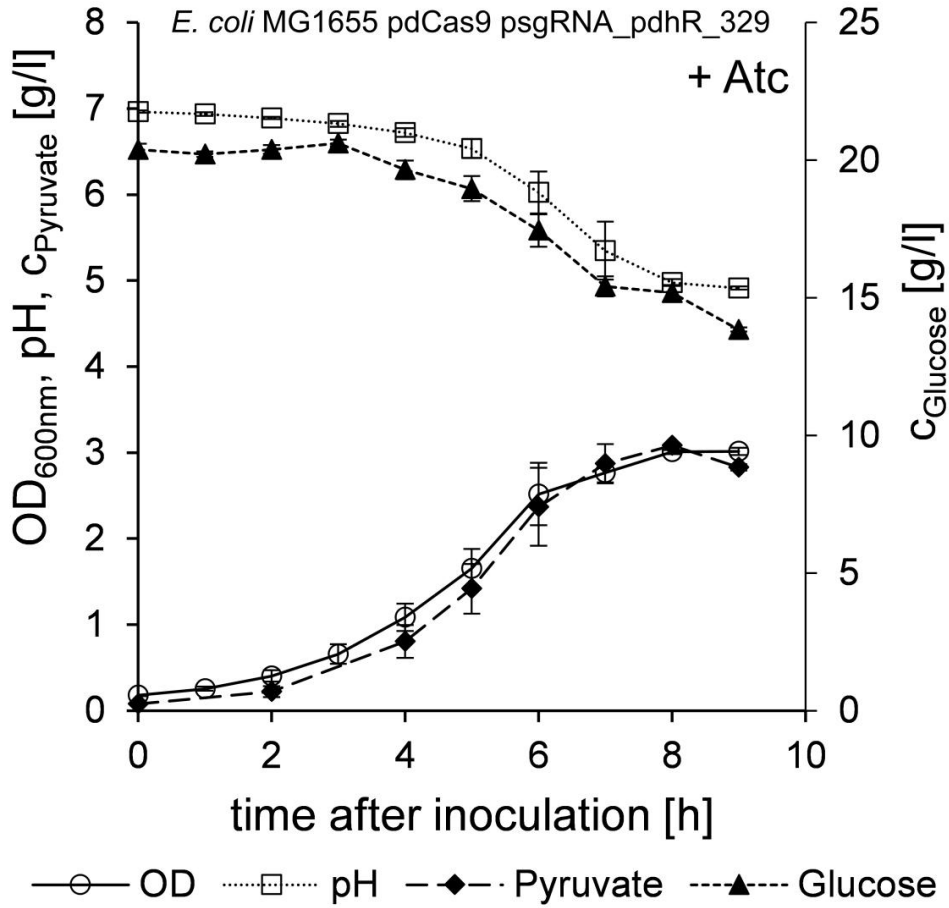
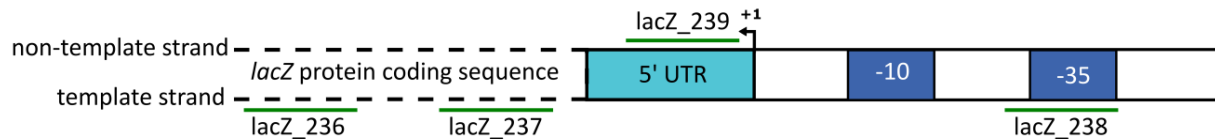


Figure 6: Shaking flask fermentations of the single knockdown strain *E. coli* MG1655 pdCas9 psgRNA_aceE_pdhR_329. Error bars indicate SEM (n = 3).

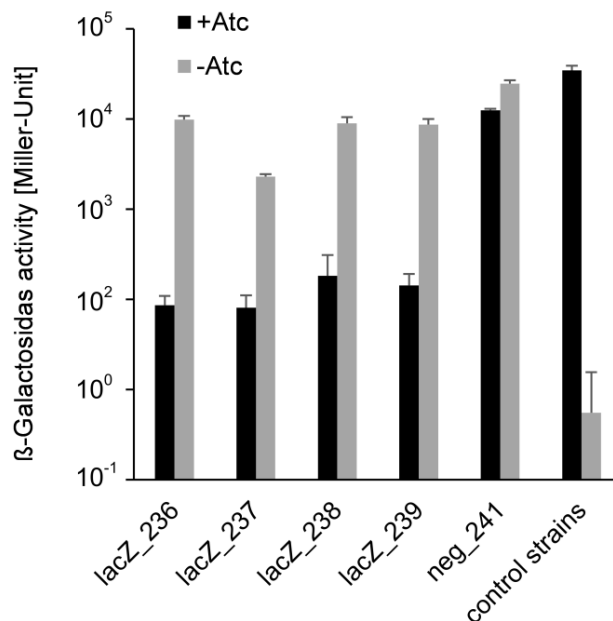
937x937mm (96 x 96 DPI)

Supporting Information S1: Knockdown of *lacZ*

We designed 3 sgRNAs targeting *lacZ* (237, 238 and 239, Suppl. Fig. 1) and used a previously described sgRNA (236) targeting *lacZ* and an empty sgRNA vector (241) as a control for the functionality of the CRISPRi system (Qi et al., 2013). *E. coli* MG1655 was used as the reference strain with high β -galactosidase activity and *E. coli* DH5 α λ pir was used as a control strain lacking any β -galactosidase activity. We performed β -galactosidase assays and found that all sgRNAs targeting *lacZ* reduced β -galactosidase activity by at least one order of magnitude (Suppl. Fig. 2). In all cases significant downregulation compared to the control strain *E. coli* MG1655 was also observed in the absence of inducer which points towards leaky expression of dCas9 from pdCas9. Enzymatic activity was also reduced with an empty sgRNA vector and more pronounced in the presence of anhydrotetracycline which indicates that small side-effects not related to the presence of sgRNA exist. Presumably, the metabolic burden of plasmid replication and dCas9 expression reduces available cellular resources for β -galactosidase expression. A residual activity remained in all assays except for the β -galactosidase assays of the *lacZ* control strain *E. coli* DH5 α λ pir.



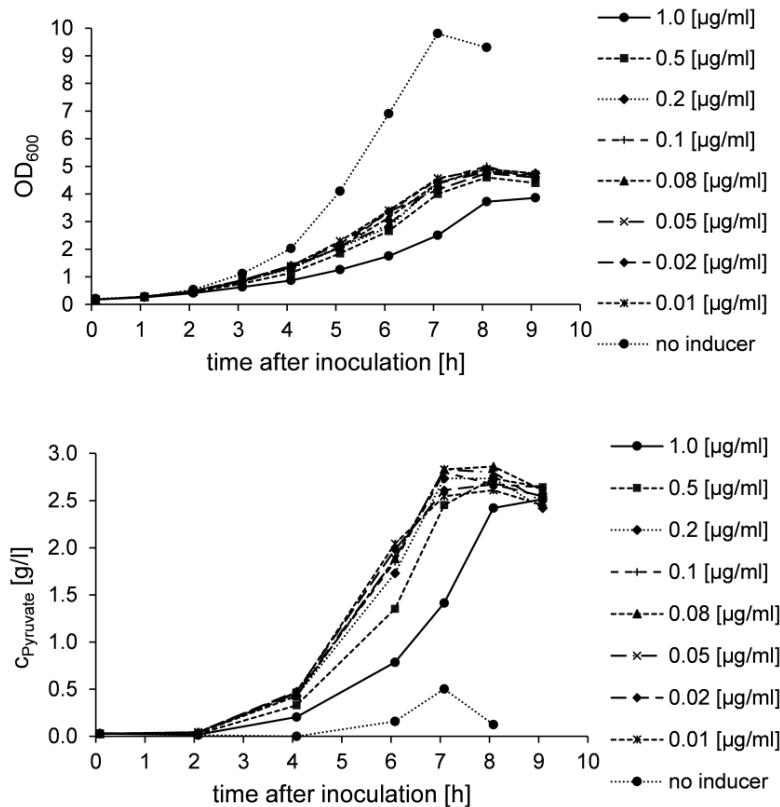
Supporting Figure 1: sgRNA binding sites for CRISPRi mediated knockdown of *lacZ*.



Supporting Figure 2: Knockdown of *lacZ*. β -galactosidase activity of *E. coli* MG1655 pdCas9 with different psgRNAs targeting *lacZ* (236, 237, 238, 239) or an empty psgRNA (241) with (black bars) or without (grey bars) inducer anhydrotetracycline. *E. coli* MG1655 (black bar) and *E. coli* DH5 α λ pir (grey bar) were used as control strains without anhydrotetracycline addition. Error bars indicate SEM (n = 3).

Supporting Information S2: Inducer Concentration

E. coli MG1655 pdCas9 psgRNA_aceE_233 was cultivated in shaking flasks with anhydrotetracycline concentrations ranging from 0.01 $\mu\text{g/ml}$ to 1.0 $\mu\text{g/ml}$ (Suppl. Fig. 2). Anhydrotetracycline serves as the inducer of dCas9 expression from pdCas9. A control fermentation with no addition of anhydrotetracycline was conducted to estimate the effects of leaky expression of dCas9. In all other shaking flask experiments and bioreactor cultivation anhydrotetracycline was added to a final concentration of 0.1 $\mu\text{g/ml}$ as described in the main text.



Supporting Figure 3: Inducer Concentration. Shaking flask fermentations of *E. coli* MG1655 pdCas9 psgRNA_aceE_233 were conducted with varying addition of anhydrotetracycline as indicated in the figure legend. Data on optical density (upper panel) and pyruvate concentration (lower panel) from single experiments is shown.

References

Qi, L.S., Larson, M.H., Gilbert, L.A., Doudna, J.A., Weissman, J.S., Arkin, A.P., Lim, W.A., 2013. Repurposing CRISPR as an RNA-guided platform for sequence-specific control of gene expression. *Cell* 152 (5), 1173–1183. <https://doi.org/10.1016/j.cell.2013.02.022>.